16th Symposium on

High-Performance Marine Vehicles

HIPER'24

Drübeck, 10-12 June 2024

16th Symposium on

High-Performance Marine Vehicles

HIPER'24

Drübeck, 10-12 June 2024

Edited by Volker Bertram

Sponsored by

tutech.de

www.hasytec.com

www.norsepower.com

www.numeca.de

www.idealship.de

theoceanly.com

www.hdhyundai-erc.com

www.siemens.com

Media Partners

https://hansa-online.de/

https://www.rina.org.uk/

Index

Volker Bertram 6
Trim Optimization – In Simple Terms

Karsten Hochkirch, Carsten Hahn, Heikki Hansen, Volker Bertram 10
Smart Energy Efficiency – Optimization for Ship Design, Retrofit and Operation

Tracy Plowman, Volker Bertram 21
AI Tools for Maritime Training Applications – Stories of Success and Failure

Oliwia Gałecka 29
Case Studies Examining the Impact of Employing Robust Voyage Optimization Techniques on Enhancing a Vessel's CII Rating

Volker Bertram 36
Savings from Route Optimization: Myth or Reality

Lennart Cederberg, Eleonor Marmefelt, Jan Snöberg 43
The Arctic Tern: AI + Soft Values = Save Fuel

Sven Albert, Thomas Hildebrandt, Benoit Mallol, Leo Poppelier 49
Robust Design Optimization for More Efficient Ship Propellers

Rodrigo Perez Fernández, Emily Arens, Sean Pearson, Dmitry Ponkratov 73
Innovative Approaches in Vessel Design: Pioneering Integrated Multidisciplinary Analysis and Digitalization for Enhanced Performance

Alessandro Castagna 89
Impact of Energy Saving Devices on EEXI and CII: Theory and Practice

Klas Reimer 101
Maritime IoT: Onboard Energy Data as Key to Operational Optimization

Matija Vasilev, Milan Kalajdžić 107
CFD-Driven Ship Trim Optimization: Simplifying Complexity of ANN with User-Friendly Software

Changbae Jin, Yoichi Wakabayashi, Nobuyuki Onishi, Yoshihiko Sugimoto 118
Wind Challenger Project - Updates & Future Plans

Roland Lindinger, Volkmar Wasmansdorff 131
The Design of the Ships' Hulls based on Application of Aircraft Wing and Fuselage Engineering Principles

Christina Warmann, Tobias Melloh, Torsten Dunger 140
Digital Twin for Port Energy Infrastructure

Hanna Pruszko, Krzysztof Czerski, Marek Necel, Sören Brüns, Sven De Brie, Michael Hübler, Jörg Mehldau, Shivaraj Kudari, Maciej Reichel 149
Evaluation of the Twin-CRP-Pod Propulsion Concept for Ultra-Large Container Ship – Conclusion From the Project Study

Kiran Ramesh, Anirban Bhattacharyya 164
Hydrodynamic Performance of a Propeller within a novel Partial Duct

Robert Dane, Nick Rozenauers, Ian Milliner 177
Sustainably Powered Autonomous Surface Vessels

Teemu Kuusisto, Mona Kanafi 184
Possibilities for Hybrid Cruise Vessel Performance Optimization through Data-Driven Battery Usage

Kadir Burak Korkmaz, Sofia Werner, Rickard Bensow, Ruihua Lu 197
Trim Optimisation – CFD, Model Test and Full Scale

Fabian Thies, Hannes Renzsch 218
Hull Form Variations for Improved Sailing Balance of Wind-Assisted Propelled Ships

Karthik Sankaramoorthy, Manuel Cerro Diaz de Teran 226
A New Paradigm in CSOV Ship Design – A Performance Study

Ville Paakkari 245
Smart Sails for Decarbonizing Heavy Shipping

Lukas Kistner, Kevin Koosup Yum 252
How to Design and Assess Multi-component Ship Power Systems

Hannes Renzsch, Andrew Spiteri, Eduardo Blanco-Davis, Milad Armin, Alex Routledge 268
Optimisation of an Air Lubrication System for Geometry and Topology: A Proposed Solution for Ship Retrofitting

Frederike Engels, Josefin Klindt, Lars Ravens 281
How to Retrofit 400 kW of Green Hydrogen Power into an Offshore Supply Vessel as an Add-on System

Dirk Höflich 290
100 Years Rotor Sails: A Rediscovered Invention to Meet the Net-Zero Goal

Stav Jacob, Matan Nice 308
Reimagining Proactive Cleaning: Benefits of High-Frequency Cleaning by Means of an Autonomous In-Transit Hull Grooming Robot

Ove Hagel, Matti Früchtenicht 315
Ultrasonic Antifouling - An Approach to Mitigate Biofouling on Ship Hulls and Niche Areas

Angela Craciun, Ivana Melillo, Fotis Papadopoulos, Mia Elg 324
Digital Tools Enabling Net-Zero Cruise Vessels

Kenneth Goh 339
Machinery Design Considerations of Future Fuel Cell Powered Vessels

List of authors

Call for Papers for next HIPER conference

Trim Optimization – In Simple Terms

Volker Bertram, DNV, Hamburg/Germany, volker.bertram@dnv.com

Abstract

This paper gives an overview of different approaches to trim optimization, discussing first-principles approaches (based on simulation) and machine-learning approaches. Key jargon used in marketing is explained. Both approaches work well and can save significant amounts of fuel if properly used.

1. Introduction

All standard references for ship energy efficiency, such as the 2nd IMO greenhouse gas (GHG) report, *Buhaug et al. (2009)*, the Oil Companies International Marine Forum (OCIMF) study for emission-mitigating measures, *OCIMF (2011),* or https://glomeep.imo.org/, have ranked trim optimization highly as a recommended measure.

Indeed, trim optimization is easy to refit and generally gives short payback times, typically in the order of several months. But customers are faced with an ever-increasing array of vendors which use incomprehensible jargon. Should I take a "dynamic performance model based on advanced machine-learning technology" or rather the "RANSE with VoF"? (The quotes are taken from actual brochures from vendors of trim optimization solutions.)

Simple advice: Don't be blinded by science; don't be impressed by a smoke screen of jargon. You don't need to code the software; you just want to understand the basic principles and the pros and cons of the different approaches.

The following gives an introduction to available options, explains some of the jargon and discusses strengths and weaknesses of the different approaches.

2. Crucial knowledge base

There are several commercial trim optimization tools on the market. These vary in price, user friendliness, fundamental approach, and performance. However, they all combine two key elements:

1. A ship specific database (often called the hydrodynamic "knowledge base") for resistance or power as function of operational parameters. This knowledge base is akin to the baseline curves in performance monitoring.
2. A user interface displaying the trim recommendation. Virtually all systems use an intuitive traffic-light scheme for good, acceptable, and poor trim options.

Key operational parameters considered are speed, displacement (respectively draft) and in rare cases also water depth.

Other factors, such as seaway, are seen as secondary for trim optimization and therefore not considered. For certain cases, such as ferries or ships trading frequently in shallow waters (e.g. Baltic Sea), the inclusion of water depth as a parameter makes sense. For most other ships, water depth may be neglected. On very shallow water, aspects of safe manoeuvring overrule energy efficiency considerations.

The hydrodynamic knowledge base should be a dense matrix of speed, trim, and draft values. Its range should cover all feasible operational combinations. Typically this requires 300-400 data sets (combinations of trim, draft and speed) for deep water, and 3-5 times as many if also shallow water variations are to be covered. The discrete data sets are connected by smooth interpolation (multi-dimensional

response surface in jargon), allowing consistent interpolation for whatever operational conditions are specified by the user.

While each trim optimization tool must have a hydrodynamic knowledge base, the chosen approach to generate this knowledge base decides costs and performance of a trim optimization system.

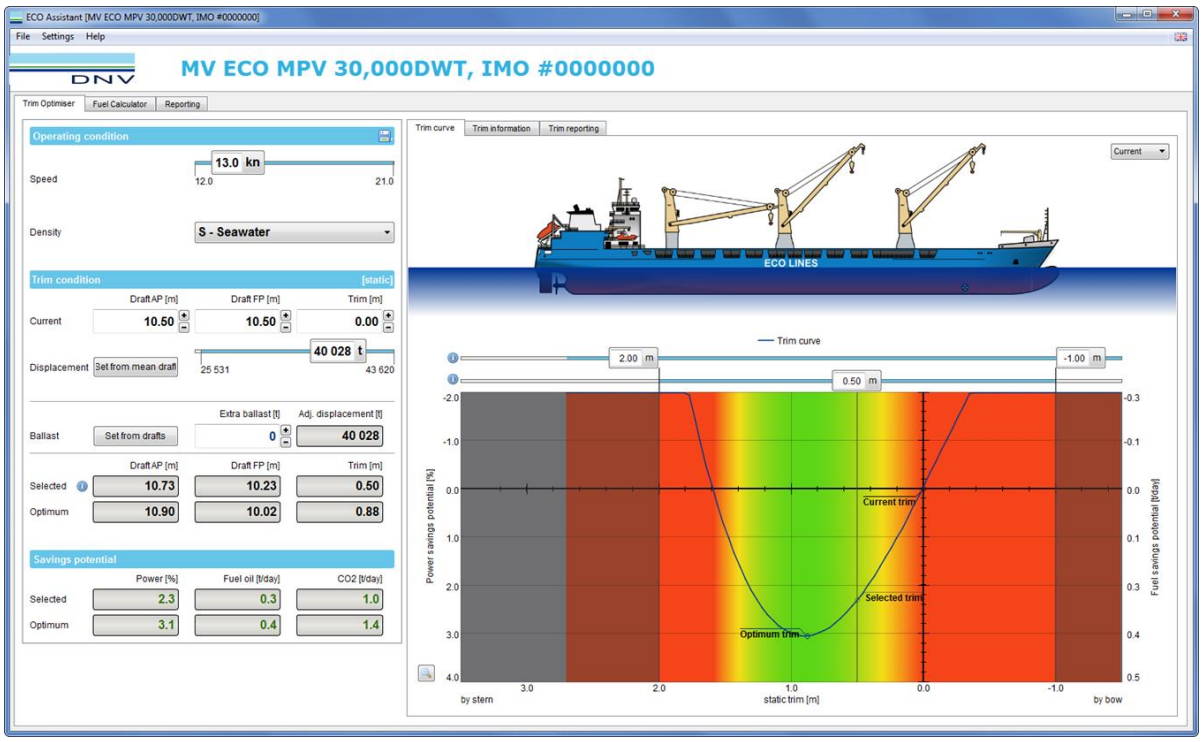


Fig1: Behind the typical user interface lies a ship-specific hydrodynamic knowledge base

3. Building the knowledge base

3.1. First learn, then apply your knowledge – The CFD based approach

There are two fundamentally different approaches to develop trim optimization tools. The first group of systems is based on a "laboratory" hydrodynamic model which creates the knowledge base systematically and completely, before the trim optimization software is used.

The system goes to school first and learns the knowledge base before being sent out to the real world. This school training may be through model tests or numerical simulations. As this approach does not require interfacing with onboard systems or sensors, it makes installations much more cost effective on most ships, especially for fleets of sister vessels. However, the approach requires a geometry model of the hull, which may have to be re-engineered from available cross sections and main dimensions or from 3D scanning.

Model tests are in principle an option, but the creation of dense knowledge base involves much more time and cost than CFD (computational fluid dynamics). In addition, model tests suffer from scale effects (different wave breaking from full-scale ship) and have thus also a slight accuracy handicap. Hence, some of the older trim optimization systems were based on model tests, but today CFD-based approaches are now preferable.

Older CFD approaches used simpler flow models (using jargon such as potential flow, panel or Rankine singularity methods). These fail for breaking waves and have poor or no propeller models, leading to less accurate results. Better flow models give more accurate results and thus better trim recommendations and higher fuel savings.

Such high-fidelity simulations (using jargon such as full-scale RANSE simulations, viscous CFD, two-phase flow, Volume-of-Fluid (or VoF) method) may be more aptly called "numerical sea trials" than "numerical towing tank" tests, as they mimic the full-scale ship rather than the scaled-down model of a model basin. They are capable of modelling breaking waves accurately, which is essential in conditions where bulbous bows partially emerge or transom sterns partially immerse.

3.2. Learning on the job – Beware of incomplete training

The second group of trim optimization systems is based on system identification of the actual ship. Typically some machine learning techniques are employed. This approach does not need any information about the ship hull geometry. However, it requires rather extensive sensor information. Ships must then be equipped with advanced data acquisition systems. These systems have to cope with changing ambient conditions (wind, waves, current, water temperature, etc.), which affect the resistance of the ship.

Even if sophisticated correction methods are used, the uncertain nature of the ambient conditions introduces unavoidable scatter in the target data. Machine learning techniques perform in essence the task of putting a smooth "curve" through the scattered data. The more parameters are involved, the slower the computer learns, *Bertram (2022)*. Therefore machine learning approaches work best for ships which feature fewer changes in operational and ambient parameters, such as ferries or cruise vessels.

While the first group (model test and CFD-based knowledge base) had the benefit of a proper school education, the second group has to learn on the job. Typically there is an apprentice period, though: Initial dedicated training periods vary draft, trim, and speed, ideally during days where the ambient conditions do not contaminate the data sets too much. After that, it is life-long learning to fill missing patches in the knowledge base and to update existing knowledge. This continuous learning is called "dynamic" in trim optimization jargon.

In a shipping fairy tale one captain was faced with a dilemma; the story goes like this: Once upon a time, there was a shipowner who was looking for the best trim optimization for his vast empire of ships. He looked for suitable candidates and installed a CFD-based system and a machine-learning system on one of his ships. One fine day, the captain asked both systems for advice. The CFD-based system said: 1 m down by the bow. The machine-learning system said: 1 m down by the stern. Who should the captain trust?

It sounds like a fairy tale, but rumor has it that this happened more than once. But, the solution to the puzzle was that the comparison was made shortly after installation. The captain had never before driven the ship on that draft and at that speed other than with trim by stern. The machine learning system had, therefore, never "seen" that by trimming by bow the fuel consumption was lower and picked the best solution from its limited experience. Its knowledge base was patchy and thus its recommendation not good. The CFD-based system had covered the whole knowledge base before installation and thus gave the right recommendation.

In all fairness, had the machine-learning system been trained on all possible conditions, it would have given the same recommendation. The vendor no doubt wrote this in his instructions. But, there is always the danger that we don't read the instructions.

4. Integrated or stand-alone?

Trim optimization may come as part of larger advisory systems, e.g. coupled with stowage planning, voyage optimization, or performance monitoring. Trim optimization software in itself is good, but even better if combined properly with other functionality. The coupling to stowage planning is attractive as optimum trim should be achieved without extra ballast.

Similarly, automated reporting functions are nice to have. The automated reporting serves a double purpose: as proof of energy efficient operation (for SEEMP documentation, national and port authorities, between charterers and shipowners, charterers and cargo owners, etc.) and as incentive for increased usage of the system.

5. Use with caution and exploit economies of scale

Trim optimization is highly advisable for virtually all ship types. CFD-based trim optimization is the most cost-effective trim optimization option for fleets of sister vessels. Care should be taken that the CFD approach used is not based on outdated potential flow methods.

The big advantage of CFD is that one can exploit the advantages of parallel computing. Dense knowledge bases can be typically generated in one or two weeks on high-performance computers with several thousand parallel processors. This is a unique advantage over model tests and system identification on real ships.

Machine-learning systems may give similarly good results, but must be trained properly, which requires more time and crew awareness.

References

BERTRAM, V. (2022), *Capabilities and Limits of Machine Learning*, 7th HullPIC Conf., Tullamore, pp. 16-23, http://data.hullpic.info/HullPIC2022_Tullamore.pdf

BUHAUG, Ø.; CORBETT, J.J.; ENDRESEN, Ø.; EYRING, V.; FABER, J.; HANAYAMA, S.; LEE, D.S.; LEE, D.; LINDSTAD, H.; MARKOWSKA, A.Z. (2009), *2nd IMO GHG Study*, Int. Mar. Org., London

OCIMF (2011), *GHG Emission-Mitigating Measures for Oil Tankers*, Oil Companies International Marine Forum, London

Smart Energy Efficiency – Optimization for Ship Design, Retrofit and Operation

Karsten Hochkirch, Carsten Hahn, Heikki Hansen, Volker Bertram, DNV, Hamburg/Germany,
karsten.hochkirch@dnv.com

Abstract

This paper gives an overview of the application of formal optimization in ship design, retrofit of ships, and operational procedures. The application cases are taken from industrial practice and recent research projects, reflecting the state of the art and near-future trends. In design, optimization based on parametric form description and CFD may be applied to global hull optimization considering realistic operational profile matrices, or local optimization, e.g., for appendages. Allowing asymmetric sterns may lead to additional fuel savings of 2-3%. In retrofits, formal optimization for bulbous bows for different operational profile (slow-steaming and partially loaded conditions) offers significant saving potential in many cases. In operation, trim optimization and weather routing are widely used applications. For ships with wind assisted propulsion systems (WAPS), weather routing needs to consider the WAPS characteristics.

1. Introduction

1.1. Energy efficiency improvement as first phase in decarbonization

IMO is set to cut the carbon footprint of shipping. The Big Zero is the long-term goal for "around" 2050, with the mandatory EEXI (Energy Efficiency Design Index) and CII (Carbon Intensity Indicator) being introduced since 2023. As a very brief recap, the EEXI is the Energy Efficiency Existing Ship (Design) Index, akin to the EEDI (Energy Efficiency Design Index) for newbuildings, expressing the theoretically achievable energy efficiency for the ship as designed, in prime condition as in initial sea trials. The CII (Carbon Intensity Indicator) is calculated based on IMO's fuel oil DCS (Data Collection System), where the requirement to just monitor is now enhanced by grading the performance each year from A to E. Poor operational performance (E once or three consecutive years D) will entail mandatory action to improve performance, planned, documented, tracked, and audited in a SEEMP (Ship Energy Efficiency Management Plan). The CII will be subject to increasingly stricter thresholds over time, driving the industry towards decarbonization.

Most vessels will be able to comply with EEXI requirements by using EPL (Engine Power Limitation). Some may have to resort to more significant retrofit options, as discussed below. The Carbon Intensity Indicator (CII) will have a more profound impact, driving design and operational changes both for the existing fleet in service and future newbuildings. In addition, the EU ETS (Emissions Trading System) will impose gradually from 2024 to 2027 surcharges on CO_2 emissions, leading eventually to an expected 50% increase of fuel cost for classical fuels.

The goal of reducing carbon footprint is clear for everyone, and so is the prospect of increasing regulatory and market pressure. But how will we get there? In essence, there are four levers to progress towards lower carbon footprints for ships:

- Low/no-carbon fuels – "Decarbonization" makes most people think first of alternative fuels, such as biofuels, methanol, ammonia, or hydrogen, *Bertram (2021)*. The problem is that these fuels generally will be significantly more expensive than Heavy Fuel Oil (HFO), the standard shipping fuel of pre-2020 times. Alternative fuels will certainly play a role, but more at a later stage, post 2030. EU ETS is likely to close current price gaps, e.g. for biofuels, post 2027.
- Market-based measures - Economic frameworks, such as CO_2 compensation schemes or taxes/ surcharges for CO_2 emissions respectively carbon-content of fuels, most notably the coming EU ETS scheme. Such schemes will make traditional carbon-based fuels more expensive.

- Wind-assisted propulsion systems (WAPS) – The idea of using renewable energy sources directly for ship propulsion is not new, but has been enjoyed exponential growth in installations over the past few years after decades of being rather dormant, *Hochkirch and Bertram (2022)*. Business cases are difficult to establish due to the highly nonlinear nature of exploitable wind conditions. Harnessing the wind is also an option which we will invoke on a wider and larger scale at a later stage, post 2030.
- Energy efficiency – With increasing fuel prices, there will be renewed scrutiny of energy-saving measures in design and operation, https://glomeep.imo.org/. This lever is likely to be the dominant contributor to decarbonizing shipping in the short term (i.e. next decade), not least because many energy saving measures pay for themselves.

In the following, we will discuss the measures for the short term, employing formal optimization technique, with a focus on energy efficiency.

1.2. Getting the terminology straight – what is "optimization"?

The term (hull) "optimization" is widely used and in many cases abused. Often the term "improvement" would be more appropriate than "optimization". Muddy terminology creates confusion. We should get our terminology straight. We distinguish then the following design approaches:

- Simulation-based design - Simulation-based design commonly employed in industry. Typically, less than 10 variants are generated and assessed by more or less sophisticated simulations. Human experts look at details of the simulation (e.g. pressure distribution in critical areas) and derive recommendations for design changes. For hydrodynamic design, CFD (Computational Fluid Dynamics) techniques are applied, *Bertram (2012)*. This by now standard design procedure is employed by many design offices and model basins around the world, but frequently we see that significant improvement beyond this approach are possible.
- Concept exploration - Concept exploration models (CEMs) have been proposed as an alternative to 'automatic' optimization. More recently, "design of experiment" (DoE) has been used as a term for the same design strategy: A large set of candidate solutions is generated by varying design variables. Each of these solutions is evaluated in key performance indicators and stored. CEMs thus generate a "map" of the unknown design space. Using suitable graphical displays, the designer gets a feeling how certain variables influence the performance of the design. The approach was deemed impractical for ship design in the 1990s due the then excessive computational requirements, *Erikstad (1996)*. However, parallel computation has changed this, and concept exploration is now used in commercial projects.
- Optimization - Optimization looks at thousands or even tens of thousands of designs and uses an optimization algorithm to find the best design. For many modern optimization problems, genetic algorithms (GAs) or related evolutionary optimization algorithms are the preferred choice these days. GAs are significantly less efficient than older gradient-based search algorithms. However, they are easily parallelized and robust in finding global optima, i.e. they do not get stuck at local optima. (Single-objective) optimization is in theory a mathematically well-posed problem. However, objective and all constraints must be expressed as mathematical functions. This is not easy in practice, *Bertram (2003)*.
- Multi-objective optimization - Optimization for multiple objectives is strictly speaking nonsense. Mathematically you can only optimize for one objective, respectively an optimum is only defined for one objective function. In layman terms, finding the fastest (objective: speed) and cheapest (objective: price) car will result in the question: Make up your mind, what do you want? Multi-objective optimization in practice is short for a combination of concept exploration and optimization. The concept exploration helps in making up one's mind. Then objectives may be reformulated as constraints or combined in one artificial objective function using weights for the individual objectives. The "best compromise" objective function can then be determined formally by the optimization algorithm of choice.

The borderline between concept exploration and multi-objective design becomes indistinct in practice. The process of concept optimization resembles a formal optimization. A concept design family is described through parametric variations; however, concept exploration uses typically fewer parameters and fewer candidate evaluations. The key difference is that the final design solution is selected without employing a formal optimization algorithm.

The highest energy saving potential lies in design. However, advanced simulations and optimization techniques are also applied to make ship operation more energy efficient. Key applications in this respect are trim optimization and weather routing.

2. Applications

2.1. Optimization in ship design (shapes)

Hull optimization has become a powerful and widely accepted tool in professional ship design, *Hochkirch and Bertram (2012), Bertram and Campana (2020)*. State-of-the-art projects employ CFD ("numerical towing tank" or "numerical sea trials"), where for final verification high-fidelity CFD at full-scale conditions is recommended, *Hochkirch and Mallol (2013)*, and consider a spectrum of operational profiles rather than a single design point, *Hochkirch et al. (2013)*.

Typically, hull optimization projects obtain 4-6% improvement on expected yearly fuel consumption in calm-water for a specified representative operational profile over a design developed by an experienced ship designer, as quantified in subsequent final model tests.

Higher savings are feasible if base designs are older or if the optimization projects start earlier with more freedom in hull modifications, e.g. starting with concept exploration.

2.1.1. Concept exploration projects

In a project for a fleet of containerships, a concept exploration study found the best main dimensions and key design parameters before a classical hull optimization was performed. The core objective of the study was requirements elucidation for the ship owner, exploring what may be possible when varying length, beam, block coefficient or average TEU weight. Hull shapes were generated automatically using commonly used CAD distortion techniques (Lackenby approach). The power requirements were assessed by means of a simplified numerical towing test: A fully nonlinear wave resistance code with simplified propeller model and viscous flow effects was employed.

Such a tool is not sufficient for a proper numerical propulsion test, but known to give correct ranking of alternatives for similar designs and significant changes in global geometry. The advantage is that the tool is very fast and allows rapid design exploration, as needed in such concept exploration. Each concept resulted in main dimensions, simplified pocket plan, speed-power curve, and initial stability assessment. In total, some 8000 designs were explored. The result is "virtual map" of the design space, allowing an informed decision on the main dimensions and configuration for the intended trade mission. The logical next step after this decision was then a refinement of the design in a formal hull optimization.

Another concept exploration study investigated an envisioned hull extension of the German Navy frigate F123. Key objectives were stability (to be increased) and power performance (to be decreased). Some 10000 variants of the new aftbody were investigated numerically, Fig.1 and Fig.2. Based on the resulting design knowledge, we recommended a detailed geometry with significantly improved stability and no hydrodynamic penalty.

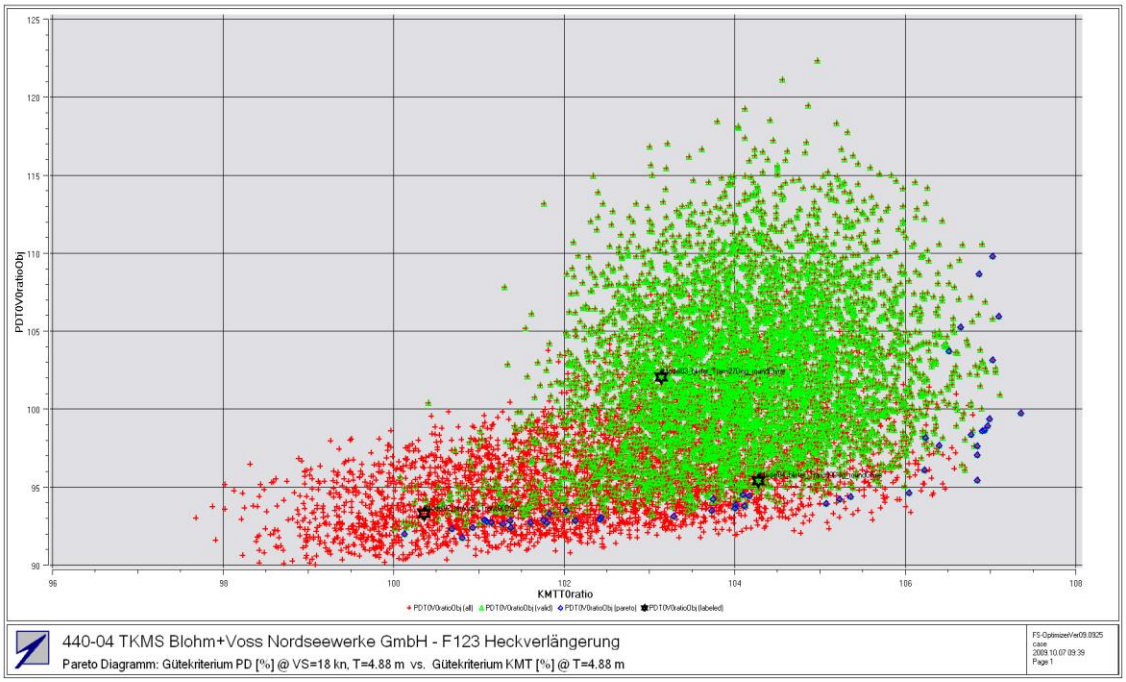


Fig.1: Pareto-diagram of required power (y-axis) and KM-values (x-axis). Green dots are permissible variants.

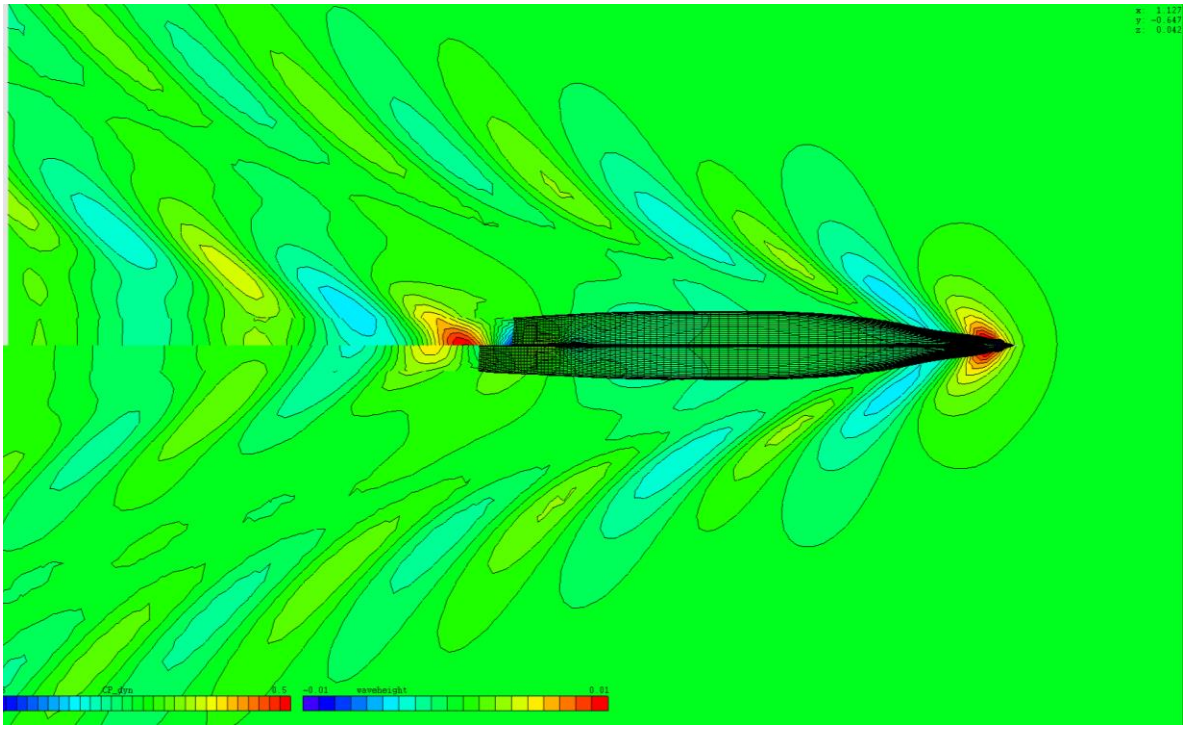


Fig.2: Wave pattern for original hull (top) and recommended extended version (bottom)

2.1.2. Hull optimization for large container ship

A typical optimization project starts with a good design, ideally with main dimensions determined in a concept exploration study. Then the hull optimization fine-tunes the vessel performance.

As a typical example, a 14000 TEU container ship project employed more than 60 free parameters with the objective of reducing fuel consumption as much as possible, taking into account hydrodynamic power requirements, the specific fuel oil consumption of the respective engines and the ship owner's

specific operational profile for speed-draft combinations. More than 35000 hull shape variants were investigated. For final validation, model tests at the Hamburg Ship Model Basin confirmed the CFD predictions of 4% improvement.

2.1.3. Hull optimization for small navy vessel

In a project for a Latin American navy, the hull for a new OPV (offshore patrol vessel) design was optimized for power requirements, considering a representative operational profile (six combinations of speed and draft). Constraints came in the form of several hard points for the hull and lower thresholds for initial stability (KM values). In total, 14000 design variants were considered. Overall power requirements were reduced by more than 20%, Fig.3. The unusually high savings can be partially explained by the longer cycles for ship replacement in many smaller navies (sometimes exceeding 30 years). Such large savings are also found for very unusual designs where the designers have no intuitive knowledge or base geometries.

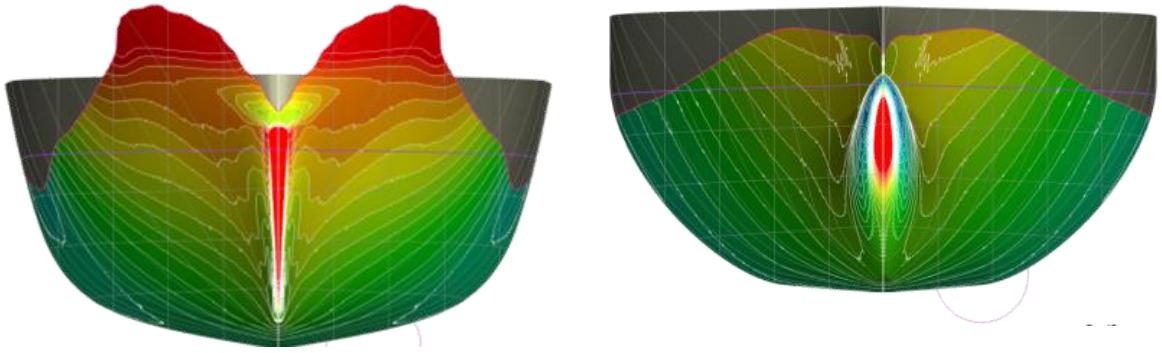


Fig.3: Hull lines optimization for OPV design; bow wave and bow pressures for original hull (left) and optimized hull (right)

2.1.4. Hull optimization for ship with asymmetric stern

Asymmetric sterns are a special case. Here the geometry model and the CFD model release the usual constraint of imposing symmetric hulls. The larger design freedom converts into additional savings in calm-water fuel consumption for realistic operational profiles of 1-5%, depending on initial design, propeller loading, ship type and optimization model, *Hochkirch and Krebber (2017), Van der Ploeg and Schuiling (2018)*.

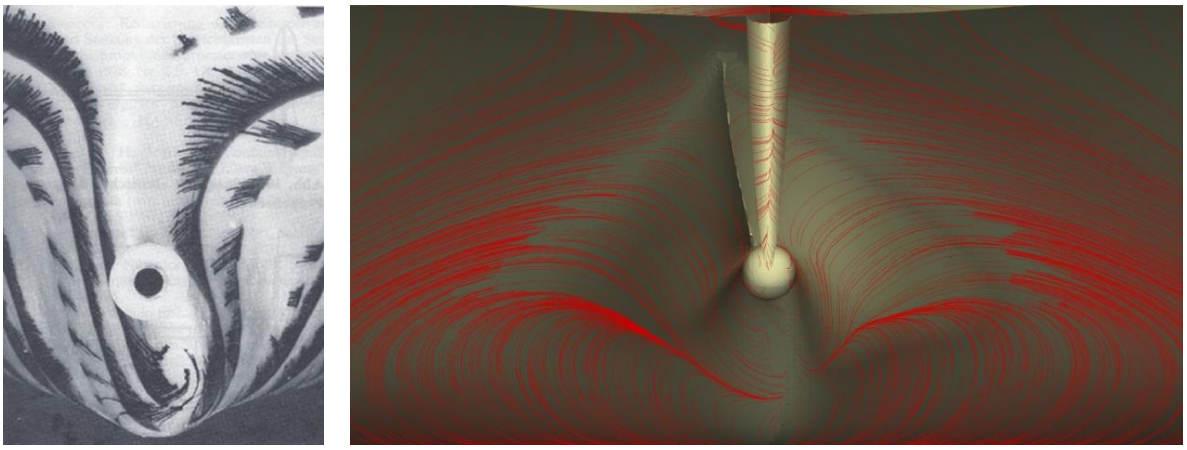


Fig.4: Model test (left) and CFD (right) evaluation of asymmetric stern

To design an optimal asymmetric aft ship, resistance and propulsion figures must be assessed and brought to an optimum. DNV's approach couples viscous RANSE (Reynolds-averaged Navier Stokes

equations) simulations for ship and rudder with a state-of-the-art propeller analysis code. The approach is computationally efficient and allows using the required power as a direct measure in the optimization.

As an example, a 3000 TEU containership was optimized for minimum power requirement, Fig.4. Starting from a well optimized symmetric baseline design, the additional freedom for an asymmetric aft ship design achieved a propulsion power reduction of 3% as confirmed by model tests, Fig.5.

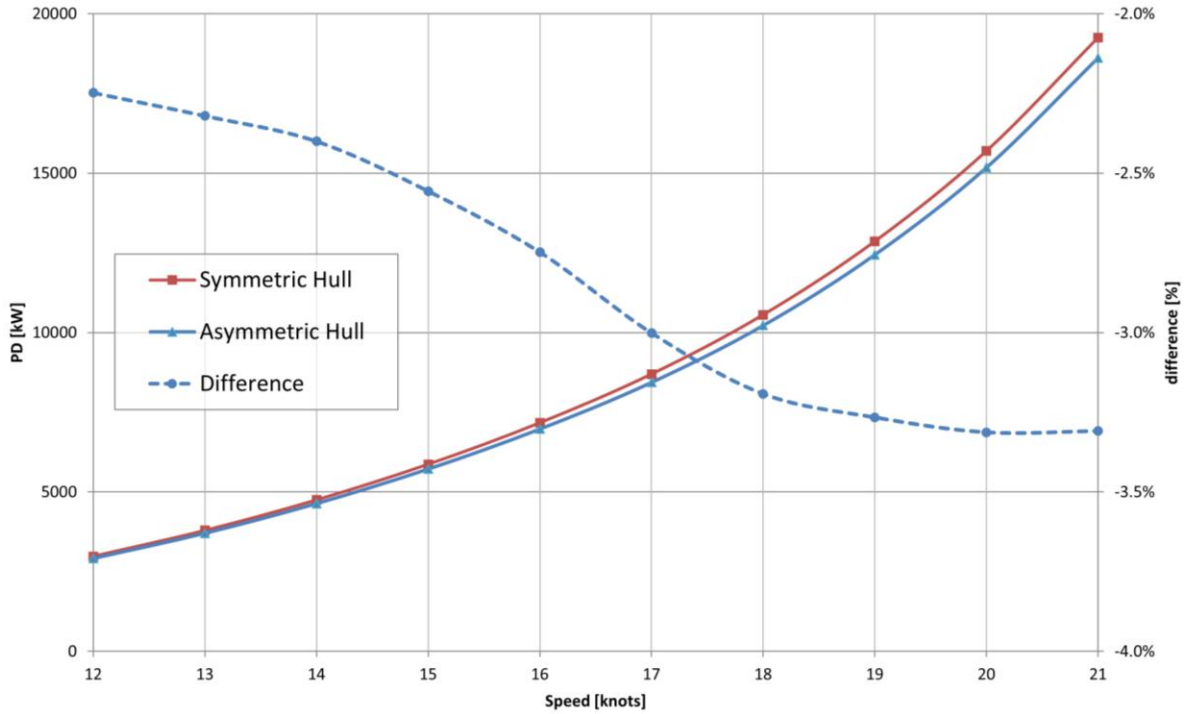


Fig.5: Model test predictions for optimized symmetric hull and asymmetric hull showing 3% improvement for asymmetric hull near design speed of 17 kn

2.2. Retrofit applications

2.2.1. Bow retrofit

While obtainable fuel savings are significantly larger for complete hull optimization, optimization of the bulbous bow region alone still offers often very attractive potential fuel efficiency gains. Such projects have enjoyed great popularity in recent years, as the quest for energy efficiency has imposed lower speeds in shipping. As a result, older ships, designed for higher speeds, then were operating in inefficient off-design conditions. In such cases, redesign of bows can offer good business cases.

A bow retrofit project for a 2700 TEU containership may illustrate this, Fig.6. The operational profile for the vessel was investigated and represented by a matrix of 9 speed-draft combinations, with weights (based on power and percentage of time in operation) as given in Table I.

Table I: Representative operational profile matrix with weights

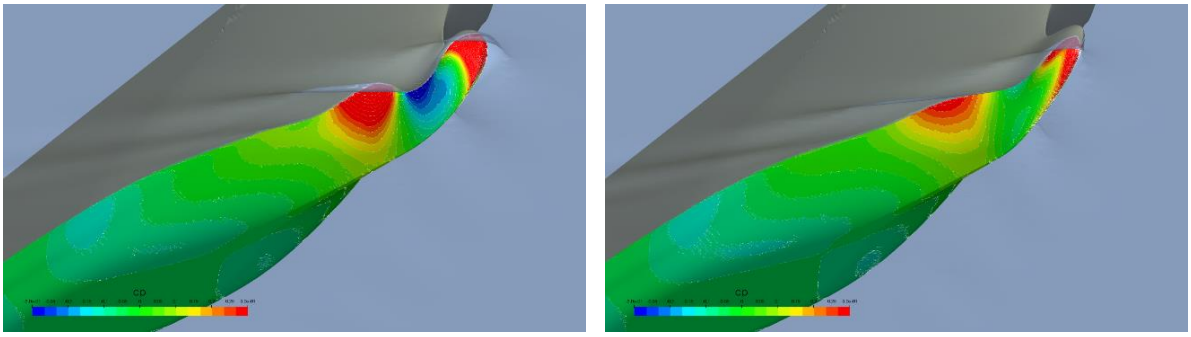
	14.5 kn	16.5 kn	18.5 kn
T_A = 8.0 m, T_F = 7.0 m	12.2%	11.3%	7.5%
$T_A = T_F$ = 9.5 m	5.4%	16.4%	1.8%
$T_A = T_F$ = 11.5 m	21.2%	22.4%	1.8%

The optimization created 4800 bow design variants as potential candidates. Table II shows the achieved savings in power for the optimized bow. The weighted average savings in power (as first approximation

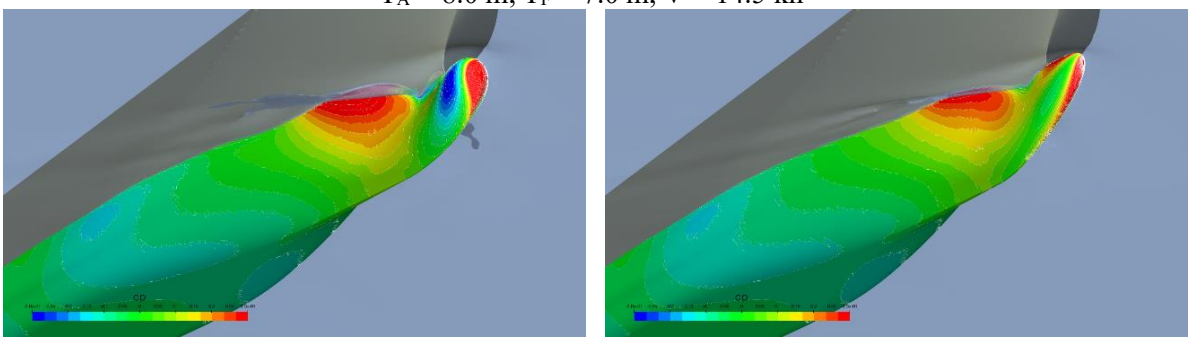
for yearly fuel consumption) summed up to 17.8%, coming largely from the off-design conditions, as typical for such projects. These savings correspond to a payback time of ~0.4 years, including conversion costs.

Table II: Savings in delivered power PD for optimized bow

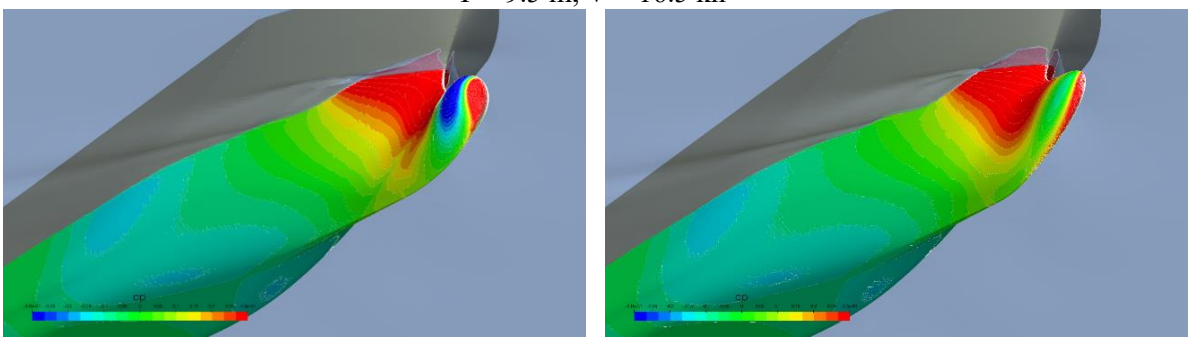
	14.5 kn	16.5 kn	18.5 kn
T_A = 8.0 m, T_F = 7.0 m	32.7%	34.6%	21.1%
$T_A = T_F$ = 9.5 m	28.4%	19.2%	10.9%
$T_A = T_F$ = 11.5 m	11.8%	4.4%	0.0%



T_A = 8.0 m, T_F = 7.0 m, V = 14.5 kn



T = 9.5 m, V = 16.5 kn



T = 11.5 m, V = 18.5 kn

Fig.6: Selected CFD results for bow retrofit analyses; original (left) and optimized (right)

2.2.2. Rudder optimization

Local optimization may also be applied to appendages, such as rudders, propulsion improving devices (PIDs), side thruster outlets, etc. For example, DNV tutored a project on optimizing a twisted rudder with a Costa bulb, Fig.7, *Echeverry Jaramillo (2016)*. In this case, the delivered power was reduced by 4.5%. However, formal optimization for ship appendages is still the exception rather than the rule. In many cases, selected CFD analyses are preferred, often due to time and budget constraints.

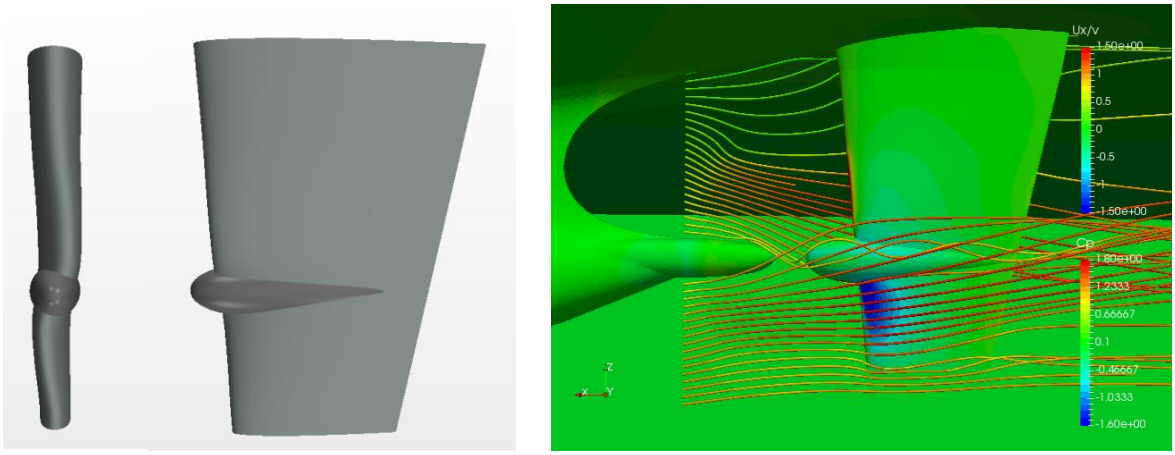


Fig.7: Rudder CAD model (left) and CFD results for optimized twisted rudder with Costa bulb

2.3. Trim optimization

In trim optimization, key operational parameters considered are speed and displacement (respectively draft). For most ships, water depth may be neglected. At the heart of any trim optimization software is a knowledge base that relates speed, trim and draft for a given ship to required power. This knowledge base should cover all feasible operational combinations with sufficient data density. Typically, this requires 300-400 data sets (combinations of trim, draft, and speed), *Bertram (2014)*. The discrete data sets are connected by multi-dimensional response surface, allowing consistent interpolation for whatever operational conditions are specified by the user. Today, CFD is the preferred choice to create trim knowledge bases. For some critical cases, such as surface-piercing bows, full-scale CFD calculations are important, *Hochkirch and Mallol (2013).* Parallel computations make the CFD approach better respectively more reliable than model tests, *Bertram (2014)*. Alternatively, the knowledge base may be created using machine learning from the real ship in operation. Here, care has to be taken that the training data sets cover the whole relevant space of data sets during the training period of several months.

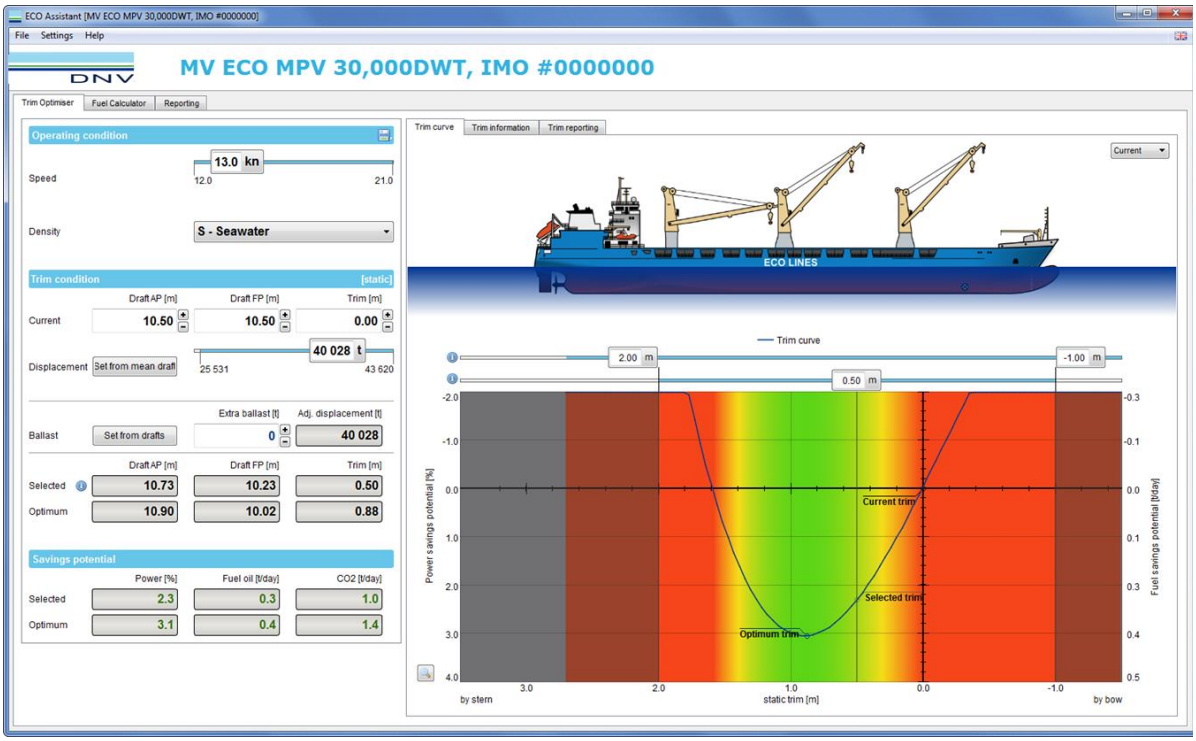


Fig.8: User interface of trim optimization software ECO Assistant

The approach is then a “simple” optimization application. The shape of the immersed ship is changed by trim and possibly by increasing draft (via ballast water). As a map of the “solution space” is created beforehand, the actual optimization is very rapid and results are displayed immediately for the user, Fig.8. The option to allow larger drafts via ballast water has proven to open better results for modern containerships. These very large containerships operate often in partial drafts where the bulbous bow may pierce the water surface creating significant resistance due to breaking waves. Counter-intuitively, adding ballast water to bring the bow down can then lead to reduced fuel consumption. For a 13000 TEU containership, the addition of 10000 t ballast water resulted in 5% or 4 t fuel saved per day.

2.4. Weather routing

Route optimization (or routing) has been a topic for research projects for probably 50 years by now. Route optimization for energy efficiency combines weather forecasts (predicting seaways for ocean areas on potential ship routes), ship response to seaways (for energy efficiency, the relevant response is the added power required) and an optimization algorithm. As an added complexity, weather forecasts become increasingly uncertain beyond a time horizon of three days. Assorted constraints (e.g. in the form of strategies of ship owners or charterers) may complicate the optimization problem and explain the diversity found in doctoral theses and service providers.

Realistic estimates for the saving potential of weather routing range from 0.1% to 1.5%, *OCIMF (2011),* https://glomeep.imo.org/, falling significantly short of vendors’ claims. The errors in predicting added resistance in waves are much larger than the claimed savings due to route optimization, *Bertram (2016).* Popular methods, such as semi-empirical formulae or strip method approaches, feature errors ranging from 20% to 200%, *Bertram and Couser (2014)*. This renders savings from weather routing as rather uncertain.

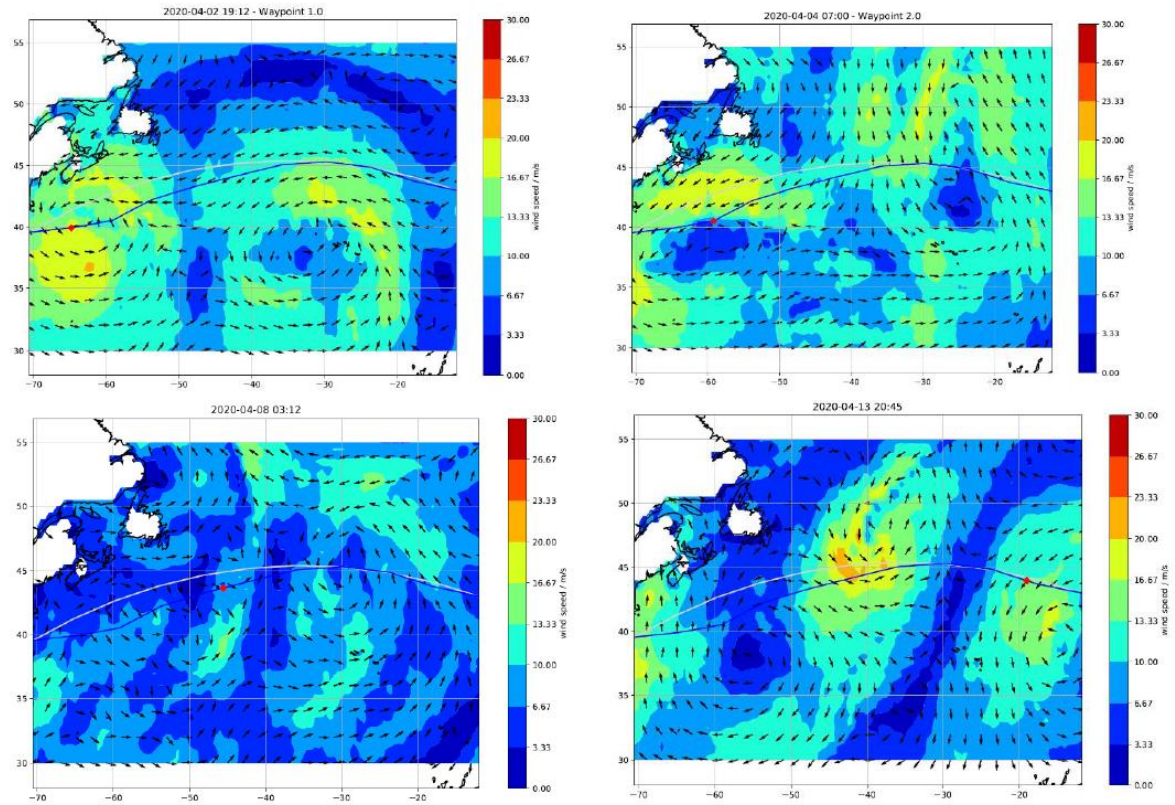


Fig.9: Optimized route for eastbound passage using Rotor Sails in April 2020. Ship position marked in red. Blue: optimized route. Grey: Great circle line (shortest distance)

Route optimization for ships equipped with WAPS offers higher energy savings, improving the business case, *Hansen et al. (2023)*. *Hollenbach et al. (2020)* describe such a dedicated route optimization model (ROM) considering the characteristics of the WAPS. Fig.9 shows the vessel's position (red dot) and the wind pattern for four stages of the optimized eastbound passage with WAPS for April 2020. Fig.10 shows the obtained average fuel savings through weather routing as a function of voyage time for a tanker without and with Flettner rotors. The average fuel savings from weather routing are 0.8-2.6% for the ship without WAPS, and 2.5-4.1% for the ship with WAPS on various transatlantic voyages simulated. Thus dedicated WAPS route optimization offers significant additional savings.

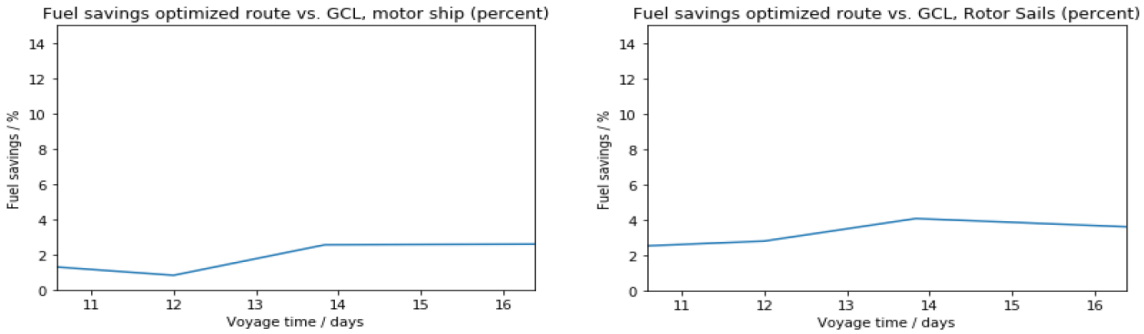


Fig.10: Average fuel savings by using weather routing. Ship without (left) and with (right) WAPS

3. Conclusions

Over the last fifty years, optimization in ship design and ship operation has progressed from "exotic" research applications to widely accepted state of the art. Refits of ship with bows optimized for current operational profiles may have payback times of less than one year. Trim optimization should be based on full-scale high-fidelity CFD. Ballast water offers additional saving potential for large containerships. Routing for energy efficiency is doubtful, as long as methods for calculating added power in waves feature high errors. For ships with wind assisted propulsion systems, routing should reflect the WAPS characteristics.

References

BERTRAM, V. (2003), *Optimization in Ship Design*, In OPTIMISTIC – Optimization in Marine Design, Mensch & Buch Verlag, pp.27-53

BERTRAM, V. (2012), *Practical Ship Hydrodynamics*, Butterworth & Heinemann

BERTRAM, V. (2014), *Trim Optimization – Don't blind me with science*, The Naval Architect, July/August, pp.66-68

BERTRAM, V. (2016), *Added Power in Waves – Time to Stop Lying (to Ourselves)*, 1st HullPIC Conf., Pavone, pp.5-13, http://data.hullpic.info/HullPIC2016.pdf

BERTRAM, V. (2021), *Fuel Options for Decarbonizing Shipping*, 13th HIPER Conf., Tullamore, pp.12-20, http://data.hiper-conf.info/Hiper2021_Tullamore.pdf

BERTRAM, V.; CAMPANA, E.F. (2020), *Ship Hull Optimization – An Attempt to Determine Position and Course of the State of the Art*, 19th COMPIT Conf., Pontignano, pp.271-279, http://data.hiper-conf.info/compit2020_pontignano.pdf

BERTRAM, V.; COUSER, P. (2014), *Computational Methods for Seakeeping and Added Resistance in Waves*, 13th COMPIT Conf., Redworth, pp.8-16, http://data.hiper-conf.info/compit2014_redworth.pdf

ECHEVERRY JARAMILLO, S. (2016), *Optimization of Twisted Rudder (With Bulb and Hub Cap),* Master Thesis, Univ. Liege, https://matheo.uliege.be/bitstream/2268.2/6189/1/Echeverry%20Sara%20-%20Full%20Thesis%205th%20Cohort,%20Feb%202016%20%20(URO).pdf

ERIKSTAD, S.O. (1996), *A decision support model for preliminary ship design*, PhD thesis, NTNU, Trondheim

HANSEN, H.; HOCHKIRCH, K.; HOLLENBACH, U.; BERTRAM, V. (2023), *Where Wind Power Makes Business Sense for Bulk Carriers,* 15th HIPER Conf., Bernried, pp., pp.116-126, http://data.hiper-conf.info/Hiper2023_Bernried.pdf

HILDEBRANDT, T.; ALBERT, S.; CARUGNO, S.; MIGEOTTE, G.; HARRIES, S.; VON ZADOW, H. (2023), *Hydrodynamic Optimization of an E-Powered Catamaran in Early Design*, 15th HIPER Conf., Bernried, pp.19-31, http://data.hiper-conf.info/Hiper2023_Bernried.pdf

HOCHKIRCH, K.; BERTRAM, V. (2009), *Slow Steaming Bulbous Bow Optimization for a Large Containership,* 8th COMPIT Conf., Budapest, pp.390-398, http://data.hiper-conf.info/compit2009_budapest.pdf

HOCHKIRCH, H.; BERTRAM, V. (2012), *Hull Optimization for Fuel Efficiency – Past, Present and Future*, 11th COMPIT Conf., Liege, pp.39-49, http://data.hiper-conf.info/compit2012_liege.pdf

HOCHKIRCH, K., BERTRAM, V. (2022), *Wind Assisted Propulsion – Economic and Ecological Considerations*, Maritime Technology and Research 4(3), https://so04.tci-thaijo.org/index.php/MTR/article/view/254498/173271

HOCHKIRCH, K.; KREBBER, B. (2017), *Optimization of ships with asymmetric aftbodies*, Whitepaper, DNV, Hamburg, https://www.dnv.com/maritime/publications/optimization-of-ships-with-asymmetric-aftbodies.html

HOCHKIRCH, K.; MALLOL, B. (2013), *On the Importance of Full-Scale CFD Simulations for Ships*, 12th COMPIT Conf., Cortona, pp.85-95, http://data.hiper-conf.info/compit2013_cortona.pdf

HOCHKIRCH, K.; HEIMANN, J.; BERTRAM, V. (2013), *Hull Optimization for Operational Profile – The Next Game Level*, 5th Int. Conf. Computational Methods in Marine Engineering (MARINE), Hamburg, pp.81-88

HOLLENBACH, U.; HANSEN, H.; HYMPENDAHL, O.; RECHE, M.; RUIZ CARRIO, E. (2020), *Wind Assisted Propulsion Systems as Key to Ultra Energy Efficient Ships*, 12th HIPER Symp., Cortona, pp.278-276, http://data.hiper-conf.info/Hiper2020_Cortona.pdf

OCIMF (2011), *GHG Emission-Mitigating Measures for Oil Tankers*, Oil Companies International Marine Forum, London

VAN DER PLOEG, A.; SCHUILING, B. (2018), *Improving an already optimized ship by making its stern asymmetric*, 17th Conf. Computer and IT Applications in Maritime Industries (COMPIT), Pavone, pp.84-97, http://data.hiper-conf.info/compit2017_pavone.pdf

AI Tools for Maritime Training Applications – Stories of Success and Failure

Tracy Plowman, DNV, Hamburg/Germany, tracy.plowman@dnv.com
Volker Bertram, DNV, Hamburg/Germany, volker.bertram@dnv.com

Abstract

We investigated various AI-based tools advocated for various functions of training – text generating tools, image generating tools, and training material. The focus of our test cases was on maritime applications. The results for specialized maritime training material applications were soberingly poor, but results for general text and image applications sometimes very good. In summary, AI has the potential to accelerate and improve development of training material, but should not be tasked with complete training development for highly specialized areas as frequently found in maritime training.

1. Introduction

Artificial Intelligence ("AI"), https://en.wikipedia.org/wiki/Artificial_intelligence, is en vogue. Even if the term is often used with only a sketchy understanding of the technology. "40% of AI start-ups don't use AI", *Collé and Morobé (2022)*. AI is widely perceived as revolutionizing our world, and impacting all industry segments, including the maritime industries and the training world.

Machine learning is the most prominent AI application, and frequently "using AI" means "using machine learning" these days. Machine learning is also at the core of machine vision and natural language processing, both often seen as AI branches in their own right, *Bertram (2018)*. Machine learning builds models and produces results based on empirical knowledge. If underlying data bases are sparse or biased, or if the software attempts extrapolation beyond the scope of the data base, errors occur. Resulting dangers from uninformed use of AI in maritime applications were already pointed out by *Bertram (2018)*, and *Collé and Morobé (2022)*.

Gaspar and Bertram (2023), *Gaspar et al. (2023)* tested various AI-based tools for maritime applications, with the conclusion that the tools gave rather disappointing results. The experience since then with AI-based tools supporting assorted tasks in developing maritime training courses has led to a more differentiated view. The conclusion and advice of using AI may then be summarized as: Be aware of limitations, but embrace the possibilities of evolving AI technologies – also in maritime training. AI offers opportunities to develop better training material in shorter time. We will illustrate that in concrete cases in the following.

2. Tools for text applications

AI may help in scientific writing, especially for non-native speakers. For automatic translation, DeepL (www.deepl.com) and Reverso (www.reverso.com) have produced good results in our experience for general texts, and reasonable results for technical translations, where occasionally specific marine, engineering, or mathematical terms were not correctly translated. Fig.1 shows an example of such a translation from a German text on numerical ship hydrodynamics, *Bertram (1994)*, to an English equivalent. The AI-based automatic translation saves significant time in re-using texts from native languages for wider, international publication.

The performance of tools like DeepL is similar to that of human translators who have a good command of languages for common vocabulary, but lack the specific vocabulary of a narrow technical domain. Even if resulting texts need some final editing, the automatic translation saves significant time and eliminates grammatical and spelling mistakes. The highly technical terms are generally the easy parts for non-native speakers with an engineering background.

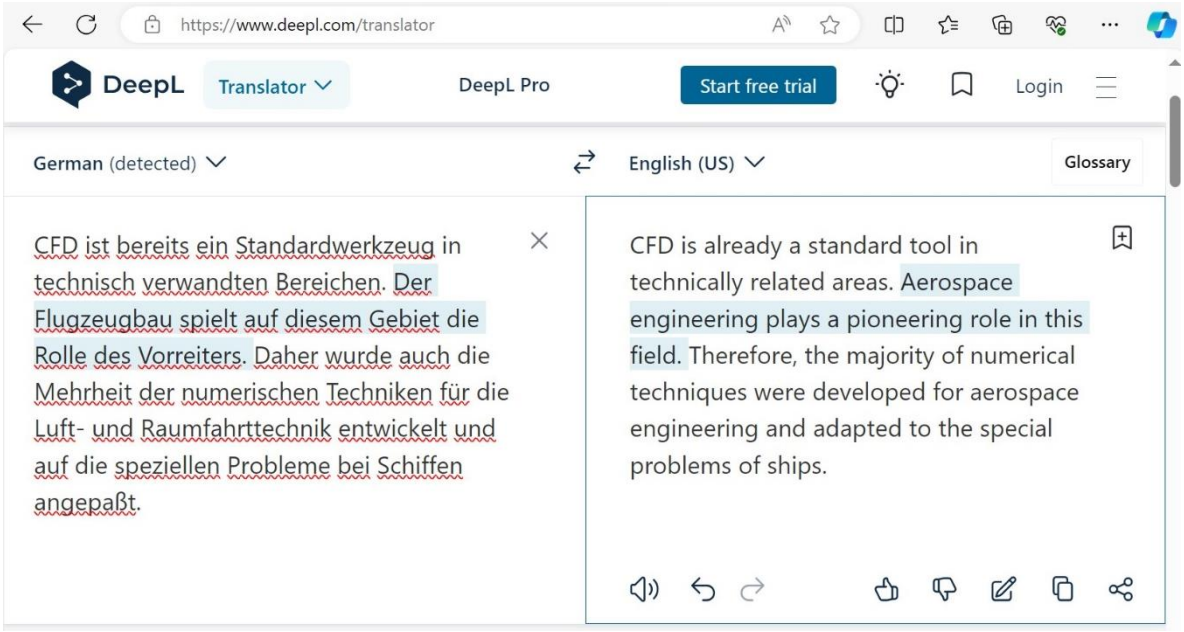


Fig.1: DeepL translation example – German to English

DeepL is limited to translations from/to 26 languages, including British and American English. ChatGPT, https://chat.openai.com/, may be used for another "special" type of translation, namely that from stilted writing into easy language, from cumbersome jargon to plain English. This is useful for native speakers as well, as their wider range of vocabulary and idiomatic expressions may introduce inadvertently linguistic hurdles for a non-native audience. Again, often some human post-processing is needed, e.g., in judging with context information what jargon is useful and what harmful for the intended audience.

ChatGPT is also good for bringing structure into larger texts. *Gaspar and Bertram (2023)* describe testing it on drafting a chapter structure for a book and a maritime paper, finding the tool very efficient in itemizing and synthetizing information. ChatGPT's suggestions were largely valid and worth considering. As a positive surprise, ChatGPT suggested some topics that the human authors had not considered, especially when asked for more information, i.e., when asking ChatGPT to "Explain".

Sometimes, it may be useful to convert images to text, e.g., when scanning older texts that are only available in analogue form, as in books or conference proceedings typically dating from pre-2000. Here, the power of pattern recognition of AI can be harnessed effectively and efficiently. Examples of online tools we have used for such purposes are https://www.jpgtotext.com/ and https://www.onlineocr.net/.

As ghost-writer for technical texts with maritime topics, ChatGPT did not write usable text and did not create usable lists of references. The texts produced needed so much reworking that any time savings as compared to writing yourself disappeared, *Gaspar and Bertram (2023)*, *Gaspar et al. (2023)*. In addition, ChatGPT tends towards "creative writing", making up wrong statements and adding non-existing references.

3. Tools for image and video creation

While ChatGPT deals with text, Dall-E from the same company OpenAI, generates images based on text prompts. For example, https://www.dallewizard.com/prompts/van-gogh advertises that you can prompt the tool to paint a specified object in the style of Vincent Van Gogh, Fig.2. We tested Dall-E 2 prompting for a ship stability curve (aka GZ curve), *Gaspar et al. (2023)*. The tool responded very quickly with a sine curve, plotted over x rather than heel angle. After 20 minutes of chat, trying to prompt Dall-E 2 into plotting a GZ curve, it still did not reach an acceptable result, see Fig.3 for the final attempt. Trying to get Dall-E 2 to draw a general arrangement plan for a frigate failed similarly,

Gaspar et al. (2023). Dall-E 2 raised high hopes looking at the Van Gogh paintings, but for technical drawings and diagrams in naval architecture, it failed.

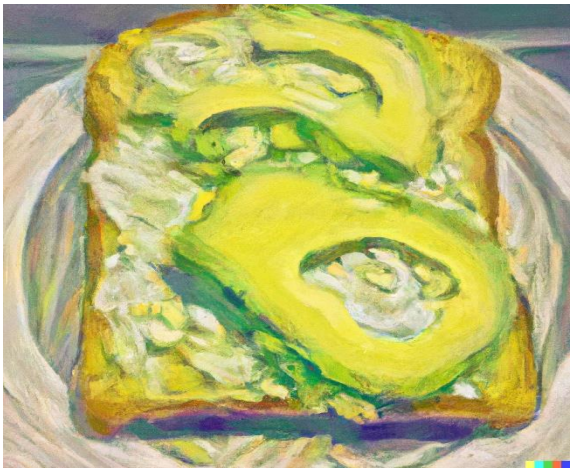


Fig.2: Dall-E 2 response to prompts for Van Gogh style avocado toast

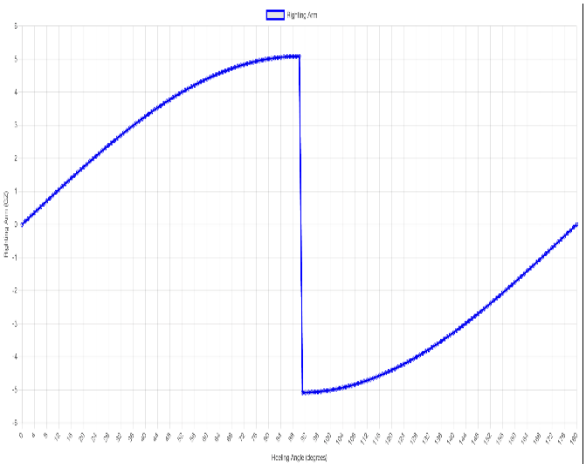


Fig.3: Failed attempt to obtain a GZ curve

A year later, we tried Dall-E 3 (as integrated in Microsoft Copilot), for more generic maritime images with good, photorealistic results. Fig.4 (left) shows a result for the prompt "worker hand holding a valve in a factory environment". Fig.4 (right) shows a result for the prompt "small Caterpillar engine inside an engine room of a small fishery vessel. Show also the other equipment of an engine room in the background. Place an engineer who is working on the Caterpillar engine in front of the engine." The results for these test cases were very good, even impressive.



Fig.4: Dall-E 3 results for valve in worker hand (left) and diesel engine on fishery vessel (right)

There are some limitations to the current versions of Dall-E or MS Copilot, though. The AI software has been trained on filtered data sets. For privacy reasons, images of celebrities were not used. For example, "show a captain on a bridge who looks like King Charles" will not work. Similarly, obscene images were not used in training; thus a naked King Charles will work even less. More annoying for our line of work is however the "dyslexic handicap" of the software. Requests to include specific words in an image often result in garbled text. For example, we requested a photorealistic image of a truck with 'ammonia' written on it in front of a ship in port. Fig.5 shows two results. While truck, ship, and port satisfied our expectations, the word 'ammonia' got garbled in different ways (Amnoina and Aminona), and we gave eventually up to get an image with correct spelling.



Fig.5: Dall-E 3 results for truck with ‘ammonia’ in front of a ship; misspelling from software

Dall-E (respectively MS Copilot) can produce tailored images to illustrate training material on generic maritime topics, without copyright issues. It is in some respect more useful than image databases like iStock or Shutterstock. Finding images to visually support a theme on PowerPoint slides or in e-learnings is a frequent task in training development, and harnessing the power of AI for this task offers definite improvements.

There has been similarly impressive progress on “moving pictures”, i.e., video creation using AI. State-of-the-art tools create storylines and dialogues from some prompts, and generate videos with lip-synced speakers. The tools are user-friendly and easy to use for beginners. “I keyed in some [DNV Maritime] Academy related words and it was pretty quick. It automatically made a starting theme with landmark Dubai buildings in the backdrop of the boat. Then I selected the conversation scene. […] I don’t think it took more than 10 minutes including me experimenting and figuring out the edits,” Michelle Kurian (DNV Maritime Academy in Dubai). Some editing is needed typically for dialogues and details, similar to repeating prompting for images to tailor the product to your needs. 1980s Vyond cartoon-style videos (www.vyond.com), Fig.6, are evolving to photorealistic, tailored avatars. The image for the avatar in Fig.7 was created using MidJourney, www.midjourney.com, which is akin to Dall-E in versatile image generation, given the right prompts. The avatar and its speech and motion in the video clip was made with D-ID, www.d-id.com, an AI video generator creating videos from videos and avatars. While our applications for such videos is mainly for the “nice-to-have” introductions (akin to the roaring lion introduction in Metro-Goldwyn-Mayer movies, https://en.wikipedia.org/wiki/Leo_the_Lion_(MGM)), the progress in AI in video generation, especially in realistic lip-synced speech, saves a lot of time and makes it accessible for general use, not requiring lengthy training.



Fig.6: Vyond video



Fig.7: D-ID video

4. Tools for more complex training material

4.1. AI-generated presentations

Developing presentations (such as for a conference) and trainings, whether based on presentations or e-learning frameworks, generally takes a lot more time than outsiders suspect, *Bertram and Plowman (2019)*. And time is money, especially in industry. Against this backdrop, DNV management stumbled across an advertisement: "Get AI-based learning content in minutes - Content can make or break your learning programs. Let Shape's AI do the heavy lifting.", https://www.docebo.com/products/shape/.

We tested Docebo Shape on DNV's "Train the Trainer" course aimed at giving an initial training for ship technology experts with no previous pedagogical experience, *Gaspar et al. (2023)*. Within a minute the uploaded original PowerPoint file was converted to the suggested online content for a training. But the result was largely useless, sometimes amusingly so, as the AI software just picked up keywords and assigned images that matched the keywords, but out of context: In introducing the trainers for the course, which hold post-graduate degrees in pedagogy, an image for a fitness trainer was selected, Fig.8 (top left). Or for training workshops, an industrial workshop with a worker welding was chosen as visual aid, Fig.8 (top right). The verb "train" was visualized with an image of a train, Fig.8 (bottom left). Text was chopped into fragments and reassembled, adding apparently random text snippets to form new sentences, which were often nonsensical, Fig.8 (bottom right). For example, "Bernhard Löbermann has a master [degree] in teaching. He has developed trainings in maritime applications for specific purposes." was converted into "Bernhil Loesbermann has a Masters in Teaching for Specific Purposes". (Typos were introduced by Docebo Shape.)

In summary, the AI-based software created useless and often nonsensical material. We looked at other AI tools to create complete trainings and presentations "within minutes" and they fell similarly short of the marketing promises and our requirements, *Gaspar and Bertram (2023).*

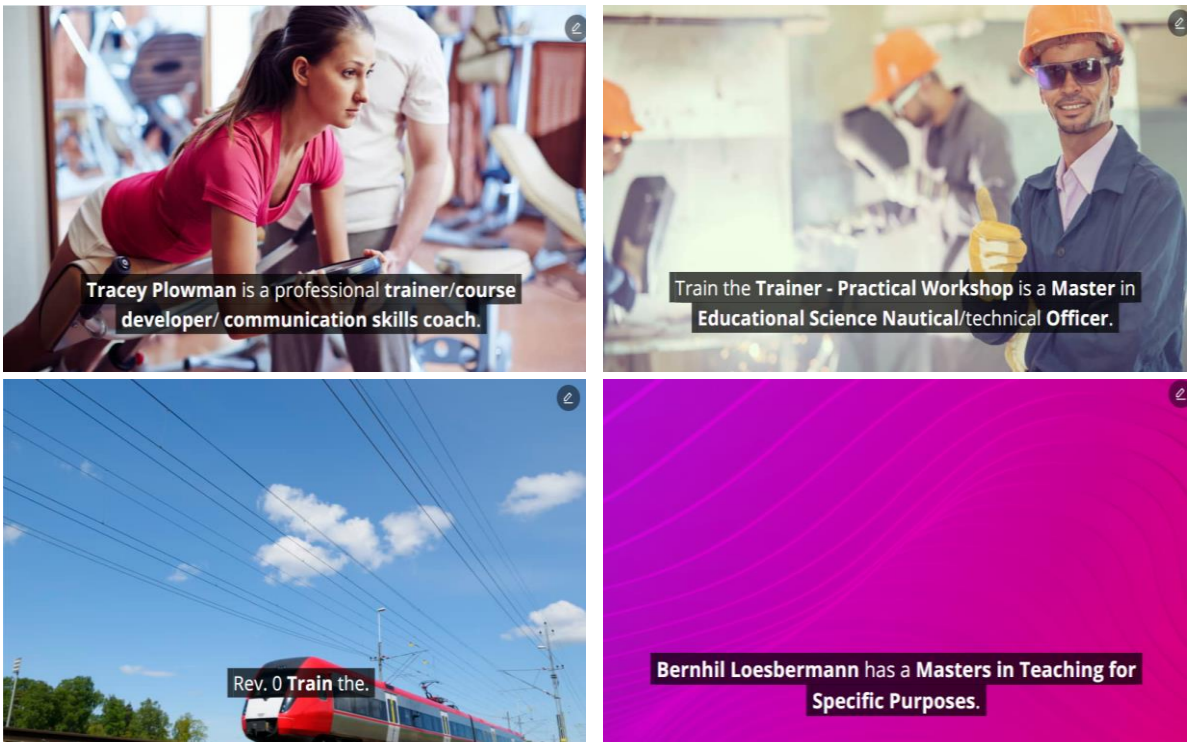
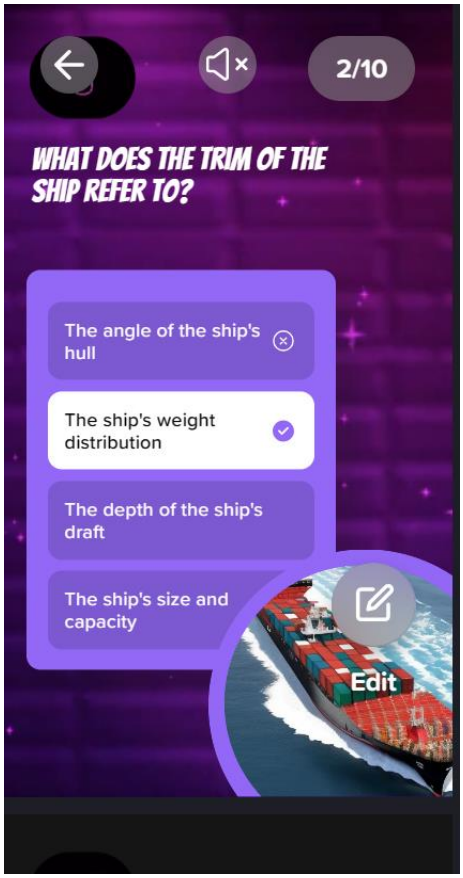
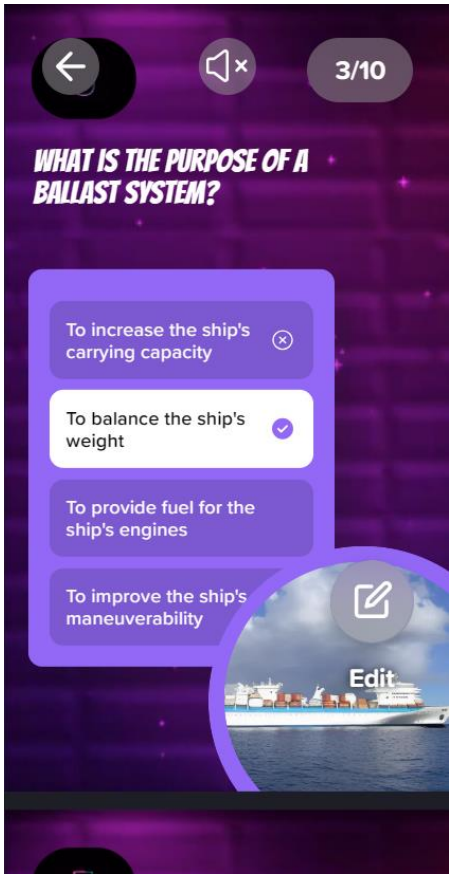


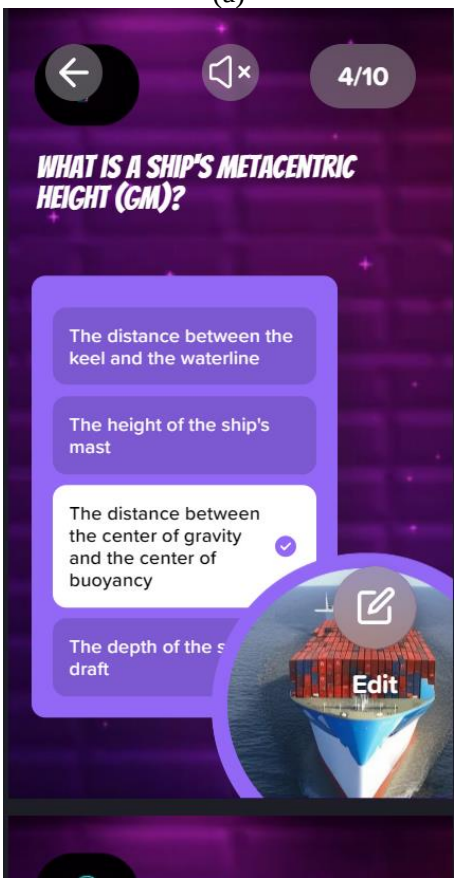
Fig.8: Images are selected based on keywords without context resulting in "nonsense"



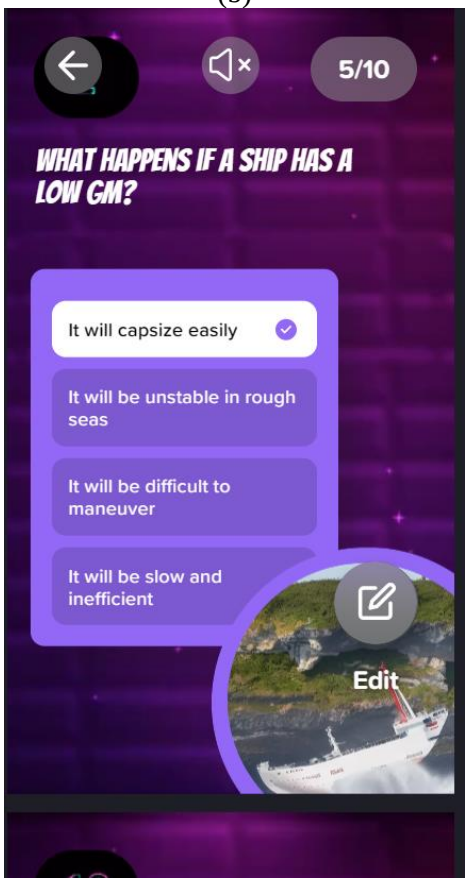
(a)



(b)



(c)



(d)

Fig.9: Sample pages for ship stability quiz from Piggy

4.2. AI-generated assessment quizzes

In training development at DNV, the starting point is often a rather factual PowerPoint presentation, for purely frontal teaching. Both for pedagogical reasons and for required assessment of learning success, we then add quizzes that can be automatically assessed in the learning platform. Typical question types are multiple choice, multiple response, matching and filling in blanks. Multiple choice questions are used the most in our applications.

Piggy is a "visual, creative, and interactive mobile documents creator", https://piggy.to/. Its website states that it is intended to "create social stories, presentations, and quizzes", designed for use on mobile phones. We asked Piggy to create a quiz on "ship stability", *Gaspar et al. (2023)*. Some of the quiz questions were OK, some wrong or nonsense, Fig.9:

a) The trim refers rather to an angle of the hull (first choice) than the ship's weight distribution (second choice, given as the correct answer).
b) The purpose of ballast tanks is certainly not to balance the ship's weight.
c) The effect of low GM is given correctly as ship "will capsize easily", but "ship gets unstable in rough sea" is arguably also possible, and ship will be difficult to manoeuvre or be slow and inefficient can be easily ruled out in a quiz on stability.
d) The metacentric height GM is not the distance between centre of buoyancy and centre of gravity.

With various other maritime topics, results were similarly problematic. The quizzes created by Piggy contained serious errors. With increasing level of specialization, the results deteriorated. Piggy may be a good tool for party games or ice breakers in training, but otherwise failed to convince.

Designing suitable quizzes for a given training requires context information into learning objectives and background of target audience. It is a high-level task in training development. Quiz tasks should assess the learning success, i.e., they should not be so easy to guess the correct answer before the training, but reflecting key training material, such that they are answered correctly after the training.

5. Conclusions

Our assessment of the state of the art of AI for maritime training development may be summarized as: the glass is half full or half empty, depending on your perspective and your expectations.

- Capabilities have progressed rapidly over the past few years to sometimes impressive levels, and AI-based tools can be used effectively for base tasks, such as translation, image generation, or the generation of lip-synced videos.
- We still don't have the "make training" button which magically designs complete training material. High-level tasks requiring context information and sometimes even creativity are best performed by human experts, e.g., core tasks of pedagogy such as defining what to teach and through what means.

The tools tested performed sometimes well, sometimes poorly, but always worse than in the marketing demos for non-maritime applications. That should not come as a surprise. Always test software for your own test cases, not the vendor's test cases. Many of the failures of AI-tools for training described here were to be expected. The fundamental shortcomings of statistical methods (such as machine learning) are known as such, *Bertram (2018)*, even if the wider public is not so aware yet.

The development of software tools for training design may be seen in analogy to the development of tools for computer aided ship design. For four decades, efforts to use AI to develop "computer generated ship design", i.e., a magic "make ship" button where just the requirements are specified and the computer generates the complete design, Fig.10, have failed, *Bertram (2013)*. However, we have seen

continuously increased efficiency in the design process, shifting low-to-medium complexity tasks to the computer. It may well be that we see a similar development for designing trainings, where training developers get increasingly efficient in the product development, as the computer handles more basic tasks with increasing autonomy. Computer-aided training development, rather than computer-generated development.

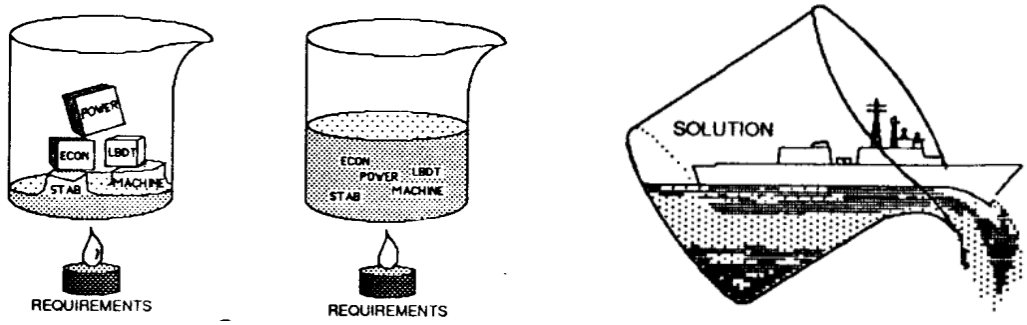


Fig.10: The vision of a magic "make ship" design, *Mistree et al. (1990)*, never materialized

Acknowledgements

We are grateful for many colleagues sharing success and failure stories on using AI-based tools discussed here, namely Bjørnar Krukhaug, Michelle Kurian, Bernhard Löbermann, and Alessio Vicini all DNV), Henrique Gaspar (NTNU).

References

BERTRAM, V. (1994), *Numerische Schiffshydrodynamik in der Praxis*, Schriftenreihe Schiffbau 545, https://d-nb.info/1071620541/34

BERTRAM, V. (2013), *A survey on knowledge-based systems for ship design and ship operation*, Int. J. Intelligent Engineering Informatics 2/1, pp.71-90

BERTRAM, V. (2018), *Demystify Artificial Intelligence for Maritime Applications*, 17th COMPIT Conf., Pavone, pp.22-35, http://data.hiper-conf.info/compit2018_pavone.pdf

BERTRAM, V.; PLOWMAN, T. (2019), *A Hitchhiker's Guide to the Galaxy of Maritime e-Learning*, 18th COMPIT Conf., Tullamore, pp.7-23, http://data.hiper-conf.info/compit2019_tullamore.pdf

COLLÉ, C.; MOROBÉ, C. (2022), *Saving AI from its Own Hype: Getting Real about the Benefits and Challenges of Machine Learning for Ship Performance Modelling Aimed at Operational Optimizations*, 7th HullPIC Conf., Tullamore, pp.198-206, http://data.hullpic.info/HullPIC2022_Tullamore.pdf

GASPAR, H.; BERTRAM, V. (2023), *The Use of ChatGPT and Similar AI in Marine Engineering: Limitations and Opportunities*, 24th COMPIT Conf., Drübeck, pp.73-83, http://data.hiper-conf.info/compit2023_drubeck.pdf

GASPAR, H.; BERTRAM, V.; PLOWMAN, T. (2023), *Hic Rhodus, Hic Salta: ChatGPT and other A.I. Tools for Maritime Applications*, 15th HIPER Symp., Bernried, pp.41-52, http://data.hiper-conf.info/Hiper2023_Bernried.pdf

MISTREE, F.; SMITH, W.F.; BRAS, B.; ALLEN, J.K.; MUSTER, D. (1990), *Decision-based design: A contemporary paradigm for ship design*, Trans. SNAME 98, pp.565-595, https://www.researchgate.net/publication/236686681_Decision-Based_Design_A_Contemporary_Paradigm_for_Ship_Design

Case Studies Examining the Impact of Employing Robust Voyage Optimization Techniques on Enhancing a Vessel's CII Rating

Oliwia Gałecka, Ardmore Shipping, Cork/Ireland, ogalecka@ardmoreshipping.com

Abstract

This study examines the impact of employing robust voyage optimization techniques to enhance a vessel's Carbon Intensity Indicator (CII) rating. Emphasis is placed on the advantages of utilizing the current findings from vessel performance evaluations to determine the ship's behaviour within the weather routing program. The convergence of human expertise and automated computation represents a core component of weather routing procedures used by Ardmore Shipping. Additionally, this study explores the prospects of voyage optimization by integrating dynamic propulsive power control systems through a real-world case study.

1. Introduction

The Carbon Intensity Indicator (CII) of a vessel, as defined by the International Maritime Organization, is the total mass of CO_2 emitted per cargo carrying capacity. Given this, by reducing the mass of CO_2 emitted by the vessel over the year, the CII rating of the vessel may be improved. There are several ways to achieve this: running on low-carbon fuels, installing wind-assisted propulsion or solar power onboard, or through speed and routing optimization. Of the many options available to owners to improve CII ratings, one of the most easily attainable is to improve the quality of the voyage optimization techniques used, which in turn will improve fuel efficiency. Voyage optimization, in this paper, is defined by three distinct elements: pre-voyage planning, voyage execution, and post-voyage analytics, allowing the voyage to be adequately planned for, efficiently conducted and thoroughly reviewed for future improvements.

2. Pre-voyage planning

Several factors are involved in efficiently planning a voyage, which starts when a contract is signed with the charter party. The current calculated TCE and bunker prices are used to influence commercial decisions regarding ETA and the agreed vessel speed. Post-voyage analytics will provide information for expected fuel consumption rates, which will be relayed back to the vessel. A route can only begin to be planned once these terms are established.

2.1. Weather routing

Before the voyage, the vessel will be sent an optimized weather-routed voyage plan. Having a reliable source of weather routing is imperative and will become increasingly necessary as the time a vessel spends in adverse weather is predicted to increase owing to the effects of climate change. The ability to predict and avoid adverse weather conditions is crucial for the safety of the ship and crew onboard, not to mention the fuel savings provided by having reliable information at hand. These fuel savings can be seen clearly during the weather routing optimization processes used by Ardmore and are outlined in the case study below.

Ardmore Shipping uses WetterWelt's MeteoPilot software to provide the vessel with the suggested route based on the predicted weather for the voyage. The active routing system will also update the suggested route and inform the vessel of any changes to the predicted weather while underway, ensuring that the vessel always has the most up-to-date and accurate information available, which in turn allows the Master to make the most informed decisions possible regarding the speed of the vessel and the route to take.

2.2. Example of Voyage from Adelaide to Cochin

Fig.1 shows an example of a voyage from Adelaide to Cochin, where the planned route was altered while underway to avoid heavy weather, in turn giving savings on the vessel's fuel consumption. The vessel departed from Adelaide, as shown in Fig.1, and was routed in a more northerly track to avoid heavy weather conditions to the south and southwest of Australia. After sailing through this area, the vessel was sent information about a port change. It initially headed towards Singapore and was rerouted later to Cochin. The new route followed a more north-westerly track to bring the vessel to Cochin on time in addition to following slightly better ocean conditions, which is what the Master now followed. When comparing the cases of the planned route versus the executed route, it can be assumed that the vessel was always to head for Cochin with no port change, as the initial leg for both destinations was the same. When comparing the data from both the weather-optimized route and the initial route, the vessel had to travel 9.7 nm further than expected; however, it saved 4 hours by doing so. It is also worth noting that by following this longer route, 2.8 tons of heavy fuel oil and 0.8 tons of marine gas oil were saved. This voyage is an excellent example of the Master trusting the information provided and, therefore, not only arriving earlier than predicted but also saving fuel during the voyage.

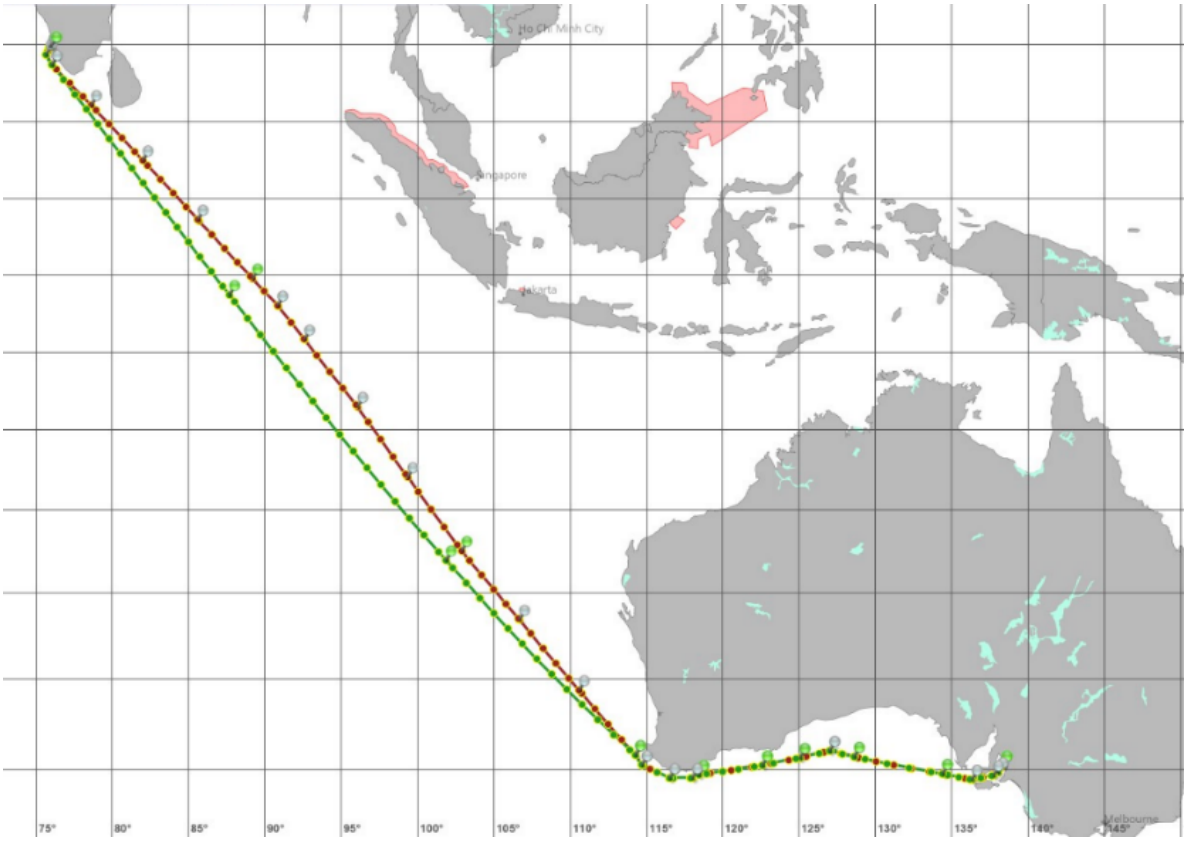


Fig.1: Voyage from Adelaide to Cochin

3. Voyage execution

During the voyage, a vessel is inclined to have power variations due to continuous load and RPM changes, leading to operational inefficiencies. To reduce this, Ardmore has deployed Yara's FuelOpt system, which adaptively optimizes the speed and fuel consumption rate (FCR) of the vessel. The system is designed to increase fuel efficiency by taking control of the main engine based on commands from the bridge and ensuring power peaks are minimized. This can be done using several strategies. Firstly, a speed is chosen by setting the shaft power to constant; this allows for the speed of the vessel to automatically decrease in bad weather as the consumption of the vessel will remain constant. Exiting the bad weather may require a manual change of speed to meet the ETA. Other operational strategies for FuelOpt include voyages where full speed may be required, which can be set to an optimum

consumption for that corresponding speed to minimize losses. Alternatively, voyages with a critical ETA may require that speed is set to a constant to meet the given laycan, ensuring precise arrival and avoiding speed and therefore power fluctuations. The system can also be operated in tandem by setting both a speed and a maximum fuel consumption if the voyage requires a contract speed below a given weather condition. This will allow the vessel to sail at the given speed until the set maximum consumption has been reached due to severe weather, for example, when it will reduce vessel speed until consumption is also reduced, *NN (2021).*

3.1. Voyage simulation from Singapore to Bangladesh

Below is an example of the fuel savings that can be achieved by using FuelOpt. It follows a voyage completed by 'Ardmore Sealion' from Singapore to Bangladesh. The voyage was carried out as usual and subsequently recreated using a digital twin to prove the fuel savings which would have been achieved by operating the vessel in constant power mode. The vessel was modelled using a digital twin, which was based on collected performance data over a two-year period. Both the weather and sea conditions were precisely simulated using historical satellite data for the specific route. The voyage was then executed virtually to match the ETA of the actual voyage, except the power was now kept constant. Fig.2 compares actual versus simulated power and speeds, in addition to the simulated weather conditions. During the actual voyage, the power fluctuations are clear, especially in the first and last quarters of the voyage. The average actual speed of the vessel was recorded to be 11.6 kn, and the actual consumption of the 1544 nm voyage was 99.2 tons. During the simulation, the power was set to a constant 4000 kW, which meant that the speed was automatically adjusted to the actual experienced weather during the voyage. When the fuel consumption of this new voyage was calculated, it came to 94.9 tons, equating to a 4.3% reduction, evidence that operating at constant power is more fuel-efficient.

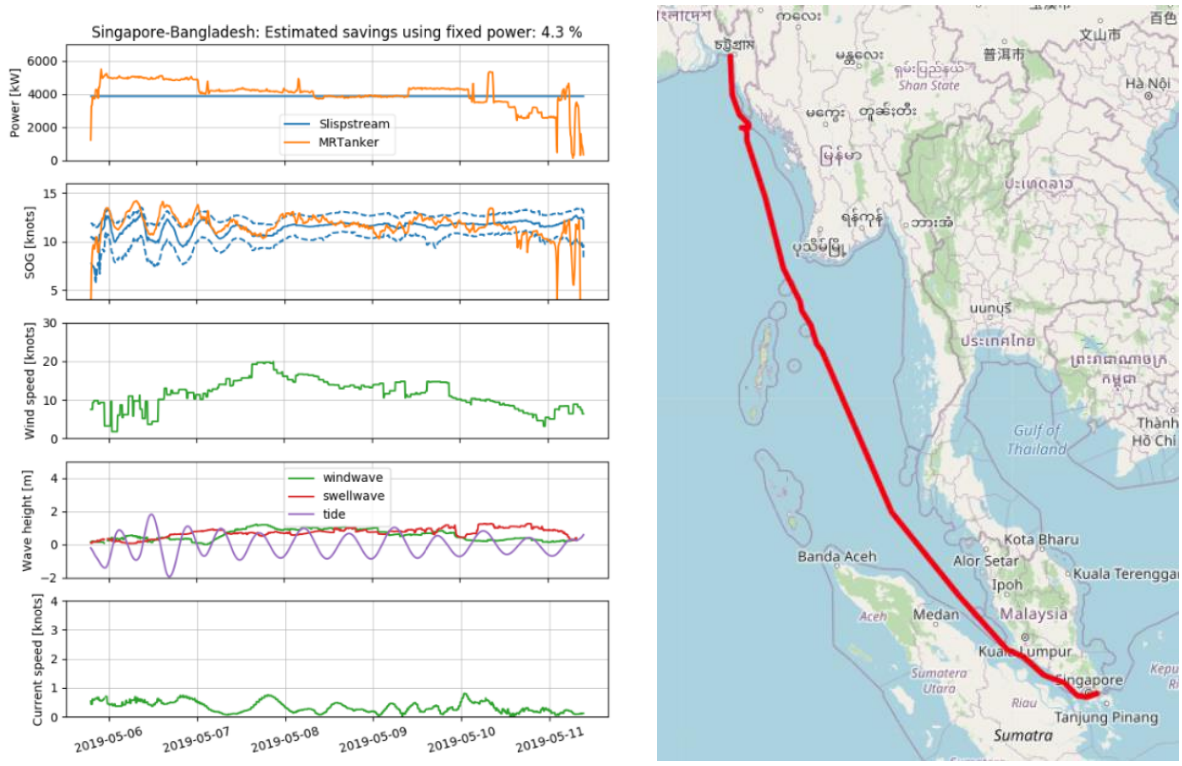


Fig.2: Actual and simulated voyages of 'Ardmore Sealion'

Independent of which strategy is used when the vessel operates using FuelOpt, the concept of the system can only be utilized to its full potential if the Navigation Officer understands how the system works and why it is being implemented. A culture shift is crucial for a change in operating style allowing for a move away from the traditional, continuous manual adjustment of the engine power to a more technologically supported approach. For successful voyages to be conducted in this way, Ardmore

ensures that the crew is adequately educated on the purpose of the system and continuously encouraged to engage it to its full potential.

4. Post-voyage analytics

There exists an abundance of data from a vessel; however, how this data is processed and interpreted is imperative, as trustworthy data can provide the owner with valuable insights into fuel efficiency and opportunities for improvement. Current post-voyage analysis at Ardmore exists via vessel performance management provided by Albis. This system allows for thorough analysis, including efficiency monitoring, voyage reporting, speed optimization, trim optimization, weather influences, and monitoring of main engines and auxiliaries, among others, by collecting and processing high-frequency data, *Fritz (2013)*.

4.1. Optimum trim tables

One of the tools that Albis provides, which allows Ardmore to maintain high CII ratings across the fleet, is the generation of empirical trim tables using historical vessel data, thus ensuring the vessel is operated at the optimum trim for any given voyage. These are produced through the collation of data for consumption in relation to the trim at a given draft for each vessel class. Trim tables are used to ensure that the vessel is operating at the optimum trim, which is a cost-effective operational solution to reduce excessive consumption. In addition, by utilizing historical trim data, expensive CFD modelling and towing tank tests can be avoided. Fig.3 shows an example of the trim tables received by Albis, which were conducted for various drafts when the vessel was being operated at the normalized speed of 12.4 kn. In this table, green values indicate lower FCR, and red indicates higher FCR as per the key. These tables are used by the Deck Officers onboard to correlate the speed and draft to the trim conditions that will result in the lowest FCR. When comparing the potential for savings on fuel consumption, on average, for any given draft at a particular speed, there may exist a 20% difference between the consumptions at different trim conditions. In severe cases, such as for the draft of 12 m of the below table, the difference can be over 30%. In this example, the best FCR is observed at a trim condition of -1m where the FCR is at 96%, correlating to 15.8 t/day as compared to the worst FCR at a trim of 2.25 m which shows a 130% consumption rate, correlating to 21.4 t/day. The difference between these conditions is 5.6 tons of fuel. Evidence that it is imperative to ensure that the trim condition in which the vessel operates is always optimal.

Measured Fuel Consumption Rates in Percent of Average

Center Draft [m]	Trim [m] Bow Down -1.50	-1.25	-1.00	-0.75	-0.50	-0.25	0.00	0.25	0.50	0.75	1.00	1.25	1.50	1.75	2.00	2.25	2.50	2.75	3.00	3.25	Bow Up 3.50
5.00																					
5.50																					
6.00																	85%	87%			
6.50				90%	83%	73%	78%	84%	83%	85%	81%	84%	84%	80%	84%	85%	86%	84%	83%		
7.00			88%	82%	79%	79%	87%	79%	83%	80%	87%	84%	86%	85%	88%	86%	85%	87%	89%	90%	88%
7.50		87%	85%		88%	86%	86%	83%	88%	86%	87%	87%	86%	85%	85%	85%	88%	89%	87%	86%	91%
8.00			85%			92%	89%	87%	89%	84%	88%	89%	86%	88%	90%	87%	90%	90%	89%	84%	
8.50	93%	93%	92%	91%	91%	89%	91%	95%	94%	85%	88%	92%	95%	94%	96%	92%	89%				
9.00		88%	96%		95%	92%	84%	89%	88%	89%	86%	95%	75%	92%	96%	93%					
9.50		96%	97%	90%	91%	88%	94%	97%	98%	98%	95%	94%	98%		97%						
10.00			84%	93%	95%	97%	96%	99%	98%	103%	93%	100%	102%	102%					95%	98%	
10.50	95%	97%	101%	100%	98%	98%	97%	99%	100%	102%	96%	99%	112%	100%							
11.00	102%	99%	102%	102%	99%	101%	99%	101%	100%	100%	101%	104%	104%		100%						
11.50	100%	103%	98%	100%	99%	103%	103%	103%	105%	99%	99%	102%	100%								
12.00	101%	98%	96%	106%	104%	102%	101%	103%	104%	108%	104%	112%	114%	113%	122%	130%					
12.50	91%	101%	101%	102%	107%	103%	108%	107%	105%	111%	109%	111%	112%	110%							
Scale	73%	76%	79%	82%	85%	88%	90%	93%	96%	99%	102%	105%	107%	110%	113%	116%	119%	122%	124%	127%	130%
FCR [t/d] at 0-4 Bft and 12.4kn	12.1	12.6	13.0	13.5	13.9	14.4	14.9	15.3	15.8	16.3	16.7	17.2	17.7	18.1	18.6	19.1	19.5	20.0	20.5	20.9	21.4

Fig.3: Trim table using historical data

4.2. Hull monitoring

Another critical factor that influences the overconsumption of a vessel is the hull condition. Albis provides Ardmore with an insight into how much any given vessel may be overconsuming based on the time between hull cleanings through the hull and propeller degradation reports. As the hull gets progressively more fouled, the resistance of the vessel will increase, requiring more propulsive power,

which is why the hull condition must be monitored closely. An example of the data received is shown in Fig.4, where the consumption of the vessel is plotted against time, with propeller or hull cleanings being marked for comparison. The scatter compares against the baseline consumption, which is taken as the FCR after drydock with new hull and propeller coatings having been applied. Each plot on the graph represents data for the median FCR per day extrapolated to fit the conditions of 13 kn, 12 m draft and 0-4 Beaufort wind conditions, ensuring that the data is unbiased towards operating conditions. The actual FCR plots are color-coordinated so that points of overconsumption can be easily spotted. When looking at Fig.4, there is a significantly higher number of spikes in overconsumption before hull or propeller cleanings compared to after; an excellent example of this is the cluster of overconsumption points around the 1st of July 2022. After the hull and propeller cleaning, the number of these points is minimal until the following year. This is why at Ardmore, reports are produced each month to monitor the consumption of the vessels and the condition of the hull and propeller, ensuring both are cleaned in a timely manner to avoid this. In addition to this, resident drones are used when in port to check the physical condition of the hull and a cost-benefit analysis is performed to determine the best time to conduct hull cleaning.

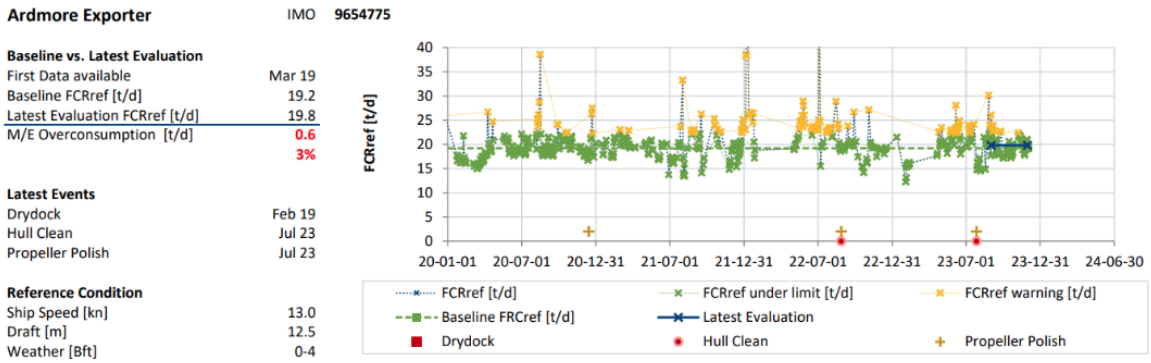


Fig.4: Example of hull and degradation reports

4.3. Charter warranties

The reports which are produced by the post-voyage analytics solution are also crucial to feeding back into the commercial decisions when agreements are made with charterers before any voyages. These come in the form of charter warranty reports, which collect actual FCR data for each ship and compare the correlating speeds when the vessel is laden at various drafts. These reports allow the commercial team to compare the established speed to an expected fuel consumption rate to be agreed upon, as mentioned at the beginning of this paper.

5. CII ratings of the Ardmore Fleet

All the strategies outlined in this paper improve the efficiency of operations at Ardmore, not just from a fuel consumption perspective but also from how all parties involved in operations interact with each other and the above systems. They were not solely employed with the specific aim of increasing CII ratings. The good CII rating of the fleet is evidence that the employment of these is effective and has a positive impact.

Fig.5 shows the CII ratings of the fleet for the year 2023. Of the 22 vessels in the fleet, 12 have an A rating, constituting 55% of the fleet, 8 have a B rating, and only 2 have a C rating. When looking closer at these two instances, ‘Ardmore Seaventure’ is just on the boundary of a B and the lower rating was due to the fact she had a long river passage prior to and post docking. The second instance occurs for the Ardmore Encounter and can be put down to high waiting times for a cargo for this vessel early in 2023. No vessels achieved a rating lower than C. The effect that more stringent CII regulation will have on the fleet is yet to be determined, but Ardmore is confident that the fleet will continue to perform well under the current systems and processes.

Vessel	Total Time [d]	Steaming Time [d]	Weather >=5Bft at Sea [d]	Total Fuel Consump. [t]	Total CO_2 Emissions [t]	CO_2 for Cargo Heating [t]	Total Dist. [nm]	Vessel DWT	AER [g/tnm]	Latest CII Rating
Ardmore Seavaliant	197	121.0	46.6	2894.3	9032.4	35.8	34678.3	49998	5.21	A
Ardmore Seaventure	283	134.1	73.6	3588.2	11229.2	49.3	35449.1	49998	6.34	C
Ardmore Seavantage	320	223.9	131.3	6053.8	18892.7	34.2	66120.8	49997	5.71	B
Ardmore Seavanguard	261	160.7	101.8	4094.6	12826.9	44.7	43376.2	49998	5.91	B
Ardmore Seafarer	328	191.2	106.9	4725.8	14849.3	286.4	50748.4	49999	5.85	B
Ardmore Cherokee	288	169.5	74.6	2964.1	9266.4	566.2	45522.7	25215	8.07	A
Ardmore Cheyenne	319	196.7	97.7	3928.2	12298.5	731.0	55652.5	25217	8.76	B
Ardmore Chinook	256	150.8	67.8	2965.3	9275.0	589.9	43269.6	25217	8.50	B
Ardmore Chippewa	313	201.6	76.4	3596.8	11222.7	649.5	56527.4	25217	7.87	A
Ardmore Dauntless	323	159.0	66.0	3501.2	11015.9	193.0	44800.1	37764	6.51	A
Ardmore Defender	306	163.8	63.9	3706.8	11620.8	555.2	47024.6	37791	6.54	A
Ardmore Sealion	305	205.4	113.4	5025.9	15669.4	81.8	62213.0	49999	5.04	A
Ardmore Seafox	322	176.5	89.8	4159.2	13039.8	93.8	51611.9	49999	5.05	A
Ardmore Seawolf	315	161.5	76.6	3763.9	11812.5	25.9	45863.3	49999	5.15	A
Ardmore Seahawk	323	198.0	88.5	4692.9	14718.0	163.5	54707.7	49999	5.38	A
Ardmore Endeavour	296	184.0	73.8	5057.3	15790.5	143.7	53363.3	49997	5.92	B
Ardmore Engineer	317	214.2	99.6	4929.8	15387.7	99.7	60279.8	49500	5.16	A
Ardmore Enterprise	292	142.0	57.7	3441.2	10753.7	49.0	39368.3	49500	5.52	A
Ardmore Endurance	299	167.2	65.3	4603.4	14359.9	167.8	46175.1	49500	6.28	B
Ardmore Explorer	329	153.8	69.7	4499.7	14074.1	198.0	40757.3	49500	6.98	C
Ardmore Encounter	281	168.4	74.1	4188.8	13076.2	48.6	47042.2	49500	5.62	B
Ardmore Exporter	232	148.6	54.2	3619.9	11324.4	121.2	41700.7	49500	5.49	A

Fig.5: CII ratings for Ardmore fleet (2023)

6. Future of voyage optimization

The three core systems used by Ardmore are imperative to complete voyage optimization. Weather routing provided by WetterWelt allows for pre-voyage planning and real-time adjustment in operations; however, it still requires the human operator to interpret and use the data as they see fit. Voyage execution provided by Yara's FuelOpt removes the amount of intervention needed by the human operator by automatically adjusting speed or FCR; however, the set points still need to be monitored and changed manually. The post-voyage analytics provided by Albis can model past voyages in a new light and provide in-depth analysis for future improvements; however, it does not allow for changes to be made in real-time due to the nature of the retrospective analyses.

The vision for the future of voyage optimization at Ardmore is to be able to integrate all three of these systems to reap all the individual benefits, improve fuel efficiency and increase ease of operation for the crew onboard. Work is being carried out to trial the amalgamated solution by using WetterWelt to provide optimum speed or FCR suggestions basis the weather routing to the voyage execution system, which will automatically input those values as the set points and adjust them when new information is received, the post-voyage system should then be able to keep track of this data and analyze it for a complete overview of the system. This would provide the crew with one complete system rather than several separate ones, in addition to moving into the future world of autonomous operations in incremental steps. Ardmore is also trialling systems which utilize the power of Artificial Intelligence to explore how these solutions will fit into the future of voyage optimization and how they can be effectively taken advantage of in today's operations, especially from a pre- and post-voyage viewpoint as well as to assist in the commercial decision-making process.

7. Conclusions

Effective voyage optimization can be split into three distinct elements: pre-voyage planning, voyage execution and post-voyage analytics. By utilizing all three methods, Ardmore obtains a complete picture of how best to operate the vessels to increase fuel efficiency and, in turn, maintain high CII ratings for the fleet. The WetterWelt system provides robust and trustworthy information about route planning as well as real-time changes and suggestions to the vessel route. Yara's voyage execution system allows the crew to be more efficient when it comes to speed and FCR optimization. Albis post-

voyage analytics gives an in-depth insight into completed voyages, providing access to numerical savings and areas of improvement, as well as feeding back into the commercial decision-making process, which is imperative for future voyages.

This paper demonstrates that the pay-off of utilizing these processes effectively will result in positive CII ratings for the vessels without the need to invest in expensive solutions such as wind-assisted propulsion or future fuels in the near term.

A view of the future of voyage optimization for Ardmore is the amalgamation of all three systems to introduce an element of automation into the operation of the vessels and reduce the amount of human intervention in the execution of the voyages. It is important that a change of culture and mindset must be undergone for a system such as this to be utilized to its full potential. The exploration of the integration of artificial intelligence into the processes which go into voyage optimization is also being undertaken, with a focus on how this may improve pre-voyage commercial decision-making.

Acknowledgements

With thanks to Garry Noonan, Director of Innovation at Ardmore Shipping, for his continuous support and guidance. Thank you to the teams at WetterWelt, Albis and Yara for their input and advice, in addition to providing the required data and figures needed to complete this study.

References

FRITZ, F. (2016), *Practical experiences with vessel performance management and hull condition monitoring*, 1st HullPIC Conf., Pavone, pp.128-136, http://data.hullpic.info/HullPIC2016.pdf

NN (2021), *FuelOpt General Introduction*, https://leanmarine.com/2021/03/29/fuelopt-a-smart-way-to-derate-engine-power-output-and-meet-eexi-requirements/

dijSavings from Route Optimization: Myth or Reality

Volker Bertram, DNV, Hamburg/Germany, volker.bertram@dnv.com

Abstract

This paper takes a critical view at alleged fuel savings from routing. The key components of routing, namely meteo-marine (waves, wind, current) forecasts and hydrodynamic response model (added fuel consumption in given weather), have much larger uncertainty than the alleged savings, which are in most cases derived from comparing results from the hydrodynamic model on direct and optimized routes. The paper argues in favour of more validation for the employed hydrodynamic models.

1. Introduction

Ship routing (a.k.a. routeing or route optimization) denotes generally the optimization of a ship's course and speed with respect to some objective. As such, the term encompasses a wide variety of approaches and software products. First developments date back at least to the 1970s, e.g., *Journée and Meijers (1980)*, and have proliferated since then with many variations on the key elements of any routing application, which have also been nicely summarized in *Walther et al. (2014)*:

- Optimization algorithms - moving from classical approaches to evolutionary algorithms such as Genetic Algorithms, see e.g. *Harries and Birk (2003)* for an overview of optimization algorithms.
- Objectives – initially, ship routing focused on safety aspects, such as (relative) motions to avoid water on deck or slamming, or accelerations to avoid e.g. loss of deck containers. With increasing fuel prices after 2008, and subsequent IMO and EU pressure to reduce CO_2 emissions in shipping, the focus of most publications on routing systems have moved towards fuel savings, sometimes employing proxies like added resistance or added power. An important difference is that weather routing for safety is based on first-order seakeeping quantities (motions and accelerations), while routing for energy efficiency is based on second-order seakeeping quantities (added resistance and possibly drift forces).
- Meteo-marine models – forecasting of wind, waves, and currents as key ambient conditions is required as "input signal" for the ship's response. The meteo-marine models generally come from external providers. The state of the art has developed over the decades, with main progress coming from satellite remote sensing. In short-distance routing, e.g. for electrically powered ferries as in *Bellingmo et al. (2021)*, meteo-marine models may be extremely simplified or omitted completely, mainly reducing the problem to speed profile and distance optimization.
- Ship performance models – forecasting the ship's response to the ambient conditions, i.e. motions, accelerations, added resistance, etc. Initially, ship performance models for routing were all based on first-principles simulations, albeit with large variations in computational accuracy and computational effort, see e.g. *Bertram (2016)* for an overview. Over the last two decades, increasingly performance models based on machine learning have been advocated, not least because of their popularity in performance monitoring applications, e.g. *Deymier et al. (2021).*

We will consider in the following only routing for energy efficiency objectives where ambient waves have a significant impact. Claims to how much fuel routing saves differ widely, with vendors being more optimistic by nature. The following list is non-exhaustive, but illustrates the point:

- "[The] fuel consumption of the optimized route is reduced by 7.84% compared with that of the Rhumb Line." *Pan et al. (2021)*
- "For deep-sea shipping, route optimization is estimated to reduce emissions by 7%." *Bellingmo et al. (2021)* with reference to *Lindstad (2013)*

- "The actual saving was 5.7%." *Shields and Weber (2015)*
- "The optimal route […] leads to 4.9% fuel savings compared with the […] shortest path." *Kytariolou and Themelis (2022)*
- "According to the International Maritime Organization, weather routing saves more than 3% in fuel consumption. For container ships, etc., that number increases substantially, up to 10%." Various vendors (including https://www.dtn.com/, https://www.sofarocean.com/, www.stormgeo.com/) with reference to *IAMU (2015)*, which in turn refers to *Armstrong (2013)*
- "[…] weather routing can lead to significant fuel consumption savings per voyage […]. In the majority of the papers reviewed in this survey, fuel consumption savings are typically reported to reach values between 3% and 5%." *Zis et al. (2020)*
- "The potential [of weather routing] has been assessed to between 0% to 5% on main engine fuel consumption dependent on ship size and type and the typical trade for the different ship segments." https://glomeep.imo.org/technology/weather-routing/
- "[F]or fuel-optimal routing, […] GL experts estimate the saving potential to less than 1% for conventional displacement hull and most realistic scenarios." *Bertram and Vordokas (2010)*
- "We estimate the saving potential beyond what is already widely done today to 0.1%." *OCIMF (2011)*

The statements on the saving potential differ widely, from almost zero to up to 10%. This should not surprise. Serious estimates should always come as a bandwidth, as the honest answer on saving potentials of any measure will be the time-honoured "it depends". Numbers given by vendors or selected (positive) cases are invariably higher than numbers by third-party consultants, *Bertram (2020)*. But which of the estimates should we then believe? I believe the correct answer to this question is – none. The uncertainty in the results of any optimization depends largely on the accuracy of the used functions for the objective. The next chapter will discuss the key elements of routing in more detail with focus on the uncertainties or errors associated with each element.

2. Routing components

2.1. Meteo-marine forecasting

The meteo-marine forecasting, https://en.wikipedia.org/wiki/Weather_routing, predicts the ambient conditions:

- Wind (speed and direction)
- Wind waves (height and direction; typically given as a spectrum with significant wave height and main direction)
- Swell (height and direction)
- Current (speed and direction)

These ambient conditions drive the ship's response, in our case the added fuel consumption, directly or through proxies. Obviously, errors in the ambient conditions (input signal) will propagate to errors in response (output signal). The weather forecast is based mainly measurements from satellites and buoys to feed numerical weather simulation models. Weather forecasts can be obtained from various, mostly governmental, service providers, such as the Japan Meteorological Agency, the United States National Weather Service, and the United Kingdom Met Office. Some commercial routing providers use these publicly available sources, merge and filter to provide their own predictions.

Error sources are:

- Wind is highly nonlinear and thus difficult to predict over longer periods; beyond 3 days, the predictions become noticeably fuzzy, which is often referred to in popular science as the Butterfly effect, https://en.wikipedia.org/wiki/Butterfly_effect.

- The wind sea follows from the wind. Here the problem is rather that we approximate actual distributions of energy over wave frequency and direction by standard spectra (with given function over wave frequencies and directional spread around main direction) with just two parameters: significant wave height and main direction. The standard spectra were derived fitting a smooth curve through many measured spectra (histograms) with some physical insight on how these curves should decay towards very high and very low frequencies. Taking a standard spectrum (e.g. the Pierson-Moscowitz spectrum) as an approximation for actual instances of wave distributions (histograms) comes always with an error. This is akin to some regulations using a standard weight of 75 kg per passenger, where at least in my case this is flatteringly far away from the truth.
- Some meteo-marine forecasts use only the standard Pierson-Moscowitz spectrum, https://en.wikipedia.org/wiki/Pierson%E2%80%93Moskowitz_spectrum, with one maximum, approximating wind sea but neglecting swell (which would give second local maximum at low frequency). Ignoring the swell component can lead to significant errors, *Gatin and Boxall (2021)*.
- Large global currents, like the Gulf Stream, are often imagined as steady conveyor belts with rather steady speed and direction. In reality, the local current speed and direction varies over time and space, with large and small eddies. In particular, the spatial resolution of meteo-marine measurements is often not fine enough for accurate predictions.

The errors in predicting highly nonlinear meteo-marine weather are often mitigated by using rolling updates as the ship progresses, adjusting forecasts e.g. daily and accordingly the optimum routing recommendations. Even then, the forecasts in themselves are an error source, which is qualitatively understood, but difficult to quantify. "While weather routing theoretically offers […] benefits, the detrimental impact of stochastic weather forecasts is unknown," *Mason and Gallego-Schmid (2022)*.

2.2. Ship performance model

The performance model predicts the "performance" (e.g. power requirement or fuel consumption) as function of various input variables, e.g. speed, draft, trim, significant wave height, encounter angle, wind speed, apparent angle of attack, etc. Such performance models are needed for a variety of applications: trim optimization, performance monitoring, routing, etc. While it makes sense to reuse knowledge for setting up such models the requirements for models differ according to their intended purpose:

- Trim optimization neglects ambient conditions generally completely, getting a much simpler performance model for the ship in calm water, *Bertram (2024)*
- Performance monitoring models mostly filter for sea states, e.g. above Bft 4. As below Bft 4, the wind plays generally a larger role than the wind sea, added resistance in waves is often completely neglected.
- Routing generally requires the inclusion of higher waves in the performance model. The associated challenges are higher than for the previous two applications.

The ship performance model may be built using various approaches:

- First-principles simulations ("white box"), using more or less sophisticated approximations of fundamental fluid dynamics equations describing conservation of mass, momentum, energy, etc. More sophisticated approximations are called high-fidelity digital twins (CFD, Computational Fluid Dynamics); simpler models based on potential flow are then often marketed as "well-proven" or "popular in many practical applications" rather than low-fidelity digital twins. *Bertram (2016)* gives an overview of seakeeping simulation tools, *Bertram and Peric (2021)* on CFD methods to predict calm-water resistance.
- Machine learning ("black box"), using numerical statistics to fit measured data. This approach needs large amounts of data, especially if there are many input variables affecting

the output. Data needs to be statistically independent, i.e. a too high data frequency, recording essentially the same conditions again and again, is useless. For ship performance models, using assembly averages of 6-minutes recordings with a filter criterion based on excessive variation within the assembly interval is recommended. Data also needs to cover the whole range of possible values for the input variables. If machine-learning models are fitted only to subsets, the models need to extrapolate later if data occur outside the original training set range, and such extrapolations generally results in large errors and wrong recommendations, *Bertram (2024)*.

- Mixed models ("grey models") combine physical insight with some calibration to measured data. Simulation models use semi-empirical constants, e.g. for viscous phenomena, and machine-learning models are dubbed as physics-informed models. Grey models are often a good choice as they reduce the number of variables or lead to relations for the remaining variables that are easier to approximate.

"All models are wrong, but some are useful". Measured input data introduce errors and uncertainties, but so do models. There is no approach that can determine added power requirements in medium-to-large seaways, especially if there is a significant contribution from waves that are relatively short compared to the ship length (say less than half a ship length):

- For full-scale measurements, generally the information on ambient waves is highly uncertain for high waves, and the added power is relatively small compared to the calm-water power requirements. The signal to measure is then "drowned out" by the background noise.
- For high-fidelity CFD, the calm-water power requires different grids for accurate computation than for the ship in waves. Especially for shorter waves, the numerical grid errors can introduce significant errors in the added power prediction. Computational effort may also be excessively high for required spatial and time resolution; with coarser grids and larger time steps, errors are introduced.
- For potential-flow 3D methods, results are very sensitive to sufficient grid resolution for added resistance (and power). Variation in added resistance of 100% are quite possible with coarser grids, even if motions like heave and pitch show only small variation, suggesting trustworthy results.
- For strip methods, semi-empirical methods are used for added resistance in waves, which were fitted to data in head waves and wave lengths close to ship length. I deem these approaches as hopeless.

Virtually all computational approaches for responses in natural seaways assume the "superposition principle". The superposition principle assumes that any sea state can be decomposed into elementary sinusoidal waves (Fourier decomposition), the response for each elementary wave then computed, and the total response given as sum of all responses for the elementary waves. Nonlinear interaction destroys this assumption, especially for higher waves and higher speeds.

Our collective knowledge of uncertainties and errors for added resistance in waves (as a simplified proxy for added power requirements in waves) is at best sketchy. Model tests with controlled conditions for waves and the simplest case of ship in head waves show already significant scatter if performed repeatedly in the same model basin. The scatter increases when comparing different model basins.

For computational methods, validation workshops such as the Tokyo 2015 workshop, *Hino et al. (2020)*, give some indication on scatter even if the same type of code or even same codes with different grids and parameters are used.

Various researchers have come to similar conclusions for assorted semi-empirical approaches for added resistance in waves, *Bertram (2016)*, e.g.:

- *Nabergoj and Prpić-Oršić (2007)* compared five approaches for a ro-ro vessel, with large scatter of results (factor of four (400%) between lowest estimate and highest estimate).
- *Boom et al. (2013)* at MARIN compared a different set of empirical wave correction methods for a product tanker. Results showed scatter by more than a factor 10 (1000%). "The results were shockingly different".

In conclusion for the ship performance model, assuming errors of 30% in the computation of added power requirements in natural seaways is rather optimistic.

2.3. Route optimization

Assorted algorithms are used in routing, most variations of Dijkstra's shortest path algorithm, https://en.wikipedia.org/wiki/Dijkstra%27s_algorithm. But neither the optimization algorithm nor the path approximation are key issues here. Variations affect mainly response time, but all algorithms used in practice are likely to give essentially the same result if everything else is kept same.

3. 3% savings with 30% inaccurate functions?

The published fuel savings from routing are not real. There is no possibility to have two identical ships sailing at the same time on the shortest route and the determined optimum route to measure the difference in fuel consumption. Instead, any such published fuel saving refers to the difference according to the ship performance model. And while the shortest route is clearly determined, the computed optimum route depends also on the other elements of routing optimization, foremost the meteo-marine weather forecast.

The various elements in routing, especially the uncertainties for the natural seaway and the ship performance model prediction for added power requirements in natural seaways, come with large errors, at least in the order of 30%. Routing savings are given in the range of 0-10%, but let's say often by more serious sources at 3%, i.e. an order of magnitude smaller than the error in the function to be optimized. If errors cancel out partially, or if errors are systematically added in same magnitude, the optimization process may still find an almost optimum solution (in our case the best route), but the associated savings will be wrong, possibly lower, possibly higher than what the ship performance model gives as result. But in any case, the results are highly doubtful, or "myth".

Orlandi et al. (2018) found that results vary significantly based on input (e.g., wave direction) and ship performance model. It would be interesting to see the effect of variations on the results (sensitivity analyses):

- what different routing solution products predict for a given route as best route and as saving;
- what a given routing solution product gives for variation of input within margins of uncertainty for the input (meteo-marine, ship operation parameters).

In general, more validation and quantification of error margins, especially for the ship performance model, would be helpful to assess saving potential of routing software seriously, and to get guidance on where current software and models can be improved. For example, one could take a given route, record speed profile, hindcast meteo-marine data, and predict consumed fuel in blind tests to get an idea how well or not a given software or ship performance model performs.

Most ship performance models have little to no validation. It is not surprising then that performance models from different vendors give different results for the same ship and the same data. A positive exception of this rule is the work of *Orihara and Yoshida (2015,2018)*. Cross-checking different approaches and comparing to on-board measurements, even if only for accumulated integral values rather than details for want of data, instils at least some confidence into the approach and results.

4. Conclusions

Routing considers weather forecasts and added power requirements as function of seaway, speed and course. The usefulness of routing advice depends on the accuracy of the predicted seaways and the accuracy of the ship performance model. Savings of "up to 8%" as given by some vendors appear doubtful as both input for ambient seaways and ship performance model have generally much higher margins of errors than the purported savings.

Continue using routing, even if we cannot quantify savings; it probably saves some fuel, just how much we don't know (in collective ignorance), and likely less than vendors claim. Routing for safety aspects is more accurate and is in itself an argument to continue the current practice.

Collectively, both users (ship operators) and vendors should spend more efforts on validation of ship performance models and routing software.

References

ARMSTRONG, N.V. (2013), *Review - Ship optimisation for low carbon shipping*, Ocean Eng. 73, pp.195–207

BELLINGMO, P.R.; POBITZER, A.; JØRGENSEN, U.; BERGE, S.P. (2021), *Energy efficient and safe ship routing using machine learning techniques on operational and weather data*, 20th COMPIT Conf., Mülheim, pp.272-281, http://data.hiper-conf.info/compit2021_muelheim.pdf

BERTRAM, V. (2016), *Added power in waves – Time to stop lying (to ourselves)*, 1st HullPIC Conf., Pavone, pp.5-13, http://data.hullpic.info/HullPIC2016.pdf

BERTRAM, V. (2020), *Fairy tales revisited: Energy efficiency options*, 5th HullPIC Conf., Hamburg, pp.7-13, http://data.hullpic.info/HullPIC2020_Hamburg.pdf

BERTRAM, V. (2024), *Trim optimization: In simple terms*, 15th HIPER Conf., Drübeck, pp.6-9

BERTRAM, V., PERIC, M. (2021), *Chronological and critical review of steady free-surface flow computations*, 23rd Numerical Towing Tank Test Sym. (NuTTS), Mülheim, https://www.uni-due.de/imperia/md/content/ist/nutts_23_2021_mulheim.pdf

BERTRAM, V.; VORDOKAS, H. (2010), *Reducing fuel consumption in moderately fast displacement ships*, 7th HIPER Conf., Melbourne, pp.38-45, http://data.hiper-conf.info/Hiper2010_Melbourne.pdf

BOOM, H.v.d.; HUISMAN, H.; MENNEN, F. (2013), *New guidelines for speed/power trials level playing field established for IMO EEDI*, Hansa 150/4, http://www.hansa-online.de/sta-jip.pdf

DEYMIER, C.; ANTOLA, M.; DANIEL SCHMODE, D. (2021), *Using publicly available data to assess hull and propeller performance*, 6th HulPIC Conf., Pontignano, pp.124-131, http://data.hullpic.info/HullPIC2021_Pontignano.pdf

GATIN, I.; BOXALL, D. (2021), *Calculating speed loss due to swell using CFD*, 6th HullPIC Conf., Pontignano, pp.63-71, http://data.hullpic.info/HullPIC2021_Pontignano.pdf

HARRIES, S.; BIRK, L. (2003), OPTIMISTIC – Optimization in Marine Design, 39th WEGEMT Summer School, Berlin, https://wegemt.com/wp-content/uploads/2019/04/39th_WEGEMT_Summer_School_on_Optimistic_Optimization_in_Marine_Design.pdf

HINO, T.; STERN, F.; LARSSON, L.; VISONNEAU, M.; HIRATA, N.; KIM, J. (2020), *Numerical Ship Hydrodynamics: An Assessment of the Tokyo 2015 Workshop*, Springer Nature

IAMU (2015), *Improving Energy Efficiency of Ships through Optimization of Operations*, Int. Association of Maritime Universities, https://gmn.imo.org/wp-content/uploads/2017/10/20140301-ITUMF_Ship-optimization.compressed.pdf

JOURNÉE, J.M.J.; MEIJERS, J.H.C. (1980), *Ship routeing for optimum performance*, Trans. IME 21, pp.12-21, https://repository.tudelft.nl/islandora/object/uuid:805c45f7-bbc0-4baa-802d-637871416490/datastream/OBJ/download

KYTARIOLOU, A.; THEMELIS, N. (2022), *Ship routing optimisation based on forecasted weather data and considering safety criteria*, J. Navigation 75(6), pp.1310-1331, https://www.cambridge.org/core/journals/journal-of-navigation/article/ship-routing-optimisation-based-on-forecasted-weather-data-and-considering-safety-criteria/AAB546D746C2EC966F8C655760E3EF88#

LINGSTAD, H. (2013), *Strategies and measures for reducing maritime CO2 emissions*, PhD thesis, NTNU, Trondheim, https://ntnuopen.ntnu.no/ntnu-xmlui/handle/11250/238419

MASON, J.; GALLEGO-SCHMID, A. (2022), *Stochastic uncertainty in fuel-optimised ship routing: How weather forecasts hinder the carbon savings from wind-assisted weather routing*, 14th HIPER Conf., Cortona, pp.201-205, http://data.hiper-conf.info/Hiper2022_Cortona.pdf

NABERGOJ, R.; PRPIĆ-ORŠIĆ, J. (2007), *A comparison of different methods for added resistance prediction*, 22nd Int. Workshop Water Waves and Floating Bodies, Plitvice, http://www.iwwwfb.org/Abstracts/iwwwfb22/iwwwfb22_38.pdf

OCIMF (2011), *GHG emission-mitigating measures for oil tankers – Part A: Review of reduction potential*, Oil Companies International Marine Forum, London

ORIHARA, H.; YOSHIDA, H. (2015), *Verification of energy saving capability of optimum routing by full-scale trial navigation*, 14th COMPIT Conf., Ulrichshusen, pp.343-354, http://data.hiper-conf.info/compit2015_ulrichshusen.pdf

ORIHARA, H.; YOSHIDA, H. (2018), *Weather routing simulation as a tool for evaluating ship's performance in operation*, 17th COMPIT Conf., Pavone, pp.391-402, http://data.hiper-conf.info/compit2018_pavone.pdf

ORLANDI, A.; BENEDETTI, R.; MARI, R.; COSTALLI, L. (2018), *Sensitivity analysis of route optimization solutions on different computational approaches for powering performance in the seaway*, 17th COMPIT Conf., Pavone, pp.341-353, http://data.hiper-conf.info/compit2018_pavone.pdf

PAN, C.; ZHANG, Z.; SUN, W.; SHI, J.; WANG, H. (2021), *Development of ship weather routing system with higher accuracy using SPSS and an improved genetic algorithm*, J. Mar. Sci. Technol. 26, pp.1324-1339

SHIELDS, M.; WEBER, T. (2015), *Challenges and solutions in speed and route optimization*, 14th COMPIT Conf., Ulrichshusen, pp.473-479, http://data.hiper-conf.info/compit2015_ulrichshusen.pdf

WALTHER, L.; BURMEISTER, H.C.; BRUHN, W. (2014), *Some systems, and basic approach: Safe and efficient autonomous navigation with regards to weather*, 13th COMPIT Conf., Redworth, pp.303-317, http://data.hiper-conf.info/compit2014_redworth.pdf

ZIS, T.P.V.; PSARAFTIS, H.N.; DING, L. (2020), *Ship weather routing: A taxonomy and survey*, Ocean Eng. 213, https://www.sciencedirect.com/science/article/abs/pii/S0029801820306879

The Arctic Tern: AI + Soft Values = Save Fuel

Lennart Cederberg, NoorCare AB, Norrköping/Sweden, Lennart.Cederberg@noorcare.se
Eleonor Marmefelt, NoorCare AB, Norrköping/Sweden, Eleonor.Marmefelt@noorcare.se
Jan Snöberg, Linnaeus University, Kalmar/Sweden, jan.snoberg@lnu.se

Abstract

This paper summaries three years of technical development and research in close collaboration with several major shipping companies. Besides the technical AI-based decision support systems, the project has focused on soft values, how the support systems become efficient support for real, both ashore and onboard. It is important to create knowledge among technical-, commercial- and operation-departments within the organisations on how to implement new methods. Different types of vessels operate under vastly different commercial realities that impact the performance and energy effectiveness. Technical systems must be adapted to each actor's reality to achieve a change and drive more climate-friendly transportation. The Arctic Tern shows fuel savings of 2-14%.

1. Introduction

This is not the first time a new and innovative tool within "Weather routing" is introduced. AI is an impressive and efficient technique to handle large amount of data, but it is neither the first nor the last. For instance, wave models were introduced in the early 1990s, with a significant impact on what became possible at that time. This was followed by naval architect-based ship models that relied on noon reports and could calculate the impact of winds, waves, and currents on ships in the 1990s and early 2000s, using the best technology available at that time. When new models and systems for calculating ship movements and parametric roll were introduced around the same time, many in the industry believed this would revolutionise the market.

The advancements in weather and ocean current forecasts over the past 30 years, where the accuracy of long-term forecasts has greatly improved, have been crucial for enabling today's applications that rely not only on current but also future winds, waves, ocean currents, ship movements, and more. However, despite these advancements, the perception persists, even in academia in 2023, that forecasts beyond +72 hours are hardly considered useful.

10-20 years ago, client-based onboard systems for route planning gained widespread popularity. Now, these systems are partially being replaced by many even better online-based apps and other functionalities that offer high-quality (sometimes even free) weather forecasts. The visualisation of weather forecasts has also played a significant role. This proliferation has contributed to the increased trust in the forecasts among users onboard ships who have access to these modern systems today. Rightfully so.

In the 2020s, AI-based systems are being introduced to better optimise short and long sea passages for individual vessels and entire fleets. Ship models based on ANN (Artificial Neural Networks) and supervised machine learning are utilised. These models which rely on robust sensor data from the ship, collected every minute or even every 10 seconds. This has proven to be a groundbreaking development, surpassing previous methods in terms of accuracy and efficiency.

However, introducing new tools is not just about technical aspects. It also involves building trust and understanding of what the new tools actually can do and what they cannot. A broader understanding is needed throughout the organisation or the entire chain of actors who are all affected. Users of these now transparent systems come from different departments with different roles and expertise, both within their own organisation and others. These soft values and communication certainly involve the onboard team, the navigational and the engineering officers. But also includes the entire technical, operational, and commercial departments of the shore organisation, sometimes with watertight compartments in

between, as well as additional actors in the customer or logistics chain. No longer is it solely the Master's responsibility to find the silver bullet for this issue. Even within traditional shipowner and charterer organisations, it is common for technological advancements to not immediately resonate with all individuals or the entire organisation. Both technology and people may need time to adapt to the change. Timing is crucial.

Ten years ago, there were approximately 10 service providers in the traditional weather routing/ optimisation field. Around 5 of these were more prominent in bidding processes with major shipping companies. Today, there are hundreds of system providers that, in one way or another, "optimise" what is considered best, often using AI, today's state-of-the-art technology. Soon to be replaced by something new and more advanced.

Notably, several of these early prominent traditional service providers in weather optimisation at sea seem to struggle with building something new. Likely because innovation takes a lot of time and effort while maintaining and operating the existing 24/7 service is a heavy daily workload. It is much easier for start-ups to emerge and deliver. However, when today's start-up companies grow and eventually face a major technological generational shift, they are likely to encounter the same challenge. Many have experienced this journey, and more will undoubtedly follow.

Introducing new technologies on the global maritime market is one of NoorCares' core business. By actively exploring and testing new ideas and methods from a pragmatic perspective, NoorCare identify what works. Being receptive and understanding even the unspoken needs, regularly engaging with our valuable network of more than 60 shipowners/operators in Europe and Asia, as well as partners and competitors, is the key. This approach has been our practice for over 30 years. Additionally, contributing to the education of new captains and engineers by showcasing the latest market developments and gaining a better understanding of what the next generation of seafarers truly needs and expects allows further contribution to the future of maritime industry. It is an iterative process, and NoorCare are certainly still learning.

2. Background

For three years, the research and development project, The Arctic Tern, (Swedish: Tärna) has been focusing on route optimisation using Artificial Intelligence. The project has been carried out by a consortium consisting of NoorCare AB, Möller Data Workflow Systems AB (Molflow), Linnaeus University, and the Swedish Maritime Administration. The consortium has extensive experience in sea voyage optimisation, both in theory and practice, from the perspectives of both the ships and the shore organisations.

Four reputable shipping companies, headquartered in Europe and Asia, took active part with vessels in the project. Three of these companies have fleets of 50 ships or more and operate both short and long sea passages across the world's oceans, representing both liner service and tramp shipping.

Molflow´s route planning tool, Slipstream, were set up and run by the shipping companies and Linnaeus University. Slipstream utilises multiple neural networks to estimate the vessel's performance. The networks are trained on ship data logs in combination with state-of-the-art Met-Ocean data that is collected multiple times every day. Slipstream continuously monitors the vessel's condition, including hull condition, and provides updated and precise status information. It has global coverage and considers factors such as tidal currents and water depths. The system includes Digital Twins for each vessel, accessible to users through a graphical user interface or via API. The optimisation tool also incorporates performance monitoring, including biofouling.

Energy efficiency and reduced environmental impact of shipping is a fundamental part of our shared responsibility to contribute to a better life on our planet for future generations for a long time to come. The optimisation tool Slipstream is based on machine learning and unique solutions that can use significantly more details and parameters compared to the traditionally available tools that dominate

the market. This enables a new way to frequently be updated on the optimal result of any operation or machine settings that is the best considering all small and large changes that occur during the voyage. This is especially important for shorter sea passages where the traditional and less precise tools are rarely useful or relevant.

Alongside with the technical development of the AI-based support system, a large part of the project has been focused on soft values and the challenges the traditional and commercial drivers in international shipping meet. The focus has been on ensuring that users understand how the new precision tools should be used, preferably in combination with other already existing systems. Within the Arctic Tern project NoorCare has trained both the teams on commercial ships and the land organisation on how to better use new data. People with long practical experience. The Arctic Tern project has also carried out practical experiments for aspiring ship officers to become better equipped for the increasing demand of energy efficient sea transport before they start their professional career. The Arctic Tern project shows how a transparent and precise tool can be used for the whole organisation to obtain energy-efficient sea transports, for shorter as well as longer voyages, with a reduced environmental impact. The NoorCare Advisory concept shows results of fuel savings/reduced emissions between 2-14%.

Table I: Fuel savings indicated in the The Arctic Tern project

Type of vessel	**Sea passage length**	**Fuel saving**
Liner service	1-2 days	10-13%
Liner service	2-6 days	2-4%
Liner service	10-14 days	10-14%
Crude oil tankers	+20 days	3-5%
Students experiments at The Maritime Academy (Liner service)	10-12 days	12-25%

3. Soft Values – Our strength in combination with AI

One of the most crucial aspects of succeeding in energy efficiency can be summarised as attitude and willingness. Add perseverance and you may reach or even exceed your goals. This applies not only to the personnel onboard but also to the entire shore organisation within a shipping company and the surrounding maritime cluster that influences the vessel's chartering and port logistics.

3.1. Introducing Innovation to the Maritime Industry - The devil is in the details

Artificial Neural Networks (ANN) with supervised deep learning, including a naval architect ship model, are, truth be told, a black box where it is not always clear why the results turn out as they do. You may accept the result, but not always fully understand. In some situations, you may understand more afterwards. That’s learning. With old technique, it was necessary to filter out a significant amount of data points before plotting a graph based on a few points only. Assuming a robust flow of data from sensors, AI can handle a large amount of data with multiple precision and efficiency, which is remarkable. Even so, it is crucial to understand the bigger picture and be able to distinguish significant information from trivial - from the customer´s perspective.

For a larger high consuming vessel on shorter sea passages, minor unplanned deviations, such as a half-hour engine stop, can easily disrupt the optimisation of a smooth shaft power and completely negate the intended fuel savings since they are of the same magnitude as what is needed to compensate for the lost half-hour or so. Similarly, a delay due to unexpected traffic congestion in a busy area like the Singapore Strait can have the same impact on the energy consumption. Also, such details as a large vessel requires time for acceleration and deceleration at the beginning and end of the sea passage will affect the detailed setting of the system. The squat effect in shallow water, all examples of things that were never an issue during longer deep-sea passages, can suddenly become highly relevant and sometimes decisive. On a

longer sea passage, there is often enough time for things to even out before the vessel reaches its destination. This can also apply to the end of a long voyage when regular or daily monitoring requires more details towards the end of the passage to be accurate. It is a different perspective to consider more details and have the ambition to reduce unnecessary margins when appropriate. The handling of modern precision tools, therefore, differs from what many have learned over the years.

So even though with the new tools, decimals are handled to diligently save fuel and reduce emissions, suddenly something bigger can disrupt everything, such as a very poor weather forecast or diversion to a new destination. Or just a modified piece of information about when the berth that is being aimed for will be available.

3.2 Learning by Doing - Towards more Climate-Smart operations

Personnel onboard and ashore that use the result from an AI-based tool like Slipstream must be given the opportunity to understand the tool and critically review the results. They should be allowed to use it sensibly, experiment, and sometimes fail in order to learn. They should be able to feel involved in a larger process with a common direction. As a next step, based on the new experiences and conclusions, new Standard Operating Procedures (SOPs) can be established with the aim of finding the efficient method that best suits the specific organisation.

In the Artic Tern project, experienced captains occasionally discovered and questioned the results of Slipstream. For example, before a voyage with unusual draft/trim, Slipstream had never been trained on such extreme loading data and simply did not know how the ship would behave, despite being based on supervised deep learning and having a ship model in the background. On another occasion, a completely different ship was going to round South Africa for the first time. The digital twin, the model for this particular ship was not trained on the very long and high swell from abeam, resulting in the output not matching reality. In practice, the ship rolled more than what the untrained Slipstream had calculated, and the speed was consequently lower. In both cases, the model learned quickly after the first passage and new data from the sensors automatically trained the ANN. However, it was important for the project to prevent similar mistakes from happening again for any other ship at any other time. And there are some good methods to ensure that this never happens. But the truth is that the more reliable data you have, the better the results will be. The amount of reliable data is crucial.

But AI and machine learning can be so beautiful when they provide new detailed explanations and insights. For example, when the model helps discover and explain details in a specific ship's behaviour in varying wind and sea conditions from the stern. Behaviours that both the captain and an experienced marine meteorologist previously attributed to "perhaps some minor variation in the ocean current," due to a lack of better explanations. Or the example where it's finally possible to measure/quantify biofouling in a way that traditional methods based on noon reports and old-school mathematics have never quite succeeded in despite more than 20 years of work. But with good AI tools and reliable high-frequency data, this is suddenly achievable.

These and many other examples build genuine and solid trust in new detailed AI-based tools like Slipstream. When users gain trust in how the new precision tool works, they can more easily reduce their margins in a different and improved way compared to before. By transparently sharing this information throughout the organisation, the risk is distributed, whether it's either some excessive fuel saving or the just-in-time performance not being entirely perfect. In an encouraging and tolerant corporate culture, it becomes natural for the Master not to bear the entire responsibility alone. As is often still the case today.

3.3 The NoorCare Advisory concept

The NoorCare Advisory concept has been demonstrated and “tested” at numerous shipping companies, with the ambition to encourage more shipowners and charterers to find methods for operating in a more environmentally friendly manner that suit their specific needs. It is striking how significant the

differences are between different shipping companies with the same types of ships and similar operating methods, depending on where they are in the process. Often, the realisation is that robust high-frequency data must first be generated before moving on to the next step. The International Maritime Organisation's latest global regulations regarding EEXI and CII, as well as the European Union's new ETS (Emission Trading System), which will be implemented in 2024, are all in line with the current transformative process for the entire industry. All opportunities and contributions that help society move towards even better energy efficiency and completely ceasing the release of carbon dioxide into the atmosphere are welcome. The expectations for the industry to deliver are increasing.

There are today thousands of vessels that still rely on traditional suppliers in weather routing. Many of them do so out of tradition, even though they often need only a small portion of the traditional and partly outdated concept. Many shipowners and charterers are also in a transition period, where they realise they would benefit from an upgrade of at least some of their used methods/ algorithms/ systems. But time is a valuable asset, and the market offers a wide range of options, and it is now harder than ever to distinguish between excellent and subpar providers and solutions.

3.4. The Shipping Industry's future decision-makers

Within the Arctic Tern project, three cohorts of students in the maritime captaincy program have been able to use Slipstream during a real-time project voyage between Gothenburg/Sweden and New York/US, during winter season.

It can be summarised that the system has provided good decision support on how to set the speed considering the current weather, forecasts, and the required ETA given to the students.

The students who frequently performed updated optimisations achieved the lowest fuel consumption and minimised environmental impact. It was also noted that the students who used Slipstream instead of solely relying on conventional methods based on available weather data were able to carry out the project voyage in a significantly more energy-efficient manner.

4. Conclusions

AI-based route optimisation systems with ANN and supervised machine learning for ships that have robust and high-frequency sensor data are a prerequisite for more detailed calculations/ optimisations of set values for speed and machinery.

These modern and much more precise tools for faster and easier decision-making regarding speed and engine settings for a particular vessel on a specific route with an unique loading condition are highly significant for the ability to operate ships more energy-efficiently and in a climate-smart manner on a broad scale.

Introducing these AI-based decision systems into shipping has significant similarities to the introduction of previous groundbreaking technologies over the past thirty years, primarily targeting the ship's captain.

The similarity lies in the fact that it takes time to build trust and understanding among users regarding what the new optimisation system can or cannot do. People need time to adjust.

The difference in introducing AI in the 2020s is that there are more people involved in the onshore organisation, and the systems today are more complex. Small changes during the sea passage can have a greater impact on the results when current margins and tolerances are streamlined.

The Arctic Tern project deliberately selected some vessels/companies that have commercial conditions that make it significantly more challenging to save fuel compared to many others.

1. Large container ships in liner service, on short sea passages of 2-6 days, in a part of the world where it is practically almost impossible to obtain a reliable berth slot time closer than 1-2 days in advance. During the same sea passage, the required ETA and thus speed can vary anywhere between maximum and min/eco speed, sometimes multiple times.
2. Crude oil tankers on the spot market, on long voyages for several weeks across the world's oceans, where the commercial aspect requires that speed and fuel consumption on a 24-hour basis are within very tight ranges. Therefore, it is almost never possible to optimise the entire sea passage.

Both examples illustrate different instances of "Hurry up and wait" behaviour deeply ingrained in the shipping companies because it is the best way to make money. At least it has been so far. Despite this, the project demonstrates fuel savings. Of course, the savings would have been even greater without these commercial realities.

Knowing when the berth at the destination port will become available already at commence of the sea passage (1) and replacing the outdated Charter Party contract system with a more transparent and reliable system that creates sufficient trust for both shipowners and charterers (2) are two things with enormous potential for significant energy efficiency improvements in maritime transportation.

It is also desirable to introduce more industry standards and common regulations that facilitate all service providers in creating and encouraging “proper behaviour" regarding overall energy efficiency and smoother traffic flow. This can facilitate better interaction between different systems and thereby reduce the number of stand-alone systems. It may involve the format of route exchange, class-approved methods for calculating ships' expected impacts on weather and traffic situations, common standards for acceptable safety levels or risks at sea, in the ports, and at the terminals etc. This may help ensure that the Safety-Environment-Economy requirements within the maritime and transportation sectors develop in a harmonious balance between feasibility and desirability.

Calculating and optimising a single sea passage and thereby contributing to smoothing out the traffic flow between Port A and Port B is relatively straightforward in this context, especially now in 2023 with systems based on the latest technology, including AI, Artificial Intelligence.

Acknowledgement

The Arctic Tern project (Swe: Tärna) have been financed by the Swedish Energy Agency, NoorCare AB and Möller Data Workflow Systems AB.

Robust Design Optimization for More Efficient Ship Propellers

Sven Albert, Thomas Hildebrandt, NUMECA Ingenieurbüro, Altdorf/Germany,
sven.albert@numeca.de, Thomas.hildebrandt@numeca.de
Benoit Mallol, Cadence Design Systems, Brussels, Belgium
Leo Poppelier, SIP Marine BV, Drunen/Netherlands

Abstract

This paper presents a robust non-deterministic optimization of a ducted marine propeller. In this test case, the statistical moments of the propeller efficiency are optimized while axial thrust is constrained, and cavitation occurrence is considered. The manufacturing uncertainties are derived from the ISO geometrical tolerances S-class. Eventually, a robust optimum is compared with a deterministic optimum in order to underline the benefits of the non-deterministic design methodology.

1. Introduction

The manufacturing of propellers comes with geometrical variability that lies within predefined tolerances decreed by standardized accuracy classes. Although controlled by these tolerances classes, the variation in the design might result in a degradation of the expected propeller behaviour.

In the recent year, the design time has been drastically reduced thanks to modern computing involving computational fluid dynamics (CFD) and embedded and automated frameworks for the simulation-based design optimization (SBDO). Nowadays, hydrodynamics SBDO of a marine propeller is currently run with a unique set of inputs, such as geometry parameters and operating conditions. This overwhelming deterministic approach produces a single value response that mainly drives all the optimization strategies. But the actual operating conditions are subject to uncertainties coming from manufacturing tolerances, operating conditions and long-term life cycle involving the slow degradation of materials because of cavitation or fouling. Aware of these variabilities, modern designers currently use tools that generally do not provide means to assess their impacts. And consequently, they need to impose very strict and costly manufacturing tolerances to make sure the newly optimum design is not influenced.

This paper presents a non-deterministic methodology that allows assessing quantitatively the effect of these variabilities, and is applied on the design optimization of a ducted marine propeller. This newly optimization procedure, called RDO, aims at improving the performances, but also guaranteeing a stable behaviour given an inputted variability. Hence, the RDO provides a range of confidence with the simulation results and might help future designers in their design strategy.

In this work, two operating conditions are studied. The manufacturing tolerances come from *ISO (2015)*.

2. Test case

2.1. Background

The background of the project consists in optimizing a propeller mounted on an inland vessel, Fig.1, Table I, with a single propeller system and twin-blade rudder appendages.

Table I: Main particulars of inland vessel

AIS vessel type	Tanker – Haz C	Design draft	2.80 m
LOA x B	109.70 m x 11.40 m	Max. draft	3.35 m
Deadweight	2810 tdw	Design speed	5.4 kn
Year built	2010	Max. speed	6.2 kn



Fig.1: The inland vessel under different loadings

The inland vessel market is expected to grow at over 4.5% from 2017 to 2024, *GTM (2018)*, justifying the recent trend at improving the performances of such vessel for economic and ecological reasons, *Sihn et al. (2015)*. Therefore, propulsion device optimization could be a worthwhile task for naval architects.

2.2. The ducted propeller

The propeller studied is a fixed pitch ducted propeller, Table II.

Table II: Main particulars of fixed-pitch propeller

Diameter	1.70 m	Mean pitch	2.25 m
Diameter with duct	2.08 m	Chord length (0.7 R)	0.68 m
Number of blades	5	Revolutions/s	5.385 rps

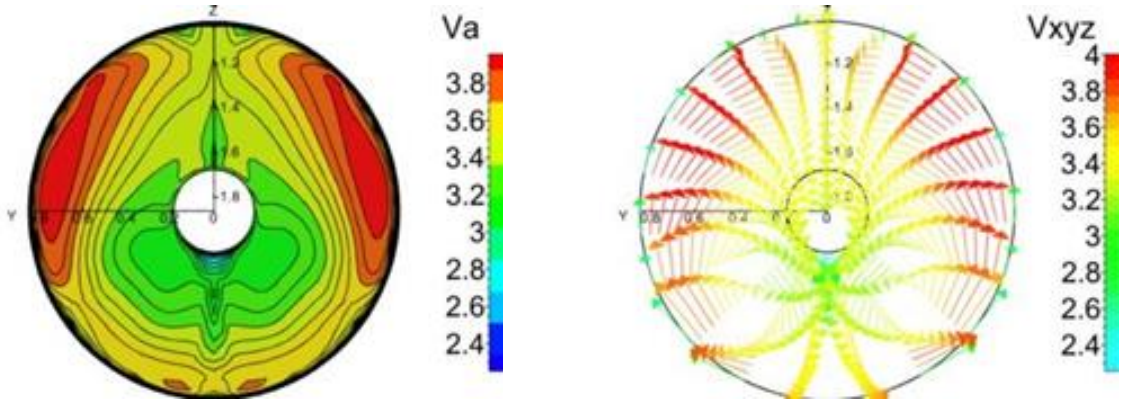


Fig.2: Nominal wake of ship at design speed



Fig.3: Propeller with (left) and without (right) duct

According to the *BAW (2016)*, all newly designed inland vessels have propellers with a nozzle. The main reason is the capacity to carry on higher thrust loading with better efficiency.
The studied case is a replacement propeller for the vessel. No design specifications were formulated for the nozzle, because it is embedded in the hull of the ship, Fig.4.



Fig.4: Final propeller mounted on the ship; the duct is part of the hull

In general practice, this type of propellers is based upon the Wageningen Ka-series ducted propellers. Hence, the empirical formulas, based on J-K_t/K_q, determine thrust and power as a function of speeds and engine characteristics. The coefficients J-K_t/K_q are defined as followed:

$$K_t = \frac{T_{prop} + T_{nozzle}}{\rho \cdot n^2 \cdot D_{prop}^4}$$

$$K_q = \frac{Q_{prop}}{\rho \cdot n^2 \cdot D_{prop}^5}$$

$$J = \frac{V_a}{n \cdot D_{prop}}$$

T is the axial thrust (of propeller and nozzle, respectively), Q_{prop} the propeller torque, ρ the water density, n the revolution rate, D_{prop} the propeller diameter, and V_a the incoming flow velocity.

The working area of the propeller is eventually defined, and therefore the blade area ratio and the required pitch. Then, the ship resistance is computed in order to extract the wake field, Fig.2. This field helps to finalize the design loop by adjusting the section profile, and more shape-determining parameters. Hence the optimization procedure can be applied during those final iterations in the design process.

3. Deterministic optimization framework

3.1. General principle

The most straightforward optimization approach is to sample the design space and use CFD at the selected point, and try to find a design for which the performances are better. However, each optimization iteration requires a CFD computation, increasing the time and computation power. Instead, an efficient methodology is implemented in FINE™/ Design3D, and relies on two building blocks, pre-exploration of the design space, performed by a design of experiments (DoE), and a surrogate assisted optimization.

3.2. Design of experiment for design space exploration

The first step consists in pre-exploring the design space, by using a near-random DoE. This pre-exploration allows creating a metamodel or a response surface that is going to be used during the optimization. For that purpose, a Latin hypercube sampling (LHS) is applied to sample the design space.

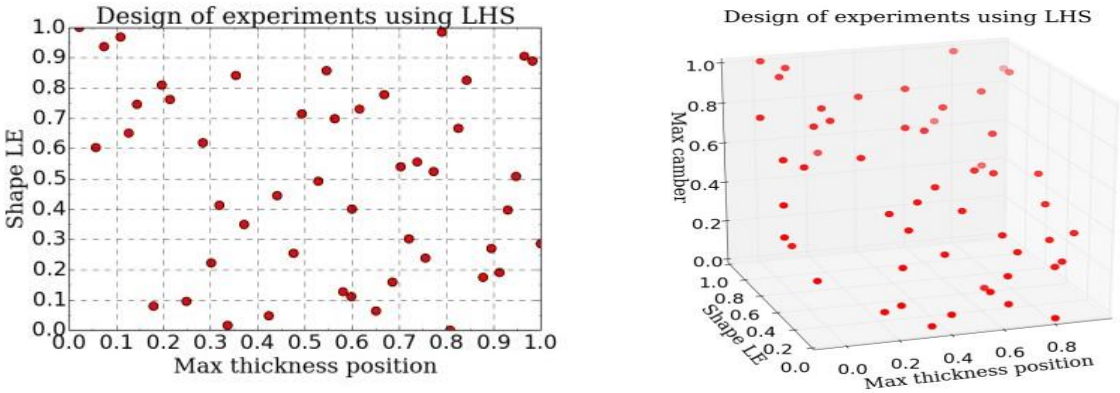


Fig.5: DoE of 30 samples for two and three design parameters

As the response surface accuracy depends on the DoE, the number of initial designs to generate is a compromise between:

- a high number of samples creating an accurate approximate model, but refining in area of low interest and requiring more computation power;
- a low number to limit as much as possible the CFD effort.

For a full benefit of this pre-exploration, the DoE is populated with 5 times the number of design parameters, in this study.

3.3. Surrogate model

From the DoE, the metamodel can be created. This approximate model, also called surrogate model, provides global design trends. The aim of the surrogate model is to mimic the propeller performances at points in between the DoE samples with a significant lower cost than CFD.

3.4. Deterministic surrogate assisted optimization

The optimizer uses a genetic algorithm (GA) to locate the interesting area. GA has the advantage to search globally in the design space, *Coley (1999)*, and mimics the natural evolution process by extracting the best design candidates over a population based on the surrogate results. Once the GA coupled with the surrogate model finds the expected optimum. A CFD simulation is performed in order to check the validity of this expected optimum design and fine-tuned the response surface for higher accurate prediction capacity with the aim of advancing further towards the global optimum. The objectives and constraints formulations can be:

- Single objective, in case of several operating conditions, the objectives and constraints can be aggregated;
- Multi-objectives, where the outcome of the optimization is the Pareto front. The Pareto front represents a set of non-dominated designs, meaning there is no better design for the respective combination of objectives.

The non-deterministic optimization, discussed in the next section, shares a common workflow with the deterministic one. The main difference lies on the definition of the objectives and constraints.

4. Non-deterministic optimization framework

Any industrial design is influenced by a superposition of several uncertainties. In order to understand the impact of these uncertainties, an uncertainty quantification (UQ) method needs to be applied.

4.1. Uncertainty quantification method

4.1.1. Brief technical overview of the methodology

To allow the propagation of uncertainties, the method, used within this work, is the non-intrusive probabilistic collocation method (NIPColM), *Loeven et al. (2007)*. This approach was implemented and successfully applied on the NASA rotor 37 validation case by *Nigro et al. (2017).*

The basis of this method is formed by the expansion of the solution into Lagrange interpolating polynomials. The base points are the collocation points, which correspond to the Gauss quadrature points weighted by an input uncertainty defined as probability density function (PDF). In order to compute the Gauss quadrature, the *Golub and Welsch (1969)* algorithm is used to provide the collocation points and it weights. A system of uncoupled deterministic simulations can be eventually derived.

Once the N_p uncoupled simulations are solved, statistical moments of any output φ_i are automatically computed by taking the weight ω_i from the Gauss quadrature. The mean and variance are calculated as follows:

- For non-centered moments, such as the mean (n=1):

$$\mu_{n,non-centered} = \sum_{i=1}^{N_p} \omega_i (\varphi_i)^n$$

- For centered moments, such as the variance (n=2):

$$\mu_{n,centered} = \sum_{i=1}^{N_p} \omega_i \left(\varphi_i - \mu_{1,non-centered}\right)^n$$

These statistical moments express the measure of the uncertainties influence over the quantities of interest.

4.1.2. Sparse grid quadrature for solving multiple uncertainties

In order to handle multiple uncertainties simultaneously, the NIPColM is usually applied with a full tensor product. This eventually leads to an exponential number of CFD simulations which is referred in the literature by “the curse of dimensionality”, and therefore cannot be used at industrial scale. To solve this issue, *Nigro et al. (2018)* applied the sparse grid technique, based on Smolyak’s quadrature method, *Smolyak (1963).*

The sparse grid technique consists in truncating dimensional function terms higher than a level of accuracy. Thus, Smolyak’s quadrature is not subject to the curse of dimensionality, and therefore offers a more efficient way of approximating function in high dimension, allowing so to make simultaneous treatment of many uncertainties in complex 3D CFD simulation.

Table III: Full tensor product grid with 3 points in each dimension vs Smolyak grids using a level 1

Dimension (number of uncertainties)	Tensor product grid (number of CFD)	Smolyak grid Level=1 (number of CFD)
1	3	3
2	9	5
10	59049	21
20	3^{20}	41

4.1.3. Sensitivity analysis for understanding the relative uncertainty influence

When facing multiple uncertainties, the analysis of the relative influence of each input uncertainty is an important element. This analysis is based on the scaled sensitivity derivatives, *Borggaard et al. (2001)*, and is used to identify the most important uncertainty over an output quantity.

In practice, the sensitivity derivative is defined as the partial derivative of the solution, from the system of uncoupled equations, with respect to the input uncertain parameter. The result is then scaled by multiplying the standard deviation of the same random input. The scaled sensitivity derivatives provide so the influence of each parameter separately, so no combined effects are taken into account.

Moreover, by providing a measure of the influence of uncertainties over the output, this analysis allows to reduce the number of uncertain input, by removing input with little influence. This can have the positive effect of using less deterministic simulations.

4.2. Robust design optimization

The main difference between the deterministic and nondeterministic optimization is the definition of the objectives and the constraints. The prior considers single values, and the latter takes into account statistical moments, represented by the mean and the variance. The most direct approach is to apply the UQ method for every single design in the DoE, hence the surrogate model is constructed based on the statistical moments of each sample. However, the cost of the nondeterministic DoE corresponds to the cost of the deterministic one times the number of UQ simulations. For a usual hundred of samples in the DoE, this approach is beyond any industrial application. For this reason, *Nigro et al. (2018)* proposed the solution to build the DoE including both design parameters and uncertainties.

Here is the example of 18 design variables and 4 uncertainties assuming the distribution is symmetric, it gives 9 deterministic simulations to run. Using 3 points in each direction of the DoE, we can obtain the following:

- DoE with UQ simulations: 18 * 3 * 9 = 486 CFD simulations
- Mixed DoE: (18+4) * 3 = 66 CFD simulations

This gain in the computational time is achieved at the expense of not having the statistical moments directly available in the surrogate model. In this manner, the surrogate is updated with UQ simulations during the optimization procedure.

5. Pre-optimization study

5.1. Numerical modelling

5.1.1. Grid generation and grid dependency study

AutoGrid5™, used for the meshing, is an automated multi-block structured mesh generator, which gives a high-quality mesh on the surface, for a short generation time. In our case, a 5 million points mesh is generated in 2 minutes on 4 threads.

Moreover, templates can be used to project same topology grid into newly design geometry shape, which is a main advantage in the frame of an optimization.

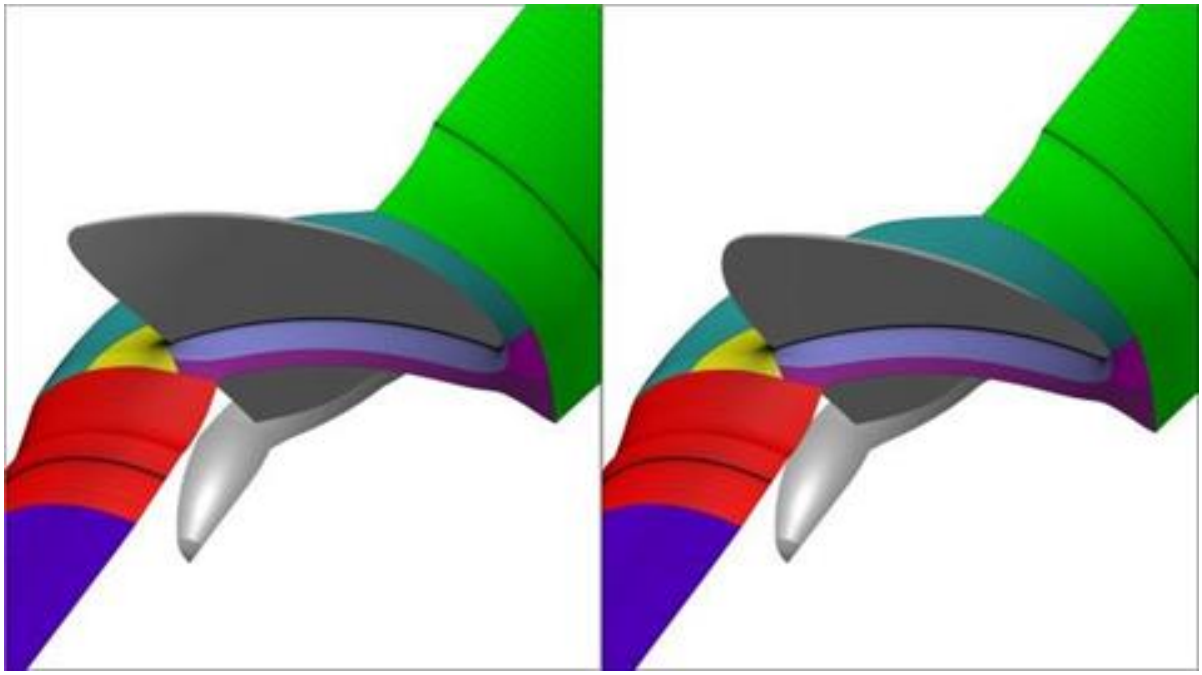


Fig.6: Template in AutoGrid5™ helps to keep the exact same mesh topology for different geometry shape. It can be seen the structured block topology is maintained for 2 different geometries.

A O4H topology is used to generate a series of five nested meshes. The targeted y^+ is 100, since the study is carried out on full scale. It gives a first layer size normal to the surface equal to 0.08 mm. The O4H grid topology consists in a O-block in the skin block of the blade and H-blocks around the main skin block. The quality of the nested meshes is summarized in Table IV. The meshes are obtained by adjusting the number of points in the O4H topology without modifying the first layer thickness. It shows that the meshing strategy has maintained the high-quality mesh and the y^+ requirements.

Table IV: Overview of the quality of the five nested meshes

Mesh	1	2	3	4	5
Million points	3.9	5.0	6.2	7.8	9.76
Min. skewness [°]	10.4	10.4	10.4	10.4	10.4
Max. exp. ratio	2.8	2.9	2.6	2.3	2.0

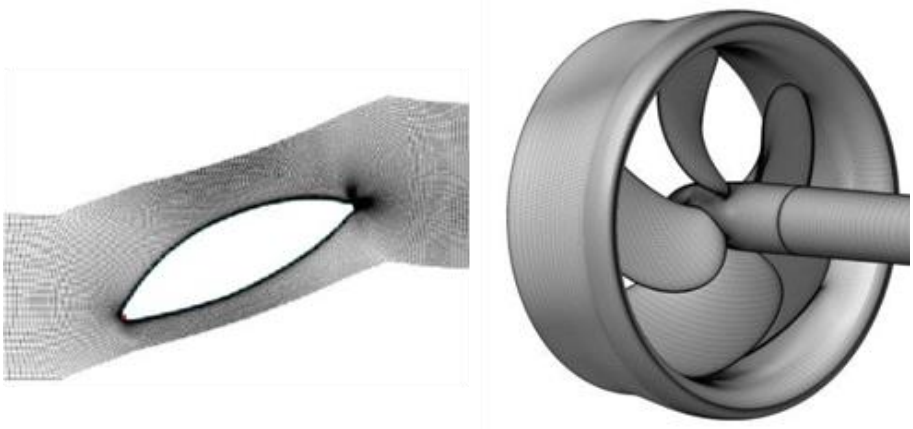


Fig.7: Final mesh: blade-to-blade view at 0.2R (left) and mesh repetition (right9

At the end, we found that a mesh of 5 million points provides an excellent trade-off between accuracy and computation time, Fig.8.

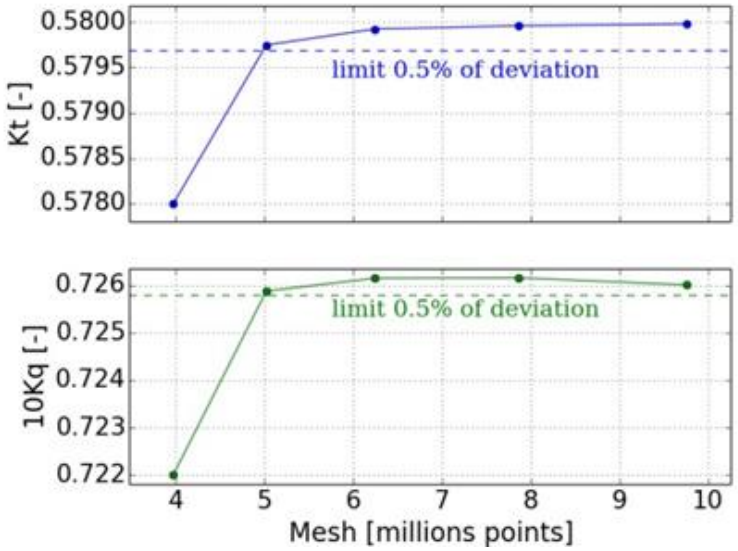


Fig.8: Grid convergence curve for the design operating condition

5.1.2 Physics and boundary conditions

The flow solver FINE™/Turbo has been validated for open-water computations, with excellent agreement with experiments, and also for cavitation patterns, *Salvatore et al. (2009)*. FINE™/Turbo is a three-dimensional density-based structured multi-block Navier-Stokes solver using finite volume. Central-space discretization is employed along with multi-grid, local time-stepping and implicit residual smoothing, in order to speed-up the convergence.

For the current propeller, the grid density allows to get a 4 levels grid and a V-cycle for the multi-grid method. In case of low Mach number incompressible fluid, time-marching density-based solvers lack efficiency and a low-speed preconditioning is often required to improve the convergence rate. The preconditioning method presented by *Choi and Merkle (1985)* is applied.

Standard boundary conditions for a typical open-water computation are applied:

- Static velocity profile and static turbulence conditions are specified at the inlet.
- Atmospheric pressure is applied at the outlet.
- A slip wall is set on the side wall of the cylindrical domain, which allows monitoring the internal mass flow for convergence behaviour.
- Periodic conditions are used to simulate only one blade passage.
- The fluid is set to be incompressible, with $\rho = 998$ kg/m^3 and $\upsilon = 1.0453 \cdot 10^{-6}$ m^2/s.

The choice of the input velocity distribution is dictated by the simulation of the ship at 10 km/h and 11.5 km/h. It eventually gives the velocity profile at the propeller location, Fig.2.

In order to take into account the highly non-uniform wake while assuming a steady state periodic computation, the wake is averaged in the circumferential direction over different radius locations.

The radial component can be neglected, as shown in Fig.9, and the tangential one remains small. Hence only an axial profile is used at the inlet.

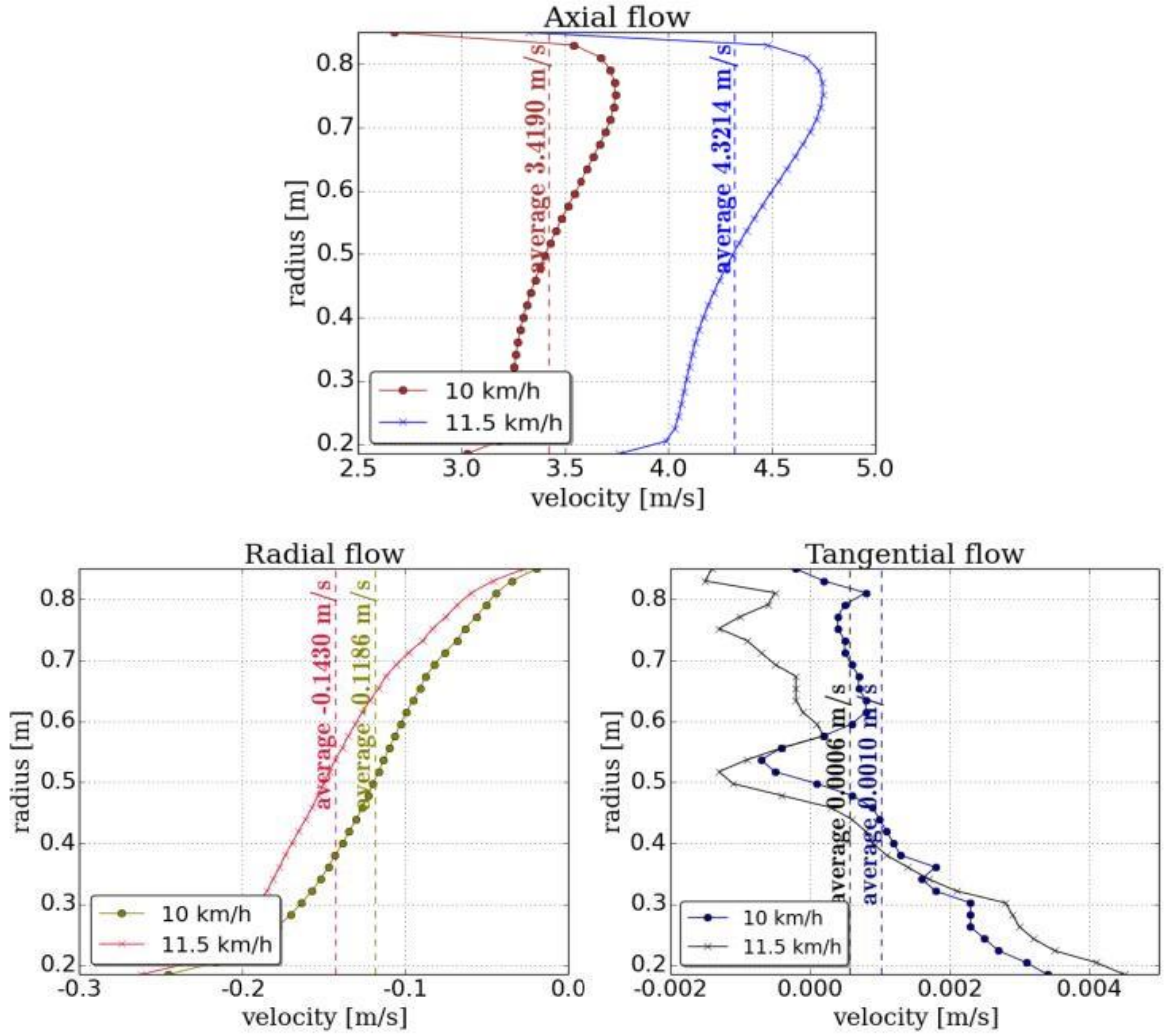


Fig.9: Circumferential averaging of the wake flow field

The position of the boundary is also important and requires considerations.

The inlet position should be selected in order to ensure an interaction between the velocity profile and the blade, without creating an upstream extrapolated lower pressure level.

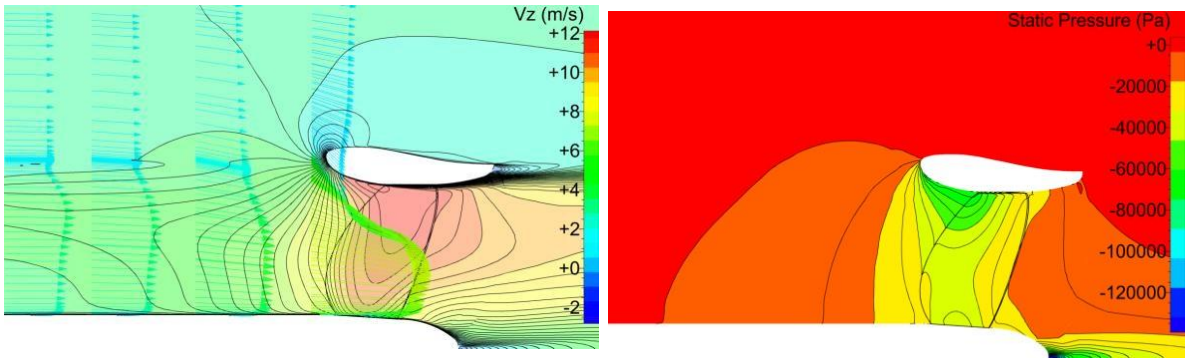


Fig.10: Meridional view of the simulation using the 11.5 km/h velocity profile, axial velocity (left) and extrapolated pressure (right)

The distance is manually adapted and set to 1 diameter length, and 5 diameter length for the outlet. This configuration is used for both operating conditions (10 km/h and 11.5 km/h).

To simulate the three-dimensional environment, Spalart-Allmaras model of turbulence is selected. At the end, a single computation, for 1 operating condition, lasts 26 min on 48 cores.

5.1.3 Cavitation inception

Cavitation can have a significant influence over the open water characteristics of the propeller, and thus should be considered when designing and optimizing any marine propeller. The complexity of the physics is real, and designers often use costly cavitation model, to evaluate its presence and the impact of this two-phase phenomenon. In the frame of the optimization, the usage of cavitation model is source of higher CPU cost and can be contradictory with the expected short design process. Hence a meaningful way to predict the cavitation is to compare the pressure level on the blade with the vapour pressure.

In our study, a 15°C fresh water is assumed with a vapor pressure equal to 1700 Pa.

In order to monitor the cavitation, the cavitating volume, or cavity, must be extracted. As the propeller tip position is quite close to free surface position at the design condition, the column of water is neglected. Hence the cavity is computing by mean of an iso-surface of static pressure below the vapour pressure.

This method has proved to give a first idea of the cavitation pattern, *Salvatore et al. (2009)*, but must be validated by a more accurate model afterwards. But in the case of the optimization, it is an excellent quantity to monitor.

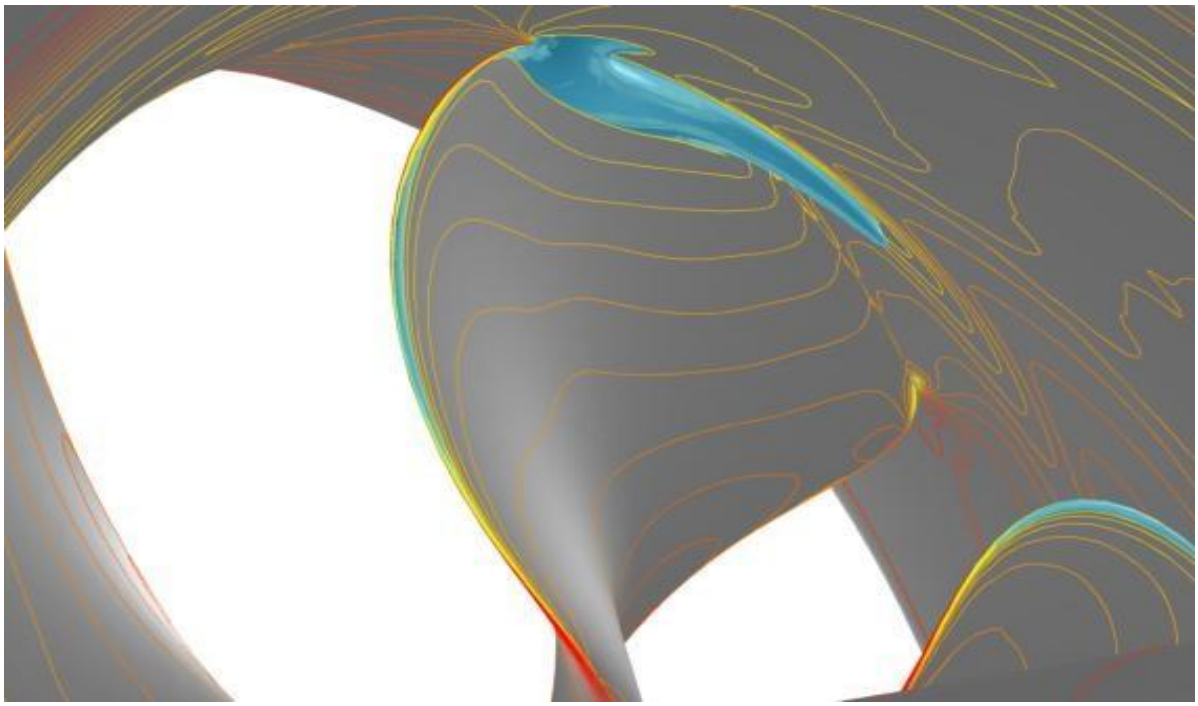


Fig.11: Static pressure isolines and cavitating cavity, represented by an iso-surface in blue, for the design condition (10 km/h)

The cavity of about 400 ml remains small compared with the overall size of the propeller. Besides, *Carlton (2012)* indicates that a moderate level of cavitation may not affect the propeller hydrodynamics performances, so the constraint on the cavitation volume should not be too strict during the optimization.

5.2. Selection of the uncertain parameters

5.2.1. Geometrical uncertainties

Manufacturing tolerances, for marine propellers, are ruled by ISO norms such as the *ISO (2015)* for any marine propeller between 0.80 and 2.50 m. The tolerances are usually expressed as a lower and an upper deviation from a nominal value. Those extrema are taken to represent a statistical tolerance by means of a probability density function, Fig.12.

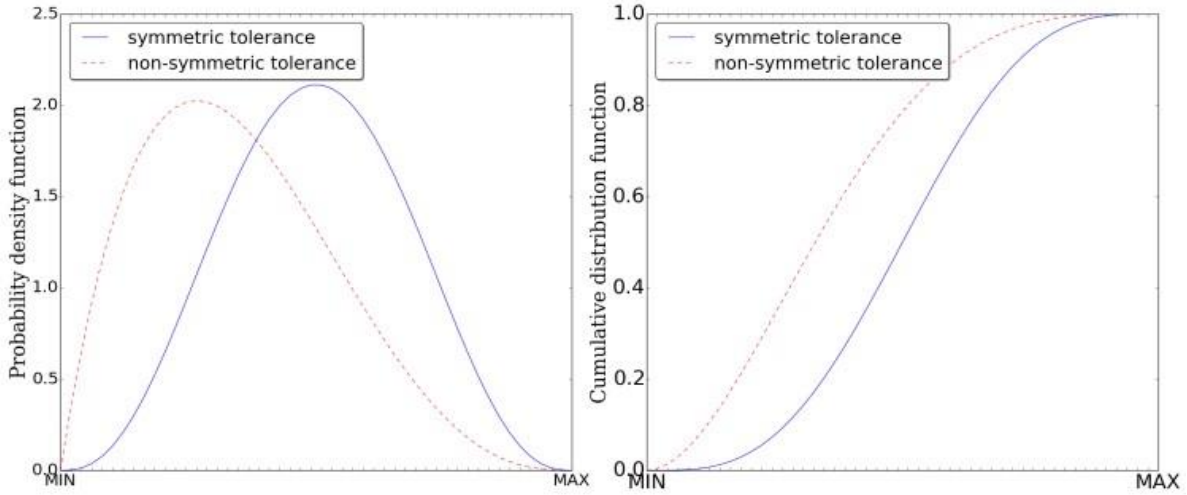


Fig.12: PDF and CDF for symmetric and non-symmetric distributions

In this paper a beta-distribution is used and determined from the ISO extrema which is a percentage of the deviation compared to the nominal design value.

Table V: Definition of each tolerance in case of an S-class accuracy

	Plus tolerance	Minus tolerance
Radius	0.2% (not less than 1.5 mm)	0.2% (not less than 1.5 mm)
Rake	0.5%	0.5%
Blade thickness	2% (not less than 2 mm)	1% (not less than 1 mm)
Blade chord	1.5% (not less than 7 mm)	1.5% (not less than 7 mm)

Those extrema are globally prescribed by four accuracy classes, ranging from the most restrictive to the widest tolerances. In this test case, the S-class tolerance is used, which represents the most accurate and restrictive one. The tolerances definition is of importance, because the final parametric modeller of the propeller has to be defined taking into account the means of tolerance measurements.

5.2.2 Operational uncertainty

Inland vessels operate seldom at the same working regime. The ship may be navigating at different speeds, especially speeds higher than the design point, or with different loadings inducing different draughts, Fig.1. Those variations might change the ship wake, influencing the operating regime of the propeller.

In this manner, two resistance computations are performed with two different draughts, nominal and maximal draughts, Table I. The nominal wake is then computed. Fig.14 shows the difference in the velocity field at the propeller location. In order to enlighten the variation of the axial velocity, a radial averaging is performed, and shows a maximal variation of 3%. Hence, a symmetric PDF is defined using as extrema the maximal variation. The wake axial profiles, Fig.9, are going to be shifted by this variation during the UQ computations.

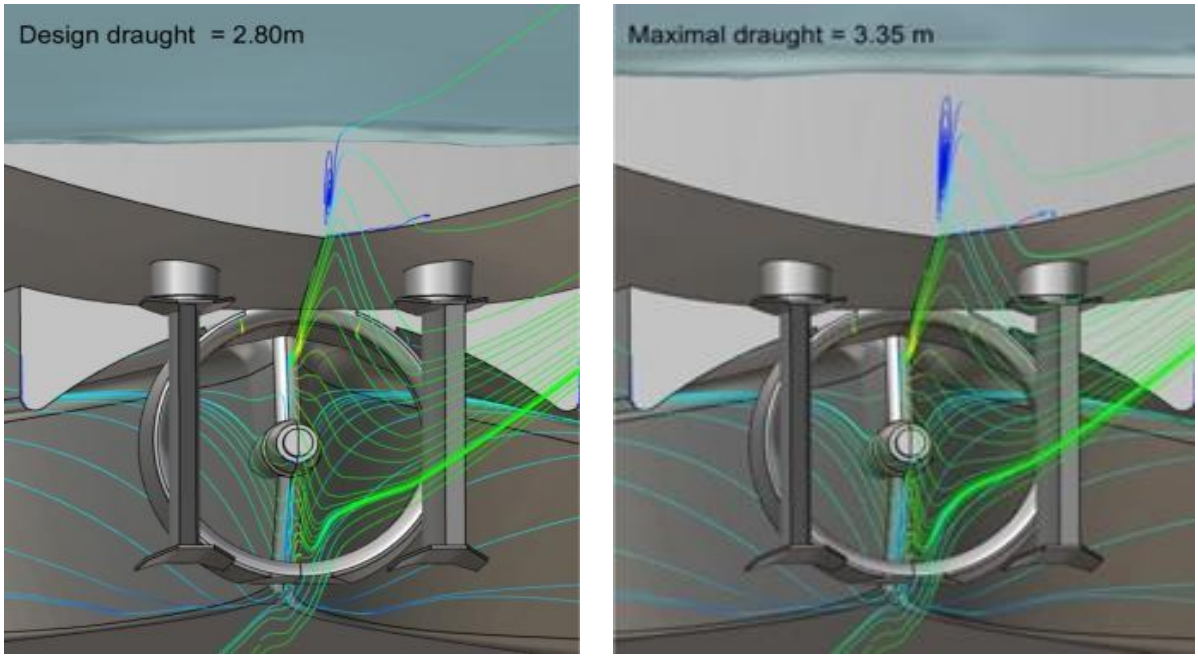


Fig.13: Streamlines, colored by the velocity magnitude, at the wake of the ship for different draughts

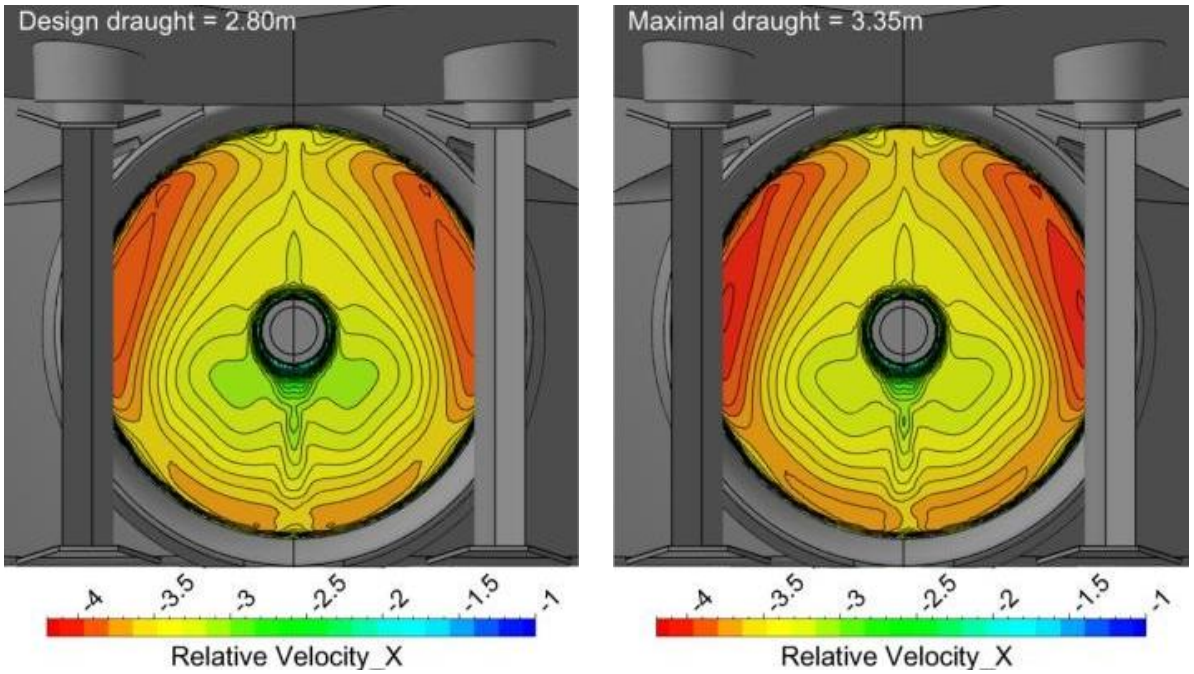


Fig.14: Relative axial velocity at the propeller location for the design speed condition under two different draughts

5.3. Parametric description of the propeller

In order to construct the parametric model, the target is first sliced at different radius locations, Fig.15. From those sections, a parametric topology is used to define the section profile and camber. The stacking of each section, in other words, their relative positions, defines the rake in the meridional direction and the skewness in the tangential one. Both meridional and tangential laws are parametrized using a Bezier of 6 control points. The profile is defined using a B-spline curve of 6 control points and the camber using a Bezier of 3 control points. This Bezier curve also defines the local profile pitch and chord.

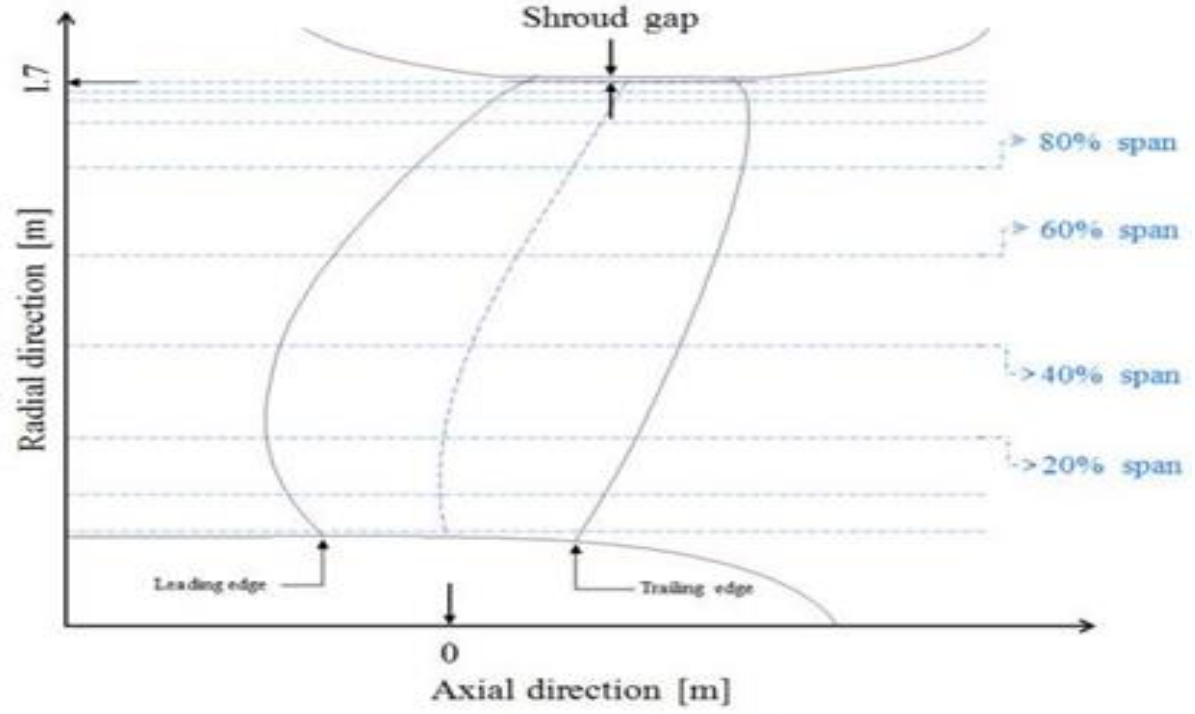


Fig.15: Location of the slicing sections along the span

The choice of the sections locations is determined by the ISO. Indeed, the ISO requests manufacturers to verify the deviation at different locations on the blade, i.e. 20%, 40%, 60% and 80% of the radius. Thus, it is better to control the uncertainty parameter and apply a correct evaluation of its impact when both manufacturing measurement and parametric modification are performed at the same radius.

As suggested by *Nigro et al. (2018)*, the parametrization induces modifications and deviations from the initial target geometry. In case of uncertainty study, it is crucial to represent the initial target geometry with a high accuracy, such that the previously discussed deviations are significantly lower than the geometrical uncertainty.

This verification is performed on two levels:

- First the parametric and the target geometry are visually compared;
- Then the CFD simulations are juxtaposed.

5.3.1. Accuracy of the geometry parameterization

During the parametrization, a global visual inspection is performed, in order to detect strong deviations and therefore adapt the parametric topology to fit accurately the initial target geometry.

The result of this process is demonstrated by figure 16. It can be seen that both geometries do not display significant differences. The parametric model respects globally the shape of the initial target one, so a close-up is performed on different sections of the blade. It eventually shows discrete geometrical deviations and amount locally up to 500 microns, Fig.17, where the uncertainty is equal to 2 mm for the thickness and 7 mm for the chord.

In conclusion, the local modifications are in the overall lower than the manufacturing tolerances.

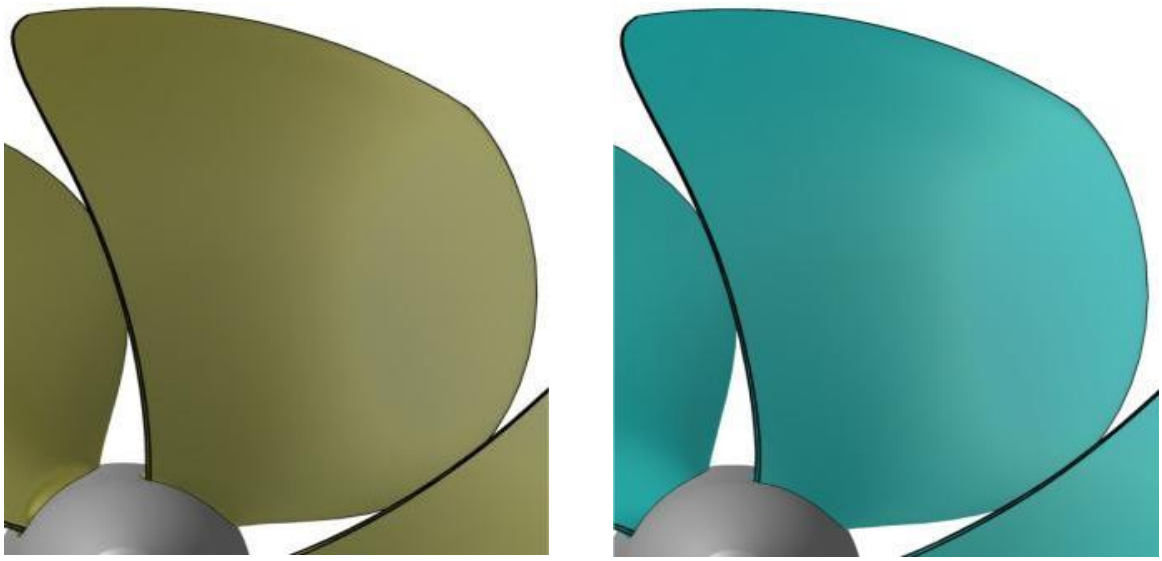


Fig.16: Comparison between the target (left) and the parametric geometry (right)



Fig.17: Close-up at the leading-edge part at 60% of the span

5.3.2. Influence of the parametric model on the deterministic results

The influence of the error introduced by the parametric model on the CFD results must be assessed. This also allows validating the parametric model as starting design for the optimization.

Eventually, the flow field does not show any serious difference, Fig.18, and the overall results are within 1%. It validates the parametric model and also implicitly confirms that even a small variation in the geometry discretely affects the performances. It is important to underline that the evaluation of the parametric model accuracy has an importance in the RDO framework. For deterministic optimization, this procedure can be more flexible, since the geometry is deformed in any case.

Table VI: Comparison of the target and parametric geometry

	Target	Parametric	Rel. Difference
T	141.1 kN	140.2 kN	-0.71%
Q	29.59 kNm	29.85 kN	+0.87%
cavity	400 ml	398 ml	-0.5%

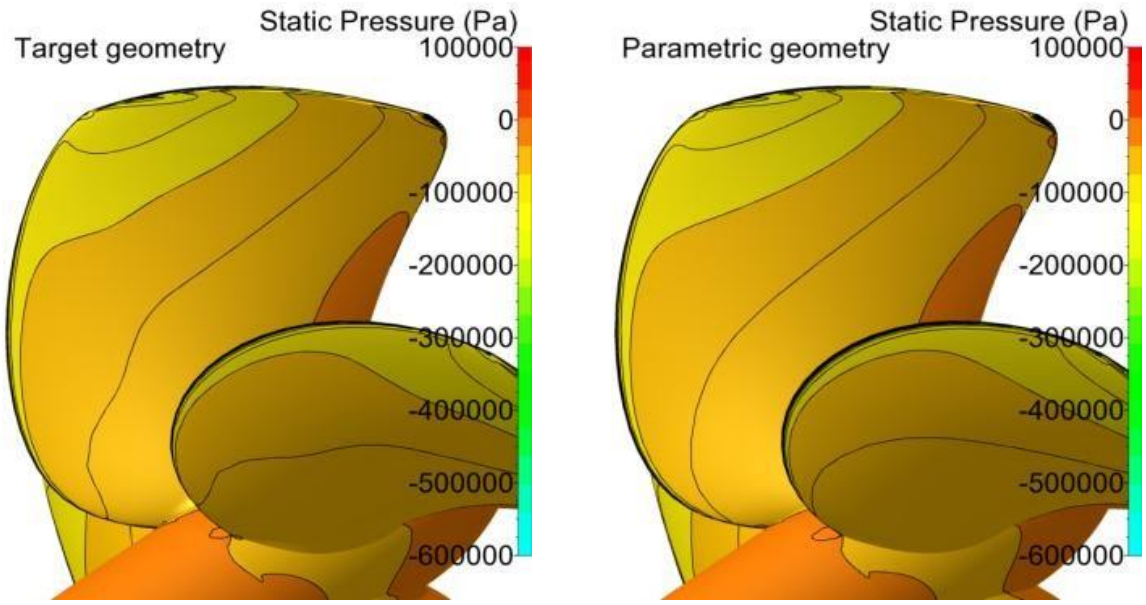


Fig.18: Comparison of pressure field between target (left) and parametric geometry (right)

6. Deterministic and non-deterministic optimization

6.1. Deterministic optimization

6.1.1. Overall formulation

The design parameters consist in a total of 18 variables:

- 4 for the sections profile law;
- 2 for the chord law;
- 3 for the local pitch law;
- 3 for the camber law;
- 6 parameters for the skewness and the rake laws.

The thickness is kept constant, as the modification would induce a change on the structural computation of the bending moment. As suggested in section 3.2, the DoE is sampled by 90 designs. For each design in the DoE, the overall quantities K_t and K_q are automatically postprocessed, along with the cavitation volume and the open-water efficiency η:

$$\eta = \frac{K_t}{K_q} \cdot \frac{J}{2\pi}$$

Two operating conditions are considered and linked to the ship speeds, Table I, 10 km/h and 11.5 km/h. The revolution rate of the propeller is kept constant. Thus, only the inlet flow condition is changed, Fig.9. The overall objectives and constraints are the following:

- Improving the overall open water efficiency η by using an aggregated formulation of both operating conditions: 70% design speed + 30% off-design speed
- Maintaining the axial thrust (as required for the contractual ship design speed): K_t = 0.58.
- Not deteriorating the performance, by keeping similar cavitation behaviour. As this constraint should be flexible, it is decided to keep the volume below 800 ml;
- Simulation should be converged. The criteria, to decide whether the simulation is converged or not, is based on the difference between the inlet and outlet mass flow. This deviation should not exceed 0.1%, otherwise the sample is rejected.

6.1.2. Optimization outcome

The deterministic mono-objective optimization reaches an optimum meeting all constraints within 30 iterations. The final optimum shows an increase in the weighted efficiency of about 2.26% relatively (i.e. almost 1% in absolute), while the thrust is maintained, and cavitation below the fixed threshold.

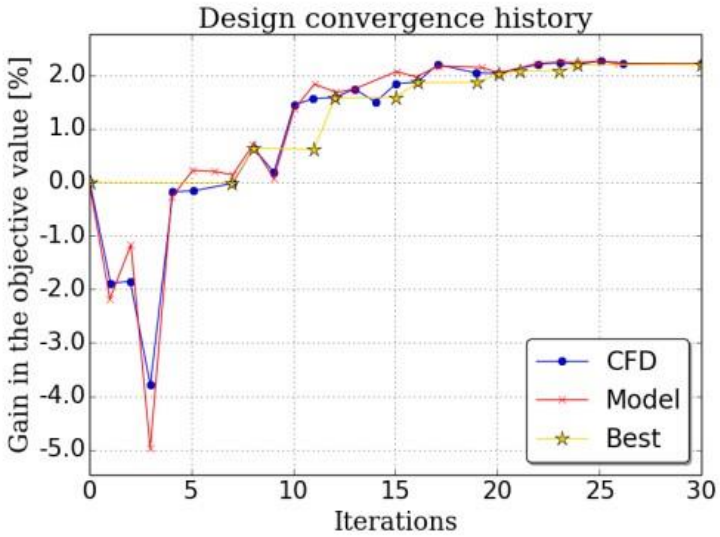


Fig.19: Convergence history of the mono-objective deterministic optimization, model represents the surrogate model results

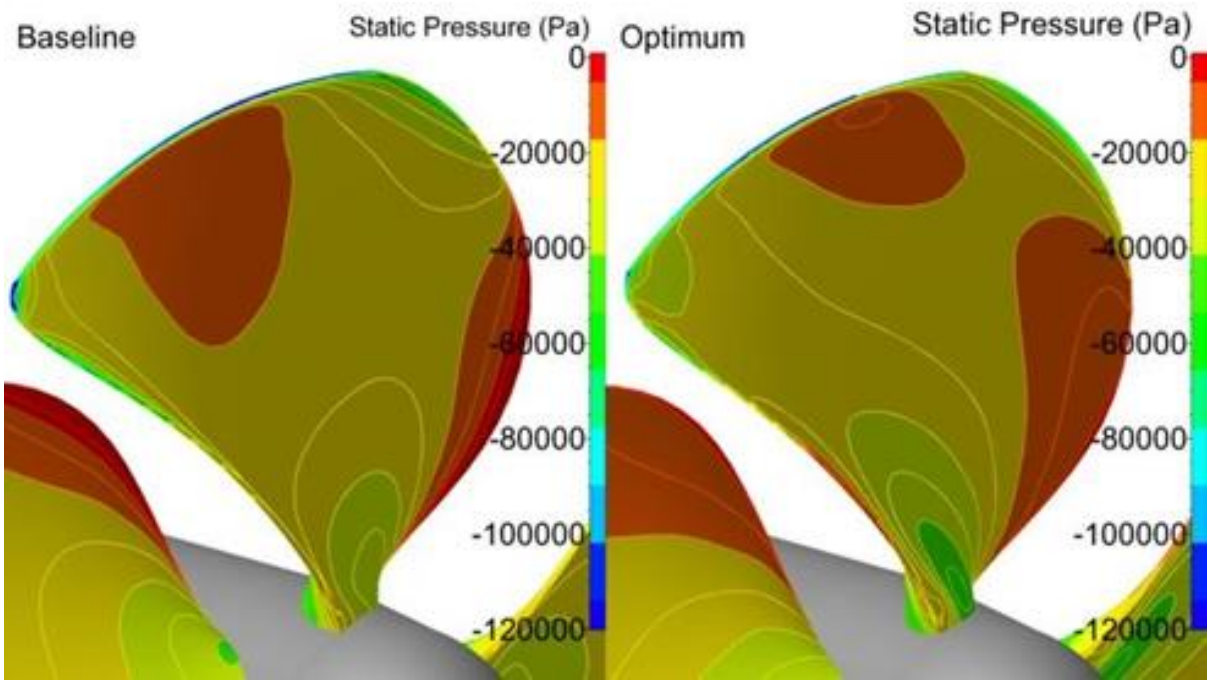


Fig.20: Static pressure comparison between the baseline (left) and the deterministic optimum (right)

Table VII summarizes the performances of the deterministic optimum compared to the baseline, the initial parametric geometry, and Fig.24 shows the geometrical differences.

In the downstream velocity field, Fig.21, the tangential component of the optimum is less pronounced than the baseline. This indicates a more aligned flow and consequently a higher efficiency.

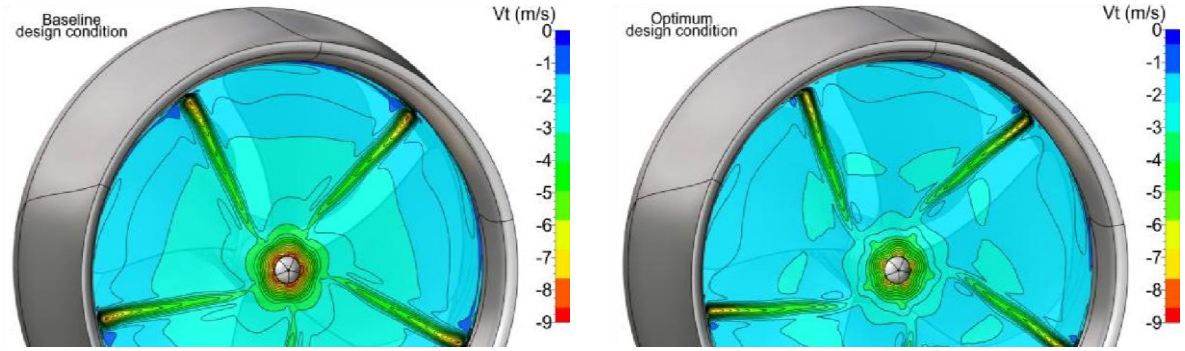


Fig.21: Tangential velocity behind trailing edge for baseline (left) and deterministic optimum (right)

This is also implied by Fig.22, where the midspan profile drag of the baseline is higher.

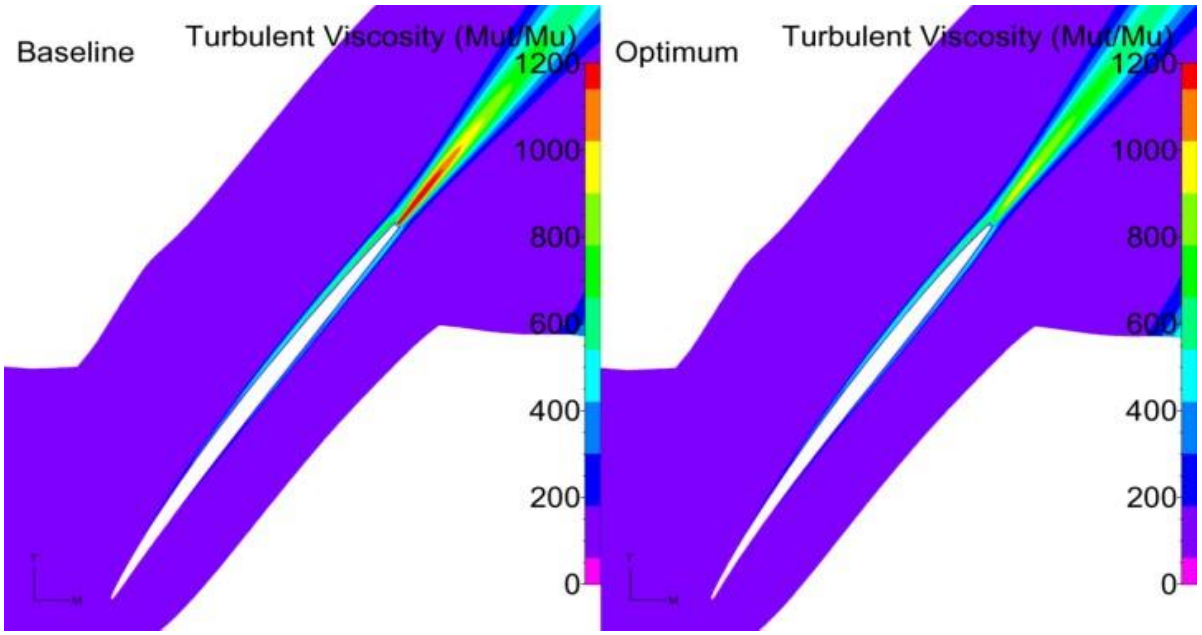


Fig.22: Midspan blade-to-blade view of turbulent viscosity ratio between baseline (left) and deterministic optimum (right), at design condition

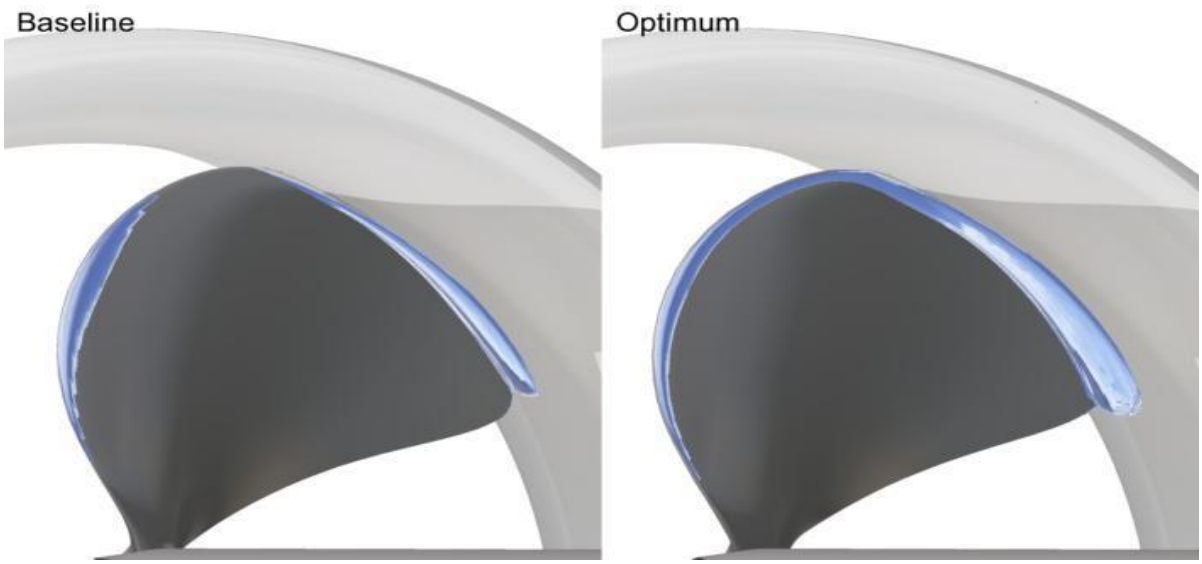


Fig.23: Cavitation simulation for the baseline (left) and the optimum (right)

Table VII: Comparison of baseline and optimum performance

		Baseline	Optimum
Design condition 10 km/h	K_t	0.58	0.58
	K_q	0.0720	0.0705
	η	0.390	0.401
Off-design condition 11 km/h	K_t	0.506	0.505
	K_q	0.0680	0.0667
	η	0.419	0.428
Weighted η		0.399	0.408
Cavity [ml]		398	769

For the cavitation modelling, it can be seen that the improvement in the propeller performances is highly constrained by the cavitation volume, Table VII, as the final optimum features a cavity close to the limit 800 ml. The optimizer cannot find a better optimum without exceeding this constraint.

Two steady cavitation simulations are eventually run to validate the actual performances of the propeller, Fig.23, and demonstrate that both designs suffer minor losses in their respective performances, validating the optimization procedure.

However, both designs feature bubbles-like cavitation at the tip. This is problematic in terms of vibration and comfort. As it is suggested in Fig.11, the cavity is attached to the nozzle shape, which indicates that the interaction between the propeller blade and the duct influences strongly the cavity size. Thus the nozzle shape should be also optimized, which we did not do in this project.

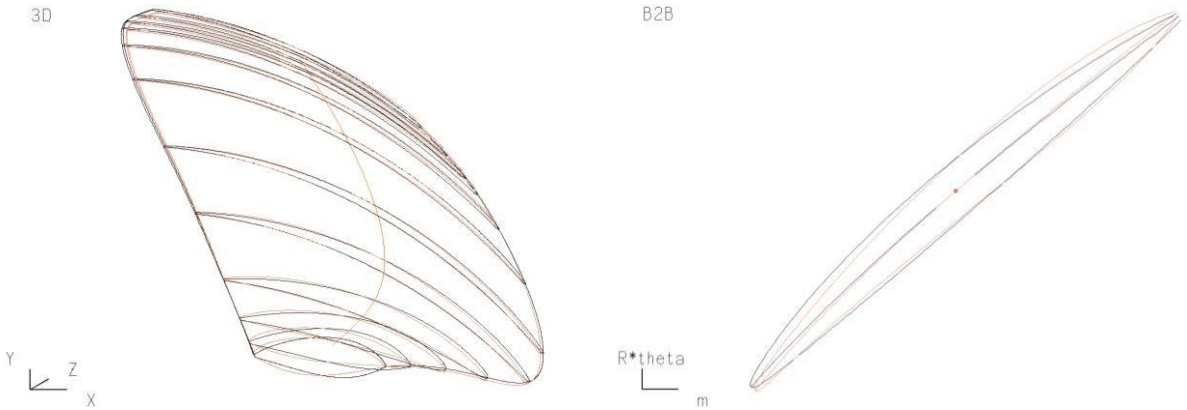


Fig.24: Overlapping of optimum (red) and baseline (black) for 3D and blade-to-blade (at 0.2R) views

6.2. Non-deterministic optimization

6.2.1. UQ simulations

An initial UQ study is performed with 13 uncertainties:

- 4 uncertainties for 4 different sections chord defined with a symmetric beta PDF;
- 4 uncertainties for 4 different profiles thickness defined with a non-symmetric beta PDF;
- 1 uncertainty for the rake, which represents the linear position of the tip compared to the root of the blade, defined with a symmetric beta PDF;
- 1 uncertainty for the gap between the blade and the duct, defined with a symmetric beta PDF;
- 1 uncertainty for the axial velocity

By using a sparse grid level 1, 32 deterministic computations need to be run. Indeed, *Nigro et al. (2017)* proved that a level 1 already provides accurate results on the mean and the variance, which is sufficient for the RDO.

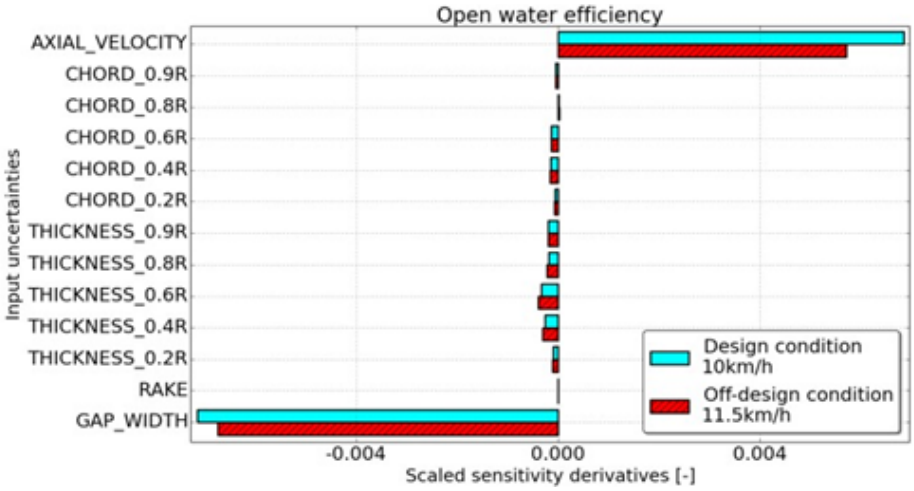


Fig.25: Scaled sensitivity derivatives of open-water efficiency for both operating points, with 13 uncertainties

Scaled sensitivity derivatives are then computed, and show that the main influencing components are the axial velocity and the gap between the duct and the tip. This analysis is quite logical, because the efficiency η is function of the advance ratio J, the blade diameter and the axial velocity.

Moreover, the uncertainties for the thickness having the lowest standard deviation are clearly more important than those for the chord. This is also logical considering the fact the thrust and torque are directly influenced by each blade profile thickness.

From that analysis, it is decided to merge all chord and thickness uncertainties together. The change in the shape of the blade profile is controlled by a single section. And the rake uncertainty is neglected. This reduces the number of uncertainties to 4, and the number of deterministic computations is now 10, for a single operating condition.

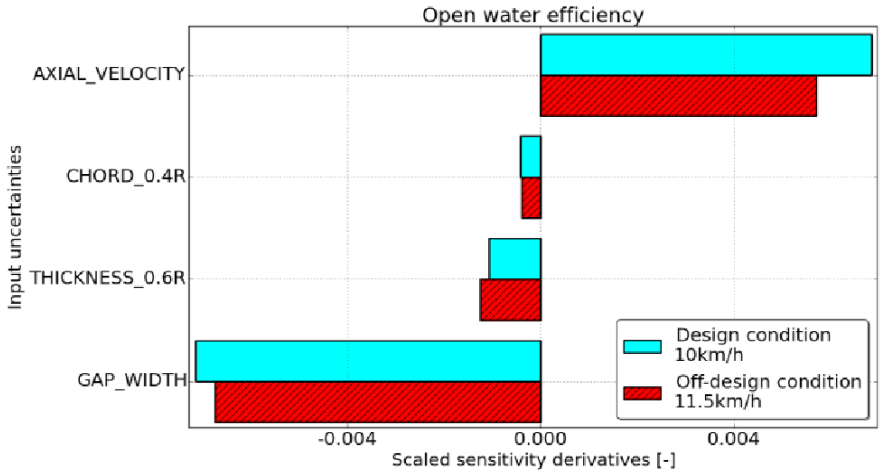


Fig.26: Scaled sensitivity derivatives of open-water efficiency for both operating points with 4 uncertainties

The scaled sensitivity derivatives show similar trends between 13 and 4 uncertainties, Figs.25 and 26. Moreover, a normal distribution is reconstructed in order to display the difference in the mean and the variance, Fig.27.

It can be concluded that the reduction of the number of uncertainties did not impact the statistical moments results. Hence, 4 uncertainties are used during the RDO.

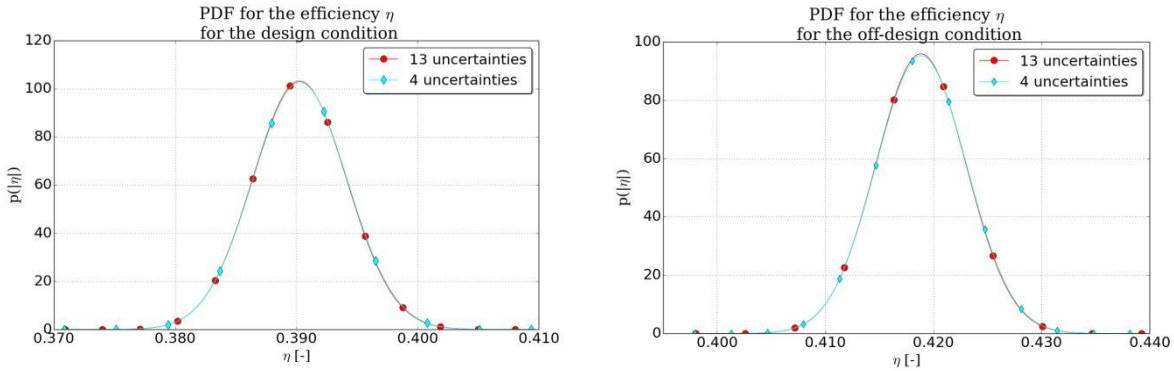


Fig.27: Normal distribution using the mean and standard deviation for both operating conditions and 13 and 4 uncertainties

The scaled sensitivity analysis can also be useful for analysing the uncertainties influence over other key quantities, such as the cavitation volume, helping to identify critical variabilities. Indeed on Fig.28, it can be seen that all geometrical and operating conditions strongly impact the cavity size, and might increase its volume by 4% when decreasing the axial velocity and 3.5% when increasing the propeller duct gap distance.

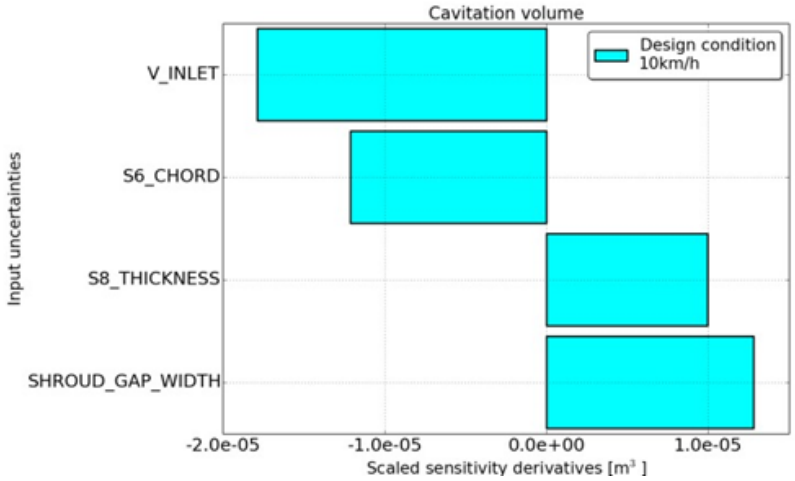


Fig.28: Scaled sensitivity derivatives of the cavity volume for design condition

6.2.2. Robust optimization outcome and comparison with the deterministic optimum

The same design parameters are used, with 4 additional uncertainties for the DoE generation. The same operating points are considered.

However, the formulation of the RDO is as follows:

- Improving the overall open water efficiency η by maximizing its mean value $\mu(\eta)$, using the same aggregated formulation for both operating conditions.
- Also improving the robustness of the design by minimizing the standard deviation of the same efficiency $\sigma(\eta)$.
- Maintaining the mean axial thrust, $\mu(K_t) = 0.58$.
- Not deteriorating the performance, by keeping μ(cavity) below 800 ml.

In consequence, it can be seen that the RDO formulation is multi-objectives and the outcome is the Pareto front. The same number of iterations is used. For each iteration, 10 deterministic CFD computations, per operating condition, are performed in order to compute the statistical moments.

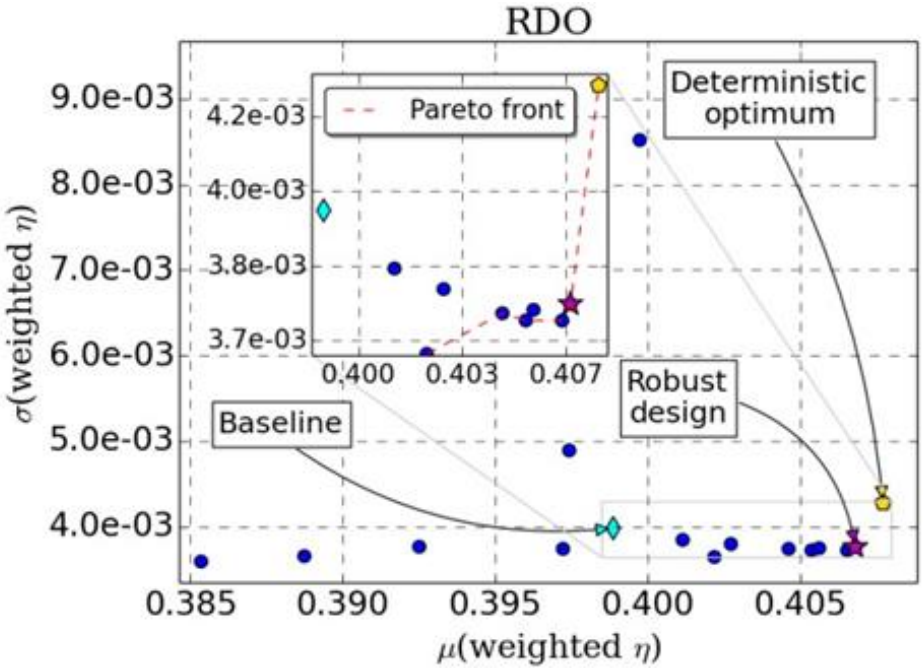


Fig.29: RDO history and Pareto front outcome

Fig.29 clearly displays a robust design among the nondominated samples, which manages to reduce the standard deviation by 6 % and the mean efficiency is increased by 2%.

We selected a single robust design, because it features the best trade-off in terms of statistical moments enhancement.

Moreover, a UQ study is performed on the deterministic optimum and also shows an increase of the mean efficiency, but also an increase of the standard deviation of about 7.4%, Fig.30. Hence, the deterministic optimum is consequently less robust, but is still located on the Pareto front.

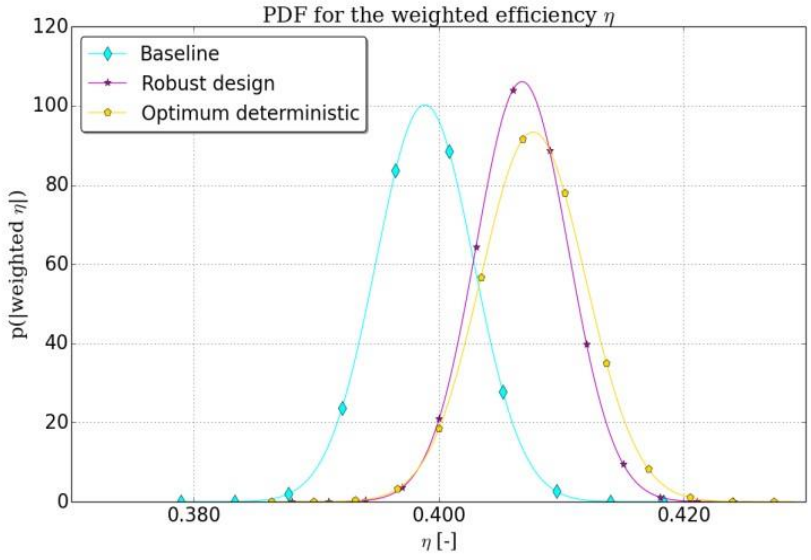


Fig.30: Normal distribution of the baseline, the robust and deterministic optima

Moreover, the scaled sensitivity derivatives (cf. fig.31) reveal that the influence of the axial velocity and the diameter are still the largest. However, the geometrical uncertainties show a discrete reduction in their respective influences for the robust design. This explains the decrease of the standard deviation.

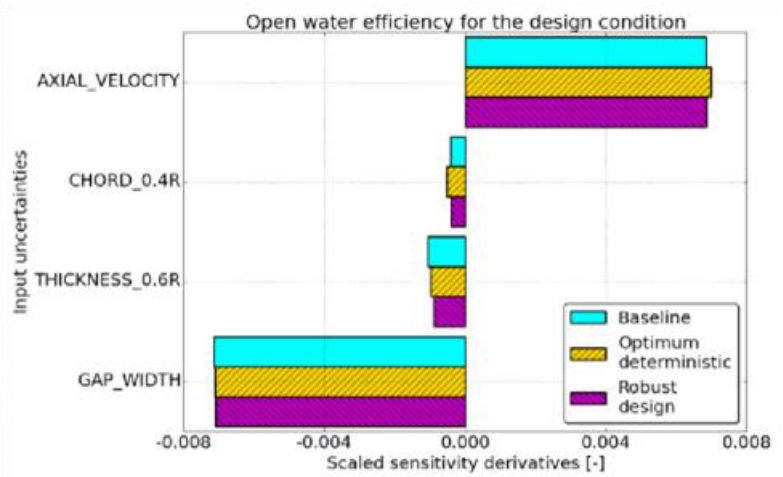


Fig.31: Scaled sensitivity derivatives at design condition for baseline, and robust and deterministic optima

Fig.32 compares the propeller blade shapes, the deterministic and the robust. The robust design features a higher skewness in contrast to the deterministic optimum and the baseline, Fig.24. The explanation of the geometrical differences comes from the robust optimization formulation.

Indeed, the deterministic optimization aims at localizing the best design for a single objective formulation, whereas the RDO proposes a set of non-dominated designs with the objective to improve both performances and robustness.

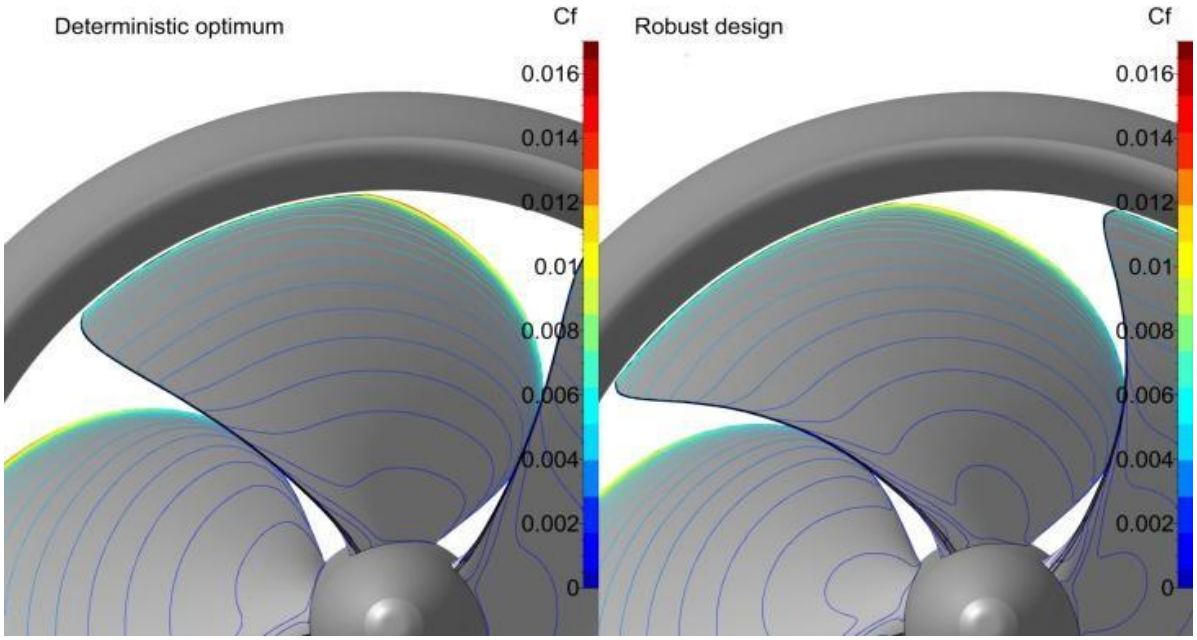


Fig.32: Comparison between deterministic optimum (left) and robust design (right)

6.2.3 Computational cost of robust design optimization vs deterministic optimization

In both cases, 5 samples per dimensions are used in the initial DoE. The non-deterministic DoE have 4 extra uncertainties, leading to an increase of 20 additional designs in the DoE.

For the optimization, the same number of iterations is used. However, each robust iteration performs UQ simulations. At the end the robust optimization leads to a computational overhead of 3.42.

Table VIII: Detail of the computational cost comparing a robust design optimization and the deterministic optimization. The computation of the CPU Hours assumes that 1 CFD has a cost of 20.784 CPU hours (26 min on 48 cores).

	Deterministic optimization	Robust design optimization
Number of samples in the DoE	90	110
Total number of CFD runs for the DoE	180	220
Number of CFD per optimization iterations	2	20
Number of optimization iterations	30	30
Total number of CFD runs for the optimization	60	600
Total number of CFD runs	240	820
Computational cost [CPU Hours]	4988.16	17042.88

7. Conclusion

In this paper, two design optimization studies were performed: a deterministic optimization and a robust optimization accounting for uncertainties. Since the investigated ducted propeller was subject to several operating conditions, two were considered: the design condition, which was used to draw the initial baseline geometry, and an arbitrary off-design condition based on the maximal cruising speed of the vessel. As the cavitation was also of importance, a low CPU cost modelling based on the pressure field was used and provided interesting information.

Indeed, the first deterministic optimization indicated the relevance of considering cavitation modelling. Indeed, the optimization outcome demonstrated the trade-off between performances improvements and cavitation criteria.

Strictly speaking, the optimizer was restrained in the search of a better design due to the constraint in the cavitation volume. However, the performances can be further improved by including the nozzle shape parameters in future optimizations.

The second optimization was the robust design optimization that aimed at improving the performances while reducing the vulnerability of the design performances with respect to both operational and geometrical variabilities. The evaluation of those variabilities was performed by uncertainty quantification simulations. It was also observed that the UQ simulations can also play a major role in the design process for identifying critical manufacturing variabilities over key quantities of interest, such as cavitation or efficiency. Eventually, both deterministic and robust optimum were compared, and as expected the robust design increased the performances and the robustness.

Moreover, the deterministic optimum was also located on the Pareto front, which might indicate that the inputted manufacturing variabilities were small enough to guarantee an acceptable stable behaviour, which was the expected results when using the most precise and costly S-class tolerance. Knowing the real-life performances can be assessed, the propeller designers can now try to apply coarser and less expensive manufacturing tolerance, and use the proposed approach to optimize the design accounting for several variabilities and operating conditions.

Acknowledgements

We thank our CADENCE colleagues for their generous and detailed input to this paper: Charles Hirsch, Benoit Mallol, and Kevin Vidal. We also thank Volker Bertram for his help in finalizing this paper.

References

BAW (2016), Driving Dynamics of Inland Vessels, Bundesanstalt für Wasserbau, Karlsruhe, https://izw.baw.de/publikationen/pianc/0/BAW_VBW_Driving_Dynamics_of_Inland_Vessels.pdf

BORGGAARD, J.; PELLETIER, D. ; TURGEON, E.. (2011), *Parametric uncertainty analysis for thermal fluid calculations*, Nonlinear Analysis 47/4, pp.4533–4543

CARLTON, J.S. (2012), *Marine Propellers and Propulsion*, Butterworth-Heinemann

CHOI, D.C.; MERKLE, C.L. (1985), *Application of Time-Iterative Schemes to Incompressible Flow*, AIAA J. 23/10, pp.1518-1524

COLEY, D.A. (1999), *An Introduction to Genetic Algorithms for Scientists and Engineers*, World Scientific

GOLUB, G.H.; WELSCH, J.H. (1969), *Calculation of Gaussian Quadrature rules*, Math. Comp. 23, pp.221-230

GTM (2018), *Inland Waterways Vessels Market to Hit $2.25 Billion by 2024*, Global Trade Magazine, April Issue

ISO (2015), *ISO 484-2: Ship screw propellers - Manufacturing tolerances - Part 2: Propellers of diameter between 0,80 and 2,50 m inclusive*, Int. Standard Org., Geneva

LOEVEN, G.J.A.; WITTEVEEN, J.A.S.; BIJL, H. (2007), *Probabilistic Collocation: An Efficient Non-Intrusive Approach for Arbitrarily Distributed Parametric Uncertainties*, 45th AIAA Aerospace Sciences Meeting and Exhibit

NIGRO, R.; WUNSCH, D.; COUSSEMENT, G.; HIRSCH, C. (2017), *Uncertainty Quantification in Internal Flows*, 55th AIAA Aerospace Sciences Meeting

NIGRO, R.; WUNSCH, D.; COUSSEMENT, G.; HIRSCH, C. (2018). *Robust design in turbo-machinery application*, Findings and Best Practice Collected During UMRIDA, a Collaborative Research Project (2013–2016)

SALVATORE, F.; STRECKWALL, H.; TERWISGA, T.V. (2009), *Propeller Cavitation Modelling by CFD - Results from the VIRTUE 2008 Rome Workshop*, SMP'09, Trondheim, https://www.researchgate.net/profile/Tom-Terwisga/publication/237569766_Propeller_Cavitation_Modelling_by_CFD_-_Results_from_the_VIRTUE_2008_Rome_Workshop/links/00b7d52b2cfc687ff9000000/Propeller-Cavitation-Modelling-by-CFD-Results-from-the-VIRTUE-2008-Rome-Workshop.pdf

SIHN, W.; PASCHER, H.; OTT, K.; STEIN, S.; SCHUMACHER, A.; MASCOLO, G. (2015), *A Green and Economic Future of Inland Waterway Shipping*, Procedia CIRP 19, pp.317–322, https://www.sciencedirect.com/science/article/pii/S2212827115004850

SMOLYAK, S. (1963), *Quadrature and Interpolation Formulas for Tensor Products of Certain Classes of Functions*, Doklady Akademii Nauk SSSR 4, pp.240-243

Innovative Approaches in Vessel Design: Pioneering Integrated Multidisciplinary Analysis and Digitalization for Enhanced Performance

Rodrigo Perez Fernández, Siemens, Madrid/Spain, rodrigo.fernandez@siemens.com
Emile Arens, Siemens, London/UK, emile.arens@siemens.com
Miles Wheeler, Siemens, Bellevue/USA, miles.wheeler@siemens.com
Sean Pearson, Siemens, Hamburg/Germany, sean.pearson@siemens.com
Dmitry Ponkratov, Siemens, London/UK, dmitry.ponkratov@siemens.com

Abstract

This paper delves into a highly innovative project aimed at revolutionizing vessel design methodologies. Our approach centers on the integration of cutting-edge multidisciplinary analysis, with digitalization serving as the cornerstone for this transformative process. The focal point is the strategic infusion of computer-aided engineering (CAE) throughout the entire design continuum, offering a distinct competitive advantage. Illustrated through the lens of a fast search and rescue vessel, this paper showcases the project´s avant-garde features. Furthermore, the paper discusses automated design exploration as the catalyst for achieving optimal hull structures.

1. Introduction

The pursuit of enhanced vessel performance is a perpetual endeavor driven by evolving technological advancements and increasingly diverse maritime operations. From cargo transport to naval defense and search and rescue missions, electrical vessels are expected to operate efficiently, safely, and with optimal performance characteristics across a spectrum of environmental conditions. Achieving these objectives necessitates a paradigm shift in vessel design methodologies, one that embraces innovation, integration, and digitalization.

In response to these challenges, our research endeavors have been focused on pioneering an integrated approach to vessel design, leveraging cutting-edge multidisciplinary analysis techniques and digitalization tools to optimize performance while maintaining safety and reliability standards. This paper presents the culmination of our efforts, highlighting the transformative potential of our approach through the lens of a fast search and rescue vessel.

Traditional vessel design processes often rely on fragmented workflows, where different aspects such as hydrodynamics, propulsion, structures, and safety are addressed independently. This compartmentalized approach can lead to suboptimal solutions, as interactions between various components are not fully considered during the design phase. Moreover, the reliance on physical prototypes and testing can be time-consuming and cost-prohibitive, limiting the exploration of design alternatives and hindering innovation. In contrast, our integrated approach seeks to break down disciplinary silos and harness the power of digital tools to create a cohesive design environment. Central to this methodology is the utilization of Computer-Aided Engineering (CAE) software, which enables the simulation of complex interactions between different subsystems and facilitates rapid iteration and optimization of design solutions. By incorporating advanced simulation techniques such as Computational Fluid Dynamics (CFD), Finite Element Analysis (FEA), and multibody dynamics, it is feasible to gain insights into the performance of the vessel across various operating conditions with unprecedented accuracy.

A fast search and rescue vessel serves as case study to illustrate the efficacy of our approach. In the design of such a vessel, Fig.1, high-speed manoeuvrability, stability in rough seas, and crew safety are paramount. By leveraging integrated multidisciplinary analysis, it is possible to evaluate systematically the impact of design decisions on these key performance metrics. For instance, CFD simulations can be used to optimize the hull form and appendages for minimum resistance and maximum maneuverability, while FEA helps ensure structural integrity under dynamic loads.



Fig.1: Design of a Search and Rescue Vessel. Engineered to be fast and safe…because every second counts when saving lives.

Furthermore, digitalization plays a crucial role in streamlining the design process and facilitating collaboration among stakeholders. Virtual prototyping allows designers to explore a wide range of design alternatives quickly, while digital twin technologies enable real-time monitoring and optimization of vessel performance throughout its lifecycle. By embracing digitalization, it is possible to accelerate the pace of innovation and adaptability in the maritime industry, ultimately leading to more efficient, safer, and environmentally sustainable vessels.

The integrated multidisciplinary analysis and digitalization approach presented in this paper represent a significant departure from traditional vessel design methodologies. By embracing innovation and leveraging advanced digital tools, it is viable to unlock new possibilities for enhancing vessel performance while meeting the evolving demands of maritime operations. The fast search and rescue vessel serves as a tangible example of the transformative potential of this approach, paving the way for a new era of maritime engineering excellence.

2. Integrated Multidisciplinary Analysis

Central to our innovative approach is the integration of multidisciplinary analysis throughout the vessel design process. Traditionally, vessel design has been compartmentalized into distinct disciplines such as hydrodynamics, structural engineering, propulsion, and safety analysis. However, this siloed approach often leads to suboptimal designs, as the interactions between different subsystems are not fully accounted for.

In contrast, our methodology employs a holistic approach, where various aspects of vessel performance are analyzed concurrently using advanced simulation tools and techniques. By integrating hydrodynamic analysis, structural analysis, propulsion system design, and safety assessment within a unified digital environment, it is achievable to capture the complex interdependencies between different design parameters and optimize the overall performance of the vessel.

Hydrodynamic analysis forms the cornerstone of our integrated approach, as it provides crucial insights for hull and appendages. Using CFD simulations, it is practicable to predict accurately hydrodynamic forces such as resistance, wave-induced motions, and maneuvering performance under different operating conditions. This allows us to optimize the hull form including appendages for maximum performance, ensuring that the vessel performs optimally across a range of sea states.

Simultaneously, structural analysis plays a vital role in ensuring the integrity and safety of the vessel´s hull and superstructure. FEA techniques are employed to evaluate the structural response to various

loads, including wave-induced loads. By iteratively refining the structural design based on FEA results, it is reasonable to minimize weight while ensuring a good margin of safety, thereby improving performance, and reducing construction costs.

Propulsion system design is another critical aspect that is integrated into our methodology from the outset. By considering the interaction between the hull, propulsion system, and hydrodynamic forces, it is realistic to optimize the selection and configuration of propulsion components such as engines, propellers, and waterjets. Through advanced simulation techniques, it is practicable to evaluate the performance of different propulsion configurations and identify the most optimal solution for the vessel´s intended mission profile.

Safety assessment is also paramount in our integrated approach, as the protection of crew and passengers is of utmost importance in maritime operations. Using virtual testing and analysis tools, it is workable to assess the vessel´s response to various safety scenarios, including collision, grounding, and capsize events. By incorporating advanced occupant safety features and emergency response protocols into the design, it is sufficient to mitigate risks and ensure compliance with regulatory requirements.

The integration of multidisciplinary analysis within a unified digital environment enables us to overcome the limitations of traditional design methodologies and achieve superior vessel performance. By considering the holistic interactions between hydrodynamics, structures, propulsion, and safety, it is possible to optimize the design process, reduce development time and costs, and ultimately deliver vessels that are safer, more efficient, and more capable of meeting the demands of modern maritime operations.

3. Digitalization as the Cornerstone

At the heart of our integrated approach lies digitalization, which serves as the cornerstone for transforming the vessel design process. Digitalization encompasses the use of advanced computational tools, simulation techniques, and data-driven methodologies to streamline the design, analysis, and optimization of marine vessels.

By leveraging digitalization technologies such as *Automated Design Exploration*, it is viable to iterate rapidly through design concepts, explore a wide range of design alternatives, and assess their performance characteristics with unprecedented accuracy and efficiency. This not only accelerates the design process but also enables us to identify and mitigate potential design flaws early in the development cycle, reducing costly design iterations and enhancing overall design quality.

One of the key advantages of digitalization is its ability to facilitate seamless collaboration and communication among interdisciplinary teams involved in the vessel design process. Through digital platforms and virtual design environments, engineers, naval architects, and other stakeholders can collaborate in real-time, share design data, and exchange feedback, regardless of their geographical locations. This fosters greater innovation and creativity, as diverse perspectives can be integrated into the design process, leading to more robust and optimized solutions.

Furthermore, digitalization enables the integration of data-driven methodologies and machine learning algorithms into the design process, allowing for predictive modeling, optimization, and decision support. By analyzing vast amounts of data collected from simulations, physical tests, and operational data, it is feasible to identify patterns, trends, and correlations that inform design decisions and improve performance predictions. This data-driven approach not only enhances the accuracy of our design models but also enables us to continuously learn and adapt, driving ongoing improvements in vessel performance and efficiency.

Virtual prototyping is another critical aspect of digitalization that revolutionizes the way vessels are designed and tested. By creating digital replicas or digital twins of physical prototypes, it is achievable

to simulate and evaluate the behavior of the vessel under various operating conditions, without the need for costly and time-consuming physical testing. This enables us to explore a wider range of design alternatives, optimize performance parameters, and validate design solutions more efficiently, ultimately accelerating the time-to-market for new vessel designs.

Digitalization fundamentally transforms the vessel design process by enabling rapid iteration, seamless collaboration, data-driven decision-making, and virtual prototyping. By harnessing the power of digital tools and methodologies, it is practicable to unlock new possibilities for innovation and optimization in maritime engineering, leading to safer, more efficient, and environmentally sustainable vessels that meet the evolving needs of the maritime industry.

4. Case Study: Fast Search and Rescue Vessel

To illustrate the transformative potential of our integrated approach, a case study is introduced focusing on the design and optimization of a fast search and rescue vessel. It is a roughly 9.75 m. The weight with a standard diesel powerplant is approximately 3,494 kg.

Search and rescue operations pose unique challenges for vessel design, requiring a delicate balance between speed, manoeuvrability, stability, and safety. Using an integrated multidisciplinary analysis framework, it is realistic to embarked on the design of a next-generation search and rescue vessel optimized for performance in diverse operating environments. Key aspects of the design process included:

- Marine Propulsion System Design: Leveraging advanced simulation techniques, the design of the vessel´s propulsion system is optimized, including the selection of waterjet propulsion technology to maximize speed and maneuverability while minimizing fuel consumption and emissions. By simulating the hydrodynamic performance of different propulsion configurations, it is adequate to identify the most efficient and effective solution for the vessel´s mission profile. Additionally, computational models of the propulsion system were integrated with overall vessel dynamics to ensure seamless integration and optimal performance across a range of operating conditions.
- Virtual Wave Tank Testing: Through virtual wave tank testing using CFD simulations, it is realisable to evaluate the vessel´s seakeeping performance under various sea conditions, ensuring superior stability and maneuverability for effective search and rescue operations. By simulating the interaction between the vessel and waves, it is meaningful to assess factors such as motion sickness, slamming loads, and overall ride comfort, optimizing hull form and appendage design to minimize wave-induced motions and maximize operational effectiveness.
- Structural Integrity Assessment: Utilizing FEA simulations, the structural integrity of the vessel´s hull and superstructure was assessed, ensuring compliance with regulatory standards and safety requirements while minimizing weight and material usage. By subjecting the digital model of the vessel to simulated loads and environmental conditions, it is possible to predict accurately stress distribution, deformation, and fatigue life, allowing us to optimize structural design parameters such as material selection, thickness, and reinforcement to achieve optimal strength-to-weight ratios and ensure long-term durability.
- Occupant Safety Evaluation: Employing advanced occupant safety analysis techniques, the vessel´s crashworthiness and crew survivability were evaluated in the event of a collision or capsize, incorporating features such as impact-absorbing structures and secure onboard systems. Through virtual crash simulations and human factors analysis, it is probable to assess the effectiveness of safety measures such as compartmentalization, seat restraints, and emergency egress pathways, ensuring the highest level of protection for crew and passengers in emergency situations.

By integrating these key aspects of design analysis within a unified digital environment, it is promising to optimize the performance, safety, and reliability of the fast search and rescue vessel, demonstrating

the transformative potential of our integrated approach in revolutionizing maritime engineering practices. This case study (workflow in Fig.2) serves as a testament to the power of multidisciplinary analysis and digitalization in addressing the complex challenges of vessel design and ensuring the success of critical maritime operations. So, the main outcomes of this case study have been:

- Identify how to efficiently share data between both internal and external colleagues.
- Designing a propulsion system.
- Validating the propulsion system through virtual sea trials in both calm water and waves.
- Looking at a strength assessment and then optimizing the hull structures for weight.
- As well as looking a passenger safety on real human models.

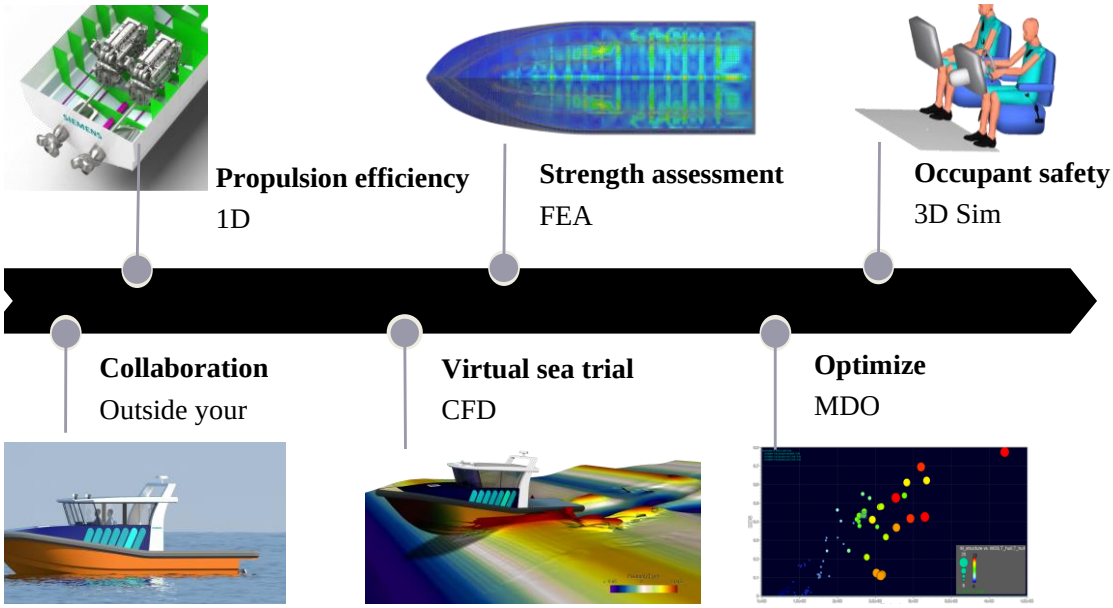


Fig.2: Design of a fast and safe planning Search & Rescue vessel

Electrifying a watercraft involves a meticulous process that integrates advanced technologies and careful analysis to ensure optimal performance and efficiency. Let us delve into the key steps and technologies involved in electrifying a vessel.

- Initial Analysis using CFD: The process begins with determining the estimated power requirements by analyzing the hull using a CFD tool such as Simcenter STAR-CCM+. This tool helps in understanding the hydrodynamic behavior of the vessel, including resistance, and flow patterns, which are crucial for estimating power needs.
- Integration with system simulation: Utilizing the data from CFD analysis, Simcenter Amesim, a 1D systems tool, comes into play. This tool helps in integrating various components of the propulsion system, such as motors, batteries, and power electronics, to determine absorbed power and overall efficiency. By simulating the system in a virtual environment, engineers can optimize the configuration for maximum performance and energy efficiency.
- Selection of Off-the-Shelf Components: Based on the absorbed power and mission profiles, off-the-shelf solutions for propulsion systems, battery packs, and other components are evaluated. This involves determining the appropriate sizing of battery packs and power requirements to meet the vessel´s operational needs while considering factors like weight, space constraints, and cost.
- Validation and Iterative Analysis: After selecting components, the initial powering estimation is revalidated by running CFD analyses with updated weight configurations. This iterative process ensures that the chosen propulsion system and battery pack sizing align with the vessel´s requirements. Simcenter Amesim is used to validate the range and performance of the electrified watercraft under various operating conditions.

- Designing Customized Components: In cases, where off-the-shelf solutions may not fully meet the requirements, designing customized components becomes necessary. Tools are available to design high-fidelity battery packs and electric motors tailored to the specific needs of the watercraft. This involves optimizing parameters such as energy density, power output, and thermal management to achieve the desired performance and reliability.

The key technologies and challenges involved are:

- Battery Technology: Selecting the right battery technology is crucial for electric propulsion systems. Factors such as energy density, weight, charging time, and lifespan need to be considered to ensure sufficient power and range for the watercraft.
- Electric Motors: Efficient electric motors are essential for converting electrical energy into mechanical propulsion. Designing motors with optimal power-to-weight ratios and torque characteristics is critical for achieving high performance and responsiveness.
- Integration and Optimization: Integrating various components of the electrified propulsion system and optimizing their interactions pose significant challenges. Balancing factors like power distribution, thermal management, and system efficiency requires advanced modeling and simulation tools.
- Range and Endurance: Ensuring adequate range and endurance for the watercraft under different operating conditions is a key consideration. Optimizing the energy management system and battery pack sizing is essential to meet the vessel´s mission requirements while maintaining reliability and safety.

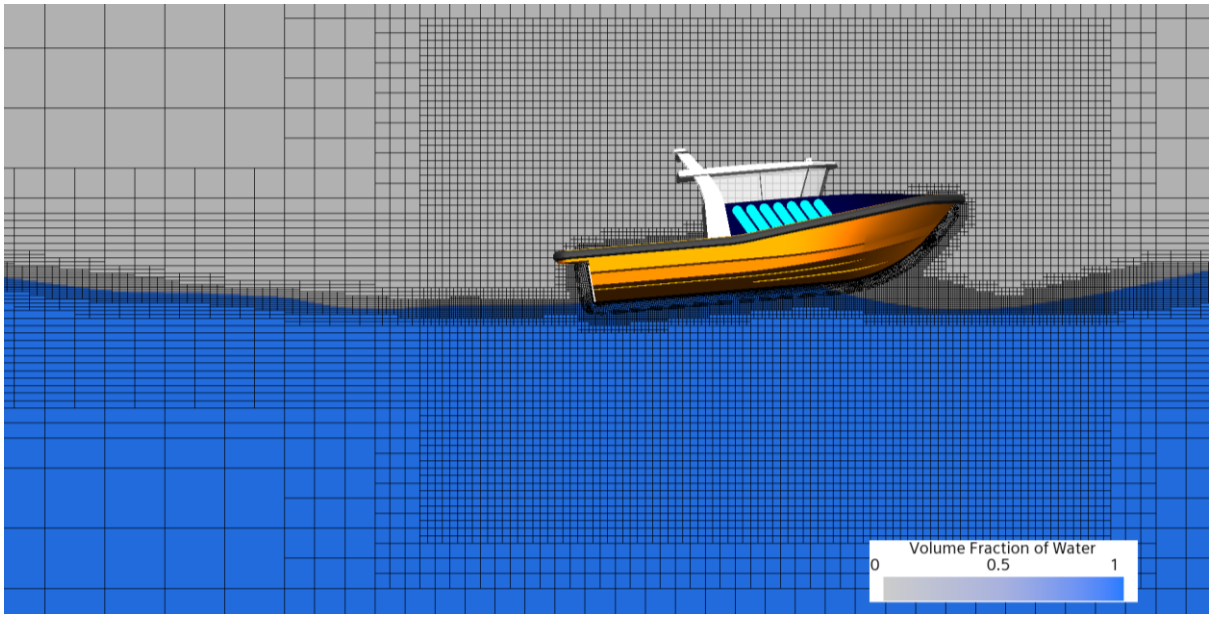


Fig.3: Virtual Towing Tank using Simcenter STAR-CCM+

The first crucial step, following the creation of a CAD model, involves employing our cutting-edge virtual Towing Tank approach using Simcenter STAR-CCM+, Fig.3, a powerful multi-physics CFD solver tailored for marine applications. There were harnessed a suite of tools to meticulously model the intricate physics of marine hydrodynamics. This includes the capability to accurately capture phenomena such as the free surface or the air-water interface, as well as dynamic vessel motions during propulsion. Whether it´s simulating waves, manoeuvring, self-propulsion, or calm water resistance, or any combination thereof.

Furthermore, there were a complete parameterization of key inputs such as weight, centre of mass, speed, and even hull geometry. This allows for iterative simulations with varying inputs to assess their impact on performance and effortlessly generate resistance or powering versus speed curves. Such

parametric analysis enables engineers to fine-tune design parameters and optimize the vessel´s performance efficiently.

The flexibility provided by Simcenter STAR-CCM+ allows for seamless design exploration through parameterization and easy updating of simulations. Using a bi-directional connectivity between the simulation and the CAD model, in this case Siemens NX, simulations can be swiftly adjusted to explore various design scenarios.

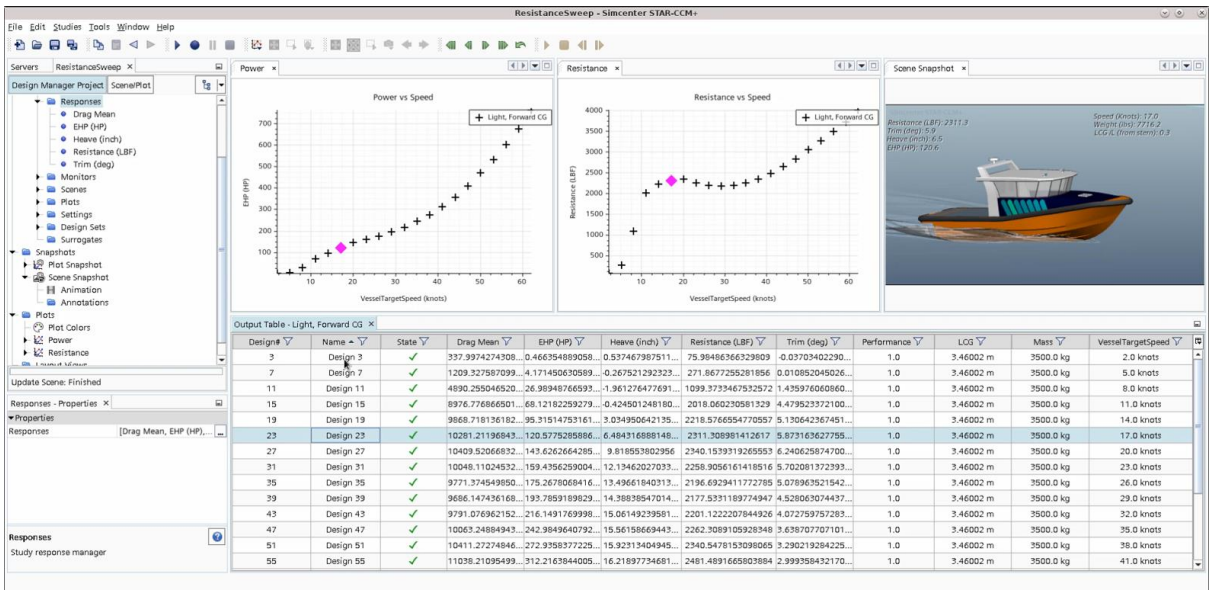


Fig.4: Virtual Towing Tank Design Manager Post Processing, showing power and resistance vs. speed curve for a single design and operating condition

Here´s how it is plausible to generate power and resistance vs. speed curve for our existing vessel using Simcenter STAR-CCM+, Fig.4:

- Parameterization and Simulation Setup: The first step is to define key parameters within the simulation environment. This allows for easy adjustment of inputs to explore different design configurations. To get the power and resistance vs. speed curve for our *existing* vessel we only need to update the value for our speed parameter. But since the simulation setup also have parameters for the weight and centre of mass, we could analyse powering and resistance characteristics under various operating conditions, e.g., different drafts.
- Design Exploration: The key for automated design exploration is the ability to easily update parameters within the simulation. Besides operating conditions like speed and mass these also includes modifications to hull geometry, so we can investigate changes in any aspect of the vessel design.
- Generating Power and Resistance Curves: Simulations are run for each design iteration to generate power and resistance data at different speeds. By varying parameters and running multiple simulations, we can create comprehensive curves illustrating the relationship between power requirements, resistance, and vessel speed.
- Data Analysis and Assessment: Once all simulations are completed, we have instant access to the required data. We can analyze individual design points to assess their performance characteristics, including power consumption and resistance. This allows us to identify optimal design configurations based on specific criteria such as efficiency, speed, or range.
- Exporting Results for Propulsion System Design: The powering estimates obtained from simulations are exported into tables for further analysis and integration into the propulsion system design process. This data serves as valuable input for selecting components such as motors, batteries, and propellers, ensuring they meet the vessel´s performance requirements.

This paper facilitates a streamlined process for generating power and resistance curves, allowing for efficient design exploration and optimization of vessel performance. Parameterization and simulation capabilities enable rapid iteration and data-driven decision-making in the electrification of watercraft.

The resistance data obtained from simulations developing a system-level model to assess energy losses within the entire propulsion system, working seamlessly integrating sea states, vessel performance, and different propulsion systems, allowing to quickly evaluate absorbed power and energy efficiency.

The first step involved importing the ship model. With CFD data it is possible enhance the accuracy of the model by incorporating the resistance data obtained from simulations. For this paper, it was considered calm water conditions. The propulsion system, including the propeller model, was integrated into the simulation.

The simulation allowed for the variation of propeller rotation rates to study their impact on vessel speed and energy consumption. By adjusting the rotation rates, it was possible to analyse the performance of different propulsion configurations and optimize for efficiency.

As the rotation rate of the propellers is varied, it was calculated the corresponding vessel speed based on the resistance characteristics of the ship model and the applied propulsion system. This provided insights into how changes in propulsion parameters affect the overall performance of the watercraft.

Using the developed model, the absorbed power within the drive train was computed, considering energy losses and inefficiencies. This absorbed power represents the actual power required to propel the vessel under specific operating conditions and serves as a critical metric for performance evaluation.

The simulation ran quickly, allowing rapid exploration of different propulsion system configurations and operating scenarios. Engineers could iteratively adjust parameters and evaluate the impact on absorbed power and vessel performance, facilitating decision-making in the design process, Fig.5.

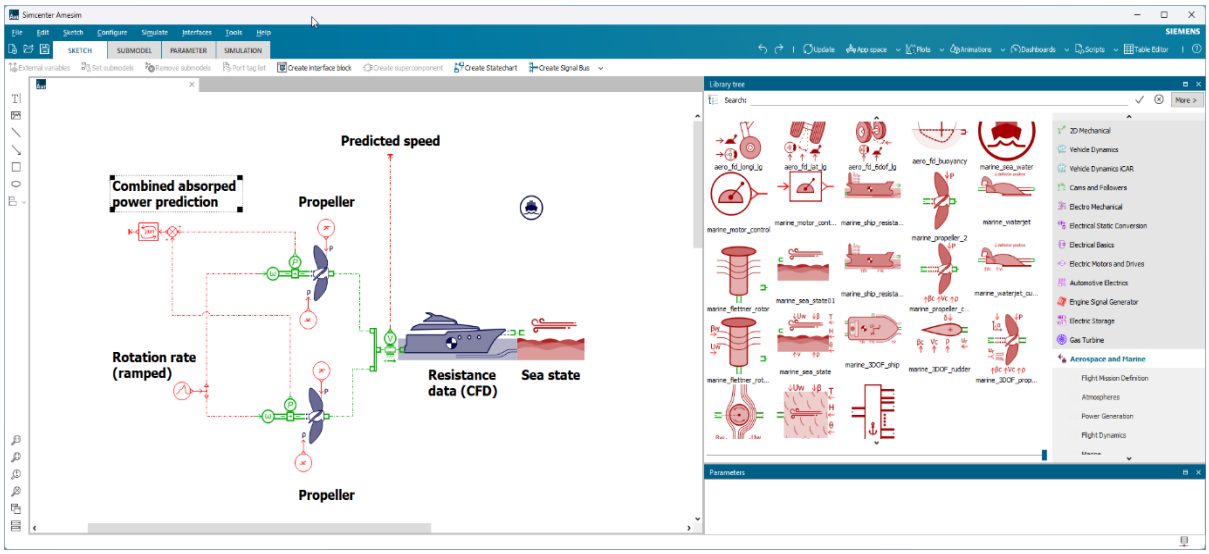


Fig.5: Propulsion efficiency

The seamless integration of sea states, vessel dynamics, and propulsion components allows comprehensive analysis and rapid iteration towards achieving energy-efficient marine propulsion systems. It explored alternative propulsor options, Fig.6. For instance, swapping traditional propellers for waterjets allows us to compare their respective efficiencies and performance characteristics.

- Efficient Simulation: By substituting propellers with waterjets, we can assess how each option impacts vessel performance and energy efficiency.

- Propulsor Comparison: The simulation results reveal distinct differences between traditional propellers and waterjets. Traditional propellers demonstrate higher efficiency at slower speeds, whereas waterjets excel at higher speeds, as anticipated. This comparison provides valuable insights into the most suitable propulsor option based on the vessel´s intended operating speed range.
- Optimal Speed Considerations: Analyzing the powering requirements across different speeds unveils important trends. We observed relatively low changes in power between 20-40 kn, followed by a significant increase in powering requirements as we approach 60 kn. Notably, there is a substantial power saving of almost 150 HP at 40 kn compared to higher speeds (compared to a conventional propeller). This suggests that aiming for a cruising speed below 40 kn may be ideal for maximizing efficiency while balancing performance.
- Efficiency-driven Design Decisions: In electric craft design, efficiency is paramount, and it was made informed decisions that optimize performance. By swiftly assessing how various design choices affect efficiency and power consumption, we can refine our design to meet performance targets while maximizing energy efficiency.

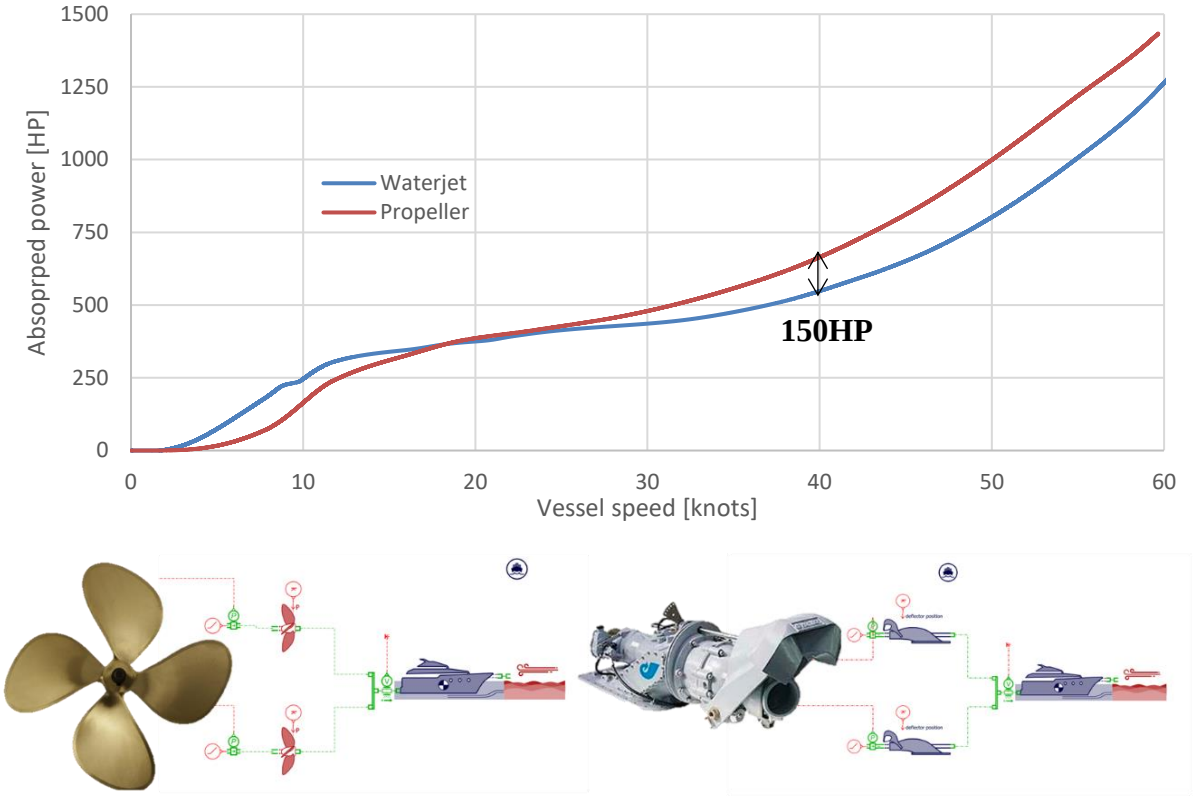


Fig.6: Comparison of propulsive power

Rapid simulation capabilities enabled us to evaluate alternative propulsor options, understand their performance characteristics, and make efficiency-driven design decisions. This iterative process ensures that our electric watercraft is optimized for performance, efficiency, and sustainability, aligning with the goals of electrification in marine transportation.

Once we determined the most suitable propulsor for our electric watercraft, the next step is to analyze various configurations to determine the appropriate battery pack sizing, Fig.7. This involves expanding on the existing simulation model to incorporate electric motors, gear ratios, and electro-chemistry models to accurately convert electrical energy into power. Here´s how we approach this process:

- Integration of Electric Motors: Electric motors, sized at 250 kW (335 HP) each based on propulsion analysis, are integrated into the simulation model. These motors serve as the primary

propulsion system, driving the watercraft forward.

- Investigation of Gear Ratios: Different gear ratios are applied to explore how various couplings affect the powering of the vessel. This allows us to optimize the transmission system for maximum efficiency and performance.
- Electro-Chemistry Models: Simple electro-chemistry models are employed to convert electrical energy from the battery pack into power for the electric motors. These models consider factors such as voltage, current, and energy consumption to accurately simulate the behavior of the battery system.
- Voltage Supply Variation: To understand the impact of different voltages on performance metrics like peak amps and energy consumption, simulations are conducted with varying constant voltage supplies. This analysis helps in selecting an optimal voltage level for the battery system.
- Mission Profile Integration: The calculations are tailored to the specific mission profile of the watercraft. By inputting parameters such as desired speeds and operating durations, a Proportional-Integral (PI) controller regulates the motor speeds accordingly. This ensures that the watercraft operates efficiently under different operating conditions.
- Battery Pack Sizing: Based on the given mission profile and power requirements, the total battery pack size is calculated. This calculation considers factors such as energy consumption, desired range, and operational constraints to determine the optimal battery capacity for the watercraft.

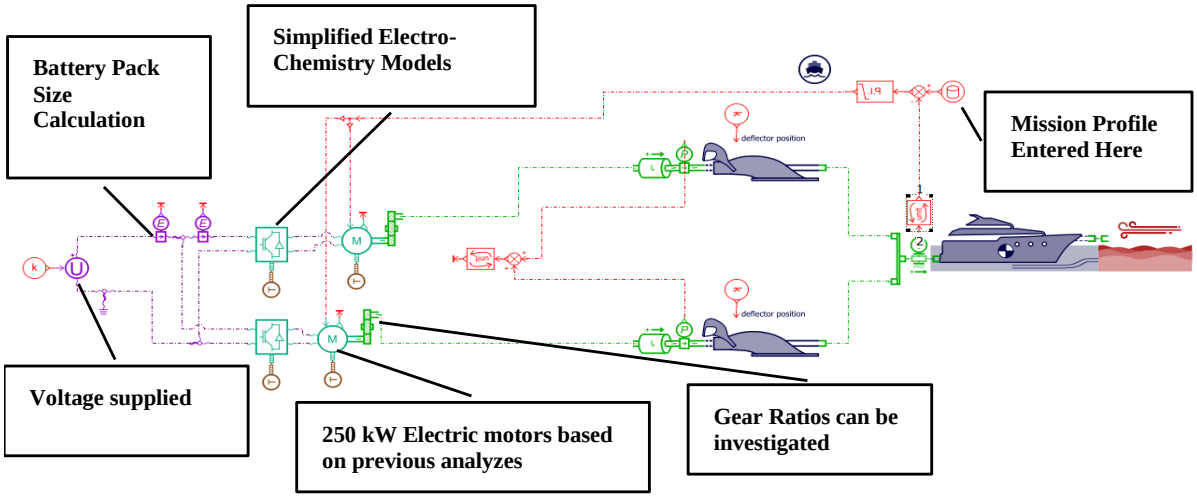


Fig.7: Battery pack sizing

By iteratively adjusting parameters (automatically) and analysing simulation results, we can derive an optimal battery pack sizing to meet the performance and efficiency requirements of the electric watercraft. This comprehensive approach ensures that the vessel is equipped with an appropriately sized battery pack to support its mission profile while maximizing energy efficiency and range.

Once a suitable propulsor is chosen, the next step is to determine the battery pack sizing by examining various configurations:

- Model Expansion: Incorporating the full propulsion system, by including electric motors, gear ratios, and electro-chemistry models for converting electrical energy into power, the initial model has been enhanced adequately.
- Gear Ratio Analysis: Different gear ratios are applied to investigate how various couplings affect the powering of the vessel. This allows us to optimize the drivetrain configuration for efficiency and performance.
- Voltage Variation Analysis: Simple electro-chemistry models are used to study how different voltage levels affect performance metrics such as peak amps and energy consumption. By

varying the voltage supply, we can assess the impact on overall system efficiency and battery utilization.

- Mission Profile Integration: We input a proposed mission profile into the model, specifying cruising speeds, durations, and periods of idle operation. For example, a typical mission profile might involve cruising at top speed for half an hour, near hump speed for another half hour, and at intermediate speed for half hour, while running idle for the remainder of the time, Fig.8.

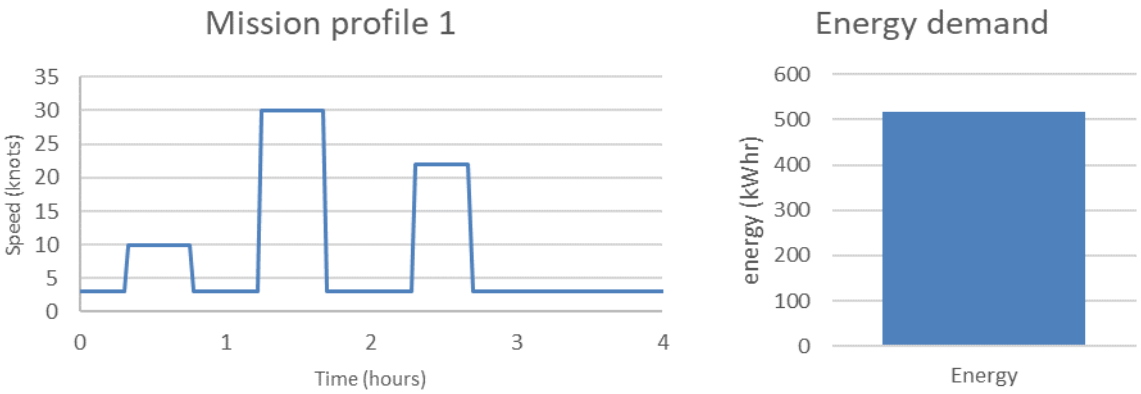


Fig.8: What battery is required for a specific mission profile?

- Battery Pack Sizing: Based on the specified mission profile, the model calculates the total energy consumption and determines the required battery pack size. For instance, if the proposed mission requires just over 500 kWh of energy, we can size the batteries to be 600 kWh. This ensures sufficient energy reserves for the specified operation, Fig.8.

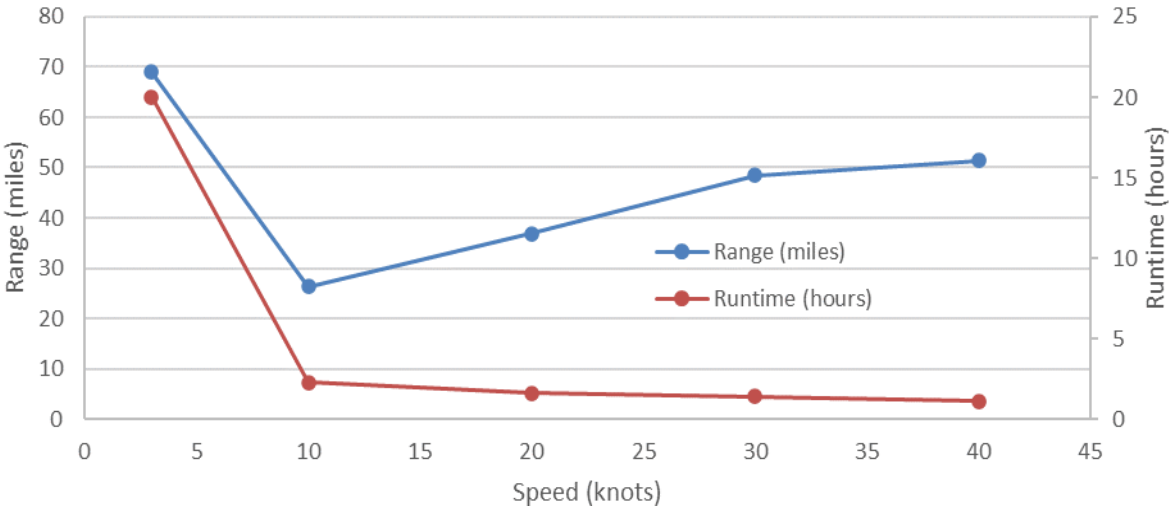


Fig.9: How far and long can the vessel run at various speeds?

- Range and Run Time Analysis: Using the model, we can analyze the range and run time of the vessel at constant speeds with the determined battery pack size. The simulation outputs provide insights into the vessel´s performance characteristics, including the distance it can cover at various speeds and the duration it can operate on a single charge, Fig.9.
- Operational Considerations: The analysis also considers operational factors such as idle speed capabilities and emergency return to port scenarios. For example, the simulation might show that the vessel can operate for over 20 h at idle speed, providing important insights for design considerations and operational planning, Fig.9.

By integrating mission profiles and evaluating different configurations, Fig.8, designers can optimize the electrification of watercraft for efficiency, range, and operational flexibility.

Once the battery pack sizing requirements are determined, the next step is to package it within a CAD program to obtain weight estimates and new Longitudinal Centre of Gravity (LCG) values. This information is crucial for updating the resistance vs. power curves to account for changes in vessel weight and balance.

- CAD Packaging: The battery pack sizing data is integrated into the CAD model of the watercraft. Using the CAD program, we can accurately position and dimension the battery pack within the vessel´s structure to obtain realistic weight estimates and determine the new LCG.
- Updating Parameters: With the revised weight and LCG values, the simulation model is updated accordingly. This includes adjusting parameters to reflect the changes in vessel configuration due to the added weight of the battery pack.
- Identifying Stability Issues: The simulation results may reveal differences in behavior between loading configurations, indicating potential stability issues. For example, a rearward CG configuration may exhibit dynamic instability, leading to concerns about vessel safety and performance.
- Regenerating Power and Resistance Curves: The simulation is rerun with the updated parameters to regenerate the power and resistance curves. The increased weight from the added battery pack will result in a higher powering requirement, affecting the performance characteristics of the watercraft.
- Insight into Dynamic Behaviour: In addition to static performance changes, the simulation provides insights into the dynamic behaviour of the vessel. By analysing the transient history of metrics obtained from CFD runs, such as trim angle and dynamic forces, we can identify potential dynamic instabilities caused by changes in weight distribution, particularly the LCG.
- Iterative Analysis and Design Optimization: The simulation allows iterative analysis and design optimization to address stability issues and ensure the safe and efficient operation of the electrified watercraft. By adjusting parameters and configurations, engineers can mitigate stability concerns while maximizing performance and efficiency. They key for automated design exploration is a seamless connection between the CAD model and the different simulation tools.

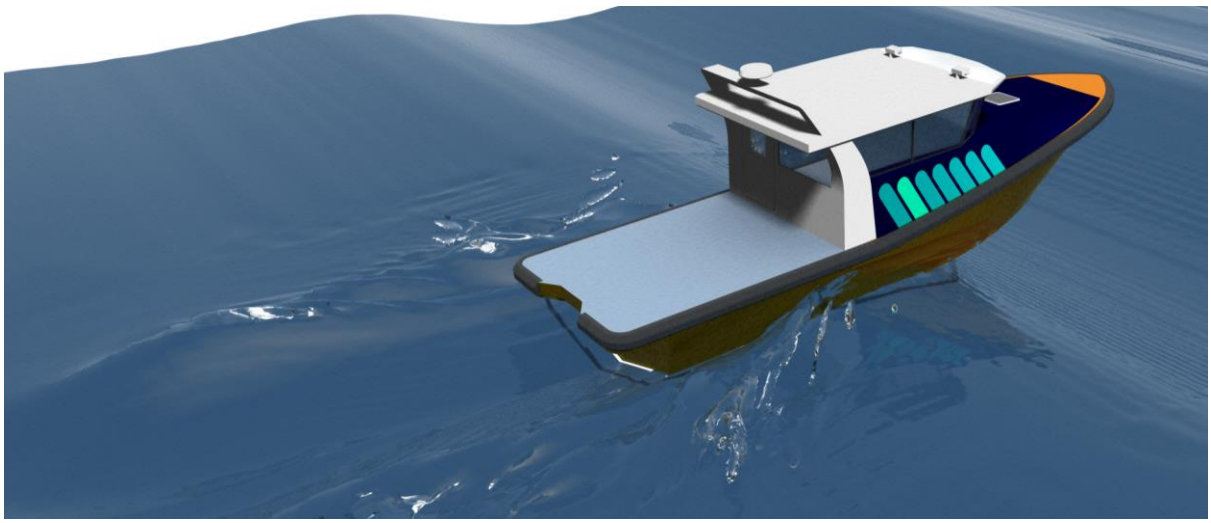


Fig.10: Revalidating Virtual Sea Trial

Integrating battery pack sizing data into the CAD model and incorporating the propulsion system within the CFD simulation using a Functional Mock-Up (FMU) interface allow for a comprehensive assessment of the watercraft´s performance and stability. By leveraging simulation tools, Fig.10., designers can optimize the electrification process while ensuring the safety and reliability of the vessel in real-world operating conditions.

In Fig.10, a sea trial was performed with CFD of the vessel with incorporated power train (FMU) where the vessel accelerates from rest with full power and will encounter waves after 40 s. Again, the full 1D

marine propulsion is included and hence thrust is modelled as two force vectors at the corresponding location of the waterjet, but no detailed water jet was modelled. It is feasible to see that 40 kn are achieved within 15.6 s and the top speed is 48.2 kn. It is also possible to visualize that the vessel slows down while moving in waves, Fig.11. In this case the full vessel including the waterjet propulsion comes out of the water while jumping on the waves hence no thrust is generated.

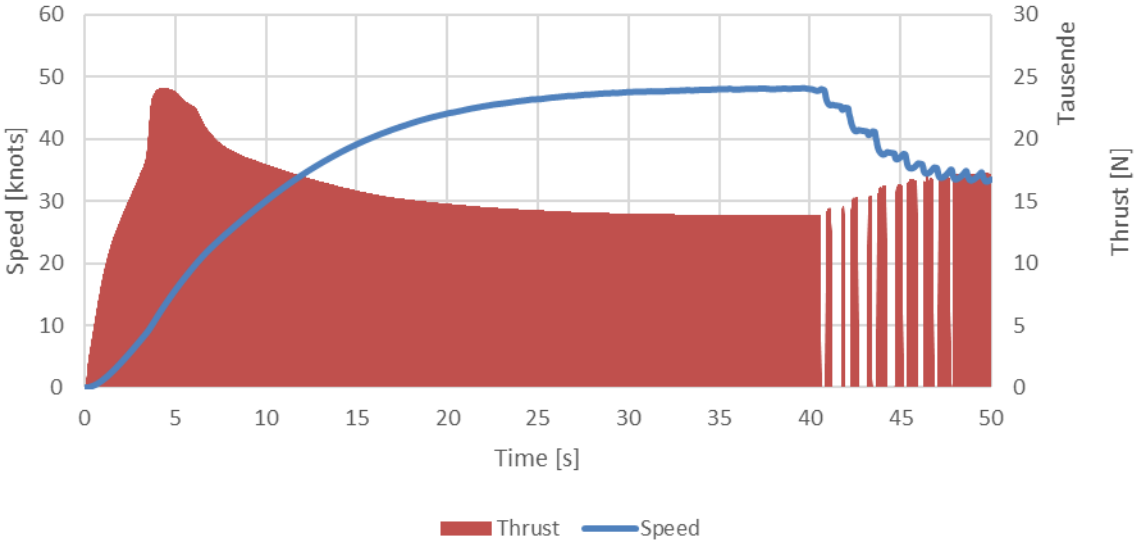


Fig.11: Revalidating Virtual Sea Trial

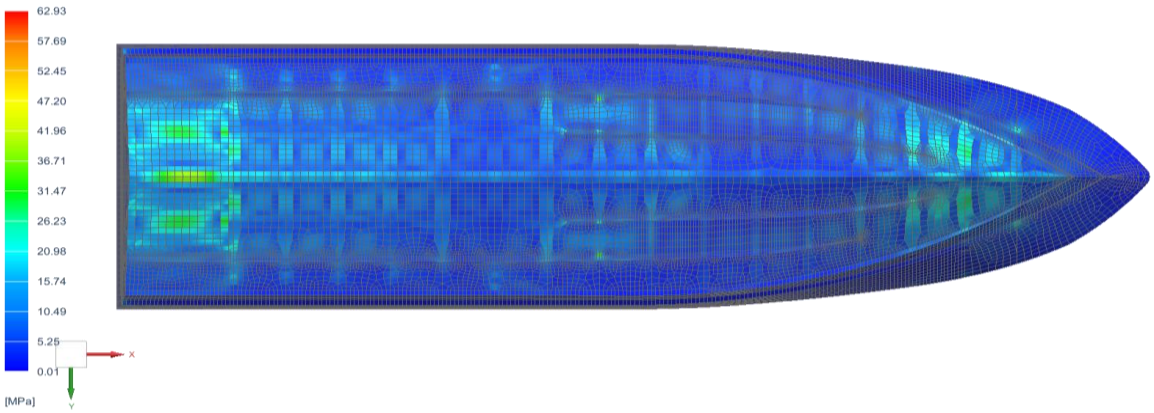


Fig. 12. Maximum stress from sea trial

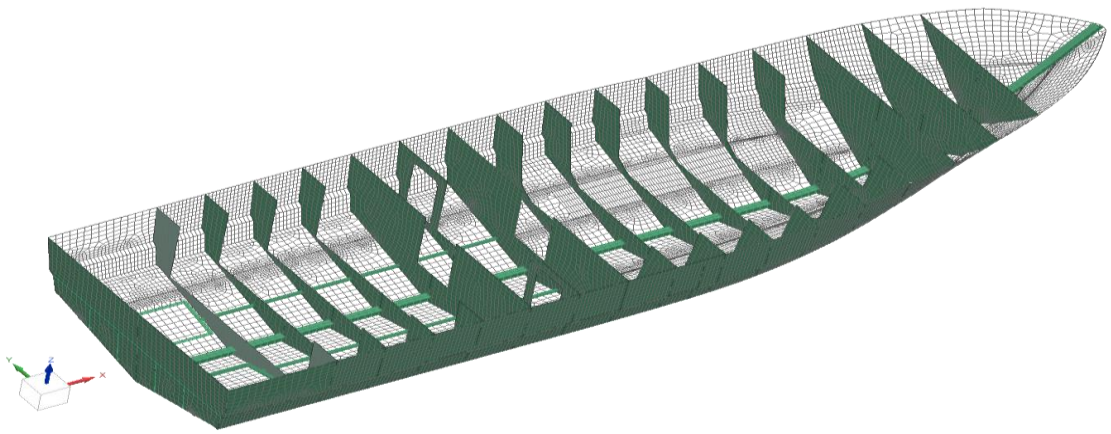


Fig.13: Structural model

Fig.12 shows that CFD can map the impact of the waves to our structural model, Fig.13, consisting of shell and beam elements and do a strength assessment.

To illustrate the power of automated design exploration a quick mass optimisation of the hull structure was performed. The objective is to minimize the mass while keeping a positive margin of safety by modifying 29 geometric parameters for the thickness of hull and plates and the geometry of the stiffeners. The study was run on a simple laptop taking less than 2 days to run 150 designs. HEEDS is used for the design exploration. HEEDS contains a unique search strategy called. SHERPA, which stands for Simultaneous Hybrid. Exploration that is Robust, Progressive and Adaptive. During a single search, SHERPA uses multiple search methods simultaneously (not sequentially). This approach takes advantage of the best attributes of each method and reduces a method´s participation in the search if/when it is determined to be ineffective. Therefore, even though we had 29 variables it was able to achieve quite a significant performance increase within 150 design iterations.



Fig.14: HEEDS is used for the design exploration

The resulting accelerations from the CFD simulation when the vessel is in waves are used to simulate the dynamics of an occupant. To model the occupant, a co-called active human model was used, Fig.15.

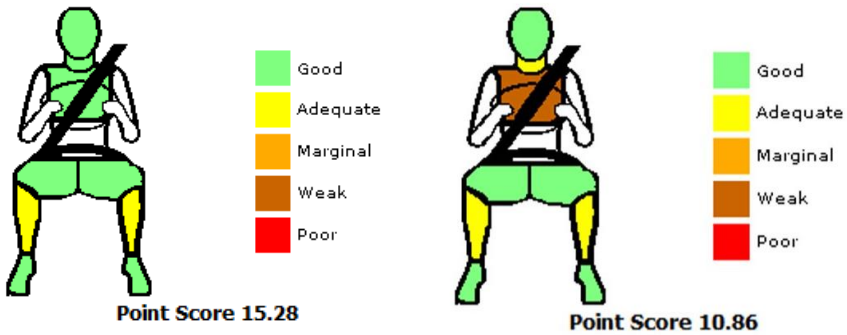


Fig.15: Passenger right, driver left

In contrast to a passive behaviour, where no stabilization occurs and the model behaves as an unconscious human or Post-Mortem Human Subject (PMHS), a (re)active behaviour model stabilizes to its initial posture or moves to a user-defined position as an aware human would do. The active human model delivers dynamic data (forces and moments) of head, neck, chest, spine, femur, and tibias. Injury values calculated based on the dynamic loadings and definitions of the safety protocols in the industry. The point score below is based on the rather violent jumping on the waves and evaluated for the Frontal impact Euro NCAP, which is an automotive standard. The lifeboat standard would be a better set of criteria, but it does not generate this kind of pictures that everybody knows. Although the motions look

harsh there is no hard hit on critical parts. The seats have quite some energy absorption to get still some more descent kinematics. Something not evaluated by this Frontal impact Euro *NCAP* score are whiplash injuries, which might be more relevant in this case. Maybe a four-point belt would be better, and simulation can easily investigate these options and optimize for occupant safety.

5. Results and Discussion

The integration of cutting-edge multidisciplinary analysis and digitalization techniques yielded significant improvements in the design performance of the fast search and rescue vessel. By optimizing the vessel´s propulsion system, hull form, and structural configuration, we were able to achieve superior speed, maneuverability, stability, and safety characteristics compared to conventional designs.

The propulsion system optimization was a key aspect of our approach, where we utilized advanced simulation tools to fine-tune the selection of waterjet propulsion technology. Through detailed computational models, we assessed the performance of different propulsion configurations, considering factors such as thrust efficiency. This optimization process resulted in a propulsion system that not only maximized speed but also minimized fuel consumption and emissions, enhancing the vessel´s operational efficiency and environmental sustainability.

In addition to propulsion system optimization, our integrated approach enabled us to refine the hull form and appendage design to further enhance vessel performance. Using CFD simulations, we could analyze the hydrodynamic behavior of the vessel and optimize hull shape, keel design, and appendage placement to minimize drag and wave resistance. This led to improved speed, maneuverability, and seakeeping performance, allowing the vessel to operate effectively in a wide range of sea conditions while maintaining stability and comfort for crew and passengers.

Structural optimization was another critical aspect of our design process, where FEA simulations were used to assess the structural integrity of the vessel´s hull and superstructure. By subjecting the digital model to simulated loads and environmental conditions, we could identify potential areas of stress concentration, deformation, and fatigue, allowing us to optimize structural design parameters for maximum strength and durability. This resulted in a lightweight yet robust structure that met stringent safety standards and regulatory requirements, ensuring the vessel´s long-term reliability and seaworthiness.

Furthermore, the use of advanced simulation tools enabled us to explore a wider design space, identify innovative design solutions, and validate design performance with a high degree of confidence. This iterative design process allowed us to quickly iterate through design alternatives, assess their performance characteristics, and make informed decisions based on simulation results. As a result, we were able to significantly reduce design cycle times and development costs while enhancing the overall effectiveness and reliability of the vessel for search and rescue missions.

In summary, the integration of multidisciplinary analysis and digitalization techniques enabled us to push the boundaries of vessel design, achieving unprecedented levels of performance, efficiency, and safety for the fast search and rescue vessel. By leveraging advanced simulation tools and methodologies, we were able to optimize every aspect of the design process, from propulsion system selection to structural configuration, resulting in a vessel that sets new standards for excellence in maritime engineering.

6. Conclusion

In conclusion, this paper has presented an innovative approach to vessel design that leverages integrated multidisciplinary analysis and digitalization for enhanced performance. Through the integration of advanced simulation techniques and digitalization tools, we have demonstrated the transformative potential of our approach in optimizing the design of marine vessels for diverse operational requirements.

By adopting a holistic approach to vessel design and embracing digitalization as the cornerstone of our methodology, we have been able to achieve significant improvements in vessel performance, efficiency, and safety. Our integrated approach breaks down traditional disciplinary silos and allows for a comprehensive understanding of the complex interactions between different aspects of vessel design. This holistic perspective enables us to optimize design decisions across multiple domains simultaneously, resulting in synergistic improvements in overall vessel performance.

The benefits of our integrated approach are evident across various stages of the design process. During the conceptual design phase, advanced simulation techniques allow for rapid exploration of design alternatives, enabling us to identify innovative solutions that may have been overlooked using conventional methods. Virtual prototyping and simulation-based optimization techniques facilitate iterative design refinement, ensuring that the final design meets or exceeds performance targets while minimizing development time and costs.

In addition to improving performance, our integrated approach also enhances safety and reliability. By incorporating advanced safety analysis techniques into the design process, we can systematically evaluate and mitigate risks associated with vessel operation, ensuring the highest standards of crew and passenger safety. Structural optimization techniques enable us to design vessels that are not only lightweight and efficient but also robust and resilient, capable of withstanding the harsh marine environment.

Looking ahead, we believe that our integrated approach will continue to drive innovation in the field of maritime engineering. As technology continues to evolve and computational capabilities expand, the possibilities for design optimization and performance enhancement are virtually limitless. We envision the development of next-generation vessels that push the boundaries of performance, sustainability, and safety, setting new standards for excellence in maritime engineering.

The seemless integration of multidisciplinary analysis and digitalization represents a paradigm shift in vessel design methodology, unlocking new possibilities for innovation and optimization. By embracing this integrated approach, we can create vessels that are not only more efficient and reliable but also safer and more environmentally sustainable, shaping the future of maritime transportation for generations to come.

Impact of Energy Saving Devices on EEXI and CII: Theory and Practice

Alessandro Castagna, Becker Marine Systems, Hamburg/Germany, aca@becker-marine-systems.com

Abstract

The EEXI and CII requirements challenge shipowners to achieve compliance. While current technologies may not offer substantial savings, a 5-10% improvement can prolong compliance until alternative fuels or new propulsion concepts (e.g. WASP) emerge. Energy Saving Devices (ESDs) like ducts and fins offer cost-effective solutions. Their installation results in a speed gain (at same power) leading to an increased V_{ref} for the EEXI calculation or a power saving (at same speed), which is reflected in fuel saving and consequently in an improved CII. Despite proven efficiency in CFD or model tests, scepticism persists among many shipowners. They argue that real-world variables such as data accuracy, weather conditions, hull condition, and crew awareness may adversely affect the performance of ESDs if not carefully considered and mitigated.

1. The regulatory Framework

The roadmap developed during the initial IMO strategy for the reduction of GHG emissions of ships, which was approved at MEPC 70, stated that the strategy adopted in 2018 would be reviewed and subsequently revised after 5 years. During the MEPC 80 session held in July 2023, the Revised IMO Strategy was officially adopted.

Compared to the initial approach, the revised strategy enhances the targets, aiming to achieve net-zero GHG emissions by or close to 2050. This is supported by two intermediate checkpoints: the first one based on a reduction in the total annual GHG emissions from international shipping by at least 20%, striving for 30% by 2030 compared to 2008, and the second one by at least 70%, striving for 80% by 2040 compared to 2008, Fig.1.

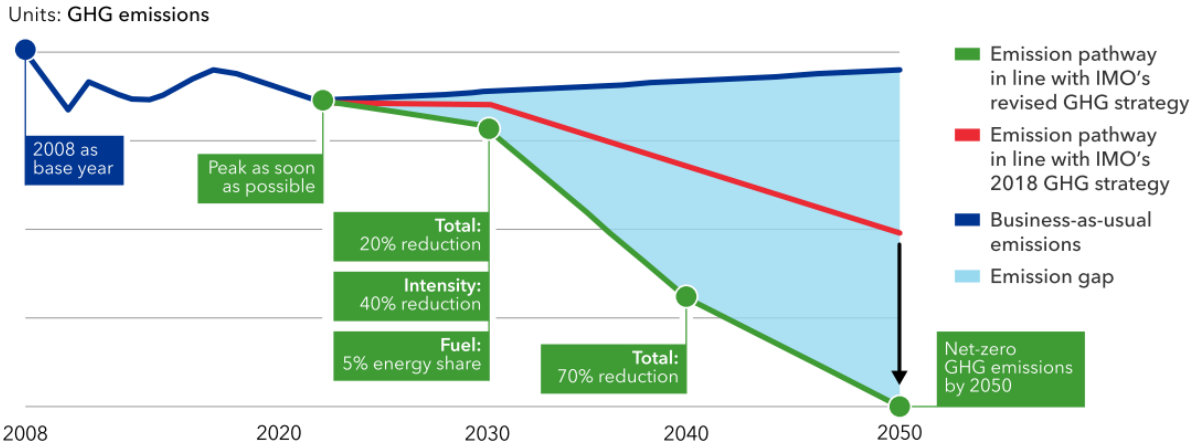


Fig.1: Revised IMO Strategy, *DNV (2023)*

The revised regulation represents a significant improvement over the IMO's initial GHG strategy, which aimed to cut GHG emissions by only 50% by 2050 and contained no absolute emissions reduction targets for the intermediate years.

While the focus has now shifted to the assessment (both technical and economical) of mid-term measures and related technologies, particularly alternative fuels and alternative propulsion concepts (e.g., WASP), the short-term measures introduced during MEPC 76 (Energy Efficiency eXisting Ship Index, EEXI, as a technical measure, and Carbon Intensity Indicator, CII, as operational measures) remain valid, as do the technologies associated with meeting these measures.

Additionally, during the MEPC 80 session, a discussion took place regarding the review of the effectiveness of the short-term measures, expected to be completed by January 1st, 2026.

The requirements for EEXI and CII are effective since January 1st, 2023. All ships of 400 GT and above are required to calculate their EEXI and implement technical measures to improve their energy efficiency. Additionally, all ships of 5,000 GT and above must calculate and report their CII, which correlates CO_2 emissions to the ship's capacity over the distance travelled. In 2024, ships will be rated (A, B, C, D, E, where A is the best) against a reference line and required reduction factors. Ships rated E or D for three consecutive years will have to implement a plan of corrective actions, demonstrating how the required index (C or above) would be achieved.

Shipowners have various options for complying with the EEXI and CII. The easiest way is probably to reduce speed by adopting either engine power limitation (EPL) or shaft power limitation (ShaPoLi). These techniques are mostly used on older ships because they require minimal changes to the ship and do not alter engine performance.

However, it's important to note that employing these techniques might compel many operators to significantly expand their fleets to meet the additional capacity demand that will arise. Consequently, not only does this potentially nullify the overall carbon savings, but it also results in a substantial increase in operational costs.

Furthermore, one should bear in mind that a ship must not reduce its engine power below the minimum propulsion power guidelines set by *IMO (2013a)* ensuring that the installed propulsion power remains sufficient to maintain the ship's manoeuvrability also in adverse conditions.

A good compromise, in terms of cost and efficiency gain, especially when neither EPL nor ShaPoli proves sufficient, is the installation of energy-saving devices (ESDs), also referred to as propulsion improving devices (PIDs). These devices are mainly intended for propulsion improvement or thrust augmentation.

Other technologies, such as alternative fuels, air lubrication, or employing the Wind-Assisted Ship Propulsion (WASP) concept, come with either high costs (due to retrofit installation, modification of existing systems, etc.) or substantial uncertainties (such as a lack of model tests or sea trial data). Ultimately, early retirement of the ship can also be taken into consideration.

2. Energy Saving Devices (ESDs)

Hydrodynamically based propulsion-improving devices are proven technologies that began proliferating in the 1980s when oil prices peaked following the 1970s energy crisis. These devices can be considered operating in three basic zones of the hull (see *Carlton (2019)* for more details): some are located before the propeller (zone 1), some at the propeller station (zone 2), and some after the propeller (zone 3).

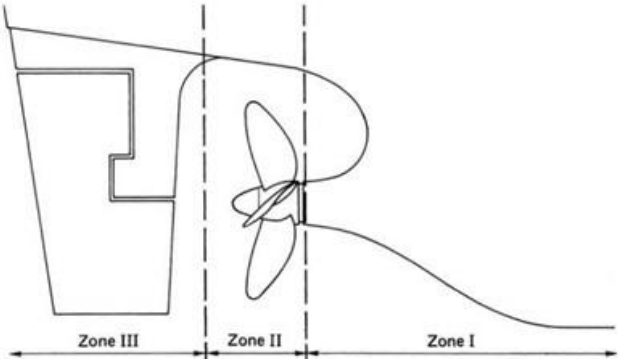


Fig.2: Zones for classification of propulsion improving devices, *Carlton (2019)*

In zone I, the ESD reacts with the final stages of the growth of the boundary layer over the stern of the ship. This is either to gain direct benefits from the boundary layer or to present the propeller with a more advantageous flow regime, and in some cases, perhaps both. Devices in zones II and III work within both the hull wake field and modifications to that wake field caused by the slipstream of the propeller. In this way, they attempt to recover energy that would be lost otherwise.

Well-known devices for reducing wake losses include the WED (Wake Equalizing Duct), *Schneekluth (1986),* and the SILD (Sumitomo Integrated Lammeren Duct), *Sasaki and Aono (1997).* Devices for reducing rotation losses include the SVA fin system, *Mewis and Peters (1986),* the Daewoo pre-swirl fin system, *Lee et al. (1992),* and the Hyundai Thrust Fin system fitted to the rudder, *NN (2005).* A well-known solution for reducing losses in the propeller hub vortex is the PBCF (Propeller Boss Cap Fins), *Ouchi et al. (1990).* The Kappel propeller utilizes a special tip fin integrated into the propeller blades to reduce tip vortex losses, *Andersen et al. (1992).*

In 2008, a revolutionary hydrodynamic energy-saving device, the Becker Mewis Duct® (BMD) for full-form vessels, like tankers and bulk carriers, was introduced in the market, Fig.3 (left). This device operates within zone 1 and is characterized by a duct and a fins system targeting a combination of flow loss types. The working principle and the theory behind it are described in the next section.

In response to customer demand, the application of the BMD concept was extended in 2012 to include faster vessels with lower block coefficients, such as container ships. This led to the development of a new product named Becker Twisted Fin® (BTF), Fig.3 (right). Conceptually, the BTF is similar to the BMD, consisting of a radial series of pre-swirl fins encased by an optimized pre-duct. Additionally, there is a series of radial outer pre-swirl fins that are twisted for optimal pre-swirl generation.



Fig.3: Becker Mewis Duct® (left) and Becker Twisted Fins® (right) after installation at the shipyard

Both the BMD and the BTF, along with the devices listed above, have an impact on the EEXI and CII. These technologies are defined as Energy Efficiency Technologies (EET) of category A, *IMO (2013b).* This category groups all the technologies that shift the power curve, resulting in a change in the combination of Pp (Propulsion Power) and V_{ref} (Reference speed). For example, when V_{ref} is kept constant, Pp will be reduced, and when Pp is kept constant, V_{ref} will be increased.

Due to the relatively low return on investment (ROI) and the simplicity of the installation process during regular dry docking, without the need for propeller removal, many shipping companies are opting for such devices as a countermeasure for timely compliance with the new requirements.

2.1. Becker Mewis Duct® and Becker Twisted Fin®

The Becker Mewis Duct® (BMD), also called "pre-swirl duct" in the literature, is based on a combination of two fully independent working principles, *Mewis (2009), Mewis and Guiard (2011).*

- The contra-propeller principle, well known for more than 100 years, *Wagner (1929)*.
- The pre-duct principle, first published by *Van Lammeren (1949)*.

The design goal of the Mewis Duct® in comparison with other ESDs is to improve two fully independent loss sources, namely:

- Losses in the ship's wake via the duct.
- Rotational losses in the slipstream via the fins.

The duct's function is to straighten and accelerate the hull's wake into the propeller, producing net forward thrust, while the pre-swirl fin system reduces rotational losses in the propeller slipstream. Additionally, the improved slipstream behind the duct significantly reduces hub vortex losses, and further positive effects are associated with less propeller cavitation (less noise, fewer vibrations), and improved course keeping.

Over the years, and also thanks to the experience collected during several tank tests conducted in independent model basins and advanced CFD calculations, the geometry of the BMD evolved from a typical full ring duct to a semi-ring duct, leading to further benefits related to weight optimization and drag reduction.

For the newest ship designs with already well-optimized hull lines, the shape of the duct is further optimized by using twisted fin profiles that extend the duct for more pre-swirl effect, Fig.4.

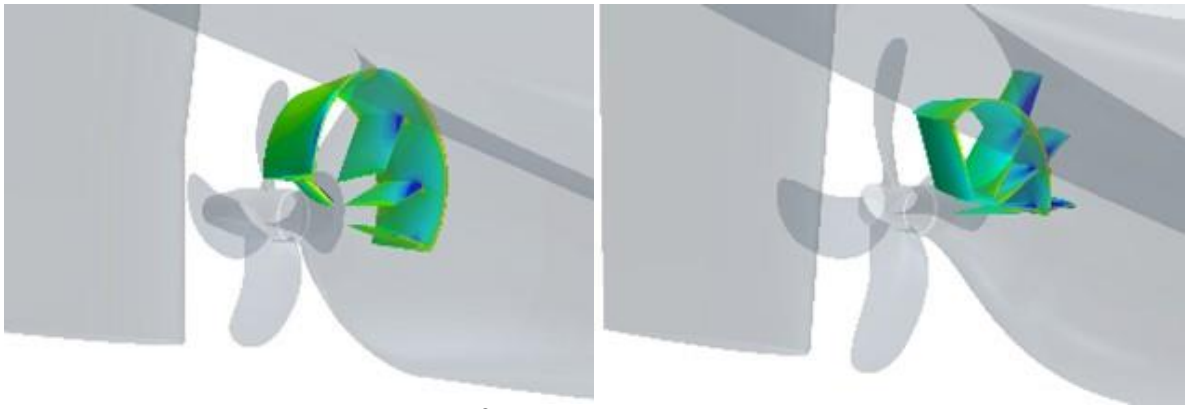


Fig.4: Becker Mewis Duct® - newest design for well optimized hull lines

For each ship design, the BMD is optimized through CFD calculations and finally tested in an independent model basin. Alternatively, an extended CFD analysis can substitute the tests in the model basin. During the optimization process, the design is further refined by choosing the best combination of fin angles.

The design process is quite complex and iterative. It begins with the computation of the wake field evaluated at various planes and operating conditions. Then, a preliminary duct design is taken as a starting point, and up to 45 parameters can be optimized to find the best duct design in terms of performance (power savings). Typically, and also for time reasons, the parameters that are changed during the design optimization are limited to around 10-12: duct diameter, duct profile length, duct profile thickness, duct profile pitch, number of fins, fins circumferential location, fins profile thickness, fins pitch, and fins profile radial variation.

An average power savings of 6% has been measured across approximately 200 different tested ship designs. Generally, the power saving remains constant over the speed range, and the occasional small fluctuations observed in the results are usually due to inaccuracies in the measurement system of the model basin.

The application of the BMD becomes increasingly challenging as the block coefficient of the vessel decreases, typically for high-speed vessels. Such vessels have finer hull lines, resulting in cleaner, more uniform nominal wake fields. Due to higher flow speeds, there is a greater risk of cavitation in the duct. Additionally, the duct and fins are subject to higher dynamic pressure loads, resulting in higher stress values and, therefore, a more challenging structural design.

The Becker Twisted Fin® (BTF) is a logical development of the BMD that incorporates alternative and new design features designed to overcome the difficulties outlined previously. All fins are twisted in the span-wise direction, enabling a more uniform hydrodynamic fin loading and controllable pre-swirl. For retrofit projects, due care must be taken to limit the degree of pre-swirl generated to minimize the reduction of shaft speed and consequent 'heavy' propeller running.

The design process of the BTF is very similar to the BMD, including the selection of the best combination of various parameters and the optimization process based on finding the optimal fin angle (either in the model basin or through advanced CFD calculations).

To date, more than 200 BTF units, corresponding to over 20 different ship designs, have been installed on various sizes of container ships, achieving an average power saving of about 3.5%.

3. Energy Saving Devices for EEXI and CII compliance

The influence of the ESDs, particularly the BMD and BTF, on the EEXI and CII is of different nature. The EEXI is improved through the increase in V_{ref} resulting in a speed gain. Since the relationship between speed and power can be approximated with a cubic function: $P \approx V^3$, the speed gain (at the same power) is less than the power saving (at the same speed). In numbers, a power saving of 4-8% can be quantified as 1-2% speed gain, which also corresponds to the EEXI improvement as shown in Table I. The calculation of the V_{ref} for a ship fitted with ESD is explained in section 3.2.

In the CII calculation, the effect of the ESD is taken directly into account in form of fuel consumption. It can be noted that the improvement in CII roughly corresponds to the measured (or calculated) power saving, bearing in mind fuel and power saving may vary slightly as explained in section 3.4.1.

Additionally, the CII relies on operational data from the IMO DCS, where fuel consumption data are stored. Consequently, the rating is sensitive to external factors not directly linked to vessel performance. These factors include the quality of the data, precision of onboard sensors, weather conditions, hull condition, and the crew's familiarity with the new systems and regulations. Further details can be found in sections 3.4.2 to 3.4.4.

Table I: Improvement on EEXI and CII due to installation of ESDs like BMD and BTF

Power reduction	4-8%
Ship speed increase	1-2%
EEXI improvement	1-2%
CII improvement	4-8%

3.1. Impact of the ESD on EEXI

The reference speed V_{ref} is part of the denominator of the EEXI formula, which can be simplified to:

$$Attained\ EEXI \approx \frac{P_{ME}\ C_F\ SFC}{Capacity\ V_{ref}} \qquad (1)$$

P_{ME} = engine power, SFC = specific fuel oil consumption, C_F = CO_2 conversion factor and V_{ref} = reference speed.

Since the improvement of the EEXI due to ESD installation is limited to 1-2%, Table I, in the majority of cases, additional measures are required to achieve compliance. One common approach is Engine Power Limitation (EPL) as explained at the end of section 1. A further benefit of installing ESD combined with EPL is that, due to the resulting increase in speed, the EEXI is reduced. Consequently, the EPL can also be decreased, leading to an additional increase in speed.

In the following case study, this behaviour is explained.

- A 115000 dwt Bulk carrier is going to be fitted with a Becker Mewis Duct®.
- At Pme = 75% MCR the reference speed V_{ref} of the ship without Mewis Duct is 14.45 kn and the attained EEXI is 3.62.
- The required EEXI for this ship is 2.97, so an EPL is needed in order to reach compliance.
- After EPL, the new V_{ref} is calculated as 83% of the limited engine power (Pme_lim).
- The Becker Mewis Duct® results in a speed increase of 0.23 kn at 83% of Pme_lim
- The speed gain improves the EEXI from 2.97 to 2.92. This results in a larger remaining engine power and thus in a further increased V_{ref} (additional 0.11 kn, in total 0.34 kn)

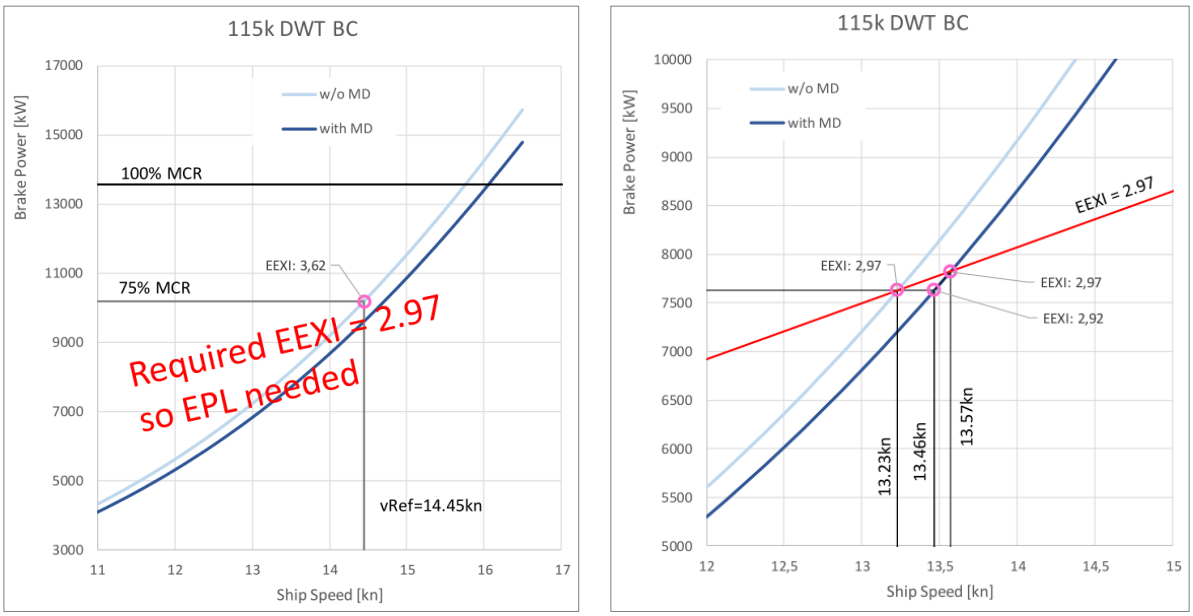


Fig.5: Impact of the BMD on EEXI and EPL for a 115000 dwt bulk carrier

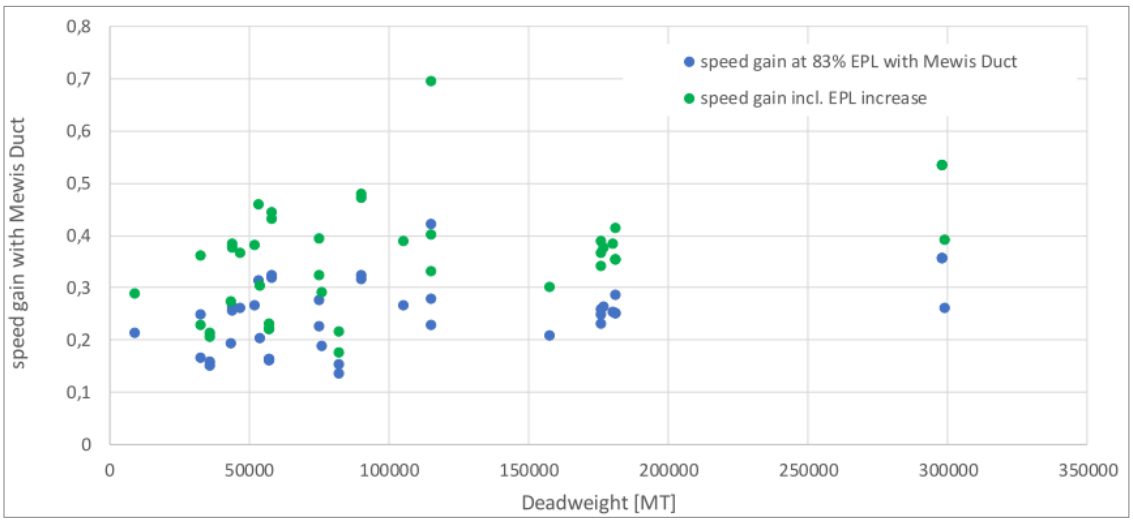


Fig.6: Speed gain obtained after the installation of the BMD for over 40 vessels. The green points represent additional speed gain, accounting for the larger remaining engine power.

A similar investigation was conducted on several other ship types and sizes confirming the results seen in the above case study: the application of an ESD for a vessel with EPL results in a speed gain due to the ESD effect and a further speed gain due to the larger remaining engine power.

Instead of limiting the engine power, or in cases where it is not allowed to further reduce the power due to regulatory or technical constraints, a combination of multiple ESDs can also be taken in consideration. In such case a comprehensive numerical calculation or dedicated model tests, including all fitted devices, must be conducted.

3.2. Calculation of the V_{ref} for a ship fitted with ESD

As per MEPC resolution 333(76) the effect of the ESD on V_{ref} can be calculated according to the following methods:

- Sea trial
- Dedicated model tests
- Numerical calculations

Since in most of the cases there is a time and cost constrain for dedicated sea trial or model tests, numerical calculations are preferred, especially for projects where the energy saving devices are installed as retrofit (and a reduced lead time is highly appreciated).

Numerical calculations are intended as computer aided calculations in which the Navier-Stokes equations are resolved by means of a Computational Fluid Dynamics (CFD) software, which requires to implement at least Reynolds-Averaged Navier-Stokes equations as governing equations with the consideration of viscosity and in presence of free-surface (MEPC 78/INF.16).

As per resolution MEPC.333(76), numerical calculations can be used in complement of model tests or as a replacement of the latter. The methodology and numerical model used needs to be validated/calibrated against parent hull sea trials and/or model tests, with the approval of the verifier. The mentioned resolution contains all the minimum requirements to be implemented in the numerical modelling and to be included in the final report: from a detailed description of the geometry of the hull and all appendages, to the turbulence model to be used (commonly the k-ω model). Additionally, the CFD 3D model must be validated through a mesh sensitivity analysis and convergence plots have to be included to assess the convergence of the calculations.

The calibration of the results is a crucial part. In case model test or sea trials for the ship being fitted are available, the numerical models used are to be calibrated against the parent hull. For the calibration a factor is calculated as the ratio between the sea trial power and/or model tests and the numerical calculation found power. In case model tests and/or sea trials are not available, which is possible for very old ships, the calibration needs to be conducted against a similar ship or a set of comparable ships.

3.3. Impact of the ESD on CII

Starting in 2024, each ship will be assigned a CII Rating from A to E based on the prior year's IMO DCS data. Each ship needs a rating of C or better, Fig.7. Vessels that achieve a D rating for three consecutive years or an E rating in a single year must develop an approved corrective action plan as part of the SEEMP. Otherwise, they risk becoming unattractive to the charter market or unable to trade internationally.

In accordance with MEPC.352(78), the CII is derived from the Annual Emissions Ratio (AER), calculated as the annual fuel consumption multiplied by the CO_2 emissions factor, divided by the transport work (distance sailed by a ship multiplied by capacity). Furthermore, correction factors for specific ship types are applied.

$$CII = \frac{Annual\ Fuel\ Consumption\ x\ CO_2 Emission\ factor}{Distance\ sailed\ x\ Capacity}\ x\ correction\ factors \quad (2)$$

The attained CII must be documented and verified against the required annual operational CII. This enables the Recognized Organization to determine the operational CII rating.

Thus, the CII is directly based on fuel consumption, influenced by how a specific ship operates in combination with its technical efficiency. Its value varies with the type of fuel used, the efficiency of the vessel, and operational parameters such as vessel speed, cargo transported, weather conditions, and the general condition of the vessel.

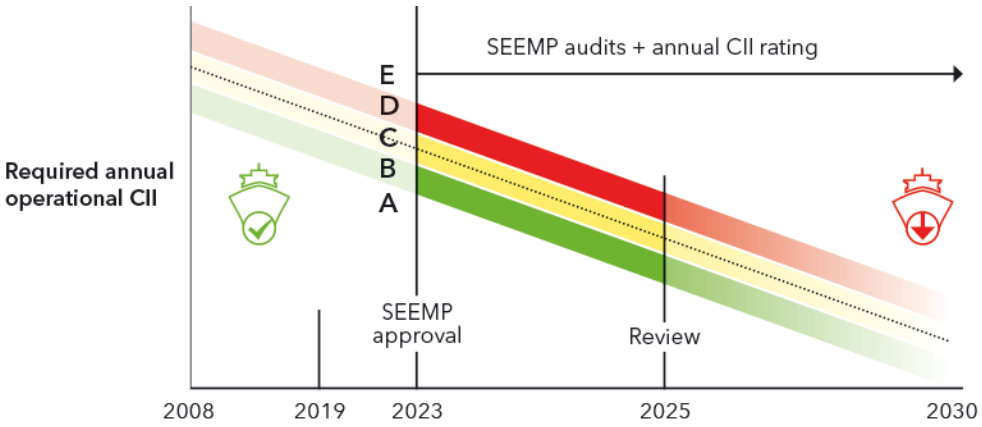


Fig.7: CII rating and development over time, source: DNV

As per the values in Table I, the improvement of the CII given by the energy-saving devices is directly related to the power saving. Again, it's important to note that power savings do not equate to fuel savings, as explained in section 3.4.1.

3.4. Challenges on using the ESDs for CII compliance

Differently from the EEXI, the CII cannot be verified by numerical calculations, model tests, or sea trials, but is based on operational data from the IMO DCS, where fuel consumption data are stored. The CII is, therefore, sensitive to external factors not essentially related to vessel performance, such as the quality of the submitted data, the precision of onboard sensors, weather conditions, hull condition, and, last but not least, the crew's awareness of how to deal with the new systems and regulations.

The first challenge, however, lies in the definition of the CII itself. While energy-saving devices are part of the solution to achieve a better CII rating, the influence of operational parameters, especially the distance traveled, plays a significant role. It is also worth noting that the current definition of CII is criticized by various stakeholders in the shipping industry, and changes may come in the near future. Several proposals are under evaluation, and even a complete abolition of the index is on the table. The next set of decisions will be made by 2026.

3.4.1. Difference between power and fuel savings

The CII rating is based on the annual fuel consumption, but the savings given by the ESD are mostly referred to as power or energy savings. Power savings and fuel savings are not identical, and converting between them requires careful consideration, especially regarding the difference in specific fuel oil consumption of main engine and generators.

In the following example, taken from a real case, the difference between power and fuel savings is explained.

An MR Tanker fitted with a Becker Mewis Duct® is expected to achieve a power saving of about 6% over the full speed range. The engine shop test data provided by the engine manufacturer gives information in the table below about the Specific Fuel Oil Consumption (SFOC).

Table II: SFOC vs Engine Load

Engine load [%MCR]	SFOC [g/kWh]
50	177
55	176
60	175
65	174
70	174
75	174
80	174

The effect of the Mewis Duct on the fuel savings in evaluated for the following two cases.

Case 1: operation at 70% MCR and 6% power savings given by the BMD.

In order to achieve the same speed without BMD a higher engine load is required:

$$P_{D(with\ MD)} = (1 - 0.06)\ P_{D\ (wo\ MD)}$$

Or

$$70\%\ MCR = 0.94 * 74.5\%\ MCR$$

The SFOC is almost constant when changing from 74.5% to 70% MCR and the fuel saving is equal to the power saving.

Case 2: operation at 50% MCR and 6% power savings given by the BMD.

In this case the situation is different:

$$50\%\ MCR = 0.94 * 53\%\ MCR$$

The SFOC changes from ~176 g/kWh to ~177 g/kWh; the fuel saving is less that the power saving.

$$fuel\ saving = 1 - \frac{consumption_{withMD}/h}{consumption_{woMD}/h} = 1 - \frac{50\%MCR \times 177\ g/kWh}{53\%MCR \times 176\ g/kWh}$$

$$= 1\text{-}\left[(1 - power\ saving) \times \frac{177\ g/kWh}{176\ g/kWh}\right]$$

$$= 1\text{-}[(1 - 0.06)x177/176] = 0.055\ or\ 5.5\%$$

3.4.2. Data quality and accuracy

The quality and accuracy of the data collected on board are of paramount importance. Historically, noon reporting has been the means of collecting data from vessels. Nowadays, while manual data input is still widely used, automatic data collection is being implemented on more and more ships, driven by the need to improve efficiency and reduce human errors. Unlike manual data collection, high-frequency data logging provides accurate data sets, making it easier to assess and verify the impact of operational changes on a vessel's performance.

Since the monitoring system on board is fed by sensor data, the accuracy and precision of the various sensors installed on board plays a critical role. Each sensor has its accuracy in measurements; for example, fuel flow meter accuracy ranges between 0.05-3%, depending on the type, manufacturer, flow characteristics, and installation. Fuel readings by tank soundings are estimated to have an accuracy of 2-5%, *Faber et al. (2013)*. Additionally, all other sensors on board have their accuracy, which depends on calibration and manufacturer, and errors can occur if the devices are poorly maintained or calibrated. Inaccurate sensors will lead to measurement errors that are inevitably reflected in the overall ship performance characteristics.

In general, an overall measurement error of 5% is common, which, for the purpose of CII calculation, is significant. Therefore, particular attention should be given on having a reliable dataset based on calibrated instruments.

3.4.3. Weather and hull condition

Weather and hull conditions are external factors that are always present and difficult to control. Heavy weather and hull fouling increase ship resistance, resulting in more CO_2 emissions and consequently, a worsened CII rating, Tables III and IV.

Weather routing programs and anti-fouling hull coatings can mitigate operational risks and enhance fuel efficiency by optimizing vessel paths based on weather conditions and reducing the impact of marine growth on the hull, respectively.

Table III: Estimated average increase in resistance for ships navigating the main routes, *MAN (2018)*

North Atlantic route, navigation westward	25-35%
North Atlantic route, navigation eastward	20-25%
Europe-Australia	20-25%
Europe-East Asia	20-25%
The Pacific routes	20-30%

Table IV: The Effect of hull fouling on ship performance, *NN (2004)*

Slime	1~2% increase in vessel drag
Weed	up to 10% increase in vessel drag
Shell	up to 40% increase in vessel drag

Examining the above tables makes it clear that the positive impact of ESD on ship performance and CII becomes negligible when the hull is fouled or when the ship is navigating in regions impacted by heavy weather.

3.4.4 Crew Awareness

Ships are operated by technical managers on shore and crew members on board; thus, they are directly involved in implementing energy efficiency operational measures.

The Master and Deck Crews are directly involved in implementing the ship’s navigation and port operation-related energy efficiency measures, such as speed optimization and weather routing. Meanwhile, the Chief Engineer and Engine Crews are responsible for all ship propulsion-related energy efficiency measures, including main engine performance monitoring, waste heat recovery, and propeller performance monitoring.

Onshore Technical Managers hold responsibility for the technical and navigational operations of ships. They oversee 5 to 10 ships and supervise vessels’ Masters and Chief Engineers by providing technical and necessary support from the ship owner's side, *Dewan and Godina (2023)*.

Many vessels are equipped with performance monitoring systems that transmit real-time data to the ship operating office onshore. This technology enables technical managers to check and analyse the vessel's data from their office, provide feedback to the onboard ship crews, and offer advice on improving the energy-efficient operation of the vessel.

According to *Dewan et al. (2018)*, the four main barriers to implementing energy efficiency measures are the lack of knowledge, awareness, and competence among seafarers, along with operational challenges. Raising awareness and understanding among seafarers is crucial for adopting and effectively implementing energy efficiency measures onboard ships. Providing necessary education and training for onshore managers and onboard seafarers should be facilitated and treated as a vital part of ship operations.

When the ship is retrofitted with propulsion improving devices, such as ducts or pre-swirl devices, it is important that the onboard crew is trained on how to harness the benefits provided by these devices. It should be emphasized that these technologies can either increase speed with the same power or achieve power savings while maintaining the same speed. Additionally, the crew should receive adequate training on how to monitor the ship's performance, and the technical managers onboard should be equipped with the skills to analyse the received data and take the right decisions.

4. Conclusions

The shipping industry is actively working on enhancing its environmental sustainability by adopting strategies and implementing measures to improve energy efficiency. The focus on ESDs, such as BMD and BTF, indicates a practical approach to achieving short-term emission reduction targets, but several challenges need to be addressed for successful implementation.

Unlike EEXI, CII relies on operational data from the IMO Data Collection System (DCS), making it sensitive to factors such as data quality and the accuracy of sensors installed on board vessels. Without a reliable performance monitoring system based on precise and well-calibrated sensors, obtaining trustworthy information about fuel consumption becomes difficult, potentially negatively impacting the CII significantly.

The impact of external factors, such as weather and hull conditions, must also be considered, as they can completely nullify the benefits of energy-saving devices. A ship navigating in adverse weather or with a fouled hull experiences significantly higher resistance compared to normal conditions. Fortunately, mitigation measures like weather routing and low-friction coatings are available to enhance control over these external factors.

Finally, the awareness of both onboard and onshore personnel plays a crucial role. A well-trained crew onboard can operate the vessel in the most efficient way, and the onboard technical managers, when properly instructed, can draw the right conclusions from the data received from the vessel.

The upcoming assessment of the CII is scheduled for 2026. It will be insightful to observe the developments up to this date and assess the persistence of the existing challenges.

References

ANDERSEN, P.; KAPPEL, J.J.; SCHWANECKE, H. (1992), *On Development of Tip-Fin Propellers*, Jahrbuch der Schiffbautechnischen Gesellschaft 86, Springer

CARLTON, J. (2019), *Marine Propellers and Propulsion*, Elsevier

DEWAN, M.H.; GODINA, R. (2023), *Seafarers Involvement in Implementing Energy Efficiency Operational Measures in Maritime Industry*, Procedia Computer Science 217, pp.1699-1709

DEWAN, M.H.; YAAKOB, O.; SUZANA, A. (2018), *Barriers for adoption of energy efficiency operational measures in shipping industry*, WMU J. Maritime Affairs. 17, pp.169-193

DNV (2023), *Maritime Forecast 2050*, report, DNV, Hovik

FABER, J.; NELISSEN, D.; SMIT, M. (2013), *Monitoring of bunker fuel consumption*, Report, CE Delft

IMO (2013a), *Interim Guidelines for Determining Minimum Propulsion Power to Maintain the Manoeuvrability of Ships in Adverse Conditions*, MEPC.1-CIRC.850-Rev.2, Int. Maritime Org., London

IMO (2013b), *Guidance on treatment of innovative energy efficiency technologies for calculation and verification of the attained EEDI*, MEPC.1/Circ.815, Int. Mar. Org., London

LEE, J.T., KIM, M.C., SUH, J.C., KIM, S.H.; CHOI, J.K. (1992), *Development of a Preswirl Stator-propeller System for Improvement of Propulsion Efficiency: a Symmetric Stator Propulsion System*, Trans. SNAK 29/4, Busan

MAN (2018), *Basic Principles of Ship Propulsion*, MAN, https://www.man-es.com/docs/default-source/document-sync-archive/basic-principles-of-ship-propulsion-eng.pdf

MEWIS, F. (2009), *A Novel Power-Saving Device for Full-Form Vessels*, 1st Int. Symp. Marine Propulsors (SMP'09), Trondheim

MEWIS, F.; GUIARD, T. (2011), *Mewis Duct – New Developments, Solutions and Conclusions*, 2nd Int. Symp. Marine Propulsors (SMP'11), Hamburg

MEWIS, F.; PETERS, H.-E. (1986), *Power Savings through a Novel Fin System*, 15. SMSSH Conf., Vol. 1, Varna, pp.9.1-9.6, Varna

NN (2004), *Hull Roughness Penalty Calculator*, Akzo Nobel

NN (2005), *Hyundai Thrust Fin Improving Propulsion Efficiency*, Flyer, Hyundai Maritime Research Institute, Ulsan

OUCHI, K.; KAWASAKI, T.; TAMASHIMA, M. (1990), *Propeller Efficiency Enhanced by PBCF*, 4th Int. Symp. Marine Engineering (ISME 90), Kobe

SASAKI, N.; AONO, T. (1997), *Energy Saving Device "SILD"*, J. Shipbuilding 45/135

SCHNEEKLUTH, H. (1986), *Wake equalising ducts*, The Naval Architect

VAN LAMMEREN, W.P.A. (1949), *Enkele Constructies ter Verbetering van het Rendement van de Voorstuwing*, Ship en Werf 7

WAGNER, R. (1929), *Rückblick und Ausblick auf die Entwicklung des Contrapropellers*, Jahrbuch der Schiffbautechnischen Gesellschaft 30. Band, Springer

Maritime IoT: Onboard Energy Data as Key to Operational Optimization

Klas Reimer, Hoppe Marine, Hamburg/Germany, k.reimer@hoppe-marine.com

Abstract

The integration of precise sensors and timeseries data acquisition through the Maritime Internet of Things (MIoT) paves the way for effective energy balancing and operational optimization. This approach focuses on installing flow meters for accurate fuel monitoring and sophisticated data transmission systems, laying the groundwork for enhanced energy management. Such methodologies are relevant for adhering to CII guidelines and preparing for the challenges posed by the EU ETS from 2025. The integration of Continuous Emission Monitoring Systems (CEMS) and energy measurement devices build the foundation for energy balancing. This allows operational optimization and validated reporting solutions and shows the critical role of data-driven decision-making and reporting in achieving sustainability and efficiency enhancements.

.

1. Introduction

The maritime industry faces the dual challenge of improving its operational efficiency while simultaneously reducing emissions to comply with growing international regulations and environmental standards. Innovative technologies such as the Maritime Internet of Things (MIoT) allow new ways to meet these demands. In this context, Hoppe Marine, a leading maritime systems supplier, plays an essential role by leveraging MIoT to perform precise measurements and analyses of maritime operational data. This data is relevant for optimizing and promoting the sustainability of ship operations.

Another important aspect in regulating maritime emissions is the introduction of the "CII Voyage adjustments and Correction Factor according to MEPC 355 (78) by the Marine Environment Protection Committee (MEPC). This regulation allows the exclusion and deduction of certain energy-intensive activities like cargo cooling and heating from the calculation of the Carbon Intensity Indicator (CII) in order to make vessels energy demand comparable. Although this helps achieve improved emission values, the practice is not merely about looking good on paper. Instead, it is essential to holistically understand, account for, and optimize ship operations to achieve genuine, sustainable improvements in efficiency and environmental compatibility.

The efficiency and sustainability of ship operations significantly depend on the accuracy and availability of operational data. For a long time, the traditional maritime industry relied on manual measurements and manual reported noon data. However, given the increasing emission regulations and a need for efficiency improvements, a paradigm shift is necessary. The saying "You cannot optimize what you do not measure" highlights the need to precisely capture operational data to make informed decisions.

2. Energy Accounting

With the introduction of the EU Emissions Trading System (EU ETS) in 2025, the focus on reducing CO2 emissions in the maritime industry will intensify. The Maritime Internet of Things (MIoT) plays a crucial role in measuring and optimizing ship operational processes to ensure compliance with new regulations while simultaneously reducing operational costs. A deeper look, where does the energy shows:

- Energy Supply (100%): Fuel that is fed into the main engine and auxiliary generators.
- Useful Work (~25-30%): The portion of energy that is actually converted into propulsion and electrical power. This value can vary depending on the efficiency of the engine and the entire propulsion system.
- Waste Heat (~30-35%): A large part of the energy is lost as waste heat through the cooling system and exhaust system.

- Auxiliary Systems and Peripherals (~5-20%): Pumps, fans, auxiliary units Exhaust (~15-20%)

The exact percentage depends on the type of fuel, the efficiency of combustion, and the effectiveness of after-treatment systems.

3. Balancing through Precise Measurement of Energy Input and Usage

A central element in optimizing maritime operations and increasing energy efficiency is energy accounting. It enables a profound understanding of how energy is generated, distributed, and consumed aboard a ship. Similar to a Sankey diagram, which visualizes energy flow through various systems, effective energy accounting requires precise data on energy input and usage.

Fuel consumption as the primary energy input plays a crucial role in a ship's energy balance. Measuring fuel consumption using flow meters provides direct data on the amount of energy supplied to the propulsion system and generators. This data is fundamental to assessing the efficiency of the main engine and auxiliary generators and identifying optimization opportunities.

Power measurement in various ship systems, including the main engine, auxiliary generators, and propulsion systems, enables an understanding of how energy provided by fuel consumption is transformed and utilized. Monitoring performance data helps identify losses, assess the efficiency of machinery and systems, and develop approaches to improve the overall energy efficiency of the ship.

Exhaust measurement provides important insights into the efficiency of combustion processes and the environmental impact of ship operations. Continuous monitoring of exhaust composition not only ensures compliance with emission regulations but also assesses and optimizes combustion efficiency, *Müller and Schmidt (2021)*. In particular, measuring CO2, NOx, SOx, and particle emissions helps relate energy consumption to emissions and develop strategies to reduce the ecological footprint.

Integrating these measurement points into a comprehensive MIoT system enables detailed and dynamic energy accounting. Through the continuous collection and analysis of data regarding energy input and usage, vulnerabilities can be identified, operational adjustments can be made, and long-term strategies for increasing energy efficiency and reducing emissions can be developed. This precise form of energy accounting is key to achieving more sustainable and efficient ship operations.

4. Reduction of Operating Costs through Energy Measurement - Theoretical Example of Energy Measurement

The concept of energy data collection serves not only to optimize the Carbon Intensity Indicator (CII) to remain competitive and avoid disadvantages that could arise from the assessment of energy-intensive goods but also enables smarter control of energy consumers. For example, a device with a power rating of 120 kW consumes approximately 190 tons of fuel annually, costing €155,000 and causing 600 tons of CO2 emissions.

Particularly in oil tankers, cargo heating and cargo transfer can account for up to 25% of the energy demand (Crude oil tankers utilize boiler energy to maintain the cargo in a liquefied state at about 50°C. Heat conduction depends on the temperature difference, surface area, and heat loss coefficient for each surface. The required heating rate depends on the cargo mass, specific heat constant, temperature difference, and target time for heating up). This can correspond to a difference of at least one energy class in the CII rating.

This underscores the importance of more accurate measurement and adjustment in assessing energy consumption to ensure a more realistic assessment of environmental impact and efficiency.

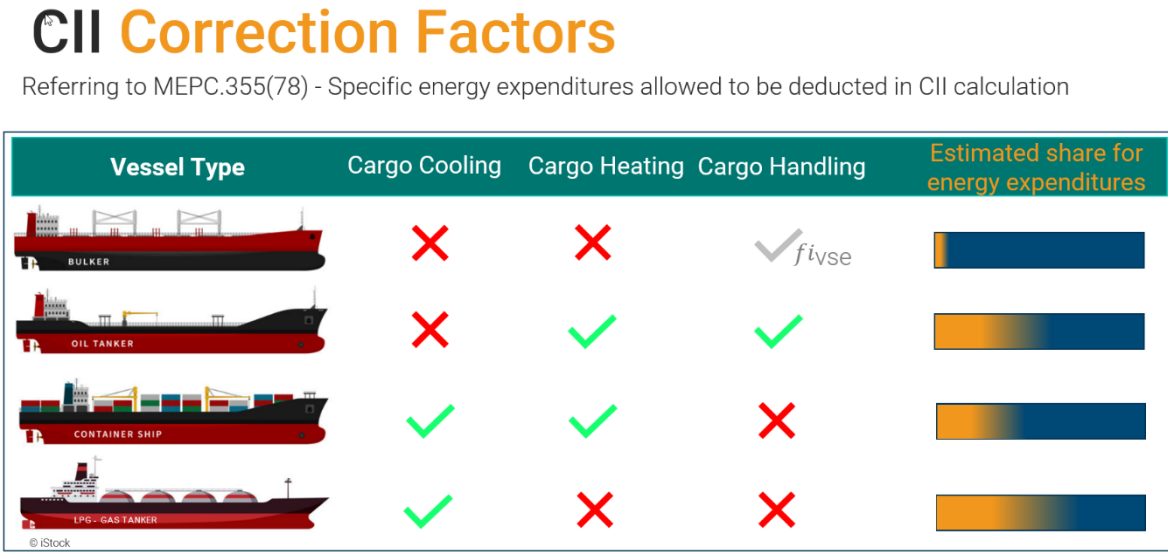


Fig.1: Energy Intensity and possible Correction Factors for different vessel types (source: MEPC.355(78) – Reefer, Reliquefaction & Refrigeration Plant)

Integrating MIoT into the existing ship infrastructure presents technical and operational challenges, particularly in data collection and validation. Ensuring data quality and integrity is crucial for reliable analyses and optimization strategies, *Reimer (2020)*.

5. Use Case Energy

Energy measurement onboard merchant ships is trends towards the installation of energy measurement devices by Rogowski coil principle, which allows for contact-free current measurement via magnetic fields. The coils, Fig.2, can be easily clamped onto existing cables or busbars and are capable of measuring currents up to 10,000 amperes. Connecting all energy measurement devices via a bus line enables centralized and efficient capture of electrical power, for both individual and combined consumers, such as individual fans or junction boxes of refrigerated containers.



Fig.2: Retrofitted Energy Measurement Device (Rogowski Principle)

Numerous generators—from auxiliary generators to shaft generators, shore power connections (cold ironing), and modern energy sources like fuel cells or battery systems—as well as various consumers such as refrigerated containers, cargo pumps, and air conditioning systems can be precisely monitored.

In addition to these advantages, the devices can be easily retrofitted in the switchboard room due to short connection paths. Communication via bus allows for cost-effective, efficient, and space-saving installation. This makes the system particularly valuable for all types of ships by enabling precise energy accounting for operational optimization and cost reduction. The cost for an energy measurement point with energy consumption and counter is ~500 € per measurement point.

6. Reduction of Operating Costs through Optimization

In terms of measurement and data acquisition of primary parameters for modeling, the use of flow meters to measure fuel consumption and sensors to monitor the performance of ships and generators enables the collection of precise real-time data. These measurements are essential to understand the actual energy consumption and identify potential savings.

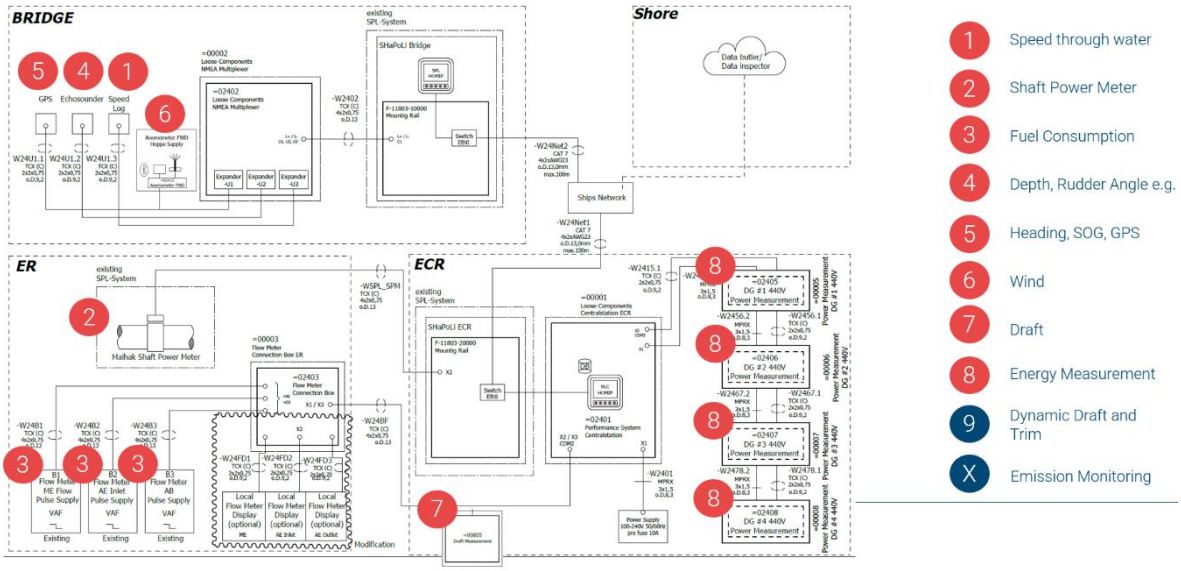


Fig.3.: Relevant Data Sources for Energy Balancing

As shown in Fig.3 with the most important data sources, integrating MIoT into the existing ship infrastructure presents technical retrofit possibilities, particularly in data collection and validation. Ensuring data quality and integrity is crucial for reliable analyses and optimization strategies.

7. Data Transmission and Analysis

A stable, cyber secure and bidirectional data transmission channel allows secure and efficient transmission of collected high quality data to shore, https://docs.hoppe-sts.com/docs/doc2#security, *Harcke (2019)*. There, the data can be analyzed and used to support decision-making. This is particularly relevant for planning structural measures to improve energy efficiency and comply with CII guidelines.



Fig.4.: Data Processing with “Data Highway”

7. Examples for Operational Optimization

In addition to energy accounting, operational optimization of ships through a variety of approaches offers potential for significant improvements. In addition to Fig. 4, trim optimization can lead to a decrease in speed by 5% or an increase in power requirement by more than 20% with just a few decimeters difference in draft.

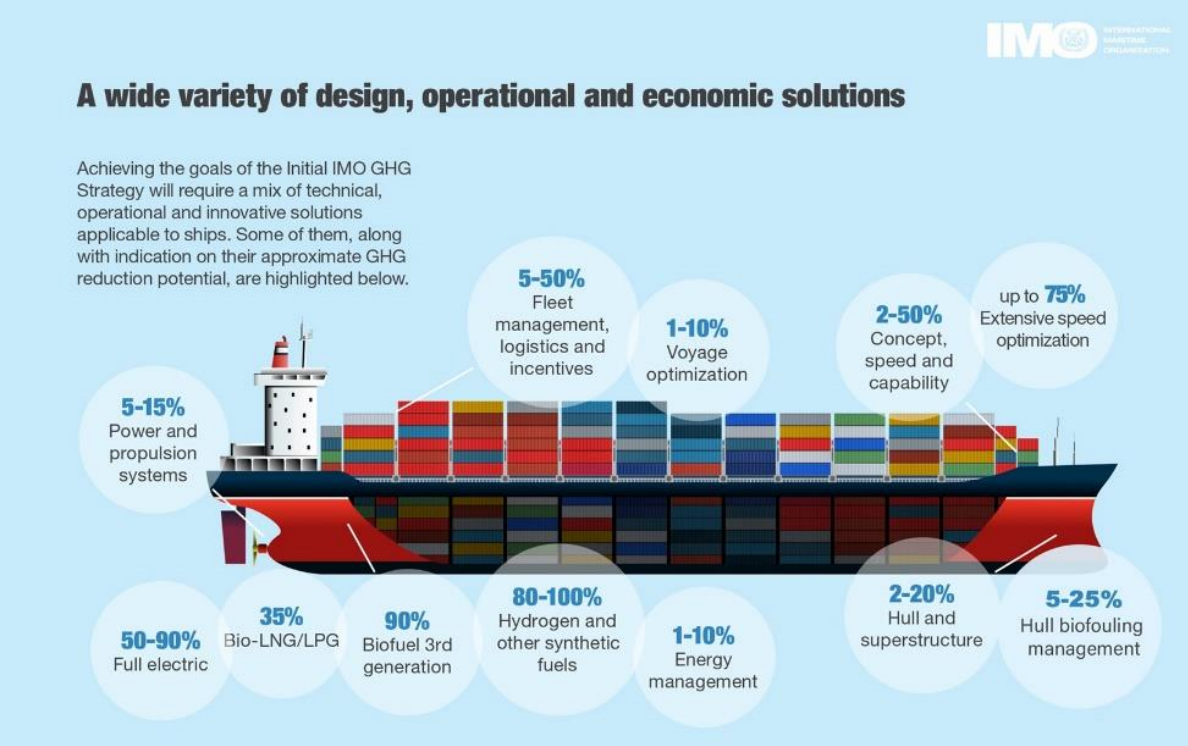


Fig.4: Different optimization potentials in vessel operation

Optimizing the ship's alignment in the water minimizes resistance and can significantly reduce energy consumption. Fan control is another example where adjusted ventilation not only optimizes onboard comfort but also energy demand. This prevents ventilation systems from running unnecessarily, thus avoiding energy waste.

Route optimization, which includes weather data and ocean currents in the planning, can also lead to substantial fuel savings, e.g. *Brown and Johnson (2022)*. Choosing the most economically favorable route makes the journey more efficient without unnecessarily burning fuel. Setting an economical speed, the so-called "Economic Speed," ensures that the ship operates at the optimal speed that minimizes fuel consumption relative to time and distance. Furthermore, rudder position optimization can lead to reduced fuel consumption by making the rudder work less against the direction of travel, thus reducing flow resistance.

The influence of wind represents a significant factor. Wind-induced resistances can be responsible for an increase in fuel consumption of over 20%. Accurate weather data and adjusted navigation can minimize the impact of wind, *White and Martin (2021)*. The operation of auxiliary engines in port often reveals that two generators are running simultaneously at 30% to 40% load. A detailed analysis of operating behavior can save fuel and increase efficiency through optimized load distribution or the shutdown of surplus generators, *Green and Harper (2023).*

These examples demonstrate that significant savings in terms of both costs and environmental impact can be realized through intelligent control and analysis of ship operational data.

8. Conclusion

This paper highlights the critical importance of capturing and analyzing precise operational data to achieve efficiency gains and emission reductions in the maritime industry. Hoppe leverages the Maritime Internet of Things (MIoT) to facilitate comprehensive measurement of ship operational parameters, utilizing flow meters for fuel measurement and robust data transmission systems. This methodology not only supports structural decision-making in line with CII guidelines but also addresses the upcoming challenges posed by the EU Emissions Trading System (ETS) set to take effect in 2025. By integrating energy measurement devices with the acquisition of operational data, the paper outlines a framework for reducing operational costs and CO2 emissions. It also sheds light on both the technical and operational challenges and opportunities that MIoT presents for the maritime sector. This approach illustrates how intelligent control and precise data analysis based on retrofitted sensor and measurement devices can lead to substantial cost savings and a lower environmental impact, underscoring the transformative potential of digital technologies in maritime operations.

References

BROWN, A.; JOHNSON, M. (2022a), *Economic Speed: Balancing Fuel Consumption and Travel Time in Maritime Operations*, J. Navigation 75(1), pp.120-134

BROWN, A.; JOHNSON, M. (2022b), *Fuel Savings through Optimized Maritime Routes: Incorporating Meteorological and Oceanographic Data*, J. Maritime Eng. 163(A2), pp.201-210

GREEN, F.; HARPER, S. (2023), *Optimizing Auxiliary Engine Usage in Ports for Better Fuel Economy*, Energy Policy 141

HARCKE, N. (2019), Einfluss der Datengüte auf die Optimierung des Schiffsbetriebs, Schiff&Hafen, pp.24-26

MÜLLER, R.; SCHMIDT, S.K. (2021), *Kontinuierliche Emissionsmesssysteme (CEMS) für die maritime Industrie: Technologien, Vorschriften und Marktperspektiven*, J. Cleaner Production

REIMER, K. (2020), *How to achieve performance optimization potential considering high quality data?*, 5th HullPIC Conf., Hamburg, http://data.hullpic.info/HullPIC2020_Hamburg.pdf

WHITE, G.; MARTIN, S. (2021), *Minimizing Wind Resistance in Maritime Transport: Strategies and Implications*, Marine Policy 123

CFD-Driven Ship Trim Optimization: Simplifying Complexity of ANN with User-Friendly Software

Matija Vasilev, Ocean Pro Marine Engineers, Belgrade/Serbia, matija@oceanpro.eu
Milan Kalajdžić, Ocean Pro Marine Engineers, Belgrade/Serbia, mdkalajdzic@mas.bg.ac.rs

Abstract

This paper presents a ship trim optimization strategy, employing user-friendly software tool integrating Computational Fluid Dynamics (CFD) and Artificial Neural Networks (ANNs). It evaluates parameters like brake power, shaft speed, and fuel consumption. The tool streamlines complex models into an accessible interface, providing optimized recommendations swiftly. CFD-informed ANN models ensure precise predictions. This advancement minimizes fuel usage, cuts operational costs, and promotes maritime sustainability. By bridging advanced computation and practicality, the tool enhances operational efficiency. The interdisciplinary integration of CFD, ANN, and user interface software underscores technology's role in advancing greener, cost-effective ship trim optimization for the maritime industry's future.

1. Introduction

Since the International Maritime Organization (IMO) introduced the Energy Efficiency Design Index (EEDI) in 2013, and later for existing ships (Energy Efficiency for Existing Ships Index - EEXI) in 2023, the shipbuilding industry has been compelled to change. The primary goal of implementing these parameters is to reduce global CO_2 emissions by 40% by 2030 and 70% or at least 50% by 2050, compared to 2008 levels. Energy efficiency criteria are based on nominal ship data and apply to all ships falling under MARPOL Annex VI and over 400 GT. Each ship has its attained EEDI/EEXI, which must be lower than the required EEDI/EEXI. The required EEDI is based on the formula $a(DWT)^{-c}$, where a and c are parameters determined from the regression curve fit *IMO* (*2013*) of data from ships built between 1999 and 2009, depending on the type of ship. Over the years, the required EEDI decreases according to reduction factors shown in *IMO (2011)* through four phases. The required EEXI is based on the required EEDI, with a reduction factor shown in *IMO (2021a)*, and the plan is for the required EEDI and required EEXI to match from 2025, with the EEXI criterion being slightly stricter until then. In addition to nominal efficiency parameters, there are also operational efficiency indicators. The idea of the Energy Efficiency Operational Indicator (EEOI) was first conceived in *IMO* (*2009*), but it never became mandatory, only voluntary. It was not until 2023 when the Carbon Intensity Indicator (CII) officially came into force, providing a real picture of pollution originating from ships. Similar to EEDI and EEXI, there are attained CII, *IMO* (*2022a*), and required CII, *IMO* (*2022b*), with the attained CII having to be lower than the required, and the required CII decreasing over the years, *IMO* (*2021b*). Based on this indicator, each ship falls into one of 5 energy efficiency grades (A, B, C, D, or E), with the boundaries between them and the method of determining them for each ship separately, depending on *DWT*, defined in *IMO* (*2022c*). The basic data considered when calculating CII are distance travelled, time spent underway, and the amount of fuel consumed over a one-year period. Recording these three pieces of information has been mandatory since 2019 under the Data Collection System (DCS) for all ships with 5000 GT or more, *IMO* (*2016*). Ships that achieve class D for three consecutive years or class E for at least one year must create a plan of measures to be taken in the next steps to reduce CO_2 emissions and enter at least class C, *IMO* (*2022d*).

Measures that can be implemented to reduce CO_2 emissions and improve energy efficiency are diverse and can be divided into operational and technical measures. Operational measures are: improved voyage planning, weather routeing, “just in time“ voyage, speed optimization, optimized shaft power, optimum trim, optimum ballast, optimum use of rudder and heading control systems (autopilot)... Technical measures include: hull maintenance, propulsion system upgrading and maintenance, waste heat recovery, fuel type change, hull retrofit (bulb modification, stern modification, energy saving device installation), wind-assisted propulsion...

Trim typically refers to the variance between the draft at the aft and forward sections of a ship. Positive trim indicates that the stern is deeper in the water than the bow, while negative trim signifies the opposite. Achieving optimum trim minimizes the required propulsive power, a goal facilitated by careful planning and executing a ship ballasting plan. Adjusting ballast water and redistributing fuel between tanks can optimize trim, especially when the ship is fully loaded. The relationship between a ship's resistances and its trim is closely related to each other. Trim influences the ship's wetted surface area and waterplane area, consequently impacting the forces impeding its movement through the water. The conventional method to find the best trim involves conducting model tests in still water to assess resistance across different drafts and trims, resulting in a set of curves highlighting the trim with the lowest resistance for a specific draft. This information is seamlessly integrated into onboard tools, with tests being commonplace and basins typically equipped with established procedures and recent insights to aid in their execution, aiming to measure slight power fluctuations within the anticipated range of 0 to 4% of the total installed power, *ABS* (*2013*), or 2% to 4% reduction in fuel consumption, *Ziarati et al.* (*2017*). Today, advancements in accuracy have reached a point where trim tables derived from CFD software calculations can rival the outcomes obtained from traditional resistance model tests for less investements. Beside model test and CFD method there are another two ways to determine optimum trim: sea trials and machine learning method. Sea trials require a lot of time and amount of fuel to determine optimum balast, while machine learning method requires a massive amounts of data from ship past navigarional voyages, *MTCC-Asia* (*2017*). The scope of this study is focused only on trim optimization with CFD method applied on one RO-RO car carrier.

Various studies already exist in the field of trim optimization using CFD methods applied to different types of ships. For instance, *Sherbaz et al.* (*2014*) demonstrated that optimizing the trim of a container ship like MOERI (KCS) can reduce total resistance by 2%, similar to the benefits seen in optimizing the trim of a US Navy ship, *Le et al.* (*2021*). Some studies even report greater benefits, such as *Petursson* (*2009*), highlighting potential fuel savings of up to 5%, *Lee et al.* (*2014*) showing a 6% reduction in delivered horsepower. Results from trim optimization can vary significantly depending on the trim condition; *Lyu et al.* (*2018*) emphasize that total resistance in the Series 60 varies by up to 11% between the worst and best trims. Even greater potential benefits are highlighted in *Moustafa et al.* (*2015*), where trim optimization of bulk carriers can reduce total resistance by up to 14%. Concerning RO-RO ships, savings of up to 10.4% in delivered power or 1.2t fuel/day can be expected, *Demir* (*2019*). In addition to the trim optimization calculations themselves, specialized software is often mentioned that can quickly determine the optimal trim based on input parameters, *Lee et al.* (*2014*), *Reichel et al.* (*2014*).

2. Methodology

The conducted work focused on Trim optimization of the RO-RO ship by using CFD simulations and guidelines *ITTC* (*2014a,b*), *ITTC* (*2017*), *ITTC* (*2021a,b), IMO* (*2022e*). Firstly, the focus was on the development of a 3D model of the RO-RO ship, utilizing the available documentation. The digital twin encompassed the hull, rudder, and propeller, aiming to replicate the ship's characteristics and behavior accurately. To ensure the fidelity of the 3D model as a representative digital twin, its hydrostatics were compared against data from the Trim & Stability booklet.

In order to assess the performance of the ship's propulsion system, two simulations of open water tests (OWT) were conducted. The scope of the first simulation was to verify the calculation methodology. An analysis of an equivalent B series was carried out due to lack of original model test data. The CFD analysis results were compared against the expected performance curves of the subject B series propeller with the same geometry particulars as per *IMO* (*2022e*). The scope of the second set of open water tests simulations was to predict the performance curves of the original propeller. In both cases, the following methodology is aligned with *IMO* (*2022e*).

Following the open water tests simulations, an analysis of steady resistance and self-propulsion with actuator disk tests at the design draft for three different speeds was completed. These simulation results were then compared against data from model tests.

Furthermore, the work included trim optimization simulations conducted for a range of speeds of 12.5, 15 and 18 kn at 7.5, 8 and 8.7 m draft, and seven different loading conditions. The aim was to optimize the trim settings and assess their impact on performance parameters under calm water conditions. The results of these simulations were presented as percentage savings in brake power and estimated fuel consumption, based on the available data.

3. Results

Results of conducted open water test simulation with B series propeller have been compared with the available results obtained with mathematical model. As per *IMO* (*2022e*) guidelines, K_t, K_q, and η_0 evaluated in CFD simulation have to be no more than 3% different from the target values in the relevant propeller operating range. Graphical representation of CFD results from conducted OWT for original propeller, B series corresponded propeller with mathematical model data for that B series propeller is shown in the Fig.1.

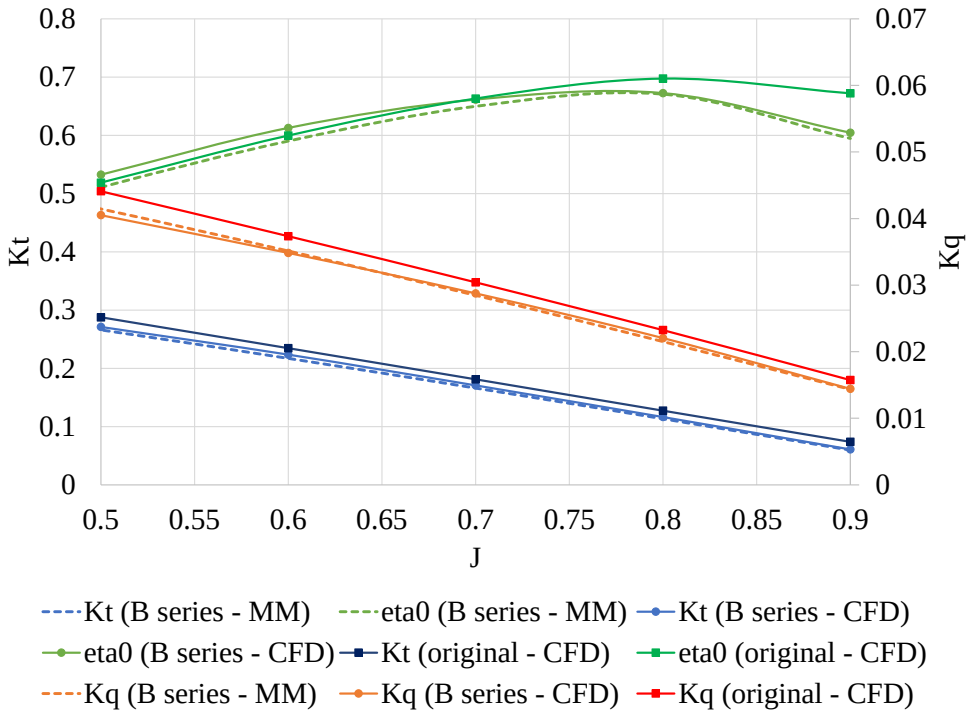


Fig. 1: Propeller characteristics – MM: mathematical model, CFD: simulated OWT

As the results for each of the advance coefficients are within the prescribed 3%, the CFD calculation methodology is considered valid therefore, the OWT CFD results for original propeller are used in self-propulsion simulations with actuator disk to estimate thrust, torque and shaft speed. Steady resistance simulations were used to obtain total resistance and nominal wake fraction coefficient. In the numerical simulations conducted for this study, the direct consideration of roughness effects and air resistance resulting from the presence of a superstructure is not included. However, these effects are accounted for in the post-processing stage by following the recommended procedures and guidelines outlined in *ITTC* (*2017*). The ITTC guidelines provide specific methodologies for incorporating the effects of roughness and air resistance into the analysis, allowing for assessment of the overall performance and characteristics of the ship. Hence the real propeller was not implemented in simulations just actuator disk, the relative rotative efficiency is adopted to be 1. The shaft efficiency coefficient is adopted to be 0.99.

Table I provides a detailed overview of the relevant parameters and their corresponding values estimated by CFD analysis for the speeds of 17, 19 and 21 kn because for these speeds model test data are available.

Table I: Results with included roughness effects and air resistance

V [kn]	Fp [kN]	Fv [kN]	Ft'[kN]	t [-]	w [-]	T' [kN]	Q [kNm]	η_0 [-]	n' [rpm]	P_D [kW]	P_B [kW]
17	125.454	292.216	475.936	0.1746	0.2487	576.644	466.316	0.6736	103.1	5032	5083
19	178.852	366.869	622.133	0.1579	0.2479	738.831	595.864	0.6721	116.0	7236	7309
21	321.762	438.076	857.035	0.1600	0.2458	1020.295	820.407	0.6656	132.8	11408	11523

As per *IMO* (*2022e*) guidelines, shaft speed and brake power should not deviate more than 5% from model test or sea trials data for the same ship speed. In this case, the calibration factors are 1.05 for shaft speed and 1.04 for brake power, which means that obtained CFD results should be multiplied by these calibration factors. Calibrated power curves are presented in Fig. 2 and Fig. 3.

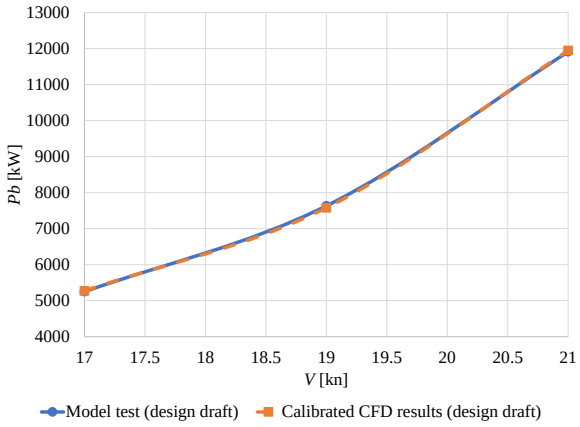


Fig.2: Brake power vs ship speed

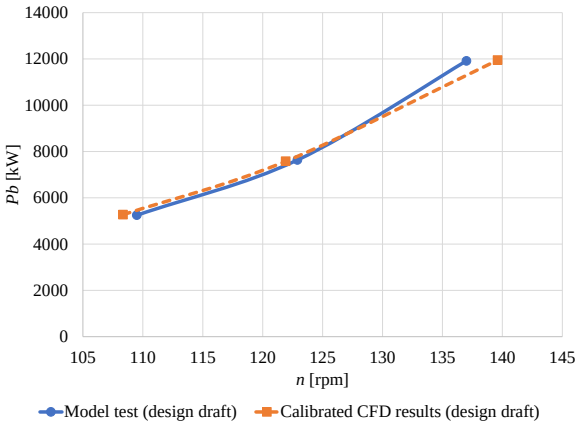


Fig.3: Brake power vs shaft speed

Trim optimization simulations were conducted for a speed of 12.5, 15 and 18 kn at 7.5, 8 and 8.7 m draft and -1.5, -1, -0.5, 0, 0.5, 1, and 1.5 m trim. Negative sign means trim by bow and positive sign, trim by stern.

With available specific fuel oil consumption (SFOC) curve as a function of brake power, a possible reduction of fuel consumption was also calculated. Table II presents brake power change for each trim, speed and draft. Relative difference is calculated based on trimmed condition and even keel condition. Cells marked in green indicate areas of savings in the brake power, while red cells represent the zone to be avoided as greater power is needed compared to even keel condition. The biggest reduction in power can be achieved at 1.5 m trim by bow, 7.5 m draft and speed of 15 kn (11.5%), while for the 8 and 8.7 m draft, the biggest reduction is at 12.5 kn (8.6%, 7.5%, respectively). Estimated possible fuel oil consumption reduction is presented in Table III.

Table II: Brake power reduction

trim [m] / V [kn]	-1.5	-1	-0.5	0	0.5	1	1.5	draft [m]
12.5	-8.1%	-4.6%	-3.1%	0.0%	6.3%	11.9%	16.0%	7.5
15	-11.5%	-7.6%	-4.9%	0.0%	4.2%	11.3%	17.1%	
18	-7.5%	-3.9%	-1.5%	0.0%	3.5%	10.6%	16.1%	
12.5	-8.6%	-5.8%	-3.0%	0.0%	3.9%	13.0%	22.3%	8.0
15	-7.3%	-3.9%	-1.3%	0.0%	5.3%	12.5%	19.9%	
18	-5.0%	-5.4%	-2.8%	0.0%	2.6%	13.5%	15.1%	
12.5	-7.5%	-5.0%	-3.0%	0.0%	3.5%	11.8%	23.0%	8.7
15	-6.6%	-5.4%	-2.8%	0.0%	4.7%	13.7%	18.8%	
18	-5.9%	-4.3%	-3.7%	0.0%	5.0%	14.2%	17.0%	

Table III: Fuel oil consumption reduction

trim [m] / V [kn]	-1.5	-1	-0.5	0	0.5	1	1.5	draft [m]
12.5	-7.6%	-4.2%	-2.9%	0.0%	5.8%	11.0%	14.6%	7.5
15	-10.5%	-6.9%	-4.4%	0.0%	3.8%	10.3%	15.5%	
18	-7.1%	-3.7%	-1.4%	0.0%	3.4%	10.1%	15.4%	
12.5	-8.0%	-5.4%	-2.8%	0.0%	3.6%	12.0%	20.4%	8.0
15	-6.7%	-3.5%	-1.2%	0.0%	4.8%	11.3%	18.0%	
18	-4.8%	-5.2%	-2.7%	0.0%	2.5%	13.0%	14.5%	
12.5	-7.0%	-4.7%	-2.8%	0.0%	3.2%	10.9%	20.9%	8.7
15	-6.1%	-4.9%	-2.6%	0.0%	4.3%	12.5%	17.2%	
18	-5.7%	-4.1%	-3.6%	0.0%	4.9%	13.8%	16.4%	

For 7.5 m draft, up to10.5% of fuel can be saved by trimming the ship 1.5 m by bow and sailing at 15 kn. For higher drafts, more fuel can be saved by sailing at 12.5 kn instead of 15 or 18 kn and even keel. By following the trend of the power curves as a function of trim, more fuel could be saved by going from trim by stern to the trim by bow. Maybe more amount of fuel could be saved by going to -2 m trim, but this condition on current ship cannot be achieved.

4. Advanced mathematical model for ship performance prediction

In the realm of modern engineering and transportation systems, the estimation of crucial parameters such as brake power, shaft speed, and daily fuel oil consumption plays a pivotal role in enhancing performance, optimizing efficiency, and minimizing operational costs. To address this imperative need, a sophisticated mathematical model has been developed, leveraging the power of ANNs. Unlike conventional approaches that primarily focus on simulated loading conditions, this innovative model is uniquely tailored to tackle the challenges posed by non-simulated loading conditions. By harnessing the capabilities of ANNs, this model promises to offer a reliable framework for estimating these critical parameters, thereby contributing significantly to the advancement of engineering solutions in real-world scenarios.

So far, ANN has been applied in predicting fuel consumption based on NOON reports *Bal Besikci et al.* (*2016*), *Jeon et al.* (*2018*) and for predicting ship speed *Bassam et al.* (*2023*). Additionally, research has been conducted on applying ANN for predicting both ship speed and fuel consumption based on data from sails, specifically for a barquentine, *Tarelko et al.* (*2020*).

A feedforward artificial neural network (FFANN) is one of the most common and fundamental types of neural networks used in machine learning and deep learning. It is a basic architecture where information flows in one direction, from input to output, without any feedback loops or recurrent connections. It consists of layers of interconnected neurons, including an input layer, one or more hidden layers, an output layer, Fig.4, and biases. A bias is a learnable parameter associated with each neuron. It allows neurons to introduce an offset or shift in their output, making the network more flexible in modeling complex data patterns. By adjusting bias terms during training, the network can fit data better and learn non-zero outputs even when inputs are close to zero. In this network, data flows in one direction, from the input layer through the hidden layers to the output layer. Within an FFANN, neurons compute weighted sums of inputs, apply activation functions, and transmit results to subsequent layers. Activation functions introduce non-linearity, facilitating the modeling of complex data relationships. Connections between neurons are characterized by weights that govern connection strength. Backpropagation is an algorithm used for training FFANNs. This is named "backward propagation of errors" because it works by iteratively adjusting the weights and biases of the neurons in the network to minimize the error between predicted and actual outputs.

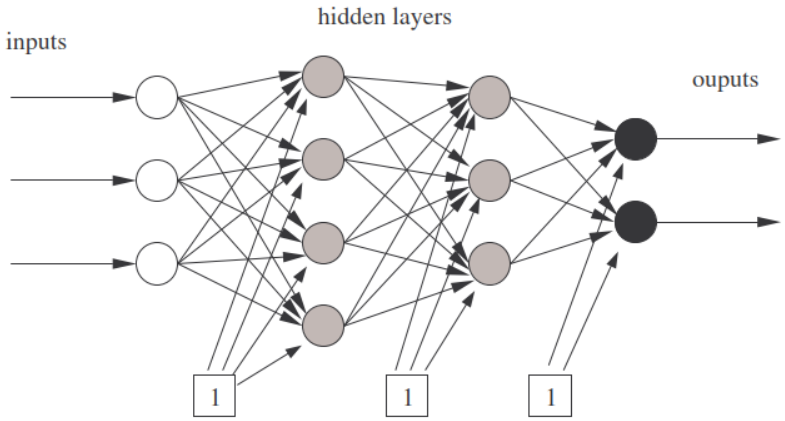


Fig. 4: Layers of interconnected neurons (circles) and biases (squares)

The training process involves two primary phases: the forward pass and the backward pass. During the forward pass, input data is fed into the network to make predictions. Subsequently, during the backward pass, the error is propagated backward through the network, with weights and biases being updated based on the gradient of the error. This iterative process continues until the network's error is minimized, enabling it to make accurate predictions. When a neuron receives input, it collects all these input values and multiplies each of them by their corresponding weights. These weighted inputs are then combined with the neuron's bias. After this, the sum is processed using an activation function to determine the neuron's output:

$$S_{x,i} = f\left(\sum_{i} S_{x-1,i} \cdot w_{x,i} + b_{x,i}\right)$$

f – activation function, $S_{x,i}$ – output signal, of i^{th} neuron in x^{th} layer, $S_{x-1,i}$ – output of i^{th} neuron in $x-1^{\text{th}}$ layer, $w_{x,i}$ – weights connected to neuron and $b_{x,i}$ – corresponding bias. Two of the most frequently used functions are sigmoid and hyperbolic tangent functions; here we used sigmoid function:

$$f = \frac{1}{1+e^{x}}.$$

The general form of the function is:

$$Y_u = \frac{f_p\left(p + \sum_{w=1}^{r}(P_w \cdot f_{p-1}(\dots \cdot f_2(b_i + \sum_{j=1}^{m}(B_{ij} \cdot f_1(a_j + \sum_{k=1}^{n}(A_{jk} \cdot (P_k \cdot X_k + R_k))))) \dots))\right) - G_u}{L_u}$$

- X_k – Input parameters (number of neurons in input layer);
- Y_u – Output parameters (number of neurons in output layer);
- $f_1, f_2, \dots, f_{p-1}, f_p$ – activation function;
- $k, j, i, \dots, v, w$ – number of neurons in each layer;
- $A, B, \dots, P$ – weights between layers;
- $a, b, \dots, p$ – weights between neurons in each layer and bias.

The software that has been used for training the ANN in this study is called aNETka, *Zurek* (*2007*), developed in LabVIEW. The output file from this software is not direct mathematical model, just weights coefficients and four additional parameters called Down offset Input (DI_k) , Down offset Target (DT_u), Up offset Input (UI_k) and Up offset Target (UT_u).

$$DI_k = \min(X_k);\ DT_u = \min(Y_u);\ UI_k = \max(X_k - \min(X_k));\ UT_u = \max(Y_u - \min(Y_u)).$$

Therefore, the rest of parameters are calculated as follows:

$$P_k = \frac{0.9}{UI_k};\ R_k = -\frac{0.9 \cdot DI_k}{UI_k} + 0.05;\ L_u = \frac{0.9}{UT_u};\ G_u = -\frac{0.9 \cdot DT_u}{UT_u} + 0.05.$$

5. Mathematical model for brake power, shaft speed and daily fuel oil consumption assessment

The output data derived from the CFD analysis in the trim optimization study, including parameters such as brake power, daily fuel oil consumption, shaft speed, were employed as input for training the ANN. Through this approach, the ANN establishes a unique mathematical correlation between draft, speed, trim, displacement, and the aforementioned performance parameters of brake power, daily fuel oil consumption, and shaft speed.

Subsequently, the applicability range of this model is defined within the boundaries: T= 7.5 - 8.7 m, V = 12.5 – 18 kn, Trim = -1.5 - +1.5 m, D = 18079 – 22884 m^3. The input dataset for training consists of a 63x7 matrix, where 63 represents the total number of conducted CFD simulations, and 7 denotes each parameter. Among these parameters, four are designated as the input layer, while the remaining three represent the output.

In the initial phase, all data was automatically normalized within the range of 0.05 to 0.95 before the training process. This normalization step is essential due to the sensitivity of activation functions to input data values that are excessively small or large.

For testing purposes, 8% (5/63) of the total input parameters were reserved, while the remaining data was allocated for training. The training process was programmed to do iteratively and stop when the target Root Mean Square (RMS) percentage error reached 1%.

$$RMS = \sqrt{\left(\sum\left[\left(\frac{T-O}{T}\right)^2\right]/N\right)}$$

where: T – targets, O – ANN outputs, N – number of values.

In the process of designing a neural network model, it is crucial to make informed decisions regarding the number of neurons in each layer and the quantity of hidden layers. These choices should align with the problem's complexity and the dataset's characteristics. Unfortunately, a single, unique mathematical model failed to achieve the desired RMS within a reasonable timeframe and the necessary number of iterations for training. Consequently, two distinct mathematical models were developed: one for brake power and daily fuel oil consumption, and the second for shaft speed.

The general form of the function for brake power is:

$$P_b = \frac{f_3\left(c_{Pb} + \sum_{i=1}^{7}(C_i \cdot f_2(b_i + \sum_{j=1}^{10}(B_{ij} \cdot f_1\left(a_j + \sum_{k=1}^{4}(A_{jk} \cdot (P_k \cdot X_k + R_k))))))\right) - G_{Pb}}{L_{Pb}}$$

The general form of the function for daily fuel oil consumption is:

$$DFOC = \frac{f_3\left(c_{DFOC} + \sum_{i=1}^{7}(C_i \cdot f_2(b_i + \sum_{j=1}^{10}(B_{ij} \cdot f_1(a_j + \sum_{k=1}^{4}(A_{jk} \cdot (P_k \cdot X_k + R_k)))))\right) - G_{DFOC}}{L_{DFOC}}$$

The general form of the function for shaft speed is:

$$n = \frac{f_3\left(c_n + \sum_{i=1}^{5}(C_i \cdot f_2(b_i + \sum_{j=1}^{8}(B_{ij} \cdot f_1(a_j + \sum_{k=1}^{4}(A_{jk} \cdot (P_k \cdot X_k + R_k)))))\right) - G_n}{L_n}$$

Configurations of neurons for both mathematical models are presented in Fig.5 and Fig.6.

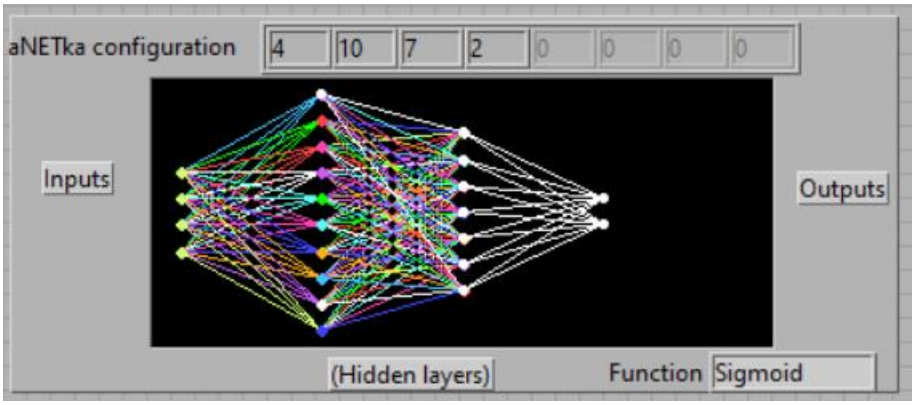


Fig.5: Configuration of neurons for brake power and daily fuel oil consumption model

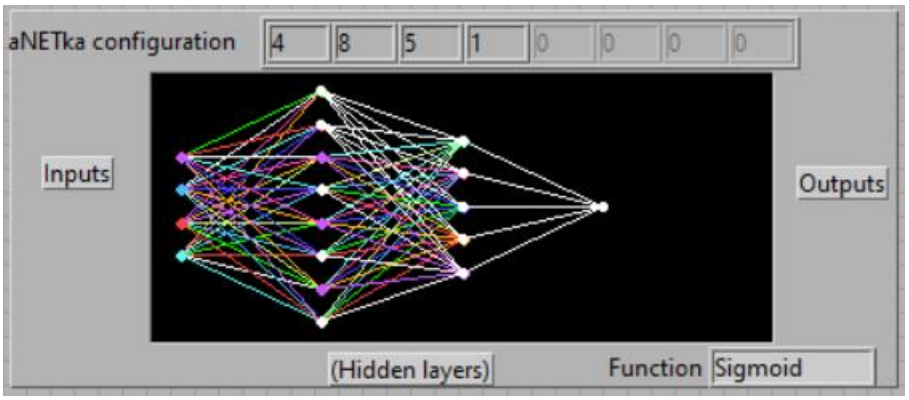


Fig.6: Configuration of neurons for shaft speed model

Standard deviations for relative differences between $P_b, DFOC$ and n obtained with ANN and by CFD are 0.6%, 0.6% and 0.2%, respectively.

6. Application for brake power, shaft speed and daily fuel oil consumption assessment

The obtained formulas in this form are not suitable for easy use; therefore, an application in the form of a *.exe* file was created in the MATLAB software under App Designer package, where these formulas have been programmed.

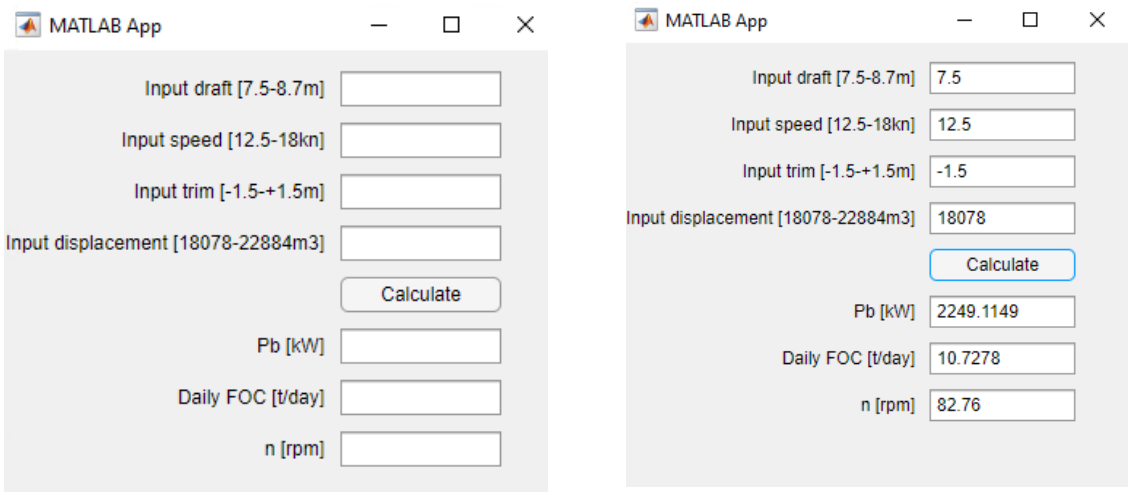


Fig. 7: Interface of developed application – Blank (left), Example (right)

The application has interface as shown in Fig.7. In the same figure, one example is shown. After entering four input parameters, and by clicking the "Calculate" button, the output values estimated

based on the previous formulas, are displayed. This means that at a certain draft and desired speed, the main engine should be run at 82.8 rpm. At this speed, the estimated brake power is 2249 kW, and the estimated daily fuel oil consumption will be 10.7 t/day.

7. Conclusions

Efficiency optimization within maritime operations is paramount for both economic viability and environmental sustainability. This article presents an investigation into trim optimization for the one RO-RO ship, employing CFD simulations and adhering to established guidelines. The research aims to elucidate the potential for fuel savings through seven trim adjustments under calm water conditions. The methodology employed in this study underwent typical validation to ensure its alignment with recognized industry standards. Utilizing CFD simulations and OWT, researchers conducted an in-depth analysis of the ship's propulsion system performance across varying operational profiles.

Trim optimization emerged as a main point of the investigation, offering a pathway towards significant fuel consumption reduction, up to 10.5%. Through systematic simulations at different speeds, drafts, and trim settings, researchers identified specific conditions convenient to substantial fuel savings. These findings underscore the significance of trim optimization as a strategic approach for enhancing maritime operational efficiency.

Furthermore, the study went into the development of advanced mathematical models leveraging ANN. These models are tailored to predict parameters such as shaft speed, brake power and daily fuel oil consumption under calm water conditions. Despite initial challenges in creating a unified model, the development of separate models for distinct parameters demonstrates methodological adaptability.

Looking ahead, the developed software tool will be put on a test to validate obtained predictive models to ensure its applicability in the real-world scenarios. Integrating this methodology into operational practices holds the potential to unlock substantial efficiency gains for this specific RO-RO ship and make a path beyond for the others. By embracing scientific innovation and leveraging data-driven optimization techniques, the maritime industry can chart a course towards enhanced efficiency and sustainability.

Acknowledgements

Authors would like to thank to Ocean Pro Marine Engineers LTD who provided necessary support in CFD simulations and guidelines. This work was supported by Ministry of Education, Science and Technological Development of Serbia (Project no. 451-03-65/2024-03/200105 from 5 February 2024).

References

ABS (2013), *Ship Energy Efficiency Measures, Status and Guidance*, American Bureau of Shipping, TX 05/13 50000 13015

BAL BEŞIKÇI, E.; ARSLAN, O.; TURAN, O.; ÖLÇER, A.I. (2016), *An Artificial Neural Network Based Decision Support System for Energy Efficient Ship Operations*, Computers & Operations Research 66, pp.393-401

BASSAM, A.M.; PHILLIPS, A.B.; TURNOCK, S.R.; WILSON, P.A. (2023), *Artificial Neural Network Based Prediction of Ship Speed Under Operating Conditions for Operational Optimization*, Ocean Eng. 278

DEMIR, U. (2019), *Evaluation of Operational Factors for the Energy Efficiency Optimization of High-Speed RORO Vessels by Trim Optimization*, MSc. Thesis, Piri Reis University

IMO (2009), *Guidelines for Voluntary Use of the Ship Energy Efficiency Operational Indicator (EEOI)*, Resolution MEPC.1/Circ.684, Int. Mar. Org., London

IMO (2011), *Amendments to the Annex of the Protocol of 1997 to Amend the International Convention for the Prevention of Pollution from Ships, 1973, as Modified by the Protocol of 1978 Relating Thereto*, Resolution MEPC.203(62), Int. Mar. Org., London

IMO (2013), *2013 Guidelines for Calculation of Reference Lines for Use with the Energy Efficiency Design Index (EEDI)*, Resolution MEPC.231(65), Int. Mar. Org., London

IMO (2016), *Amendments to the Annex of the Protocol of 1997 to Amend the International Convention for the Prevention of Pollution from Ships, 1973, as Modified by the Protocol of 1978 Relating Thereto*, Resolution MEPC.278(70), Int. Mar. Org., London

IMO (2021a), *Amendments to the Annex of the Protocol of 1997 to Amend the International Convention for the Prevention of Pollution from Ships, 1973, as Modified by the Protocol of 1978 Relating Thereto*, Resolution MEPC.328(76), Int. Mar. Org., London

IMO (2021b), *2021 Guidelines on the Operational Carbon Intensity Reduction Factors Relative to Reference Lines (CII Reduction Factors Guidelines, G3)*, Resolution MEPC.338(76), Int. Mar. Org., London

IMO (2022a), *2022 Guidelines on Operational Carbon Intensity Indicators and the Calculation Methods (CII Guidelines, G1)*, Resolution MEPC.352(78), Int. Mar. Org., London

IMO (2022b), *2022 Guidelines on the Reference Lines for Use with Operational Carbon Intensity Indicators (CII Reference Lines Guidelines, G2)*, Resolution MEPC.353(78), Int. Mar. Org., London

IMO (2022c), 2022 *Guidelines on the Operational Carbon Intensity Rating of Ships (CII Rating Guidelines, G4)*, Resolution MEPC.354(78), Int. Mar. Org., London

IMO (2022d), *2022 Guidelines for the Development of a Ship Energy Efficiency Management Plan (SEEMP)*, Resolution MEPC.346(78), Int. Mar. Org., London

IMO (2022e), *Development of Draft 2022 IACS Guidelines for the Use of Computational Fluid Dynamics (CFD) for the Purposes of Deriving the V_{ref} in the Framework of the EEXI Regulation*, Resolution MEPC.78/INF.16, Int. Mar. Org., London

ITTC (2014a), *7.5-03-02-03, Practical Guidelines for Ship CFD Applications*, ITTC Quality System Manual, Recommended Procedures and Guidelines

ITTC (2014b), *7.5-03-03-01, Practical Guidelines for Ship Self-propulsion*, ITTC Quality System Manual, Recommended Procedures and Guidelines

ITTC (2017), *7.5-02-02-03, Resistance and Propulsion Test and Performance Prediction with Skin Frictional Drag Reduction Techniques*, ITTC Quality System Manual, Recommended Procedures and Guidelines

ITTC (2021a), *7.5-03-02-04, Practical Guidelines for Ship Resistance CFD*, ITTC Quality System Manual, Recommended Procedures and Guidelines

ITTC (2021b), *Uncertainty Analysis in CFD Verification and Validation, Methodology and Procedures*, ITTC Quality System Manual, Recommended Procedures and Guidelines

JEON, M.; NOH, Y.; SHIN, Y.; LIM, O-K.; LEE, I.; CHO, D. (2018), *Prediction of Ship Fuel*

Consumption by Using an Artificial Neural Network, J. Mech. Science and Technology 32, pp.5785–5796

LE, T.H.; VU, M.T.; BICH, V.N.; PHUONG, N.K.: HA, N.T.H.; CHUAN, T.Q.; TU, T.N. (2021), *Numerical Investigation on the Effect of Trim on Ship Resistance by RANSE Method*, Applied Ocean Research 111

LEE, J.; YOO, S.; CHOI, S.; KIM, H.; HONG, C.; SEO, J. (2014), *Development and Application of Trim Optimization and Parametric Study Using an Evaluation System (SoLuTion) Based on the RANS for Improvement EEOI*, ASME 2014 33rd Int. Conf. Ocean, Offshore and Arctic Eng. (OMAE2014), San Francisco

LYU, X.; TU, H.; XIE, D.; SUN, J. (2018), *On Resistance Reduction of a Hull by Trim Optimization*, Brodogradnja 69/1, http://dx.doi.org/10.21278/brod69101

MOUSTAFA, M.M.; YEHIA, W.; HUSSEIN, A.W. (2015), *Energy Efficient Operation of Bulk Carriers by Trim Optimization*, 18th Int. Conf. Ships and Shipping Research, NAV 2015, Lecco

MTCC-Asia (2017), *Guidelines on Ship Trim Optimization – Based on Machine Learning Method*, The Global MTCC Network

PETURSSON, S. (2009), *Predicting Optimal Trim Configuration of Marine Vessel with Respects to Fuel Usage*, University of Iceland

REICHEL, M.; MINCHEV, A.; LARSEN, N.L., (2014), *Trim Optimization – Theory and Practice*, TransNav Int. J. Marine Navigation and Safety of Sea Transportation 8/3, http://dx.doi.org/10.12716/1001.08.03.09

SHERBAZ, S.; DUAN, W. (2014), *Ship Trim Optimization: Assessment of Influence of Trim on Resistance of MOERI Container Ship*, Hindawi Publishing Corporation, DOI: http://dx.doi.org/10.1155/2014/603695

TARELKO, W.; RUDZKI, K. (2020), *Applying Artificial Neural Networks for Modelling Ship Speed and Fuel Consumption*, Neural Computation & Application 32, pp.17379–17395, https://doi.org/10.1007/s00521-020-05111-2

ZIARATI, R.; BHUIZAN, Z.; DE MELO, G.; KOIVISTO, H.; LAHIRY, H.; OZTURKER, E.; AKDEMIR, B. (2017), *MariEMS Train the Trainee (MariTTT) Courses on Energy Efficient Ship Operation*, MariEMS

ZUREK, S. (2007), *Labview as a tool for measurements, batch data manipulations and artificial neural network predictions*, National Instruments, Curriculum Paper Contest, Przeglad Elektrotechniczny, NR 4/2007, pp.114-119

Wind Challenger Project - Updates & Future Plans

Changbae Jin, Mitsui O.S.K. Lines, Tokyo/Japan, changbae.jin@molgroup.com
Yoichi Wakabayashi, Mitsui O.S.K. Lines, Tokyo/Japan, yoichi.wakabayashi@molgroup.com
Nobuyuki Onishi, Mitsui O.S.K. Lines, Tokyo/Japan, nobuyuki.onishi@molgroup.com
Yoshihiko Sugimoto, Mitsui O.S.K. Lines, Tokyo/Japan, yoshihiko.sugimoto@molgroup.com

Abstract

A telescopic type of hard sail solution for large vessels called Wind Challenger has been developed by Mitsui O.S.K. Lines and Oshima Shipbuilding Co. Ltd. through joint research with research institutions, and a classification society. The Wind Challenger has been installed on a large bulk carrier named Shofu-maru and has been successfully constructed and delivered for operation in 2022 and has completed 8 voyages. In addition, there are plans to install it on various types of large vessels in the future, and development and design for this purpose are currently underway. This paper provides a general introduction to the Wind Challenger project, its technical background, the performance measurement, and evaluation of the Shofu-maru during actual seagoing, the lessons learned from the Shofu-maru installation, and future plans.

1. Introduction of the Wind Challenger project and solutions using the Wind Challenger from Mitsui O.S.K. lines

In April 2018, the IMO (International Maritime Organization) adopted a greenhouse gas (hereafter referred to as GHG) reduction strategy in the wake of ever-increasing efforts to prevent global warming since the entry into force of the Paris Agreement and decided to reduce total GHG emissions from ships by 50 percent by 2050. In recent years, the movement toward carbon neutrality has become more active around the world.



Fig.1: Shofu-maru the 100,000 deadweight ton class bulk carrier installed the Wind Challenger

A wind-assisted propulsion system uses sails to convert the renewable energy of the wind to provide thrust directly to a vessel. Large commercial vessels today depend on fossil fuels for almost all of their propulsion, but by adding wind power as direct propulsion, they can reduce fossil fuel consumption without changing speed. By maximizing and utilizing the sail installation, or technology

of old sailing ships, with modern technology, we reduce fuel consumption and significantly reduce GHG emissions on large cargo ships.

Since the start of the joint industry project organized by the University of Tokyo in 2009, an innovative telescopic hard-sail system has been proposed, and in 2015, its effectiveness was confirmed through tests on a 40% scale model.

Mitsui O.S.K. Lines (hereafter referred to as MOL) partnered with Oshima Shipbuilding to take over this project. In 2019, the Approval in Principle certification was issued by Class NK, and finally, in October 2022, the first Wind Challenger vessel "Shofu-maru" was delivered from Oshima Shipbuilding.

2. What is the Wind Challenger?



Fig.2: The hard wing sail named Wind Challenger has been developed by MOL

The mechanism for generating thrust with the sail is the same principle on a yacht. The hard wing sail, which combines fibre reinforced plastic (hereafter referred to as FRP) and steel frames, can always maintain an optimal wing shape, and lift is generated from that wing shape. The forward component of this lift and drag becomes auxiliary thrust. The sail is automatically controlled to maintain the optimal angle of attack relative to the wind direction. An illustrative diagram of thrust generation by the sail is shown in Fig.3.

Thrust can be generated in the forward direction if the wind is blowing from any direction other than about 30° to the left or right of directly ahead. The most efficient wind comes diagonally from behind and contributes to both the lift and drag generated by the sail in the forward direction.

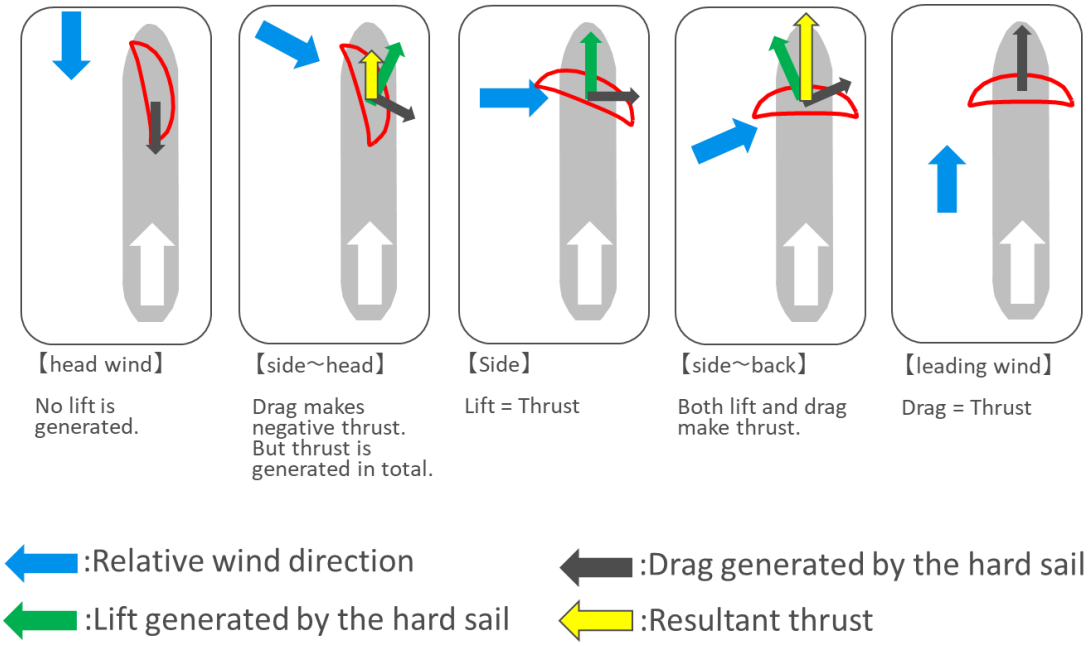


Fig.3: Wind-assisted thrust mechanism for Wind Challenger

2.1. Technical features of Wind Challenger

The sail is composed of rigid materials and structural components, and is designed as a hard sail that can maintain its wing shape at all times. It can be adjusted in stages at a time from one stage (reefed state) to four stages (full sail state). In addition, the angle and height of the sail are automatically controlled according to wind direction and wind speed. Even seafarers without sailing experience or knowledge can operate it just like a normal ship.

2.1.1 Main materials and the symmetric wing section

The material for the sail is made of glass fibre reinforced plastic (GFRP) because it is important to reduce the weight of the sail so that it does not affect the volume of cargo that can be loaded on merchant ships. The weight reduction allows for a larger total sail area and maximizes utilization for thrust, and the installation of sails minimizes the impact on the ship's balance and dramatically increases operational safety.

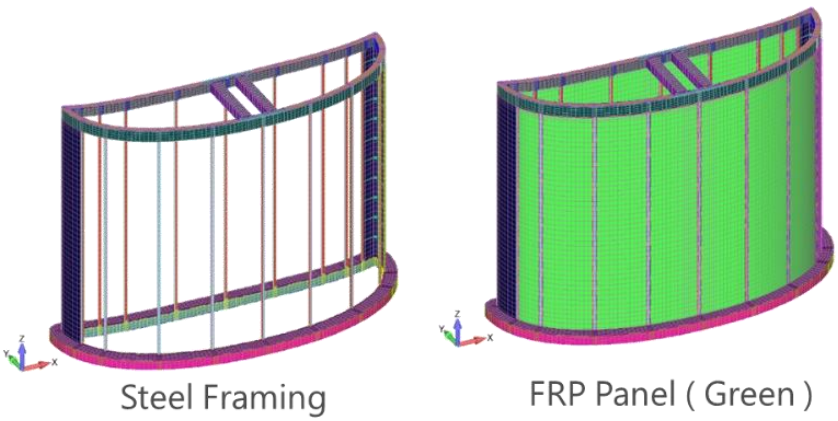


Fig.4: Sail structure

The Wind Challenger has a symmetrical wing section on its sail to maximize the operating angle range where wind propulsion can be generated. It also minimizes resistance from the sail at angles where propulsion cannot be generated.

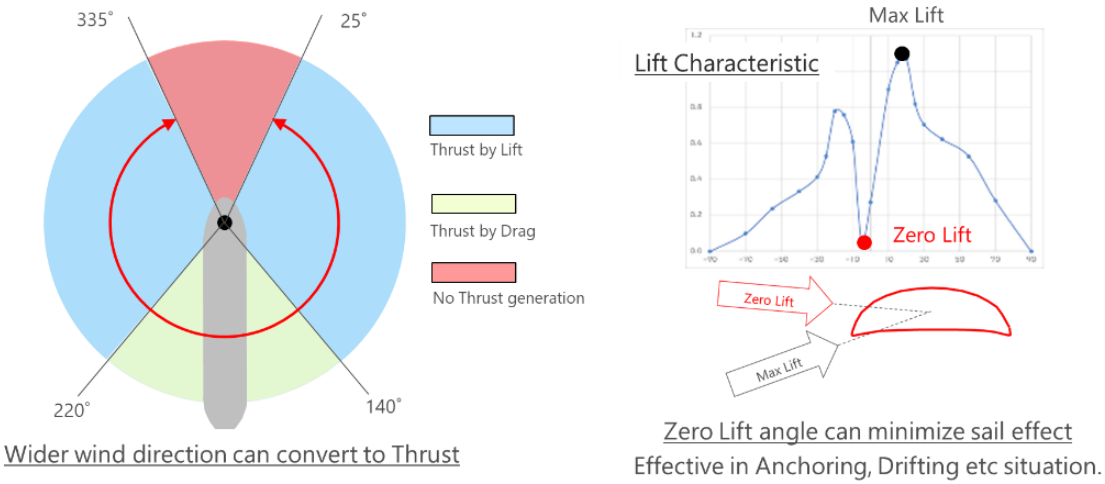


Fig.5: Operatable wind directions and lift characteristics

2.1.2 Telescopic structure

The Wind Challenger has a telescopic structure to maximize wind-assisted propulsion depending on various sailing situations. In situations where it is necessary to maximize wind propulsion, it operates in "Extend Sail" mode, expanding the sail to its maximum size. In cases where wind propulsion is not needed, such as in-port navigation, it operates in "Reef Sail" mode, folding the sail to its minimum size and maintaining an angle to ensure the maximum field of view for the navigator.

The control of the sail is not only about the angle of attack but also includes the control of the telescopic mechanism, which is an important feature of the sail of this ship. The purpose of this control is to control the overturning moment applied to the base of the sail. It can also be described as a kind of safety device.

The sail receives two kinds of forces: the wind pressure, such as the lift generated by the wing, and the inertial force of the sail itself caused by the ship's motion. In order to detect both the ship's motion, which has amplitude and period, and the wind pressure simultaneously and comprehensively, a strain sensor is installed at the base of the sail, and the extension and contraction control of the sail is performed according to the strain level.

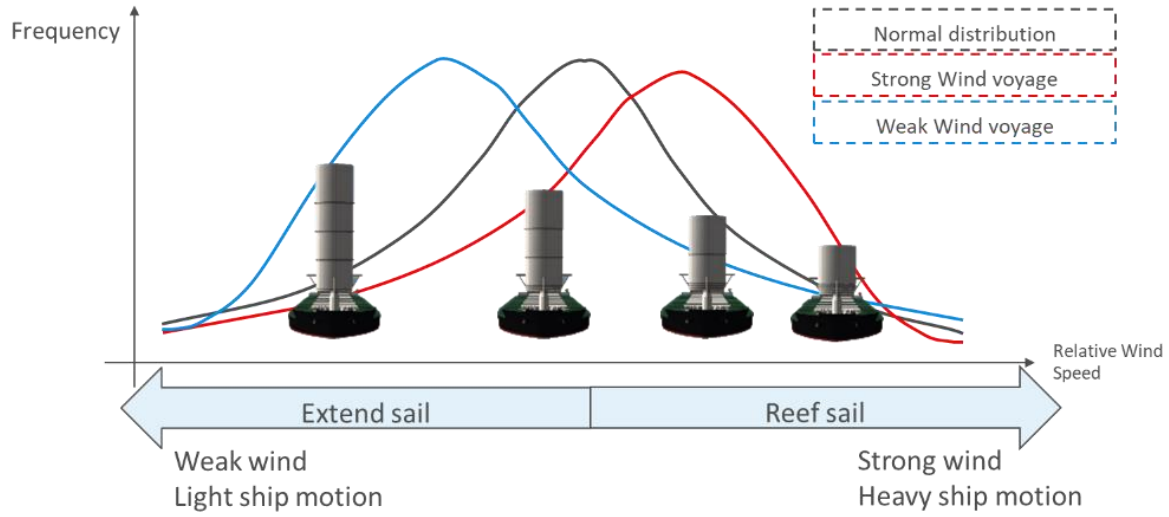


Fig.6: Height controls for Wind Challenger

Specifically, when the stress is high (i.e., the wind is strong or the ship's motion is large), the sail is shortened by one stage, and when the stress is low (i.e., the wind is weak or the ship's motion is small), the sail is extended. By controlling in this way, the stress on the base structure can be kept within a certain range, thereby limiting the range of risk in terms of operational strength.

Since waves have a certain correlation with wind speed, Fig.6 shows a guideline for wind speed and the state of the sail on a certain assumed route.

2.1.3 Automatic control system

Sailing ships need to adjust the direction and tension of their sails depending on wind conditions (strength and direction) and require advanced knowledge and experience. The Wind Challenger automatically controls sails to make it easier for ordinary crew members to use wind power as efficiently as possible. Sails detect the strength and direction of the wind with sensors, extend (lengthen) the sail when the wind is weak, reef the sail when the wind is strong, and rotate the sail automatically.



Fig.7: On-board sail status and control panel

3. The first Wind Challenger vessel, Shofu-maru

3.1 Design of the Shofu-maru

The 100,000 deadweight ton (hereafter referred to as DWT) class bulk carrier Shofu-Maru, owned and operated by MOL, is equipped with a Wind Challenger, a wind-assisted, rigid-wing sail wind propulsion system that uses the wind received by the vessel while underway as propulsion. Shofu-Maru was built at the Oshima Shipbuilding Co. Ltd., Nagasaki Prefecture, Japan in October 2022. The vessel carries coal from Australia, Indonesia, and North America for use in thermal power plants in Japan.

As shown in Table I and Fig.8, the size of the sail is about 15 m in width, about 54m in height from the upper deck in the full sail state, and about 23 m in the reefed state. In the full sail state, it is approximately the height of an 18-story building.

Table I: Principal particulars of Shofu-maru

Length (LOA)	235.00 m
Breadth (Mid)	43.00 m
Depth (Mld)	20.00 m
Draft: Designed	12.80 m
Draft: Scantling	13.80 m
Deadweight	104,422 DWT

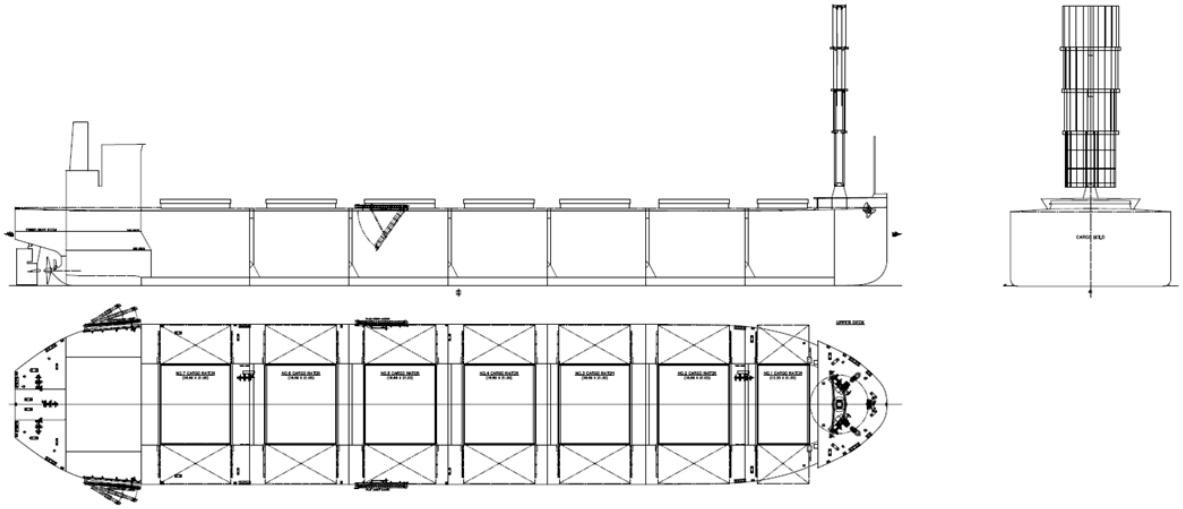


Fig.8: General arrangements of Shofu-maru

3.2. Effect of reducing GHG emissions by installing sails

In this project, the computation fluid dynamics (hereafter referred to as CFD) and wind tunnel experiments have been conducted to estimate the thrust generated by sails, and polar plots were generated.

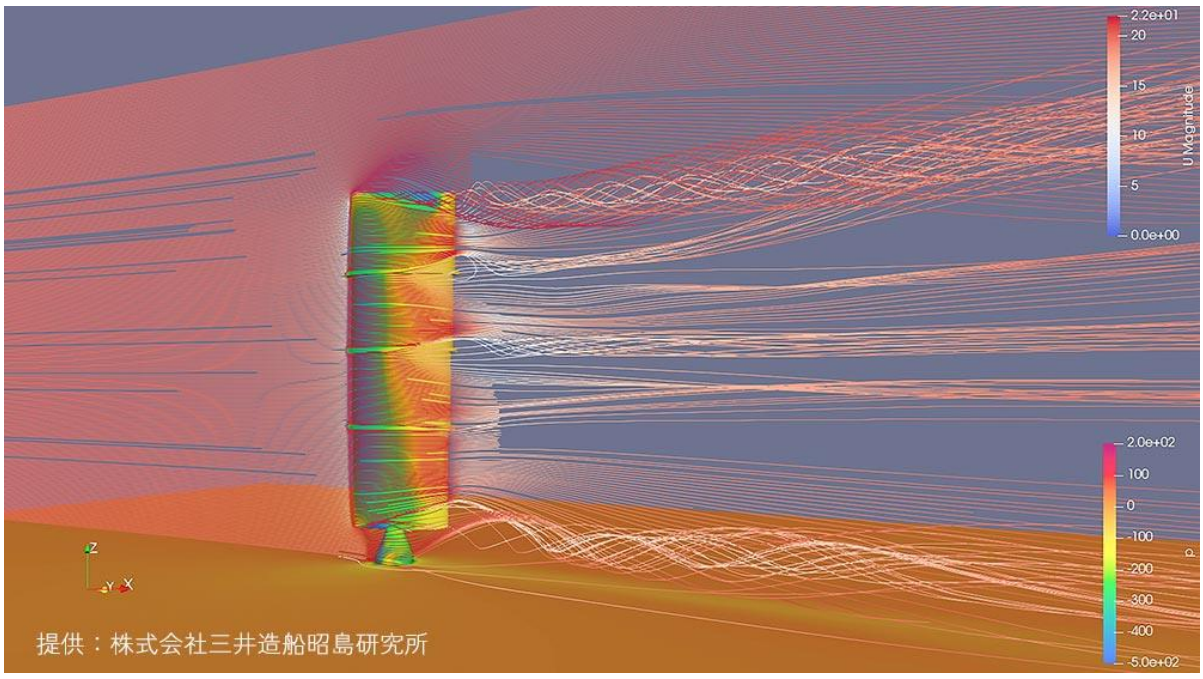


Fig.9: Performance calculations for the Sail using CFD by Akishima Laboratory

By multiplying the polar diagram with the estimated wind conditions and ship speed, the total amount of wind assistance (auxiliary thrust) in the route was calculated and compared with the absence of auxiliary thrust by sail. Considering the size of the vessel, the auxiliary thrust is expected to be converted into fuel efficiency, and for Shofu-maru the 100,000 DWT class bulk carrier, it is validated to be reduced by 5% on the Japan-Australia route and 8% on the Japan-North America West Bank route on year-average basis.

3.3. Impact on navigational performance

The impact on navigational performance is directly related to operational safety and therefore requires careful consideration. There are two specific items to consider under navigational impact: impact on bridge visibility and impact on manoeuvring performance. Both items have international standards that should be met.

After these reviews, a motion model and a 3D model of the harbour are used for a comprehensive review. A 360° bridge simulator, which is used for crew training, is also used to evaluate the port entry and exit simulation.

3.3.1 Impact on bridge visibility

The international standard for the range of visibility obstruction on ocean-going vessels is a total of 10° or less for an obstruction from the bridge observation position within 5°. On the proposed vessel, the angle of visibility obstruction by the sail from the bridge is 4.6°, which meets the standard. Ideally, there should be no obstruction angle, so an Augment Reality system with some cameras that can capture the front of the sail and confirm it from the bridge is equipped as an auxiliary monitoring device.

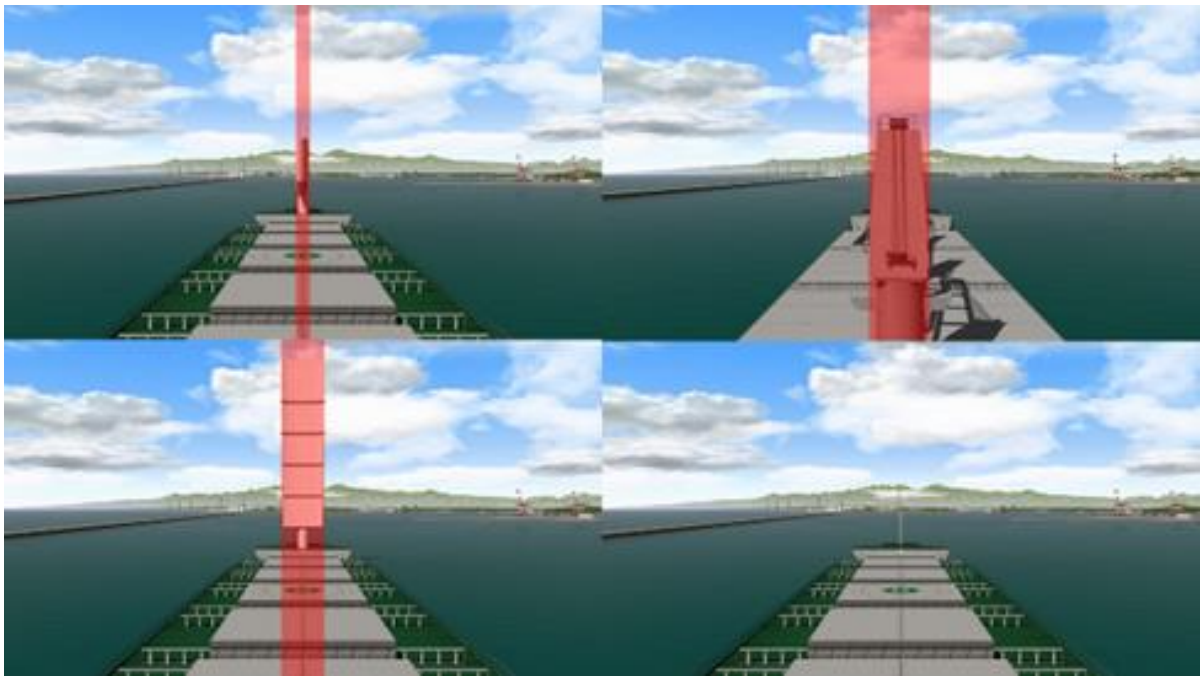


Fig.10: Impact on bridge visibility

3.3.2 Impact on manoeuvring performances

A motion model of a 100,000 DWT bulk carrier without sails had already been created in previous simulations by MOL, and this motion model was calibrated with actual ship trial

information. Based on this motion model, a motion model for the Wind Challenger was created with modifications to account for the effect of the sails, and verification was conducted in standby mode. Standby mode is the mode used when navigating in harbours or narrow straits, and if the navigational impact is significant at that time, there may be restrictions on entering and leaving the harbour. Basic manoeuvring performance such as course-keeping performance, turning performance and zig-zag navigations were verified and confirmed to be equivalent to normal vessel operation. Operations such as leaving the berth with tug assistance and turning on the spot were also confirmed in various wind conditions. An example of the results of these considerations is shown in Fig.11.

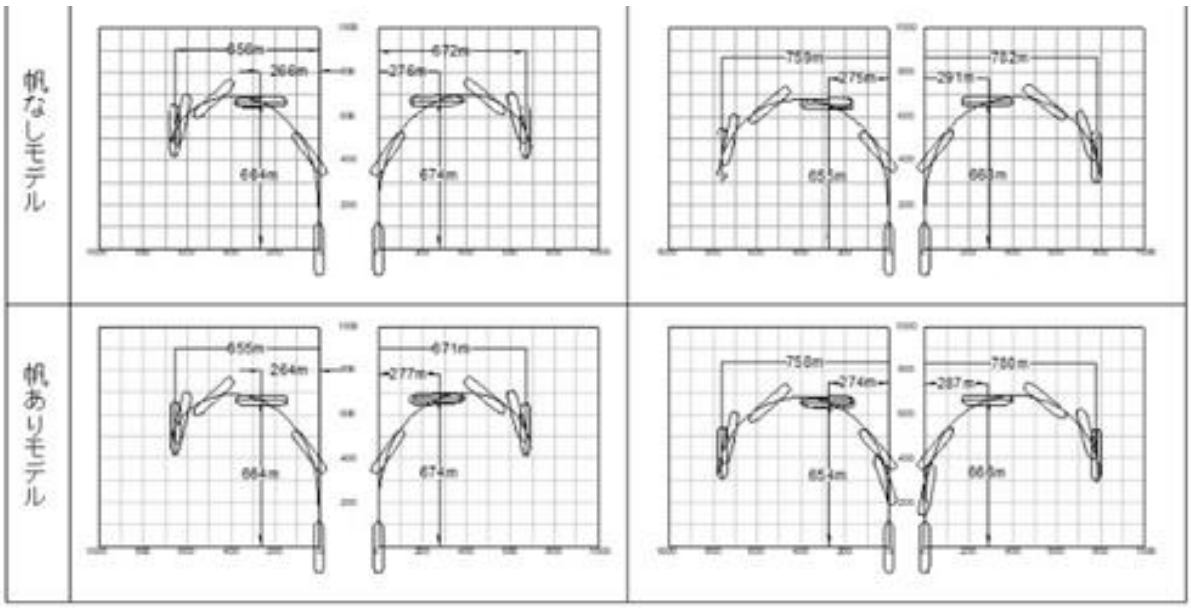


Fig.11: Turning ability simulations

3.3.3 Bridge simulations

A domestic port was used as a model port, the prevailing sea and wind conditions at that port were reproduced, and it was checked whether the ship could safely enter and leave the port using general navigational techniques, referring to standard pilotage guidelines, etc., from the pilot's association.

First, as a method, a ship without sails was navigated into and out of the port, referring to the pilot's navigation guidelines, and then the Wind Challenger ship was navigated to track the course of that ship. Not only the navigational parameters of the ship, but also the changes in the performance of the tugboats that assist in entering and leaving the port were recorded by the simulator. This allowed the impact of the presence or absence of sails on navigation to be quantitatively extracted and verified. Especially pilots and a harbour-master from the Port of New Castle have been invited and validated to the bridge simulator.

After several patterns were verified, it was confirmed that it could be handled with normal navigation techniques. These results were compiled into a report and more than 30 pilot associations, port authorities, loading and unloading terminals, both nationally and internationally, were visited. The project was explained, the impact on navigability associated with port entry was demonstrated, and port entry permits were obtained.



Fig.12: Full mission bridge simulator

3.4. Construction and sea trials of the Wind Challenger on Shofu-maru

As a wind propulsion system installed on actual ships, not only the FRP panel and steel framing parts of the optimized sail design for the Wind Challenger, but also the operating parts with pumps and the spar parts that bear the load of the sail were well designed and constructed, and successfully installed on the Shofu-maru.



Fig.13: Wind Challenger construction for Shofu-maru

After the construction was completed, various tests were carried out to verify whether it operated as designed and could withstand sufficient load. After launching, the wind assist effect was validated with numerical data through the actual sea trials.

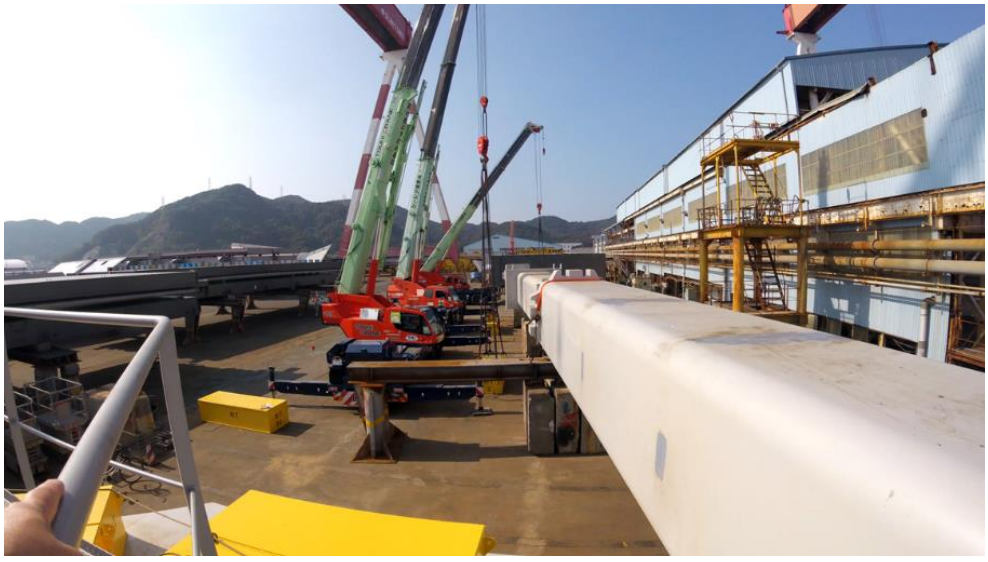


Fig.14: Load test carried out by Class Surveyor for strength verification

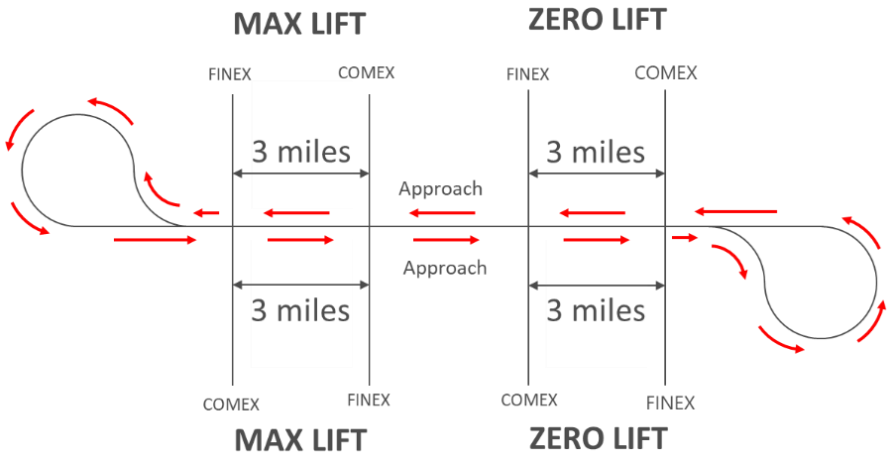


Fig.15: Performance trials running sequence

4. Actual monitoring of ocean-going for Shofu-maru

4.1 Summary of the maiden voyage

As shown in Table II and Fig.16, the records and evaluations of the Wind Challenger during the maiden voyage have been summarized and reported.

Table II: Summary of maiden voyage for Shofu-maru

	Ballast Voyage	Laden Voyage
Departure port	OSHIMA, JAPAN	NEWCASTLE, AUSTRALIA
Departure date	7th Oct 2022	25th Oct 2022
Destination port	NEWCASTLE, AUSTRALIA	NOSHIRO, JAPAN
Arrival date	24th Oct 2022	15th Nov 2022
Hard sail operation rate(*1)	70.1%	87.6%
25-335deg rel. wind direction rate(*2)	73.7%	64.6%
Hard sail assist rate(*3)	52.0%	54.0%

*1: Percentage of time when the hard sail was in Auto. mode

*2: Percentage of time when the relative wind direction was between 25 and 335 deg.

*3: Percentage of time when the sail was generating thrust

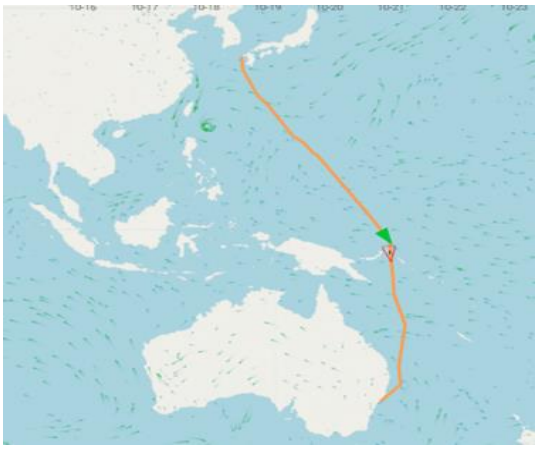


Fig.16: Route of the maiden voyage for Shofu-maru

4.2 Verification methodology of fuel savings for Wind Challenger

A Classification Society has been asked by MOL to validate the fuel saving calculation method of the Wind Challenger project, which uses CFD and wind tunnel test data to estimate the performance of the wind-assisted ship propulsion.

The validation method consists of the standard power calculation process with and without sail thrust, the adjustment of relative wind directions and wind speeds based on CFD analysis, and the calculation of the average performance for the wind-assisted ship propulsion based on 18 in-service trials.

At the end of the validation, the Classification Society confirmed that the proposed method and the fuel saving calculation tool were appropriate and correctly defined and functional. They also noted that the method was in good agreement with the ISO 15016:2015 and ISO 19030:2016 standards.

5. Future plans for installation to various kinds of vessels

Since the installation and operation of the prototype Wind Challenger on the Shofu-maru, MOL is planning to install the Wind Challenger on various types of vessels, including VLCCs and LNGCs. The plans are in the process of developing optimal designs, and the appropriate number and size of sails will be optimized and applied to these different types of vessels.



Fig.17: Installation example for VLCC (4 sails)



Fig.18: Installation example for LNGC (2 sails)

The Wind Challenger project will be able to produce an average of 10 vessels per year and will be installed on three vessels by 2025 and on 25 vessels by 2030. In addition, after 2035, it is planned to develop a next-generation hull form specializing in wind power utilization with multiple MOL-developed Wind Challenger sails beyond the wind-assist concept.

A 1% reduction in GHGs means also a 1% reduction in fuel costs. Currently, fuel oil is being run on, however, with the use of next-generation fuels such as ammonia, methanol, and hydrogen in the future, the value of 1% will increase.



Fig.19: Wind Hunter of the future concept vessel

6. Conclusions

MOL has successfully delivered the Shofu-maru, the first ship equipped with a new concept of wind-assisted propulsion system named the Wind Challenger. It is successfully contributing to actual navigation, and we are monitoring and analysing it to reflect a more efficient improved design. In addition, a special weather routing system is being developed for the Wind Challenger to appropriately catch good winds, which will be applied to the next vessels.

The second vessel equipped with the improved Wind Challenger design is scheduled for delivery in 2024, and there are also plans to install units on an existing operational vessel as a retrofit design. The Wind Challenger enables significant fuel savings in the installation of multiple sails. It has the potential to solve fuel cost and tank space issues in the rapidly advancing transition to renewable energy.

The Wind Challenger project is planning to install it on various types of vessels, and development and design for this purpose are currently underway. The appropriate number and size of sails will be optimized and applied to these different types of vessels.

References

ISO (2015), *Ships and marine technology – Guidelines for the assessment of speed and power performance by analysis of speed trial data*, ISO 15016:2015, Int. Standard Org., Geneva

ISO (2016), *Ships and marine technology - Measurement of changes in hull and propeller performance Part 2: Default method*, ISO 19030-2:2016, Int. Standard Org., Geneva

ONISHI, N.; FUKUSHIMA, H. (2019), *Wind Challenger Sail fitted on 100,000 DWT bulk carrier*, RINA-IWSA Wind Propulsion Conf., London

OUCHI, K.; SHIMA, K.; KIMURA, K. (2023), *Wind Hunter - The Zero Emission Cargo Ship Powered by Wind and Hydrogen Energy*, RINA-IWSA Wind Propulsion Conf., London

WAKABAYASHI, Y. (2023), *Delivery of the 1st Wind Challenger ship "SHOFU MARU"*, RINA-IWSA Wind Propulsion Conf., London

The Design of the Ships' Hulls based on Application of Aircraft Wing and Fuselage Engineering Principles

Roland Lindinger, LR-Shipdesign ("LRSD"), Zug/Switzerland, r.lindinger@lr-ship-design.com
Volkmar Wasmansdorff, Movena, Bremen/Germany, wff@movena-group.com

Abstract

This paper presents the application of new findings of fluid sciences in order to significantly reduce the overall ships' resistance and to improve the propulsion. "AFT OPT" technology applied to ship hulls originates from the transfer and application of principles used in the design of aircrafts. The application of these physical principles to hydrodynamical and hydromechanical principles using proprietary CFD software leads to a new design approach for the aft hull. Hull shape and lower hull resistance lead to a much better filled propeller disk, wake flow and rudder characteristics. As a result, the main engine power may be reduced by more than 6%.

1. Introduction

Corporate responsibility for environmental protection, sustainability and IMO regulations to limit emissions from shipping require more measures than ever before for maritime stakeholders.

For compliance w/IMO regulations, EEDI, CII, investors must apply all measures available to protect their investment on long-term basis. Besides fuel selection, design of ships' hulls is an option for sustainable compliance. Main unique selling points for the holistic AFT OPT solution include the facts that AFT OPT vessels always consume substantially less fuel – whatever fuel is used. AFT OPT vessels therefore establish a new "best-in-class" benchmark. Substantial OPEX reduction increases the competitiveness of market participants.

In order to generate OPEX savings already at the birthplace of ships evaluation of hull design and performance according to a speed profile must be added to the most important selection criteria in addition to "easy-to-evaluate" criteria "price + delivery time + performance at design speed", LRSD had invited and involved a limited number of interested parties for joint development projects (JDP). World's top container liner companies are involved in technology review, get access to model basin results to verify these new applied sciences.

The first contract has been signed with a leading Chinese ship building and financing group in 2023 for a series of container feeder vessels after technology verification and validation of superiority of AFT OPT. Ship model tests were executed, among others, at MARIN (NL). These vessels shall be built for a world leading container liner company.

A joint development project (JDP) and with a Korean Shipbuilding Group for ultra large container vessels started in April 2024, model tests shall be done in Q3/2024 in South Korea.

Earlier, the technology has been developed for and applied to optimize vessels at SVA Vienna (since 2018) and a bulk carrier at HSVA (2022) for the purpose of validating the technology as such. Classification societies and flag states are usually invited to join the tests at site as impartial witnesses.

2. Challenges in shipbuilding

Due to the holistic U-shape - common in shipbuilding - with attached bow and stern, there are only a few development opportunities to generate cost-effective advantages for the shipyard and the shipowner or charterer to increase their competitiveness. LRSD with AFT OPT offers a new approach and extends progress in ship technology.

The main problem is the increasing hull resistance due to the above proportion increasing block coefficient (volume resistance of the submersible part of a ship when fully loaded) and the displacement pressure due to the speed. All this increases the power required exponentially and the fuel consumption increases significantly while at the same time the propulsion efficiency is reduced.

Historically, the analysis of fuselage flow, the flow of air around the wings of aircrafts, led to the question at LR-Shipdesign, whether with a specific new approach can be made to improve the flow of water underneath of the keel from bow to stern and to modify the stern region. Slight bow modification allows to deliver best "starting point" for AFT OPT calculations and best results for the holistic approach as the water regime is interconnected from bow to stern.

Based on shipbuilding theories, the basic design conditions in new buildings are regulated by validated rules. However, not all solutions based on physical possibilities of fluid dynamics and especially fluid mechanics are applied nowadays in shipbuilding. Applied physics offers several possibilities that have previously been only used in aviation, but not in shipbuilding.

3. Original observations as basis for technology development of AFT OPT

3.1. MIRAGE 2000, Fig.1

The "area rule" (developed in 1943) influences the laminar flow through a negative pressure form on the wing/fuselage. This significantly postpones the separation of the flow of air from the aircraft's body at a speed range close to speed of sound (transonic).

3.2. Wing airliner, Fig.2

Triangles and flaps used as vortex generators on the wing increase the resistance during normal flight operations only slightly. During take-off and landing, the angular position of the wing creates a very special type of vortex ("bag vortex"), which generates a higher lifting moment by compressing the flow and thus reduces the landing speed of an aircraft. This is necessary for safety reasons at slow landing speeds.



Fig.1: Mirage



Fig.2: Wing airliner

4. AFT OPT technology

AFT OPT is nothing less than a detailed analysis of the flow of water cells underneath of a ship's hull – from bow to rudder – with a unique LRSD calculation and CFD approach with application of previously unutilised physical effects for ship design in order to create a more efficient hull form.

The core result of AFT OPT technology application includes a slightly modified rear hull bottom area to keep the water flowing longer along the hull through displacement. This reduces energy losses and the energy gained is fed through the shape to the effectors of the propulsion comparable to a water jet.

The cascade effect: Less energy is lost from the hull, fewer waves are generated, and more water is directed towards the propeller disk. Furthermore, the wake field is more uniform, the better preconditioned water pattern reaches the propeller disk, so that the entire disk surface is filled more evenly. In consequence, both, propeller and a twisted rudder – designed to deal with the vortex flow and to increase propulsion – contribute to the much more efficient energy utilization. All this can be implemented in ship newbuildings with minimum commercial engineering effort compared with the OPEX savings. Fig.4 shows a design example for a 76000 dwt bulk carrier.

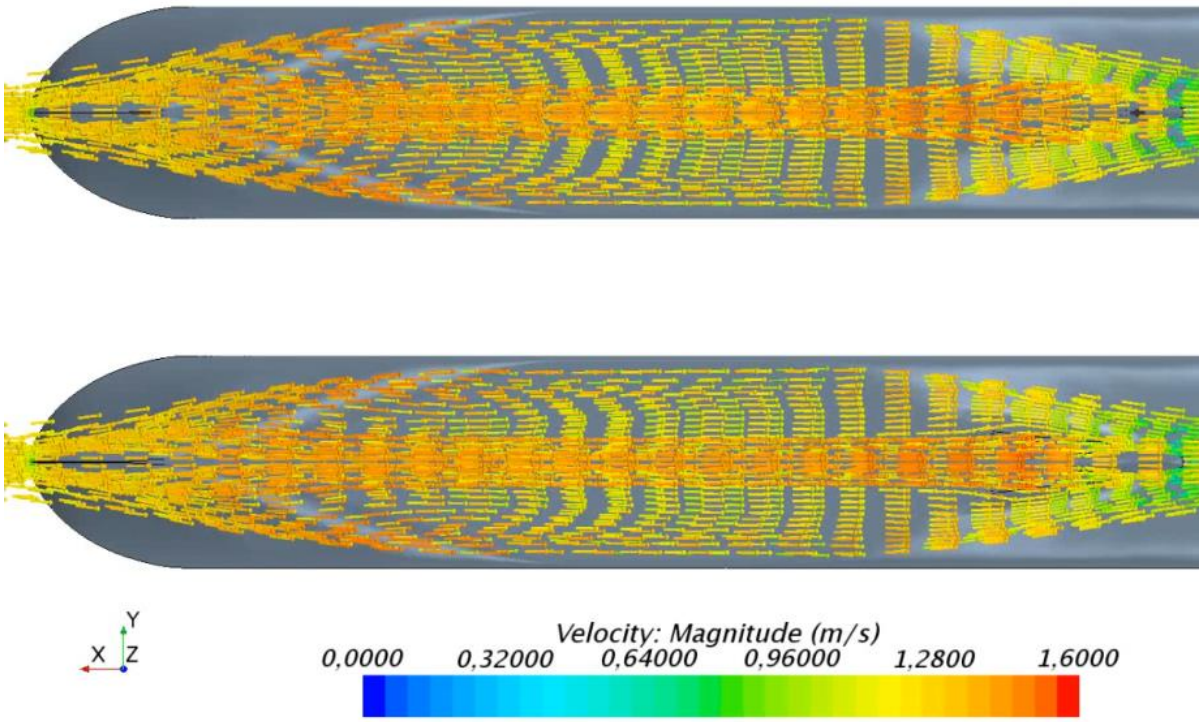


Fig.3: Influence of LRSD aft ship on the flow at the ship's hull. Original design (top) and LRSD design with narrower streamlines, closer in parallel to the x-axis

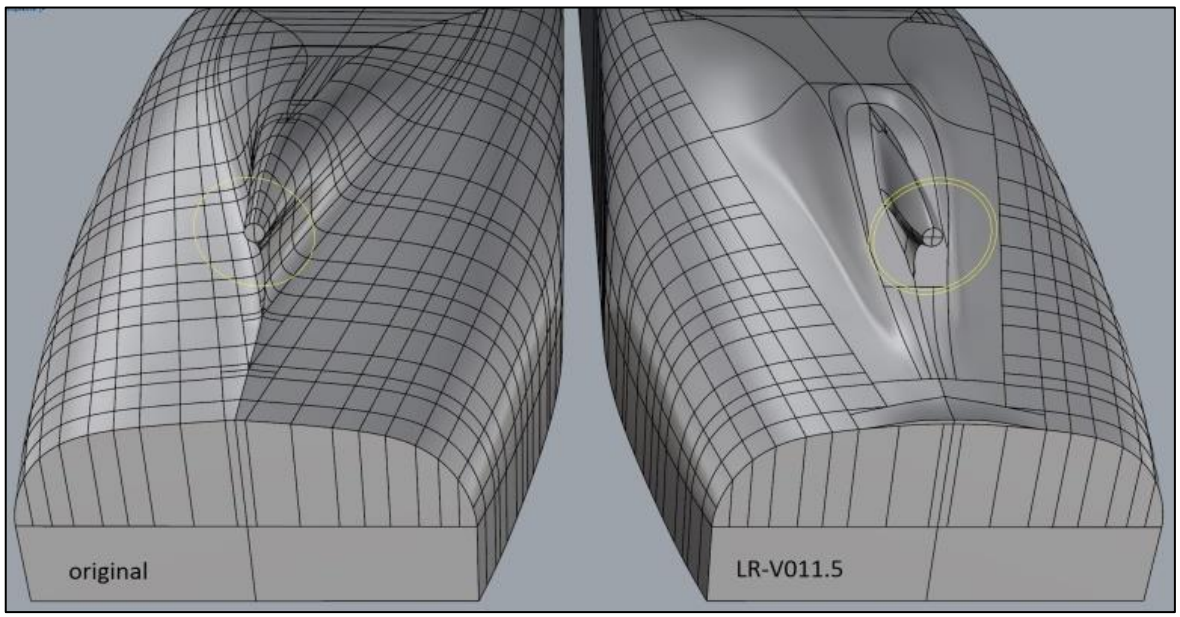


Fig.4: Bulk carrier tested in 2022 at HSVA; special shape of AFT OPT hull modification with 2 propeller options

4.1. Application of Coandă effect et al. to ship design

LRSD has investigated how to use the findings of fluid sciences (such as the "Coandă effect", etc.) to significantly improve the overall ships' resistance and propulsion for ship propulsion while adhering to the given shipbuilding regulations. LRSD has developed an own CFD software for this, as even latest standard programs for CFD only partially cover possible improvements. LRSD utilises the aft bow in connection with the ramp to apply the Coandă effect, for example.

LRSD always looks at the entire hull and on a holistic approach to record all parameters for an efficient hull design. The result of AFT OPT® technology application is a precisely calculated shape for aft ship bottom area and stern, designed for maximum improvement of hydrodynamics and propulsion and for hydro-mechanical optimisation of propeller and rudder.

4.2. Practical approach

LRSD follows the design specification with regards to sailing speed, design draft, main engine performance and the lowest ship construction effort while adhering to the freight volumes. The unique LRSD shape in the aft ships bottom area, the stern of the ship, improves the induced resistance and reduces energy losses due to displacement. An additional adapted pressure impulse is transmitted to the propeller for higher propulsion efficiency.

All this results in the following technical and physical advantages:

- The overall resistance of the hull decreases by reducing the peaks of the pressure fluctuations along the hull (by minus 3 to 6 %).
- The improved flow to the propeller means that more thrust can be generated at lower main engine speed, resulting in more efficient propulsion. The required power amounts to abt. minus 6-8% PD.
- In some cases (mainly for tankers, bulk carriers) minor modifications of the main engine room might be necessary as an adaptation to the modified aft ship lines. This will be done in accordance with the main engine manufacturer's requirements.

4.3. The physical effects, impressions, charts

Induced by the special AFT OPT form and input edges of the ship's bottom semi-circular form, the applied pressure is reduced, and the water flow is accelerated due to the indentation. Thus, energy losses are reduced and the flow pattern along the edge lines (shoulder) and stern as well as the trailing whirl are optimized.

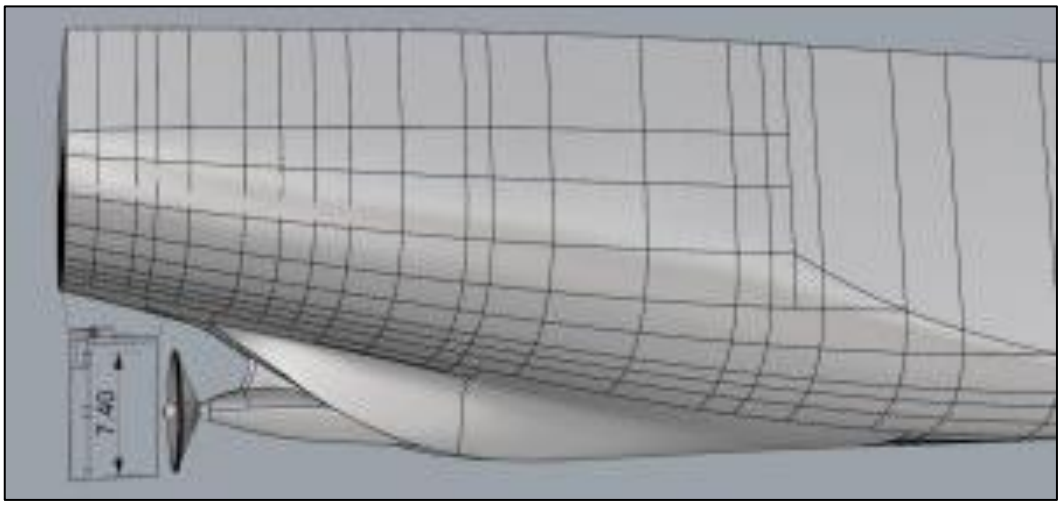


Fig.5: Bulk carrier, tested in 2022 at HSVA, Hamburg. 7.4 m propeller diameter

This system essentially improves the water flow to the propeller and rudder. The propeller gains more pressure due to a more uniform inflow, especially in the 12 o'clock position and by an adaption of the transmission and/or propulsion further savings are generated.

The resistance of hull without attachments was improved for container vessels and bulk carriers, by more than 3-4% in full scale (4-5% in model scale). The overall result for the container vessel and bulk carrier reached much more than 6% improvement in full scale with propeller and rudder attached during first trial. Further minor improvements can be made possible and verified in future tests.

Fig.6 shows of streamlines at the stern for a Panamax bulk carrier, as an example. Compare line thickness, smaller red zone in the aft area; reduced pressure regime, reduced resistance. Fig.7 shows the propeller wake for the same vessel, as determined in a steady-flow CFD analysis at model scale, Fig.8 the wave field. The better distribution of forces is recognizable already in model scale. The full-scale vessel should have an even better predicted wake flow in the propeller disc.

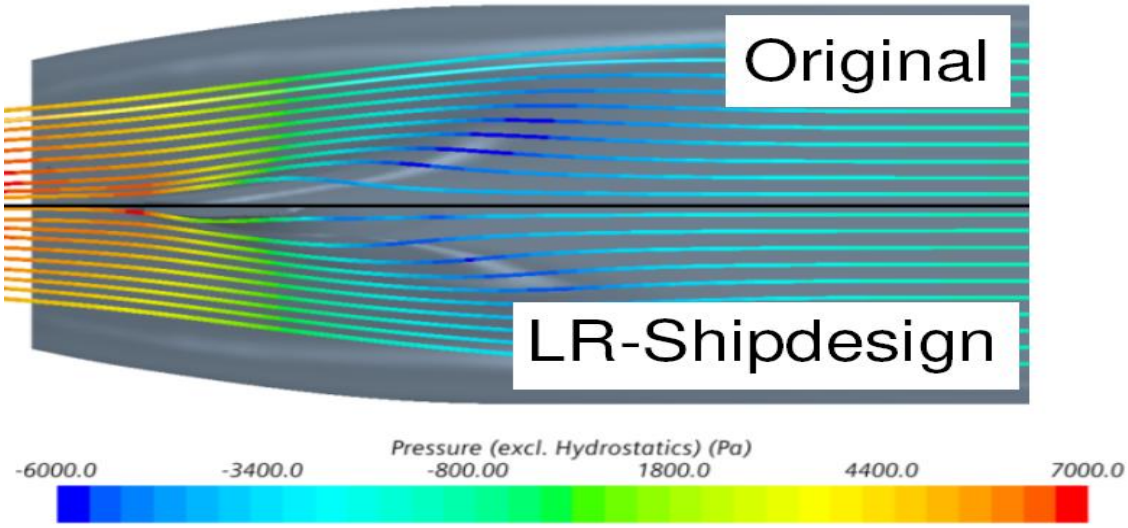


Fig.6: Streamlines in aftbody for original design (top) vs. LRSD AFT OPT (bottom)

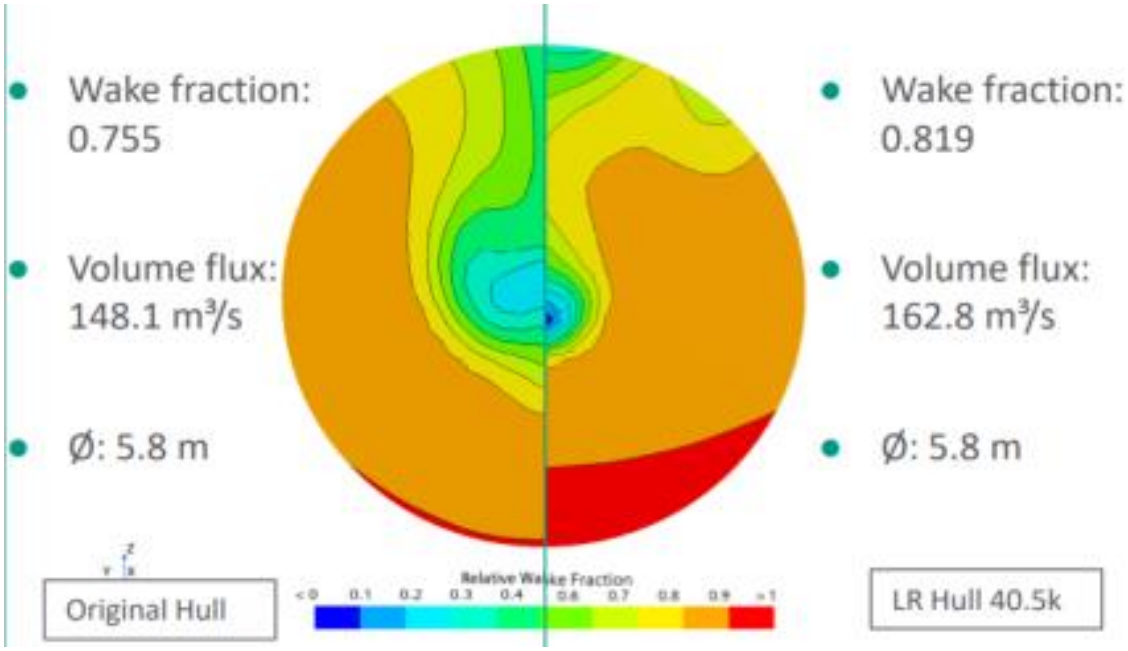


Fig.7: Wake field for bulk carrier at 14 kn, original hull (left) and AFT OPT (right)

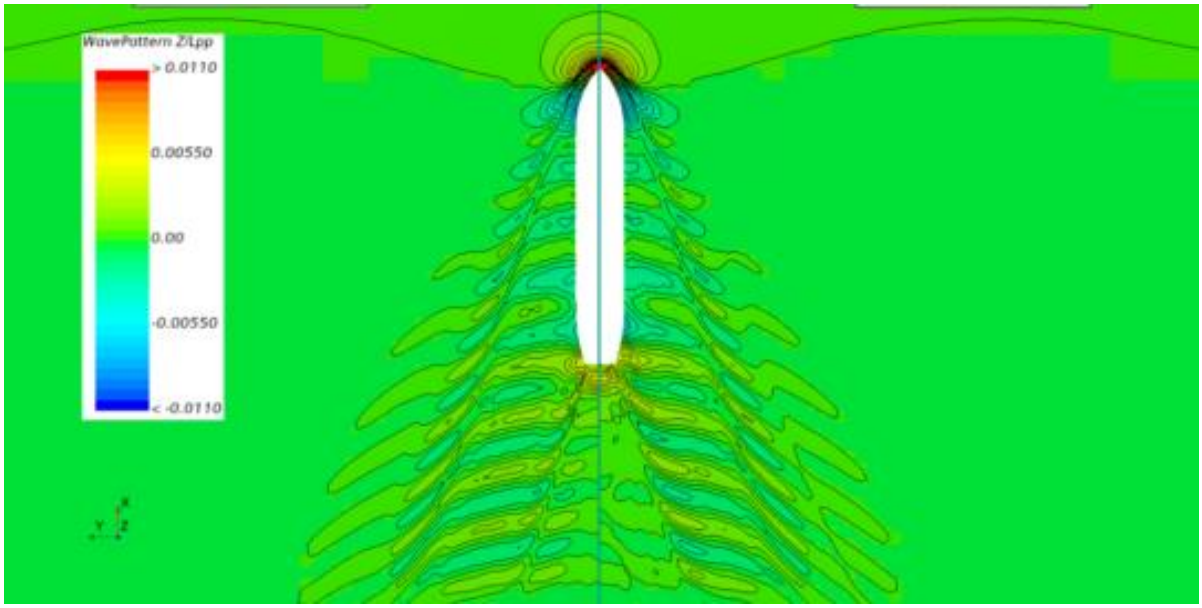
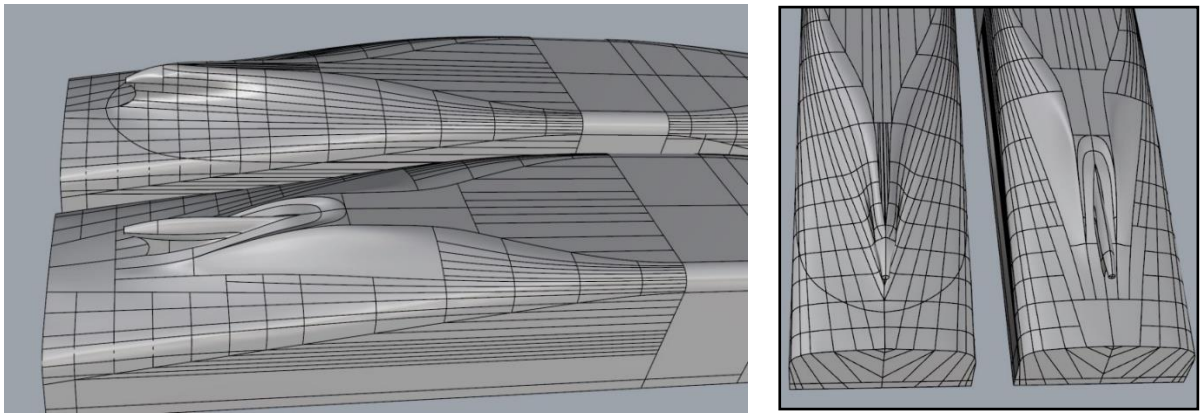


Fig.8: Wave pattern for bulk carrier at 14 kn, original hull (left) and AFT OPT (right)

Figs.9 and 10 show the hull geometries for another illustrative example, namely a 2900 TEU container ship. Figs.11 to 14 show CFD results for the full-scale ship. Note the equalizing effect of the AFT OPT design in each case. The new bow section improves the overall pressure distribution and thus wave formation, Fig.11. Fig.13 shows the very even wake distribution in the propeller disc, which enables high propeller efficiencies. Fig.14 shows streamlines in the aftbody, forming a slight vortex, but without stall.


Fig.9: Side view 2900 TEU container vessel, LRSD design


Fig.10: 2900 TEU container vessel designs, original vs. AFT OPT

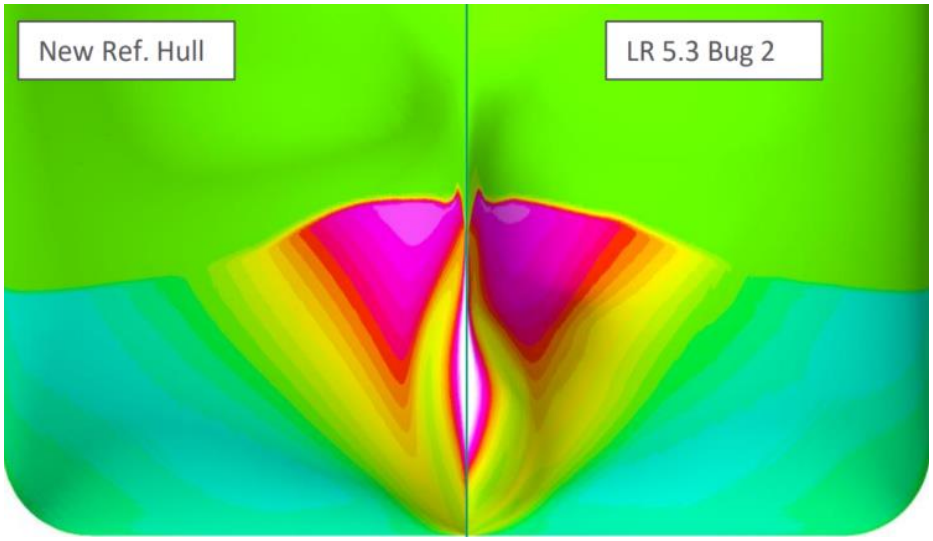


Fig.11: Pressure distribution on bow area for 2900 TEU container vessel

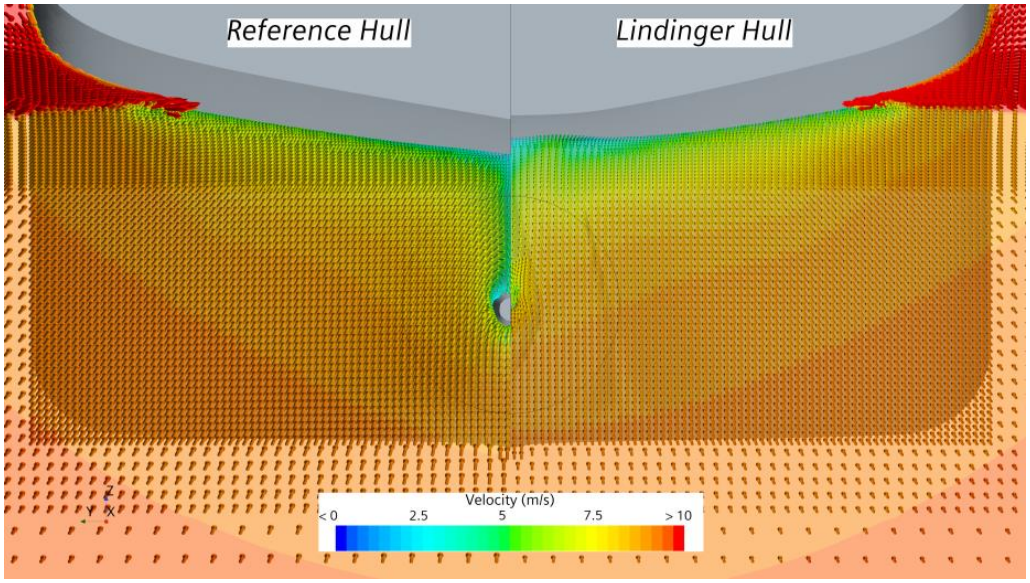


Fig.12: Velocity field 1 m upstream of propeller for 2900 TEU container vessel

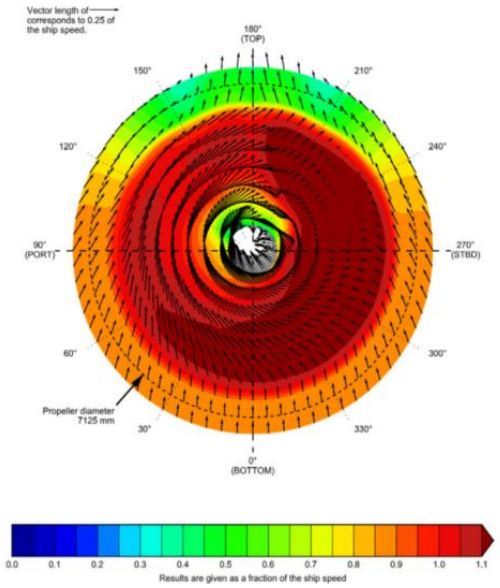


Fig.13: Wake distribution for 2900 TEU container vessel at 19 kn (AFT OPT dsign)

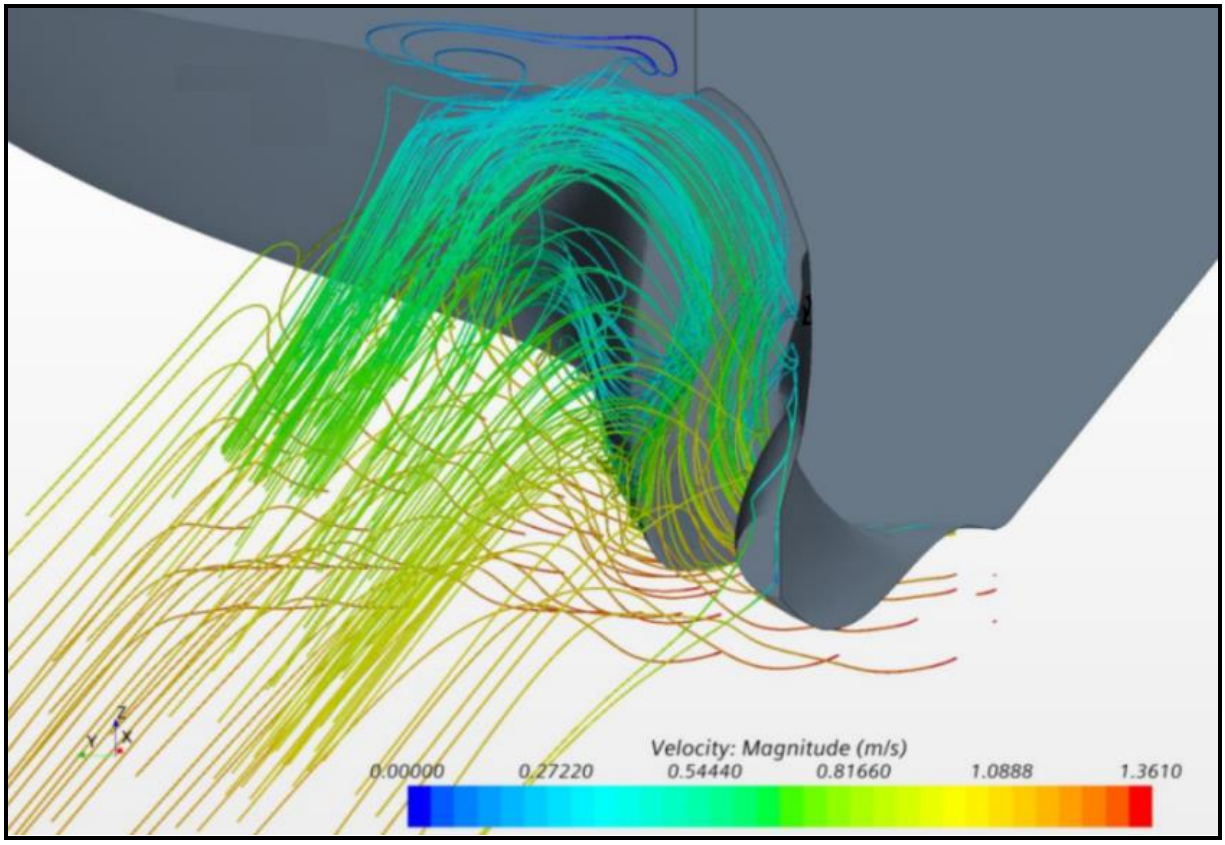


Fig.14: Aftbody streamlines for 2900 TEU container vessel (AFT OPT design)

5. Resume

The competitive advantages of the Patented Lindinger Hull are as follws:

- Fuel reduction of more than 5% (up to 10 %) during regular operation just due to the innovation AFT OPT; benchmark always: “best design” without AFT OPT
- Substantial main engine power reduction accordingly
- Lower main engine RPM at design speed
- Better rudder efficiency, especially at a neutral steering angle of ±4°
- Effectiveness of AFT OPT over the entire speed/draft range
- No attachments or ESD required; therefore, no additional (ESD) maintenance expenses
- Enhanced efficiency of the propeller due to increased thrust, reduced suction value and slip
- Less vibration and lower noise level due to the smoother propulsion
- Propeller with less weight is possible (smaller thickness possible)
- Reduced drifting tendency of the hull during sailing
- Functional for all semi-glider and displacement hulls
- Applicable for single screw vessels and for twin screws as well

6. Conclusions

Ships are only sustainable future assets when combining all latest requirements of builder and user. Ship owners should not be shy to use their purchasing power to combine more economical ship building know-how with their own ship operational requirements. The cost for new merchant vessels is relatively low compared with the OPEX during a ships’ lifetime. AFT OPT helps the ship owner and the party paying for fuel to stay ahead of other market participants. The savings have been confirmed by renowned ship model basin and classification society DNV.

Result of AFT OPT application:

- Reduction of main engine power demand for same cargo load, speed, draft, by at least 6% compared with so-called "latest optimised design" which was based on traditional or proprietary design technologies.
- Analysis of all ship model basin test result shows that full scale results for the real vessels will be better than in model scale. Here, however, we report model scale results only.
- Statements of Fact (by class, flag state) and worldwide patents for hull lines issued including of China, South Korea, Japan, EU.

Acknowledgements

LR-Shipdesign AG ("LRSD") is a Swiss based engineering company with private investors. Movena GmbH is the exclusive partner of LRSD for ship building activities in Asia/Pacific. LRSD is grateful to their industry partners for providing hull lines and support for developing holistic solutions for propeller design, main engine setup and for rudder design (LOEWE MARINE). LRSD would like to thank in particular Prof. Dr.-Ing. Stefan Krüger, Head of Institute of Ship Design and Ship Safety at Hamburg University of Technology (TUHH) and Chairman of the Board of "Schiffbautechnische Gesellschaft" (STG) (The German Society for Maritime Technology) for his technology review, valuable input information, advice and encouragement. Last but not least, LRSD would also like to thank the managers of SVA Vienna, MARIN and HSVA for their scientific support and all participating classification societies, flag states and third-party experts for their commitments, data verification and Statements of Fact regarding the results achieved with AFT OPT technology application.

References

LINDINGER, R.; WASMANSDORFF, V. (2022), *Rethink Shipbuilding*, HANSA 09, pp.82-83

MEYER, M. (2022), *AFT OPT – "Keine TikTok-Geschichte"*, HANSA 11/2022, pp 46-47

Digital Twin for Port Energy Infrastructure

Christina Warmann, ITK Engineering, Braunschweig/Germany, christina.warmann@itk-engineering.de
Tobias Melloh, ITK Engineering, Braunschweig/Germany, tobias.melloh@itk-engineering.de
Torsten Dunger, ITK Engineering, Braunschweig/Germany, torsten.dunger@itk-engineering.de

Abstract

This article presents a digital energy twin for the design and optimization of a port energy system. First, the methodological approach is described and then the implementation and optimization results are presented using the example of shore power supply in a Baltic port. With the help of the Digital Energy Twin, complex relationships, and the optimal dimensioning of individual components in different future scenarios with changed energy requirements, costs and political framework conditions are investigated. Based on the current state of the energy system, general optimization goals and boundary conditions are formulated as scenarios and iteratively refined.

1. Introduction

The EU's "Fit for 55" package addresses European ports with a requirement to provide sufficient shore-side power for certain ships from 2030 onwards, and thus to supply the docking ships with energy with as low emissions as possible, *BMDV (2015)*. This poses major challenges for the port infrastructure and requires a restructuring of the energy systems in ports. The Digital Energy Twin takes a holistic approach with the aim of sustainably transforming port energy systems. In the current phase of major changes, special attention must be paid to the planning phase of port energy systems. Digitalization, the digital twin, and intelligent optimization algorithms are key technologies for planning sustainable investments in port infrastructure, e.g., for shore power supply and future alternative fuels, as well as renewable energy systems. The digital twin also provides the basis for efficient and safe operation of the port energy system. The aim is to ensure a safe and reliable energy supply while at the same time achieving profitability for the port operator and meeting the specified EU emission targets.

2. The challenges of energy supply in the ports

The optimal energy supply in the ports is a very complex task due to the very individual requirements and framework conditions, which has become considerably more complicated by the directives of the European Union for achieving the climate targets, *EC (2022)*. The climate targets and the associated political requirements involve the minimization of emissions. This in turn requires a precise analysis of the energy demands and the energy potentials for renewable energies (RE) and the conversion and storage of these.

The availability of renewable energies is subject to large fluctuations due to the influence of weather (wind, sun, etc.), the annual and daily rhythm. This requires new concepts for energy storage and conversion. Which are the future energy sources? What storage requirements exist? How well equipped is the port infrastructure for this? How does the connection to power plants, decentralized generation systems and the public grid look like? Who are the various energy consumers in the port and how can a safe and efficient, but also economical, energy supply be sustainably implemented for the port operator?

There are major changes in the pipeline, for which there is little or no experience to draw on. If experience is missing, it is even more important to use new technologies such as digital twins, simulations and optimization algorithms to support investment decisions. In this way, decisions can be made consciously and based on comprehensible data and facts.

3. The basis for a sustainable energy system

By creating a digital twin for a port, all physical objects and systems in the real port can be digitally recreated and simulated under real-time information as well as designed and optimized in the planning phase under the influence of various framework conditions. The digital twin should also make it possible to collect and evaluate data during operation and to achieve the best possible operating objective defined based on artificial intelligence. In this paper, the focus is on the planning phase of the electrical energy systems for a reliable shore power supply of the docking ships.

Fig.1 shows the typical real and virtual objects and their manifold relationships and interactions of a digital twin of a port. The respective characteristics for a specific port are very individual, even if individual objects such as a photovoltaic system or an energy storage unit can occur repeatedly as building blocks in the modeling. A port is a complex system consisting of energy, goods, and mobility flows and systems and can be controlled by a virtual system.

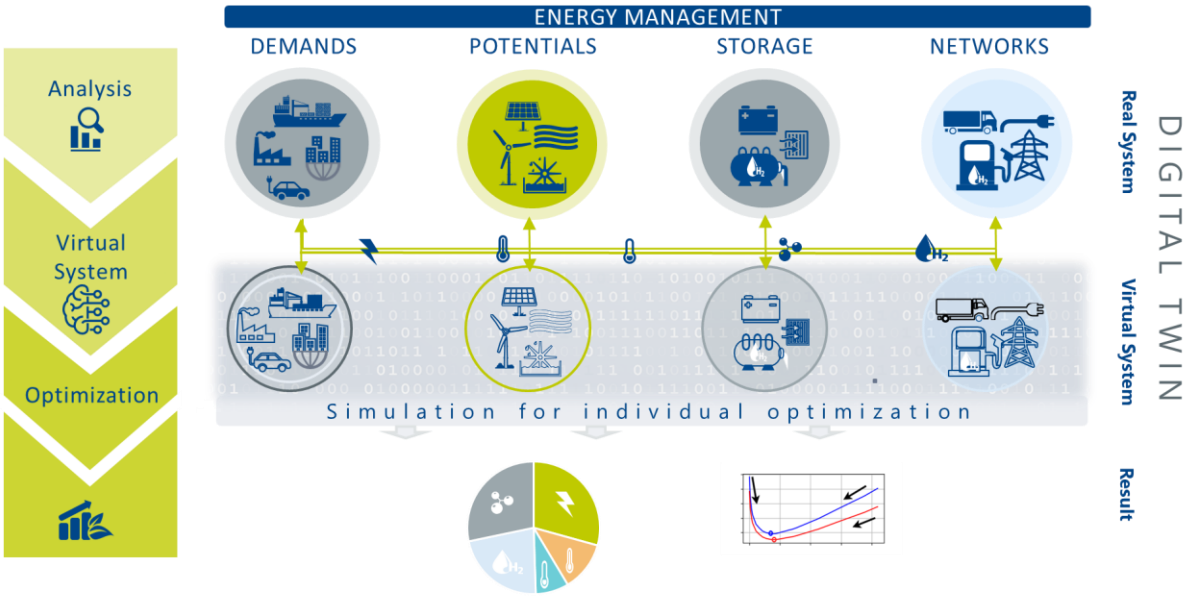


Fig.1: The digital twin as a holistic energy approach from analysis to optimization

3.1. Analysis

The analysis phase includes both the energy potential analysis and the energy demand analysis. For the creation of the virtual system as a representative of the real system, the energy potential analysis and the energy demand analysis are of particular importance. The development of information and data sources is a prerequisite and thus part of this phase. Data is checked for availability, relevance and quality and, if necessary, interfaces are established.

The energy potential analysis aims to maximize the supply of renewable energy to the ports. This includes the potential of energy generation as well as the potential of energy storage. The consideration of energy generation in the port area and in upstream grids is initially limited to wind and solar energy, although other forms of energy (e.g. wave and tidal energy) could also be interesting in the future. In the potential analysis, geo-information data, information on the usability of areas, possible restrictions due to shipping, etc. and weather data such as wind speed and direction, temperature and solar radiation (global and diffuse) are considered, *DWD (2023)*. In addition, initial technological decisions (e.g. power and number of suitable wind turbines) and corresponding load curves are obtained.

Within the demand analysis, the relevant forms of energy and the respective demands are determined. The demand for shore power for the hotel operation, the energy for the port infrastructure and logistics

applications are differentiated and classified according to energy forms. The energy demands are quantified and resolved over time.

3.2. Creation of the virtual system

In the creation of the virtual system, the information and data gathered during the analysis phases are incorporated into the digital model of the port energy system and form the digital twin. In this context, the digital twin means a digital energy system, which is supplied with real-time data, capable of simulation and learning, and self-optimized, in which all associated components (energy sources, storage and consumption) are modelled, *DEA (2023).*

Modelling the physical behaviour of the system offers the advantage that the interactions between the components are made transparent and the data collection effort is also reduced. Various system topologies are mapped, simulated, and evaluated using performance indicators such as total costs, energy efficiency, and self-sufficiency. The robustness and sensitivity of the system can also be assessed by varying the input parameters. This provides the basis for sustainable planning and optimal operation.

3.3. Optimization

The optimization of very complex systems, as in the case of the port energy system, usually includes large solution areas and often several conflicting objectives. Methods of artificial intelligence provide us with the appropriate equipment for mastering such problems, which are characterized by the fact that there is no global optimum. The multicriteria optimization provides the best possible solutions for these tasks. In addition, expert knowledge is used to optimize the port energy system and prioritize the objectives.

3.4. Sustainability through digitalization

As already mentioned, the digital twin makes a special contribution to sustainability, as it can be used for optimization in all phases of the life cycle of a port. Especially in the planning phase, the preliminary simulations support decisions on investments and construction measures for scenarios that are close to the future, but also those that are still far away in terms of time, among other things, by adding parameters for achieving the "Fit for 55" climate targets. In the planning phase, new technology and investment decisions can be modelled with the digital twin and then their impact can be estimated using AI forecasts. "First simulate then invest" is quite easy with a digital twin, even with highly individual requirements. Different scenarios can be simulated, and the respective benefits shown. Not yet identified forecasts can be derived from such model-based data analysis and developed and prioritized in the form of use cases.

4. The concrete implementation on a port example scenario

Our exemplary elaboration refers to a Baltic Sea port and focuses on a reliable and safe shore power supply for the docking ships.

4.1. Electrical potential and demand analysis

When planning and analyzing possible renewable energy generation plants, the usable areas for such generation plants are calculated from the evaluations and existing plants are included in the calculation. The potential analysis on the example scenario has resulted in a total usable area of approx. 40,000 m² that can be built with photovoltaic (PV). According to approximate projections, this results in a PV output of 4 MWp. For the simulations, we have selected different scenarios that represent the gradual expansion of renewable energy systems up to the maximum potential, which is limited by the available space. This variation in the share of renewable energy provides a good evaluation measure of total costs or the ratio of investment costs versus potential savings and profit through the sale of electricity.

In analyzing shore-based energy demands, historical data and real-time data are collected for the ships from online ship monitoring providers, so that nautical data as well as further data on the type, size, propulsion, etc. of each ship can be determined and thus the energy demands of the ships in the ports of call can be resolved over time. In addition, this data can be supplemented with information from the ships' schedules. This makes it possible to analyze the necessary shore power demand.

By simulating energetic potentials and demands in terms of time, it is possible to calculate demands from the power grid, which can still deviate using storages or under further target variables through power purchase and sale. Fig.2 shows the potential energy generation and the onshore power demand for the hoteling of the ships over a period of one year. The potential of PV energy is significantly lower than the potential of wind energy when averaged relatively over the day due to its dependence on the sun. The demand for shore power is calculated in the average one-day cycle, firstly for all ships docking in port and secondly limited to the criteria of the "Fit for 55" package. The EU resolution stipulates that ships must be supplied with shore power if they are container or passenger ships, have a retention time of more than two hours and exceed a size of 5,000 GT. This results in an averaged energy over the whole year for the shore-side demand of about 3 MWh.

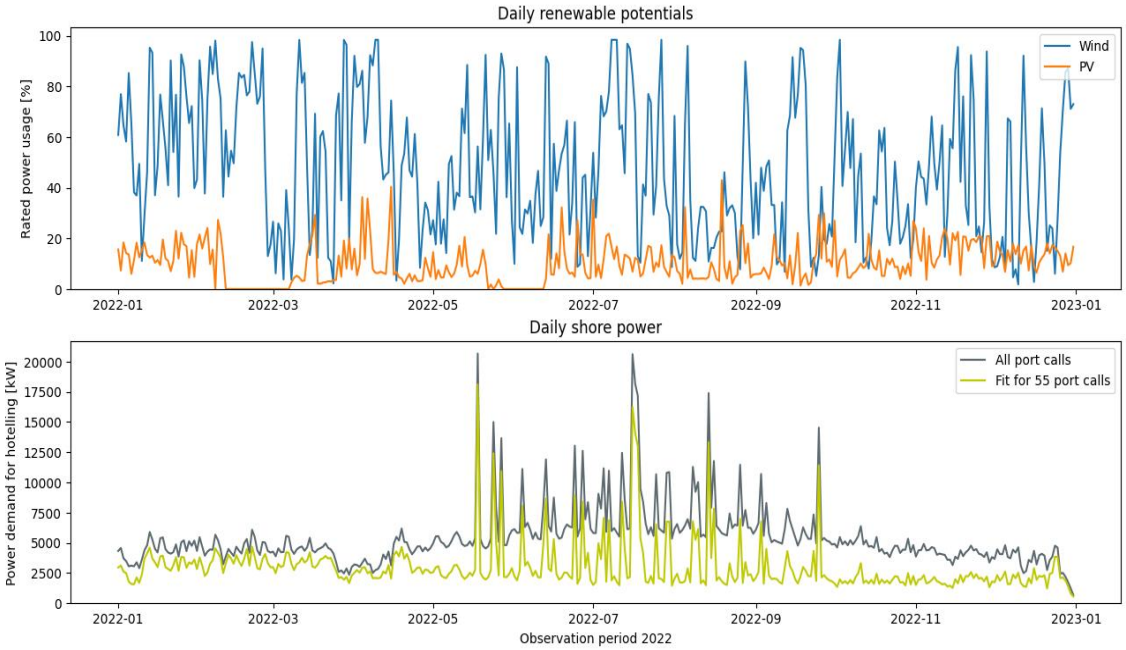


Fig.2: Calculation of the potential RE generation (top) and the shore power demand of the ships a) for all docking ships b) for ships limited by the "Fit for 55" package (bottom) over one year.

4.2. Scenario simulation for the electrical energy system

For the simulation of the modelled energy system, various scenarios have been developed (see table 1), which optimize the overall system in the direction of different objective variables. Scenario 0 represents the basis without renewable energy generation plants with 100% energy grid supply. In comparison, the focus for scenarios 1 is on self-use of the renewable energy generated and the purchase and sale of energy on the electricity market. Scenario 1a assumes contractually fixed purchase and selling prices, while scenario 1b considers purchase and selling prices at current exchange prices. In scenarios 2, the increase in economic efficiency is analyzed by including electrical energy storage devices. Here as well, we assume contractually fixed purchase and selling prices in scenario a, and in scenario b that purchase and selling prices at current exchange prices. Scenarios 3-5 simulate the gradual exploitation of renewable energy potential.

Table I: Calculation of the potential renewable energy generation

	PV rated output	Wind rated output	Grid purchase and grid sales costs	Energy storage capacity
Scenario 0	-	-	variable	-
Scenario 1a	4 MWp	7.5 MW	fix	-
Scenario 1b	4 MWp	7.5 MW	variable	-
Scenario 2a	4 MWp	7.5 MW	fix	3 MWh
Scenario 2b	4 MWp	7.5 MW	variable	10 MWh
Scenario 3b	2 MWp	3.5 MW	variable	-
Scenario 4b	4 MWp	3.5 MW	variable	-
Scenario 5b	2 MWp	7.5 MW	variable	-

Fig.3 shows the annual electrical energy shares to cover the demand for shore power as well as the sale of electricity to the public grid for variable electricity exchange prices based on historical data for 2022. Renewable energies have a visible impact on the amount of energy purchased and sold. Due to the weather conditions at the Baltic Sea port, wind energy has a significantly greater influence on the generation of renewable energies, which could be different at more southern latitudes. Including an energy storage system reduces the energy from the power grid (comparison 1b and 2b). The annual overall costs (right) show the energy costs, which add up over the year from the purchase and sale of electricity, as well as the annual investment costs for the installed technologies, which depreciate over 25 years. By exploiting the full RE potential and without investing in electrical energy storage (scenario 1b), the lowest annual total costs are achieved in the example considered.

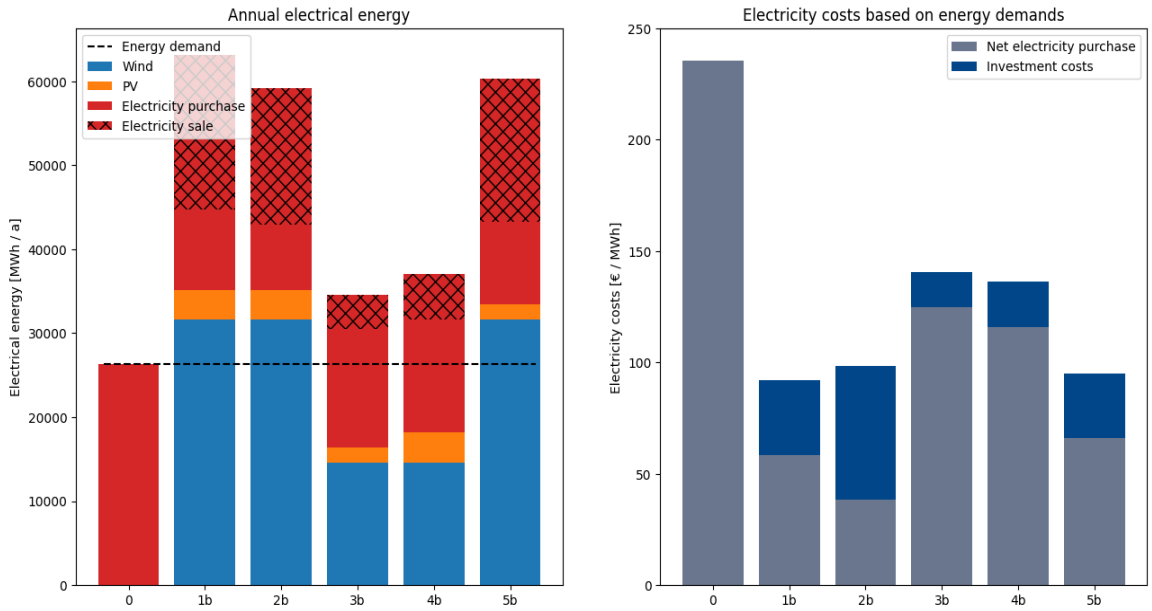


Fig.3: Electrical energy shares from renewable energy generation as well as the energy flows between port and grid add up over a year for the scenarios with varying electricity exchange prices (left) and investment and energy costs of the scenarios (right)

Fig.4 compares the scenarios with fixed and variable electricity exchange prices, taking full advantage of the RE potential, as energy costs can lead to an underestimated cost factor in energy system planning. The comparison of the determined energy costs for scenarios 1a and 1b shows that the consideration of variable electricity prices is important. The difference in costs makes it clear that the simplified assumption of fixed electricity prices leads to an incorrect evaluation of the scenario. Scenarios 2a and 2b show, on the one hand, the positive impact of the installed energy storage systems through reduced energy costs since the demand for power can be limited at times of high grid load and the energy storage can be filled at low grid charges. In scenario 2a, an electric energy storage capacity of approximately

3 MWh and for scenario 2b a capacity of approximately 10 MWh is simulated. However, a look at the total costs shows that the investment costs to be incurred for energy storage are not offset by lower energy costs, so that under today's technology costs, energy storage systems in these example scenarios are not profitable.

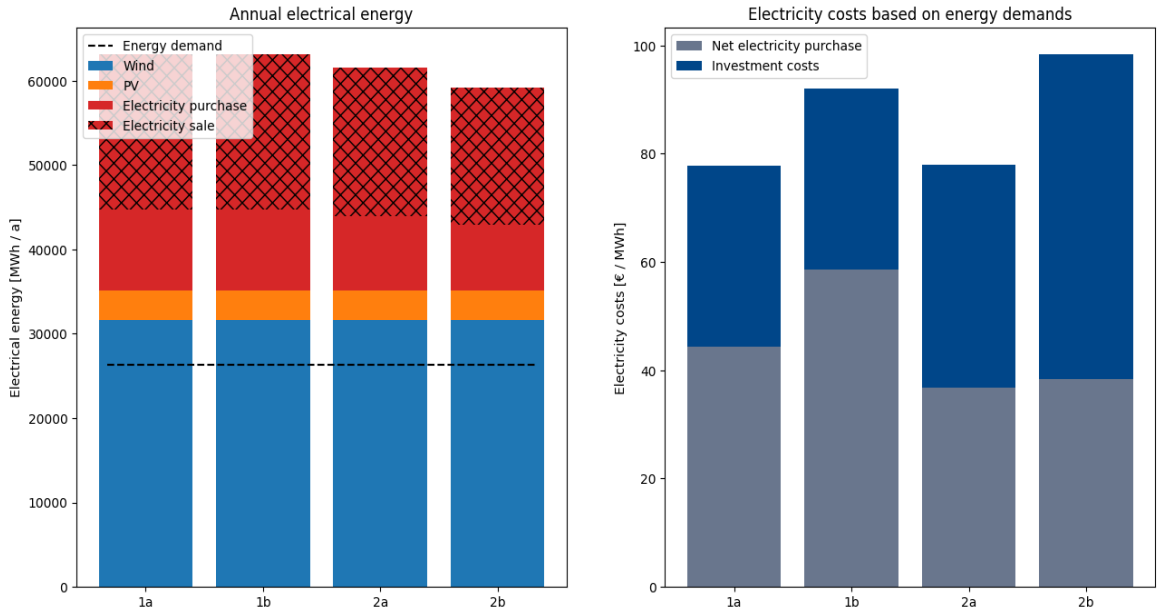


Fig.4: Electrical energy shares from renewable energy generation as well as the energy flows between port and grid add up over one year for scenarios with fixed electricity prices and varying electricity exchange prices (left) and investment and energy costs of the scenarios (right)

The annual CO2 emissions for the various scenarios with variable electricity exchange prices are shown in Fig.5. The emissions values for an electricity mix are included in the calculation for purchasing electricity from the grid.

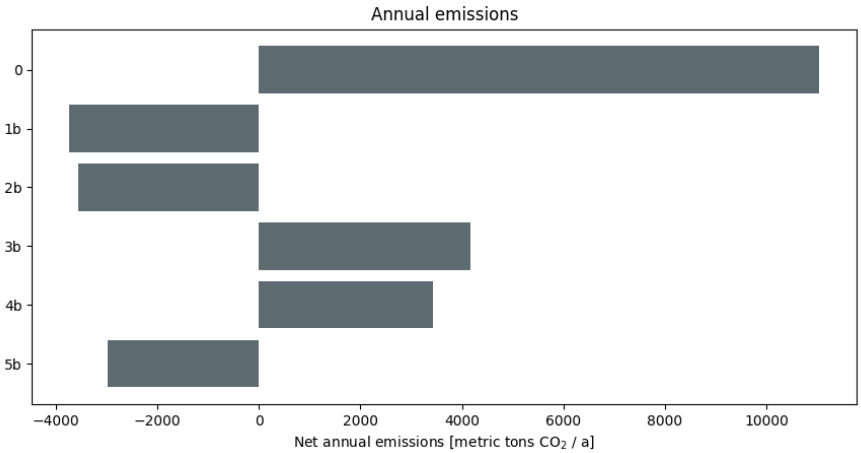


Fig.5: CO_2 emissions in metric tons added up over a year for all scenarios

The sale of electricity from renewable energies has a positive effect on the emissions generated, so that negative emissions result when renewable energies are fed into the grid. For grid purchase, emissions are calculated at 0.42 $kgCO_2$/kWh, and for grid sale, emissions are calculated at - 0.42 $kgCO_2$/kWh, *BMUV (2022), Juhrich (2022)*. This results in climate-neutral operation of shore-side electricity supply for scenarios 1, 2, and 5, as more energy from RE generation is fed into the public grid than electricity is purchased. Comparing scenarios 1b and 2b, the scenario without energy storage proves to be the better performing in terms of emissions, as more energy is released to the grid. Due to the reduction of wind power output in scenarios 3 and 4, the annual emissions are in the positive value range, so that no

climate-neutral shore power supply is realized. Since the energy input of the PV systems in the example studied is rather low compared to wind power, the reduction of solar energy (scenario 5) has a correspondingly lower effect.

5. Energy scenario outlook for the future

By developing future scenarios and preliminary simulations, investments in energy infrastructure can be planned more sustainably, as the example calculations show. To assess these future scenarios, studies are used that make predictions about shipping volumes, shipping traffic, energy demand, energy generation, forms of energy, energy prices, etc. These can also be supplemented with expert interviews.

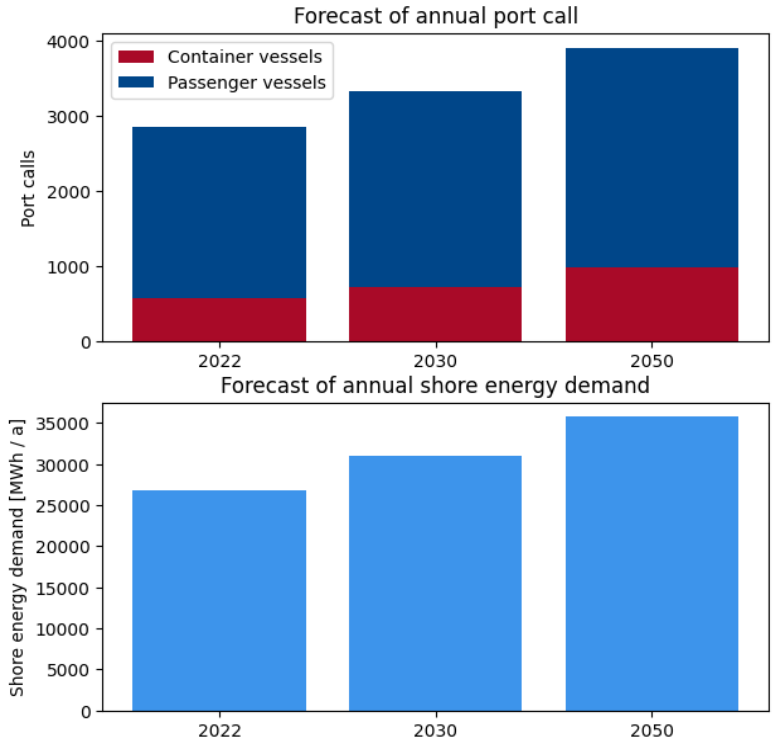


Fig.6: Outlook for the number of ship calls to the exemplary port (top) and for the expected shore-side energy demand of ships constrained by the "Fit for 55" package (bottom) based on assumptions from DNV, Region North Europe, Maritime Forecast to 2050, 2022

Fig.6 shows the forecasts of the development of the annual port calls as well as the resulting annual energy for the shore power demand for the exemplary Baltic Sea port, *Fintraffic (2023)*. The port calls relate to the ships limited by the "Fit for 55" package and show an increasing course until 2050 for container and passenger ships. For the annual energy demand, the extrapolations under current circumstances of energy consumption and ship volume of today's data are used. Based on these assumptions, an increase in shore power demand of approximately 34% is expected by 2050 from today's perspective. Contrary to these assumptions, shore power demand could be mitigated by 2050 through increased energy efficiency, meeting demand from green fuels, and new technologies.

6. Classification, opportunities and maturity level of the approach

The concept presented represents an important contribution in the context of digitalization with the goal of a CO_2-neutral port. Digitalization has already found its way into energy systems and their management in many areas. There are several projects that have overcome the first important hurdles and have thus established a basis to be used by collecting and monitoring data. We see our approach as a holistic method that can build on these foundations, if available.

In addition to the holistic approach, our approach is characterized by the combination of AI and physical modeling. This combination is the important basis for stable energy management. Compared to purely AI-based approaches, our approach is less dependent on existing training data.

The application shown to an example port makes it clear how the necessary high investments can be planned sustainably through the analysis of energy demands and potentials and the subsequent simulation of future scenarios. In the example, a cost saving of more than 3 million euros can be achieved annually for the onshore power supply alone by exploiting the potential for renewable energy. In comparison, the simulation costs are negligible.

A look at the emission values and the savings potential shows once again how important the expansion of renewable energies is. This applies to the climate and with increasing extent, it will also become increasingly visible on the cost side.

The approach of the virtual intelligent port offers far more potential. By 2055, the ports will not only have to ensure the onshore power supply, but also plan and implement the supply of alternative fuels for the marine powertrain. The example shown is just a beginning that can be expanded and can grow with the requirements of the future.

In addition, we can also apply the described method to the energy system of the ship, which includes both the propulsion engine and all other energy consumers on the ship.

Here, too, we see the application in the design phase as well as for the development of suitable operating strategies and an optimized energy management during the drive and at the berth for very profitable. The proof of the carbon intensity index to be provided would also be included.

ITK Engineering GmbH has been distinguished for almost 30 years by its methodical, technological and cross-industry expertise. The application of the described methodology in the context of the port energy system is good proof of this. Thanks to our many years of experience gained in similarly complex energy systems, we are the right partner for ports.

Acknowledgments

This paper was created as part of the competition "MCN Cup 2023 - Maritime Innovations from the North" of the Maritime Cluster Northern Germany. ITK Engineering has won the competition in category C: Digitization of the maritime economy with the “VIPort - virtual intelligent port - sustainable energy supply through digitization”.

References

BMDV (2015), *The 2030 maritime traffic forecast*, https://bmdv.bund.de/SharedDocs/EN/Documents/G/flyer-2030-maritime-traffic-forecast.pdf

BMUV (2022), *CO_2-Emissionen pro Kilowattstunde Strom steigen 2021 wieder an*, BMUV, Bundesrepublik Deutschland, https://www.umweltbundesamt.de/themen/co2-emission

DEA (2023), *Technology Data for Generation of Electricity and District Heating*, Danish Energy Agency, https://ens.dk/en/our-services/technology-catalogues/technology-data-generation-electricity-and-district-heating

DWD (2023), Index of climate environment observations Germany, Deutscher Wetterdienst, https://opendata.dwd.de/climate_environment/CDC/observations_germany/

EC (2022), *Vorschlag für eine Verordnung des Europäischen Parlaments und des Rates über die Nutzung erneuerbarer und kohlenstoffarmer Kraftstoffe im Seeverkehr und zur Änderung der Richtlinie*

2009/16/EG, European Council, https://data.consilium.europa.eu/doc/document/ST-10327-2021-INIT/de/pdf

FINTRAFFIC (2023), *Marine traffic, open data from Finnish waterways*, https://www.digitraffic.fi/en/marine-traffic/

JUHRICH, K. (2022), *CO2 Emission Factors for Fossil Fuels*, section v 1.6 emissions situation. German environment agency (UBA)

Evaluation of the Twin-CRP-Pod Propulsion Concept for Ultra-Large Container Ship – Conclusion from the Project Study

Hanna Pruszko, Gdańsk University of Technology, Gdańsk/Poland, hanna.pruszko1@pg.edu.pl
Krzysztof Czerski, Seatech Engineering Ltd, Gdańsk/Poland k.czerski@seatech.com
Marek Necel, Seatech Engineering Ltd, Gdańsk/Poland, m.necel@seatech.com
Sören Brüns, HSVA, Hamburg/Germany bruens@hsva.de
Sven De Brie, BRABO, Antwerp, Belgium, sven.debrie@brabo.com
Michael Hübler, CMT, Hamburg/Germany, huebler@cmt-net.org
Jörg Mehldau. CMT, Hamburg/Germany, mehldau@cmt-net.org
Shivaraj Kudari, CMT, Hamburg/Germany, kudari@cmt-net.org
Maciej Reichel, Gdańsk University of Technology, Gdańsk/Poland, maciej.reichel@pg.edu.pl

Abstract

This article presents the concept of a twin contra-rotating propulsion system and determines its sustainability for an ultra-large container ship. Its performance is assessed from a number of perspectives. These include the design phase and propulsion efficiency determined by means of towing tank tests and CFD calculations. Manoeuvrability and safety of navigation were evaluated using manned model trials on the lake. A cradle-to-grave life cycle analysis was carried out to determine the economic efficiency and environmental impact. The overall assessment is that the twin-CRP-pod propulsion system is a very promising solution, particularly in terms of manoeuvrability and navigational safety.

1. **Introduction**

The current requirements of the IMO, ambitious decarbonisation goals and the need to reduce the Green-House Gases emissions push the need to investigate the green ships' propulsion solutions. The research project "Application of hybrid CRP-POD propulsors on ultra-large twin screw containerships to increase propulsive efficiency, reduce GHG emissions and improve navigational safety" was established to answer this need and other related issues.

Ultra Large Container Ships (ULCS) are those that, on the one hand, have the highest carbon footprint individually but, on the other hand, take advantage of economy of scale and transport a vast amount of goods worldwide. Therefore, this type of ship is a perfect target for taking action to investigate energy-efficient solutions. The project's overall goal is to minimize fuel consumption, improve manoeuvring abilities, and increase navigational safety of an Ultra Large Container Ships by introducing three innovations: twin-propeller arrangement, pod propulsors, and contra-rotating propellers concept. All solutions investigated in the project are commonly known as separate means of high-efficient propulsion systems. However, never before three proposed solutions have been applied jointly on one ship. Thus the project goes beyond the state-of-the-art and opens new research fields on the topic.

In general, the project takes a holistic approach to the life cycle of the ULCS with a novel propulsion system. All aspects, from the design and building process, including costs for possible retrofitting, through operation, i.e., manoeuvring and propulsion up to the ship handling by skilled masters and pilots, will be considered.

2. Scope and aim of the project

This paper aims to describe the project findings focussing on four aspects of twin-CRP-pod propulsion system. The analysis covered design phase, investigation into propulsion efficiency, evaluation of the manoeuvring properties and cost efficiency analysis. The project objectives were:

- to recognize the increase of propulsive efficiency of the twin-propeller based propulsion configurations on the ULCS, including the development of model test set-up and results of

extrapolation method;
- to identify the manoeuvring abilities of ULCS with the twin-propeller based propulsion arrangement configurations, including fulfilment of IMO standard tests and restricted waters navigation;
- to summarise the technical and technological threats related to the design, production, and operation of ULCS with twin-propeller based propulsion configurations, including life cycle analyses;
- to prepare masters and pilots for operational challenges regarding the handling of the ship with such an innovative and intricate steering system.

Each of aforementioned aspects will be addressed, described and analysed in the further course of this paper.

3. Project assumptions, limitations and description of methods

3.1. Design Phase

The vessel main particulars were elaborated based on the study of existing container ships of similar capacities described in **Fehler! Verweisquelle konnte nicht gefunden werden.**.

Table I: Main particulars of existing Ultra-Large Container Ships

Vessel name	**TEU capacity**	**Principal dimensions**	**Service speed**	**Propeller**	**Engine(s) output**
Maersk-McKinney-Moller	18 000	LOA: 399.0 m LBP: 377.4 m Breadth moulded: 59 m Draught (scant.): 16 m Deadweight (scant.): 196 050 dwt	23 kn	2x FPP D =9.65 m	2x 29 680 kW at 73.1 rpm
Al Murabba	15 000	LOA: 368.52 m LBP: 352.0 m Breadth moulded: 51 m Draught (scant.): 15.5 m Deadweight (scant.): 194 967 dwt	21 kn	1x FPP D = 10 m	1x 54 900 kW at 84 rpm
CSCL Globe	19 000	LOA: 400.0 m LBP: 383.0 m Breadth moulded: 58.6 m Draught (scant.): 16.0 m Deadweight (scant.): 183 800 dwt	23 kn	1x FPP D = 10 m	1x 56 800 kW at 84 rpm
CMA CGM Marco Polo	16 000	LOA: 396.0 m LBP: 378.4 m Breadth moulded: 53.6 m Draught (scant.): 16.0 m Deadweight (scant.): 186 470 dwt	25.1 kn	1x FPP D = 9.1 m	1x 80 080 kW at 102 rpm

After a deep insight into the existing solutions, the decision about the vessel's main dimensions was taken. It was assumed that the designed ship capacity would be 16000 TEU, and due to current design trends toward the slow steaming, the design speed would be equal to 21 kn.

In the design of a new container vessel, present environmental regulations need to be taken into account, for example NOx - ECAs along US coastline and in Northern and Baltic Seas in Europe, which influences the choice of the fuel type. Therefore, as the main fuel for propulsion, LNG was applied.

For podded contra-rotating propulsion, typically the shaft line propeller takes between 50% and 70% of the total power and azimuting pod takes the remaining 30% - 50%. Assumed for this project ratio is

60% for shaft line propeller and 40% for azimuthing pods. For the design of the power plant concept four following scenarios were considered:

- seagoing mode;
- slow steaming (pods only);
- manoeuvring mode;
- cargo loading / unloading.

This design study included determination of the challenges, defining power balance, selection of the main engines, auxiliary systems and 3D design of the power plant.

Design phase included also generation of the 3D model of the hull, pod housing and propellers proceeded by the study of current azimuth pods market solutions and desired geometric parameters of the propellers. The ratio of aft to front propeller diameters was assumed as 0.78. The ratio has been chosen based on simplified propeller momentum theory to achieve the highest utilisation of front propeller axial losses, thus to work most efficiently in a slipstream of the front propeller.

The 3D model of the hull was done in four stages, as the final shape of the hull evolved in order to accommodate the parts of the machinery and have little resistance:

- generation of the midship and bow section based on the lines plan of the reference vessel;
- generation of the twin screw aft section based on the photogrammetric measurements of the existing manned model for manoeuvring training;
- redesigning the aft section to accommodate the machinery;
- second redesigning to lower the transom and reduce the resistance by elimination of the pod housing head boxes.

The first two stages of the 3D model generation are described in detail by *Bielski et al. (2021)*. The final 3D model of the ship hull is presented in Fig.1.



Fig.1: 3D model of the final hull version of the ULCS with the twin-CRP-pod propulsion system

Table II presents the selected main particulars for the new-designed ULCS with the twin-CRP-pod propulsion system.

Table II: Table captions above table with roman numerals

Length overall	LOA	399.90 m		Draught (scant.)	Tscan	16.00 m
Length between perpendiculars	LBP	378.40 m		Container capacity		15 918 TEU
Breadth moulded	B	53.60 m		Service speed	v	21 kn

The last phase of the design process included the design study of the retrofitting an existing ship into the twin-CRP-pod propulsion system. It was assumed that the retrofit process could be only favourable if the twin screw vessel is retrofitted. It was concluded that integration of the pod into single screw aft ship geometry within the retrofit process would lead to massive structural challenges and unfavourable hydrodynamic compromises. The retrofit design study included determination of the challenges, defining power balance selection of the main engines, auxiliary systems and 3D design of the power plant. Nevertheless, in our paper we will focus on presenting the solutions only for the new build, since the retrofit concept did not vary a lot form the new build concept.

3.2. Hydrodynamic analysis

Hydrodynamic analysis covered the primary numerical study for determination of the optimum propeller revolution, pod housing position and comparison of the calm water resistance between the single screw benchmark vessel and twin-screw ship. Further studies focussed on the numerical determination of the propulsive efficiency for the single screw ship, twin screw ship and twin screw ship with CRP-pod propulsion system. This study was performed in full-scale. For determination of the propulsion efficiency, it was necessary to assess the open-water propeller simulation for the separated propellers, and propellers operating in CRP-pod configuration. Finally, the multiscale analysis of geo-sim models was done to determine the scale error and indicate possible advances in the extrapolation methods for the ship with twin-CRP-pod propulsion system. Parallel to that, the towing tank investigation was done. It included four campaigns:

- resistance and propulsion (R&P) of the single screw benchmark vessel to determine the total delivered power;
- R&P of the twin screw vessel to determine the total delivered power;
- R&P of the twin-CRP-pod vessel to determine the total delivered power;
- R&P of the twin-CRP-pod vessel with the redesigned aft part of the hull to determine the total delivered power.

Fig.2 presents the hull model for the towing tank tests. It was manufactured in scale of 37.416.



Fig.2: Twin-CRP-pod hull model for towing tank experiments

The first approach to the hull design resulted in the aft part of the hull that had too little space inside to accommodate pod bearings. Therefore, they were inserted in very large head boxes, which produced significant amount of the drag (they are visible in Fig.2b). It was decided to redesign the aft part of the vessel by lowering the bottom and considerably decrease the head boxes size. It was decided that the shape of the pod housing remain the same. Fig.2c) presents the new pod head boxes. Table III presents the data of the propellers chosen for the hydrodynamic analysis.

Table III: The operational states of the Twin-CRP-pod ULCS

	Single screw		**Twin screw**		**Twin-CRP-pod**			
	Exp.	**CFD**	**Exp.**	**CFD**	**Front propeller**		**Aft propeller**	
					Exp.	**CFD**	**Exp.**	**CFD**
Z	6	6	4	5	5	5	4	4
D	9.121	9.09	9.50	7.68	7.63	7.68	5.99	6.00
P/D	0.935	0.9368	1.002	1.0221	1.016	1.0221	1.062	1.016
A_E/A_0	0.908	0.908	0.52	0.8014	0.849	0.8014	0.670	0.5184

3.3. Life Cycle Analysis of the ship

When new solutions or services wish to be used, the assessment is not only limited to the technical and operational feasibility but also to the cost and even further to the environmental impact. Based on the EU directive 2014/24/EU, "Life Cycle Cost (LCC) shall to the extent relevant cover parts or all of the following costs over the life cycle of a product, service or works:

a) costs, borne by the contracting authority or other users, such as:
   • costs relating to the acquisition;
   • costs of use, such as consumption of energy and other resources;
   • maintenance costs;
   • end of life costs, such as collection and recycling costs.
b) costs imputed to environmental externalities linked to the product, service or works during its life cycle, provided their monetary value can be determined and verified; such costs may include the cost of emissions of greenhouse gases and of other pollutant emissions and other climate change mitigation costs."

The Life Cycle Analysis (LCA) in the project will bring information about the emissions level and external costs caused by the emissions that could be reduced by applying innovative solutions for the propulsion system. In Twin-CRP-POD, the LCA will be used to assess the solutions proposed in newbuilding and retrofitting cases. To validate the integration of the innovative technology in the Ultra Large Container Ship (ULCS), in the LCA study a minimum of two ship models will be defined. They will be defined as reference ships and Twin-CRP-POD ships. Twin-CRP-POD ship will represent the state of the ship (the changes in terms of the propulsion system, weight, cost, etc.) after the integration of the innovative technology. Both ships will be modelled for three phases of the product life cycle:

• Production Phase - ship is in production or retrofitting process at the shipyards;
• Operational Phase - the ship is in its operation at sea;
• End of Life Phase - the operational life of the ship is over, either will be scrapped or resale.

For newbuilding project, an Ultra Large Container Ship (ULCS) called Twin-CRP-POD I is developed by using references from CMA CGM Marco Polo ULCS. While the hull lines are similar, the major difference between these two ships is laying on the propulsion system, the fuel type, and the design. As the Twin-CRP-POD I has twin screws with the POD system, there are significant changes on the aft part construction of the ship. For this project, it is expected the building process will be executed in the Asian shipyards as no ULCSs are built in Europe.

The second model is focusing on the assessment of retrofitting projects. For this project, a ULCS called

Twin-CRP-POD II is developed by using references from Maersk Triple E. While the hull lines are similar, the major difference between these two ships is laying on the propulsion system. Same as newbuilding, as the Twin-CRP-POD II has twin screws with the POD system, there are significant changes on the aft part construction of the ship. Furthermore, it is assumed the retrofitting project will be executed in the European shipyards, not in the Asian shipyards.

For LCA study, it is assumed the expected lifetime for newbuilding is 30 years and 15 years for the retrofit ship. To measure all operating expenses, it is assumed the ship averagely operates for 308 days a year. Furthermore, for the assessment, five different operational states (Table IV) will be used to define the fuel consumption during the operation.

Table IV: The operational states of the Twin-CRP-pod ULCS

No	Operational state	Percentage	Duration (h)
1	Sea going mode	30 %	554.4
2	Manoeuvring mode	20 %	369.6
3	Slow steaming mode	30 %	554.4
4	Cargo load / unload	15 %	277.2
5	Idle	5 %	92.40

In LCA various scenarios was considered with the regard to the ambitions of CO_2 and NO_x reduction for the future as well as future fuel price.

3.4. Manoeuvring and safety of navigation

According to many authors, additional advantage of application of CRP-pod arrangement is improvement of manoeuvring abilities and redundancy in case of loss of power by one of propellers, *Backlund and Kuuskoski (2000).* In general, manoeuvring abilities of ships equipped with pod propulsors are extremely different from conventional propeller-rudder ships, *Haraguchi et al. (2006), Reichel (2010,2017),* thus masters and pilots have to be prepared for handling of such ship. The compliance of investigated ULCS with twin-CRP-pod propulsion system with International Maritime Organisation requirements has been checked through a set of standard manoeuvres like turning circle and zig-zag.

Second part was to investigate the “human-machine” interaction, i.e. how the masters and pilot behave and perform on a ship with unusual steering-propulsion system. A specific programme for ship handling training has been elaborated with help of masters and pilots. Furthermore, experienced seafarers checked the perspectives on handling a twin-CRP-pod ULCS in various hydro-meteorological conditions, including wind, waves and current, both in unrestricted and restricted areas.



Fig.3: Manned model of a ULCS

Model used for the manoeuvring and ship handling tests was a manned model built to a scale 1:24, Fig.3. The manoeuvrability tests have been executed at open-air station at Ship Handling Research and Training Centre near Iława in Poland. The lake is 59 ha (146 acres) large and provides unique

opportunity to check manoeuvring abilities of ships both on deep and shallow water, *Kobylinski (2011,2016)*. The model was fully equipped with all necessary navigational aids and the trajectory was measured with the use of a GPS system, with RTK reference station owned. The tracking system used gives a nominal position monitoring accuracy of 10 mm, while the heading is measured with the use of gyrocompass with 0.1° accuracy.

3.4.1. IMO model tests programme

The Standards for ship manoeuvrability have been adopted by *IMO (2002)*. However, the specifics of pod propulsors or more general vectoring thruster devices has not been taken into consideration during preparation of these standards. Therefore, the procedures presented in these regulations are not fully suitable for pod-driven ships, however there are no alternative methods for pod-driven ships.

Regarding the test parameters that relate to steering device settings, the Standards say:

- Turning circle manoeuvre is the manoeuvre to be performed to both starboard and port with 35° rudder angle or the maximum rudder angle permissible at the test speed, following a steady approach with zero yaw rate.
- The 10°/10° zig-zag test is performed by turning the rudder alternately by 10° to either side following a heading deviation of 10° from the original heading
- The 20°/20° zig-zag test is performed using the procedure given above using 20° rudder angles and 20° change of heading, instead of 10° rudder angles and 10° change of heading, respectively.

According to IMO procedure, the approach test speed used in the standard manoeuvre tests is speed of at least 90% of the ship's speed corresponding to 85% of the maximum engine output. Therefore, the model tests have been carried out for approach speed of 1.68 m/s, corresponding to 16 kn in full scale.

3.4.2. Ship handling session programme

The objective of this part of research was to understand better the complex physical phenomena affecting twin-CRP-pod ships manoeuvrability and to gain more detailed practical knowledge. The overall goal of this part was to provide pilots the knowledge on the difference between ultra large container ships with conventional twin-screw twin-rudder or single-screw single-rudder arrangements and twin-CRP-pod propulsion. The programme covered:

- turning in restricted basin;
- harbour basin entrance and departure;
- harbour manoeuvres (use of bow thrusters in combination with twin screw propulsion arrangement and crabbing);
- effect of wind on ship's manoeuvrability: ship in ahead and astern motion, different directions of wind;
- turning in current;
- berthing and unberthing manoeuvres for different wind direction and force;
- entering locks.

4. Results

4.1. Design Phase

At the early design phase, it was estimated that the summarized power delivered to both propellers is 35000 kW and is lower than in similar vessels, Table I. After taking into consideration sea margin, engine margin and shaft line efficiency total brake power of both main engines is ~50 000 kW.

According to available publications of CRP Azipod®, *ABB (2012)*, we assumed that efficiency of CRP-pod system comparing to conventional propulsion systems should ~10% higher. Based on evaluated power as main engines were selected 2-stroke dual fuel WinGD engines type 7X82DF with Contracted Maximum Continuous Rating (CMCR) of each engine equal 28 000 kW at 84 rpm. Power includes sea margin of 15% and engine margin of 10%. Therefore, among the others, this reduces NOx levels required by regulations, without the necessity to implement additional equipment like SCR. Carbon footprint could also be reduced compared to traditional HFO fuelled engines.

The initial summary of the electric power balance assumed for the design of the power plant concept is presented in **Fehler! Verweisquelle konnte nicht gefunden werden.**V.

Table V: Summary of the Power Balance

Electric load definition	**Sea going mode**	**Slow steaming (only pods)**	**Manoeuvring mode**	**Cargo loading / unloading**
Machinery / general ships consumers	2 329 kWe	1 810 kWe	7 016 kWe	1 873 kWe
Azimuthing pods	12 454 kWe	7 326 kWe	7 326 kWe	0
Reefer Containers	5 600 kWe	5 600 kWe	5 600 kWe	5 600 kWe
TOTAL	**20 383 kWe**	**14 736 kWe**	**19 942 kWe**	**7 473 kWe**

Propulsion system proposed for this project was based on unique concept of big shaft generators (one per each shaft line) directly coupled with main DF (dual fuel, diesel-gas) engines. The electric output of each of shaft generators was assumed to be equal to 12000 kWe. Selected shaft generators are high efficiency permanent magnet type which can be combined with the Energy Stored System (batteries modules). They have reduced fuel consumption and improved energy efficiency design index (EEDI). Further improvement could be achieved, e.g., when waste heat recovery equipment is installed (power turbine generator utilizing exhaust gases energy from main engines). Thanks to such solution, electric power needed for CRP-pod is generated, through shaft line, by main engine, which is also giving mechanical power for conventional propeller. Because in normal seagoing operations, when vessel is sailing with service speed, only 2 stroke engines are in operation, total fuel consumption is at very low level, compared with today's vessels where main engines and also 4 stroke generators are in operation.

Proposed solution with big battery pack for peak shaving of production of electric power became also very efficient in manoeuvring mode. During this mode, only main engine can operate and power from that main engine is "used" for powering shaft generator and that shaft generator is giving suppling power for CRP Pods used during manoeuvres (main propellers are disconnected).

Low fuel consumption and also savings of CO^2 emissions due to operations on LNG, gives final carbon footprint at level much lower than standard todays solutions for ULCS. Fig.4 presents the view at the engine room, including main engine, and pod machinery room.

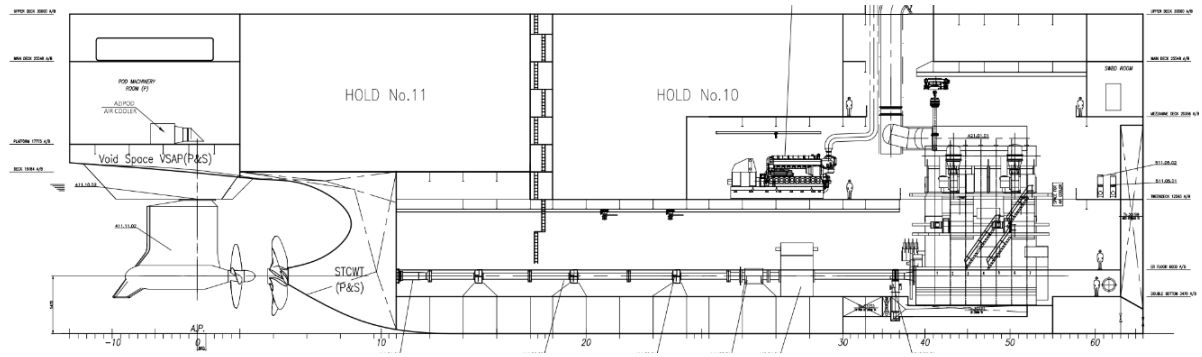


Fig.4: View at the engine room

4.2. Hydrodynamic analysis

Within the scope of the hydrodynamic CFD calculations the optimum revolution rate and pod housing position was determined. It was concluded that the optimum thrust division between the propellers should be:

- ~ 60% of the thrust generated by the front propeller;
- ~ 40% of the thrust generated by the aft propeller.

It is the similar result to what can be found in the literature. It was noticed that the right division of the power can cause the reduction of the delivered power up to 6% compared to the case when the thrust division is ~90% /~10%. Moreover, by means of full-scale CFD calculations five various pod housing positions were checked, and the most favourable one used for further towing tank experiments. The comparison of the total delivered power vs the position of the aft propeller vertical rotation axis with the regard to the aft perpendicular is presented in Fig.5. It can be noticed that it is more favourable to shift the propellers closer to each other than primary position. Further moving the pod housing to the front would result in collision with the front propeller. Optimisation of the pod housing position can bring the reduction of the delivered power equal to about 3%.

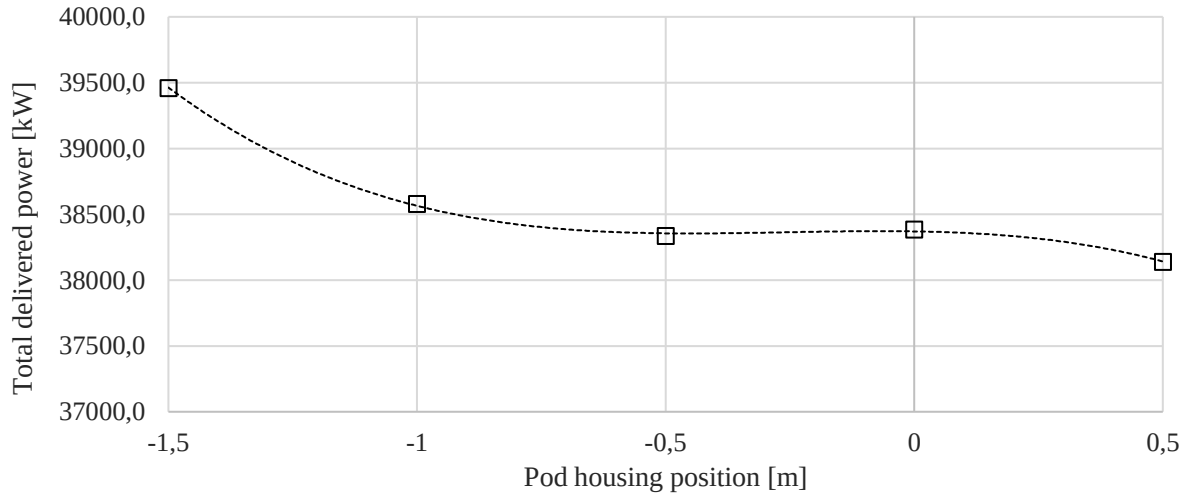


Fig.5: Results of the pod housing position optimisation

The optimisation of the position was done for the single-phase flow assumption, therefore, the total delivered power in Fig.4 should not be compared directly to the one in Fig.6.

Towing tank tests were performed for two combinations of the propeller rotation direction:

- Front propeller rotating inward / aft propeller rotating outward
- Front propeller rotating outward / aft propeller rotating inward

According to the results the more favourable from the propulsion point of view is the first combination. The potential savings in the delivered power were reported to be equal to 2%.

Fig.6 presents the formation of the wave system during the experiments for the design speed of 21 kn and the design draft of 14 m. During the self-propulsion experiment the thrust and torque of all four propellers was measured.



Fig.6: Wave system of the vessel during the towing tank test at speed corresponding to 21 kn

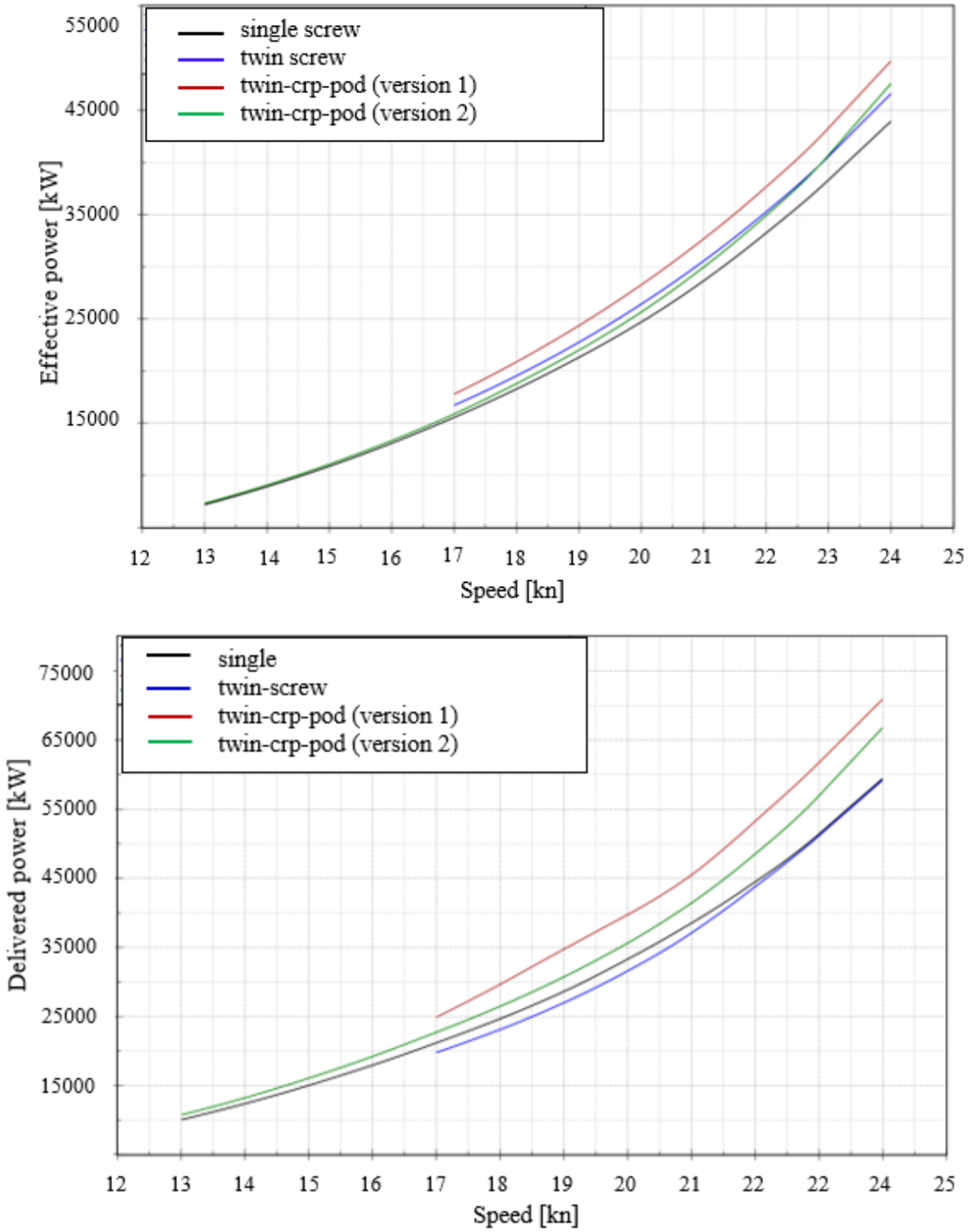


Fig.7: Comparison of the effective power (top) and total delivered power (bottom) for the tested hull forms and propulsion systems

The results of the towing tank tests are presented in Fig.7, in which the comparison of the effective and delivered power are shown. The delivered power prediction takes into account also the hull roughness, air resistance and differences between wake fraction and open water propeller characteristic for full and model scale. The results present the comparison between single screw, conventional twin screw and two versions of twin-CRP-pod arrangement: before and after modifications. For twin-CRP-pod arrangement the results are presented for optimum propeller revolutions.

The single screw ship is characterised by the effective power, which is directly related to the resistance. For the design speed the redesigned twin-CRP-pod hull has lower resistance than twin screw. The hull modification brought significant resistance reduction compared to the original twin-CRP-pod hull form, which also found the reflection in the reduction of the total delivered power. Nevertheless, according to towing tank experiments it turns out that conventional propulsion systems are more favourable for the entire range of analysed speed of the vessel when the delivered power is considered. With the single propeller vessel as the benchmark, the modified twin-CRP-pod vessel has 7.5% higher delivered power, and the twin screw vessel had 3.7% lower delivered power. There are several reasons for that, including:

- CRP-pod modified hull despite significant improvement still has 4.8% higher effective power than single-screw vessel;
- the quasi-propulsive efficiency for the twin-CRP-pod vessel was 1.8% lower than of the single screw vessel;
- the quasi-propulsive efficiency for the twin-CRP-pod vessel was 10% lower than of the twin screw vessel (twin screw vessel was equipped with the excellent efficiency propeller compared the twin-CRP-pod vessel).

Therefore, it is clear that further improvements are possible, and the first to be included is the detailed design of the propellers for the twin-CRP-pod vessel. *Krasilnikov (2022)* shows that the propulsive power improvements are possible even if the high efficiency separate propeller is compared.

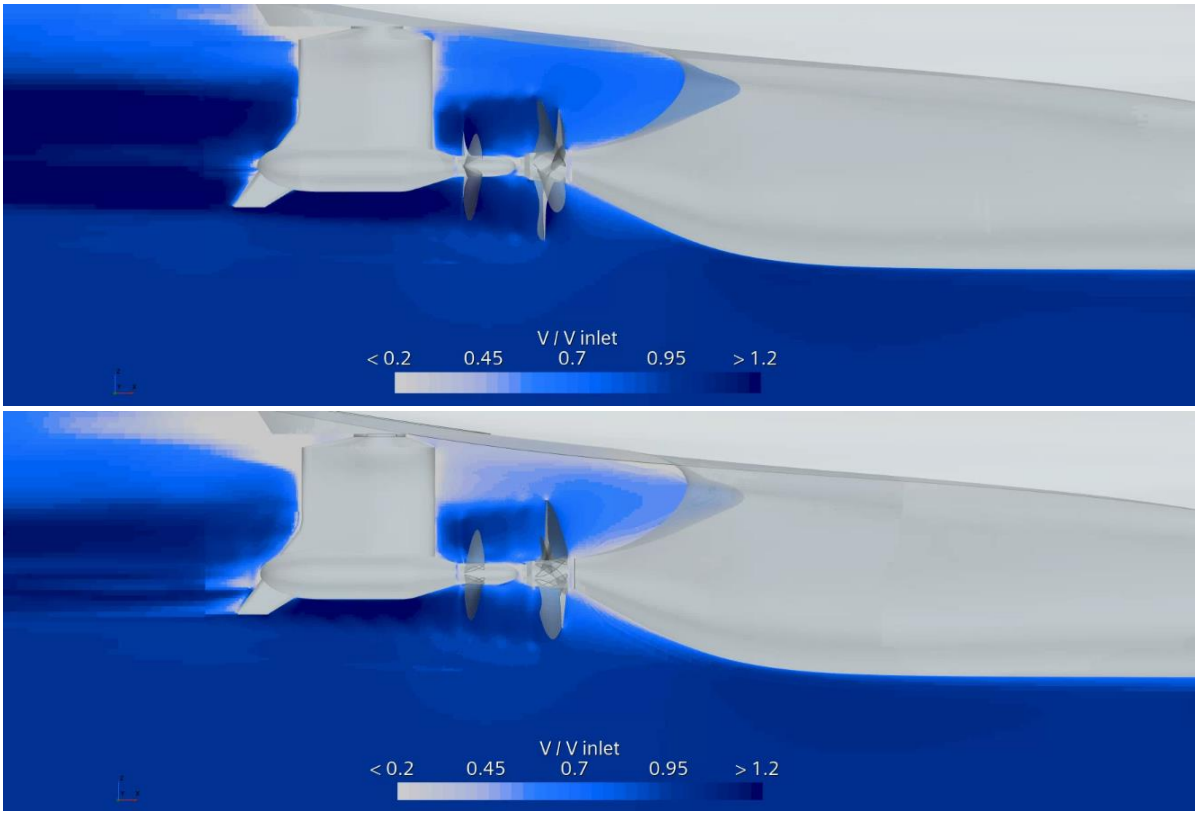


Fig.8: Comparison of the normalised velocity magnitude flow field for full scale vessel (top) and model scale vessel (bottom)

Last important aspect to be considered is the scale effect and scale error, which has more sources for the twin-CRP-pod vessel. The two that are different from vessels with the standard propulsion system are scaling of the pod housing resistance and interaction of the propellers between each other. Fig.8 shows the velocity magnitude scalar field normalised by the velocity magnitude in the free stream in the aft part of the vessel.

It can be noticed that velocity of the flow in the stern part is much smaller for the model scale than in the full scale, and also pod housing is subjected to flow of the higher velocity. Multiscale analysis to assess the sources of the scale errors shown, that standard propeller characteristics scaling is sufficient in this case. However, the pod housing should not be treated as a part of the propulsion system, and its resistance should not be included only in the thrust deduction fraction. According to our calculations the thrust deduction fraction is significantly smaller in the full scale than in the model scale. Therefore, the towing tank including this fact should give slightly smaller values of the delivered power. Nevertheless, this requires some further studies.

4.3. Life Cycle Analysis of the ship

The two considered cases of a new build twin-CRP-POD and a retrofitting on twin screw vessel with conventional rudder arrangement were calculated based on properties of existing and replaced equipment and the hydrodynamic performance results received during the project. The variants with LNG as main propulsion fuel compared to those with classical MDO prime movers, provide a lot of advantages depending on scenarios of implementation, economic prosperity, fuel prices, restrictions and external costs for operation in emission control areas due to reduced GHG, SO_x, NO_x and particular matters. The newbuilding variant with its immediate cost and emission reduction potential is clearly the preferred solution. It is showing the best economic performance and receiving highest net present values due to earlier refinancing of higher investment cost in extra LNG engine equipment, fuel gas supply systems (FGSS) and more complex tank technology. The additional investment for the LNG fuelled variants differs from estimated 28mio Euro for a new build to 66mio Euro for a retrofitting. This includes resale/scraping of old components, extra docking costs for four weeks, adaption work, additional steel for pod foundations and hull adaptions. For the retrofitting also the loss of revenues for the conversion time were considered as well as a reduction of payload of about 350 TEU due to space consumed by the newly installed LNG tank. For the new build it was assumed that the tank is installed under the deckhouse with no loss of payload.

Due to high profitability of the container vessel case in general, the return on invest of the different solutions varies in a range between a few months and about a year. But considering the net present value over the life cycle of the vessel the factors like the time of retrofitting, the development of fuel price and external cost play a major role for the economic success of such a project and make a large difference. A scenario of moderate fuel price economic, prosperity and external costs on GHG emissions was selected for comparison. In case of a new build, with higher investment for the LNG variant, the net present value performance improves compared to a vessel with standard diesel prime movers after about 5 years. For the conversion case – e.g. after 10 years operation – the values for the retrofitted LNG variant and a vessel remained fuelled with MDO equals much later approaching the end of the remaining lifetime. This might prevent ship owners from investment in LNG, if emission reduction is not considered as a major argument. Of course, the advantage of LNG increases with expected improved availability and larger price differences compared to MDO and its external costs on emissions that might give retrofitting a better economic perspective in future.

4.4. Manoeuvring and safety of navigation

Results of the tests show excellent manoeuvring abilities of investigated ULCS with twin-CRP-pod propulsion system. Both yaw-checking course keeping and turning abilities first of all satisfy the IMO requirements. The positive difference was especially visible in turning circles, where the analysed ship with twin-CRP-pod propulsion arrangement showed up to 40% smaller steady turning circle diameter, Fig.9.

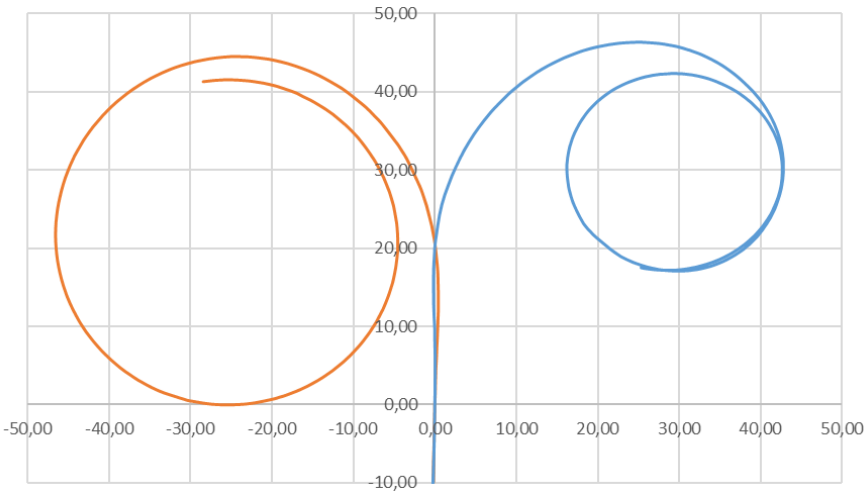


Fig.9: Turning circle (twin-propeller twin-rudder to portside, twin-CRP-pod to starboard side)

In the case of more usual manoeuvres the new ULCS with twin-CRP-pod propulsion system showed extraordinary handling capabilities. Test showing the lock passage record from the GPS is presented in Fig.10.

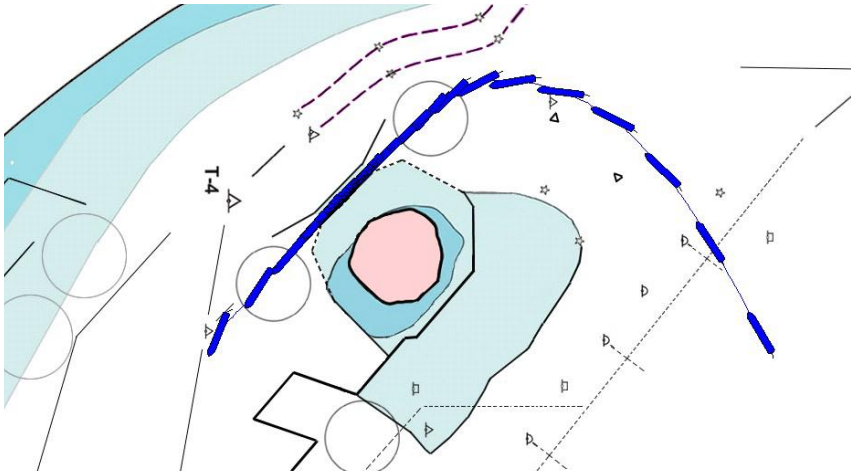


Fig.10: Manoeuvring tests records - lock approach and a passage

The subjective opinion from river and harbour pilots showed dozens of pros of the ULCS with twin-CRP-pod arrangement:

- vessel is easy to handle at slow speeds; even at speeds of less than 3 kn, the ship can keep its course / heading;
- in light weather conditions, manoeuvres can be done without any assistance of a tugboat;
- main engines are not needed while manoeuvring in port; all manoeuvres are carried out by pods only (electrical);
- as the pods are electrically powered, any number of revolutions on the pod propellers can be achieved and thus there is no minimum manoeuvring speed;
- even with the pod propellers not turning, the vessel is able to keep its course while sailing on main engines.

It shows that the twin-CRP-pod propulsion system can be extremely beneficial from the manoeuvring and safety of navigation point of view. Additionally, it offers potential savings in harbour operation due to possibility of manoeuvring without the tugboats.

5. Conclusions

This paper describes the results of the analysis of the twin-CRP-pod for ULCS propulsion solution. This novel propulsion concept was analysed from various perspectives: design, hydrodynamic performance, Life Cycle Cost and manoeuvrability and safety of navigation.

The result of the design analysis was a concept of the pod housing, machine room concept, General Arrangement and initial power estimated. The proposed system was a dual-fuel engine with a unique concept of big shaft generators (one per each shaft line) directly coupled with main DF (dual fuel, diesel-gas) engines. Selected shaft generators are high efficiency permanent magnet type which can be combined with the Energy Stored System (batteries modules). Proposed system is characterised by the great flexibility suitable for all modes of operation, and additionally, by reduction of the EEXI.

The results of the hydrodynamic analysis show that proposed twin-CRP-pod is less favourable than the conventional single and twin screw concept from the propulsion point of view. The differences in the total delivered power between twin-CRP-pod, single screw and twin screw vessel are equal to 7.4% and 10.5%, respectively. However, some actions can be taken to improve the efficiency. It was noticed that another 10% of the delivered power can be gained / lost if the right position, rotation direction and thrust division between propellers are found. Finally, the shape of the pod and propellers itself were not optimised, and that is believed to be the main source of further improvements.

The results of the Life Cycle Analysis show that for the LNG fueled cases a cost benefit over life cycle is achievable which increases with larger price difference between conventional fuels and LNG if - due to better availability of LNG - prices will further drop. Different scenarios on rising external cost and improving economic prosperity show also further benefits on higher net present values and earlier return on invest for the LNG fueled variants.

The highest gains are obtained from the safety of navigations point of view. The amount of control that can be used to manoeuvre and the possibilities to gain control over the vessel in emergency situations are optimal. Although the system is excellent to gain control of the ship, in unexperienced hands it will not come to his full potential. Therefore, we would like to emphasise the need for extensive training on staffed models and simulators, a combination of both training tools is the only correct way to gain the right amount of insight in these complex manoeuvring assets.

To conclude, we believe that the twin-CRP-pod propulsion concept is a very promising one, but its complexity opens much more ways to optimise and improve the propulsion setup. Therefore, further studies are recommended to fully explore its' full potential.

Acknowledgements

This work was supported by MarTERA and co-financed by Polish National Centre for Research and Development (NCBR) and Development (NCBR), under the grant agreement MARTERA-2/twin-CRP-pod ULCS/1/2020 and the German Federal Ministry of Economic Affairs for Economic Affairs and Climate Action (BMWK), and the Flemish Agency for Innovation and Entrepreneurship (VLAIO). Calculations were carried out at the Centre of Informatics Tricity Academic Supercomputer & Network.

References

ABB (2012), *Azipod® XO2100 and XO2300*, Product introduction

BACKLUND, A.; KUUSKOSKI, J. (2000), *The Contra Rotating Propeller (CRP) Concept with a Podded Drive*, Motor Ship Conf., Amsterdam

BIELSKI, P.; PRUSZKO, H.; REICHEL, M.; MACIKOWSKI, Z. (2021), *Photogrammetric measurements of an existing ship hull geometry for reverse engineering*, PostGradMarTec.

HARAGUCHI, T.; KAYANO, J.; TSUKADA, Y. (2006), *Prediction of the manoeuvrability on a ship with a CRP pod propulsion system and an auxiliary rudder*, Int. Conf. Marine Simulation and Ship Manoeuvrability (MARSIM), Terschelling

IMO (2002), *Resolution MSC.137(76) Standards for ship manoeuvrability*, Int. Maritime Org., London

KOBYLINSKI, L. (2011), *Capabilities of Ship Handling Simulators to Simulate Shallow Water, Bank and Canal Effects*, Int. J. Marine Navigation Safety and Sea Transportation 5(2), pp.247-252

KOBYLINSKI, L. (2016) *Impact of hydrodynamics on ship handling characteristics in training simulators*, Scientific J. Maritime University of Szczecin 45(117), pp.9-16

KRASILNIKOV, V. (2022). *Simulaton driven design of a counter-rotating propeller system for low-emission coaster vessel*, 24th Numerical Towing Tank Symposium (NuTTS), Zagreb

REICHEL, M. (2010), *Manoeuvring Abilities of Podded Ships with Different Stern Shapes*, 18th Int. Conf. Hydrodynamics in Ship Design, Safety and Operation (Hydronav), Gdańsk

REICHEL, M. (2017), *Prediction of manoeuvring abilities of 10000 DWT pod-driven coastal tanker*, Ocean Eng. 136, pp.201–208

Hydrodynamic Performance of a Propeller within a Novel Partial Duct

Kiran Ramesh, **Anirban Bhattacharyya**, IIT Kharagpur, Kharagpur/India,
kiran.ramesh92@kgpian.iitkgp.ac.in

Abstract

The thrust, torque, and efficiency of a marine propeller working within a partial accelerating duct is investigated. An elliptic half duct is placed over the propeller to induce partial flow acceleration and reduce wake non-uniformity. The specific duct profile allows the propeller blades to have a gradual transition from the fully ducted to open condition over a complete revolution. RANS-based CFD analyses indicate that the duct provides positive thrust at lower advance coefficients, resulting in a higher open water efficiency as compared to a non-ducted propeller. Nominal wake analyses with different partial duct designs on a benchmark propeller model indicate significant wake equalisation due to the partial duct.

1. Introduction

The shipping sector is one of the major contributors to global carbon emissions. Initiatives by the International Maritime Organization (IMO) aim to meet decarbonization targets of net zero by 2050. One method of achieving this is to improve the hydrodynamic performance of ships, which may be achieved by certain design modifications to optimize the efficiency of the ship-propeller combination. Certain complex effects associated with the flow in the stern of a ship can be alleviated to a certain extent by the use of devices aimed at improving the flow characteristics into the propeller, and therefore, the propeller's efficiency.

The working principles of such devices have been elucidated in multiple publications. A general description of the hydrodynamics of the working of Energy Saving Devices or Propulsion Improvement Devices can be found in *Terwisga (2013),* where the differences in momentum are assessed in terms of energy gains and losses. Pre-Swirl Stators and Wake Equalizing Ducts are among the most widely used and researched devices. Some of the popular pre-swirl duct designs are the Wake Equalising Duct, *Schneekluth (1986),* and the Becker Mewis Duct, *Mewis (2009).* It is evident that there are many such existing devices in the marine industry, each designed over years of research and optimisation, including combinations of multiple devices. With the advances being made in various Computational Fluid Dynamics (CFD) codes, the use of these solvers in the prediction of hydrodynamic performance of such devices has become a standard practice.

In the present study, numerical methods solving the Reynolds-Averaged Navier-Stokes (RANS) equations have been employed using the commercial CFD Suite Siemens Star CCM+ to extensively investigate the hydrodynamics of flow associated with the use of a novel Partial Accelerating Duct, *Bhattacharyya (2020),* in conjunction with a marine propeller. The partial duct has an airfoil cross section with sectional geometry (AA') similar to that of the Wageningen 19A duct, and is located in the propeller plane on the upper half of the propeller. The duct is configured in the form of a semi ellipse, such that the distance between the propeller tip and the duct is minimum at the vertical 0-degree position and gradually increases to the maximum value at the horizontal or 90° position, Fig.1. The duct design was conceptualised with the idea that the flow acceleration is restricted to only the upper sections of the propeller plane where wake fractions are generally higher, thereby providing a "wake equalisation". The elliptical design ensures that the blade transitions gradually from the fully ducted condition in its vertical position to the completely non-ducted condition over a quarter of a revolution. The free ends of the duct are faired to reduce the strength of end vortices and the resulting duct drag.

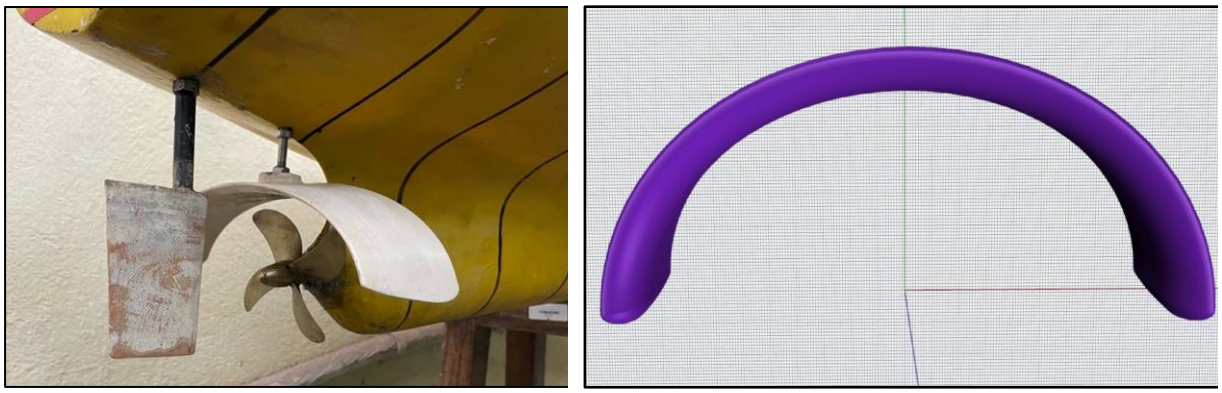


Fig.1: The Elliptic Partial Accelerating Duct

In the analysis of open water characteristics, the partial duct is considered a part of the propulsion system, integrated with the propeller. A detailed study on the open water characteristics with a B-Series propeller including associated vorticity fields and scale effects is given in *Bhattacharya and Ramesh (2024).* This is further extended in the present work with the open water characteristics of four different propellers within the partial accelerating duct being numerically investigated to arrive at certain common conclusions on the effects of the partial duct. A further effort has been made to study the effect of the partial duct on the nominal wake behind a KVLCC2 ship model, wherein the duct is considered as part of the ship's hull. Finally, a few different iterations of the partial duct design are studied to arrive at certain conclusions regarding wake equalisation effects of the partial duct design.

2. Geometry and Test Conditions

2.1. Open Water Simulations

The main focus of the present study is to understand the effect of the partial duct on the open water characteristics of different marine propellers. For the open water simulations, four propeller geometries have been used: a 5-bladed Wageningen B Series propeller, the PPTC 4-bladed propeller, a 7-bladed Kaplan Series Propeller, and the NMRI KVLCC2 propeller KP458. Whilst the first three propellers are studied at a model scale diameter of 0.25 m, the KP458 propeller is investigated at a diameter of 0.0896 m, due to published model test data from NMRI at the same scale. The principal parameters of the propeller geometries used for the study are as tabulated below:-

Table I: Propeller geometries and operating conditions used in the open water simulations

B-Series Propeller (B-5.75)	**Potsdam Propeller Test Case (PPTC)**	**Kaplan Series Propeller (Ka-7.525)**	**NMRI KVLCC2 Propeller - KP458**
D = 0.25 m	D = 0.25 m	D = 0.25 m	D = 0.0986 m
Z=5	Z=5	Z= 7	Z = 4
A_e/A_o =0.78	A_e/A_o =0.78	A_e/A_o = 0.525	A_e/A_o = 0.431
P/D = 1.635	P/D = 1.635	P/D = 1	P/D = 0.721
Skew = 18.84º	Skew = 18.84º	n =12 rps	r_b/R = 0.155
n =12 rps	n =15 rps		n = 43.62 rps

The open water simulations involve running the propeller in open water at a fixed revolution rate and changing the inlet velocities so as to cover the range of advance coefficients (J) values required. For the ducted case, the open water characteristics can be defined as follows :-

$$K_{TP}\ (Propeller\ Thrust\ Coefficient) = \frac{T_P}{\rho n^2 D^4} \quad (1)$$

$$K_{TD}\ (Duct\ Thrust\ Coefficient) = \frac{T_D}{\rho n^2 D^4} \quad (2)$$

$$K_Q\ (Torque\ Coefficient) = \frac{Q}{\rho n^2 D^5} \quad (3)$$

$$\eta_o\ (Open\ Water\ Efficiency) = \frac{K_{TP}+K_{TD}}{K_Q} \cdot \frac{J}{2\pi} \quad (4)$$

T_P and T_D are the thrusts from the propeller blade and the partial duct, respectively, ρ is the density of water and n is the revolution rate in rps.

2.2. Nominal Wake Analysis

The benchmark ship model KVLCC2 (KRISO Very Large Crude Carrier) has been used as the hull geometry for investigating the effects of the partial accelerating duct on nominal wake. KVLCC2 is the second variation made from the initial benchmark model- the MOERI tanker, and has been modified to have more U-shaped lines towards the stern. The hull form has been extensively used for various model tests and CFD studies around the world. A scaled down CAD model with scale ratio λ = 1:100 has been used in the simulations. The main particulars of the KVLCC2 hull are given in Table II. The analysis involves validating the bare hull resistance of the KVLCC2 with published model test data and then investigate the variations in the nominal wake field caused by the presence of the partial duct, now considered as part of the hull. All simulations are undertaken at the operating Froude Number of 0.142.

Table II: Principal particulars of the full scale KVLCC2 hull, *Stern (2008)*

Length Between Perpendiculars (L_{BP}) (m)	320
Breadth (B) (m)	58
Depth (D) (m)	30
Draft (T) (m)	20.8
Block Coefficient (C_B)	0.8098
Volume Displacement (∇) (m^3)	312662
Wetted Surface Area (excluding rudder) (S) (m^2)	27194
Longitudinal Centre of Buoyancy (LCB), % (fwd+)	3.48

3. Numerical Setup

3.1. Governing Equations

Computational Fluid Dynamics (CFD) codes use the Reynolds-Averaged Navier Stokes (RANS) equations with closure turbulence models to solve the complex flows of Newtonian fluids. The governing equations in integral form are (continuity and momentum equations, respectively):

$$\frac{\partial}{\partial t}\int_V \rho \, dV + \int_S \boldsymbol{v}.\boldsymbol{n} \, dS = 0 \quad (5)$$

$$\frac{\partial}{\partial t}\int_V \rho \, \boldsymbol{v} \, dV + \int_S \rho \boldsymbol{v}\boldsymbol{v}.\boldsymbol{n} \, dS = \int_S \boldsymbol{T}.\boldsymbol{n} \, dS + \int_V \rho \boldsymbol{b} dV \quad (6)$$

V denotes the control volume bounded by surface S and **n** is the normal vector outwards. Body forces are given by **b**, ***v*** is the velocity vector and **T** is the stress tensor.

Spatial and temporal discretization schemes are used to obtain iterative numerical solutions using a Finite Volume Method (FVM), with suitable pressure velocity coupling algorithms. A combination of the Boussinesq Hypothesis and the Menter's k-ω Shear Stress Transport (SST) model have been used in the simulations with a Semi-Implicit Method for Pressure Linked Equations (SIMPLE) algorithm being used for the pressure-velocity coupling. The commercial CFD suite Siemens' Simcenter STAR-CCM+ v13.06 has been used for undertaking all CFD simulations in the present work.

3.2. Open Water Simulations

A cylindrical domain with a hemispherical inlet (radius = 5D, outlet length =13D from propeller) has been defined for the fluid domain and a rotating domain has been defined around the propeller so as to ensure a clearance of 2 mm from the inner surface of the duct, Fig.2.

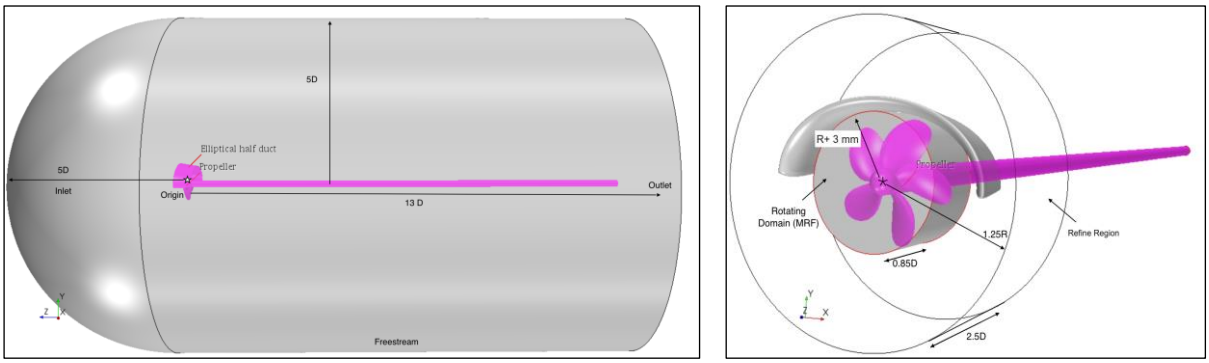


Fig.2: Domain definition for Open Water Simulations

The core mesh consists of polyhedral cells within the rotating domain, with prism layers defined around the propeller and duct for capturing complex flow gradients. The fluid domain is made of trimmed cell giving a Cartesian octree mesh. The final mesh has a wall $y^+ < 2$ over the propeller and duct, and has been obtained based on a grid refinement study undertaken as per ITTC recommendations for the B-5.75 propeller using convergence of K_T and $10K_Q$ values at J=0.2 being compared with published open water model test data, Fig.3. A geometrically similar mesh is obtained by adopting the same meshing methodology for the other three propeller designs, thereby reducing errors that may originate from different simulation setups.

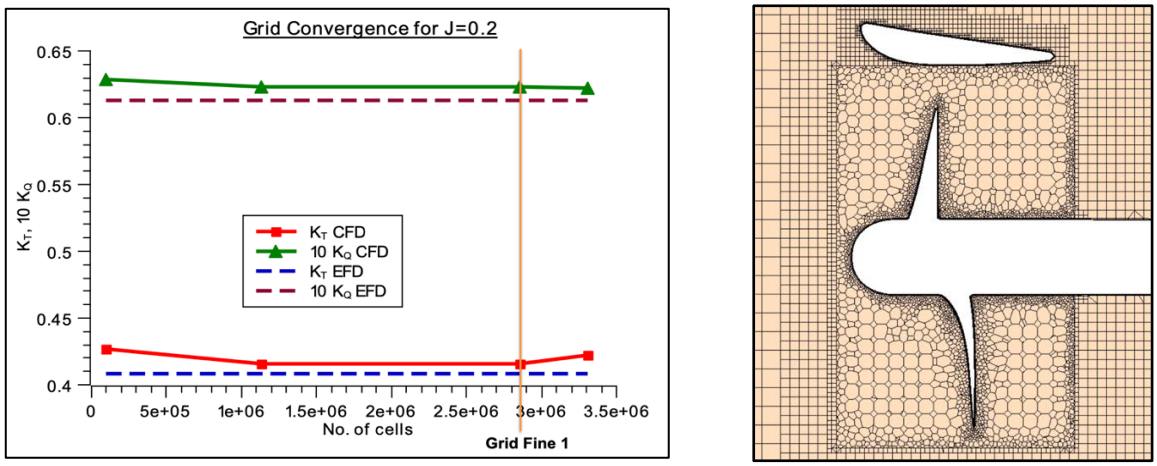


Fig.3: Grid Refinement Study and resulting final core mesh around propeller and partial duct

Propeller rotations have been simulated using the Moving Reference Frame (MRF) technique and for transient solutions, the sliding mesh technique with body rotation has been used

3.2.2. Nominal Wake Analysis

The simulations for analysing the nominal wake behind the KVLCC2 hull involve definition of a cuboidal towing tank (1L forward, 3L behind 1L below and 1.5L from the hull where L is the model length), and then moving the fluid inside it at the intended ship's speed. Due to port-starboard symmetry, undertaking simulations over half of the ship's hull, cut along its centre plane, and hence half of the numerical tank is sufficient. There is very little influence of the free surface and motions like sinkage and trim on the flow at the propeller disc and therefore, these effects can be considered negligible for wake predictions in ships running at such low speed regimes. The double-body model is used treating the free-surface as the symmetry plane to save computational effort.

The mesh for nominal wake analysis consists of a trimmed cell octree mesh with prism layers defined on the hull and duct surfaces. Further mesh refinements are provided near the ship bow, ship stern and the propeller slipstream to accurately capture possible flow separation phenomena and flow gradients

in these critical regions with a resulting y+ on the hull and duct less than 2. The final mesh for nominal wake analyses is obtained using a similar grid refinement study undertaken for the convergence of bare hull resistance at the model scale.

The velocity inlet has only x velocity component defined, the outlet is a pressure outlet; the top, bottom and sides are defined as symmetry planes and the hull and duct are defined as no slip walls. A steady simulation with the SIMPLE algorithm is used for Pressure Velocity Coupling with a segregated solver, which has more approximations but offers faster convergence. Again, the k-ω SST model with an all-wall y+ treatment have been employed in these simulations.

4. Results and Discussions

4.1. Effect of the Partial Duct on Open Water Characteristics

The open water simulations are undertaken in the model scale wherein the Reynold's number is in the range 2 x 10^5 to 1.6 x 10^6 over the range of J values. The results obtained for the B-5.75 propeller is validated with published results, Fig.4, and the average deviation is found to be within 2-3%, the errors found to be greater at higher J values.

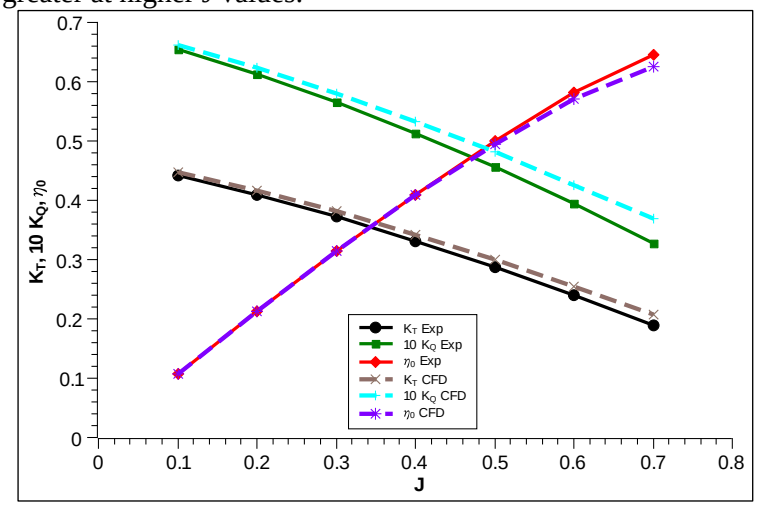


Fig.4: Validation of simulated Open water results of B-5.75 propeller with published model test data

Bhattacharyya et al (2015) compared the use of the γ-Re_θ transition model in open water simulations with the results of a standard k-ω SST model. The detailed implementation of the γ-Re_θ transition model in Star CCM+ involves defining custom turbulence intensity and turbulence viscosity ratio, through the definition of a kinetic energy source in the form of ambient or specified turbulence sources. The use of transition modelling has a definite influence over the flow patterns and the pressure and friction components of the propeller forces in model scale, especially at lower Reynolds numbers where flow transition occurs. For the B-5.75 propeller, it was observed that the use of the γ-Re_θ transition model for the given range of Reynolds numbers resulted in nearly the same results as predicted with a standard k-ω SST model, with average deviation in the CFD results being less than around 3% at the J value of 0.7. Therefore the standard model without transition capturing has been used in all open water simulations, including within the partial duct for all four propeller cases, to avoid the associated complexities in definitions of turbulence parameters. As an example, the open water characteristics of the B-5.75 propeller within the partial duct is shown in Fig.5.

The thrust generated by the partial duct in open water is found to be quite insignificant as observed in the open water diagram. The duct thrust is only 3.5% of the propeller thrust at J=0.1, and decreases steadily at higher J values. This may be attributed to the flow around the elliptical geometry as well as the higher drag due to the end vortices.

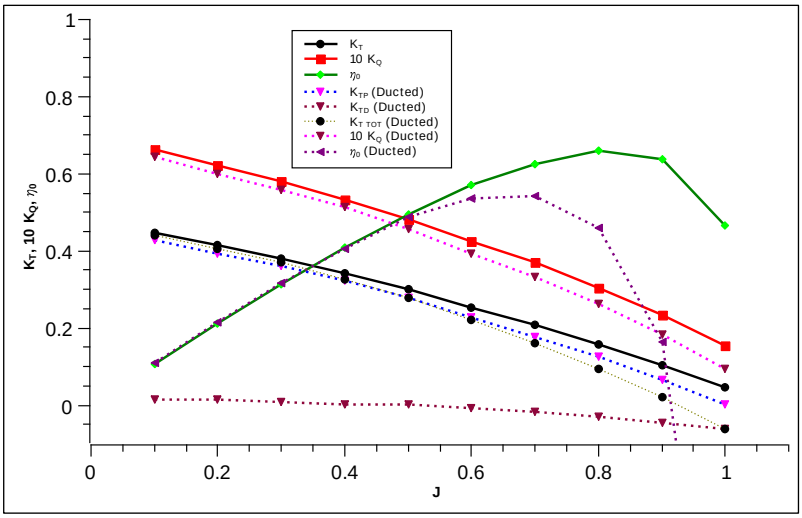


Fig.5: Open Water Characteristics of the B- 5.75 propeller within the partial duct

A detailed study on the effects of the partial duct for a B-Series propeller, in terms of pressure coefficient plots over blade and duct sections, including unsteady simulations and scale effects on duct are elucidated in *Bhattacharyya and Ramesh (2024).* The percentage variations in open water efficiency η_0 for all the four propellers, from their respective non-ducted cases, are shown for three representative J values of 0.1, 0.2 and 0.4 in Fig.6. With the partial duct fitted, the thrust and torque are found to reduce from the non-ducted case, due to acceleration of the flow, which consequently also affects the open water efficiency. The change in open water efficiency that is observed depends on the relative changes of propeller thrust and torque and also depends on the contribution to thrust from the partial duct. The small improvements in open water efficiency that has been observed are restricted to the heavy propeller loadings.

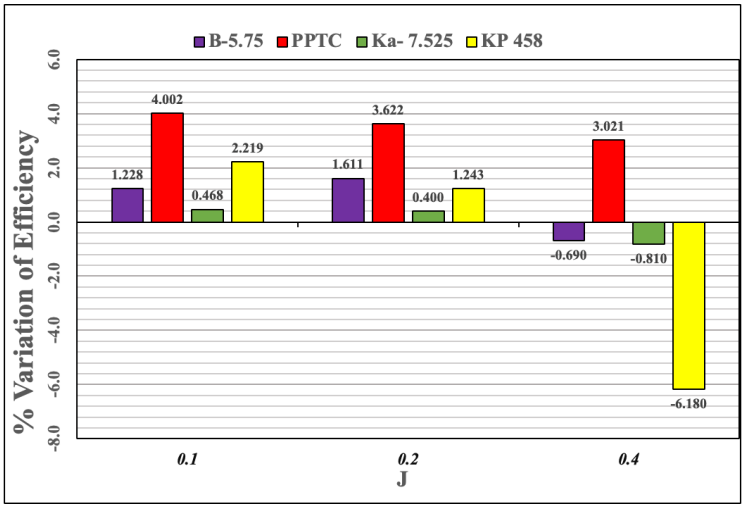


Fig.6: Variation of Open Water Efficiency with J for the various propellers within the partial duct

The pressure coefficient plotted over a representative blade section taken at 0.7R provides further insight into the effect of the partial duct. The resultant flow velocity V_R comprising of axial and rotational components is used to non-dimensionalise the pressure and the blade chord is used to non-dimensionalise the chordwise position over the blade section. At a low J value of 0.2, all four propellers show a similar decrease in pressure difference between the face and back in the presence of the partial duct, resulting in a minor reduction in propeller thrust and torque at these heavily loaded conditions. The maximum change is observed in the Kaplan propeller, possibly due to the wider tip design, Fig.7.

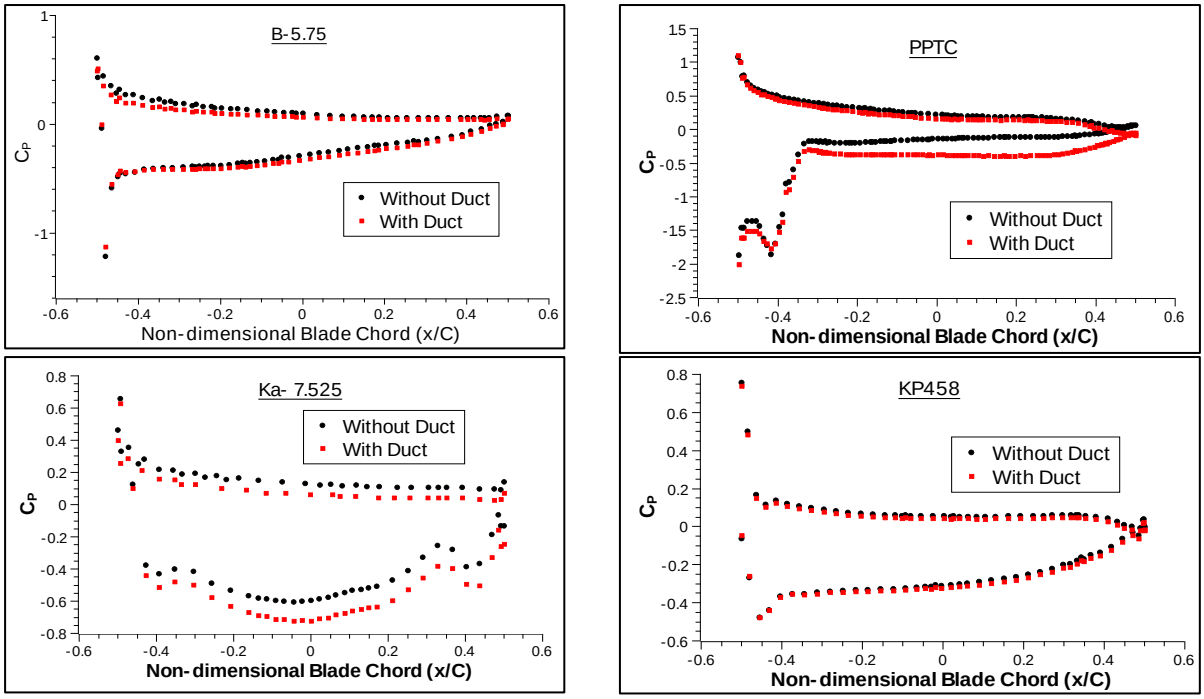
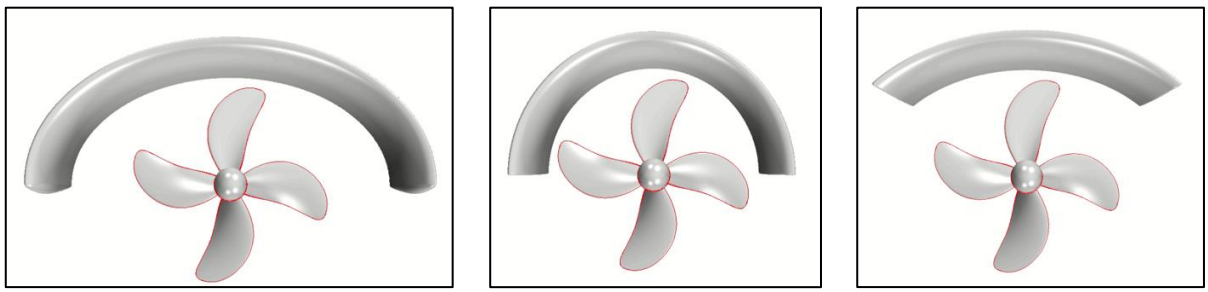


Fig.7: Effect of the partial duct on pressure coefficient over a blade section at 0.7R at J=0.2

4.2. Effect of variations in duct design

Three different variations of the partial duct design have been generated for understanding the effect of variation in duct design on open water characteristics. Duct 1 is the elliptic partial duct design with axis ratio 1.5. Duct 2 is a semi-circular partial duct with the same 19A section and Duct 3 is a modified version of Duct 1 extending only 60° on either side of the vertical along the same elliptic generating line and is hereby termed as the 60/60 partial duct. The three duct designs are shown in Fig.8.



Duct 1 -Elliptic Partial Duct Duct 2 – Semi Circular Duct Duct 3 – 60/60 Partial Duct

Fig.8: Variations in partial duct design

A comparison of the percentage variation in thrust, torque and open water efficiency and the total duct thrust in model scale for the KP458 propeller within the three different duct designs over a range of low J values (0.05-0.25) is shown in Fig.9. All three duct variants decrease the propeller thrust and torque due to flow acceleration as expected. However, the maximum open water efficiency at higher propeller loading is found to be given by the elliptic partial duct. A comparison of the contribution to total thrust by the partial duct indicates that the semi-circular duct generates maximum duct thrust.

The effect of the partial duct design is investigated further by plotting pressure coefficient over duct sections cut at 30° and 45° from the vertical blade position at J=0.1, Fig.10. At the vertical section (0°), the propeller blade is passing closest to the duct in the elliptic and 60/60 configurations, and this distance increases with increases distance from the vertical position. The rpm-based velocity ‘nD’ is used to compute C_P and the position on the duct is non-dimensionalised using duct chord with leading and trailing duct edges at -0.5 and 0.5, respectively.

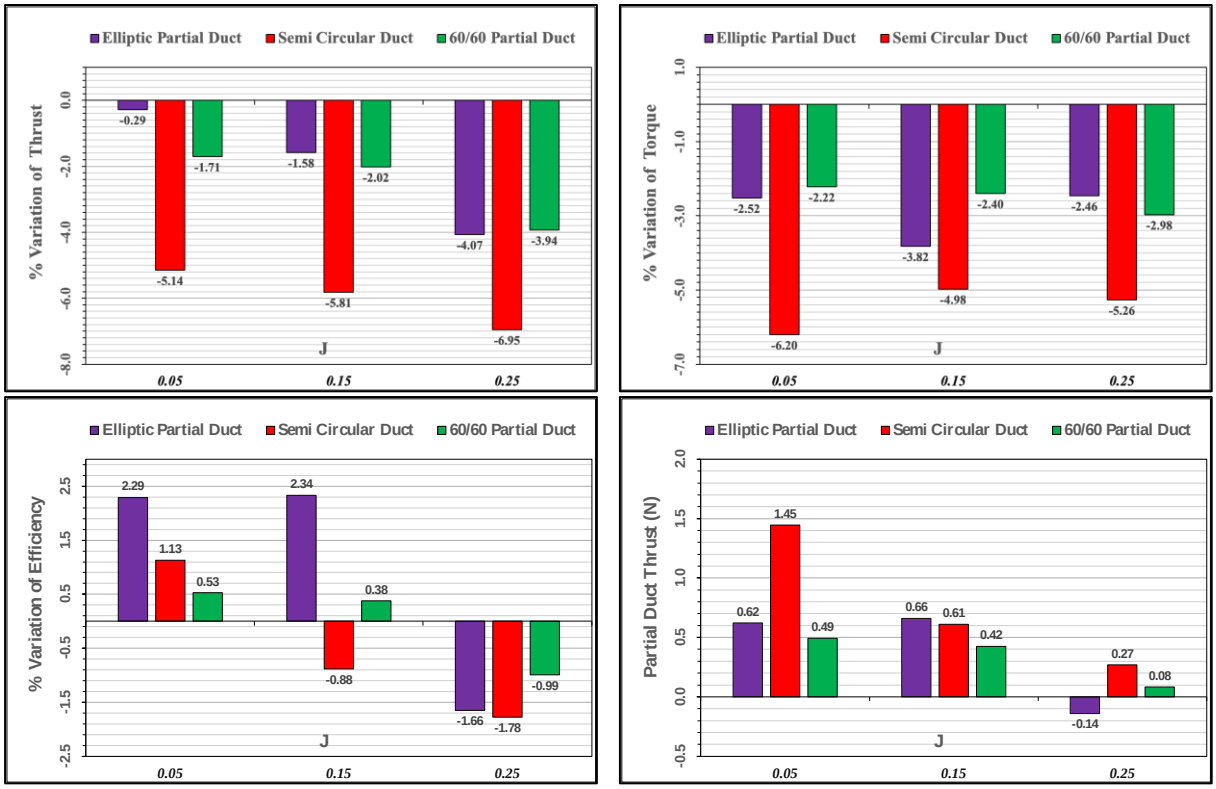


Fig.9: Percentage Variation in Propeller Thrust, Torque, Efficiency and Duct Thrust for the KP458 propeller within different partial duct designs, as compared to the non ducted condition in open water (positive % indicate higher value wrt non-ducted condition and vive-versa)

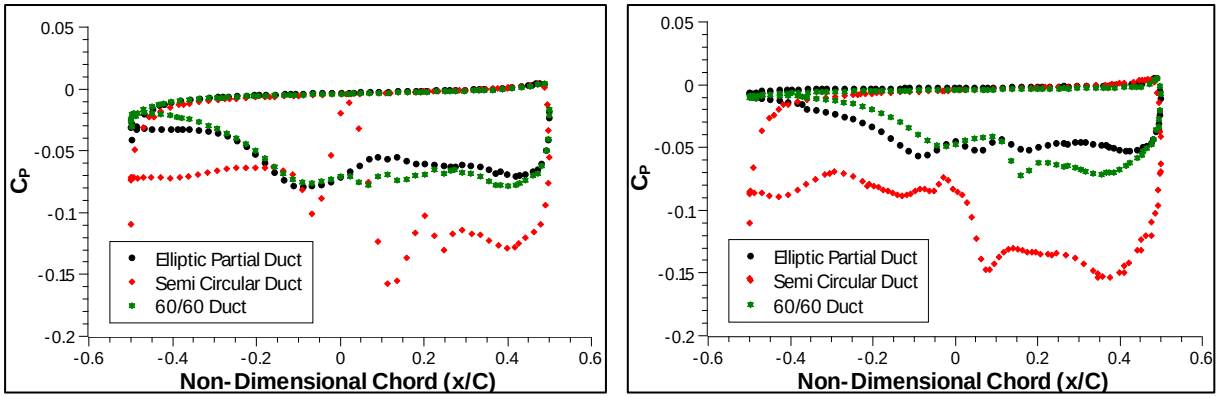


Fig.10: C_P over the duct sections at 30° (Left) and 45° (Right) for the three partial duct designs

As the proximity from the blade increases at 45° for the two elliptic designs, there is a reduction seen in the difference between pressure and suction side peaks. The semi-circular duct has maximum negative suction, and the value remains more or less unchanged with distance from the vertical, as the clearance from the blade tip remains the same.

4.3. Effect of the Partial Accelerating Duct on Nominal Wake behind a KVLCC2 hull

Any device which is placed in the ship stern adds to total vessel resistance due to its own drag as an appendage. The idea behind the partial duct is to obtain certain hydrodynamic advantages over and above its drag due to its geometry and positioning with respect to the propeller. Hence, the net intended effect including the increase in drag should be a reduction in the powering requirement. This requires undertaking a self-propulsion analysis and powering calculations based on the results on the self-propulsion tests, which have not been performed in the present study. Resistance tests form a pre-requisite for the powering calculations and the resulting nominal wake field is useful in tailoring the

duct design for improved wake characteristics and powering performance. The design of the partial duct is based on its primary intended function of is to provide flow acceleration on the propeller plane in the region above the propeller axis where the wake fraction is higher.

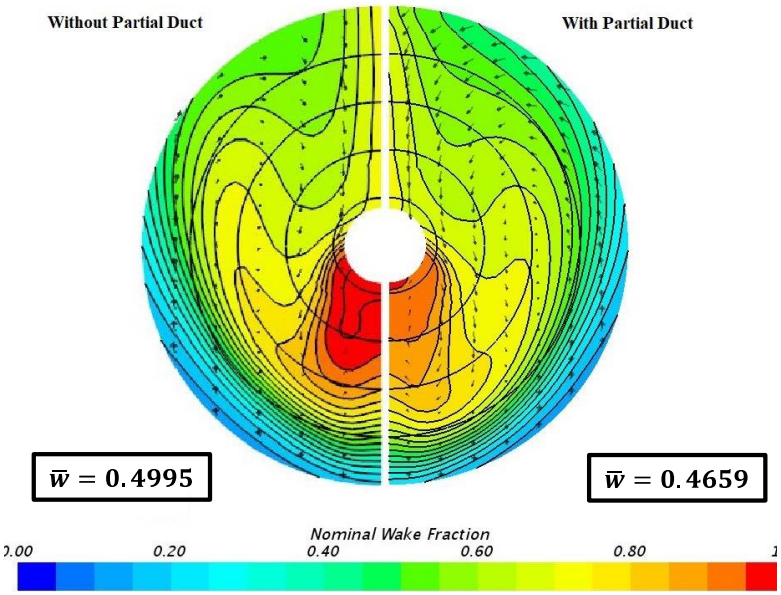


Fig.11: Nominal Wake Fields behind the KVLCC2 hull with and without the partial duct

As the partial duct is located at the propeller plane, the hydrodynamic interaction between the duct and propeller is expected to be stronger, and it becomes important to understand the effect the partial duct can have on the ship's nominal wake field. The comparison of nominal wake plot obtained with and without the partial duct behind a KVLCC2 hull is shown in Fig.11. The resulting nominal wake plot displays significant wake equalization, therefore verifying its intended advantage for the given hull configuration, with the wake fraction $\bar{w} = \left(1 - \frac{V_a}{V}\right)$= 0.4995 without duct and 0.4695 with the partial duct, where V_a is the axial velocity and V is the inflow velocity.

4.4. Effect of different duct designs on nominal wake

The three partial duct designs used for the open water simulations with the KP458 propeller are used for understanding the extent of wake equalisation caused by these different ducts. The nominal wake fields behind the KVLCC2 hull for the elliptic partial duct, the semi-circular duct, and the 60/60 partial duct are shown in Fig.12. Comparison of the contour plots indicates that the maximum wake equalisation for the present hull configuration is provided by the elliptic partial duct design. To understand this effect, further qualitative analyses of the nominal wake fields are conducted.

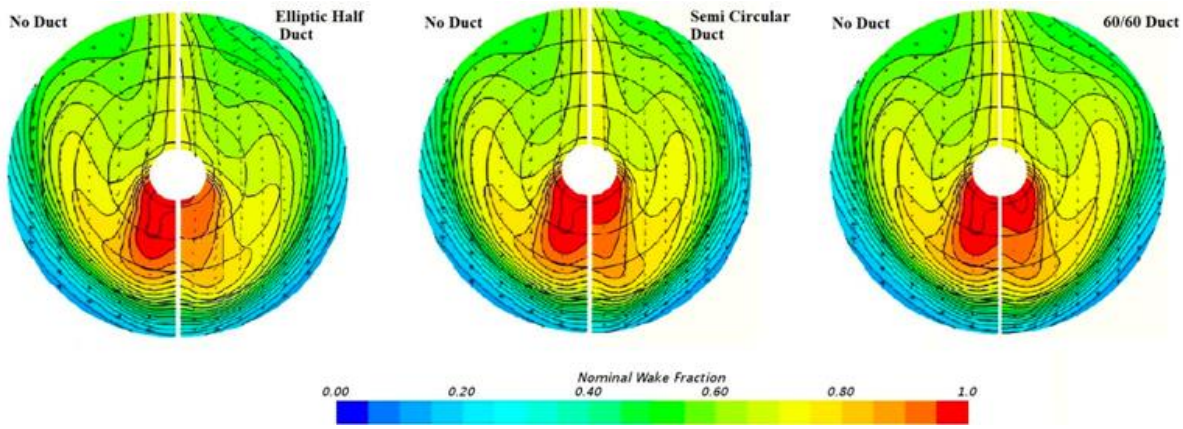


Fig.12: Nominal Wake Fields behind the KVLCC2 hull with different partial duct designs

4.5. Wake Quality Analysis

Two methods have been followed for the analysis of the nominal wake that provides a qualitative picture of the improvement in the wake field effected by the presence of the partial duct designs. Though evident in the contour plot in Fig.12 as an obvious reduction in wake fraction in the propeller disc, a better interpretation for wake equalisation can be obtained by these methods.

4.5.1. Basic Wake Quality Analysis

The first basic method involves plotting the axial (V_a) velocity components at the propeller plane, non-dimensionalised by the inlet velocity or the ship's speed (V), to obtain the axial velocity ratio. Axial velocity ratio has port starboard symmetry for a symmetric hull and the plots from the half body simulations can be mirrored to obtain variations over the full 360° peripheral disc angle. In this, the axial velocity ratio distributions are analysed to give the following parameters at each radial position.

$$\text{Maximum velocity variation-}\quad \Delta\left(\frac{v_a}{v}\right)_r = \left(\frac{v_a}{v}\right)_{r,max} - \left(\frac{v_a}{v}\right)_{r,min} \tag{7}$$

$$\text{Averaged velocity ratio-}\quad \overline{\left(\frac{v_a}{v}\right)_r} = \frac{1}{\Delta\varphi}\int_{\varphi_{min}}^{\varphi_{max}} \left(\frac{v_a}{v}\right)_r d\varphi \tag{8}$$

r is the radius being evaluated, and φ is the peripheral angle. Fig.13 shows the basic wake quality assessment undertaken the three different duct designs.

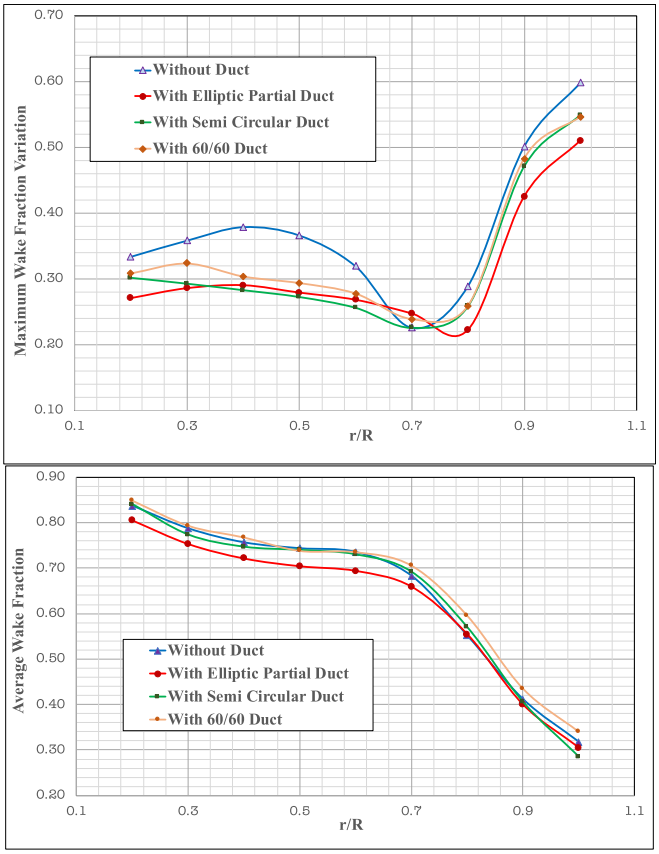


Fig.13: Comparison of maximum wake variation and mean wake fraction at different radial locations for the different cases with and without the partial duct designs

The elliptic partial duct, in general, provides maximum improvement in axial velocity in the ducted region (-90° to +90°) over the propeller disc, in comparison to the other two duct designs. In the outermost radii of the disc, the effect of the semicircular duct is more pronounced view proximity of the propeller plane to the inner surface of the duct.

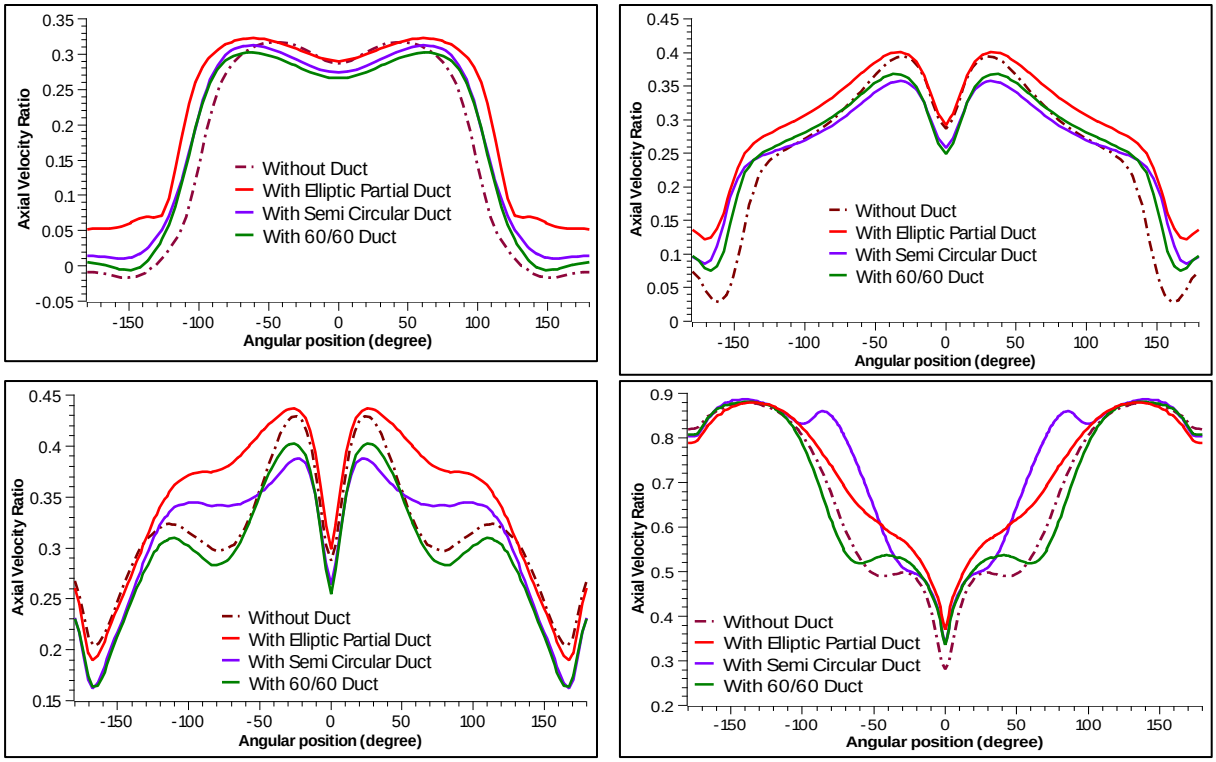


Fig.14: Variation of axial velocity ratio over peripheral angle for r/R =0.2, 0.5, 0.7 and 1.0 for different partial duct designs

4.5.2. BSRA Wake Quality Criteria (Odabasi and Fitzsimmons, 1978)

During their time in BSRA (British Ship Research Association), Odabasi and Fitzsimmons proposed five criteria to examine wake quality, with main focus being on the top dead centre region of a propeller disc, Maasch et al. (2018). The measurement points for the quality analysis requires the use of polar coordinates to depict propeller nominal wake, so that the results are available in the form of velocity distributions in radial and circumferential directions also, and an overall picture of the velocity vector faced by the propeller can be adjudged. Several criteria values were specified based on the top dead centre region and the ship hull form parameters and operational conditions to evaluate the wake field quality. In the present study, these criteria have been evaluated with and without the partial duct (including different duct designs) to understand the extent by which the partial duct influences the wake field quality. The results of the wake quality analysis with and without the partial duct designs are summarised in Table III.

Table III: BSRA Wake Quality Criteria Check

Criterion	Without Duct	Elliptic Partial Duct	Semi-Circular Duct	60/60 Partial Duct
$\bar{w}_{disc}$	0.4995	0.4659	0.4976	0.5045
$w_{max,\emptyset_B} < (0.75, C_B)_{min}$	0.725 (0.75)	0.705 (0.75)	0.743 (0.75)	0.751 (0.75)
$w_{max,disc} < 1.7\,\overline{w_{0.7R}}$	1.021 (1.1609)	0.9911 (1.121)	0.9907 (1.1759)	1.0067 (1.1999)
Width of Wake Peak at r/R=1 > Wake Shadow Area	39° (50°)	36° (50°)	40° (50°)	32° (50°)
Intersection of Wake Non-Uniformity and Tip Cavitation in Acceptable Region	Fulfilled (> 0.26)	Fulfilled (> 0.25)	Fulfilled (> 0.27)	Fulfilled (> 0.25)

Limits are specified within parentheses and criteria that are fulfilled are shown in green and those not fulfilled are shown in red. The fourth criterion indicates extent of excitation forces on the hull by

finding the intersection point between the tip based cavitation number and the wake non-uniformity at r/R=1.0, and requires this value to be above a threshold line. Though the third criterion is not satisfied in any of the cases, the partial elliptic partial duct shows maximum improvement in the wake quality parameters.

5. Concluding Remarks

A systematic investigation has been conducted on the hydrodynamic performance of a patented partial duct design with different propeller designs and a benchmark ship model. Due to flow acceleration by the partial duct, the propeller thrust and torque are reduced and a combination of these gives rise to marginally higher propeller open water efficiency, restricted however to high propeller loadings. A parametric study on the variation of the elliptical geometry indicates that the optimal influence on propeller characteristics in open water is provided by the duct with the axis ratio of 1.5. The elliptic partial duct design also provides best wake equalisation as indicated by the values in the BSRA Quality criteria. It is important to mention that the present study provides only some preliminary estimates of the hydrodynamic influence of a partial accelerating duct on the open water performance of a marine propeller and the nominal wake behind a benchmark hull form. Practical applications of this study would also need to encompass stern designs, support structures for the partial duct and clearances from the hull.

Further investigations need to estimate the hull-propeller interaction parameters due to the partial duct designs to provide a better picture on the performance of the propeller in conjunction with the partial duct. This would necessitate conduct of self-propulsion simulations with and without the partial duct and validation of the same with model tests in a towing tank. Also, considering the complexities involved while assessing Reynolds scale effects for such devices, it is envisaged that full scale CFD simulations need to be performed to better understand the hydrodynamic impacts on ship performance.

Acknowledgements

We would like to acknowledge the Sagarmala Cell, Ministry of Ports, Shipping and Waterways, Govt. of India for providing funds through the Centre for Inland and Coastal Maritime Technology (CICMT) at IIT Kharagpur.

References

BHATTACHARYYA, A. (2020), *Partial accelerating duct around a marine propeller*. India Patent No. 506503

BHATTACHARYYA, A; RAMESH, K. (2024), *A Partial Accelerating Duct over the Marine Propeller,* 8th Int. Symp. Marine Propulsors (SMP'24), Berlin, pp.659-665, https://doi.org/10.15480/882.9331

BHATTACHARYYA, A; NIETZEL, J.C.; STEEN, S; ABDEL-MAKSOUD, M; KRASILNIKOV, V. (2015), *Influence of flow transition on Open and Ducted propeller Characteristics*, 4th Int. Symp. Marine Propulsors (SMP'15), Austin

ITTC (2011), *Practical guidelines for ship CFD applications,* ITTC – Recommended Procedures and Guidelines, Vol. 7.5–03–02–03, Int. Towing Tank Conf.

ITTC (2014), *Practical guidelines for ship self-propulsion CFD,* ITTC – Recommended Procedures and Guidelines, Vol. 7.5–03–03–01, Int. Towing Tank Conf.

MAASCH, M; MIZZI, K; ATLAR, M; FITZSIMMONS, P; TURAN, O. (2018), *A generic wake analysis tool and its application to the Japan Bulk Carrier Test Case*, Elsevier Ocean Engineering Series 171(120), pp.575-589

MEWIS, F. (2009), *A Novel Power-Saving Device for Full-Form Vessels*, 1st Int. Symposium on Marine Propulsors (SMP'09), Trondheim

ODABASI, A.Y; FITZSIMMONS, P.A. (1978), *Alternative methods for wake quality assessment*, Int. Shipbuilding Progress 25/282, pp.34-42

SCHNEEKLUTH, H. (1986), *Wake Equalising Ducts*, The Naval Architect

STERN, F; AGDRUP, K. (Ed.) (2008), *SIMMAN 2008. Workshop on Verification and Validation of Ship Manoeuvring Simulation Methods*, Copenhagen

TERWISGA, T. (2013), *On the working principles of Energy Saving Devices*, 3rd Int. Symp. Marine Propulsors (SMP'13), Launceston

Sustainably Powered Autonomous Surface Vessels

Robert Dane, Ocius Technology, Randwick/Australia, robert@ocius.com.au
Nick Rozenauers, Ocius Technology, Randwick/Australia, nick.rozenauers@ocius.com.au
Ian Milliner, Ocius Technology, Randwick/Australia, ian.milliner@ocius.com.au

Abstract

This paper describes the concept of Ocius' Uncrewed Surface Vessels (USVs), the 'Bluebottles'. The drones are autonomous robots powered by solar, wind and wave energy making them also autonomous in terms of energy, allowing long periods of operation covering vast areas. The drones are team capable and approved by AMSA for operating in Australia's EEZ to conduct long-duration autonomous surveillance missions. Ocius is currently deploying Bluebottles for defence, oil & gas, and oceanography missions around Australia.

1. Our story – The long enjoyable road towards the "Bluebottles"

The Bluebottle range of USVs (Unmanned Surface Vehicles) are innovative unmanned drones designed to provide long-term autonomous surveillance and communications for defence, offshore, or oceanographic applications, Fig.1, https://ocius.com.au/. They represent a unique combination of technologies making them "doubly autonomous":

- The drones are "intelligence autonomous" in some decision-making, e.g. using Artificial Intelligence for autonomous collision avoidance and team capability. This is the normal autonomy that people have in mind when talking about autonomous underwater vehicles or autonomous (future) surface ships, e.g. *Bertram (2016).*
- The drones are also "energy autonomous" using wind, solar and wave power, with rechargeable batteries to ensure propulsion and manoeuvring at all times. Sustainably powered USVs like the Bluebottle drones could stay at sea indefinitely, in theory. A current practical limitation can be accumulating biofouling. Classical biocidal antifouling solutions have typical life cycles of 5 years before requiring replacement, but some of the evolving innovative solutions for biofouling, *Bertram (2023)*, may overcome the issue with biofouling limiting deployment times.

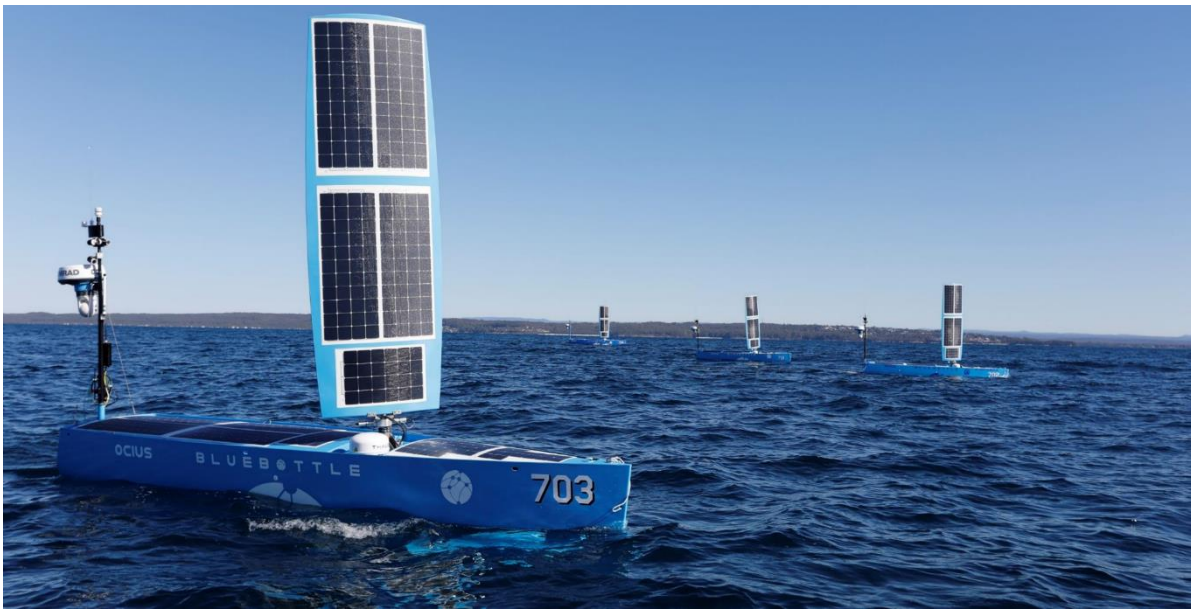


Fig.1: Bluebottle drones at sea

The Bluebottle solution is unique in its combination of intelligence and energy autonomy. It is the product of an evolution that spans almost 30 years (of trials and tribulations, as well as triumphs):

- 1997-2000
  - Winner of Advanced Technology Boat Race in Canberra with a boat with solar panels, Fig.2, that could angle to the sun and wind and fold away.
  - Formation of SolarSailor Holdings Limited.

- 2001-2014
  - Built solar ferry for Sydney Olympics, Fig.3, which won 2001 Australian Design Award of the year
  - Six hybrid ferries sold to Australia, China and Hong Kong carrying 10s of thousands of passengers

- 2015-2021
  - Enquiry from USA for building a platform that could go to sea 'forever'
  - Three successive defence innovation contracts
  - Seven USVs built and completed successful missions with Australian Border Force, RAN, Army, Ops Sovereign Borders and Marine Parks Australia, Fig.4

- 2022-Current
  - Contract for five Bluebottles for $5M with Warfare Innovation Navy (WIN) branch
  - Royal Australian Navy (RAN) operations contract
  - JAMSTEC contract, mapping underwater volcanoes off Japan
  - Marine Parks Australia
  - Oil and Gas trial
  - Trials for Royal New Zealand Navy
  - Named as a program of record by Australian Navy
  - Sold two Bluebottles to US company Thayer Mahan.



Fig.2: Boat Race winning solar-sail boat



Fig.3: SolarSailor, *Dane (2006)*

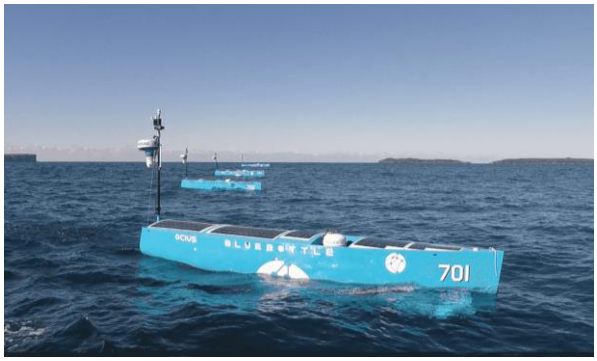


Fig.4: Bluebottle for Royal Australian Navy



Fig.5: Bluebottle trials in San Diego, USA

2. Bluebottle technology

Ocius' Bluebottle drones operate on energy harvested at sea. Thus, the 'Beth' type Bluebottle requires no fuel and no crew, hence no supplies. The 'Bathy' type Bluebottle offer enhanced power options at night and wind-still conditions using diesel hybrid propulsion. See Appendix I for technical specifications. Both Bluebottle types are self-deploying and self-retrieving and can roam widely or be kept on station virtually indefinitely. The following will focus on the 'Beth' type.

2.1. Persistent long-range ISR (Intelligence, Surveillance and Reconnaissance)

The ultimate objective of the development of the Bluebottle drones was to showcase an affordable, persistent, long-range detection capability, primarily to bolster the ability of navies and border forces to identify and monitor potential threats (e.g. submarines) from practical distances.

The "persistent" part requires rechargeable batteries for power supply when the mix of solar, wind, and wave energy was insufficient. As illustrative example, Bluebottle drones off the coast of Australia operated for 35000 nm over two years, on a long-term ISR mission, Fig.6.

The "long-range detection" is based on an array of low-cost, low-power sensors. Mission-specific sensor suites can be installed in the modular concept, fitted inside the hull and on the aft communications mast. An integrated and networked communication system supports live tracking and monitoring of the drones. They may be operating autonomously or under remote control.



Fig.6: Long-term Bluebottle deployment for ISR missions in Australia and New Zealand

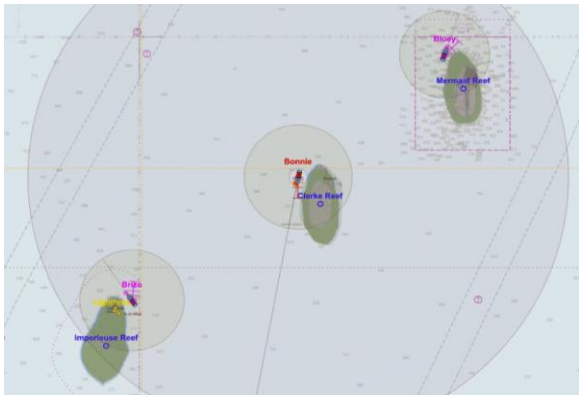


Fig.7: Bluebottles operating in a team

The drones have some "thinking" and decision autonomy including team capabilities, Fig.7, where Bluebottle drones communicate in a team and e.g. reconfigure location, selecting one vessel in a team to inspect a suspicious object, while the others continue to patrol a given area, etc.

The Bluebottle capabilities allow a variety of missions:

- Maritime Domain Awareness - Proven ISR capability with Australian Border Force, Regional Force Surveillance Group, and AMP (Australia Marine Parks).
- Enhanced ISR - Improved Radar, cameras, plus acoustic sensors and better Artificial Intelligence
- Anti-Submarine Warfare – Bluebottle equipped with a winch for a thin line array that detects and locates underwater vessels
- Communication Gateway - Bluebottle used as platform to connect with underwater assets
- Electronic Warfare - Monitoring of electromagnetic signals and spoofing
- Mine Counter Measures - Demonstrated with DST (https://www.dst.defence.gov.au/) Autonomous Underwater Vehicles

- Bathymetry - Single and multi-beam echo sounders can be fitted to Bluebottles to map underwater topography, Fig.8
- Offshore oil & gas/windfarms - Environmental monitoring, security and wildlife surveillance, Fig.9



Fig.8: Bathymetric detection of wreck on seabed



Fig.9: Offshore underwater inspection

2.2. Interoperability

Autonomous USVs like the Bluebottles can and should be part of a larger (defence) eco-system, collaborating with other Bluebottles, other robotic systems (e.g. underwater drones), or crewed vessels. Especially for countries with long coasts and sparse populations/harbours, Bluebottles can act as "satellites of the sea" with permanent surveillance of territorial waters. The combination of autonomous eyes on the front together with rapid response forces of manned vessels is an effective and also cost-effective approach to protection of security and economic interests for coastal states, as proven by the Australian Border Force, Fig.10.



Fig.10: Typical application cases for Bluebottles in ABF service

2.3. Deployability

The Bluebottle is easily deployable, using a choice of options, Fig.11:



Fig.11: Launch from a boat ramp



Fig.12: Launch by crane from ship

- Launch and recovery from a boat ramp, transport with road trailer, Fig.11
- Launch by helicopter from a ship
- Launch by crane from a ship, Fig.12

Only an area of 900 m^2 of hardstand is required. The containerised logistics support makes the Bluebottle easily deployable and operational.

2.4. Management

Support USV operations requires a skilled workforce of pilots and technicians. Ocius has supported customers with a flexible approach to vessel management, depending on their ability to support such a workforce. For customers who wish to own the platform, Ocius has sold boat and can support their operations with training, spares and maintenance. However, noting the personnel problems that navies are experiencing, Ocius developed an operational 'capability as a service' model, Fig.13, where Ocius supports depot level maintenance and operations up to the operational area, where it then hands control to a uniformed member of the navy. This model minimizes the resources needed and skilled personnel by navies to support uncrewed operations. This model is similarly used by Ocius for commercial applications of the Bluebottle, where it provides vessel time or data as a service.

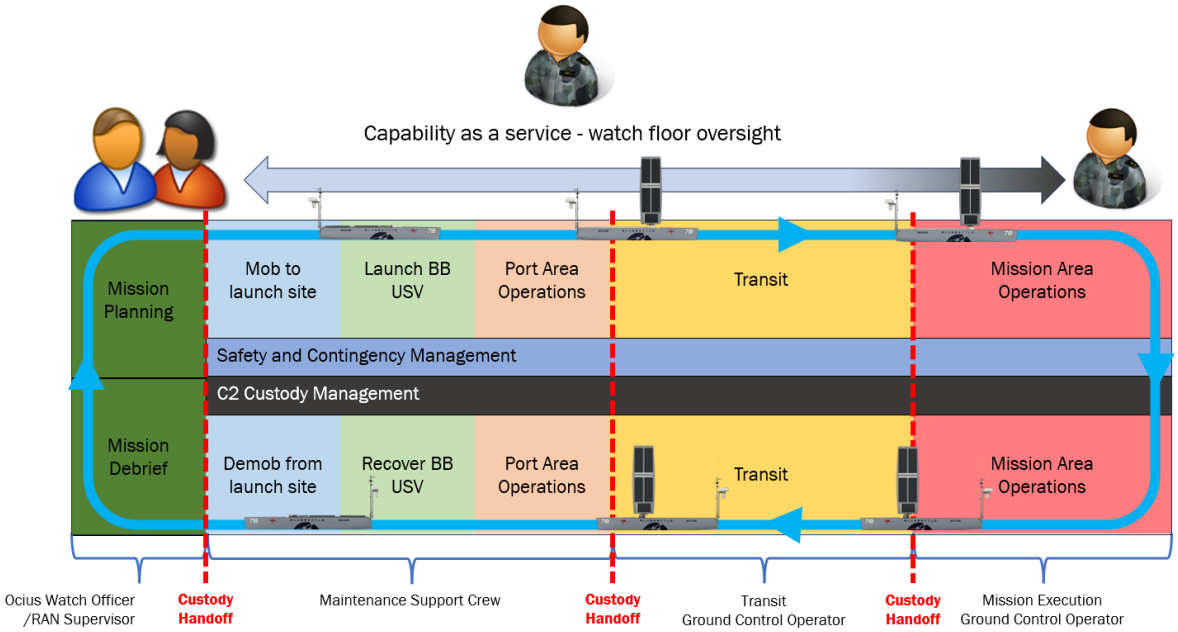


Fig.13: Example management style

3. Conclusions and outlook

The successful adoption of the Bluebottle USV by the Royal Australian and Royal New Zealand Navies for offshore surveillance validates the concept of USVs as force multipliers in border protection. However, the Bluebottle's impact extends far beyond military applications. Its long-range autonomy, low operating costs, and robust design make it ideally suited for growth industries like hydrographic surveys, environmental monitoring, and even anti-submarine warfare in a support role. Across these diverse sectors, operators are drawn to the Bluebottle's ability to minimize risk by using unmanned vessels, its alignment with environmental concerns through low emissions, and its cost-effectiveness compared to traditional methods. The Bluebottle USV is not just a technological advancement; it is a disruptive force transforming the landscape of maritime operations.

References

BERTRAM, V. (2023), *A Snapshot of Evolving Innovative Antifouling Options*, 15th HIPER Conf., Bernried, pp.53-61, http://data.hiper-conf.info/Hiper2023_Bernried.pdf

BERTRAM, V. (2016), *Unmanned & Autonomous Shipping – A Technology Review*, 10th HIPER Conf., Cortona, pp.10-24, http://data.hiper-conf.info/Hiper2016_Cortona.pdf

DANE, R.; PARKER, G.; FAHR, M.; THOMSEN, C.; PATTEN, B. (2006), *Zero Particulate and Toxic Gas Emissions at the wharf by Commercial Hybrid-Electric Powered Vessels*, 5th HIPER Conf., Launceston, pp.447-454, http://data.hiper-conf.info/Hiper2006_Launcerston.pdf

Appendix I – Bluebottle technical specifications

	"Bathy"	"Beth"
Power	Solar, Wind, Wave, Diesel	Solar, Wind, Wave
Length	6.9 m	
Beam	1.3 m	
Draft	1.7 m	
Air draft – mast up	6.0 m	
Air draft – mast down	2.4 m	
Displacement	1500 kg	1100 kg
Top speed	6.0 kn	
Average speed	1.5 kn	3.0 kn
Sailing speed in 5 kn wind	1.4 kn	
Sailing speed in 15 kn wind	3.5 kn	
Sailing speed in 25 kn wind	5.5 kn*	
Operating sea state	5	
Max. sea state	7	
Wave powered speed	0.5-15 kn	
Energy storage	Battery 14-21 kWh Diesel 750 kWh	Battery 14-21 kWh
Solar power	Up to 1.5 kW	
Power allocated for payload	Average 0.85 kW for 30 days Max: 4 kW	Average 0.15 kW for 8 h sun Min: 35 W 10 days no sun Max: 2 kW
Payload	100 kg off sensor mounting bracket incl. MBES, sidescan sonar, sub-bottom profiler	150 kg dry in payload bay 150 kg wet in keel cassette module or winch
LARS	Boat ramp, or ship	
Keel winch diameter	n/a	1780 mm
Winch torque	n/a	120 Nm
Shipping	Two per 40' ISO shipping container	

* Depending on angle of attack

Possibilities for Hybrid Cruise Vessel Performance Optimization through Data-Driven Battery Usage

Teemu Kuusisto, Wärtsilä, Helsinki/Finland, teemu.kuusisto@wartsila.com
Mona Kanafi, Wärtsilä, Helsinki/Finland, mona.kanafi@wartsila.com

Abstract

This article investigates the feasibility and optimization of battery systems in hybrid cruise vessels, focusing on environmental and economic impacts. Using literature review, qualitative interviews, data simulation, and statistical analysis, the study explores integrating Battery Energy Storage Systems (BESS) into cruise power supply. Digital twin simulations suggest that battery integration can achieve OPEX savings of 0.6% - 1.6%. Key challenges include high initial costs and long payback periods, while sensitivity analysis highlights the impact of fuel prices, battery costs, and financial conditions. Despite these hurdles, battery systems can enhance fuel efficiency and reduce emissions, requiring technological advancements and regulatory support.

1. Introduction

In the 2020s, driven by digitalization, increasing environmental awareness, and tightening emission regulations, the traditional maritime industry faces an imperative transformation. Tens of thousands of vessels sail the seas daily, with hundreds of new vessels ordered and built yearly. Maritime transport accounts for nearly 90% of global trade and freight movements, significantly impacting both the world economy and the environment, *Alnes et al. (2017)*. In 2018, shipping alone produced around 1076 million tons of Greenhouse Gases (GHG), representing 2.5–3% of global emissions, which marked an increase of almost 10% since 2014, *IMO (2020).*

Despite being a major polluter, the maritime industry can take critical decisions and actions across the entire lifecycle—from ship design to end-of-life recycling—to combat climate change. Environmental concerns have increasingly gained attention in the maritime business, where most vessels still operate on non-environmentally friendly fossil fuels. The International Maritime Organization (IMO), under the United Nations, regulates and controls maritime business, setting global short and long-term emission reduction targets and energy efficiency regulations for both newbuild and existing vessels. To meet these goals and challenges, the maritime industry needs efficient and environmentally sustainable innovations and solutions to reduce its carbon footprint.

One such solution is the introduction of onboard batteries. Operating a fully electric battery-powered vessel produces zero emissions during the voyage, offering a 100% operating emission savings potential compared to traditional vessels. However, the weight, capacity, and cost of current battery systems make it unfeasible for certain types of vessels to become fully electric. Implementing a battery system as a secondary power source supporting combustion engines has proven to reduce fuel consumption, emissions, and operating expenses by up to 30%, depending on the vessel type and operating profile, *EMSA (2020)*.

To fully utilize the benefits of hybrid power supply, operational vessel data must be collected and analyzed. This data provides insights into the optimal propulsion configuration, battery characteristics, energy control strategy, and other factors contributing to the vessel's efficiency. Energy Storage Systems (ESS) and the hybrid vessel concept are well-studied fields, with research on multiple pilot vessels and various ESS technologies. However, vessel batteries have not been studied as intensively e.g. as their automotive and stationary energy storage counterparts. Previous studies on cruise vessels with battery systems are limited and often lack comprehensive data to support feasibility estimations.

This article is based on *Kuusisto (2023)* master's thesis, aiming to fill the gap in research by providing a detailed examination of the feasibility and optimization of battery systems on hybrid cruise vessels.

2. Methodology

This study employs a mixed-methods approach, integrating both qualitative and quantitative research methodologies to provide a comprehensive understanding of the feasibility and optimization of battery systems on hybrid cruise vessels. The research design includes four primary methods: literature review, qualitative interviews, data simulation, and statistical data analysis.

2.1. Literature Review

The literature review forms the theoretical foundation of this study, involving a systematic examination of peer-reviewed publications to gather existing knowledge on battery energy storage systems in maritime applications, particularly for cruise vessels. Although the concept of a battery hybrid vessel has been studied for decades, research focusing on the cruise segment has been lacking, justifying the need for this study. Therefore, literature from other maritime segments and industries is also examined to explore the possibilities in the cruise market.

2.2. Qualitative Interviews

Qualitative data were collected through semi-structured interviews with key stakeholders in the maritime industry, including representatives from cruise lines, shipyards, and system solution providers. The interviews aimed to capture insights on the current and future market situations of hybrid cruise vessels, drivers for implementing alternative power sources, and the potential benefits and challenges associated with these technologies.

2.3. Data Simulation

The potential cost savings and operational efficiencies of battery systems were assessed using data simulation. Digital twin models of selected case vessels' power systems were developed and input with real cruise data. These simulations aimed to analyze the operating cost reduction potential of specified onboard battery systems under various scenarios. The results from these simulations were compared with baseline data from the literature to estimate the economic and environmental benefits of battery investments. Sensitivity and scenario analyses were conducted to evaluate the robustness of the simulation results against critical variables.

2.4. Market analysis

To understand the current and future market situations of hybrid vessels, statistical data from public vessel registers, such as the Det Norske Veritas (DNV) and Clarksons database, were analyzed. This analysis provided insights into market trends and the adoption rates of hybrid power systems in the cruise industry. The hybrid vessel market development was analyzed with publicly available IMO-listed vessel characteristic data. Additionally, the data from the interviews were analyzed to triangulate findings and validate the qualitative insights with quantitative data.

3. Results and discussion

The primary advantage of energy storage systems in maritime vessels is engine optimization, independent of power demand. This disconnection enables various opportunities for total onboard energy management. Cruise vessels, however, face unique challenges compared to ferries and merchant ships, resulting in slower adoption of battery technology. Despite strong drivers like regulation, brand image, and customer values, the wider adoption of batteries depends on economic feasibility. This involves comparing Capital Expenditures (CAPEX) and Operating Expenses (OPEX) of the battery to potential OPEX savings from reduced fuel consumption. Estimating battery costs is straightforward, but savings potential requires advanced approaches such as data simulations.

3.1. Battery possibilities on cruise vessels

Batteries enable multiple approaches for vessel performance and efficiency improvement, categorized into power load levelling, zero emission operations, and battery as an enabler, Fig.1.

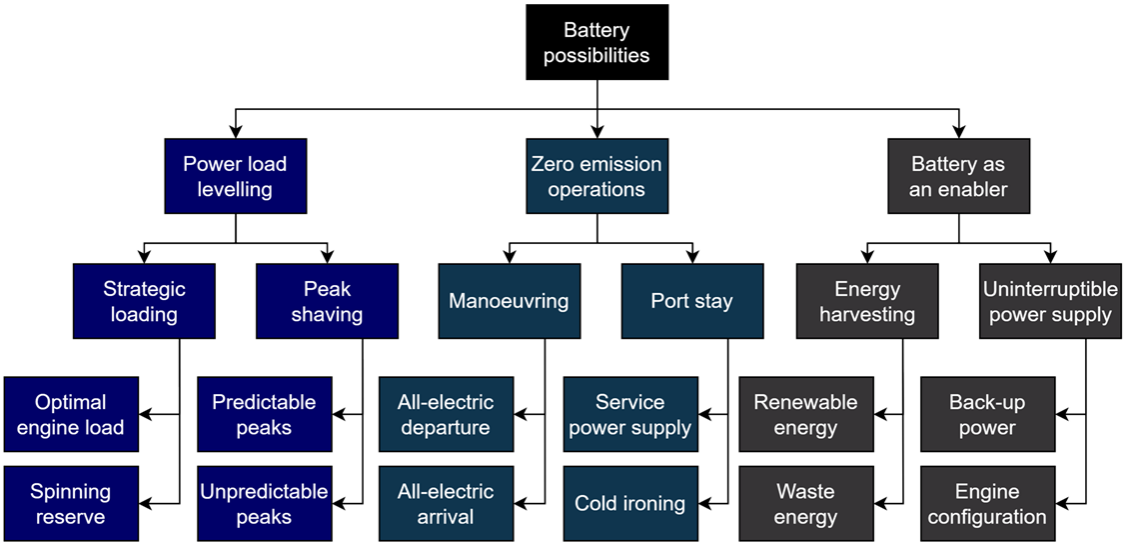


Fig.1: Cruise battery possibilities

Power load levelling is the primary use case of onboard batteries, directly creating OPEX savings. It involves strategic engine loading and shaving power demand peaks. To keep the vessel powered, the power demand must be met, often leading engines to run inefficiently in traditional systems. This can be avoided with strategic loading, either charging or discharging the battery to maintain optimal engine loads, typically around 85% of Maximum Continuous Rate (MCR), *Baldi et al. (2022)*. Additionally, the number of running engines affects total fuel efficiency. For example, during manoeuvring, power demand fluctuates rapidly due to thruster use, necessitating quick power availability for safety. Batteries can serve as a spinning reserve, enabling optimal engine load and number.

Another element of power load levelling is peak shaving, which focuses on power consumption. During manoeuvres or sudden power demands, engines may deviate from optimal load or require starting a new engine, incurring high costs and emissions. Batteries can smooth these peaks, avoiding inefficient engine use and new engine starts. Batteries also absorb small, rapid power peaks on cruise vessels caused by unpredictable electricity consumers.

Zero emission operations offer indirect benefits by operating the vessel engine-free on battery power for short periods, producing no emissions, noise, smoke, or vibration. This is feasible during manoeuvring and port stays. Batteries can supply service power or charge while cold ironing if shore power is available, enhancing brand image and regulatory compliance. For example, Norway plans a zero-emission requirement in its heritage fjords by 2026, which could restrict access to compliant vessels, *NMA (2023)*.

Batteries also enable energy harvesting from renewable sources or waste heat, storing energy for later use. This supports renewable energy sources and optimal engine operation. Lastly, batteries can function as Uninterruptible Power Supply (UPS), avoiding power shortages and blackouts, improving safety, controllability, and efficiency. This could lead to optimized onboard engine configurations, potentially reducing CAPEX and maintenance costs, and making battery investments more feasible.

3.2. Onboard battery limitations and challenges

While offering a variety of benefits through several use cases, battery technology faces notable challenges when applied into maritime power supply, especially on cruise vessels focusing on

passenger entertainment and safety. The key challenges of hybrid cruise power supply can be divided into operational and business categories.

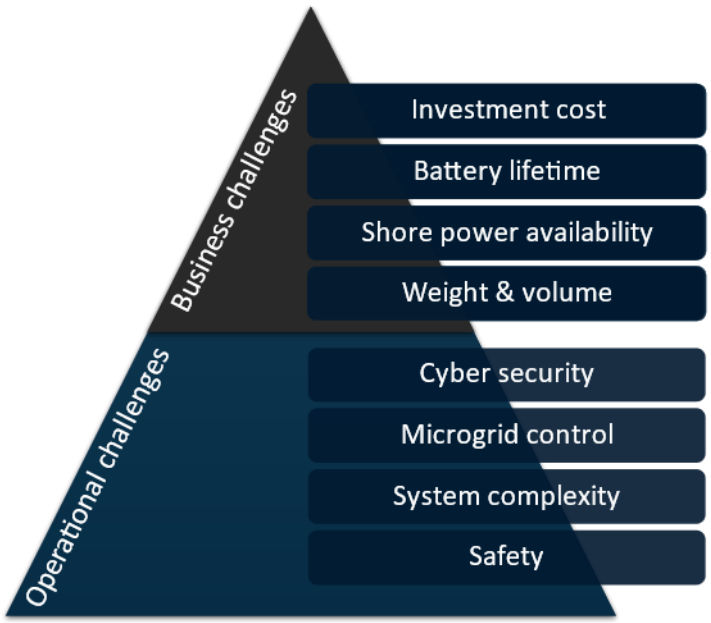


Fig.2: Hybrid power supply challenges

3.2.1. Operational Challenges

The primary concern is safety. Batteries can enhance vessel safety by providing backup power during blackouts. However, they pose risks like thermal runaway (fire hazard) and electrolyte off-gassing (explosion risk), which must be addressed in the design phase. These risks stem from operational or design issues such as overcharging, short circuits, mechanical damage, or external fire. Safety regulations and standards are continuously evolving to ensure battery safety onboard passenger vessels.

Batteries also increase the complexity of the vessel's power supply configuration, necessitating additional Battery Management Systems (BMS) and upgrade to Energy Management System (EMS). Effective battery optimization relies on seamless data flow between vessel systems. The availability and quality of data influence the viability of advanced microgrid control strategies. While simple rule-based control strategies do not fully optimize batteries, real-time multi-objective optimization strategies are complex to develop and implement. Increased data dependency also raises cyber security concerns as vessels continuously share and receive data via satellite connections.

3.2.2. Business Challenges

These challenges directly affect the feasibility of battery investments. Factors like weight, volume, and battery lifetime depend on the technology. Battery weight affects draft and stability, while volume poses a challenge as cruise vessels optimize space for revenue generation. Newbuild vessels can more easily accommodate batteries during design but retrofit projects face challenges in finding suitable space. Battery lifetime, impacted by technology and operating profile, also affects feasibility. For example, lithium-ion batteries can last up to 20 years with optimal usage but may last less than half of that with rapid charging and discharging at high C-rates, *Perry (2022).*

Battery investment cost and lifetime are directly linked to life cycle feasibility. Although data-driven battery usage can improve fuel efficiency in the cruise segment, estimated OPEX savings are unlikely to cover high installation costs, especially given limited battery lifetimes. Trends of increasing fuel prices and decreasing battery costs could drive wider adoption by improving life cycle feasibility. Another potential motivator is the global availability of shore power. Batteries enable efficiency

optimization, such as strategic loading and peak shaving, independently of shore power. Charging batteries during port stays with shore connections can utilize green onshore energy, enabling zero-emission operations during departures and arrivals. Although few ports currently offer shore power, the number is expected to increase due to more shore power-capable vessels and tightening emission regulations.

3.3. Hybrid vessel market trends and stakeholder insights

Hybridization, among other decarbonization trends, has attracted significant interest in recent years. Even though today's battery modules and energy management solutions are relatively new, the concept of hybrid power supply was introduced already in the late 1990s. The ferry segment was a natural starting point for onboard batteries, as they travel short distances between the same ports, making charging from shore easy and stable. After ferries, other small vessels with low power demand, like tugs and fishing ships, incorporated batteries in their power supply. The first larger vessels from the merchant segment were introduced with hybrid power supply in the early 2010s, after which it took almost a decade for the cruise segment to pilot onboard batteries. Fig.3 visualizes the growth in the number of battery-hybrid vessels per vessel category, with "other" including tugs, fishing ships, and inland vessels, *Clarksons Research (2023)*

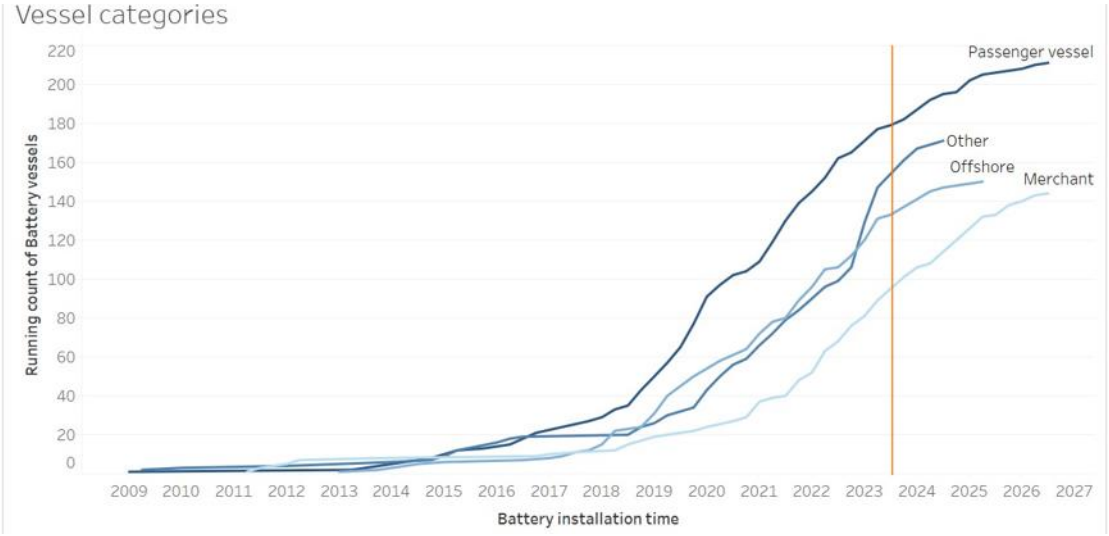


Fig.3: Battery installations by vessel category, *Clarksons Research (2023)*

The pace of the market adoption of hybrid power supply is steered by the pushing and pulling factors originating both from the operating environment and business perspectives. These drivers and barriers differ between vessel categories and continuously evolve, making the prediction of future market development challenging. Fig.4 summarizes the main factors for and against hybridization in the cruise segment. Cruise differs from other segments particularly on the opposing factors. The previously listed challenges of high investment cost, and weight and volume constraints due to high energy and power demand, are against battery adoption, especially when combined with low estimated savings potential and long payback time of the investment. Slowing factors on the other hand consist of technological challenges, like battery lifetime, safety, and shore power unavailability, and concerns from the operating environment, like global economic challenges and battery material availability.

Knowing that battery-hybrid cruise vessels have started to emerge, the drivers of adoption have been valued higher than the barriers. The pushing factors, especially emission targets and regulations like the Carbon Intensity Indicator (CII) and Energy Efficiency Existing Ship Index (EEXI), are seen as the main driver for cruise hybridization. The maritime field, often considered a relatively conservative industry, finds the most effective boost towards decarbonization through regulation. Regulation is not only a strict pushing factor but also linked to monetary feasibility. The new EU Emission Trading System (ETS) directly impacts financials.



Fig.4: Drivers and barriers of cruise hybrid power supply

For vessels with poor fuel efficiency, the EU ETS means increased cost of operation, but for an efficient hybrid vessel, it can even mean extra income through selling part of their EU Emission Allowances (EUA), *EC (2024)*. Both scenarios promote the adoption of batteries, lowering the relative installation cost and making the investment more justified. Other pulling factors include reduced engine running hours and maintenance costs, supporting other onboard systems, and better brand image responding to increasingly green customer values. As a conclusion from the comparison between the hybridization drivers and barriers, batteries are expected to become more common in the cruise segment in the near future.

The interviews provided a comprehensive picture of the current and future market situations for hybrid cruise vessels, highlighting drivers for development. Insights into alternative power supply options, such as batteries, fuel cells, shore power, and alternative fuels, were well recognized. The shipyard demonstrated an understanding of the physical challenges of various energy storage systems, while Wärtsilä and cruise lines focused on technologies likely to offer the best efficiency. Major business-related drivers included regulations, brand image, and financial considerations. The main challenges identified were the added volume and weight due to high power and energy demand, high costs, global shore power availability, and the conservative nature of the maritime industry. Despite varied opinions on battery feasibility, BESS was generally viewed as beneficial for supporting power supply and improving vessel performance.

Most interviewees believed in the future potential of batteries in the cruise segment, predicting several pilot projects and wider adoption as a supportive power source post-2030. Combustion engines were still seen as the main power source in the long run, albeit powered by green fuels. Fuel cells and shore power were expected to see future piloting and adoption due to their environmental benefits and possible tightening of port emission regulations. Fully electric power supply was deemed impractical for large ocean-going ships, though future technological advancements could alter this perspective. These insights are summarized in Fig.5.

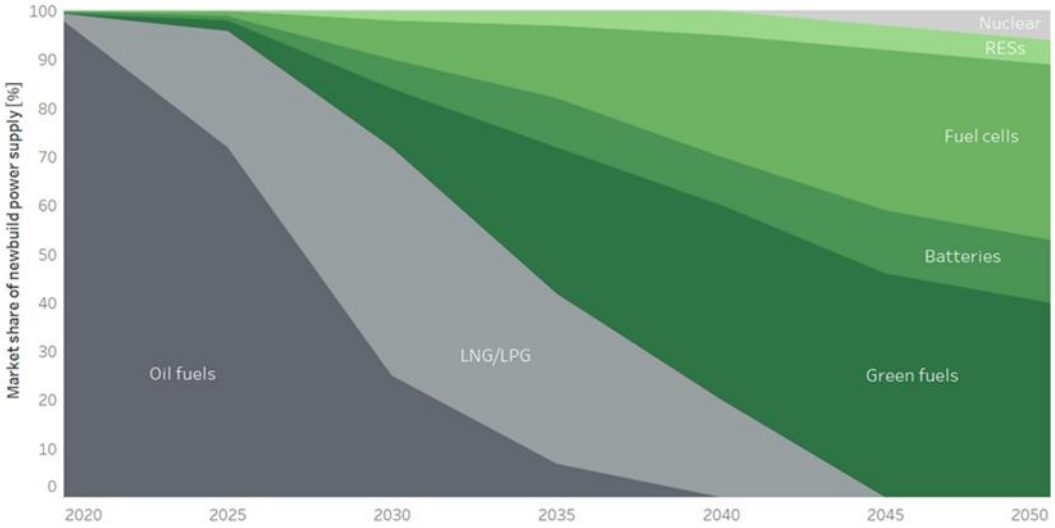


Fig.5: Diffusion of cruise power supply technologies

3.4. Feasibility analysis through battery simulations

The wider adoption of batteries in the cruise segment hinges on their overall feasibility, which involves a combination of multiple factors, as illustrated by the drivers and barriers comparison. Given that the market has only recently begun to see battery-hybrid cruise vessels, there is insufficient data, proof, and research on their usability and feasibility in the cruise segment. The greatest uncertainty concerns the potential magnitude of OPEX savings achievable through power load levelling. While some general estimates of the fuel consumption reduction potential of batteries have been presented in academic literature, they often indicate the cruise segment has the lowest savings potential among all vessel categories, with a maximum of 5%, *EMSA (2020)*. This savings potential is inherently vessel-specific, depending on the power supply configuration, operating profile, and installed battery energy storage system.

One data-driven approach to estimating the feasibility of batteries onboard a cruise vessel involves performing digital twin simulations using actual cruise operation data. In essence, this method estimates fuel savings potential by creating a digital replica of a real cruise vessel, enhancing it virtually with the chosen battery system, and then comparing performance on real-life leg examples by simulating the digital twin with and without the battery onboard. This approach is suitable for assessing the impact and feasibility of battery installations in both newbuild and retrofit projects, aiding decision-making for fleetwide hybridization to meet upcoming regulatory emission requirements, Fig.6.

3.4.1. Case Study: Digital Twin Simulation for Battery Feasibility

The simulation process begins with the creation of the digital twin model of the case vessel, which involves digitally configuring the current onboard power supply system from tank to wake. The virtual battery system is also configured with chosen characteristics. After creating the digital twin, the simulation parameters are defined, and vessel and battery control strategies are selected, such as limiting battery usage to peak shaving or enabling charging with shore power. Finally, actual high-frequency operation data of the case vessel is input into the simulator, which optimizes the power supply

and fuel consumption for the given data with the configured digital twin. The results of simulations with and without the onboard battery system can then be compared in terms of fuel consumption, emissions, and operating expenses, providing an estimate of the battery savings potential.

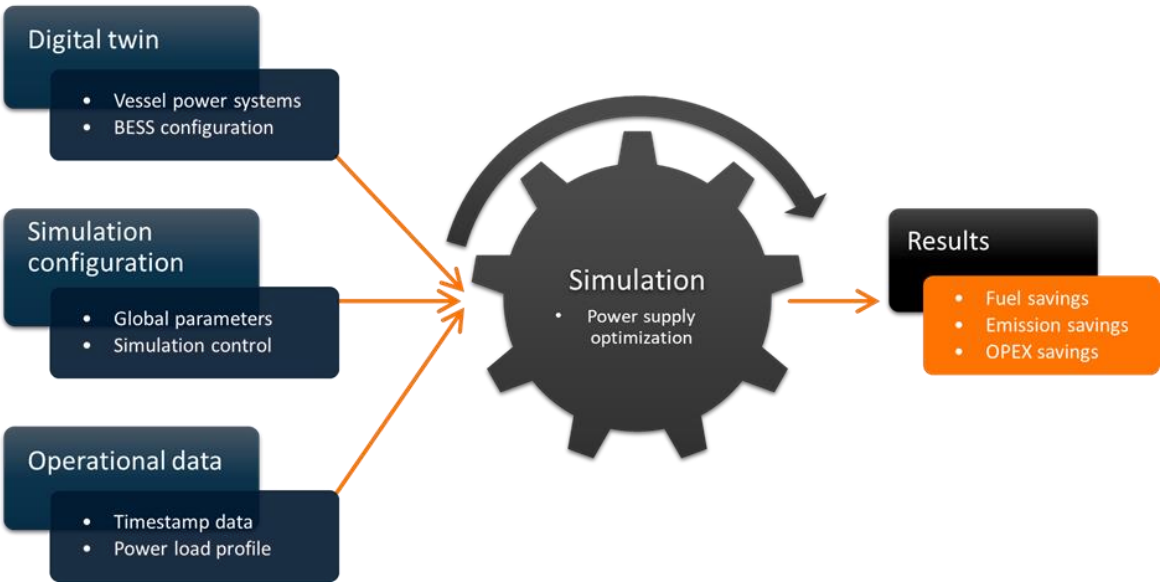


Fig.6: Digital twin simulation process

The idea of the simulation can best be demonstrated with a single-leg example. Fig.7 visualizes a sailed route from Road Town to Nassau. Despite being a rather straightforward route, it can illustrate all cruise operation modes (at port, manoeuvring, and sailing) and all battery use cases (peak shaving, strategic loading, all-electric manoeuvring, and shore power charging) incorporated in the simulation.



Fig.7: Case example route

The operating profile of the case vessel for the example leg is visualized in Fig.8. The first graph presents the vessel's power demand, divided into power consumers (propulsion, thrusters, hotel). Propulsion accounts for most of the power, thruster usage is seen as power demand peaks during manoeuvring, and the hotel load is continuously present, even during port stays. The second graph illustrates the corresponding hybrid power supply, addressing the given power demand. The case vessel has two large engines, two medium engines, and one small engine. Additionally, the digital twin model

of the vessel is virtually enhanced with shore power capability and a battery with a 6 MWh capacity. At port, the hotel load is supplied by the shore power connection, which in this example is assumed to be available in both ports. Shore power is also used for charging the battery at the beginning, as visualized in the third graph below. The beginning of the manoeuvring is performed fully on battery power, but quickly switches to run on three engines while balancing load fluctuations with battery power. The high-speed sailing is performed with three optimally loaded main engines and is supported by battery-powered load leveling. Upon arrival in Nassau, batteries are used for peak shaving and are again charged with shore power at the destination port.

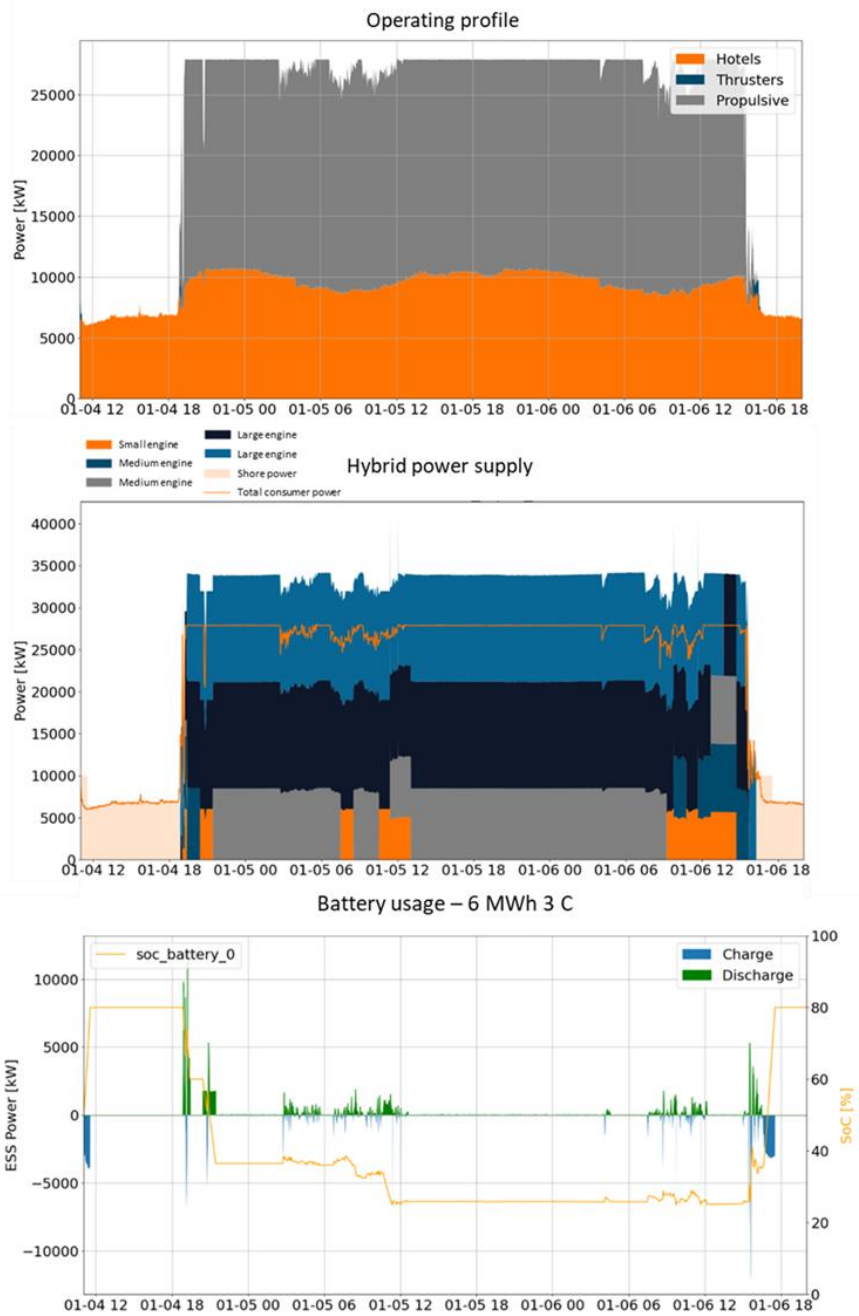


Fig.8: power demand and supply of the case vessel

3.4.2. Evaluating Battery Savings Potential: A Digital Twin Case Study

Digital twin simulations, similar to the case example demonstrated above, were conducted for two large cruise vessels with varying battery configurations. Many assumptions were necessary in the configurations, such as costs of engine running hours and maintenance, as well as constant prices and

emission factors for fuels and shore electricity. While more reliable results could be achieved by reducing these assumptions and increasing the amount of data, these case examples provided sufficient insights for estimating the general range of cruise OPEX savings potential from batteries.

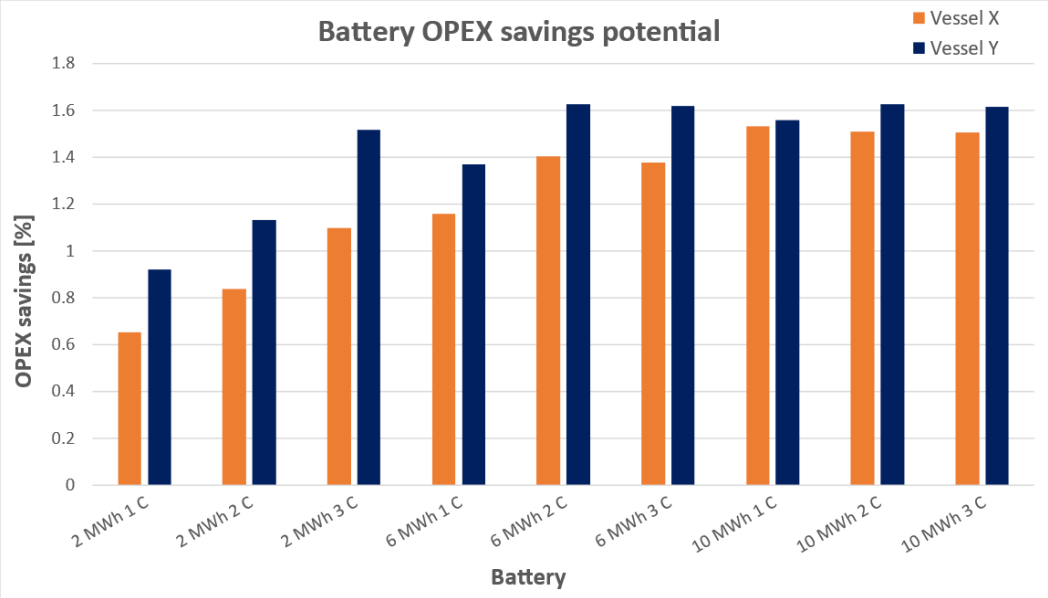


Fig.9: Cruise battery savings potential

Fig.9 summarizes the simulation results in terms of OPEX savings potential, which include fuel and running hour costs, shore power, and battery maintenance costs. The average savings potential varies between 0.6 – 1.6%, with larger battery capacities and higher C-rates providing greater savings. For case vessel Y, it is observed that beyond a 6 MWh battery with a C-rate of 2, further upgrading the battery does not yield additional savings but would increase the investment cost. On large cruise vessels, depending on the operating profile and cost elements, the OPEX reduction of 0.6 – 1.6% translates to annual savings of 100 – 600 k€. These savings must be assessed over the full battery lifetime to evaluate the monetary life cycle feasibility of the battery investment.

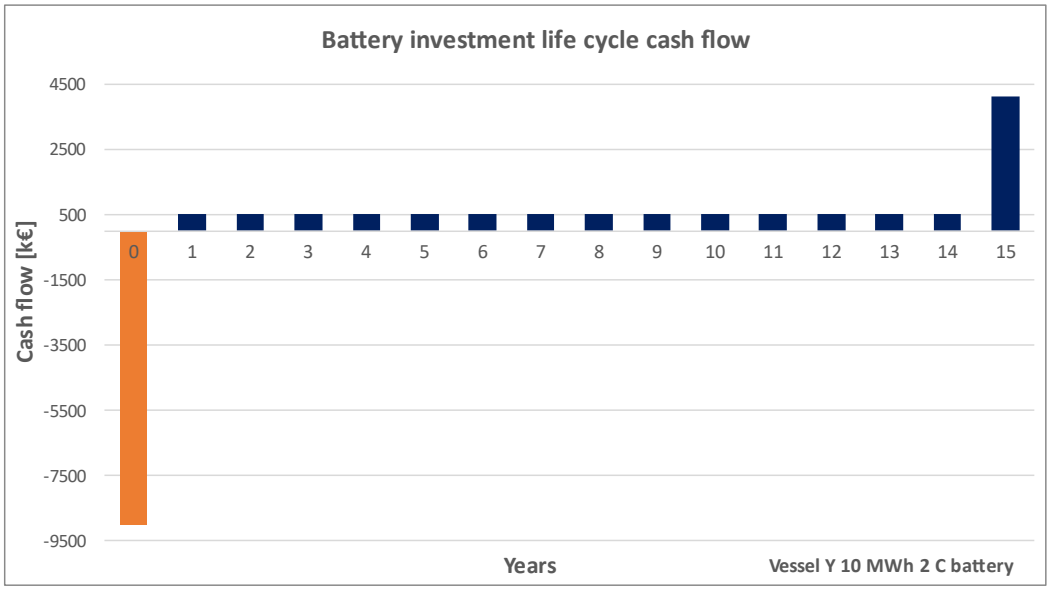


Fig.10: Battery investment life cycle feasibility

Fig.10 provides an example of the life cycle feasibility in absolute cash flow for a 10 MWh 2C battery investment on case vessel Y. Here, the hybridization investment cost is estimated to be 9 MEUR. The simulation results indicate approximately 500 k€ in annual OPEX savings, assumed to remain

constant throughout the estimated 15-year battery lifetime. When the battery reaches its end of life after performing over 7000 cycles, it can be resold to the secondary market at an assumed value of 40% of the original price. Considering all assumptions and ignoring the effect of the interest rate, the investment generates a profit of ~2.5 MEUR. However, the payback occurs in the 15th year and is heavily dependent on the battery's resale value, as the OPEX savings are relatively small compared to the substantial investment cost. Additionally, the interest rate's impact on the investment's net present value is significant, given that the largest positive cash flow is realized after 15 years.

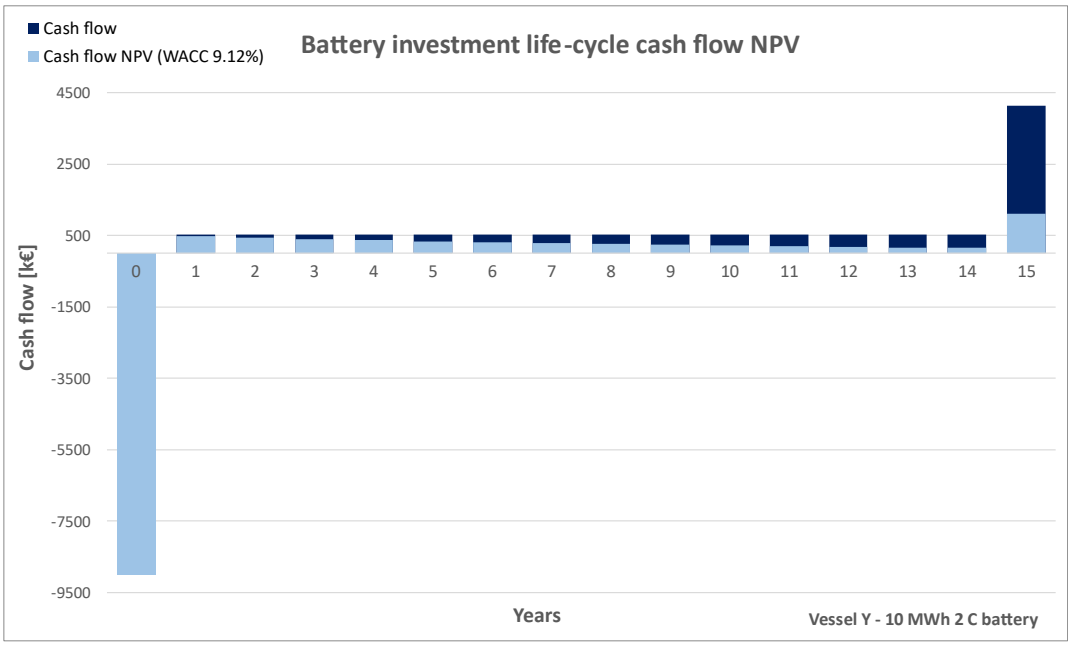


Fig.11: Battery investment life cycle feasibility

Net Present Value (NPV) analysis was conducted to evaluate the long-term financial feasibility of battery investments in hybrid cruise vessels. By discounting future cash flows associated with the investment, the NPV provides a clear picture of the potential profitability over the battery's lifetime. Typical Weighted Average Cost of Capital (WACC) in the cruise industry was considered as the Required Rate of Return (RRR) for the battery investment. The results showed that the battery NPV is highly sensitive to the discount rate used, especially due to the major cash flow coming from the battery resale in the end of the investment life cycle. Continuing the same example in Fig.11, for a 10 MWh 2 C battery investment with an initial cost of 9 MEUR, despite the positive absolute cash flow, the discounted NPV was negative under current market conditions and typical cruise RRR. To assess the full picture of the hybridization investment, it should be viewed from the vessel life cycle perspective, including potential battery pack replacements.

Sensitivity and scenario analysis were conducted to evaluate how changes in key variables impact the financial feasibility of battery investments in hybrid cruise vessels. Key variables considered in this analysis include battery price, fuel cost, shore power availability, and battery lifetime. An example of this analysis is depicted in Fig.12, which illustrates the impact of varying battery prices on the NPV of different simulated battery options. The analysis shows that lower battery prices significantly increase the NPV, making the investment more attractive, as the initial investment cost is reduced. The sensitivity and scenario analysis thus provides crucial insights into the conditions under which battery investments in hybrid cruise vessels are likely to succeed or fail, aiding stakeholders in making informed decisions.

Even though monetary feasibility is a key driver in maritime hybridization, the role of emissions is rapidly increasing. Reducing fuel consumption lowers operating costs, also reducing Greenhouse Gas emissions. Fig.13 summarizes the carbon emission savings potential with and without shore power for different battery capacities on the simulated case vessels. With shore power, the emission savings

potential increases linearly with battery capacity, as more shore electricity can be used instead of running engines on fossil fuels. Recent changes in maritime emission regulations, such as the EU ETS and FuelEU, are linking emissions with additional costs for cruise lines. Avoiding additional emission fees will significantly increase the monetary savings potential of batteries in near future, making the investment more justified.

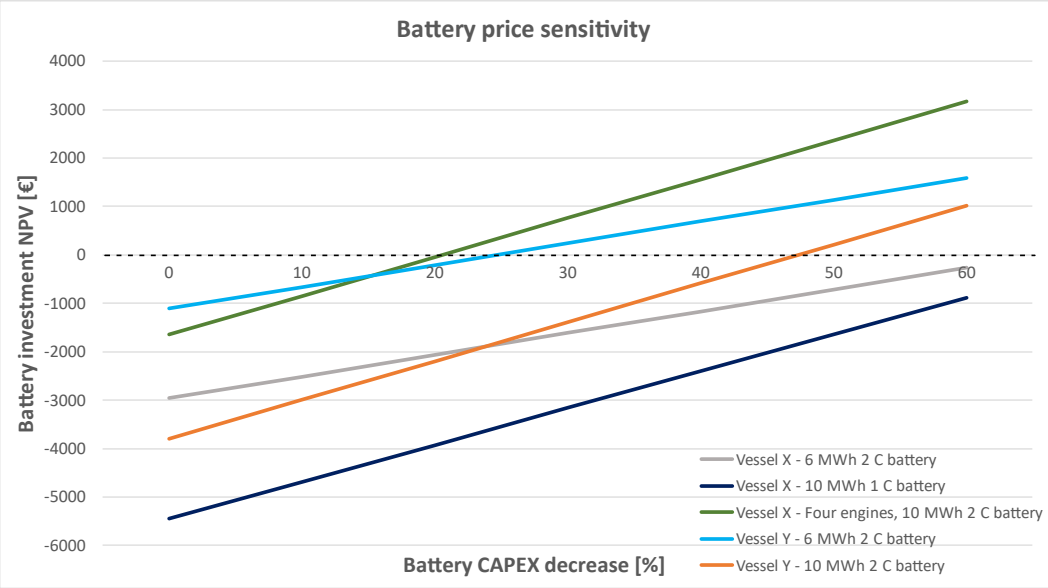


Fig.12: Battery price sensitivity

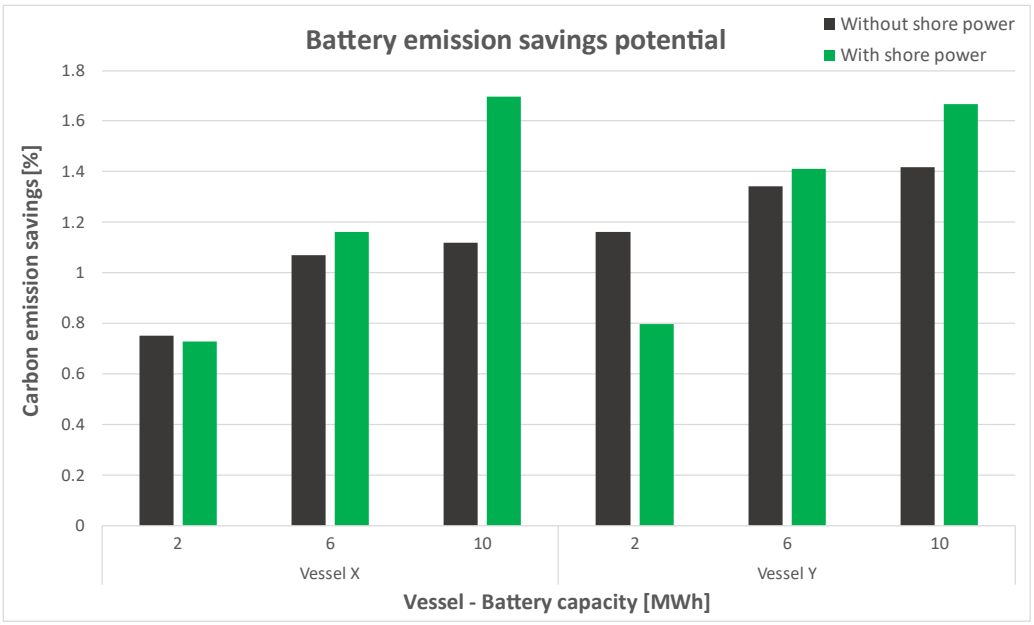


Fig.13: Battery emission savings potential

4. Conclusion

This article explored the feasibility and optimization of battery systems on hybrid cruise vessels, addressing environmental and economic challenges. Through literature review, qualitative interviews, data simulation, and statistical analysis, the study highlighted the potential and challenges of battery hybridization in the cruise segment.

Digital twin simulations indicated OPEX savings from cruise battery integration ranging between 0.6% and 1.6%, translating to significant annual savings depending on the vessel's operating profile and

battery capacity. Despite these benefits, high initial investment costs and long payback periods remain critical barriers for wider adoption of batteries. Sensitivity and scenario analyses underscored the importance of increasing fuel prices, decreasing battery costs, and favourable financing conditions to enhance the investment's net present value and Return On Investment (ROI).

In conclusion, while battery systems offer substantial benefits for cruise vessels, their economic viability depends on technological advancements and supportive regulatory measures. As the industry evolves, batteries are expected to play a crucial role in the decarbonization and efficiency improvement of maritime operations, contributing to future sustainable shipping strategies.

References

ALNES, O.; ERIKSEN, S.; VARTDAL, B.-J. (2017), *Battery-Powered Ships: A Class Society Perspective,* IEEE Electrification Magazine 5, pp.10–21

BALDI, F.; CORADDU, A.; MONDEJAR, M.E. (2022), *Sustainable Energy Systems on Ships: Novel Technologies for Low Carbon Shipping,* Elsevier

CLARKSONS RESEARCH (2023), *World Fleet Register,* https://www.clarksons.net/WFR/

EC (2024), *Reducing emissions from the shipping sector, European Commission*

EMSA (2020), *Study on Electrical Energy Storage for Ships*, European Maritime Safety Agency, pp.1-171.

IMO (2020), *Fourth Greenhouse Gas Study 2020,* Int. Mar. Org.

KUUSISTO, T. (2023), *Possibilities for hybrid cruise vessel performance optimization through data-driven battery usage*, LUTPub.

NMA (2023), *Zero emissions in the world heritage fjords by 2026,* Norwegian Maritime Authority

Trim Optimisation – CFD, Model Test and Full Scale

Kadir Burak Korkmaz, RISE-SSPA Maritime Center, Göteborg/Sweden, burak.korkmaz@ri.se
Sofia Werner, RISE-SSPA Maritime Center, Göteborg/Sweden, sofia.werner@ri.se
Rickard Bensow, Chalmers University of Technology, Göteborg/Sweden, rickard.bensow@chalmers.se
Ruihua Lu, Stena Line, Göteborg/Sweden, ruihua.lu@stenaline.com

Abstract

Seaborne transportation, vital for global trade, faces challenges from rising greenhouse gas (GHG) emissions. To align with International Maritime Organization GHG reduction goals, this study investigates trim optimization, an effective method to enhance ship energy efficiency. Utilizing model tests, CFD, and full-scale data analysis, the research underscores the pivotal role of full-scale CFD in cost-effectively predicting trim trends with reasonable accuracy. Both CFD and extrapolated model test results replicated real-time ship data with acceptable accuracy when appropriate methodologies were selected, highlighting their effectiveness in predicting trim trends.

1. Introduction

Seaborne transportation is a cornerstone of global trade, mobilizing over 80% of the world's cargo while accounting for nearly 3% of global greenhouse gas (GHG) emissions (IMO, 2021). The International Maritime Organization (IMO) predicts a potential 90-130% increase in shipping emissions from 2008 levels by 2050 if no mitigating actions are taken (IMO, 2021). To address these challenges and align with the IMO's GHG reduction goals, enhancing the energy efficiency of ships has become paramount. Among various initiatives, the IMO's Energy Efficiency Design Index (EEDI) plays a critical role by promoting energy-efficient ship designs and discouraging inefficient ones. Calculating the EEDI is mandatory during the design phase of new ships, emphasizing the importance of incorporating energy-saving solutions such as hull form optimization and energy-saving devices early in the design process, *IMO (2011)*.

In 2023, the IMO introduced two additional regulations: the Energy Efficiency Existing Ship Index (EEXI) and the Carbon Intensity Indicator (CII). The EEXI assesses the energy efficiency of existing ships, while the CII measures operational carbon intensity, defined as GHG emissions per unit of cargo carried over distance. The CII targets a 40% reduction in carbon intensity by 2030, a goal that can be achieved through operational measures like speed and route optimization, hull and propeller cleaning, and trim optimization, *IMO (2022a,b)*.

Trim optimization is a widely applicable and effective method for improving ship energy efficiency, potentially reducing fuel consumption by 0.5-5% without requiring structural modifications, *IMO (2013)*. Trim adjustments can be made by altering the vessel's loading, ballasting, or shifting ballast water between tanks. Medium and slender vessels, often operating in partial load conditions, stand to benefit the most from trim optimization. Each ship's unique design and propulsion arrangement influence the energy savings achievable through trim adjustments, *Sames et al. (2012), IMO (2023).*

The principle behind trim optimization is that ship resistance and propulsive efficiency vary with different trim angles at a given displacement and speed. During the design phase, hydrodynamic performance is typically optimized for specific loading conditions and speeds. However, in actual operations, ships often encounter a wider range of conditions. Consequently, the optimal trim angle varies, and the minimum propulsive power may not occur at an even keel or fixed trim value for all displacements and speeds. Hence, it is essential to evaluate the ship's performance across various displacements, trims, and speeds to identify the optimal trim for minimizing delivered power in real-world operations.

Trim optimization data can be derived through experimental methods, computational methods, or analysis of real operational data. Experimental methods involve model testing in towing tanks, but uncertainties in testing and scaling can affect the accuracy of full-scale predictions. The 1957 and 1978 ITTC Performance Prediction Methods, for instance, differ significantly in their approach to scaling resistance and propulsion results, *ITTC (2021a).* Simplified extrapolation methods might reduce testing scope but at the cost of accuracy, *Reichel et al. (2014).*

Computational methods, particularly the Reynolds-averaged Navier-Stokes (RANS) approach, are prevalent for studying trim optimization trends. These methods have matured to provide reliable trim trend predictions at model scale, and recent studies have expanded their application to self-propulsion simulations, *Chen et al. (2019), Islam et al. (2019), Mahmoodi et al. (2022,2023), Sun et al. (2016), Shivachev et al. (2017).* Potential flow methods offer another computational approach, though they may struggle with highly viscous effects and wave deformation issues, *Hansen (2010), Lemb Larsen et al. (2012), Korkmaz (2023).* More advanced numerical methods like Detached Eddy Simulation (DES) and Large Eddy Simulation (LES) are less common due to their high computational demands, *Kanninen (2022).*

Finally, real operational data, or ship monitoring data, provides a valuable resource for understanding trim optimization trends. This data-driven approach can predict ship behaviour under various conditions and extract vessel performance at different trims, offering insights directly applicable to operational decision-making, *Coraddu et al. (2017). Huffmeier (2020).*

The present research addresses the knowledge gap in trim trend extraction methods by conducting a comprehensive comparison. It investigates trim optimization trends for a RoPax vessel utilizing experimental, computational, and full-scale data analysis techniques. The investigation includes resistance and self-propulsion model tests, comparing model-scale trim trends with free-surface RANS computations. Additionally, full-scale power predictions are derived from multiple extrapolation methods and contrasted with both CFD predictions and ship monitoring data. This analysis provides a deeper understanding of the physics behind trim optimization trends and offers practical guidance for selecting the most suitable methods for trim trend extraction.

2. Trim Optimisation methods

2.1. Experimental method

In this study, two model-to-full-scale extrapolation methods are utilized: the standard 1978 ITTC Performance Prediction Method, *ITTC (2021a),* and the 1978 ITTC Performance Prediction Method with an empirical transom correction, *Korkmaz (2022).* The same towing tank test results are employed for different extrapolation methods to predict full-scale speed-power relations.

The standard 1978 ITTC Performance Prediction Method, or ITTC-78 method, extrapolates towing tank test results to full scale without modifications. Tests for resistance, self-propulsion, and propeller open water are performed to predict delivered power and propeller turning rate. The ITTC-57 model-ship correlation line, *ITTC (1957),* is used for resistance extrapolation, with form factors determined by CFD, *Korkmaz (2021a,b), ITTC (2021),* and the Prohaska method, *Prohaska (1966).* The resistance scaling assumes identical form factors at model and full scales, despite partial transom wetting in some conditions, *Hughes (1954).*

The second extrapolation method, ITTC-78 Method with Empirical Transom Correction, is similar to the standard ITTC-78 method but includes an empirical correction for resistance scaling. Substantial transom submergence in some loading conditions causes flow separation, invalidating the form factor approach. Therefore, different form factors are used for model and full scales, with the full-scale form factor adjusted using Korkmaz's empirical correction, *Korkmaz (2022).*

2.2. Computational method

The computational simulations utilized the Fine^{TM}/Marine computing suite version 10.2 for conducting free-surface Reynolds-Averaged Navier-Stokes (RANS) computations. The incompressible RANS equations were solved using the ISIS-CFD flow solver, which employs the finite volume method. This solver is capable of handling a variety of grid types, including three-dimensional unstructured grids. The velocity field was derived from the momentum conservation equations, while pressure was determined from the continuity equation. Turbulence modelling was achieved through the discretization and solution of the transport equations, employing the AVLSMART discretization scheme for both momentum and turbulence transport equations. All free-surface RANS computations were conducted in steady-state conditions, utilizing the k-ω SST turbulence model proposed by *Menter (1993).*

The free surface was modelled using a Volume of Fluid (VOF) multi-phase flow approach. Within the ISIS-CFD framework, the Blended Reconstructed Interface Capturing Scheme (BRICS) was employed for multi-fluid discretization. Further details on the surface capturing method can be found in the work by *Wackers et al. (2011).*

Unstructured hexahedral grids were generated using the HEXPRESS^{TM} module of the Fine^{TM}/Marine suite. The volume-to-surface approach was employed to generate non-conformal body-fitted full hexahedral unstructured grids around the hull and appendages. Boundary layers were inserted between the no-slip wall and surrounding hexahedral grids. These grids were refined with a local zone near the free surface to ensure consistent grid spacing in the z-direction. In cases involving self-propulsion, additional refinement regions were added around the actuator disc to minimize interpolation errors. Adaptive Grid Refinement (AGR) was employed during computation to further refine the grids. The AGR criterion used for all computations is based on Hessians of both pressure and velocity, which are weighted as they appear in the flux. In terms of trim optimization computation, the main advantage of the flux-component Hessian (FCH) criterion is that shear layers, wakes, boundary layers, and pressure-based flows (waves, vortices) can be tracked, and grids are refined precisely where needed. As a result, rather than generating separate grids for each loading condition and speed, one grid was generated per speed. Mesh deformation techniques were employed to adapt the initial grids for various loading conditions and then further refined by the AGR algorithm, allowing for efficient computation.

Computational domains were configured as rectangular prisms, with specified distances between the inlet and outlet boundaries. Solid wall boundaries, including the hull and appendages, were modelled using a wall-law boundary condition. For full-scale self-propulsion computations, roughness effects were incorporated using a wall function approach with the sand-grain roughness height of 30 μm as recommended by, *Schultz (2007).*

Propeller effects were simulated using the actuator disc model within the ISIS-CFD solver. The actuator disc's influence was included in the momentum equations of relevant cells. Thrust, torque, and propeller turning rate were updated at each time step based on the predicted values obtained from the propeller open water curve (POW). The thrust of the actuator disc was determined by considering drag and external force vectors, such as the towing force in model scale and air resistance in full scale.

2.3. Full-scale data

The vessel is outfitted with a diverse array of sensors designed to monitor and record various aspects of its operation. These sensors capture data pertaining to the vessel's condition, including draught at fore and aft perpendiculars, heel angle, speed over ground, and speed through water. Additionally, environmental factors such as current, depth below keel, water temperature, apparent and true wind speed and direction, as well as now-casting based swell, wave height, and period, are continuously monitored. Furthermore, the performance of the vessel is monitored through the tracking of propeller turning rate, shaft torque per propeller, and fuel consumption.

Data collection spans from 2015 to 2022, with measurements logged at regular 10-minute intervals. The installation of these sensors and subsequent data collection are overseen by the ship owners. Therefore, this study focuses solely on the analysis of the data collected within this timeframe.

3. Test case, experimental and computational conditions

The test case for this study involves a RoPax vessel with over a decade of operational history. Operating exclusively between two harbours, the vessel's route remains consistent. Equipped with a twin-screw propulsive arrangement, each shaft line is supported by shaft bossing, an I-bracket, and a V-bracket. The rudders are positioned transversely near the same y-coordinate as the shaft line. While the vessel's hull lines, shaft arrangement, propulsion setup, and propeller design are typical of a RoPax vessel, confidentiality prohibits the sharing of images or drawings in this paper.

Trim optimization parameters are determined through statistical analysis of ship monitoring data. Consequently, three speeds and two displacements—referred to as light (L) and heavy (H)—are selected. Model tests encompass three trim conditions: 1.5 m bow trim, even keel, and 1.5 m stern trim. Trim is calculated as the difference between the draught at the fore perpendicular (T_f) and the draught at the aft perpendicular (T_a). As the calculation of the trim ($Trim = T_f - T_a$) implies, positive trim values indicate bow trim, while negative values indicate stern trim.

Experimental conditions and measurement uncertainties are detailed in *Korkmaz (2023)*, with model-scale computations replicating identical conditions including speed, temperature, viscosity, salinity, and model geometry. Full-scale computations are conducted for seawater at 15°C. The vessel's superstructure is omitted, and the same geometry as the model is used. Air resistance is factored in as an external force in full-scale computations, calculated according to *ITTC (2021c)* for each loading condition (two displacements and three trims). All computations assume calm, deep, and unconstrained waters.

3. Trim optimisation trends in model scale

This section discusses results of the trim optimization tests, for 2 displacements, 3 trim conditions, and 3 speeds. The evaluation is based on towing tank test results and free-surface RANS computations in resistance and self-propulsion modes. The change in the quantity of interest, such as resistance force, between trimmed and even keel conditions for each displacement and speed is calculated as follows:

$$\Delta R_{TM} = \frac{R_{TM}(trim) - R_{TM}(trim = 0)}{R_{TM}(trim = 0)} \times 100 \quad (1)$$

where ΔR_{TM} represents the relative change in resistance force for a given trim condition, $R_{TM}(trim)$, as a percentage of the resistance at zero trim condition $R_{TM}(trim = 0)$. Although this section only presents model tests and computations performed at model scale, the vessel's speed is always indicated using the corresponding full-scale speed in kn. This approach is adopted because the same full-scale speed under different loading conditions cannot be addressed with a single Froude number, due to significant variations in waterline lengths between loading conditions.

3.1. Resistance

The results of the trim optimization towing tank tests are shown in Fig.1. Black markers represent measured data, error bars indicate the measurement uncertainties, *Korkmaz (2023)*. Each sub-figure in Fig.1 illustrates the relative change in resistance under trimmed conditions compared to even keel condition for a specific displacement and speed, as noted in the titles on top of the plots.

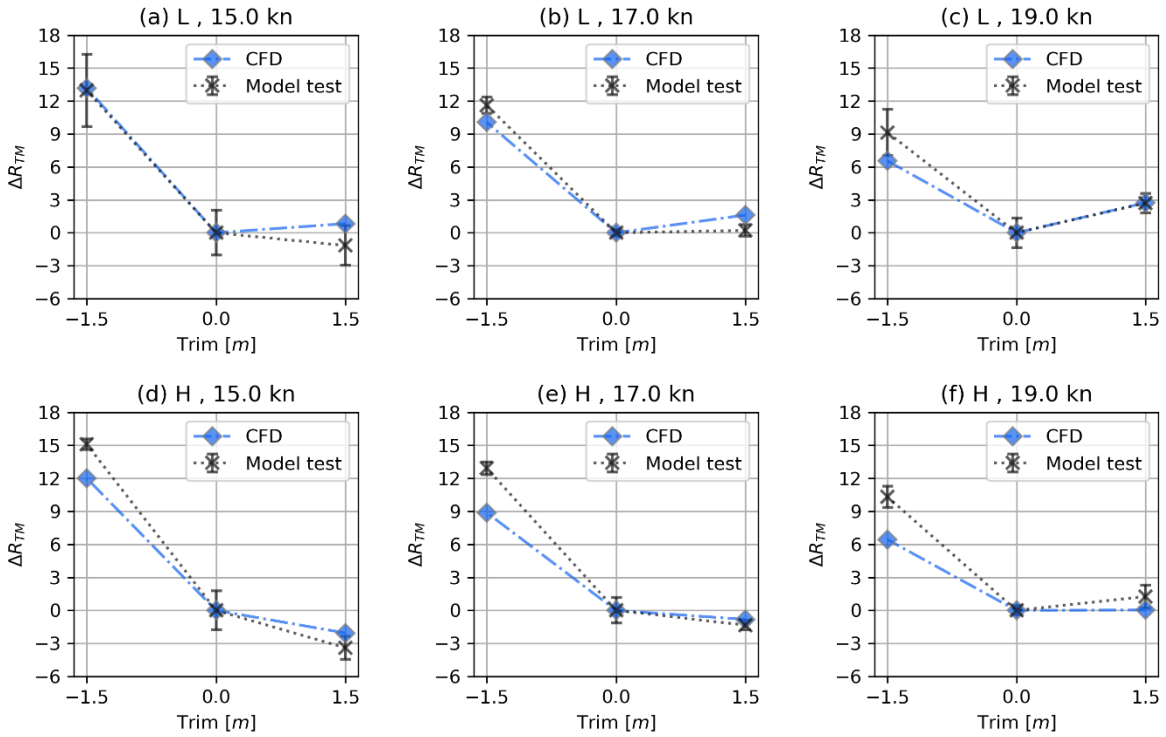


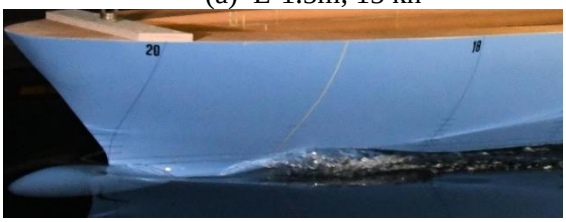
Fig.1: Change of total resistance with respect to trim relative to even keel condition, $\Delta \boldsymbol{R_{TM}}$, for model tests and CFD computations.

An overall analysis of the ΔR_{TM} trends in Fig.1 suggests that trimming the bow provides negligible resistance reduction at 19 kn, modest reduction at 17 kn, and limited reduction at 15 kn. Conversely, trimming the vessel by the stern results in increased resistance across all displacements and speeds. The potential gains are overshadowed by the resistance penalties incurred when operating the vessel under non-optimal conditions, amounting to as much as 15%.

Comparing the light (top row) and heavy displacements (bottom row) in Fig.1 at their respective speeds reveals little difference, despite the 10% difference in displacement volumes. This similarity can be partially attributed to the forebody design. The bulbous bow was optimized for narrow operational conditions, with its volume centre close to the water surface and its forward end near the tip. Consequently, loading conditions where the bulb is too close to the water surface (trim < 0) and low Froude numbers result in unfavourable wave patterns, occasionally leading to breaking waves as seen in Fig.2(a), (b) and (d). Additionally, significant flare and a relatively blunt waterline entrance angle above the design waterline cause the water surface to rise along the hull as a thin sheet (up to 30% of the draught from the water surface) before rolling off the sides when trimmed by the bow (trim > 0) at higher speeds as seen Fig.2 (c) and (d). Furthermore, aft body characteristics, such as the transom flow regime, exhibit significant variation depending on trim and speed conditions. The similarity in ΔR_{TM} trends for each speed in different displacements can largely be explained by the fact that similar flow phenomena, albeit with varying intensities, are observed in both displacements rather than entirely distinct wave patterns.

The flow regime behind the transom varies significantly with trim and speed conditions, including dry-transom, wetted-transom, and partially dry-transom flows observed in the model tests. However, regular transom flow, *Larsson and Raven (2010),* was not observed as the wave crest at the stern consistently reached the transom edge under all conditions. Dry-transom flow, with the flow smoothly leaving the transom edge tangential to the buttocks, was observed at light displacement, even keel and trim by bow, while heavy displacement exhibited dry transom only in trim by bow, while heavy displacement exhibited dry transom only in the trim by the bow conditions as seen in Fig. 3.

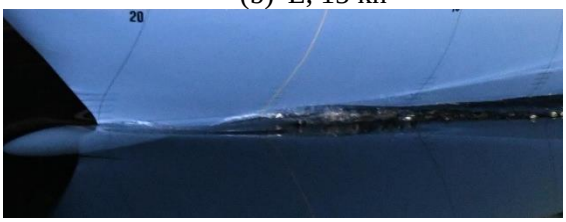
(a) L-1.5m, 15 kn



(d) H-1.5m, 15 kn



(b) L, 15 kn



(e) H, 15 kn



(c) L+1.5m, 15 kn



(f) H+1.5m, 15 kn

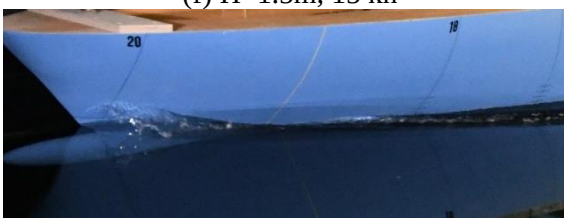
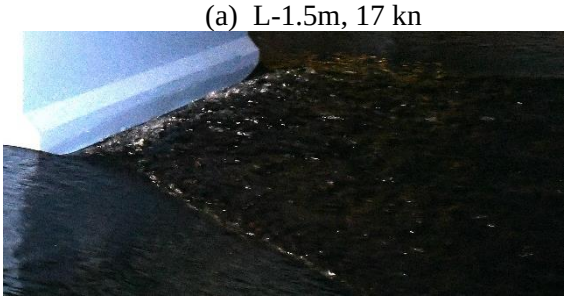
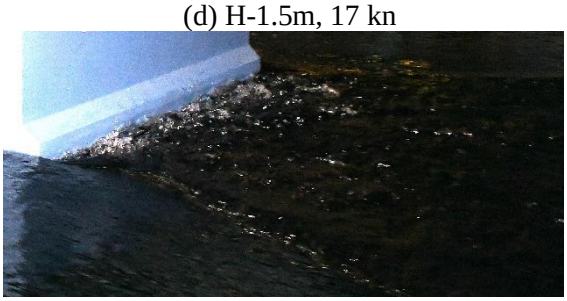


Fig.2: Wave patterns at the bow for light and heavy displacements at 15 kn

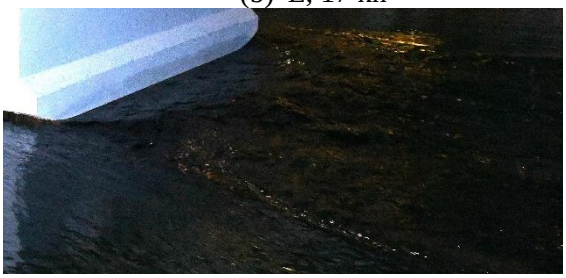
(a) L-1.5m, 17 kn



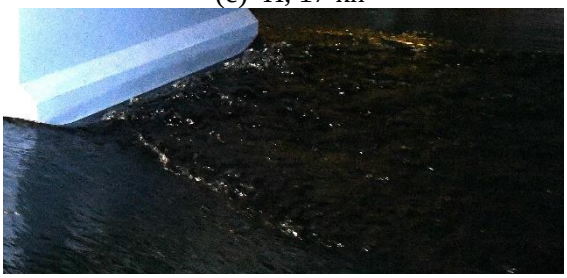
(d) H-1.5m, 17 kn



(b) L, 17 kn



(e) H, 17 kn



(c) L+1.5m, 17 kn



(f) H+1.5m, 17 kn



Fig.3: Wave patterns at the bow for light and heavy displacements at 17 kn

Most other trim conditions and speeds resulted in partially dry transom flows with the increasing intensity of flow separation and spill breakers with the increasing transom submergence; hence, explaining the high resistance penalties with trimming by the stern. The wetted transom flow regime

was observed only with the high displacement stern trim and the slowest speed ($Fn = 0.166$ and $Fn_{tr} = 2.75$).

Computational Fluid Dynamics (CFD) method is employed to analyse trim optimization, and its results are compared to those from towing tank tests. The ΔR_{TM} values, represented by blue markers in Fig.1, demonstrate that CFD predictions closely match the towing tank measurements. Additionally, the comparison error between the CFD predictions and the model tests are calculated as

$$E\%D = (D - S)/D \times 100 \quad (2)$$

where D is the experimental value and S denotes the value obtained from CFD.

As seen in Table I, half of the loading conditions and speeds resulted in comparison errors less than $\pm$1%. When these cases were cross-checked with the flow features, it was observed that the flow is mostly free from complicated and unsteady phenomena, such as flow separation, breaking waves, and spill breakers. On the other hand, the comparison error tends to be larger especially when the transom features wetted transom and partially dry transom flow. Even though the prediction accuracy is relatively high in general, as evidenced by the mean absolute comparison error of 1.2%, the prediction accuracy for the trim trends can be significantly worse (up to 3.5%) for certain loading conditions as also seen in Fig.1.

Table I: Total resistance comparison error, $\boldsymbol{E\%D}$

Loading Condition	Speed		
	15 kn	17 kn	19 kn
L-1.5m	0.57	1.55	1.68
L	0.77	0.16	-0.71
L+1.5m	-1.23	-1.23	-0.74
H-1.5	3.51	3.43	1.96
H	0.84	-0.15	-1.62
H+1.5m	-0.54	-0.67	-0.40

3.2. Self-propulsion

This section presents the results of self-propulsion towing tank tests and Computational Fluid Dynamics (CFD) simulations. The same trim optimization conditions used in the resistance tests (two displacements, three trims, and three speeds) were applied in the self-propulsion tests. Delivered power in model scale was calculated from measured torque and propeller rotation rate, with measurement uncertainties predicted as described in Korkmaz (2023). The change in delivered power, P_{DM}, between trimmed and even keel conditions is calculated using:

$$\Delta P_{DM} = \frac{P_{DM}(trim) - P_{DM}(trim = 0)}{P_{DM}(trim = 0)} \times 100 \quad (3)$$

Fig.4 displays the relative change in delivered power (P_{DM}) across different trims, displacements, and speeds. Black markers represent measured data, with error bars indicating measurement uncertainties. Trim trends from resistance tests, Fig.1, and self-propulsion tests, Fig.4, show similarities across various conditions, with stern trims resulting in significant power penalties, while bow trims yield variable outcomes based on displacement and speed.

The primary distinction between resistance and self-propulsion tests lies in the magnitude of potential gains or losses from trimming. For instance, at L-1.5m and 15 kn, $\Delta R_{TM} = 13.0\%$ and $\Delta P_{DM} = 24.5\%$. This disparity arises not only from propulsive efficiency differences but also from the differing test

setups. In self-propulsion tests, a towing force (R_a) unloads the propeller, addressing frictional resistance and roughness allowance discrepancies between model and full scale, *ITTC (2021)*. Hence, a direct comparison between the resistance and the delivered power in model scale is inappropriate. Instead, the towing force from self-propulsion tests should be subtracted from total resistance for an accurate comparison.

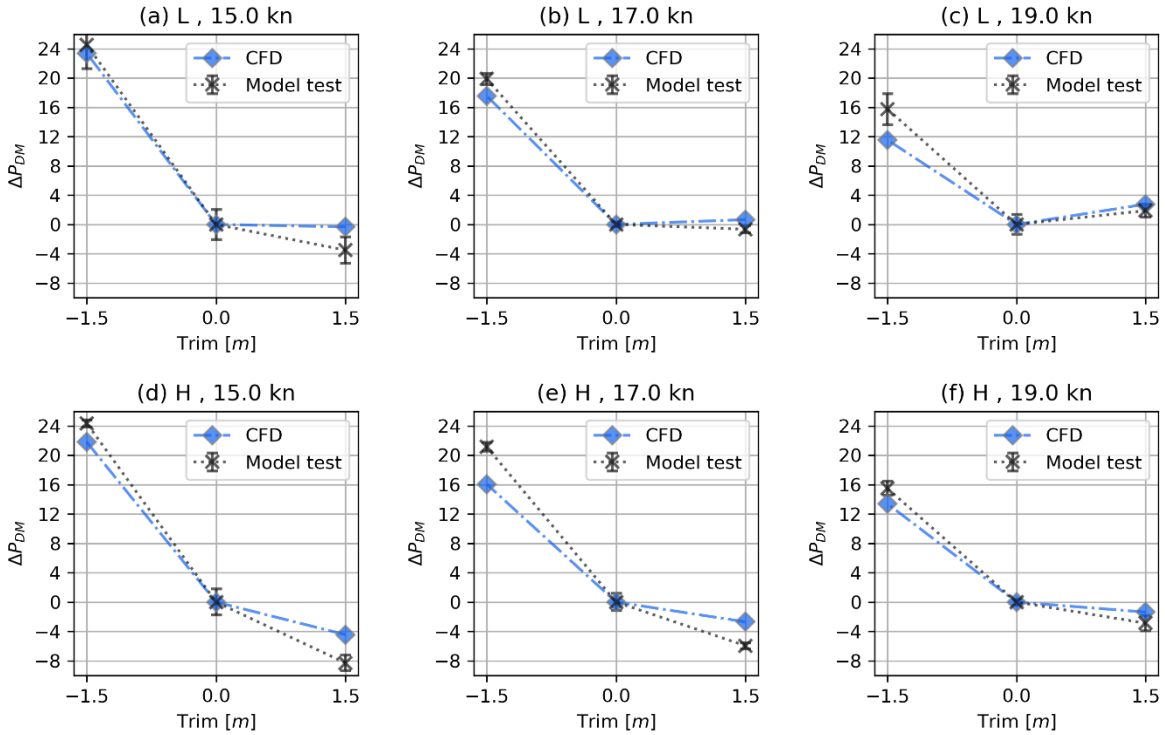


Fig.4: Change of delivered power with respect to trim relative to even keel condition, $\Delta \boldsymbol{P_{DM}}$, for model tests and CFD computations.

Table II: Comparison between adjusted resistance and delivered power at 19 kn

Loading Condition	Speed	
	19 kn	
	$\Delta(R_{TM} - Ra)$	ΔP_{DM}
L-1.5m	12.9	15.7
L+1.5m	4.3	1.9
H-1.5	13.6	15.5
H+1.5m	2.1	-2.8

Table II presents trim trends at 19 kn, showing adjusted total resistance ($\Delta(R_{TM} - Ra)$) and delivered power (ΔP_{DM}). Even after the adjustment, the gains, or losses due to trimming by bow or stern are substantially different, Table II. In the case of heavy displacement trim by the bow (H+1.5m), the trim trends do not even agree, resistance mode indicating 2.1% penalty while the self-propulsion mode suggests 2.8% reduction. Further investigations on the propulsive coefficients indicated that, aft trims (L-1.5m and H-1.5m) exhibit lower thrust increases than adjusted resistance, signifying reduced thrust deduction but a notable increase in propeller rate, leading to decreased wake fraction and hull efficiency. Aft trimming reduces hull efficiency and propeller efficiency due to increased resistance and altered propeller loading (K_{TM}/J_{TM}^2) substantially. Conversely, bow trims increase hull efficiency, particularly in heavy displacement, as they increase wake fraction and overall efficiency, highlighting gains in self-propulsion over resistance tests.

CFD computations for self-propulsion towing tank tests were conducted using the same conditions, and ΔP_{DM} values are illustrated in Fig. 3 where blue markers denote CFD results. The CFD method accurately replicated trim trends for delivered power, with a mean absolute comparison error of 2.2% compared to model tests. The simple propeller model used in CFD effectively captured thrust deduction, wake fraction, and propeller loading changes across trim conditions.

However, CFD predictions under-predicted ΔP_{DM} by 1.5% to 5.4% for stern trims, similar to R_{TM} predictions from resistance computations. This under-prediction is attributed to modelling errors in complex aft trim conditions involving breaking waves and unsteady eddies. Consequently, the under-prediction in self-propulsion computations likely stems mostly from resistance under-prediction and partially from the simple propeller modelling. CFD predictions were more accurate for bow trims, where flow conditions are less complex, again pointing towards modelling errors, such as time-averaging and turbulence modelling.

3.3. Comparison of resistance and self-propulsion results

As explained in Section 3.2, propulsive efficiency significantly impacts trim trends. Unlike resistance tests, self-propulsion tests closely resemble full-scale ship operations since the effect of the propeller is included. The operating propeller induces notable variations in pressure distribution at the aft body and modifies the local flow both upstream and downstream of the propeller. In self-propulsion tests, the pressure drop caused by the propeller at the hull and appendages, such as the rudder, increases dynamic sinkage at the aft body and alters the wave pattern in the hull's wake compared to resistance tests. Additionally, the propeller jet introduces significant flow variations downstream, extending up to the free surface and affecting the flow behind the transom.

(a) Resistance (b) Self-propulsion

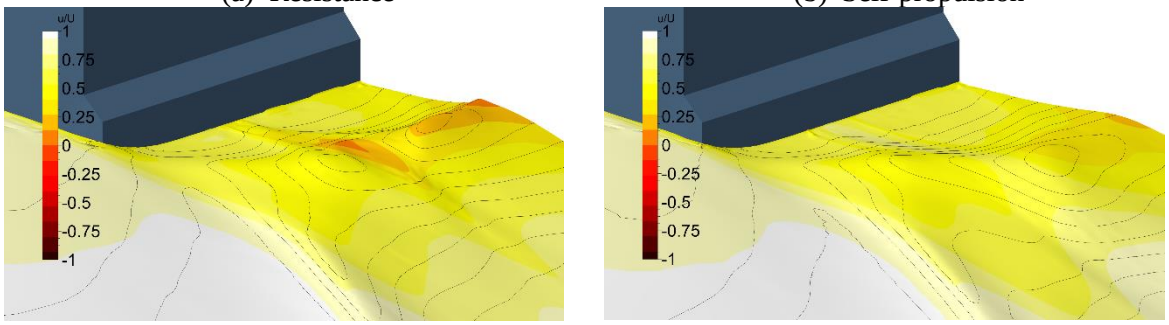


Fig.5: Wake behind the transom from the CFD computations in model scale, heavy displacement even keel condition, 19 kn.

Due to confidentiality constraints, specific pressure distributions on the hull and appendages are not disclosed. Instead, the wave pattern and non-dimensional longitudinal velocity (u/U, where u is the longitudinal velocity and the U is the free-stream velocity) at the free surface for resistance and self-propulsion computations at heavy displacement and 19 kn are presented in Fig.5. The negative u/U values indicate that water on the free surface is moving in the same direction as the model, trailing the hull. The contour lines on the iso-surface representing the wave elevation in Fig.5 mark the Z/L_{PP} (where Z represents the wave elevation and L_{PP} is the length between perpendiculars) with an interval of 0.001. The profound changes in the wave pattern behind the transom and the momentum loss in the wake due to the propeller's influence are visualised in Fig.5. The resistance computation, Fig.5**(a)**, the rudder's trace is visible as a longitudinal wave crest followed by a recirculating flow region. In contrast, the self-propulsion computation (Fig.5(b)), this trace is absent, and the recirculating flow is eliminated both behind the propeller and at the wave crest along the centreline.

To further clarify these differences, longitudinal wave cuts at three transversal positions —centreline, propeller centre, and $y/L_{PP} = 0.08$ (where y is the transversal distance from centreline) — were generated, Fig.6. Solid red lines represent resistance computations, while blue dashed lines denote self-

propulsion computations. The vertical black dotted line marks the transom's longitudinal position. These wave cuts reveal a significant difference in the steepness and shape of the first wave crest in self-propulsion tests compared to resistance tests. In addition, the wavelength of the transversal wave behind the transom is longer in self-propulsion compared to resistance computation. The diverging waves emitted from the edge of the transom shows significant differences while the wave pattern upstream of the aft body remains largely unchanged, as indicated by the wave cuts at $y/L_{PP} = 0.08$.

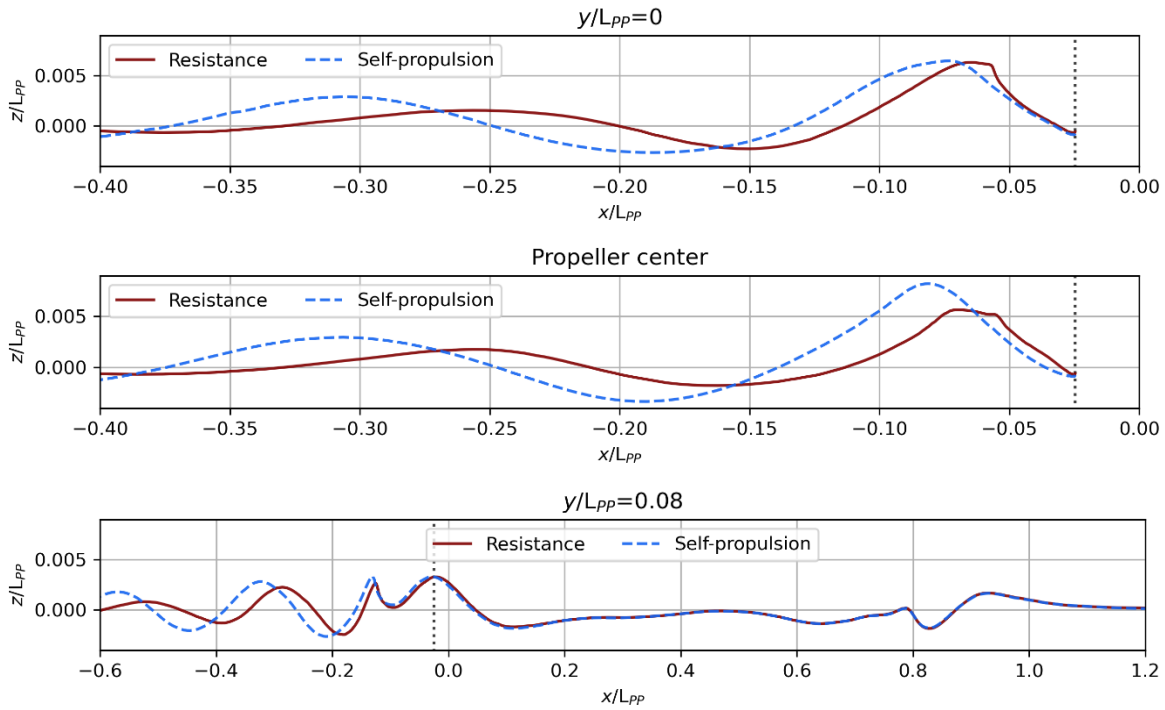


Fig.6: The longitudinal wave cuts from CFD computations in model scale, heavy displacement even keel condition, 19 kn.

As evidenced by the differences in the trim trends between the resistance and self-propulsion, the differences are not limited one or two loading conditions and speeds, but similar observations were made nearly for all combinations of speeds and loading conditions underscoring the importance of considering propeller effects for accurate ship performance predictions, i.e. trim trends.

4. Trim optimisation trends in full-scale

This section discusses the trim trends based on two different methods of extrapolation of trim optimization towing tank tests and self-propulsion computations in full scale. The methods for this extrapolation are detailed in Section 2.1. Unlike model scale experiments, where towing tank tests include uncertainty estimations, there is no experimental data with uncertainty estimations for full-scale. Although less accurate than speed trials, ship monitoring data can still be used to verify the trends predicted by different methods.

4.1. Analysis of the experimental and computational results

This section presents the trim optimization results for delivered power using the ITTC-78 and ITTC-78tr methods, and full scale self-propulsion CFD simulations. Fig.7 presents the trim optimization results of the delivered power. Similar to earlier plots, Fig.1, the non-dimensional delivered power predictions at the trimmed conditions are presented with respect to the even keel loading at each speed and displacement.

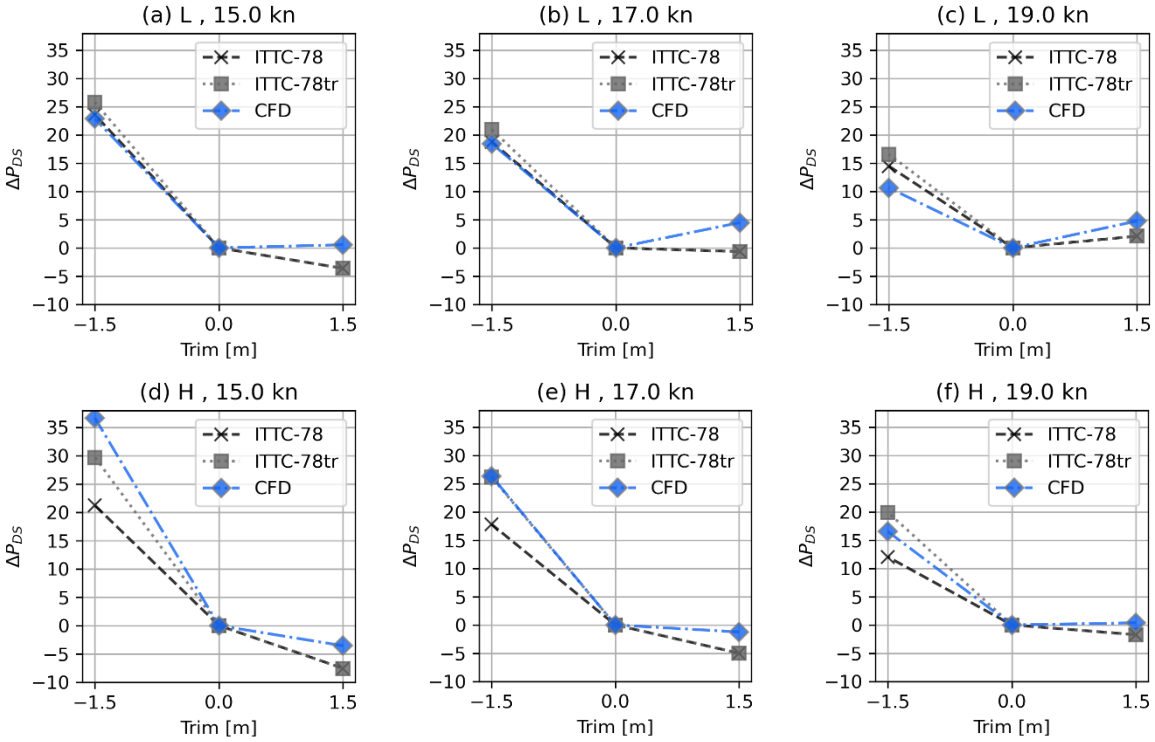


Fig.7: Change of predicted delivered power in full scale with respect to trim relative to even keel condition, $\Delta \boldsymbol{P_{DS}}$, for extrapolated model tests and CFD computations.

As seen in Fig.7, the results from ITTC-78 and ITTC-78tr are identical for the bow trim, as there is no transom submergence at trim by the bow for both displacements. On the other hand, the agreement in ΔP_{DS} predictions from the two extrapolation methods are less for aft trim (trim < 0) compared to trim by the bow. The ΔP_{DS} predictions differ up to 2.2% in the light displacement aft trim conditions. However, significant discrepancies emerge when the transom is submerged, notably in heavy displacement at 15 kn, leading to differences of up to 8.5% between ITTC-78 and ITTC-78tr. At this condition, wetted transom flow was observed in the towing tank tests. If the flow pattern behind the wetted transom is similar in the model and full scale, the ITTC-78 method is unsuitable, since the scaling of the viscous pressure resistance leads to under-prediction of the total resistance and delivered power, *Korkmaz (2023)*. This under-prediction stems from the flow recirculation (i.e., separated flow) behind the transom, which violates the form factor assumptions used in scaling the resistance. To address this limitation, the ITTC-78tr method introduces a correction, assuming that flow separation occurs both in the model and full scale, resulting in the ΔP_{DS} predictions between ITTC-78 and ITTC-78tr differing as much as 8.5%. Other speeds (17 kn and 19 kn) at heavy displacement and aft trim indicated partially dry transom flow in model scale. Therefore, the ITTC-78tr method includes a correction for the submerged transom, assuming a wetted transom both in the model and full scale. The wetted transom assumption does not hold in model scale and probably in full scale; therefore, the ITTC-78tr method likely over-predicts the delivered power in trim by the stern in heavy displacement, especially at the fastest speed.

There is no true reference in full scale to compare the ΔP_{DS} predictions from the full scale self-propulsion computations. However, the prediction accuracy of the CFD in model scale self-propulsion can be informative when full-scale predictions from the extrapolation methods and CFD are compared. The prediction pattern of CFD shows similarities in model and full scale for the loading conditions where the transom submergence is either zero or insignificant. For example, the model scale ΔP_{DM} predictions from the CFD were always under-predicted for the trim by the bow condition compared to the model tests, Fig.4. Similarly, in Fig.7, the full-scale CFD predictions are 3-4% higher than the predictions from extrapolation methods in trim by the bow condition.

At heavy displacement and aft trim conditions, the transom is substantially submerged, and the predictions from all methods, including CFD, diverge significantly, especially at the slowest speed of 15 kn. The contrast between the agreement of predictions from different methods for the light and heavy displacements with aft trim at 15 kn is significant. As argued earlier, the flow separation complicates the scaling procedure for the extrapolation methods. As a result, different extrapolation methods predict vastly different ΔP_{DS} values at the aft trim condition. Notably, CFD predictions align closely with ITTC-78tr, especially evident in heavy displacement conditions with substantial transom submergence. As speed increases, discrepancies diminish, especially in heavy displacement conditions at higher speeds, reflecting a shift in transom flow regime from wetted to partially dry and dry transom.

4.1.1. Comparison between model and full scale trim trends

Free-surface RANS self-propulsion computations were employed to compare the flow features between the model and full scale. Such comparisons are crucial since numerous loading conditions and speeds yielded partially dry or even wetted-transom flows, alongside dry transoms. Partially dry transoms are subject to large-scale effects, *Starke et al. (2007)*, potentially causing different flow regimes in model and full scale.

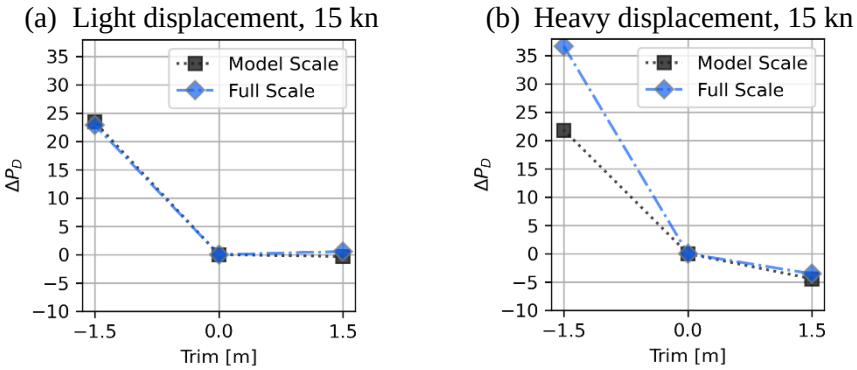
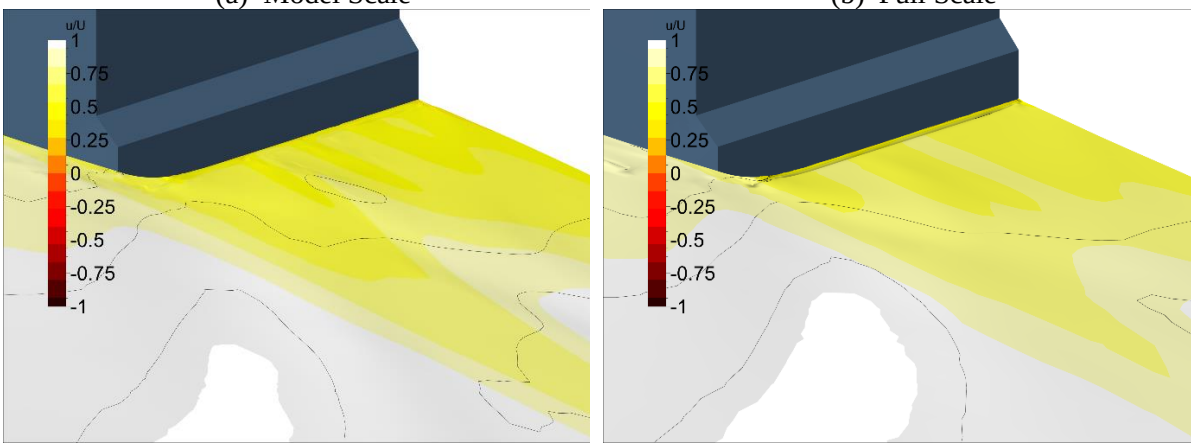


Fig.8: Comparison of the change of predicted delivered power between the model and full scale from the CFD computations.

To demonstrate the scale effects on the trim trends and the flow especially behind the transom, the speed of 15 kn has been selected. As in Fig.8(a), the model scale and full scale delivered power trends with bow and stern trims are nearly identical for light displacement. The flow is visualised in in Fig.9 through surface elevation coloured by the non-dimensional longitudinal velocity, and the wave cut at the centreline for the even keel condition at light loading condition. As seen in Fig.9, both model and full scale have dry transom flow where the flow leaves the transom edge smoothly, and no traces of flow separation can be observed in the wake. Additionally, the wave cut shown in Fig.9, suggests only limited differences between the two scales.

Similar comparisons were conducted for aft trim conditions in light displacement (L-1.5m), indicating nearly identical trim trends in both scales, Fig.8 (a). The flow for the L-1.5m condition is visualised in Fig.10 similar to the earlier Fig.9. As seen in Fig.10, both model and full scale have dry transom flow. However, the longitudinal velocity at the free surface shows significant flow retardation, even pockets of flow recirculation zones exist in both scales. Additionally, wave pattern shows considerable differences as shown in Fig.10 by the surface elevation and the wave cut at the centreline. However, a neither a major recirculation region nor a significant change is observed in both even keel and aft trim conditions; hence, the trim trends remained relatively similar in both scales.

(a) Model Scale (b) Full Scale



(c) Wave cut at the centreline

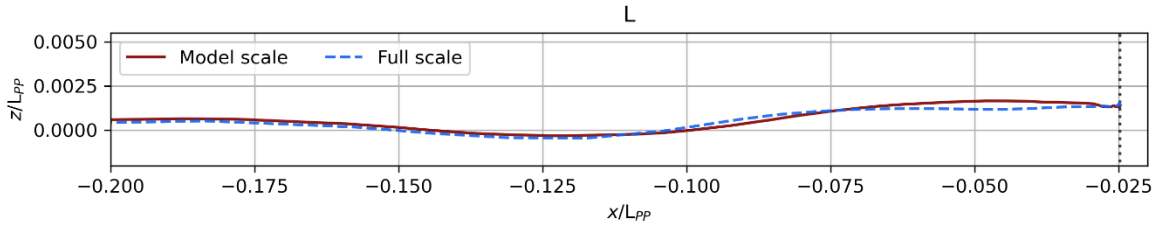
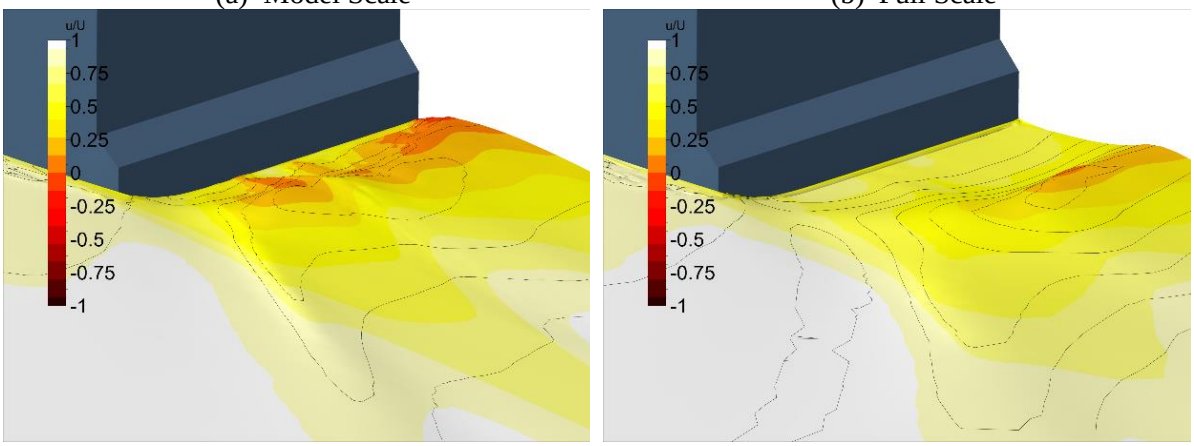


Fig.9: Non-dimensional longitudinal velocity on the free surface from CFD computations in model (top left) and full scale (top right) at 15 kn and L loading condition.

(a) Model Scale (b) Full Scale



(c) Wave cut at the centreline

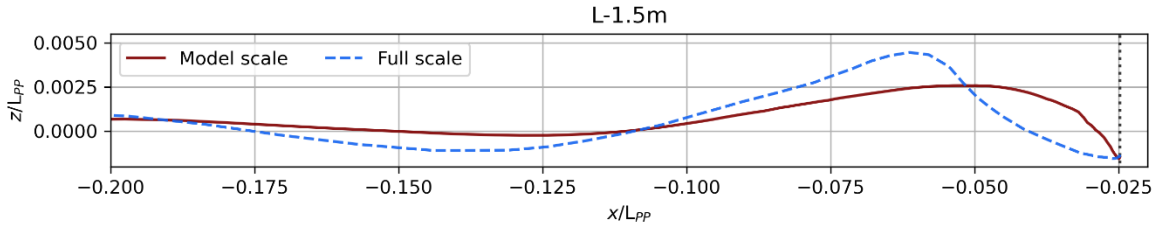


Fig.10: Non-dimensional longitudinal velocity on the free surface from CFD computations in model (top left), full scale (top right) and wave cuts at 15 kn and L-1.5m loading condition.

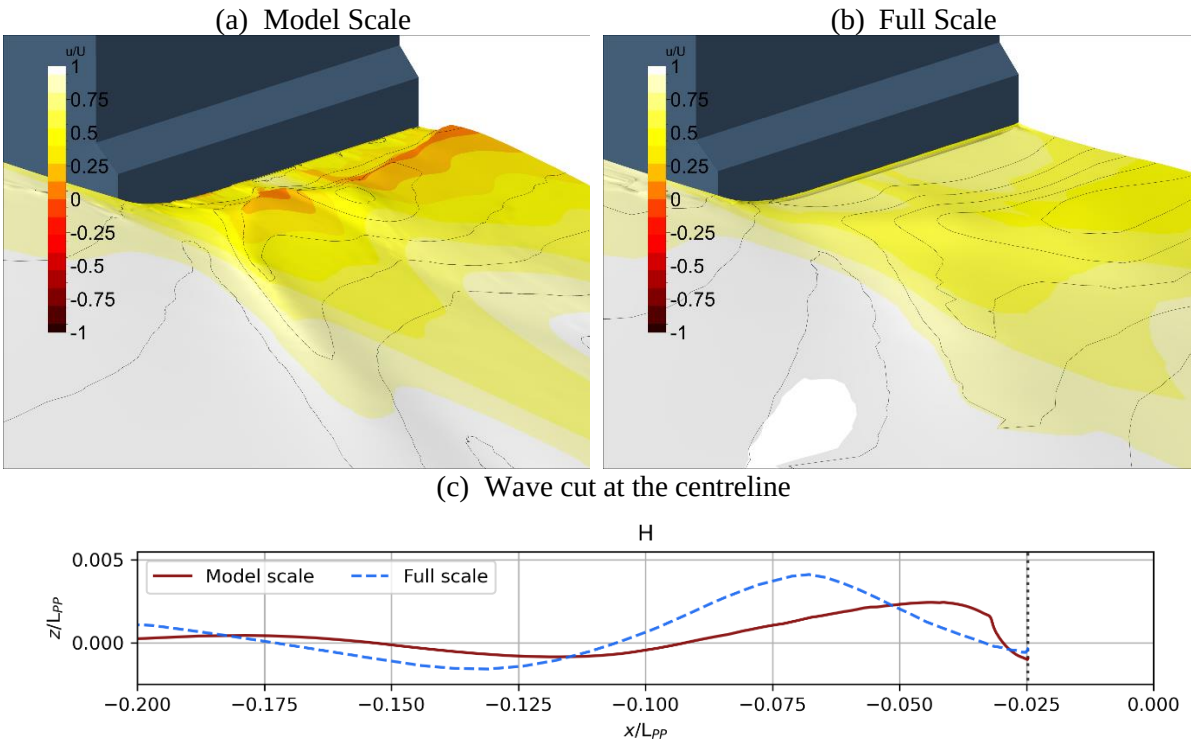


Fig.11: Non-dimensional longitudinal velocity on the free surface from CFD computations in model (top left) and full scale (top right) at 15 kn and H loading condition.

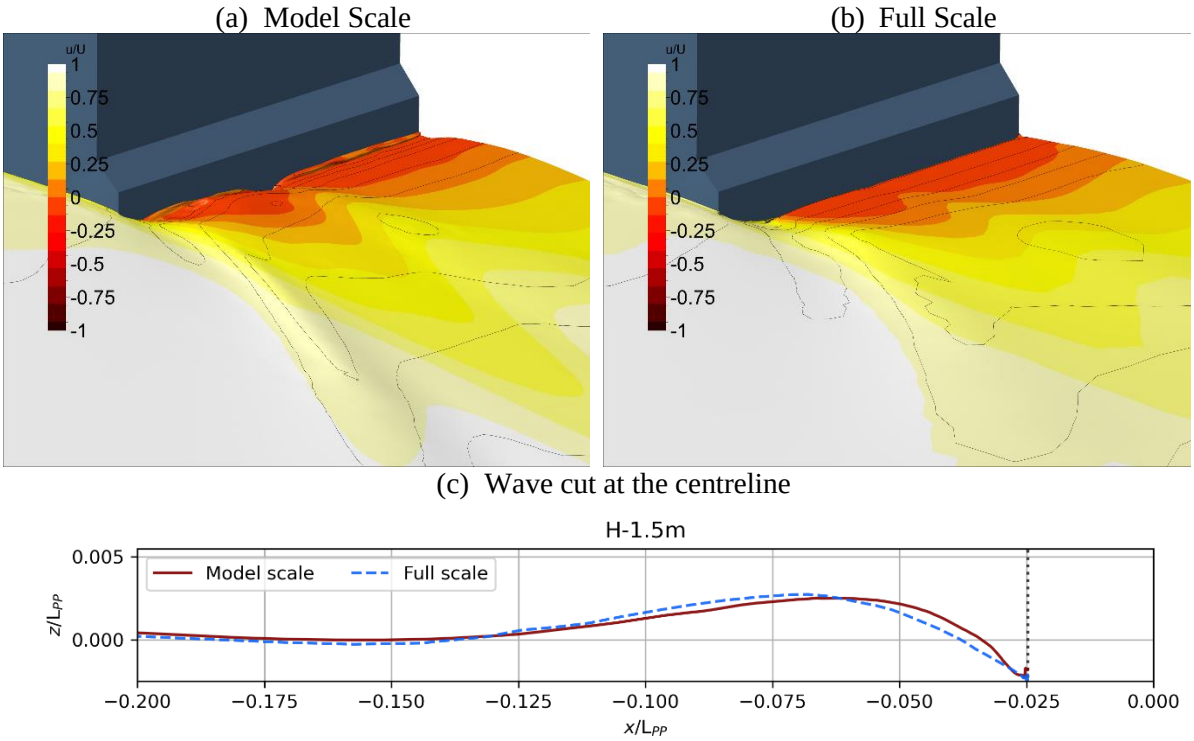


Fig.12: Non-dimensional longitudinal velocity on the free surface from CFD computations in model (top left) and full scale (top right) at 15 kn and H-1.5m loading condition.

Moving on to the next loading condition, heavy displacement at 15 kn, Fig.8(b) indicates nearly 15% difference in the trim trends for the aft trim condition, while the bow trim trend remained nearly identical for both scales. To scrutinise the large scale effect for at the aft trim, the flow is visualised in Fig.11 through surface elevation coloured by the non-dimensional longitudinal velocity, and the wave cut at the centreline for the even keel condition at the heavy loading condition. As seen in Fig.11, the

full scale computation shows dry transom flow where the flow leaves the transom edge parallel to the buttocks, and trace of excessive flow retardation can be seen on the free surface, The transom in the model scale computation is also dry; however, the transverse wave following the transom is steep as seen in Fig.11(c), and the wave crest is occupied by significant separated flow. As a result of the changed flow regime (disappearing recirculation zone) between the two scales, significant scale effects are observed in the even keel heavy displacement at 15 kn.

Unlike the even keel condition at the heavy displacement, the flow observations for the trim by the stern shows less differences between the model and full scale as seen in Fig.12, where free surface and wave cuts are visualised in a similar fashion to the earlier ones e.g. Fig.11. As seen in Fig.12(a) and (b), both model and full scale has wetted transoms. The negative non-dimensional longitudinal velocities immediately downstream of the transom for both scales indicate large flow recirculation zones. Additionally, a closer inspection on the extend of flow retardation behind the transom and the wave cut suggests little change in terms of flow recirculation zone between the model to full scale. As argued by *Korkmaz (2022)*, the resistance caused by the flow recirculation zone, i.e. wetted transom, becomes much more prominent in full scale as the frictional resistance coefficient and viscous pressure resistance coefficients (excluding the transom resistance) reduces with the increasing Reynolds number, while the part of the pressure resistance coefficient due to wetted transom remains relatively similar in both scales. Since the trim trends highlight the difference between the even keel and trimmed conditions, the difference between the model and full scale widens for the heavy displacement aft trim condition.

4.2. Preparation of the ship monitoring data and full-scale predictions for comparison

4.2.1. Experimental and computational methods

Full-scale predictions were generated for two displacements, three trims, and three speeds. However, the ship's actual operating conditions surpass these 18 CFD and EFD predicted scenarios. Therefore, a surrogate model is necessary to estimate conditions between the predictions.

The polynomial response surface approach was chosen to build the surrogate model. In this approach, the independent variables—draught at midship (T_M), trim, and ship speed—were used in a regression analysis to predict the dependent variable, delivered power. However, the limited data points for each independent variable posed challenges in selecting the polynomial degree. Initially, a linear regression was employed due to the availability of only two draughts, but it produced unsatisfactory results. To enhance the accuracy of the model, the number of data points was artificially increased through linear interpolation for draught and trim. Subsequently, quadratic and cubic polynomials were fitted to each data set (ITTC-78tr, model scale resistance CFD, full scale self-propulsion CFD), yielding maximum standard deviations of approximately 1.0% and 0.7%, respectively. The cubic fit was preferred due to its qualitative alignment with the observed trends in trim across different speeds and its lower standard deviation.

4.2.2. Ship monitoring data

Relevant variables were carefully chosen from the sensor data to characterize various aspects of the ship's operating environment. These included parameters describing the ship's loading condition (draught at fore and aft perpendiculars), environmental factors (such as current, depth below keel, apparent and true wind speed and direction, swell, wave height, and period), and speed-power performance (including propeller turning rate, shaft torque, speed over ground, and speed through water). Once the dataset was verified to ensure the existence and integrity of all selected variables for each reading, filters were applied to approximate calm and deep water conditions. Speed through water (STW) was prioritized over speed over ground (SOG) based on feedback from ship operators. Data points with STW less than 14.5 kn or greater than 19.5 kn were eliminated to align with the range of predictions from CFD and EFD.

Given that the vessel navigates through areas with shallow water sections, measures were taken to exclude the effects of shallow water. This involved calculating parameters such as the depth Froude number (Fr_H), h/T_M ratio (where h represents the water depth), and Raven's shallow water correction, *Raven (2019)*. Data points with $Fr_H > 0.6$, $h/T_M < 5$, or Raven's correction exceeding 3% were filtered out accordingly.

The twin-screw propulsive arrangement allows operational flexibility, leading to unequal shaft line loads. Data points where either shaft bore less than 30% or more than 70% of total power were removed to match prediction conditions of equal propeller loading.

Wind conditions were cross-referenced with wave data due to the consistent wind direction and sheltered operations. Data points with apparent wind speeds exceeding 18 m/s were excluded. Additionally, draught and trim values beyond the scope of the towing tank tests were eliminated.

Following the filtering process, approximately 9.5% of the original dataset remained, closely approximating the conditions for full-scale CFD and EFD predictions. Each subset of data, roughly corresponding to the full-scale prediction conditions, underwent regression analysis with ship speed, midship draught, and trim as independent variables, while total power was designated as the dependent variable.

4.3. Comparison between the predictions and the full scale data

The final step of the full-scale analysis involves comparing measured and predicted power. As explained in Sections 4.2.1 and 4.2.2, two regression models—one for predictions and one for measurements—are utilized to approximate trim optimization trends across various scenarios, including light and heavy displacements, three speeds, and a suitable range of trim values within each dataset subset. The predictions from extrapolation method (ITTC-78tr) and CFD (model scale resistance and full-scale self-propulsion), along the trim trends from ship monitoring data (denoted as data fit), are compared in Fig.13. A reference band of ±5% is placed around the data fit curve, and histograms of trim values are shown above each plot to indicate frequency and skewness in each data selection. The x-axis alignment enables a clear comparison of trim value frequencies, while the y-axis, representing either ΔP_{DS} or ΔR_{TM}, depicts the percentage change in power or resistance, respectively, with varying trim values.

The comparison, limited to data with sufficient trim values, shows that all predictions from ITTC-78tr method and full-scale self-propulsion computations fall within the 5% reference band, as observed in Fig.13. Although most conditions fall within this band, in some cases, the trim trends from model scale resistance computations lie outside of it. This agreement, despite uncertainties in ship monitoring data collection and curve fitting, indicates high similarity between predictions and measurements across all loading conditions and speeds.

As observed in Fig.13, all predictions and data fit of the measurements agree that trimming by the stern increases power demand. While predictions and measurements largely align for trim by the bow, the data fit from ship monitoring data suggests an optimum trim at smaller values compared to prediction methods. However, the trim trends from ship monitoring data exhibit some inconsistencies. For example, the data fit suggests ΔP_{DS} values of approximately -6%, -1%, and -4% for heavy displacement at ~0.75m trim for speeds of 15 kn, 17 kn, and 19 kn, respectively. This trend is not supported by towing tank tests and CFD computations, which suggest a monotonic change. Therefore, the trim trends from ship monitoring data should be interpreted cautiously, with a significant reference band to account for unrealistic fluctuations in data curve fits.

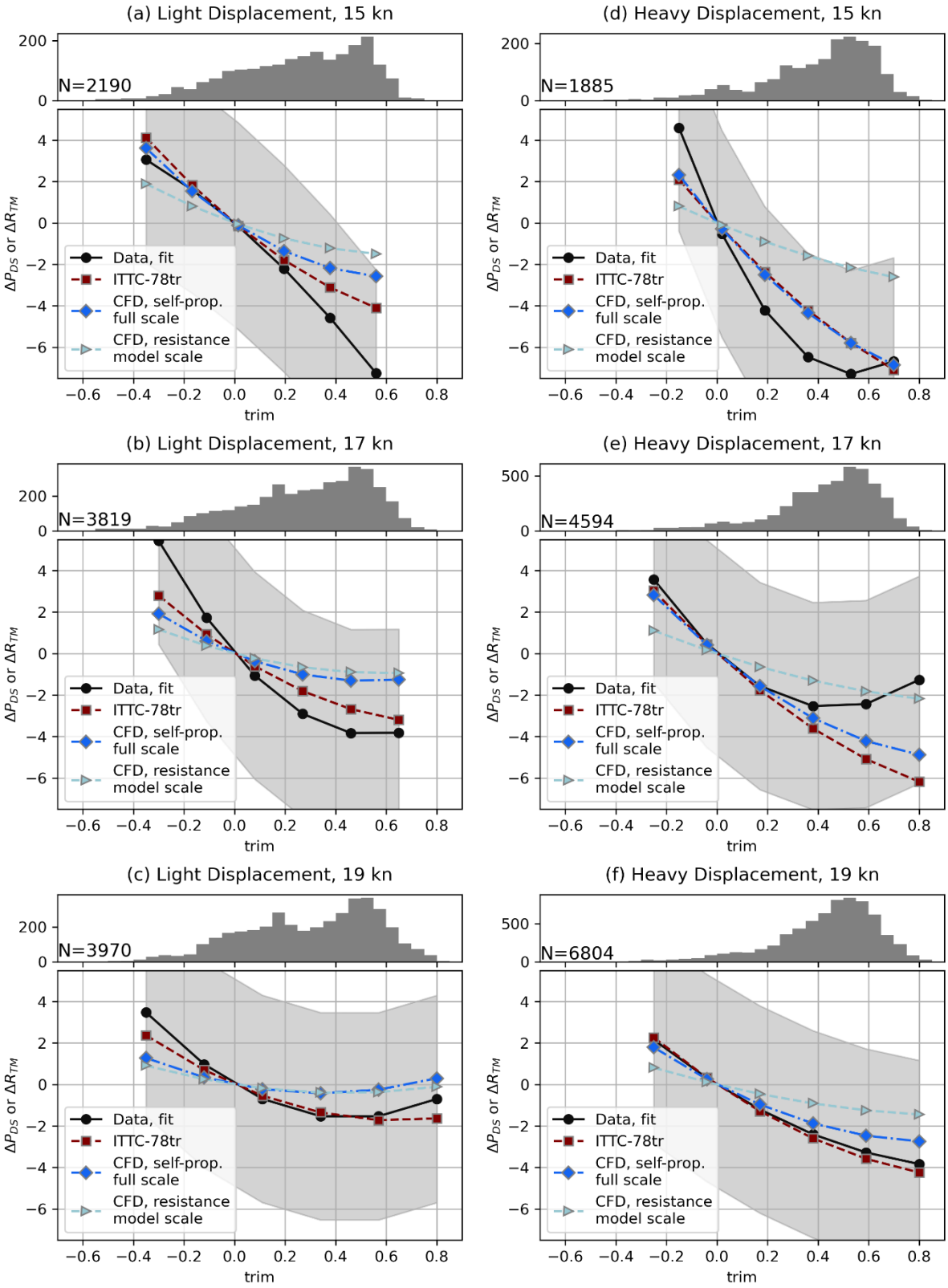


Fig.13: Comparison between trim trends from ship monitoring data, extrapolations methods and CFD

Despite observed fluctuations in the trim trends from ship monitoring data, further analysis was conducted to compare the trim trends from full-scale measurements and various prediction methods. The comparison error, denoted as $E\%D$, quantifies the discrepancy between the data fit and prediction methods, namely ITTC-78tr, CFD self-propulsion full-scale, and CFD resistance model-scale.

Table III summarizes the mean comparison error ($\overline{E\%D}$) and the mean absolute comparison error ($\overline{|E\%D|}$) for light loading (L) condition, heavy loading (H) condition, and the combined loading conditions. The $\overline{E\%D}$ values indicate the mean bias between the predictions and the actual measurements. For the ITTC-78tr method, the mean errors are relatively small, with the combined loading condition showing a minor positive bias of 0.09%. The CFD self-propulsion full-scale predictions display a larger negative bias in the light loading condition (-0.69%) and a smaller negative bias in the combined condition (-0.29%). In contrast, the CFD resistance model-scale predictions exhibit a consistently negative bias across all conditions, with the heaviest bias observed in the heavy loading condition (-0.96%).

In other terms, predictions of trim trends from ITTC-78tr are on average in good agreement with the full-scale measurements, while the full-scale CFD computations closely follow this level of agreement but with a small negative bias, indicating a general underprediction of trim trends. On the other hand, the model-scale CFD computations systematically underpredict the trim trends, which is expected in light of the investigations on scale effects (see Sections 3.3 and 4.1.1).

Table III: Comparison error between ship monitoring data and full-scale predictions

Error	ITTC-78tr			CFD self-prop. full-scale			CFD resistance model-scale		
	L	H	Combined	L	H	Combined	L	H	Combined
$\overline{E\%D}$	-0.23	0.41	0.09	-0.69	0.12	-0.29	-0.60	-0.96	-0.78
$\overline{\|E\%D\|}$	0.88	1.07	**0.98**	1.52	0.96	**1.24**	1.77	1.95	**1.86**

The $\overline{|E\%D|}$ values provide insight into the magnitude of the prediction errors regardless of their direction. The absolute errors are highest for the CFD resistance model-scale method, indicating larger deviations from the full-scale measurements, particularly in the heavy loading condition (1.95%), where the scale effects are the most prominent due to substantial transom submergence. The ITTC-78tr method shows a balanced error distribution among different loading conditions, while indicating the smallest overall error. The CFD self-propulsion full-scale method, closely following the ITTC-78tr method, gives the lowest absolute error in the heavy loading condition (0.96%).

In summary, while all prediction methods exhibit some degree of error when compared to full-scale measurements, the ITTC-78tr method generally provides the most accurate predictions, evidenced by the smallest absolute error magnitudes. The CFD self-propulsion full-scale method, though having larger biases, offers a balanced performance with moderate absolute errors. The CFD resistance model-scale method, despite having the highest errors, offers only a crude understanding of the trim trends due to its significant deviations from full-scale measurements especially.

5. Conclusions

In this study, the trim optimization trends of a RoPax vessel have been investigated using both experimental and computational methods. The accuracy of different CFD methods in the model scale was assessed through comparisons with towing tank tests, and full-scale predictions were compared to ship real-time recorded data.

The free-surface RANS computations generally replicated towing tank resistance tests accurately, particularly for trim by the bow conditions. However, its accuracy is reduced with increased transom submergence, especially for trim by the stern conditions, due to the complex flow phenomena. The use of a simple actuator disc model in self-propulsion simulations demonstrated that while the prediction accuracy for power was slightly lower than for resistance, it was sufficient to capture variations in propulsive efficiency and local flow differences in model scale. The propulsive efficiency variation with trim was found to be significant, emphasizing the necessity of self-propulsion tests or computations to accurately quantify the potential gains and losses of trim optimization.
The comparison of different extrapolation methods for full-scale predictions revealed significant

insights. The ITTC-78 method with transom correction demonstrated the closest alignment with full-scale CFD predictions, offering consistent performance across various loading conditions. Conversely, disparities were noted among different prediction methods in conditions characterized by substantial transom submergence, particularly evident in trim by stern scenarios.

Through comparisons between measured and predicted power, facilitated by regression models, the study evaluates trim variations across different loading conditions and speeds. Notably, the ITTC-78 method with transom correction (ITTC-78tr) and CFD simulations (model scale resistance and full-scale self-propulsion) generally align within a ±5% reference band around the ship monitoring data curve, indicating substantial similarity across various operating conditions. However, deviations are observed, particularly in conditions involving substantial transom submergence, where model scale resistance computations diverge from the reference band. Despite uncertainties in data collection and curve fitting, the agreement between predictions and measurements underscores the robustness of prediction methods. Notably, the ITTC-78tr method demonstrates the smallest absolute error magnitudes, suggesting superior accuracy compared to other prediction methods. Conversely, the CFD resistance model-scale method, characterized by larger deviations from full-scale measurements, offers only a rudimentary understanding of trim trends.

In conclusion, the full-scale self-propulsion CFD method is a reasonably accurate and cost-effective approach for determining trim trends, though thorough verification and validation studies are advised due to potential discretisation and modelling errors in some loading conditions. When performing towing tank tests, it is recommended to use an extrapolation method that includes corrections for substantially submerged transoms to ensure more accurate full-scale predictions. Future research should investigate the effects of shallow waters and waves on trim trends, as the current study's conclusions are limited to deep and calm sea conditions.

Acknowledgements

This research was funded by Energimyndigheten, the Swedish Energy Agency, grant 2020-018759, and the computational resources provided by RISE-SSPA Maritime Center. The authors declare no conflict of interest. The funders had no role in the design of the study; in the collection, analyses, or interpretation of data; in the writing of the manuscript, or in the decision to publish the results.

References

CHEN, J.; YU, C.; SHEN, L. (2019), *Study of trim optimization based on design of experiments and RANS simulation*, 11th International Workshop on Ship and Marine Hydrodynamics, Hamburg

CORADDU, A.; ONETO, L.; BALDI, F.; ANGUITA, D. (2017), *Vessels fuel consumption forecast and trim optimisation: A data analytics perspective*, Ocean Eng. 130, pp.351–370

HANSEN, H.; FREUND, M. (2010), *Assistance tools for operational fuel efficiency*, 9th COMPIT Conf., Gubbio

HUGHES, G. (1954), *Friction and form resistance in turbulent flow, and a proposed formulation for use in model and ship correlation*, R. I. N. A. 96

IMO (2011), *Annex 19: resolution MEPC.203(62)*, Int. Mar. Org., London

IMO (2021), *Fourth IMO GHG Study 2020*, Int. Mar. Org., London

IMO (2022a), *2022 Guidelines on operational carbon intensity indicators and the calculation methods (CII guidelines, G1), Annex 14: Resolution MEPC.352(78)*, Int. Mar. Org., London

IMO (2022b), *2022 Guidelines on the method of calculation of the attained energy efficiency existing*

ship index (EEXI), Annex 12: Resolution MEPC.350(78), Int. Mar. Org., London

IMO (2023), *Definitions of maturity levels according to uptake across the maritime industry, and degree of proven technology/principle*, Int. Mar. Org., London

ISLAM, H.; GUEDES SOARES, C. (2019), *Effect of trim on container ship resistance at different ship speeds and drafts*, Ocean Eng. 183, pp.106–115

ITTC (1957), *Subjects 2 and 4 skin friction and turbulence stimulation*, Int. Towing Tank Conf.

ITTC (2021a), *1978 ITTC performance prediction method. ITTC – Recomm. Proced. Guidel. 7.5-02-03-01.4*, Int. Towing Tank Conf.

ITTC (2021b), *Quality assurance in ship CFD application. ITTC – Recomm. Proced.Guidel. 7.5–03–02–04*, Int. Towing Tank Conf.

ITTC (2021c), *Practical guidelines for ship resistance CFD. ITTC – Recomm. Proced.Guidel. 7.5–03–02–04*, Int. Towing Tank Conf.

KANNINEN, P.; PELTONEN, P.; VUORINEN, V. (2022), *Full-scale ship stern wave with the modelled and resolved turbulence including the hull roughness effect*, Ocean Eng. 245, p.110434

KORKMAZ, K.B.; WERNER, S.; BENSOW, R. (2021a), *Verification and validation of CFD based form factors as a combined CFD/EFD method*, J. Marine Sci. Eng. 9 (1)

KORKMAZ, K.B.; WERNER, S.; SAKAMOTO, N.; QUEUTEY, P.; DENG, G.; YULING, G.; GUOXIANG, D.; MAKI, K.; YE, H.; AKINTURK, A.; SAYEED, T.; HINO, T.; ZHAO, F.; TEZDOGAN, T.; DEMIREL, Y.K.; BENSOW, R. (2021b), *CFD based form factor determination method*, Ocean Eng. 220, p.108451

KORKMAZ, K.B.; WERNER, S.; BENSOW, R. (2022), *Scaling of wetted-transom resistance for improved full-scale ship performance predictions*, Ocean Eng. 266, p.112590

KORKMAZ, K.B.; WERNER, S.; BENSOW, R. (2023), *Investigations on experimental and computational trim optimisation methods*, Ocean Eng. 288, Part 2, p.116098.

LARSSON, L.; RAVEN, H.C. (2010), *Ship Resistance and Flow*, SNAME, Jersey City

LEMB LARSEN, N.; SIMONSEN, C.D.; NIELSEN, C.K.; HOLM, C.R. (2012), *Understanding the physics of trim*, 9th Annual Green Ship Technology (GST) Conf., Copenhagen

MAHMOODI, H.; GHAMARI, I.; HAJIVAND, A.; MANSOORI, M. (2023), *A CFD investigation of the propulsion performance of a low-speed VLCC tanker at different initial trim angles*, Ocean Eng. 275, p.114148

MAHMOODI, H.; HAJIVAND, A. (2022), *Numerical trim and draft optimization of a twin-screw modern surface combatant with inverted bow*, Appl. Ocean Res. 123, p.103186

MENTER, F.R. (1993), *Zonal two-equations k–ω turbulence models for aerodynamic flows*, 23rd Fluid Dynamics, Plasmadynamics, and Lasers Conference, Orlando, pp.93–290

PROHASKA, C.W. (1966), *A simple method for the evaluation of the form factor and low speed wave resistance*, 11th ITTC Conf.

RAVEN, H.C. (2019), *Shallow-water effects in ship model testing and at full scale*, Ocean Eng. 189,

p.106343

REICHEL, M.; MINCHEV, A.; LARSEN, N.L. (2014), *Trim optimisation - theory and practice*, TransNav, Int. J. Marine Navig. Safety Sea Transp. 8 (3), pp.387–392

SAMES, P.C.; KÖPKE, M. (2012), *CO2 emissions of the container world fleet*, Procedia - Soc. Behav. Sci. 48, pp.1–11

SCHULTZ, M.P. (2007), *Effects of coating roughness and biofouling on ship resistance and powering*, Biofouling 23 (5), pp.331–341

SHIVACHEV, E.; KHORASANCHI, M.; DAY, A.H. (2017), *Trim influence on Kriso container ship (KCS): An experimental and numerical study*, Volume 7A: Ocean Engineering, ASME, Trondheim

STARKE, B.; RAVEN, H.; VAN DER PLOEG, A. (2007), *Computation of transom-stern flows using a steady free-surface fitting RANS method*, 9th Int. Conf. Numerical Ship Hydrodynamics

SUN, J.; TU, H.; CHEN, Y.; XIE, D.; ZHOU, J. (2016), *A study on trim optimization for a container ship based on effects due to resistance*, J. Ship Res. 60 (01), pp.30–47

WACKERS, J.; KOREN, B.; RAVEN, H.C.; VAN DER PLOEG, A.; STARKE, A.R.; DENG, G.B.; QUEUTEY, P.; VISONNEAU, M.; HINO, T.; OHASHI, K. (2011), *Free-surface viscous flow solution methods for ship hydrodynamics*, Arch. Comput. Methods Eng. 18 (1), pp.1–41

Hull Form Variations for Improved Sailing Balance of Wind-Assisted Propelled Ships

Fabian Thies, FRIENDSHIP SYSTEMS, Potsdam/Germany, thies@friendship-systems.com
Hannes Renzsch, FRIENDSHIP SYSTEMS, Potsdam/Germany, renzsch@friendship-systems.com

Abstract

This paper presents the influence of the hull design on the sailing balance, i.e. the centre of lateral resistance (CLR), of a wind assisted propelled (WASP) ship. The importance of the CLR on the performance of a WASP ship is discussed using results from a generic performance model. On the example of a case study ship and using fully viscous CFD computations, the influence of hull design features (e.g. forward shoulders and bulbous bow design) and the influence from additional appendages in the skeg region are presented.

1. Introduction

Wind-assisted ship propulsion continues to be one of the most important and most discussed option to reduced greenhouse gas emissions from shipping. While multiple WASP technologies have been proven to give good fuel savings, *WASP (2023)*, the effect of WASP on ship design is not yet discussed much. Recently, studies on propeller design for WASP ships have been conducted and discuss the special requirements due to large load variations due to different propulsion thrust from the sails and oblique inflow, *Gypa et al. (2023)*. In *Renzsch and Thies (2023)* the effect of hull form modifications on the added resistance due to drift has been discussed, which becomes important due to the large side forces implied by the sails. As a follow up, this paper investigates the effect of hull form on the centre of lateral resistance (CLR), i.e. the point where the side force generated by the hull acts. The importance of the CLR has already been discussed during the early rise of WASP technologies, *van der Kolk (2016)*, but few studies on suitable hull modifications to influence the position of the CLR have been conducted.

2. The case study ship

This study is based on the well-known KVLCC2, a common test and verification ship hull representing a very large crude oil carrier, *Van et al. (1998).* The dimensions of the ship are presented in Table I.

Table I: Main dimensions of the KVLCC2

	Full scale	Model scale
Lpp	320.0 m	7.0 m
B	58.0 m	1.269 m
T	20.8 m	0.455 m
c_B	0.8098	0.8098

In an exemplary study, the effects or a CLR variation on the fuel savings from a WASP system are presented in Section 3. For this study, the KVLCC2 is equipped with 6 Flettner Rotors (5 m x 30 m), arranged as presented in Fig.1.

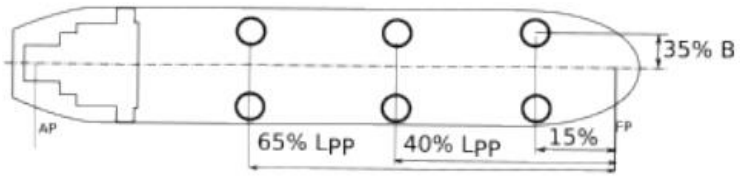


Fig.1: Arrangement of 6 Flettner rotors on the KVLCC2

3. The importance and typical position of the CLR

In contrast to a conventional propeller, a sail introduces large side forces into the system, which must be compensated by the hull and propeller. In a static sailing condition one can formulate a system of equations by:

$$0 = Y_{sail} + Y_{hull} + Y_{rudder}$$
$$0 = M_{z_{sail}} + M_{z_{hull}} + M_{z_{rudder}} = Y_{sail} * x_{sailForce} + Y_{hull} * CLR + Y_{rudder} * Lpp$$

M_z denotes the yaw moments and Y denotes the side forces. This shows that the balance between the side force created by the hull and the rudder, i.e. the rudder angle and drift angle, are defined by the position of the CLR. The further forward, the more of the side force must be taken by the rudder since the hull yaw moment decreases. This must be considered to (a) ensure course keeping capabilities, and (b) improve overall performance. To ensure course keeping capabilities, the static rudder angle should be limited, which calls for a CLR further back. From a manoeuvring and course keeping point of view, a CLR at the centre of the sail force would be ideal, meaning that the static rudder angle becomes zero. However, as shown in *Renzsch and Thies (2023)*, the added resistance due to drift can vary largely. It is not uncommon, that the added resistance from drifting is much higher than the added resistance caused by a rudder angle. In such case, it would be beneficial to load as much of the side force on the rudder as possible, i.e. moving the CLR as far forward as possible. As soon as the added resistance from drifting becomes lower (some variants in *Renzsch and Thies (2023)* even showed a negative added resistance), the rudder should be unloaded.

Fig.2 presents the influence of the CLR on the resulting sail net thrust (i.e. the thrust deducted with the added resistance from drift and steering) of the case study ship with the sail arrangement presented in section 2. The analysis was done at a true wind angle of 50 degrees, a true wind speed of 20 kn and a ship speed of 15.5 kn. The prediction was performed using the generic four degrees of freedom model ShipCLEAN, *Tillig and Ringsberg (2020).* The CLR is moved back (positive values) and forward (negative values), by 6% Lpp. Results show an increase of the net thrust when the CLR moves forward, which is due to a higher rudder loading, which for this hull reduces the total added drag. However, moving the CLR forward with more than 1% Lpp from the original value causes the rudder angle to reach the defined maximum value (5° in this case), in which case the sails must be depowered causing a decrease of the net thrust.

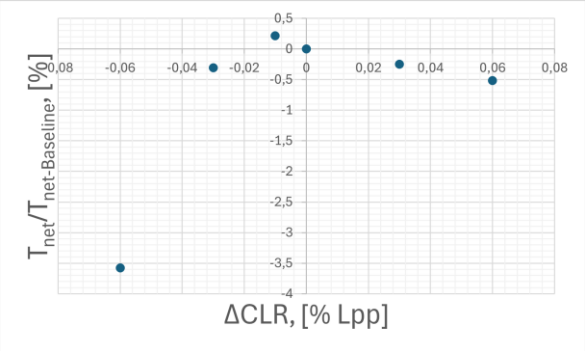


Fig.2: Relative net thrust with varying CLR position.

In summary, the position of the CLR influences the relation of the side force taken by the hull and the rudder. Thus, it directly influences the added resistance and course keeping capabilities and the efficiency of the WASP system.

As discussed in *Tillig and Ringsberg (2020),* the side force generation of a ship hull is dominated by the cross flow drag. The centre of this cross flow drag force is close to the geometric centre of the lateral plane of the hull. However, due to the pressure distribution along a slender body in oblique floe, an external moment is implied to the hull, the so called Munk moment, *Nomoto and Tatano (1979)*. The

Munk moment occurs for all 3-dimesnional bodies except spheres and is always destabilizing, i.e. it tries to turn the body perpendicular to the flow. This moves the CLR forward resulting in it possibly being well in front of the FP, as presented in, e.g., *van der Kolk (2016).*

4. CFD computations

Two CFD software were used in this study. The forebody variation and the effects of the deadwood were analysed using OpenFoam, while the LCB variation was analysed using Shipflow. For each case, the forces and moments at a drift angle of 6 degrees and a ship speed of 15.5 kn were computed.

In the first case a specialized and upgraded version of OpenFOAM® was used, *Renzsch et al. (2017), Meyer et al. (2016).* To be able to use a validated simulation setup and accelerate turnaround times, the simulations were carried out in model scale. For the simulations, body-fitted split cartesian meshes of ~5.0mio cells, incl. boundary layer refinement, were generated using snappyHexMesh. The free surface is captured by a volume of fluid approach with appropriate mesh refinement in the free surface region and bespoke differencing schemes to keep a sharp interface between air and water.

For the LCB variation, Shipflow was used with a potential free surface and a fully viscous double body computation. A mesh of around 4.8 million cells was used. As for the OpenFoam compuations, Shipflow was run in model scale.

Model to full scale transformation has been computed by Reynold's correction for straight line resistance and assuming that side-force and added resistance coefficients are independent of scale.

5. Results from hull form variations

The original hull form of the KVLCC2 is varied in several areas, the forebody and bulbous bow, the forward and aft shoulder by means of a LCB variation (Lackenby shift) and the skeg region by means of the addition of a deadwood. The skeg and forebody variations are identical to those shown in *Renzsch and Thies (2023).*

5.1. Forebody variation

The forebody variation was realised using a deformations box to vary the length, width and height of the bulbous bow and the foremost part of the hull. Fig.3 to 5 give an impression of the effect of the bulb variation.

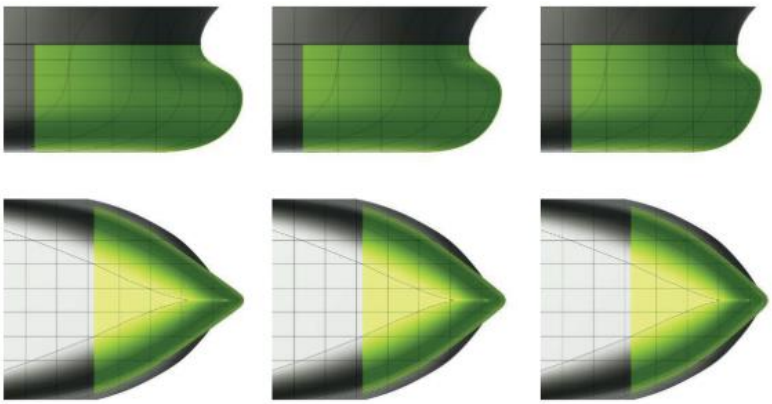


Fig.3: Effect of the length scaling of the stem region (taken from *Renzsch and Thies (2023)*)

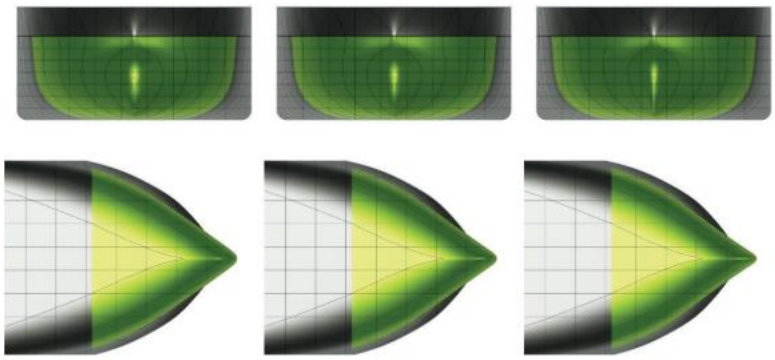


Fig.4: Effect of the width scaling of the stem region (taken from *Renzsch and Thies (2023)*).

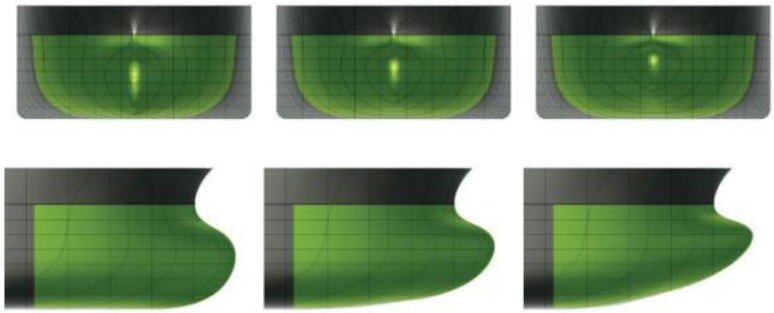


Fig.5: Effect of the height scaling of the stem region (taken from *Renzsch and Thies (2023)*).

Fig.6 presents the differences of the CLR compared to the baseline (shown on percent of the Lpp, negative values denote a CLR position further forward). The CLR of the different variants was found to be up to 1.5% Lpp forward of the CLR of the CLR of the baseline and up to 2% Lpp aft of the CLR of the baseline.

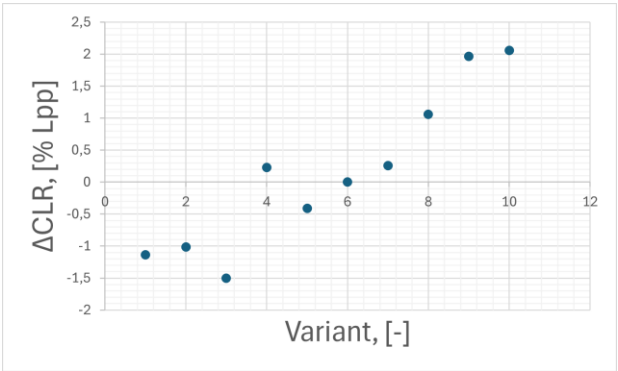


Fig.6: CLR of the created variants during the forebody variation

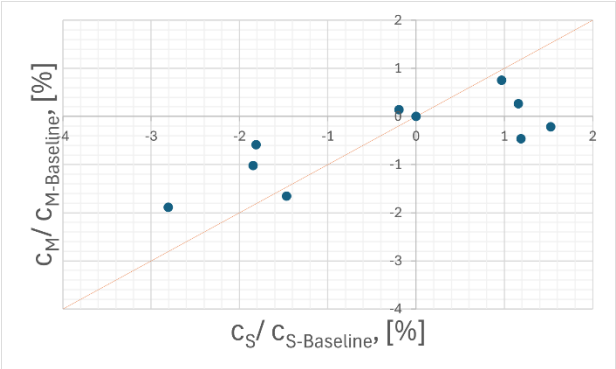


Fig.7: Relation between the changes of the side force and the yaw moment

To understand what causes the differences of the CLR location, the relation between the side force coefficient, c_S, and the yaw moment coefficient, c_M, is presented in Fig.7. It is shown that the yaw moment does not linearly follow the side force. This means that the changes of the CLR positions are dominated by the changes in the side force created of the hull and not changes to the Munk moment. However, it must be noted that the plot shows some scatter, indicating that both, the cross flow drag and the Munk moment are influenced by the hull deformations.

Finally, the changes of the CLR position can be presented over the relative side force, as shown in Fig.8. It is obvious that the CLR moves aft for hull with higher side forces created. As stated earlier, this indicates that the forebody variation mainly influences the side force, i.e. cross flow drag, and not the Munk moment. However, considering the scatter, it must be assumed that the induced Munk moment varies as well, as stated earlier.

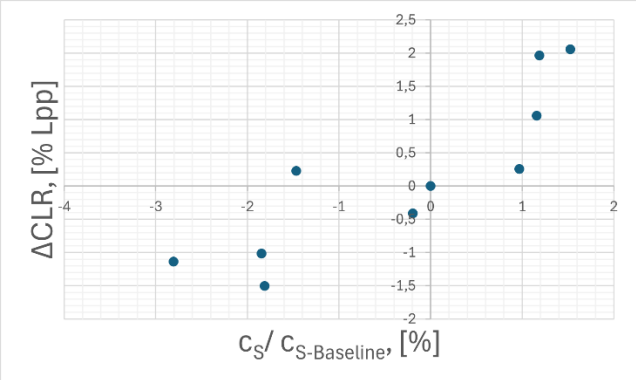


Fig.8: Changes of the CLR over the relative side force coefficient

The differences in the flow pattern and causes of the different side forces created by the hull are further discussed in *Renzsch and Thies (2023)*.

5.2. Application of a deadwood

A deadwood is commonly applied to ships with course keeping problems. Hence it seems like a suitable addition to create more side force on a WASP ship. To investigate the influence of a deadwood on the CLR, a 0.7m long plate was added to the aft end of the skeg, as presented in Fig.9.

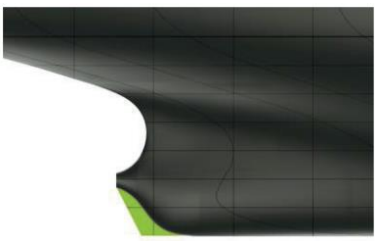


Fig.9: Deadwood in the stern region (shown in green).

Results show a CLR of about 0.8 % Lpp aft of the baseline CLR. As for the forebody variation, the yaw moment is almost constant (0.15 % higher), but the side force is increased (about 0.81 %), causing the CLR to move aft.

5.3. LCB/ shoulder position variation

The variation of the forward and aft shoulders was performed by means of a variation of the longitudinal centre of buoyancy (LCB) using a Lackenby transformation, *Abt and Harries (2007)*. The LCB was shifted by 0.8 %, forward and aft of the baseline LCB. Results are presented in Fig.10 as the differences

of the CLR in percent Lpp over the change in LCB. As shown in Fig.10, the CLR moves aft with the LCB moving forward and the bow becoming fuller.

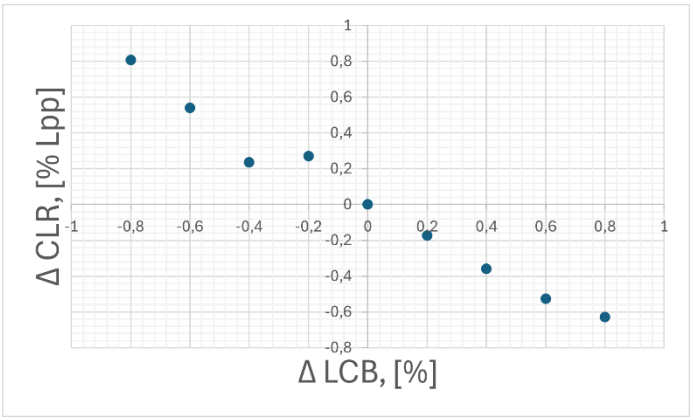


Fig.10: Change of the CLR positions due to variation of the LCB.

To understand the reason for the differences in the CLR positions, Fig.11 presents the relation between the change in moment and side force for the different variants. The figureshows that, as for the bow variations, the dominating factor is a change in the created side force.

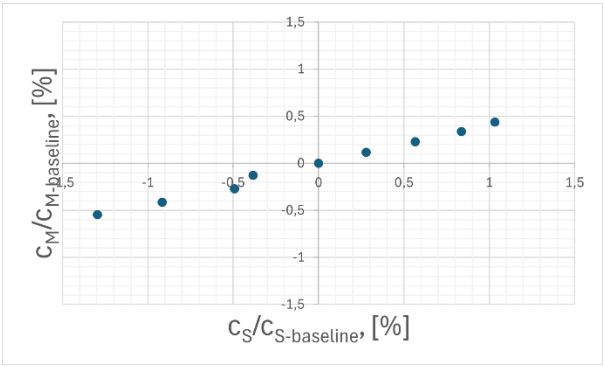


Fig.11: Relation between the changes of the side force and the yaw moment.

However, since modifying the forward and aft shoulder drastically change the pressure distribution along the hull, as shown in Fig.12, it must be assumed that the Munk moment is affected by these modifications.

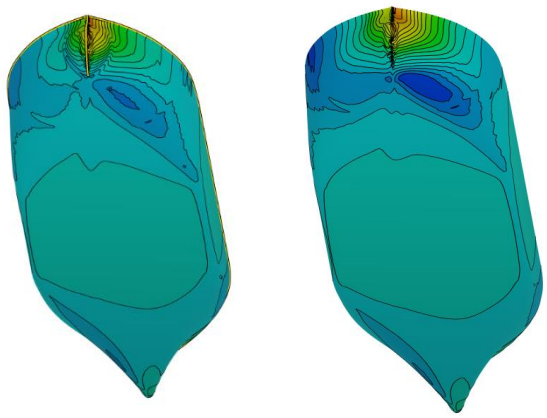


Fig.12: Pressure distribution along the hull. Left: LCB -0.8%, Right: LCB +0.8%.

To quantify the effect of the LCB modifications on the Munk moment, it is assumed that the side force caused by the cross flow drag acts at a point at half the ship's length. From this, the yaw moment

induced by this side force and its location can be deducted from the total yaw moment. The remaining part should give an indication of the Munk moment. The result of this analysis is presented in Fig.13.

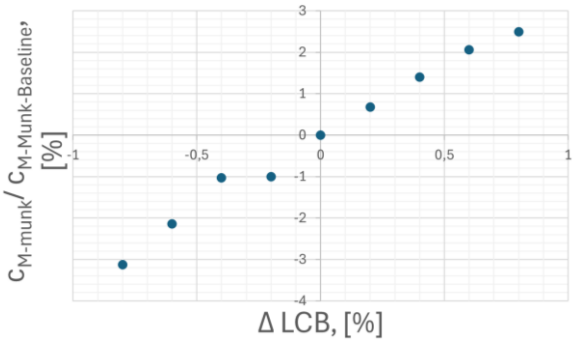


Fig.13: Relative remaining yaw moment coefficient over the LCB change

Fig.13 indicates a trend of a decreasing external yaw moment with decreasing LCB, which could be assumed from the more even and pressure distribution as presented in Fig.12. This result indicates that the Munk moment can be influenced by moving the forward and aft shoulder. However, in the present study the side force was changed due to that modification as well, overlaying the changes to the Munk moment.

6. Conclusions

This study investigated the effect of hull form variations on the sailing stability, i.e., the centre of lateral resistance (CLR) of the hull. Three different types of hull form modifications were applied, a deformation of the bulbous bow, an addition of a deadwood in the stern region and a LCB variation. In all cases the CLR could be shifted considerably. The change of the CLR was often dominated by a change of the side force instead of a change of the yaw moment. It must be concluded that the applied hull form modifications did not considerable affected the Munk moment, but more the cross flow drag of the hull. With an increased cross flow drag but a constant Munk moment, the CLR moves aft.

Further investigations could focus on the effect of the stem geometry to possibly decrease the Munk moment to move the CLR further aft. The bulbous bow variation showed some scatter in the relation between the yaw moment and side force, indicating that the bow deformation influenced the Munk moment. Further, the pressure distribution along the forebody and the difference between the low-pressure fields in the forebody and aftbody should influence the Munk moment. In the present study an attempt was made to separate the moment induced from the cross flow drag and the Munk moment by defining a fixed centre of the cross flow drag force. With this assumption it was shown the Munk moment decreases when the LCB is moved aft. However, since the side force decreased more, the CLR was moved forward. In future studies it should be aimed to research the influence of the forward and aft shoulder on the moment alone, i.e. the generates side force should be kept as constant as possible, e.g. by modifying the bulbous bow. It must be concluded that the results concerning the dependency of the Munk moment on the shoulder position assume of a fixed centre for the cross flow drag, which might not be valid.

From this study and the consideration in Section 3, it must be concluded that hull form design for WASP ships requires special consideration and multi-objective or integrated optimizations approaches using CFD in oblique flow. For the hull design of WASP ships, it could be concluded that a high side force coefficient is preferable to move the CLR aft. A further aft position of the forward shoulder can further help to reduce the Munk moment and move the CLR aft.

Acknowledgements

This research was funded by project “RETROFIT solutions to achieve 55% GHG reduction by 2030” (RETROFIT55) - Horizon Europe programme, Grant Agreement No. 1011096068”.

References

ABT, C.; HARRIES, S. (2007), *Hull Variation and Improvement using the Generalised Lackenby Method of the FRIENDSHIP-Framework,* The Naval Architect

GYPA, I.; JANSSON, M.; GUSTAFSSON, R.; WERNER, S.; BENSOW, R. (2023), *Controllable-pitch propeller design process for a wind-powered car-carrier optimising for total energy consumption,* Ocean Eng. 269

MEYER, J.; RENZSCH, H.; GRAF, K.; SLAWIG, T. (2016), *Advanced CFD Simulations of free-surface flows around modern sailing yachts using a newly developed OpenFOAM solver*, 22nd Chesapeake Sailing Yacht Symp., Annapolis

NOMOTO, K.; TATANO, H. (1979), *Balance of Helm of Sailing Yachts*, 4th Int. HISWA Symp. Yacht Design and Construction, Amsterdam

RENZSCH, H.; MEYER, J.; GRAF, K.. (2017), *Investigation of modern sailing yachts using a new free-surface RANS-code*, 4th Int. Conf. Innovation in High Performance Sailing Yachts, Lorient

RENZSCH, H.; THIES, F. (2023), *Hydrodynamic Optimization of Ships with Retrofitted WASP-Systems*, 6th Int. Conf. Innovation in High Performance Sailing Yachts, Lorient

TILLIG, F.; RINGSBERG, J.W. (2020), *Design, operation and analysis of wind-assisted cargo ships*, Ocean Eng. 211

VAN, S.H.; KIM, W.J.; YIM, D.H.; KIM, G.T.; LEE, C.J.; EOM, J.Y. (1998), *Flow Measurement Around a 300K VLCC Model*, SNAK Annual Spring Meeting, Ulsan

VAN DER KOLK, N.J., (2016), *Hydrodynamics of Wind-Assisted Ship Propulsion: Modelling of Hydrodynamic Sideforce*, HISWA Technical Conf.

WASP (2023). *Report: Work Package 3 - Engineering of Wind Propulsion Technologies,* Technical report, Intereg WASP project, https://vb.northsearegion.eu/public/files/repository/20230720150403_WP3deliverablestechnicalreport.pdf

A New Paradigm in CSOV Ship Design – A Performance Study

Karthik Sankaramoorthy, Damen Shipyards, Gorinchem/Netherlands,
Karthik.sankaramoorthy@damen.com
Manuel Cerro Diaz de Teran, MARIN, Wageningen/Netherlands, m.cerro@marin.nl

Abstract

CSOVs (Construction/Service Operation Vessels) are multi-role vessels which are key to servicing offshore wind farms, operating at wind farm locations for extended periods of time. With increasing demand for offshore wind farms and their cost-effectiveness, the performance requirements (comfort, operability, fuel efficiency) for these vessels are ever more demanding, which traditionally designed vessels can no longer fully satisfy. Hence, a radically new design was devised with a double-acting hull fitted with 4 identical azimuth thrusters (Damen DPX-DRIVE™). This paper studies the impact of such a design choice on the vessel performance, demonstrating that the design enables easier manoeuvring, more efficient DP performance, improved onboard comfort and maintenance, while reducing system complexity and operational costs, all at a small expense of lower propulsion efficiency in free-sailing.

1. Introduction

With most countries adopting global targets for energy transition and decarbonization, the demand for increasing share of renewable energy in the total energy mix is growing. Wind energy, particularly offshore wind energy forms a crucial part of this mix, and therefore the planning and mobilization of new offshore wind farms is rapidly accelerating. More and more offshore windfarms, both bottom-fixed and floating are either already in operation or are planned to be in operation in the coming years and decades around the world.

For the construction and servicing of the windfarms, different types of vessels are required for different stages and purposes, the most notable ones being – Wind-turbine installation vessels (WTIV), construction/service operations vessels (CSOVs) and crew transfer vessels (CTVs). Of the three, this paper focuses on the CSOV type vessels.

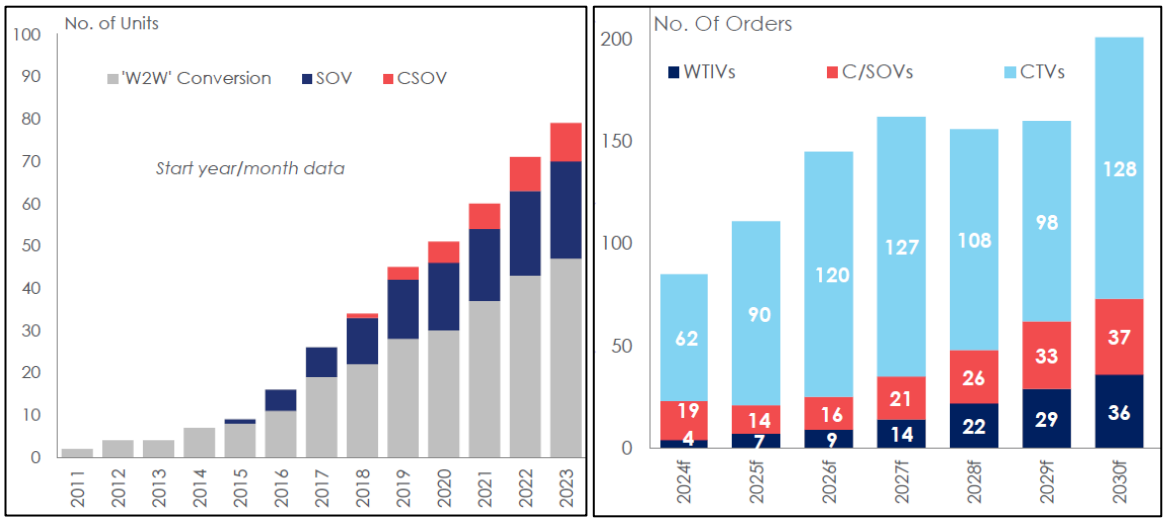


Fig.1: (Left) W2W fleet size up to 2023. (Right) Order forecast of Wind farm support vessels up to 2030. Source: Clarkson's Research, March 2024

In the past decade, the construction and servicing of the offshore windfarms were undertaken by retrofit 'Walk-To-Work (W2W)' vessels which were PSVs, or other offshore support vessels retrofitted with among other things, personnel access systems. However, with the limitations of such retrofits and increasing number of windfarms, there is now a growing demand for more dedicated Construction

and/or Service Operation Vessels (C/SOVs) as they need to not only cater to the large number of wind turbines in more severe conditions, but also perform the operations as quickly and efficiently as possible, while keeping specialized personnel safe and comfortable during extended stays offshore. This growth demand is illustrated in Fig.1.

Such a specialized operation requires a vessel concept that offers high manoeuvrability, operability and comfort while staying at sea for weeks at a time. Given the demands and challenges of such operations, a conventional vessel design solution isn't sufficient anymore. Hence, a new solution with four identical azimuth thrusters at the forward and aft of the vessel is chosen to accommodate these new demands.

This paper outlines the benefits of such a novel CSOV ship design, over a conventional offshore support vessel design. First, the motivations for this paradigm change are studied, followed by a description of the new design. Then the performance of this new vessel design is compared with other similar vessels both qualitatively and quantitatively from several aspects.

2. C/SOV Vessel Design Philosophy

2.1. Description of the operational profile

The function and operational profile of C/SOVs are quite different from traditional offshore support vessels. CSOVs are primarily intended to perform a significant number of personnel and cargo transfer operations on each working day. These operations are to be performed as effortlessly as possible, so that specialized technicians can spend their working days as efficiently as possible. Depending on the type of operation, either construction or servicing, a typical day involves covering several Wind Turbine Generators (WTGs). At each wind farm site, the vessel transits at sailing speeds towards a WTG, after which DP (Dynamic Positioning) systems takeover to manoeuvre slowly but efficiently to reach the desired approach orientation and connect with the WTG landing platform via the vessel's motion compensated access system. Personnel and cargo are then transferred via the access and crane system, after which the vessel manoeuvres away and the process is repeated at other WTGs throughout the day. Table I summarizes a typical operational profile of the SOV-type vessel.

Table I: Typical Annual Operational Profile of SOV vessels

Operation	% of Time
Port time, bunkering, crew change	2%
Transit at economical speed	16%
Operation under DP2	50%
Standby under DP1	32%

Overall, the vessels spend around 80% of their operational time annually in low-speed manoeuvring and in DP operations. Transit between WTGs within a wind farm is typically done at moderate speeds (up to 8 knots), since higher transit speeds are unsafe. Hence, it's important to have a vessel design which is optimized for this combination of operations.

2.2. Overview of the Traditional design and its Pitfalls

Keeping these operational criteria in mind, designing a CSOV using a traditional approach would result in a vessel focused on maximum sailing speed and maximum DP capability. This would perfectly satisfy all required criteria but would be less efficient and less practical in real-life operations. Some of these limitations are summarized as follows:

- A hull shape optimized purely to reduce drag while sailing ahead has significant resistance while sailing astern even at slower speeds.
- With traditional offshore vessel thruster layouts, the aft thrusters are primarily installed for free-sailing and hence are typically under-utilized during manoeuvring and DP, while the

transverse/retractable thrusters in the bow are usually the limiting units. This limits the manoeuvring and DP capability of the vessel.

- Tunnel thrusters are often used in the bow and are relatively inefficient when compared with azimuth thrusters in terms of power consumption and response times.
- Tunnel thrusters generate more air-borne and structure-borne noise which increases noise and vibration levels onboard, impacting overall comfort. This can require significant additional investment in countermeasures and equipment to minimize the induced noise and vibrations, and sometimes still not sufficient to provide the necessary comfort class notation.
- While retractable azimuth thrusters in the bow are more effective in low-speed manoeuvring and DP operations, they increase integration complexity, cost, and maintenance.

These technical and practical considerations warranted a fundamental change to SOV design and topology.

2.3. Characteristics of New CSOV Design

After several design iterations, a new concept was devised with essentially a different hull and thruster layout.

2.3.1. Thruster Layout

The most fundamental element of an offshore support vessel is the thruster layout, as this usually drives several other elements of vessel design. For the CSOV, the efficiency of personnel transfer operations can be significantly improved if the vessel's low-speed manoeuvring capability can be increased. This requires a versatile thruster layout along with quicker response times, while ensuring adequate redundancy for safety-critical transfer operations undertaken during DP.

For this purpose, Damen devised the DPX-DRIVE™ which features 4 identical non-retractable azimuth thrusters, symmetrically placed at each corner of the vessel, as outlined in Fig.2.



Fig.2: Damen DPX™ Drive with 4 identical thrusters installed on the CSOV9020. ©Damen Shipyards Group

This has the following benefit in manoeuvring and DP:

- Azimuth thrusters ensure quick response times in both propeller speed and steering speed enabling quicker omnidirectional movement & thrust vectoring.
- 4 identical thrusters ensure that at least 2 thrusters are online during a Worst-Case Single Failure (WCSF) at either end of the hull providing a safe and reliable platform for transfer operations.

- The symmetric thruster layout with quick-response azimuth thrusters ensures a smaller DP footprint (accuracy of position-keeping) for the vessel thereby increasing its operability.

2.3.2. Hull Form

A significant benefit can be achieved if the vessel can manoeuvre equally well while sailing both ahead and astern. This can allow the vessel to approach WTGs in the most efficient orientation, with minimum number of manoeuvres. Hence, in combination with the 4-thrusters layout, this led to the design of a double-acting hull which retains high efficiency while sailing ahead at service speeds while providing significant resistance reduction while sailing astern at low speeds up to 8 kn.

The hull consists of a pointed and sloped transom as opposed to a full and flat one, to minimize hydrodynamic pressure and encourage smoother flow while sailing astern. This is achieved without compromising on the valuable deck area. In the bow, the keel is raised to fit the thrusters, which can present a potential slamming issue, similar to the stern. However, at both ends, deep V-sections are made to reduce the amount of flat bottom area exposed to waves and hence minimize slamming impacts. The result is a double-ended ferry-like hull concept which has seemingly symmetric forward and aft ends.



Fig.3: Hull shape of the new CSOV Design showing the forward and aft ends of the vessel. ©Damen Shipyards Group

The resulting hull form design provides the following benefits to the CSOV platform:

- Minimized hydrodynamic drag while sailing astern at slow speeds while maintaining efficiency while sailing ahead.
- A symmetric submerged fore-aft hull shape when exposed to quartering waves exhibits a more symmetric wave and current moment behaviour which is easier to offset by the thrusters. This

in combination with the symmetric thruster layout, enables easier manoeuvring in the wind parks, and enables the DP system to be optimized for efficiency apart from positional accuracy.

2.3.3. Additional Design Considerations

The identical and symmetric main thruster layout affects other design considerations which are summarized as:

- Identical thrusters mean that all auxiliary equipment such as electric motors, drive systems, are also identical simplifying onboard electrical and control system architecture. This helps for easier troubleshooting, maintenance, spare parts availability etc.
- A simpler electrical and mechanical system layout enables a relatively easier system integration and commissioning of the various onboard systems, and an easier tuning of the DP system.

3. Performance Assessment of The New SOV Design

Throughout the design process, the new concept was developed through rigorous performance assessments, both semi-empirical and numerical, and eventually tested at model scale at the Maritime Research Institute of the Netherlands (MARIN). This chapter outlines the most relevant performance aspects of the new concept and offers both a quantitative and qualitative comparison with traditional vessels.

3.1. Dynamic Positioning

As discussed earlier, the DP capability for a CSOV vessel is very important in determining the operability window of the vessel. In combination with Seakeeping aspects of the vessel, DP capability enables safe transfer of personnel. This capability of the new CSOV vessel has been presented and compared with a traditional design.

3.1.1. Static DP Capability

Firstly, a comparison of static DP capability is performed which is a static balance of the environmental forces with the thruster forces. A simple thrust allocation algorithm is used to calculate the balancing thrust required for each heading, along with the power consumed.

To evaluate the performance of the ship at DP condition, a comparison with the Damen CSOV8720 has been performed. This comparison is performed for the actual propulsion system of the new vessel (4-thruster configuration) but also for the same hull form with a “traditional” propulsion layout taken from a previous generation SOV. This consists of 2 main aft thrusters, 2 retractable bow thrusters and one tunnel bow thruster. The hull is assumed to be the same for the purpose of this study. Hence the same wind coefficients and hydrodynamics coefficients (for waves and current) are used, along with identical wind and current areas. Table VI summarizes the propulsion arrangement used for the comparison.

Table II: Propulsion layouts for static DP Comparison

	Nominal Power	**Propeller Diameter**	**Nominal Thrust**
CSOV - 4 thruster layout			
4 x Main Azimuth Thrusters (2 x Forward + 2 x Aft)	1780 kW	2.5 m	309 kN
CSOV - Conventional Layout			
2 x Main Azimuth Thrusters (Aft)	2150 kW	2.8 m	351 kN
2 x Retractable Forward Thrusters	600 kW	1.6 m	99 kN
1 x Tunnel Forward Thrusters	600 kW	1.65 m	95 m

The comparison is made using MARIN's software TRUST which has been developed within the Thrust Hydrodynamics JIP. The program is based on components from the Extensible Modelling Framework (XMF) library, *Abbing (2015)*, which contains calculation models that are also used in many other MARIN software applications. In TRUST, the mean wind, wave, and current loads are calculated, after which the thrust required to counteract the environmental forces is determined. The performance is assessed for two environmental conditions (EC) as shown in Table VII.

Table III: Environmental condition for static DP assessment

EC	**Waves**		**Wind speed**	**Current speed**
	Hs [m]	Tp [s]	Vw [m/s]	Vc [m/s]
Medium	1.3	6.5	7.9	0.75
Heavy	3.1	8.5	13.8	0.75

Fig.4 shows the required total power to keep the vessel in position for the above environmental conditions. It is remarkable that the 4-thruster configuration needs an average of ~35% less total power compared with the traditional layout configuration (over all the headings).

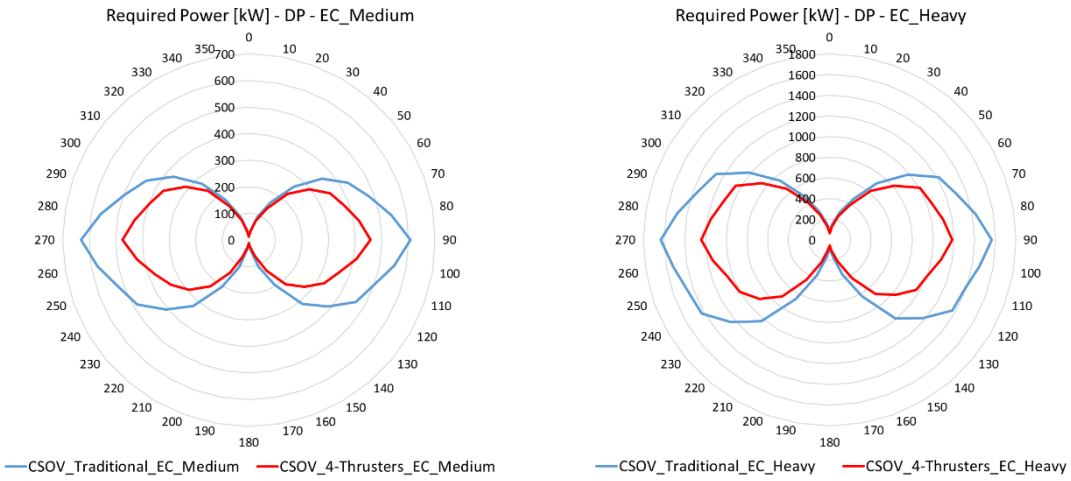


Fig.4: Required total power at DP – Medium and heavy Environmental Conditions

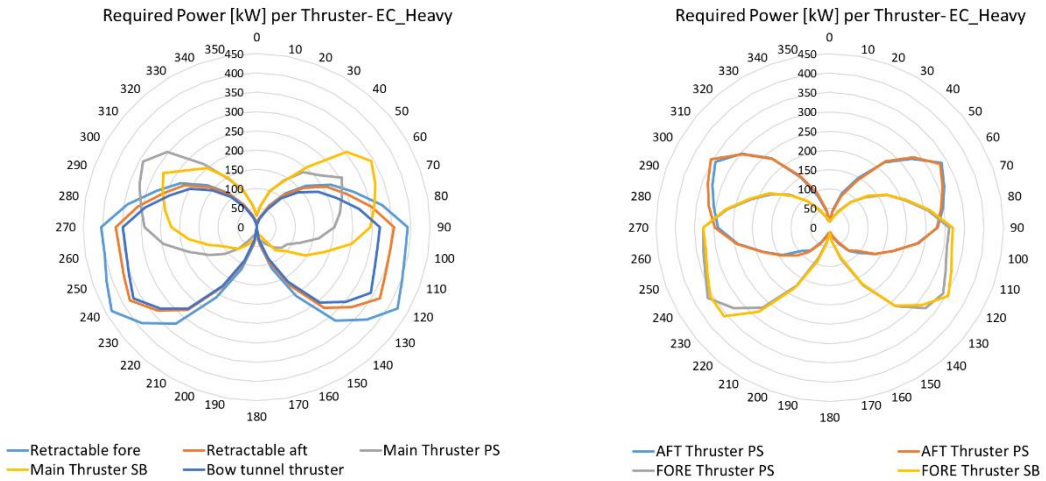


Fig.5:1 Required power at DP (Heavy EC) per thruster. (Left) Traditional layout. (Right) 4-Thruster layout

It should be highlighted that the total effective thrust (per heading) required is the same in both layouts, which is expected since the hulls and environmental conditions are the same. The difference in power therefore arises from the efficiency of the respective thrusters:

- Tunnel thrusters show a relatively high thrust degradation in current or in forward speed; in Fig.13 the required power of both propulsion configurations is compared. The 4-thruster configuration has a symmetrical power distribution between the fore/aft thrusters and SB/PS. Whereas in the case of the traditional layout, it can be seen that the forward retractable thrusters and the tunnel bow thruster require higher power to provide the same thrust.
- In general, smaller propeller diameters are less efficient (Less thrust to power ratio) than larger ones. Tunnel thrusters also incur additional friction losses due to flow through the tunnel.
- Tunnel thrusters are also directionally limited compared to azimuth thrusters whose thrust vectors can be varied omnidirectionally. This limitation is compensated by the main or retractable azimuth thrusters leading to higher usage of the thrusters overall.
- The propellers of the 4-thruster layout have been designed for DP (with maximum thrust available at 0 knots ship speed), and hence have a lower P/D. This is an advantage during DP but less efficient during free sailing. Traditional offshore vessels have main propellers designed for Free-sailing (Maximum thrust available at design speed) and hence are less efficient at 0 knots or in DP condition.

Considering the above, it can be observed that the new CSOV design with the 4-thruster layout can keep position more efficiently with less power and fuel consumption.

3.1.2. Dynamic DP Capability

In contrast to static DP capability where forces are balanced statically, the dynamic DP capability takes the dynamics of all the sub-systems into account, including the vessel hydrodynamic response, thruster dynamics and DP control reactions. This provides a much more realistic behaviour of the vessel under DP conditions.

For this comparison, a time-domain dynamic positioning study performed by Damen for a similar vessel is used (70m version). The study compares the vessel footprint while in DP and the power consumption between a conventional thruster layout (CL) and the 4-thruster layout with double-ended hull (DE). It should be noted that the CL layout in this study utilizes 2 tunnel and 1 retractable, which is different from the conventional layout used in static DP comparison where 2 retractable and 1 tunnel thruster is used. The calculations were performed with MARIN's aNySIM Simulator platform, *Serraris (2010)*, which is used for analysis of multibody dynamics in offshore operations. The two layouts for the comparison are shown in Fig.6.

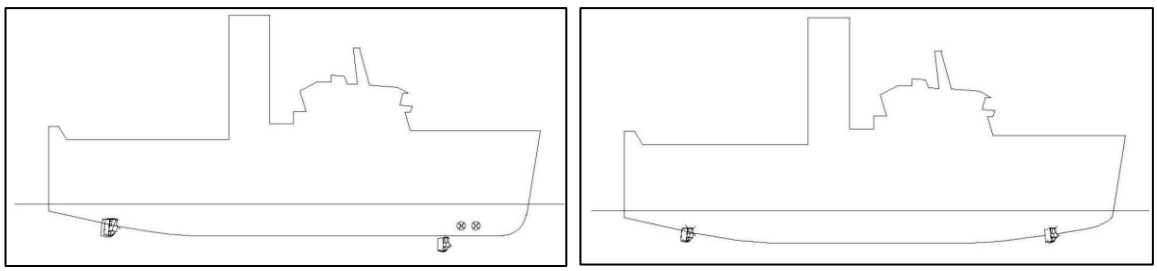


Fig.6: Comparison of the 2 layouts. (Left) conventional thruster layout (CL). (Right) 4 thruster layout (DE)

The DP control system in the model consists of a Proportional–integral–derivative (PID) controller which uses the error between the required vessel position and the measured vessel position (surge, sway, and yaw) to derive the required force/moments. An allocation algorithm calculates the thrust (magnitude and direction) to be assigned to the different thrusters. The thrust allocated to each propulsion device is such that the sum of thrust magnitudes and the sum of moments applied to the ship equals those required by the PID controller to counteract the environmental loads. The resulting allocation minimizes the required power by the propulsion devices and considers thrust magnitude and direction limitations.

As the input for the PID controller is based on the vessel motions (due to environmental influences), and the same hull form/loading condition is used for both configurations, the same control gain settings are considered applicable for both configurations. It should be noted that this study was not focused on optimizing the control system for DP performance, but rather on comparing the DP performance of the two configurations.

Using aNySIM, several fast-time simulations are performed subjecting the vessel to environmental conditions, Table VII, consisting of waves, wind, and current approaching from different headings for a time span of 3 hours. From the resulting time trace, a mean offset or the deviation from its target or reference position is plotted for each heading. Additionally, an indication is given on the average power consumption of the vessel during the simulation.

Table IV: Summary of environmental conditions for Dynamic DP Capability assessment

Condition	Waves [Hs]	Wind [Vw]	Current [Vc]
Medium	2.0 m	12.0 m/s	0.50 m/s
Heavy	2.5 m	14.0 m/s	0.75 m/s

Figs.7 and 8 present the response and behaviour of the combined vessel and DP system to the above environmental conditions.

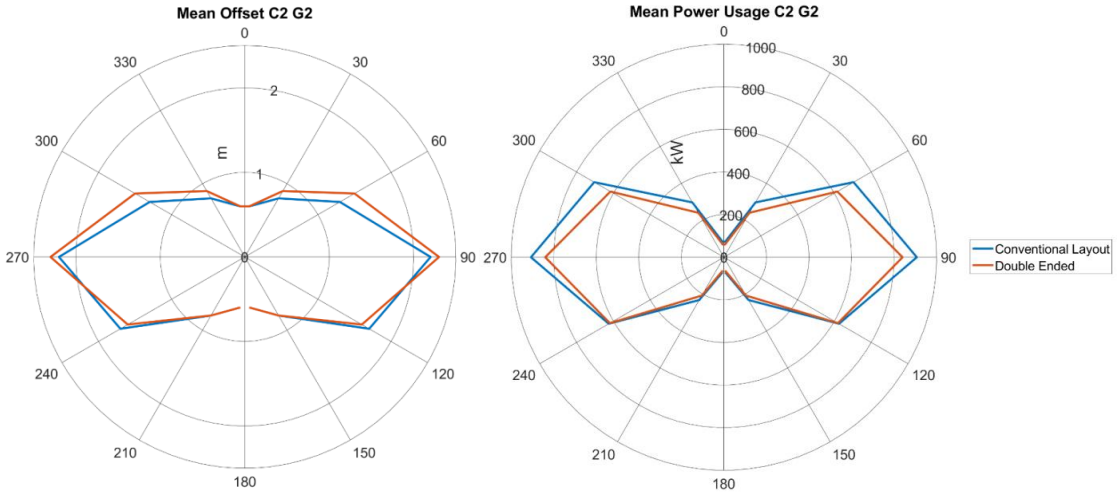


Fig.7: Medium condition - Polar plot comparison of conventional thruster layout and 4 thruster layout: (Left) Mean offset from target position in meters. (Right) Mean power usage in kW

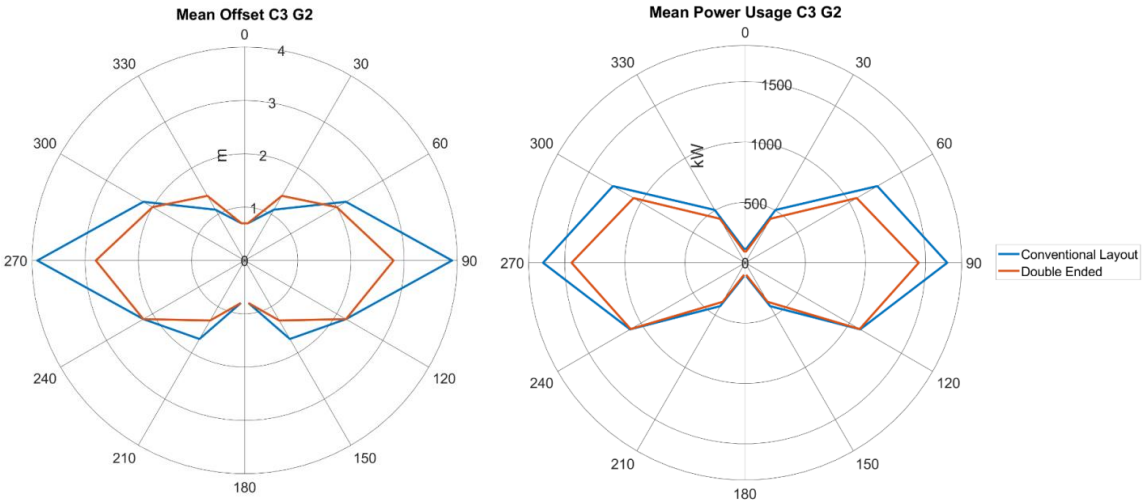


Fig.8: Heavy condition - Polar plot comparison of conventional thruster layout and 4-thruster layout. (Left) Mean offset from target position in meters. (Right) Mean power usage in kW

Comparing the mean offsets, the mean offsets in the medium conditions of both configurations are very similar. In the heavy condition, the mean offset is also similar except in beam seas where CE has higher offsets as limits of the bow tunnel thrusters are reached often. The dynamic offsets and footprint were found to be similar (not presented here).

Comparing the average power consumption, the 4-thruster layout overall is found to consume up to 19% less power in both environmental conditions, with highest reductions found in bow quartering and beam seas. This is also where the efficiency of the forward azimuth thrusters of the DE configuration is found to be better than that of the tunnel thrusters of the CL configuration.

In summary, the two configurations provide similar performances up to medium environmental conditions. However, as the conditions get more severe, the conventional layout starts to reach some of its thruster limits whereas the 4-thruster layout is able to handle it better. The average power consumption is clearly found to be lower in the 4-thruster layout in both environmental conditions.

Overall, the 4-thruster layout is found to provide significantly lower power & fuel consumption and marginally better Dynamic DP performance (DP accuracy).

3.2. Calm Water Resistance & Powering

To assess the design's free-sailing efficiency, it's important to understand the resistance and propulsion characteristics to a high degree of accuracy. Hence a systematic CFD campaign was performed both for the hull and its appendages followed by an extensive towing tank test campaign.

3.2.1. CFD Hull Optimizations

The new hull shape and all its appendages were analysed numerically using Damen's in-house CFD capabilities before model testing at MARIN. The focus during CFD was to minimize drag while sailing ahead up to 14 kn and while sailing astern up to 8 knots.

To aid in sailing efficiently both ahead and astern, several improvements were made. The volume distribution across the length of the vessel was made as symmetric as possible, while slightly favouring sailing ahead at design speed. This makes a better compromise in the wave-making resistance in both sailing directions. The transom was sloped as much as possible to avoid creating a stagnation point while sailing astern.

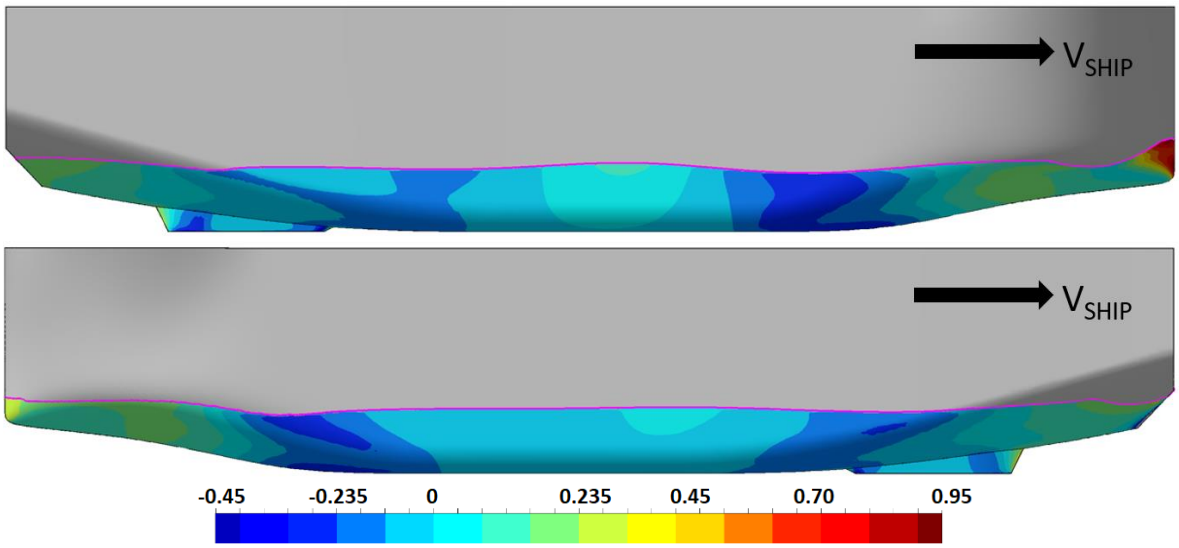


Fig.9: Hydrodynamic Pressure (Coefficient of pressure) while sailing at 12.5 kn. (Top) Ahead, (Bottom) Astern

In the Fig.9, the hydrodynamic pressure coefficient (Cp) obtained from CFD is compared at the same speed of 12.5 kn to enable a fair comparison. As intended, the stagnation pressure at the transom is reduced while sailing astern, owing to the sloped and pointed transom design. This creates a smoother wave pattern along the hull compared to the sailing ahead condition.

The resistance coefficients while sailing ahead and astern are compared along with the pressure and frictional components in the Fig.10. As expected, the astern condition has slightly higher resistance mainly from the pressure component, as the transom has a larger entrance angle compared to the bow. But overall, the difference in total resistance is ~6% at 8 kn which is deemed reasonable considering the compromised shape.

Fig.10 compares the resistance coefficients as determined from the CFD calculations, both sailing ahead and astern. The C_T also includes a correlation allowance (CA), as explained in 3.2.3. CFD Studies were also conducted to optimize the shapes of appendages such as thruster headbox, sensor housings, alignment of bilge keels etc. to keep drag to a minimum.

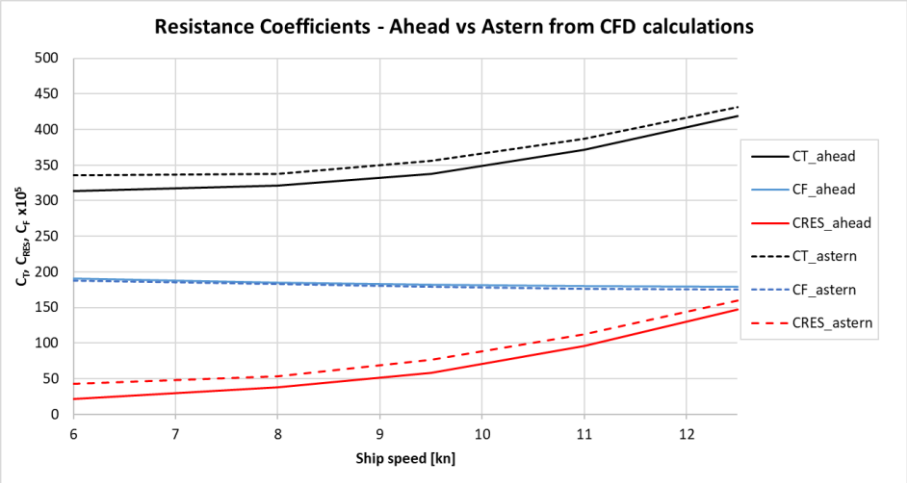


Fig.10 - Comparison of CFD resistance coefficients while sailing ahead and astern

3.2.2. Resistance & Powering Model Tests

After the CFD hull-form optimization, MARIN built a suitable ship model including all appendages and performed resistance tests in the Deep-Water Towing tank (DT). The goal was to determine the ship's resistance and validate the results of the CFD calculations. The resistance test, in combination with the self-propulsion tests, allows to determine the ship's propulsion coefficients, such as thrust deduction, wake fraction and propulsive efficiency. This information is particularly interesting in this project to make a suitable comparison with other designs.



Fig.11 – Self-propulsion model tests as performed at MARIN's towing tank (14kn)

Prior to the self-propulsion model test, MARIN performed an optimization test to determine the optimal power distribution between the forward and aft thrusters.

This test was performed at both 8 and 12.5 kn. The results are presented in Fig.12. Since the design speed of the vessel is 12.5 kn, a power distribution of 20/80 (fore/aft) was selected and used further in the self-propulsion tests. This prioritizes the design speed, while offering a good balance at the transit speed of 8 kn.

As can be seen in Fig.12, the optimal value depends on the speed. The optimal power distribution at 8kn speed would be ~15/85 (fore/aft). In practice the ship operator should take this into account during the operation of the ship to optimize the fuel consumption.

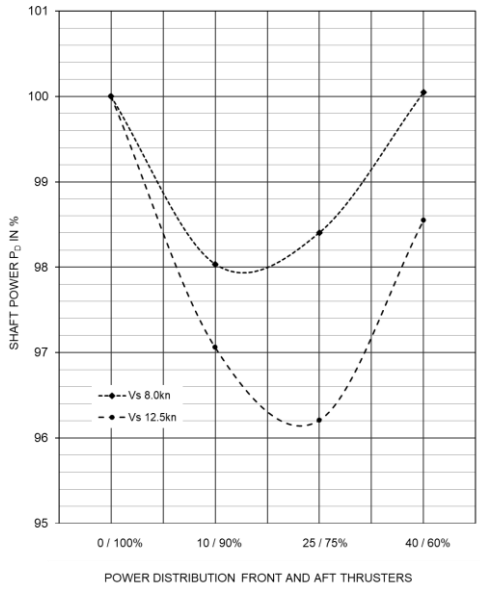


Fig.12: Results of power distribution optimization test taken from Model Tests

Fig.13 shows the net force of the forward thruster units (Fx) measured at the connection point of the thruster unit with the hull. The optimal power distribution is achieved when this Fx force is zero or when the forward thrusters are generating enough thrust to overcome their own resistance when sailing at a certain speed.

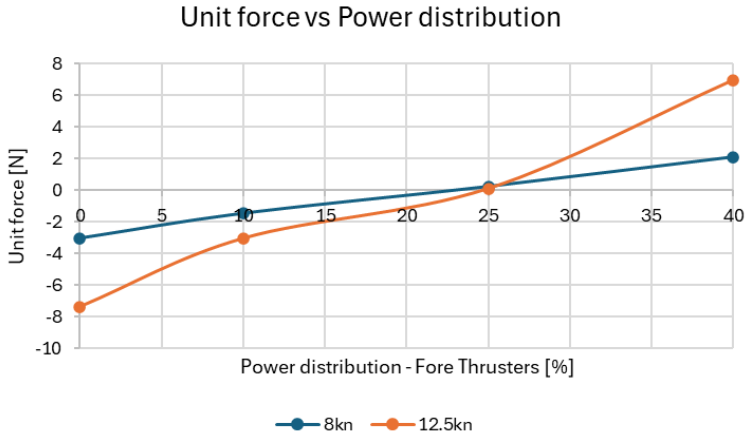


Fig.13: Unit force (Fx) measured during the model tests – The results suggest that when the Forward thrusters provide ~22% of the total power their resistance is zero.

From the Fig.13, we observe that ~20% of this power is used to overcome the resistance of the forward thrusters, and this reduces the propulsive efficiency (η_D) of the vessel.

The propulsive efficiency for a ship is defined as follows:

$$\eta_D = \frac{P_E}{P_D} = \eta_H \times \eta_0 \times \eta_R \; ; where \; \eta_H = \frac{1-t}{1-w}$$

Considering that without the presence of the forward thrusters, only 80% of the power would be required to propel the vessel at the same speed, the η_D would then have been 0.501 which is very comparable to similar vessels as will be shown later in 3.2.4.

3.2.3. Resistance Comparison - CFD and Model Tests

As mentioned, one of the objectives of the model tests was to allow the verification of the CFD resistance calculations performed by DAMEN.

Table V: Comparison of Resistance coefficients between CFD and model tests

Speed	Fn	CT_CFD	CA	CT + Ca	Comparison between CFD & Model tests
6 kn	0.11	2.49E-03	6.5E-04	3.14E-03	-6%
8 kn	0.14	2.57E-03	6.5E-04	3.22E-03	-4%
9.5 kn	0.17	2.73E-03	6.5E-04	3.38E-03	-2%
11 kn	0.19	3.07E-03	6.5E-04	3.72E-03	1%
12.5 kn	0.22	3.54E-03	6.5E-04	4.19E-03	3%

Table II shows this comparison, the difference varies between –6% to +3%. In this comparison, it was essential to add a correlation allowance (CA) to the CFD results. It was decided to use the same CA as determined for the model tests. The CA_{Basic} is determined using the Grigson friction line with the following formula, given by the MARIN 3D method:

$$CA_{Basic} = 0.0058(L+100)^{-0.16} - 0.00196$$

The CA_{Basic} would be equal to 0.000552. However, based on statistical data of MARIN it was decided to increase it to 0.00065. If a CA is not added to the CFD results, the difference would be quite large, from 34% at 6 kn to 15% at 12.5 kn.

3.2.4. Performance comparison with Similar Ships

To get a better understanding of the resistance & propulsion performance, the new Damen CSOV is compared with similar offshore support vessels with traditional thruster arrangement (2 main thrusters in the aft and one or two bow thruster(s) in the fore ship). The comparison is performed using the admiralty coefficient.

$$AC_{Res} = \frac{0.7477 \times V_S^3 \times \nabla^{2/3}}{P_E}$$

The comparison is presented in two stages. First to judge the quality of the hull (AC_{RES}) without the thrusters, and second to evaluate the propulsive performance (AC_{PROP} – which considers the delivered power instead of the effective power) and therefore the impact of the thruster's selection.

$$AC_{Prop} = \frac{0.7477 \times V_S^3 \times \nabla^{2/3}}{P_D}$$

Three additional vessels have been selected for this comparison. A PSV-type and ROV-type vessels are added here as they are traditional offshore support vessels which are usually also retrofitted for

W2W operations, and an additional ship from MARIN database (state-of-the-art SOV vessel) has been also included as reference.

Table VI: Main particulars of ships used in the comparative study

Particulars	Symbol	MARIN DB	CSOV8720	PSV	ROV	Unit
LCB position (from midship)	LCB	+1.60	-1.20	+2.20	+0.85	%
Block coefficient	C_B	0.736	0.629	0.681	0.628	-
idship (ordinate 10) coeff.	C_M	0.993	0.982	0.987	0.947	-
Prismatic coefficient	C_P	0.738	0.641	0.69	0.663	-
Length-Breadth ratio	L_{PP}/B	3.983	4.452	4.648	4.222	-
Breadth-Draught ratio	B/T	3.60	4.062	3.60	3.273	-

All the ships except the Damen CSOV8720 present a classical propulsion approach for SOV's with 2 main thrusters and two bow thrusters, Table IV.

Table VII: Propulsion Arrangement of Reference Ships used in comparative study

	Bow thrusters	**Main thrusters**	**Nozzle Type**
MARIN ref DB	2	2	HR
CSOV8720	0	2+2	19A
PSV75	2	2	19A
ROV83	2	2	19B

The data of the reference ships has been corrected for (small) differences in main dimensions, form coefficients etc., by means of the methodology of DESP (valid for displacement ships up to Fn = 0.8). This way the differences between test results only depend on the quality of the hull form and not anymore on the main dimensions and fullness. The hull form with the highest level of AC_{Res} is the best.

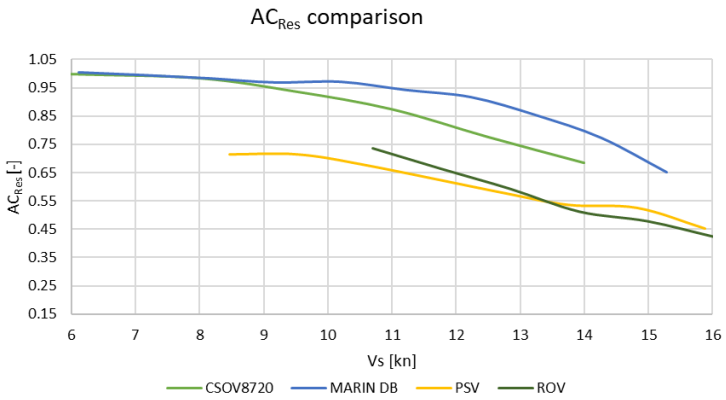


Fig.14: Comparison of Hull Quality with similar ships (higher value indicates better hull quality) - The actual values have been normalized by the AC_{RES} of the MARIN DB reference ship

In Fig.14, the two SOV-type hulls are seen to perform the best compared to the other two in terms of hull quality (hull resistance). It is worth pointing out that PSV and ROV vessels are generally designed to carry cargo and have different design constraints than the CSOVs which are designed to carry personnel mainly. So, it is not unexpected that they are less efficient than the SOVs. Comparing within the SOV type hulls, the performance between both the MARIN DB ship and the CSOV8720 is very similar up to 9 kn, after which the MARIN DB shows ~10% higher performance. This is reasonable since a compromised hull form was selected for the CSOV to improve astern sailing and to fit the forward thrusters. It also shows that the hull design of the CSOV is more efficient compared to hulls with "traditional" propulsion arrangement, such as the PSV-type and ROV-type.

In conclusion, although the new CSOV hull form was designed as a compromise to achieve better manoeuvring and DP performance, the resistance is found to be the same, if not better compared to benchmark hull forms which are of more traditional design.

The same comparison can be performed to show the effect of the propulsion arrangement, using AC_{PROP}, which uses delivered power P_D instead of the effective power.

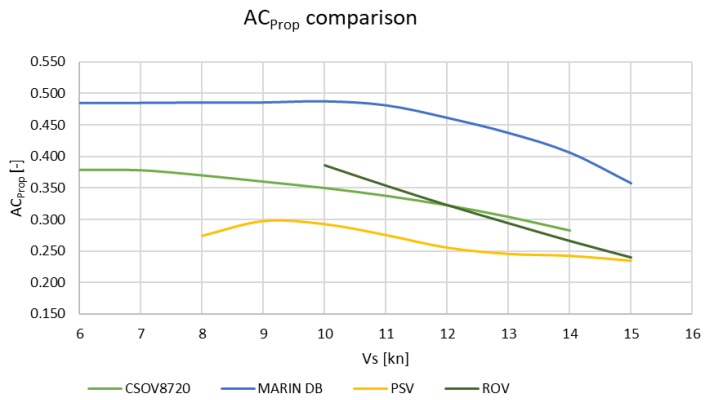


Fig.15: Comparison of hull and propulsion efficiency with similar ships (higher value indicates better hull quality and propulsion performance) - The actual values have been normalized by the AC_{PROP} of the MARIN DB reference ship

From Fig.15, the AC_{PROP} of the CSOV8720 is 20% lower than that of the MARIN reference ship. This is due to the different thruster configurations. This reduction in efficiency points out to the additional drag due to the presence of the 2 forward azimuth thrusters as discussed in 3.2.2.

Ultimately, it is also interesting to compare the relation between AC_{RES} and AC_{PROP}, or in other words, the relation between P_E and P_D, and this is represented by the propulsive efficiency (η_D).

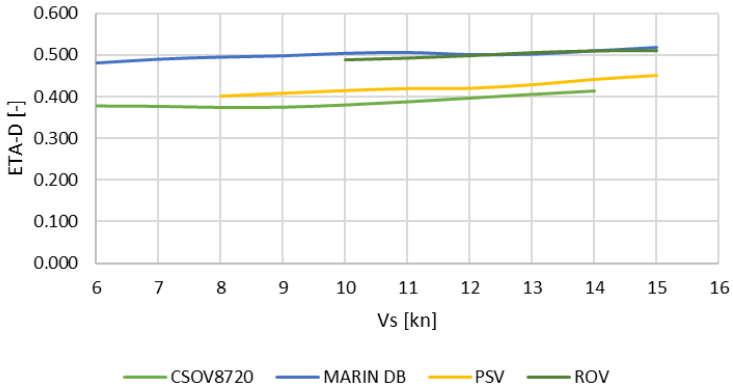


Fig.16: Comparison of Propulsive Efficiency (η_D) of the different ships

Overall, the following conclusions can be made regarding the resistance and powering performance of the vessel with regards to similar vessels:

- Considering resistance performance compared in the form of AC_{RES}, the new CSOV is one of the best ships for W2W operations.
- However, the powering performance compared in the form of AC_{PROP} clearly shows the penalty that the new CSOV8720 must pay due to the 4 thrusters' configuration, especially when compared to the MARIN DB or the ROV-type.
- The propulsive performance η_D is found to be the lowest, again due to the penalty of the forward thrusters. However, knowing that these thrusters represent a penalty of about 20%, a hypothetical ship with a hull form similar to the CSOV would achieve η_D values very similar to the MARIN DB vessel or other traditional vessel.

3.3. Seakeeping

As mentioned in 3.1, operability and comfort are paramount for the CSOV vessels. A big driving force for operability is how the ship responds to 1st order waves (dominant wave periods) and if they can stay within the limits of the compensation system. The lower the response, the higher the operability, and safer for transfer of personnel. Similarly, lower ship responses lead to lower slamming, lower accelerations onboard and better and comfortable experience overall for crew and personnel.

With a new hull and thruster concept, it was important to assess the seakeeping performance of the vessel through model tests. This was done at MARIN's Seakeeping and Manoeuvring Basin (SMB). The same model was used as for resistance & powering tests. It was self-propelled for tests at speed and in soft springs for the tests at zero speed. The model was equipped with four identical azimuth thrusters, a network of sensors and a standalone signal acquisition system. It was only connected to the carriage via power and data cables, arranged to avoid affecting its free-body motion. The vessel's U-type anti-roll tank (ART) was also optimized and installed within the ship's model to include its effects on seakeeping. The respective models are shown in Fig.17.



Fig.17 - Seakeeping model as tested at MARIN, along with the U-type ART

The tests were focused on the seakeeping behaviour of the vessel at zero speed, which is the most critical condition for transfer operations at sea. Three different sea states were tested in several vessel headings as outlined in Table V. Additionally, roll resonance tests were performed to assess the roll damping behaviour of the vessel and the ART.

Table VIII: Sea states tested for seakeeping behaviour

Sea state	Wave period (Tp)	Significant wave height (Hs)	Wave Headings
A	8.4 s	2.1 m	0°, 45°, 90°, 135°, 180°
B	9.0 s	2.5 m	0°, 45°, 90°, 135°, 180°
C	8.5 s	3.1 m	0°, 45°, 90°, 135°, 180°

The following observations and conclusions are made from the seakeeping tests at zero speed.

- The ART was found to provide a roll-reduction of ~40% at the roll resonance period for waves heights of 4m. The ART thus significantly helps reduce the roll motions and hence the comfort and operability of the vessel even in the severest of conditions.
- The vessel exhibits a marked fore-aft symmetric behaviour in roll, pitch, and heave motions because of the hull shape that was designed to improve astern performance.
- Roll and Pitch root mean square (RMS) values stayed below 1.5° for all sea states and headings. The max roll RMS was calculated at 1.1° for beam-seas.
- The most critical limit of the gangway limit to stay under is the telescoping compensation speed limit. For most gangway equipment, the technical limit is ~2.5 m/s but 2.0 m/s is used for this study. From the tests, the vessel movement at the gangway tip was found to not exceed this value up to sea state B, and exceed less than 1% of the time for sea state C.
- The measured accelerations at the bridge, mess and forward most cabins remained within acceptable comfort levels, according to the personnel criteria limits from NATO STANAG 4154.

- Green water events were not observed for any test condition.
- Slamming was observed in the bow, particularly in head sea and bow-quartering seas in sea state B and C. This is a result of the raised bow shape compared to traditional vessels and is one of the disadvantages of the design. However, additional strength and fatigue assessments were performed to ensure slamming pressures do not damage the structure or disrupt gangway operations.

3.4. Comfort

Since CSOV vessels carry specialized crew and technicians who are mostly land-based and have limited acclimatization with sailing in moderate seas, comfort is very important, as reduction in the effectiveness of the personnel lowers the operability of the complete vessel operation.

Traditional offshore support vessels, particularly outfitted for DP operations, invariably consist of one or more bow and stern tunnel thrusters (including retractable thrusters). In these types of vessels, manoeuvring and DP operations involve significant use of tunnel thrusters which generate tremendous amount of both air-borne and structure-borne noise, *Fischer (2000)*. The main sources of both noise sources are the cavitation at the propeller blades which then is permeated into the ship structure via the propeller blades as well as the tunnel, and the machinery itself.

While air-borne noise is relatively easily attenuated before it reaches the accommodation space, structure-borne noise is notoriously more difficult to attenuate. Hence the bow thruster noise can be often heard for several decks, especially in the forward area even with additional acoustical countermeasures. In offshore support vessels, most accommodation spaces are located between the midship and the bow of the ship as the aft space is used for machinery, workshops, storage, etc. Hence comfort in these vessels during DP and manoeuvring operations is relatively lower. Air injection system in newer vessels helps reduce the amount of air bubbles being generated during the thruster operation but the noise can still be disruptive in several cabin spaces. For a vessel which stays in DP conditions for 80% of the time, comfort is therefore very important.

In the new CSOV design with DPX Drive™, the tunnel and retractable thrusters are replaced with 2 L-drive azimuth thrusters. Hence the only reduction gearing is in the thruster hub, outside the hull which reduces the vibrations from the gearing into the rest of the hull. Unlike with tunnel thrusters, noise from cavitation is significantly minimized as the air bubbles don't interact and implode on the tunnel walls within the ship construction. Although cavitation does occur with azimuth thrusters, their implosion is not effectively carried through to the ship structure because the cavitation source is further away, generating less noise. Overall, some structure borne noise from the azimuth thruster operation is transferred to the hull, however the levels are significantly reduced.

Based on sea-trial measurements during DP operation in a similar Damen vessel with 2 tunnel and retractable thrusters in the bow, and 2 main azimuth thrusters in the aft, all running at 40% of nominal power, differences in sound levels can be seen in the adjacent spaces directly above these thrusters. The location of the measurement spaces is indicated in Fig.18.

The difference in sound pressure levels between the bow thruster room and the aft propulsion room was measured to be ~10 dB(A). Even with a main thruster with twice the nominal power as of the tunnel thruster, and consequently a bigger electric motor compared, the sound levels in the main propulsion room are found to be lower.

With lower structure-borne noise generated at the source, lower noise and vibration levels are expected in the forward accommodation area. This can also be observed onboard of the vessel in these 2 different locations. Hence replacing tunnel thrusters at the bow with azimuth thrusters helps in improving the overall comfort of the new CSOV vessel.

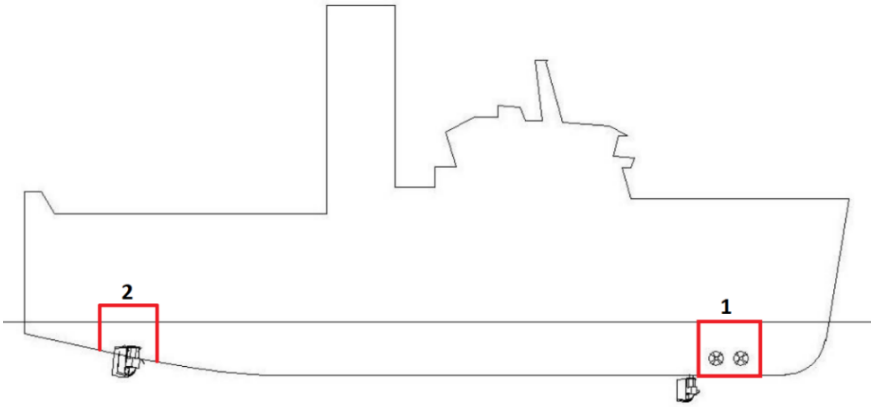


Fig.18: Locations of sound measurements while in DP operations. 1 – Bow thruster room, 2 – Main thruster room

3.5. Costs

Costs are also a big consideration for SOV operators and the competition in the offshore wind market drives operators to lower costs further. For the purposes of the comparison between the new CSOV and traditional SOVs, the costs are split into:

- CAPEX – Capital expenditure. The cost it takes to engineer, build, and deliver the vessel.
- OPEX – Operational expenditure. The cost it takes to operate the vessel.

3.5.1. CAPEX

In comparing the CAPEX between the new and old CSOV designs, the analysis showed that the costs were equal or slightly lower. This analysis is based on indicative prices of ship components and not actual quotes from suppliers. Hence the actual price differences may vary. However, based on this indicative pricing analysis, it was seen that the CAPEX difference wouldn't be significant.

3.5.2. OPEX

When comparing OPEX, the difference between the traditional and new design mainly comes down to the fuel consumption during operation, which in-turn relates to the total power consumption. As the CSOV vessels are primarily operating in DP conditions (~80% annually), a comparison of the power consumption during DP operation is considered most significant for the overall OPEX of the vessel.

As was seen from section 3.1, Damen's 4 thruster DPX drive solution consumes less average power up to 19% and even up to 22% in lighter environmental conditions. This directly translates to a lower fuel consumption assuming diesel-electric arrangement or similar.

3.6. Maintenance

During operations, normal wear and tear and occasional breakdown of components is expected. And breakdown or malfunction of critical components such as generators, propulsion motors, propulsion frequency drives, electrical switchboards etc. can lead to failures, and any operation is terminated till the problem component or issues are fixed. Breakdown of non-critical components may not cause termination of operation but would still need to be replaced.

For failures of both critical and non-critical components, the parts either must be fixed or replaced while underway or at port. And if spares aren't readily available, this can keep the vessel out of operation which can be expensive.

For traditional offshore support vessels, the thruster topology includes at least 2 or 3 different types of thrusters (Stern propulsion thruster, bow tunnel thruster, retractable bow thruster, etc.). Consequently, different types of thrusters require different auxiliary machinery such as electric motors, frequency drives, distribution cables, etc.

Finally, to avoid significant impact on operations in case of failures, spares for the different types of components must be procured and kept available onboard or at a dedicated facility designated by the owner, increasing complexity of spare parts management and with an impact on the CAPEX and OPEX of the ship that depends on inventory and logistical procedures of the Shipowner.

For the new CSOV with DPX Drive, all 4 thrusters are identical, which means identical auxiliary machinery too. This enables having just 1 or 2 sets of spares per vessel (or per fleet) for the expensive critical components. This simplifies procuring and maintaining the spares for the critical components which can only be fixed at port. The same is true for components which can be maintained onboard. Overall, onboard maintenance and spare parts inventory is expected to be easier and less expensive for the operators.

4. Conclusions

A new CSOV vessel design was found to be necessary due to the increased demand from the offshore wind industry in terms of operability, comfort, and efficiency. To suit the required operational profile of such vessels which was mostly low-speed manoeuvring and DP, Damen devised the DPX Drive™ with four identical non-retractable azimuth thrusters along with a double-acting hull. This new design is then compared with traditional designs with conventional propulsion layouts from several performance aspects.

From a DP perspective, the new CSOV is found to be notably better than its traditional counterparts. Both static and Dynamic Capability assessments show that the new CSOV requires significantly less power consumption (and hence less fuel consumption) to keep position in the same environmental conditions. The dynamic study also showed a slightly lower station-keeping footprint for the new CSOV.

The new CSOV is found to have similar if not better calm-water resistance performance while sailing ahead compared to traditionally designed offshore vessels. With a modified hull form, resistance while sailing astern was only slightly higher compared to sailing ahead. However, when including the propulsion aspects, the vessel is found to be less efficient primarily due to the presence of the two additional non-retractable forward thrusters. Overall, this is considered acceptable as free-sailing is a very small part of the operational profile.

Replacing tunnel thrusters with azimuth thrusters also reduces onboard noise and improves comfort as was shown by measurements. In terms of the costs, the CAPEX is found to be similar, while OPEX is expected to be lower due to lowering in fuel consumptions during DP operations. While maintenance and spare parts inventory is expected to be easier due to identical auxiliary systems and a simpler electrical system layout. Finally, the simpler layout also enables easier commissioning, tuning, and troubleshooting of the systems both during the build-phase and operations.

Overall, this new design paradigm provides a more efficient, comfortable, reliable, and all-round improved CSOV vessel platform which ticks all the boxes of the increased demands set by an ever-growing offshore wind industry.

Acknowledgements

The authors would like to thank several people for their contributions to this paper. From MARIN, Manuel Aguiar Ferreira (former seakeeping project manager of the CSOV) and Rene Kaufmann for assisting in the seakeeping part. For powering and static DP respectively, Peter Labee and Baderiya

were highly instrumental. And lastly, Klaas Kooiker who originally ideated to publish a paper about this project and was also involved in the model testing phase of the new CSOV. From Damen, Mark Couwenberg, Scott Terry, Piero Favero and Jorinus Kalis provided valuable input and feedback on the quality and content of this paper. Mark was also instrumental in the design of this new successful CSOVs for Damen and as such provided the background context and motivations for the new design. And Frank van Dongen for his contribution to the Dynamic DP assessment performed in cooperation with MARIN.

References

ABBING, A. (2015), *XMF leads to development of a Multi-Purpose simulation platform*, MARIN report 116, Wageningen

FISCHER, R. (2000), *Bow Thruster Induced Noise and Vibration*, Dynamic Positioning Conf.

SERRARIS, J.J. (2010), *Time Domain Analysis for DP Simulations*, ASME 28th Int. Conf. on Ocean, Offshore and Arctic Engineering, Hawaii

Smart Sails for Decarbonizing Heavy Shipping

Ville Paakkari, Norsepower, Helsinki/Finland, ville.paakkari@norsepower.com

Abstract

This paper explores the topic of decarbonizing shipping by the means of wind propulsion. Wind propulsion can support regulatory compliance (CII, EEDI/EEXI), while similarly producing operational cost savings. Special attention is given for the need of smart systems and how they can be utilized to enable more substantial use of wind energy. It is argued that increasing share of sails in the "propulsion energy mix" mandates novel digital solutions.

1. Introduction

Wind propulsion is gaining momentum as a means to provide zero-carbon propulsion energy for ship propulsion. The past years have shown rapid growth in both the installation base and the order backlog for wind-assisted ships. To put things into perspective, according to DNV's Energy Transition Outlook 2023 (DNV, 2023), wind propulsion is the fourth largest alternative energy source for shipping by the number of ships in operation. Wind propulsion is followed by technologies like methanol and hydrogen that have arguably been discussed in the industry more. In DNV's report, the technologies ahead of wind propulsion in the uptake are LNG, Batteries, and LPG. It can be expected that many of the LNG and LPG powered ships are using fossil fuel instead of the renewable alternatives in their operation.

When comparing sails to the other zero- or very-low-carbon-intensity energy sources (here low-carbon refers to carbon intensity on well-to-wake basis), the rational for using direct wind is easy to understand. To de-carbonize the whole production chain of fuels, significant amounts of renewable electricity are needed. Generally, this is done by using either wind or solar energy. Considering the losses in the "energy production chain" (conversion to electricity, transmission, conversion to liquid of gaseous fuel, losses in combustion engine and finally the losses in the propulsion), it is clear that only one fraction of the kinetic energy in the wind or the photons of the sunlight is converted to useful propulsion. In the case of sails, this chain is significantly shorter and hence the overall process is more energy efficient.

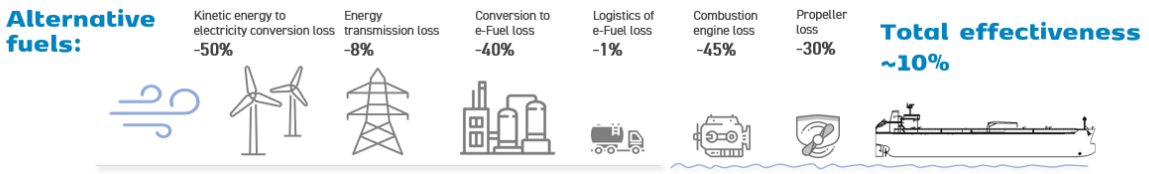


Fig.1: Schematic of energy conversions to produce synthetic fuels

The consequence of the higher total energy efficiency is that one can expect the overall cost per kWh of useful energy produced to be lower for sails than other very-low-carbon-intensity energy sources. According to a shipowner engaged in commercial operations with rotor sails, this is indeed the case in the current market, *Seatrans (2022)*.

2. Sails and environmental regulation

Sails are recognized in most of the major regulatory frameworks addressing environmental impacts of shipping. In this chapter, the most relevant current and potential future regulatory schemes are briefly discussed from the perspective of wind propulsion. The purpose is not to provide exhaustive technical information about these regulations but to compare how sails affect the performance of ships under these regulations, highlight their respective differences, and shed light on some of the caveats in the current regulations. The scope is limited to IMO and EU regulations. IMO due to its global reach, and EU due to the stringency of the regulations within the Union.

2.1. EEDI and EEXI

The technical energy efficiency of ships is considered in the EEDI and EEXI regulations. The indices (EEDI for newbuild and EEXI for existing ships) are calculated once in the ship's lifetime if no major modifications are performed. The sails are considered in the regulation via explicit terms in the calculation formula.

This means that, similar to the index in general, the impact of the sails does not change from year to year. Even if, from a technical perspective, sails are a means to produce low or zero carbon energy onboard, in the EEDI and EEXI regulation the sails are considered as an "energy efficiency device".

The guidelines allow multiple possibilities to calculate the impact of sails on the index. The selections are CFD, full-scale trial, or wind tunnel testing. The regulation also allows the use of validated lower fidelity methods. These methods enable fast and relatively low-cost assessments of the impact of the sails on the index prior to the ship installation. With this, the commercial risk can be reduced particularly for the yards, as they can assess the impact of the sails in advance. The first generation of such validated lower fidelity models is already available in the market.

What is notable about EEDI and EEXI with respect to sails is that neither the operational area nor the prevailing wind conditions impact the performance in the index calculation. This naturally makes the impact assessment simpler, but the index value does not necessarily provide a very good estimate of the actual performance.

2.2. CII

The other short-term energy efficiency measure issued by IMO is the CII. The influence of sails in the index value materializes through the lower fuel consumption with same operational profile. That being said, the CII is accounting for the actual performance of the sails even if the contribution of wind propulsion is not explicitly calculated. In contrast to EEDI and EEXI, the influence of sails on the CII is more challenging to predict, mainly due to the uncertainties related to the operational profile of the ships. For ships with constant operational areas and profiles, the wind conditions can be estimated from meteorological data so that the long-term average gains of wind propulsion can be predicted.

2.3. EU ETS

In 2024 shipping was included in the EU emissions trading system (ETS). Under this regulation, ships need to purchase emissions rights for the emissions trading market. Very much like the CII, as the sails reduce the fuel consumption, they will also reduce the required emissions rights.

2.4. FuelEU Maritime

In 2025 there will be a new regulation within the EU mandating the carbon intensity of the fuel used in shipping. While the regulation is fuel-centric, there are two notable exceptions. The first one is the use of shore power, which can lower the carbon intensity of the energy mix. The other is the use of wind propulsion. The ships which have deployed sails, can use a "reward factor" in their calculations of the carbon intensity. The factor will depend on the installed capacity of the sails and the overall installed engine capacity. The capacity calculation follows the guidelines for the EEDI / EEXI.

To provide an example, if the contribution of sails in the EEDI calculation is more than 15%, the ship gets 5% reward factor in the fuel calculations. The required carbon intensity reduction is 2% between 2025 and 2030. The legislation includes a pooling mechanism, so the 5% reward is sufficient to provide compliance for 2.5 similar ships. To put the numbers in a perspective, for a typical MR tanker, the highest reward factor can be reached with two 30m x 5m Norsepower Rotor Sails™.

Table I: Reward factor for wind propulsion under the FuelEU Maritime, *EC (2023)*

Reward factor for wind-assisted propulsion - WIND (f_{wind})	$\frac{P_{Wind}}{P_{Prop}}$
0,99	0,05
0,97	0,1
0,95	$\geqslant$ 0,15

There are various challenges with the FuelEU Maritime legislation when considering wind propulsion. More specifically, the regulation risks not rewarding the ships with significant actual contribution of wind propulsion while rewarding ships with lower utilization rate of the sails. These challenges of FuelEU Maritime stem, to a great extent, from the use of EEDI guidelines to account the effort of wind propulsion.

The other parts of the regulation are based on actual fuel consumption and fuel type used but the effort of wind propulsion is insensitive to the actual operational performance of the sail.

2.5. IMO Midterm measures

The short-term measures of IMO (EEDI/EEXI and CII) have proven to be relatively lenient or at least they are not driving substantial investments in carbon intensity reductions. Generally, in the industry the mid-term measures are expected to drive a more significant change. While the discussions on these regulations are still ongoing, IMO has issued a GHG reduction strategy in 2023, which indicates that the mid-term measures will consist of "technical element" and "economic element". It is expected that these are reminiscent of the similar regulations from the EU. This means that the economic element would essentially put a price on the carbon dioxide emissions (cf. EU ETS) and the technical element will regulate the GHG intensity of the fuel used onboard (cf. FuelEU Maritime).

2.6. Business case implication

The impact of the regulations discussed in previous chapters should not be underestimated. In this chapter the discussion is limited to the EU regulations as they are already defined. However, it is expected that the IMO regulations will have similar implications even if there might be some differences in the levels of financial implications, depending on the exact formulation and level of stringency.

As explained in the previous chapter, the impact of sails on the EU ETS are quite straightforward. When the sails reduce the fuel consumption, they reduce the emissions, and therefore the need to purchase emissions rights. The emissions price for one ton of carbon dioxide has been 60-100 EUR in recent years. Given that each ton of fuel converts to approximately three tons of CO_2 this means that the EU ETS will effectively increase the fuel cost in EU area by 200-300 EUR. This is roughly 30-50% increase to the current bunker prices for HFO and will result in similar increase in the cost savings from sails.

A less obvious but more significant impact to the business case comes from the technical measures, or in this case the FuelEU Maritime. As a source of zero-carbon renewable energy, wind propulsion contributes to the energy mix of the ship without increasing the respective carbon intensity. In the regulation this is considered via a reward factor. The business case impact of FuelEU Maritime can be assessed with a method very similar to the one introduced earlier to account for the business case of lowering CII with alternative fuels, *Paakkari and Hörkkö (2024).*

Below a business case provides the calculation for a fleet of 5 MR tankers out of which one is equipped with 2 units of 35m x 5m Norsepower Rotor Sails™. The assumed annual consumption of each of the

"conventional" ships is expected to be 6700 tons of fuel, while the one with sails is expected to save 10%. As an alternative fuel e-methanol is assumed.

The scenario "no sails" presents the case where none of the ships have sails. The scenario "Under FuelEU Maritime" illustrates the fuel cost for the fleet with one ship equipped with sails, in a situation where the fleet is FuelEU Maritime compliant. The last scenario shows the situation where only the HFO saving is considered. This last scenario is not FuelEU Maritime compliant.

Table II: Business case calculation to comply with FuelEU Maritime using e-methanol or wind propulsion

	No sails	**Under FuelEU Maritime**	**Reference (not considering FuelEU)**
Energy needed	377 GWh	377 GWh	377 GWh
HFO consumed	33034 tons	32546 tons	32 830 tons
E-methanol consumed	948 tons	578 tons	0 tons
Fuel cost*	$24.45M	$23.59M	$22.98M
Cost saving		**$860k**	**$469k**

*Fuel prices: HFO: 700 USD/ton; E-Methanol: 1400 USD/ton

3. Need for smart sails

The new regulations will further strengthen the economics of sail installation projects. Wind propulsion technologies are maturing and the industry's (ship designers, yards, classification societies) knowledge about the technology is also increasing rapidly. This enables more ambitious projects with more substantial contribution of wind propulsion. In the taxonomy laid out by *Schenzle (1985)* the industry is moving from "wind-assisted motorships" towards "hybrid ships" and even "motor-assist windships".

Table III: Hybrid wind ship taxonomy by *Schenzle (1985)*

Wind ship class	Proportion of the Wind Energy
Motor Ship	0 %
Wind-Assisted Motorship	0-25 %
Hybrid Ship	25-75 %
Motor Assisted Windship	75-95 %
Pure Wind Ship	>95 %

Taking an example from the projects completed by Norsepower, the first Norsepower Rotor Sail™ was fitted on the ro-ro ship MV Estraden in 2014, where the overall contribution of sails was about 6%, *Norsepower (2023).* Six years later, in 2021, another ro-ro ship, SC Connector was equipped with sails that produce more than 20% of the ship's propulsive energy, according to the owner, *Seatrans (2022).* The next milestone installation on this path will be the three ro-ro vessels designated to carry airplane components. These ships are expected to have 50% lower CO_2 emissions compared to current operations with conventional ships, *Norsepower (2024).*

While the examples provided above are anecdotal, they illustrate a trend that can be observed in the industry more widely. The increasing confidence in the technology and knowledge of it will likely increase the average "project scope" so that wind propulsion is further utilized. It remains to be seen what level of wind propulsion contribution will be typical or the most common one. This will depend significantly, among other things, on the regulation and what kind of economic impact GHG emissions have. Given these projections, it is worthwhile to consider the technical implications of increasing the share of wind energy in the total propulsive energy mix. The taxonomy introduced by *Schenzle (1985)* suggests an important insight about wind propelled ships - the move from motorships to windships is a continuum. Depending on where the ship in question falls on this continuum, more traits of the "archetype" it has.

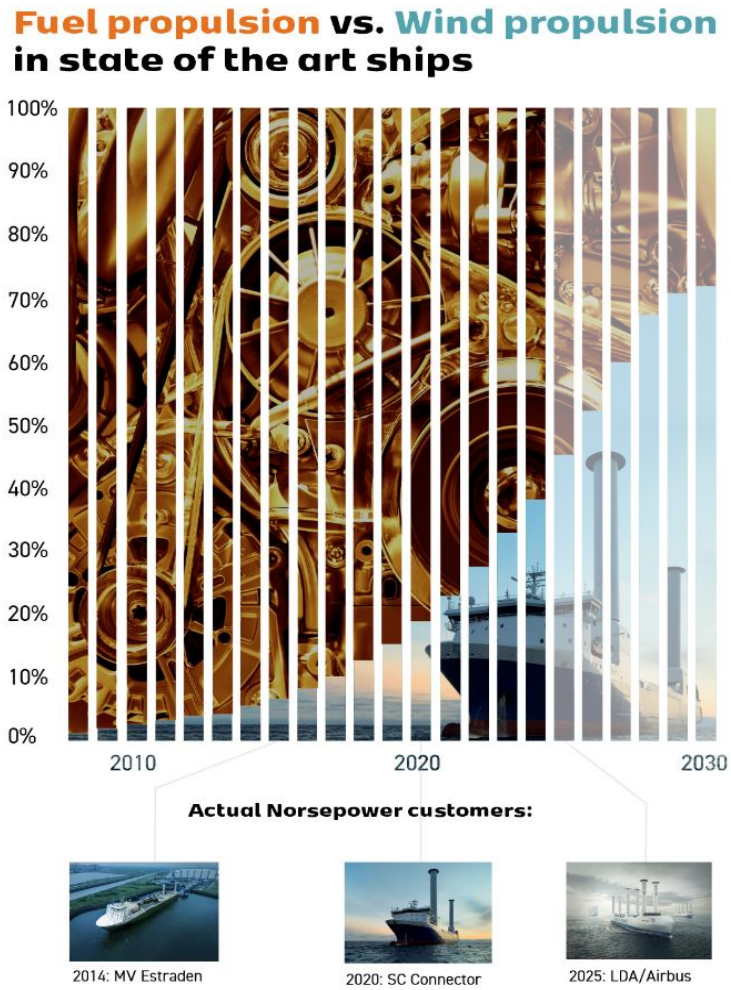


Fig.2: Trend in share of wind propulsion for "state of the art" rotor sail propelled cargo ships

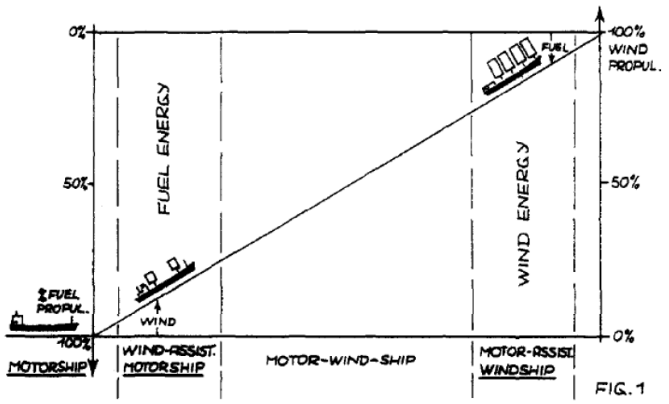


Fig.3: “Original” wind-ship spectrum, *Schenzle (1985)*

If for example a ship has on average 5% wind propulsion contribution, then it is much closer to a conventional motor ship than a wind ship, and hence its design is not too different to that of a conventional ship. In contrast, the larger the wind element, more the design deviates from conventional and more traits of the sailing ship are needed.

It is very important to remark that, in addition to different ships being located at different stages on the motorship-windship spectrum, also any ship equipped with sails and motor will experience times when the sails contribute more to propulsion, and times when they contribute less. This is natural due to the intermittent nature of wind, but it sets certain requirements for the design. Hence, when considering the

continuum, each ship has a spectrum of its own. This spectrum has a mean (average sail power), a maximum (this is the value companies write press releases about) and a minimum (the added resistance in headwind). In addition to the above, the spectrum has also a range of the most typical conditions, say a range on which 80% of the operation falls within.

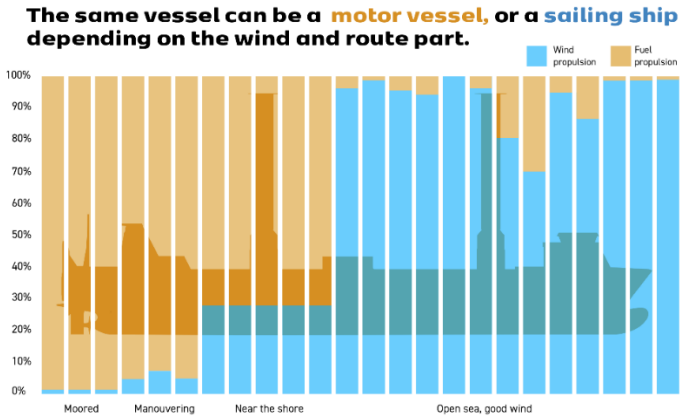


Fig.3: Operation of a hybrid ship using wind (schematic)

In a Joint Industry Project called WISP, led by Marin, it was shown that for installations where the wind contribution is modest, even fairly simple calculations can provide good estimates of the performance. As the average performance increases, one needs to include more physical phenomena. For example, if the sail effect is small, the impact hydrodynamics of the ship can be largely omitted in the performance prediction. However, for more substantial sail performance, things like ships drift, changes in rudder angles, etc. start to become more important, *Eggers (2023).*

The above-mentioned results from the WISP project were made in the context of performance predictions. However, the practical experience of Norsepower highlighted similar points. To get the full benefit from wind propulsion, particularly in cases where there is significant sail power, it is important to consider the ship holistically. Particularly this calls for smart sail systems that can incorporate accurate measurements of the sails, their effects on the ship and its performance, and use these as an input for the optimization and control.

Such advanced control systems are being developed and deployed with promising results, *Mizutani et al. (2024), Norsepower (2024).* Furthermore, it should be mentioned that when the relevance of wind propulsion is increased, the effect of smart operations and weather routing is increased too. The weather routing of modern cargo ships equipped with sails has been extensively investigated, and the performance improvement potential is very high. It is not uncommon to have the added benefit of 30-100%, *Mason et al. (2023), Dupuy et al. (2023).*

4. Smart sails = smart regulation?

As was seen in chapter 2, regulations can have a significant economic impact. One of the key hurdles in the current regulation is the lack of standardized methods to evaluate the actual, realized performance of the sail systems on a continuous basis. Many of the approaches taken or proposed so far rely on performance indicators that are measured in controlled environments, and then on extrapolating these to the conditions encountered during the actual operations. This is analogous to using sea-trial performance curves to evaluate fuel consumption based on the actual speed profile. Generally, methods like these would not be considered sufficient to measure the performance of the ships. Consequently, the applicability of similar methods for considering wind propulsion if questionable.

In order to effectively regulate the emissions and to reach the ambitious targets of IMO, it is important to consider the propulsion energy mix and its emissions as accurately as possible. In chapter 3 the need for accurate understanding of sail effort was pointed out from the optimization perspective, but it should

be noted that it is equally important from the regulatory perspective. Providing information on the actual sail performance is essential to enable more to-the-point regulation but also to enable ships that are equipped with sails to get full economic benefit of those sails.

5. Future work

Norsepower has developed a measurement and control system that enables both the further optimized sail system but also addresses the need for continuous measurement of the sail effort. There is ongoing work being undertaken to validate the latter aspect of the system. The purpose is to enable shipowners to report the contribution of sails in their energy mix continuously, without the need for extensive and often practically very challenging measurement campaigns.

References

DNV (2023). *Energy Transition Outlook*, DNV, Hovik

DUPUY, M.; LETOURNEL, L.; VILLE PAAKKARI, V.; RONGERE, F.; SARSILA, S.; VUILLERMOZ, L. (2023), *Weather Routing Benefit for Different Wind Propulsion Systems*. J. Sailing Technology, pp. 200-217

EGGERS, R.; KISJES, A. (2023), *WiSP2 Project on Wind Propulsion Performance*, RINA Wind Propulsion Conf., London

EC (2023), *Regulation (EU) 2023 of the European Parliament and of the Council on the use of renewable and low-carbon fuels in maritime transport, and amending Directive 2009/16/EC,* European Commission, https://data.consilium.europa.eu/doc/document/PE-26-2023-INIT/en/pdf

MASON, J.; LARKIN, A.; BULLOCK, S.; VAN DER KOLK, N.; BRODERICK, J.F. (2023), *Quantifying voyage optimisation with wind propulsion for short-term CO2 mitigation in shipping,* Ocean Eng. 289

MIZUTANI, N.; NAKADOZONO, N.; MASUTANI, A.; ARAI, Y.; AONO, T.; PAAKKARI, V. (2024), *Navigating a Sustainable Future with Wind-Assisted Ship Technology*, 9th HullPIC Conf., Tullamore, pp.111-128, http://data.hullpic.info/HullPIC2024_Tullamore.pdf

NORSEPOWER (2023), *Norsepower Performance Data at glance*, Norsepower, Helsinki

NORSEPOWER (2024), *LDA and Norsepower Join Forces,* Norsepower, Helsinki, https://www.norsepower.com/post/lda-and-norsepower-join-forces-in-shipping-large-airbus-aircraft-components-future-fleet-of-low-emission-roros-to-use-norsepower-rotor-sails/

PAAKKARI, V.; HÖRKKÖ, R. (2024), *Leveraging Rotor Sails to support CII compliance*, RINA CII Technical Conf., London

SCHENZLE, P. (1985), *Estimation of wind assistance potential*, J. Wind Eng. and Industrial Aerodynamics, pp. 97-110

SEATRANS (2022), *Seatrans sustainability report*, https://seatrans.no/wp-content/uploads/2022/03/Seatrans-Sustainability-report-2021.pdf

How to Design and Assess Multi-component Ship Power Systems

Lukas Kistner, HD Hyundai Europe R&D Center, kistner@hdhyundai-erc.com
Kevin Koosup Yum, HD Hyundai Europe R&D Center, kevin.koosup.yum@hdhyundai-erc.com

Abstract

While conventional ship powertrains mainly incorporate propulsion and auxiliary engines, modern designs are also integrating shaft generators, fuel cells, and batteries to enhance energy efficiency and reduce CO_2 emissions. However, due to the diversity of vessel characteristics, a universally best-performing design is not conceivable. Instead, different technologies, each with its unique efficiency characteristics and operational limitations, are favored, also necessitating tailored system control strategies. This paper introduces an early-stage modular energy management approach aimed at operational efficiency and flexibility, which can be used for model-based system design optimization tasks. Furthermore, the generalized strategy is tested with various power system configurations.

1. Introduction

The subject of this paper is a generalized energy management strategy (EMS) approach, which can be used for an early-stage direct comparison of power system designs via fuel consumption calculations, and to develop cost-optimal multi-component system configurations.

While traditional ship power systems typically consist of a main propulsion engine paired with an auxiliary genset, modern design approaches are increasingly integrating a variety of power-converting components to enhance energy efficiency and reduce greenhouse gas emissions. Technologies such as engines with variable-speed shaft generators, various fuel cell types, and energy storage devices like batteries are gaining traction for their potential contribution to meeting CO_2 reduction targets set by the International Maritime Organization, *IMO (2024)*, and the European Union, *EC (2020)*. However, the growing array of technology options, each with its unique energy efficiency characteristics, increases the complexity of both system design and operational strategies: mechanical and electric sector coupling, diverging operational limitations, and a more challenging cooperation of multiple components call for more sophisticated energy management strategies, which are not only required for real-life ship operation, but are also essential for evaluating system behavior during the design phase. Given the diverse needs of different vessels, there is likely no general best combination of technologies and tailored solutions suited to specific load profiles must be developed individually for each ship. Consequently, power system modeling and time-dependent simulation, which requires a dispatch strategy to obtain operation-dependent results, are crucial tools for assessing a system's performance. Typically, three kinds of control strategies are used for power system simulations, each of which have their own advantages and flaws:

a) Fixed operation, neglecting time-dependent specifications by using stationary assumptions or load distribution graphs, *Baldi et al. (2018)*: A stationary assessment massively reduces the complexity of the modeling approach and simplifies the operating requirements to one or few modes. However, this approach cannot consider load shift limitations of fuel cell systems or capacity limitations of energy storage systems due to the lack of energy time evolution information.
b) Highly specified power management strategies, *Bassam et al. (2017)*: While these are the most promising approaches for putting into later real-life use, they also require high commitment (i.e. neural network training, model predictive control strategies, sophisticated knowledge of the configuration and the potential synergies) and can therefore not be utilized in a general technology configuration comparison for combinatorial reasons.
c) Optimization approaches with unit commitment tasks, *Tang et al. (2020)*: The advantage of not requiring a formulated control strategy suites an initial assessment, but time-dependent optimi-

zation tasks require a specific setup of the power system models, limiting their formulation to convex objective functions and optimization constraints (i.e. linear formulations).

To address the challenge of creating niche operating approaches, this paper proposes a modular and component-independent EMS that covers the ship propulsion and the electric power demand. Emphasizing system efficiency and operating flexibility, this approach includes control strategy formulations at the power system, component group, and single-unit levels. Subsequently, an exemplary use case is presented, in which system performances for various component configurations are compared economically.

2. Methods

Fig.1 gives an overview of the method section, which is structured in analogy to the workflow of a typical optimization framework: first, the power systems under consideration, their operation requirements, and options for a design optimization are introduced. Then, the modular, generalized control strategy is schematically described. After that, exemplary power system model setups for the fuel consumption assessment are given.

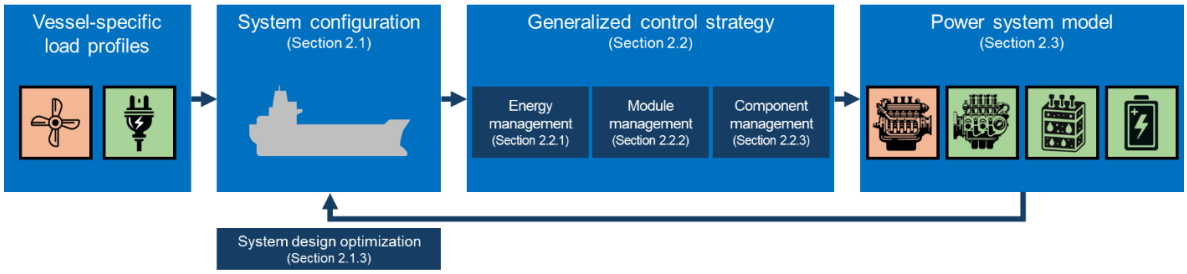


Fig.1: Typical workflow of a power system design optimization

2.1. Component characteristics and system design optimization

In this section, the assessed system components and configurations are briefly described, followed by the description of the optimization problem.

2.1.1. System components under consideration

For the exemplary system study, five main components of the powertrain are considered. Their specifications and key features are given in the following:

- **Main engine** – Many merchant ship power systems contain an internal combustion engine for propulsion, which is directly coupled to the propellor or connected to the shaft line with a gearbox. For large deep-sea ships, 2-stroke engines with slow rotational speed are favored for their high efficiency. In the present study, a dual-fuel engine operating with liquefied natural gas (LNG) is selected.
- **Shaft generator** – The main engine can also function as an electric power generator in addition to its propulsion task if a generator is coupled to the shaft line. This supportive operation is denoted Power Take Off (PTO) and is favorable due to the advantageous energy efficiency of the main engine in high part load. A secondary option is the propulsion support through the electric machine operated as a motor, also referred to as Power Take In (PTI). Depending on the operational requirements, both modes can reduce the power system's overall fuel consumption, *Perez et al. (2020)*.
- **Genset** – To fulfill the electric power demand on a ship, traditional system approaches include a group of combustion engines and electric generators, also called a genset. For the application under investigation, 4-stroke medium speed engines are selected.

- **SOFCs** – The electrochemical fuel conversion of solid oxide fuel cells (SOFCs) offers a higher energy efficiency than internal combustion engines, especially in lower part loads. As opposed to most low-temperature fuel cell technologies, an SOFC can be operated with various fuels and does not require a hydrogen storage, *Kistner et al. (2023)*. For comparability, the SOFC-based systems are operated with LNG, but ammonia, methanol, or hydrogen are also options to consider.
- **Batteries** – The benefits of energy storage systems in hybrid configurations can be categorized in two segments: system design advantages and energy efficiency improvement. For example, peak load shaving for power-intensive maneuvers enables a reduced rated power requirement for other electric power converters. Further, batteries can support gensets and prevent low-part-load operation, if the active number of engines can be reduced. In addition to the supportive measures, batteries are mandatory for SOFC-based configurations to compensate inevitable power deltas, *Kistner et al. (2021)*.

2.1.1. System configurations under consideration

Now that all components under consideration have been briefly introduced, four representative system configurations are created, Fig.2. Case 1 represents the traditional power system built from a mechanical propulsion system with a main engine and an electric power system with a genset. Case 2 introduces the potential interaction of mechanical shaft line and electrical bus bar through a shaft generator. Case 3 represents an electric propulsion system including SOFCs as a main power source as well as a genset plus battery system support. Finally, Case 4 includes all components under consideration. While this configuration is likely not put into practice for newbuilds, it could function as a reference for retrofits and as a theoretical example for an optimal component selection task.

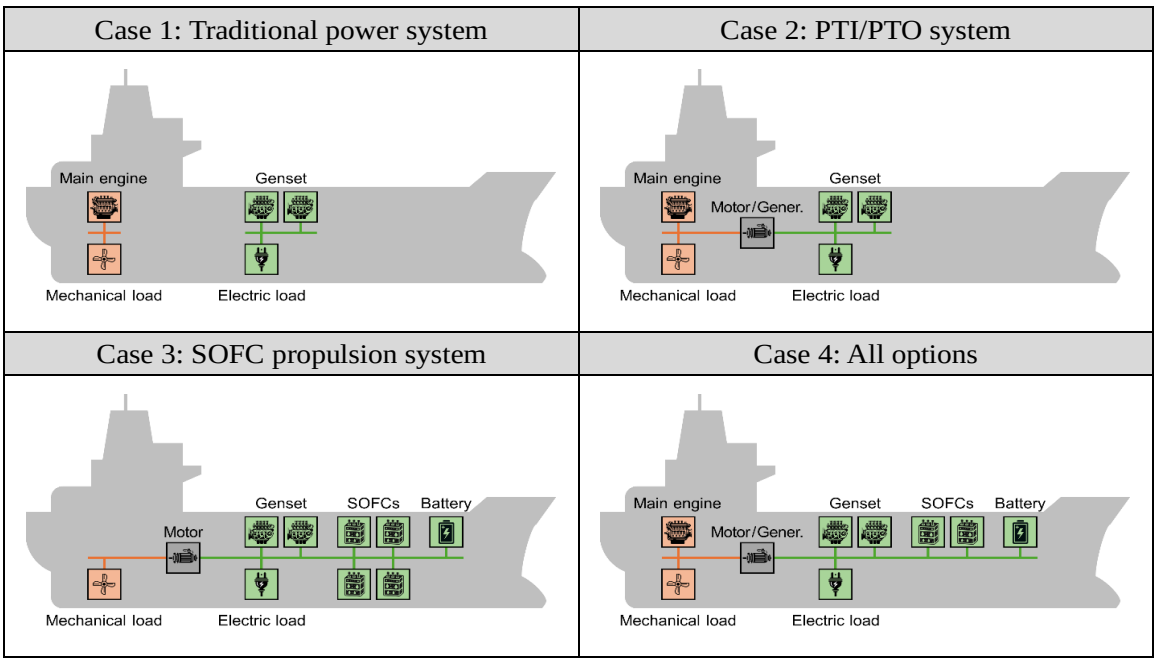


Fig.2: Investigated ship power systems with various configuration complexites

2.1.1. Typical optimization task

The main objective of an optimization task is to identify a cost-optimal system configuration, observing annual capital expenditure of the power train components $c_{\mathrm{CAPEX,a}}$ and the annual operational expenses including fuel consumption and maintenance requirements $c_{\mathrm{OPEX,a}}$. The system design, i.e. the rated

power P_r , which can be selected from available products, the rated energy capacity C, or the number of installed component modules N (indexes: main engine ME, genset GEN, shaft generator SG, solid oxide fuel cells SOFC, battery B) are typical degrees of freedom. The required coverage of the time-dependent mechanical power $P_{\mathrm{L,mech}}$ and the electric power demand $P_{\mathrm{L,el}}$ represent the constraints of the optimization problem. In the given balances, the power of the shaft generator is represented both mechanically $P_{\mathrm{SG,mech}}$ and electrically $P_{\mathrm{SG,el}}$. Furthermore, the components' operating limitations P_{lim} (e.g. maximum power, restricted load shift capabilities) and component cost calculations are part of a complete constraint formulation.

$$\begin{aligned} &\text{minimize} && c_{\mathrm{CAPEX,a}} + c_{\mathrm{OPEX,a}} \\ &P_{\mathrm{r,ME}}, P_{\mathrm{r,GEN}}, P_{\mathrm{r,SOFC}}, N_{\mathrm{SG}}, C_{\mathrm{B}} && \square \\ &\text{subject to} && \\ &\square && 0 = P_{\mathrm{L,mech}} - P_{\mathrm{ME}} - P_{\mathrm{SG,mech}} \\ &\square && 0 = P_{\mathrm{L,el}} - P_{\mathrm{SG,el}} - P_{\mathrm{GEN}} - P_{\mathrm{SOFC}} + P_{\mathrm{B}} \\ &\square && P_{\mathrm{lim,down},j} \leq P_j \leq P_{\mathrm{lim,up},j} \; \forall \, j = \mathrm{ME, GEN, SOFC, B.} \end{aligned}$$

In the presented approach, both the satisfaction of the power balance for a well-designed system and the compliance with the operating limitations are covered by the EMS. For a complete design optimization, an economic modeling approach guideline is given in the following: annual capital costs should be directly influenced by the system design:

$$c_{\mathrm{CAPEX,a}} = \sum_{i}^{\square} (P_{\mathrm{r},i} \cdot p_i \cdot A_i) + \mathrm{N_{SG}} \cdot p_{\mathrm{SG}} \cdot A_{\mathrm{SG}} + C_{\mathrm{B}} \cdot p_{\mathrm{B}} \cdot A_{\mathrm{B}},$$

where i are the investigated power converters, p are specific prices for all individual powertrain components (e.g. in €/kW) and A are annuity cost factors to include component lifetime and interest rates. For the annual operating costs, maintenance expenses and fuel consumption are to be quantified:

$$c_{\mathrm{OPEX,a}} = p_{\mathrm{fuel}} \cdot \frac{t_{\mathrm{op,a}}}{t_{\mathrm{op}}} \cdot m_{\mathrm{fuel}} + \sum_{j}^{\square} c_{\mathrm{maint},j},$$

where t_{op} is the operating time of the investigated passage, $t_{\mathrm{op,a}}$ is the annually expected operating time, and c_{maint} are the annual maintenance costs for each component j. However, in this operation-centered investigation, only the single-passage fuel consumption m_{fuel} is evaluated for prefixed system designs to directly evaluate control strategy influences.

2.2. Control strategy

The central feature of this paper is the generalized, modular system-and-component control strategy for early-stage performance evaluations. The rule-based approach is split into three segments: the energy management is represented by a hierarchical set power calculation for each power system component group. The module management further specifies the allocation of the set power values. Finally, the component management strategy ensures the compliance with the components' operating limitations.

2.2.1. Energy management strategy

When multiple components can fulfill the ship's power requirements alone or in co-operation at different operating points, an EMS is required for a reasonable decision process, also called dispatch strategy. The proposed generalized EMS therefore follows three objectives:

1) maintaining the operability of the system to ensure an uninterrupted power supply,
2) reducing the total fuel consumption, and
3) being easily adaptable to freely add new components and investigate all kinds of component configurations.

As a result, a cascading, hierarchical set-power value calculation is proposed, where highly efficient technologies are dispatched first, and more flexible-operating component capabilities are conserved for

balancing. Before providing the set-power equations, an exemplary cascading dispatch of power requirements is shown in Fig.3: the mechanical propulsion requirement (light orange) is fully covered by the main engine (dark orange), consequently no PTI is required. For the electric system, not one single component can fulfill the requirements due to their defined operating restrictions (cf. Section 2.2.3). Therefore, the power supply is shared following an efficiency ranking and based on the information of deltas between set-power (light green) and actual power values (dark green). Next, the introduced logical approach is given in form of equations.

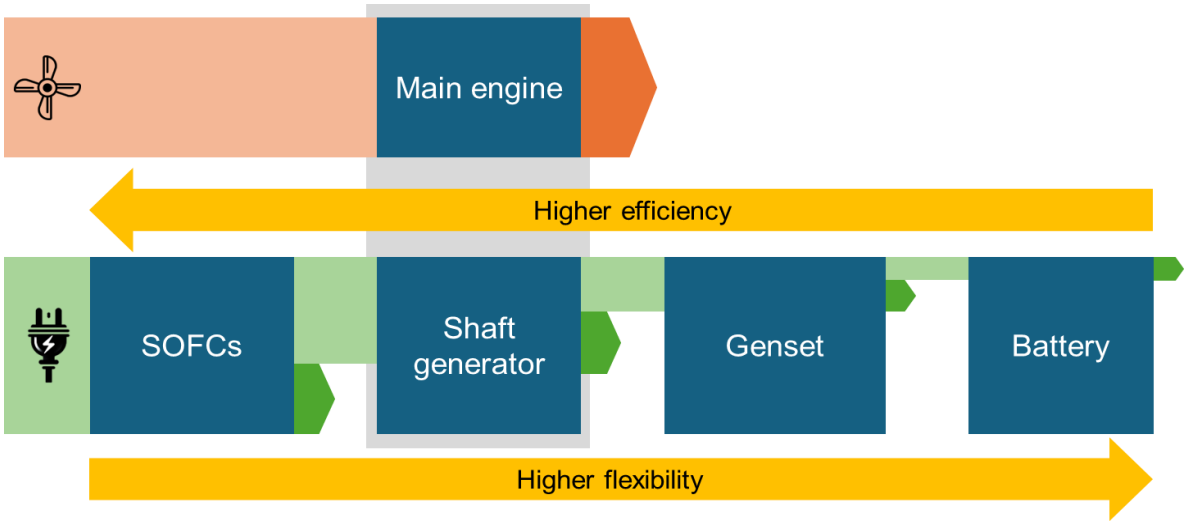


Fig.3: Hierarchy-based system control strategy for mechanical (orange) and electric (green) power demand: light-colored boxes symbolize power requests, darker arrows component responses

For every given power system configuration, which includes a main engine for direct mechanical propulsion, a first mechanical set-power value is given with

$$P_{\mathrm{ME,mech,set}} = P_{\mathrm{L,mech}} \,.$$

For the first-ranked component $i = 1$ (in this case the SOFCs), the electric power demand is given as:

$$P_{i=1,\mathrm{set,el}} = P_{\mathrm{L,el}} + N_{\mathrm{SG}} \cdot P_{\Delta,\mathrm{mech-el}} + P_{\mathrm{B,des}}(F_{\mathrm{B}}) \,,$$

where $P_{\Delta,\mathrm{mech-el}}$ symbols the open mechanical power requirement which must be covered by the shaft generator and $P_{\mathrm{B,des}}$ is an additional power requirement to potentially balance the battery systems state of energy F_{B}. Then, set values for all other electric components *i* are given consecutively with the power delta not fulfilled by the previously ranked electric component:

$$P_{i,\mathrm{set,el}} = P_{i-1,\mathrm{set,el}} - P_{i-1,\mathrm{el}} \,.$$

Shaft generator operation – electrically supported propulsion **(**PTI) operation can be suitable for various reasons but is often related to one of the following scenarios: the operation with an idling main engine due to a very small propulsion request or the operation at maximum speed or torque. Both modes lead to a delta between main engine set power and response, requiring a balancing electric power $P_{\Delta,\mathrm{mech-el}}$.

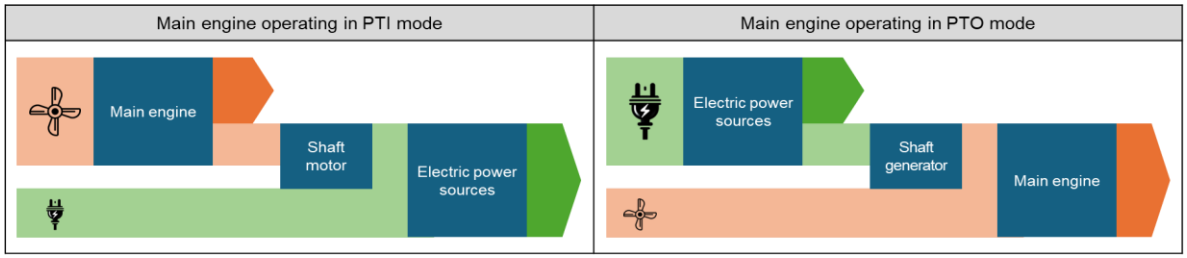


Fig.4: Power flow diagram for the mechanical-electric sector coupling through an electric engine

The additional electric power requirement is influenced by the shaft generator efficiency, as shown in Fig.4 (left). For the electric system support from the main engine (PTO), displayed in Fig.3 and Fig.4 (right), sector coupling is modeled with two decoupled set-value calculations. Note, that the cumulated mechanical and electric power output is certainly restricted in total (cf. Section 2.2.3).

Battery balancing – While battery reaction times are usually negligibly small, not only static power restrictions, but also a finite energy capacity limits the storage's operation. Consequently, the EMS considers the battery's state of energy (SOE) in the set value calculation and aims to charge or discharge the battery whenever it is beneficial:

$$P_{\mathrm{B,des}} = \begin{cases} P_{\mathrm{B,cha}} \text{ if } F_{\mathrm{B}} < F_{\mathrm{des,min}} \\ P_{\mathrm{B,dis}} \text{ if } F_{\mathrm{B}} > F_{\mathrm{des,max}} \\ 0 \quad \text{else.} \end{cases}$$

Here, a specified minimum desired SOE $F_{\mathrm{des,min}}$ should be maintained for sea operation to enable peak-load shaving, whereas a maximum SOE $F_{\mathrm{des,max}}$ only is required when compensating inevitable power deltas due to slow SOFC load shifts. The evolution of the battery's energy content is a function of the battery power P_{B} and a self-discharge factor r_{SD}:

$$\frac{\mathrm{d}F_{\mathrm{B}}}{\mathrm{d}t} C_{\mathrm{B}} = -r_{\mathrm{SD}} C_{\mathrm{B}} F_{\mathrm{B}} + P_{\mathrm{B}} \begin{cases} \eta_{\mathrm{B}} & \text{if } P_{\mathrm{B}} > 0 \\ 1/\eta_{\mathrm{B}} & \text{if } P_{\mathrm{B}} < 0 \end{cases}.$$

Additional components – Certainly, this method can be enhanced with other components like low-temperature hydrogen fuel cells (ranks between SOFCs and shaft motor), gas turbines or combined cycles (ranks between SOFCs and genset, depending on operating specifications), and supercapacitors (rankes more flexible than battery due to higher specific power ensurence).

2.2.2. Module power management strategies

One additional aspect of an EMS is to further allocate set-power values to individual operating units. Specifications are required for gensets (commonly referred to as power management strategy – PMS) and fuel cell modules, or in general for all power technologies with modular characteristics. For internal combustion engines, a high-part-load operation is beneficial to reduce the specific fuel consumption, *Skjong et al. (2017)*. Therefore, a on/off switch logic is required, as displayed in Fig.5 (left). Here, as few engines as possible are operated. On the other hand, maintaining all fuel cell units in low part load (Fig.5 right) enhances the overall fuel efficiency of SOFCs, as their main energy losses are related to electrochemical and transport processes. Of course, balance-of-plant requirements, as well as fluid-dynamic and thermal aspects of the systems limit these considerations, *Kistner et al. (2021)*.

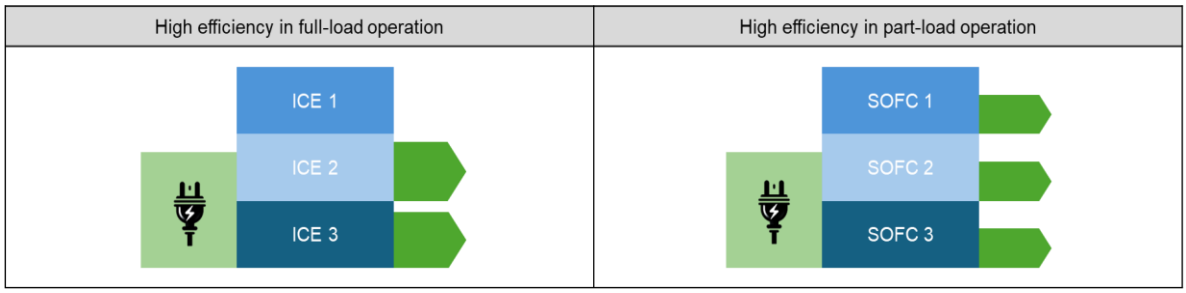


Fig.5: Module power management of a genset and SOFC maximizes the energy efficiency

2.2.3. Component management strategies

The main objective of the formulated component management strategy is aligned with the EMS requirement to be as flexible and generic as possible. Before the defined framework is introduced, typical operating limitations for the assessed components are summarized in the following:

- **Main engine** – With the exception of short-term operations, the maximum deployable power equals the engine's rated power. Also, a minimum power supply is stipulated to maintain operational stability (combustion, lubrication) and prohibit an excessive specific fuel consumption. For event of very low power requirements, either a higher power output (not recommended for mechanical propulsion) or switching to a stand-by mode are options in line with the component limitations.
- **Shaft generator** – For PTI mode, maximum power of the shaft motor drive and torque/rotational speed restrictions of the shaft line are the most relevant operational limitations. The integration of a frequency converter over a gearbox enables superior part-load operability and is therefore selected in this case study, *Souflis-Rigas et al. (2021)*. For PTO mode, the electric power supply capabilities are also limited by the main engine's maximum power.
- **SOFCs** – In addition to a maximum power output, two relevant restrictions are to be considered (cf. Fig.6): SOFCs' load shift capabilities are significantly more limited than it is the case for combustion engines or low-temperature fuel cells. The reasons behind this are the risk of thermomechanical stress impacting the cells, the potential requirement of fuel steam reforming, and the thermal inertia of the system. Also, SOFCs should operate permanently to maintain a desired temperature level and fluid dynamical behavior required for heat exchangers, *Kistner et al. (2021)*. Alternatively, SOFCs can be idled and externally heated, but then require an extended period for heating up before deploying electric power again.
- **Genset** – The internal combustion engines of the genset have very similar limitations to the main engine. However, one additional challenge of operating a genset with a switch-on-and-off control approach is the delay of power supply when starting up an individual engine due to the electric motor synchronizing requirements, *Perabo et al. (2020)*.
- **Batteries** – Energy storages entail power limitations for charge and discharge operation. These two parameters do not have to be identical, depending on the technology under consideration. For electrochemical solutions, power limitations typically are a function of the state of charge influencing the cell voltage, and the required electric current. However, since no cell chemistry has been selected for this assessment, a constant maximum power is assumed, neglecting the charge-voltage-current interdependencies. In addition to the power restriction, batteries require a state-of-energy observation, preventing an empty unit to further discharge, and vice versa for a fully charged unit, Fig.6. An implementation approach of a generic energy storage management and technology-specific descriptions can be found in *Kistner et al. (2021)*.



Fig.6: Characteristic operational limitations for the components under consideration, categorized into power limitations, time-dependent limitations, and component-specific descriptions

All operating restrictions can be compiled by a combination of predefined limitation types, and technology-specific parameters, which are given in Fig.6. Also, a visual limitation example is given for the SOFCs and depict the components response $P_{\mathrm{SOFC,1,el}}$ to a set value $P_{\mathrm{SOFC,set,el}}$.

2.3. Power system modelling approach

For the component models, operation-dependent efficiency curves and specific-fuel-consumption (SFC) descriptions $\dot{m}_{\mathrm{SFC}}$ (in g/kWh) are essential tools to display the complete powertrain behavior and calculate the overall fuel consumption. The operation-dependent fuel consumption rate of a power technology thereby includes all conversion-step efficiencies up until the switchboard or shaft interface:

$$\dot{m}_{\mathrm{fuel},i} = \dot{m}_{\mathrm{SFC},i}\overbrace{\left(P_i / P_{\mathrm{r},i}\right)}^{\substack{\text{rel.oper.}\\ \text{point}}} \cdot P_i \cdot \prod_k^{\square} \frac{1}{\eta_{i,k}},$$

where k are the different integrated conversion steps. The overall fuel consumption then is cumulated for the assessed voyage time:

$$m_{\mathrm{fuel}} = \sum_i^{\square} \int_{\square}^{t_{\mathrm{op}}} \dot{m}_{\mathrm{fuel},i}\, \mathrm{d}t.$$

For better comprehension, the utilized model structure is given for an exemplary configuration in Fig.7. Note, that an alternating-current electric grid is assumed, whereas a direct-current approach would require rectifiers for the genset, a voltage converter for the SOFCs and an inverter for the shaft engine. The investigated shaft generator setup couples the mechanical and the electric system with three conversion steps. For a PTI operation, the provided mechanical power is always smaller than the required electrical expense:

$$P_{\mathrm{SG,mech}} = \underbrace{\eta_{\mathrm{SG}} \cdot \eta_{\mathrm{CON}} \cdot \eta_{\mathrm{TF}}}_{\eta_{\mathrm{mech-el}}} \cdot P_{\mathrm{SG,el}},$$

where η_{SG} is the operation-dependent efficiency of the shaft generator, η_{CON} is the frequency converter efficiency, and η_{TF} is the efficiency of the interposed power transformer. For PTO operation, the opposite holds true:

$$P_{\mathrm{SG,mech}} = \frac{P_{\mathrm{SG,el}}}{\eta_{\mathrm{SG}} \cdot \eta_{\mathrm{CON}} \cdot \eta_{\mathrm{TF}}}.$$

For the implementation of all fuel consumption calculations and power balances, we selected the FEEMS modeling framework for programming language Python, *Sintef (2024).*

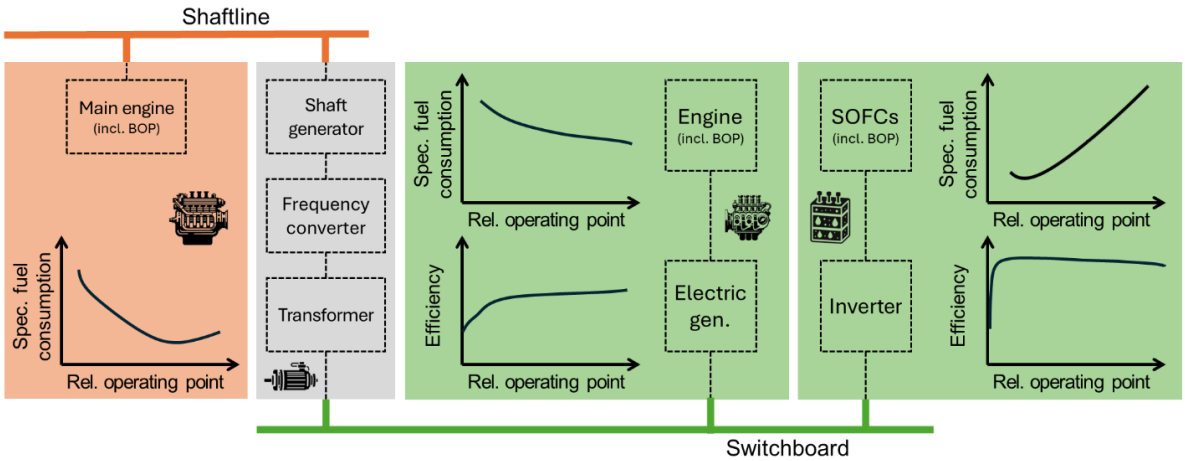


Fig.7: Structural setup of the empirical, characteristic-curve-based component models including balance of plant (BOP) by example of an engine and an SOFC in an electric propulsion system

3. Exemplary mission assessments

This section covers a description of the case study vessel and the mission profiles. Following, the system designs of the four powertrain configurations are specified. After that, the operating profiles for all configurations are generated based on the introduced energy management strategy.

3.1. Vessel description and powertrain design

For the initial EMS test, a 3.5-day operation of a Very Large Crude Carrier (VLCC) is assessed. The vessel's mechanical and electric operating profiles are given in Fig.8. The assessed mission includes deep-sea operation at the beginning and the end of the time horizon, resembled by a relatively static plateau at a10 MW power demand. In between, two calls at port and an intermediate operation of around 9.5 hours with the maximum power demand of around 13 MW at 2,500 minutes are observable. The highest auxiliary power demand results from thruster maneuvers during the intermediate period at around 1.7 MW, while the deep-sea electric power demand is given as a steady baseline with smaller fluctuations.

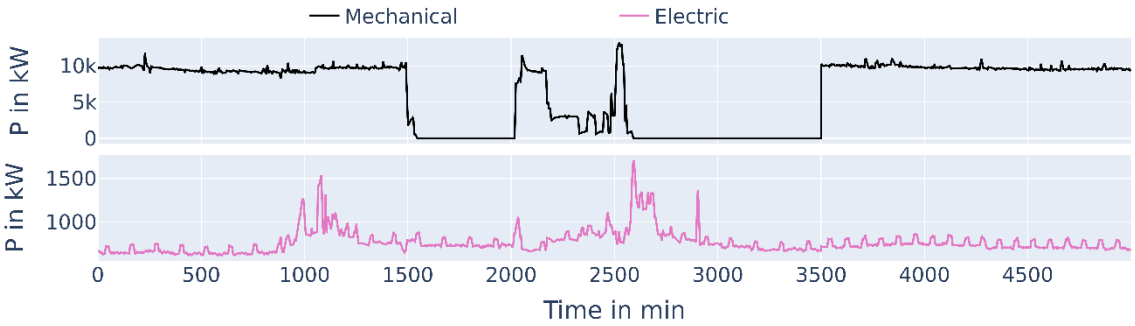


Fig.8: Mechanical propulsion load and electric power demand profiles for the exemplary case study

Fig.9 summarizes the designs of all four configurations. In Case 1, a 13.5 MW main engine rated power is selected to securely cover the propulsion demand. The auxiliary genset's total rated power is 2 MW, compromising two engines. With the addition of a shaft generator, the rated power of the main engine can be reduced to 12.5 MW in Case 2, as PTI for peak load support is granted by the identical auxiliary genset. In Case 3, a larger total rated power is required, as the SOFC load shift support constitutes an energy-intensive task for the battery. 12 SOFC modules, each with 1 MW rated power, are supported by a 2-engine 2 MW genset and a 6 MWh battery system with a specific power of 1.5 MW/MWh for both charging and discharging. For the hybrid propulsion system in Case 4, an equal split of rated power is assumed for SOFCs and main engine, resulting in an installation of two-time 6 MW. Since battery support requirements are now reduced, a 2.5 MWh storage suffices for load shift support.

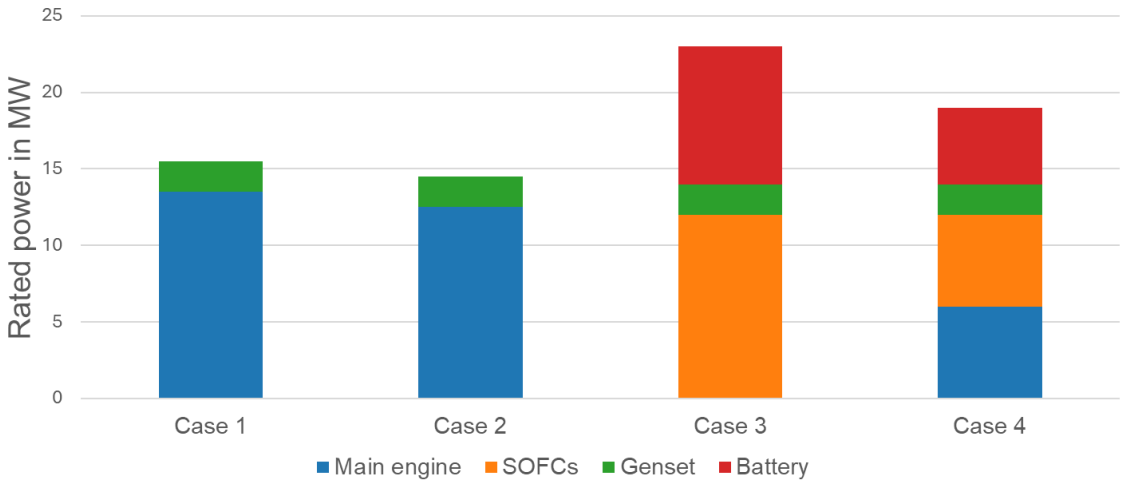


Fig.9: Rated system power for the four predefined power system configurations

3.2. Component operating profiles

In this section, the individual operating profiles of the components are briefly discussed before a direct comparison of the fuel consumption is given. Fig. 10 displays the conventional ship power system as introduced for Case 1. The load profiles are exactly covered by main engine and genset, since no operating flexibility is given. In Fig. 11, the result of incorporating a shaft generator is demonstrated (Case 2). The formulated EMS mostly results in PTO support for most operation at sea and shows events for PTI for peak-load shaving during the power-intensive intermediate maneuver. The SOFC-based power system with electric propulsion (Case 3) is shown in Fig. 12. The fuel cell modules are operating in high part load mostly and are supported by the genset to charge the battery system during initial deep-sea operation. As the cumulated rated power of the fuel power converters does not suffice for the highest electric power demand, battery peak load shaving is applied by the hierarchical set power calculation. The required design of the battery is however not specified by the amount of energy necessary during peak shaving operation, but during the second SOFC ramp-up. Note, that battery power values higher than zero equal charging operation. In Fig. 13, the hybrid, most complex system configuration of Case 4 is displayed. The main engine is operating at rated power during operation at sea, while the SOFC covers both the residual mechanical and the electric power delta. During steep power increases, the SOFCs are supported by the genset. PTI propulsion support is active for almost the whole sea operation, but PTO also supports the electric power sources during the SOFC switch-on delay. The charging process of the now smaller battery system is finalized after around 45 minutes. As the now smaller SOFC systems also require less absolute load shift support, battery peak load shaving requirements also are reduced by a factor of around 2.4. Still, the design of the battery is restricted by the amount of energy required, but now also operates close to its power limitations.

While for a complete technology comparison, a total cost of ownership assessment is certainly required, fuel costs resemble the largest share of a merchant ships' power system expenses. The traditional Case 1 powertrain configuration results in a fuel consumption of 75.1 tons for the main engine and 12.7 tons of LNG for the auxiliary genset. On this basis, Case 2 results indicate an operational benefit of shaft generators: the fuel consumption of the main engine increases to 81.8 tons (+8.9%), but a reduced operation of the genset results in 4.2 tons (- 67%) fuel consumption. The overall fuel consumption is decreased by 2.1% due to the augmented high-part-load operation and the better efficiency of the now smaller main engine. In Case 3, the expected reduction of an SOFC application to 72.2 tons of LNG is achieved. An additional decrease of genset fuel consumption to 3.7 tons is enabled due to the SOFC covering most of the electrical demand. Overall, the electric propulsion system reaches a consumption reduction of 8.4%. For the hybrid 2-stroke main engine plus SOFC design in Case 4, a close second-best result of 7.6% fuel consumption reduction is computed. This indicates that not entirely switching to SOFCs e.g. in retrofit scenarios already results in an advantageous operation, as the fuel cells cover the electrical base load as well as the propulsion power. Notably, the SOFC fuel consumption only accounts for 31.1 tons, as the modules operate in lower part load primarily.



Fig.10: Operating profiles for the Case 1 configuration: Main engine, auxiliary genset



Fig.11: Operating profiles for the Case 2 configuration: Main engine, genset, shaft generator



Fig.12: Operating profiles for the Case 3 configuration: SOFCs, genset, battery



Fig.13: Operating profiles for the Case 4 configuration: hybrid main engine plus SOFC propulsion

4. Demonstrating the influence of energy management strategy alterations

As already annotated, the proposed strategy aspects are not designed to optimize the operation, but rather for initial assessments of technologies and component configurations. However, it is already of interest, if adding specific features to the control strategy substantially alters the assessment results. While the general efficiency-based hierarchy and the monitoring of component operating limitations are required for reducing the overall logical effort, two potentially relevant module strategies are selected to demonstrate effects of revising the EMS: (a) improving the co-operation between combustion engines and batteries to increase energy efficiency and (b) analyzing the influence of altering SOFC operating limitations on the system design restrictions. For both challenges, exemplary cases are discussed in the following sections.

4.1. Influence of actively supporting the genset with a battery storage

In hybrid ship power systems, batteries represent manifold potentials and flexibilities for co-operation of components. While their most dominant task still is the peak-load-shaving operation to improve system design aspects and spinning reserve to allow for tight genset operations or SOFC load shift support, other supportive measures, including long-time part-load prevention of the genset, are suitable for common operation at sea. The idea behind this supportive measure, which neglects the approach of a strict dispatch hierarchy, is visualized in Fig.14: here, a genset without battery support can fulfill the power demand only with dispatching all three engines, whereas a battery-supported genset can and switch off one unit to momentarily reduce fuel consumption. However, the battery must be charged repeatedly to ready the support. This operation can be controlled with a state machine (charge to desired maximum SOE $F_{\mathrm{des,max}}$, then support operation until the minimum desired SOE $F_{\mathrm{des,min}}$ arises).

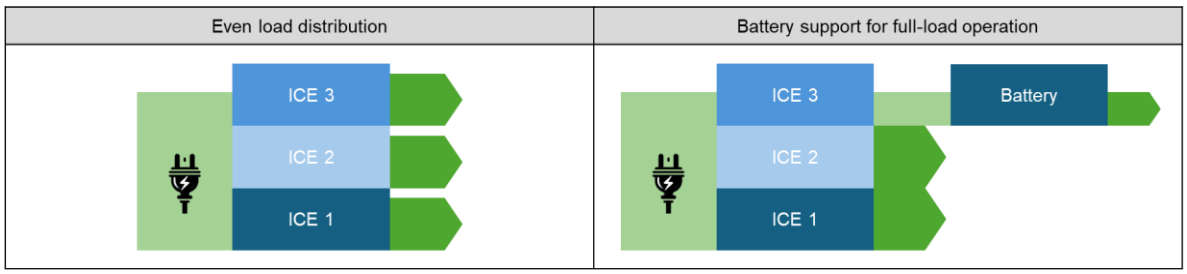


Fig.14: Genset operational options: even load distribution with no support demand; additional battery support to maximize ICE energy efficiency by increasing the relative load

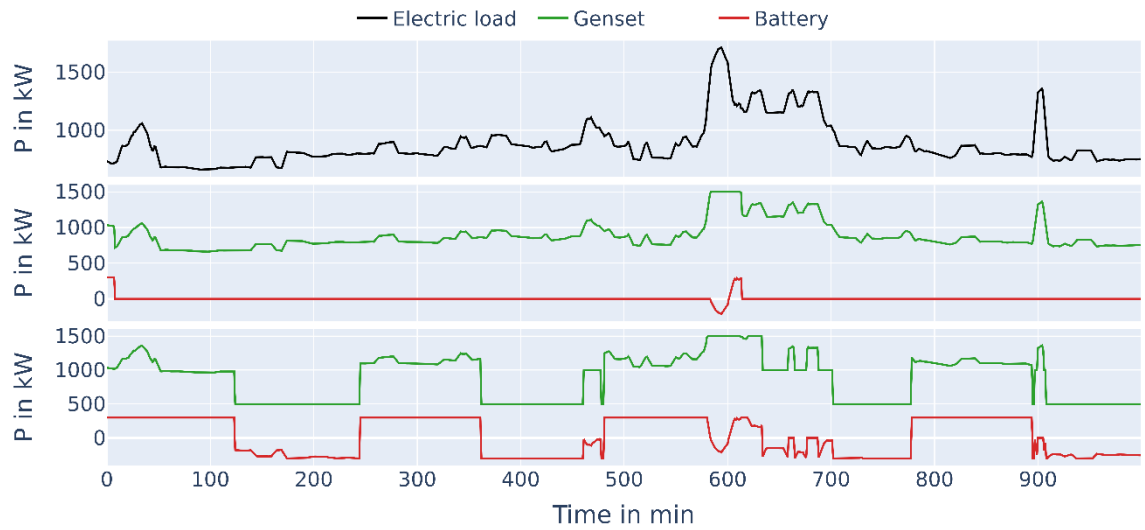


Fig.15: top: exemplary electric load profile, mid: load distribution for genset while the battery only operates during peak, bottom: battery support to increase ICE load and reduce fuel consumption

The tradeoff between battery roundtrip losses and generator efficiency can be evaluated by applying two different management strategies to a simple power system a with fixed design of 3 generators with 500 kW rated power each, and a battery with 600 kWh rated capacity and a specific power of 0.5 kW/kWh. The diverging operating profiles are given in Fig.15: Both strategies first charge the battery up until the desired state of energy ($F_{\mathrm{des,min}}$ for peak load shaving disposition, $F_{\mathrm{des,max}}$ for active battery support). While in the even-load-distribution approach the battery is idled afterwards and two generators are active in part-load operation, in the battery-support mode, two generators are idled, while the third one is operating at full power. After a period of about 120 minutes, the battery must be recharged again. For both strategies, all components are active for peak load compensation at around 600 minutes. As the batteries have not been discharged below the minimum desired state of energy, the uninterrupted power supply is effortlessly ensured at all times.

When directly comparing the gensets' fuel consumptions, a reduction of 0.6% from 2.899 tons to 2.882 tons is determined by allowing the battery unit to actively support the engines, even if electric energy is lost during battery charging and discharging. As this is evaluated to be a negligible value, it is at least questionable if these kinds of additional EMS capabilities are required for an initial assessment of a complex power system configuration. Also, what has not been taken into account for this assessment is the likely lifetime reduction of the battery due to more excessive utilization. This effect should therefore be covered in the total cost of ownership assessment by including an operation-dependent battery degradation model.

4.2. Influence of idling SOFCs on the design of the battery storage support

Another relevant strategy alteration is the idling of components with long start-up times. As SOFCs cannot be beneficially operated at very low part loads, two options are conceivable whenever no electric power is required by the vessel: continuous operation at the minimum power output and complete stand by. However, Fig.16, both operations require an operational support of another component to not produce a vast amount of excess energy, or forfeit the ability of a swift operational readiness, respectively. Even if SOFCs are kept at high temperatures during idling (hot idling), a start-up procedure can take several minutes and potentially requires a large spinning reserve. Therefore, an interesting degree of freedom is the number of idled modules at port to mitigate the amount of required support.

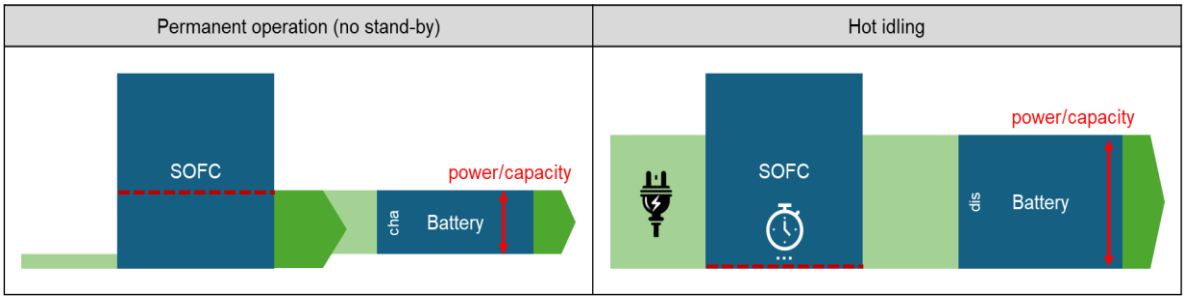


Fig.16: Battery sizing in dependence on SOFC operation during low power requirements: permanent operation buffered by charging battery; idling operation requires battery start-up support

For demonstration, three energy management strategy alterations are tested for one load profile, Fig.17 (first graph), and the required battery designs are directly compared. Twelve SOFC modules with 1 MW rated power and a minimum part load of 40% are selected. For comparability reasons, only a battery storage is utilized as operational assist, even if a genset could theoretically also support in the hot-idling scenarios. The first scenario allows to idle all twelve modules, Fig.17 (second graph) if less power than the minimum output capability is required. Here, the battery must not compensate excess energy during anchoring starting 150 minutes, but fully undertakes the power supply during the thirty-minute start-up of the SOFCs at 220 minutes and low part load, starting after around 450 minutes. In the second scenario, Fig.17 (third graph), half of the SOFCs are allowed to be idled, resulting in a 2,5 MW power output at port and during low-part-load operation, which are compensated by the battery. In turn, the required energy during SOFC ramp-up is slightly reduced. For the last scenario, no

idling is allowed, Fig.17 (fourth graph), further increasing the power surplus at port to 5 MW, while the required capacity for peak load shaving and spinning reserve is significantly decreased.

For all three design problems, the energy capacity is the design bottleneck, whereas the rated charge of discharge power only plays a subordinate role for a marine battery system. In the case that all SOFCs are allowed to be idled, a battery support with 10.8 MWh rated capacity is required to buffer the SOFC start-up time just after leaving the port. If only half of the SOFC modules can be put into stand-by operation, a 2% smaller storage (10.6 MWh) suffices to avoid excess power during anchoring and assist during start-up. While this small reduction could again be evaluated as negligible, not allowing the SOFCs into idling mode at all results in a required 10% capacity increase (11.9 MWh). This indicates that simple operating decisions could have a great influence on the optimal powertrain design. Another essential takeaway is that these kind of management decisions are greatly dependent on the characteristics of the load profile. Longer times at port advise for idling of the SOFCs, whereas fluctuating load profiles require more rapid operational readiness. This perspective also outlines the biggest flaw of a rule-based energy management strategy, which cannot easily react to every hypothetical niche case and therefore likely is bot leading to ideal results.

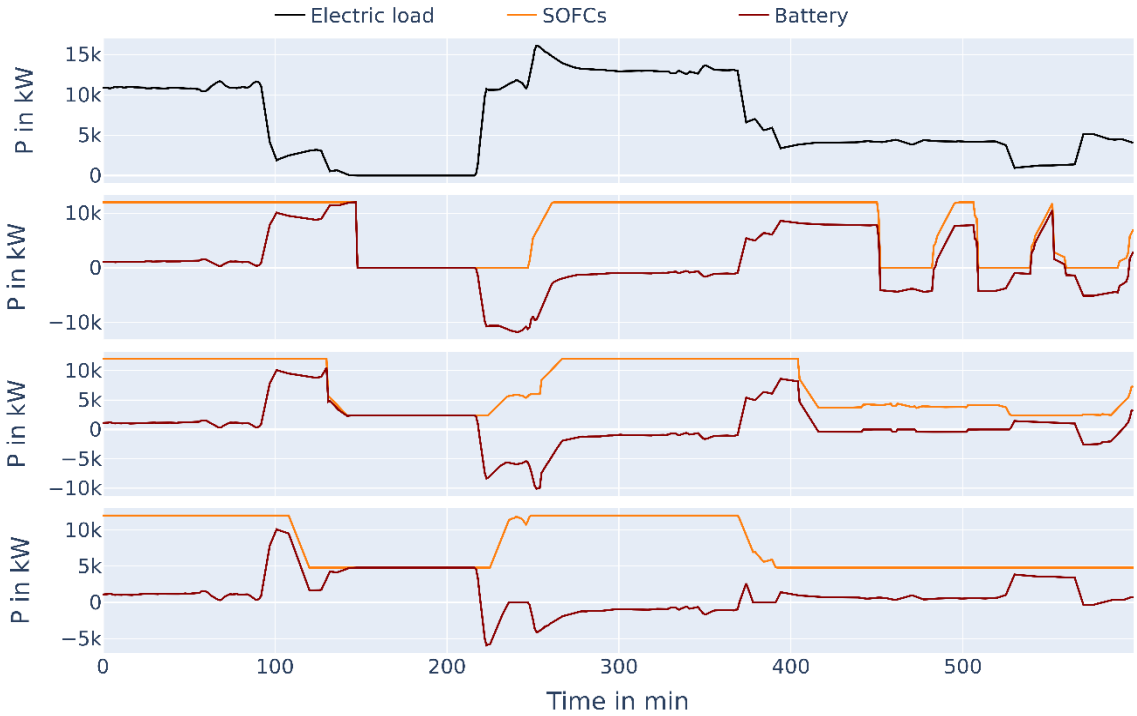


Fig.17: top: exemplary electric load profile, upper mid: SOFCs are allowed to idle and require start-up time, lower mid: only half of the SOFC modules are idled, bottom: no idling is allowed

5. Conclusion

In the present paper, a generic energy management strategy framework for multi-component ship powertrains, which can be utilized for system design optimization and techno-economic assessments, is presented. The approach covers operational constrains of the system components, interactions between units with modular structures, as well as the dispatch of power technologies with diverging efficiency and flexibility characteristics. The energy management strategy's functionality is demonstrated by calculating the fuel consumptions of four system configurations with various complexities. For an investigated vessel operation with two calls at port and an intermediate group of maneuvers, all aspired co-operation aspects between the power system components can be recognized in the operating profiles. In the assessment, the operational benefit of a shaft generator (-2.1% fuel consumption), the advantages and challenges of SOFCs in an all-electric ship (-8.4% fuel consumption, 6 MWh battery support for 12 MW SOFC rated power), and the intermediate solution of mechanical propulsion with meaningful electric support from SOFCs (-7.6% fuel consumption) are indicated.

While the initial control strategy follows a strict dispatch hierarchy, an altered approach is given by the idea of actively supporting the genset operation with a battery to allow full-load operation at specific time windows. However, this example demonstrates that fine tuning of the EMS not necessarily leads to a fundamentally different result and therefore likely can be dismissed in an initial case study. On the other hand, the example of altering the SOFC idling strategy suggests that energy management decisions can noticeably influence the design requirements. Operating profiles resulting from rule-based decisions must be subsequently evaluated with special care and strategies should be altered where appropriate. It has however been demonstrated that additional energy-saving strategies can be integrated into the presented EMS without larger effort due to the modularity of the framework.

Potential next steps to further increase the usability of the modelling framework involve adding alternative power technologies like gas turbines, combined cycles, alternative fuel cell types, and supercapacitors, as well as providing component-or-configuration-specific operating strategy alterations. Latter may include a dynamical hierarchy for dispatching the components for low and high part load, or hybrid storage strategies. Also model-predictive control approaches can be utilized to reduce the disadvantages of e.g. the SOFC operational inertia, while not relying on analytically optimizing unit commitments.

References

BALDI, F.; AHLGREN, F.; NGUYEN, T.V.; THERN, M.; ANDERSSON, K. (2018), *Energy and exergy analysis of a cruise ship*, Energies 11(10), 2508

BASSAM, A.M.; PHILLIPS, A.B.; TURNOCK, S.R.; WILSON, P.A. (2017), *Development of a multi-scheme energy management strategy for a hybrid fuel cell driven passenger ship*, Int. J. Hydrogen Energy 42(1), pp.623-635

EC (2020), *Regulation of the European parliament and of the council on establishing the framework for achieving climate neutrality and amending Regulation (EU) 2018/1999 (European Climate Law), COM(2020) 563 final*, European Commission

IMO (2024), *IMO's work to cut GHG emissions from ships*, Int. Mar. Org., London https://www.imo.org/en/MediaCentre/HotTopics/Pages/Cutting-GHG-emissions.aspx

KISTNER, L.; BENSMANN, A.; HANKE-RAUSCHENBACH, R. (2021), *Optimal design of power gradient limited solid oxide fuel cell systems with hybrid storage support for ship applications*, Energy Conversion and Management 243, 114396

KISTNER, L.; BENSMANN, A.; MINKE, C.; HANKE-RAUSCHENBACH, R. (2023), *Comprehensive techno-economic assessment of power technologies and synthetic fuels under discussion for ship applications*, Renewable and Sustainable Energy Reviews, 183, 113459

PERABO, F.; ZADEH, M.K. (2020), *Modelling of a shipboard electric power system for hardware-in-the-loop testing*, 2020 IEEE transportation electrification conference & expo (ITEC), 69-74)

PEREZ, J.R.; REUSSER, C.A. (2020), *Optimization of the emissions profile of a marine propulsion system using a shaft generator with optimum tracking-based control scheme*, J. Marine Science and Engineering 8(3), 221

SINTEF (2024), *FEEMS: a modeling framework for a marine power and propulsion system for calculation of fuel consumption, emissions, and energy balance with the input of operation mode and external power load*, https://github.com/SINTEF/FEEMS

SKJONG, E.; JOHANSEN, T.A.; MOLINAS, M.; SØRENSEN, A.J. (2017), *Approaches to economic energy management in diesel–electric marine vessels*, IEEE Trans. Transportation Electrification 3(1), pp.22-35

SOUFLIS-RIGAS, A.; PROUSALIDIS, J.; DIMOPOULOS, G. (2021), *Assessing the implementation of Power Take Off (PTO) system onboard Liquified Natural Gas (LNG) carriers*, IEEE Electric Ship Technologies Symp. (ESTS), pp.1-8

TANG, R.; AN, Q.; XU, F.; ZHANG, X.; LI, X.; LAI, J.; DONG, Z. (2020), *Optimal operation of hybrid energy system for intelligent ship: An ultrahigh-dimensional model and control method*, Energy 211

Optimisation of an Air Lubrication System for Geometry and Topology: A Proposed Solution for Ship Retrofitting

Hannes Renzsch, FRIENDSHIP SYSTEMS, Potsdam/Germany, renzsch@friendship-systems.com
Andrew Spiteri, LJMU, Liverpool/UK, A.Spiteri@ljmu.ac.uk
Eduardo Blanco-Davis, LJMU, Liverpool/UK, e.e.blancodavis@ljmu.ac.uk
Milad Armin, ENKI Marine, Liverpool/UK, m.armin@enkimarine.co.uk
Alex Routledge, Armada Technologies, Birkenhead/UK, alex.routledge@armada-technologies.com

Abstract

This paper presents the challenges of developing and optimising a second-generation Passive Air Lubrication System (PALS). After presenting the general working principle of this system, the paper focuses on the geometry optimisation of the system itself and the arrangement in the vessel. The challenges and limitations of the associated CFD computations will be discussed. Experimental test results under laboratory conditions and validation of the system's design will be presented qualitatively. An exemplary arrangement for a PALS will be shown.

1. The Challenge

Recent and future regulations require significantly reduced emissions from merchant shipping, *IMO (2023*). While current and emerging technologies offer quite a range of options for new-builds, these are considerably more limited for vessels already in operation.

One of these options available to vessels in service is to reduce the required propulsive power –and consequently fuel consumption and emissions– by reduction of resistance, e.g., by using air lubrication. Installation of an air lubrication system in an existing ship poses the dual challenge of integrating the system within pre-existing hull structures, without impacting hydrodynamic performance. And, in some cases, resolving challenges associated with limited volumetric space availability to house system components, e.g., air compressors. Further, existing auxiliary engine power is often limited, constraining the possibility of installing large-capacity air compressors.

2. Working Principle

2.1 Air Lubrication – A Short Literature Review

Hassan et al. (2006) reported that an increase in microbubble concentration leads to a reduction in the Reynolds stresses and turbulence production in the boundary layer (B.L.). *Sindagi et al. (2019)* stated that the drag reduced by microbubble drag reduction (MBDR) is due to alteration of the viscosity density of the fluid in the B.L. These changes reduce the Reynolds' stresses, which minimises shear stress. Work done by *Gao et al. (2023)* states that bubbles within the B.L. minimise the effect of formation and development of turbulence, if the air is injected into the laminar region.

The resultant net shear stress is reduced since the bubbles have lower shear stress than most solids. In some work, it is thought that the introduction of air reduces the overall viscosity of the B.L. and hinders turbulence production near the hull, *Stephani et al. (2006)*, *Hassan et al. (2008)*, and *Jiménez and Pinelli (1999)*.

Hassan and Gutiérrez-Torres (2006) reported that the increase of microbubbles within a B.L. is inversely proportional to the Reynolds stress. Reynolds stress measures the turbulent fluctuations in a fluid flow. It is responsible for the transfer of energy from large scales to small scales in fluid flow. This also holds for turbulence production. As more air is introduced, turbulence production is delayed, *Stephani et al. (2006)*.

According to *McCormick and Siddiqui (1989)*, when bubbles split, they do so by extracting turbulence energy, therefore reducing turbulence. Turbulence energy is the amount of kinetic energy present in turbulent flow. It is measured in turbulent kinetic energy (TKE), and it is the sum of the kinetic energy associated with the velocity fluctuations, related to the Reynolds stress. TKE is generated by the action of large-scale velocity fluctuations, which are transferred to smaller scales via cascading. Later this was proven to be true when a particle image velocimetry (PIV) technique was used by *Jacob et al. (2010)*. Additionally, it was found that the flow velocity gradient changes in the turbulent layer. This could be because bubbles migrate into vortical structures thus disrupting them, *Sanders et al. (2006)*, *Murai (2014)*, *Elbing et al. (2008)*.

When the bubbles split, the diameter is reduced making the bubbles smaller. When the bubbles become smaller, they will be pushed away from the wall due to buoyancy effects and turbulent eddies. This will result in a restoration of the turbulent boundary layer (T.B.L.) and reduction of void fraction. As the smaller bubbles escape the T.B.L. further away from the injection point, only the larger bubbles will be left, leading to an overall reduction of void fraction and bubble concentration, *Kawamura et al. (2003)*. The higher the Reynolds number (Re), the higher the turbulence shearing effect and bubble breaking; therefore, bubble escaping will increase. This can result in a problem of persistence down stream of injection, *Pavlov et al. (2020)*.

Sanada et al. (2009) observed that the bubble trajectory and its place within the T.B.L. is strongly dependent on the Re. *Legendre et al. (2003)* used Direct Numerical Simulations (DNS) to model two spheres to study their relative motion and direction. It was concluded that direction and motion changed in accordance with the Re.

Kawamura et al. (2002) concludes that as the bubbles flow away from the injector they converge to an equilibrium value that is dependent on the local shear rate. Splitting takes places at around 1 – 10x the B.L. thickness while coalescence takes place at 100 x the B.L. thickness.

Work done by *Sindagi et al. (2019)* shows how the coefficient of friction (CF) increases further away from the injection both longitudinally and transversely as can be seen in Fig.1.

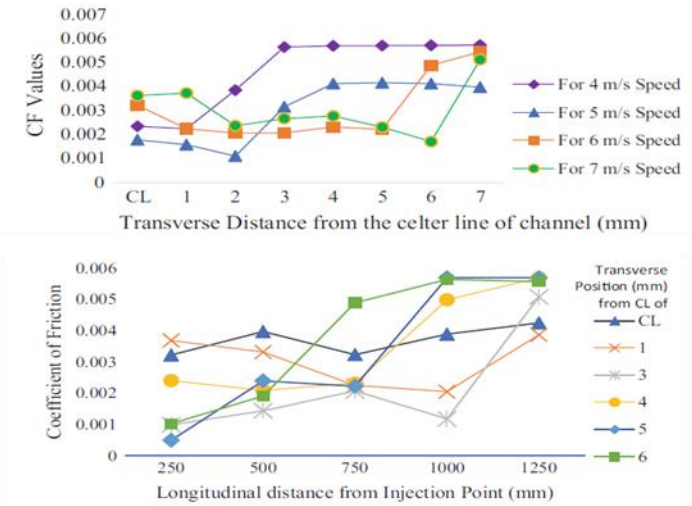


Fig.1: Increase of coefficient of friction with distance according to *Sindagi et al. (2019)*

Kodama et al. (2002) showed that drag reduction in the spanwise direction is not uniform and it decreases further away from the centreline of injection. *Sanders et al. (2006)* and *Elbing et al. (2008)* reported that the drag reduction effect is lost the further downstream the drag is measured. This was thought to be due to the near-wall shears in the B.L.

This wall shear makes the bubbles move from the wall's surface. *Harleman (2012)* later confirmed this. Therefore, the shape with respect to the injection point is also an important parameter. *Jang et al. (2014)*

did a study whereas a side wall of 10 mm height was put on a flat plate to avoid bubble escaping and using a side wall proved to be more effective.

As can be seen appreciated from this review any air injection into the boundary layer of a vessel will result in rather complex flow phenomena, not all of which can be completely resolved presently in any fluiddynamic simulations that accounts for the full-scale situation.

2.2 Passive Air Lubrication System

Armada's Passive Air Lubrication System works on the Bernoulli principle and can be considered a naturally aspirated alternative to the active ALS currently on the market. The working principle uses the ship's forward motion to create a precise pressure differential between geometrically refined inlet and outlet transition pieces. This pressure differential develops the net driving force to 'power' the system.

As the ship moves forward, seawater enters the ship through a series of inlet transition pieces (the number varies depending on the application). The water transits through a low-pressure region (inline venturi subsystem), creating a net suction of air from deck level. Subsequently, a precise mixture of air and water is delivered downstream via an outlet transition piece back to the vessel boundary layer for optimal drag reduction performance.

Between each of the inlet and outlet transition pieces, the ejector (venturi) and a diffuser sit. The unique design of these sub-components allows for the development of a refined air-water ratio and a superior level of control of bubble size and homogeneity.

The PALS performance control system and machine learning capability support the system, which is designed with logic to tune the system set points to the prevailing vessel operating condition. An isometric view of the PALS is shown in Fig.2.

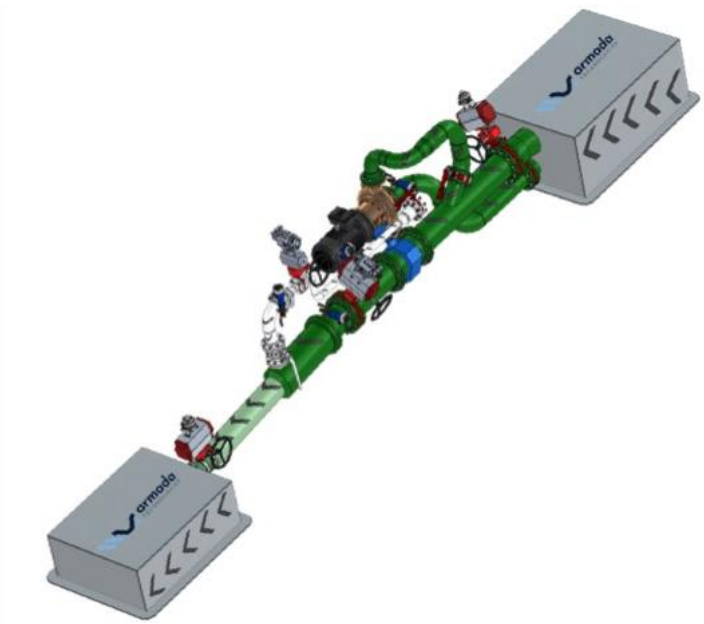


Fig.2: Isometric view of Armada's PALS

3. CFD Simulations

3.1 Global Simulations

3.1.1 CFD Methodology

The CFD simulations used for the geometry optimisation in this project have been run using a specialized and upgraded version of OpenFOAM®; details are given in *Renzsch et al. (2017)* and *Meyer et al. (2016)*. In this CFD code, the Reynolds-averaged Navier-Stokes equations (RANS) are solved on an unstructured grid using the finite volume method. Pressure velocity coupling uses the PIMPLE method, a combination of the SIMPLE, *Patankar and Spalding, (1972)*, and PISO methods, *Issa (1985)*.

Turbulent viscosity is computed using the k-ω-SST turbulence model, *Menter et al. (2003)*. The free surface is captured by applying the Volume-of-Fluid (VoF) method, *Hirt and Nichols (1981)*. The BRICS scheme, *Wackers et al. (2011)*, is used for convective transport of the VoF-scalar, providing compressive behaviour to keep the interface sharp. Bubble dynamics are disregarded; only the presence and amount of air underneath the hull are computed by this approach.

3.1.2 Case Setup Intake / Injector

To evaluate intake/injector properties and align with the tests conducted at HSVA (see section 4), the intake and injector are analysed and mounted in a channel with similar dimensions to HSVA's *Hydrodynamic and cavitation tunnel* (HyKaT). Fig.3 shows the injector and the balance plate arranged in the domain. The significant length upstream is intentional in allowing the boundary layer to fully develop.

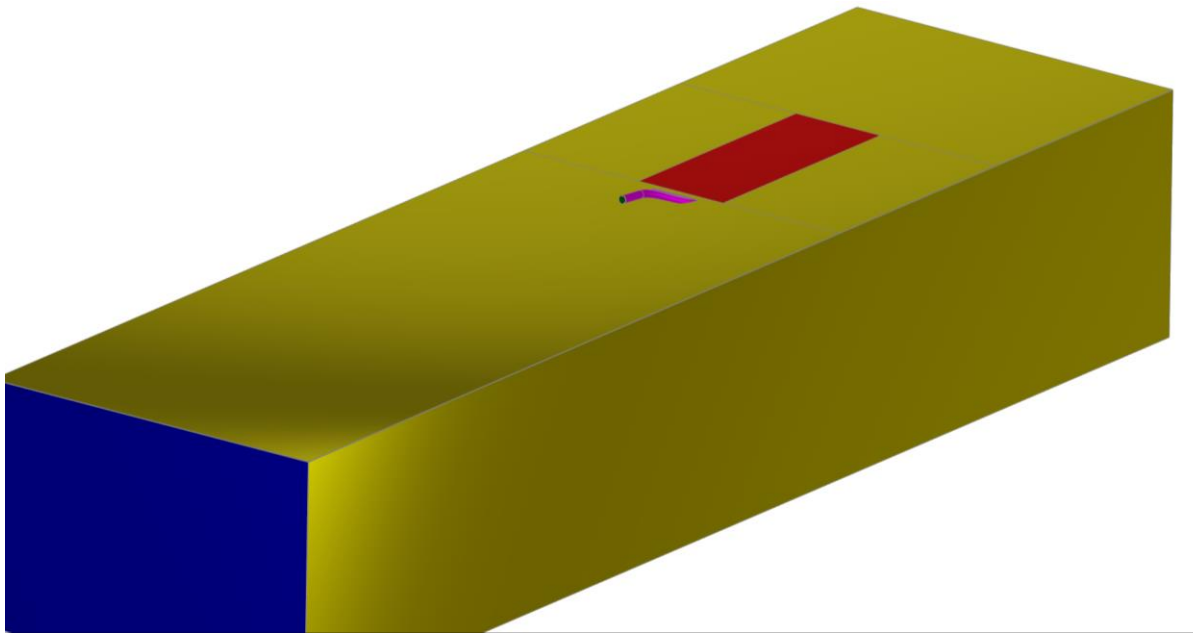


Fig.3: Schematic of injector and reference plate in domain

While the intake and injector geometries are parametrised (see section 5), design requirements fix basic dimensions like the system's length.

Due to the venturi pump's working principle and requirements, the volumetric flow rate (respectively velocity) at the inboard boundaries of intake and injector is prescribed. The pressure differential between the boundaries of intake and injector is monitored. One of the constraints during the optimisation is that a sufficient pressure differential must be maintained to drive the venturi pump.

To evaluate the quality of the air injection, the volume fraction on a plate downstream from the injector is monitored. Further, as a qualitative criterion, the stability of the air carpet is visually inspected, and geometries generating a highly transient behaviour are discarded from the optimisation process.

3.2 Simulations at Bubble Level

Experimental laboratory work done by *Qin et al. (2017)* shows oscillation in drag reduction due to bubble motion and behaviour, as seen in Fig.4. The graph depicts the coefficient of friction on the y-axis and the distance along the plate on the x-axis. As the air moves further down the plate, see section IV in Fig.4, the air turns into bubbles. This results in oscillating drag and lift due to the motions of the bubbles in the turbulent boundary layer (T.B.L.).

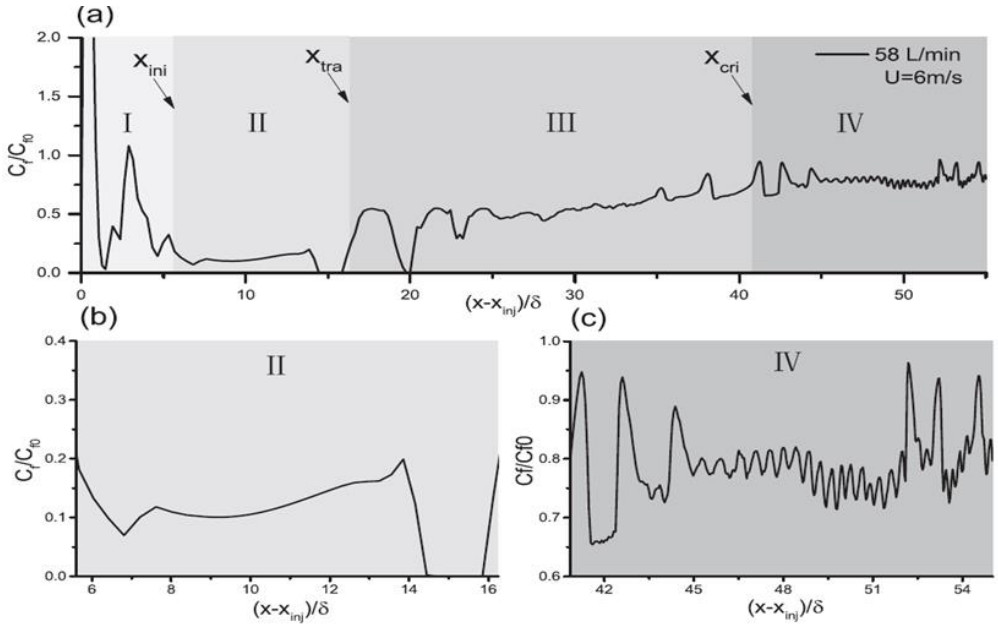


Fig.4: Bubble Oscillations Effect on drag reduction (D.R.), *Qin et al. (2017)*, with close-ups given in (b) and (c) for section II and section IV, respectively

The CFD simulations shows oscillating behaviour, Fig.5. Whilst numerical oscillations do occur, they do not happen at the same frequency and range. Hence, the behaviour of these oscillations is due to the air bubbles moving around in the T.B.L., giving confidence in the CFD model as it apparently captured such a tricky behaviour seen in experimental laboratory testing.

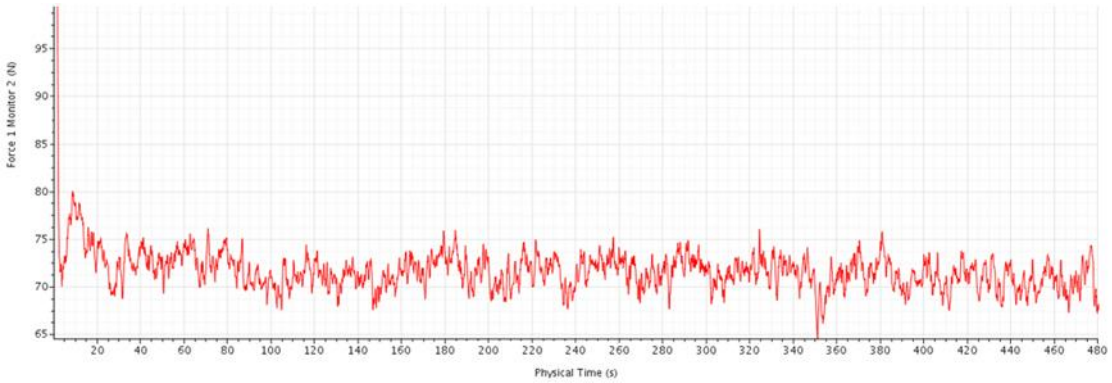


Fig.5: D.R. Across Modelled Plate with Oscillations

When the bubbles split, their diameter is reduced, making them smaller. As they become smaller, they will be pushed away from the wall due to buoyancy effects and turbulent eddies. This will result in a restoration of the T.B.L. and a reduction of the void fraction.

As the smaller bubbles escape the T.B.L. further away from the injection point, only the larger bubbles will be left, leading to an overall reduction of void fraction and bubble concentration, *Kawamura et al. (2003)*. The higher the Reynolds number, the higher the turbulence shearing effect and bubble breaking; therefore, bubble escaping will increase. This can result in a problem of persistence downstream of injection *Pavlov et al. (2020)*.

Sanders et al. (2006) prove that the shear flow of the B.L. will not let the bubbles be in contact with the hull. The bubbles will be suspended at a location underneath the surface unless the bubbles coalesce and stratify. This thin layer of liquid between the hull and bubbles is sometimes called the "liquid layer" and can be seen in Fig.6, *Elbing et al. (2008)*.

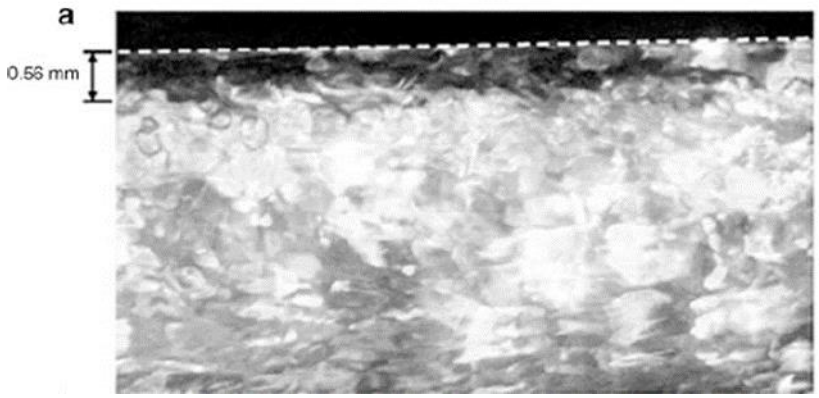


Fig.6: Observing the Liquid Layer, *Elbing et al. (2008)*

This is further explained in Fig.7. Part (a) shows how the B.L. is initially divided into a viscous sub-layer, buffer layer, outer layer, and flow region. Part (b) demonstrates how another layer is added, the bubbly two-phase layer between the outer and buffer layers, *Adrian (2007)*. This agrees with the findings from *Madavan et al. (1984)*, *Merkle et al. (1990)*, *Kanai and Miyata, (2001)*, and *Hassan et al. (2008)*, where it was deduced that the concentration increases away from the wall up to a peak value and then decreases to zero once in the free stream.

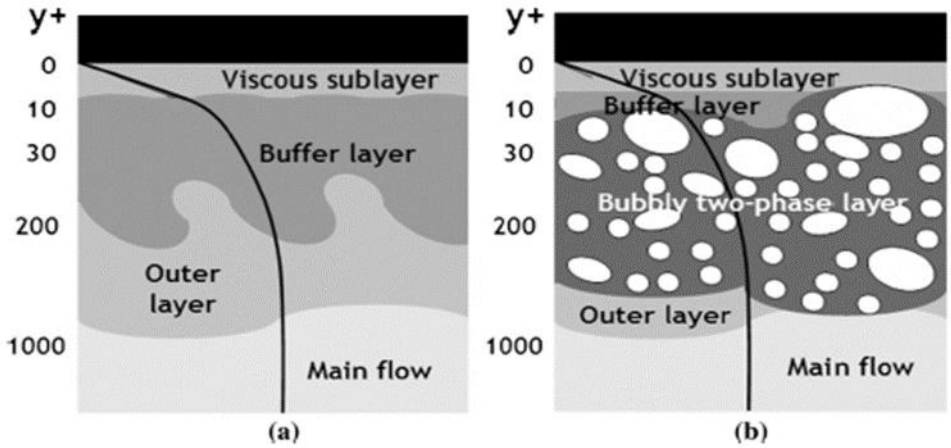


Fig.7: Boundary Layer with and Without Air Injection, *Adrian (2007)*

This also occurs in the CFD simulations, Fig.8: The bubbles do not touch the flat plate, as mentioned in the literature previously and seen in Fig.4 and Fig.5. This was noted across all models in same-plate testing, Reynolds-variance testing, and scaling-up testing. It further confirms the robustness of the CFD model and its ability to replicate sufficiently the air-water interaction behaviour observed in experiments.

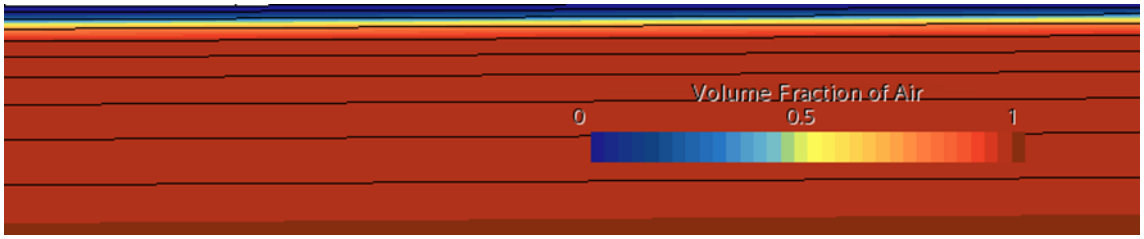


Fig.8: Liquid layer at the wall of the plate replicated by CFD

4. Experimental Testing

Armada Technologies has performed a series of targeted demonstration tests at the world-leading facility, HSVA, in Hamburg. HSVA not only operates the world's largest commercial cavitation tunnel (Hykat) but is also 'the' preeminent testing facility for Air Lubrication systems globally. Similarly, HSVA regularly attends sea trials of ALS to gain full-scale performance validation.

The test variables included:

1. Ship speed (represented by Hykat tunnel flow speed, in m/s)
2. Ship draught (represented by Hykat tunnel pressure, in kPa)
3. ATL water pump speed (m^3/hr)
4. ATL active air delivery rate (m^3/hr).

The results evidenced that the PALS design effectively introduced a layer of high-quality aerated water to the simulated vessel boundary layer. Similarly, complete passive aeration of PALS is achievable under the simulated operating conditions. The results indicate the existence of a drag reduction 'sweet spot' where two hydrodynamic phenomena are effectively balanced at every discreet operating condition, namely:

- The momentum balance between external and injected flow for favourable boundary layer behaviour.
- The optimal air-water-mixture ratio for best reduction of viscous resistance.

It was also identified that water injection alone already yields a certain drag reduction. Fig.9 gives an impression of the air bubbles coming out of the injector during the HyKaT experiments.


Fig 9: Air bubbles being injected during HyKaT experiments

5. Parametric Models and Geometry Optimisation

When optimizing a product, the effort of exploring the design space and exploiting the potential for further improvement scales up rapidly with the number of free variables of the systems, i.e., the degree of freedom (DoF). The more free variables, the more variants are needed, *Harries (2020)*.

Consequently, a deliberate variability reduction is built into a system instead of allowing any conceivable freedom. This is usually realised by defining a product with as few descriptors, typically called parameters, as possible. In Computer-Aided Design (CAD), this approach is generally referred to as parametric modelling. In this study, the Process Integration and Design Optimisation platform CAESES® by Friendship Systems has been used for parametric modelling, design space exploration, and optimisation.

5.1 Intake / Injector

As first step the intake (whose task it is to provide sufficient dynamic pressure at for the venturi at a given flow rate) and the injector which in turn shall create an efficient bubble distribution downstream are optimised.

A fully-parametric approach has been chosen for both the intake and the injector to provide large design flexibility within the intended design space. This approach allows for the variation of all relevant angles, distances, radii, and cross-sections with a very low number of design variables. Fig.10 shows a generic representation of the injector model. It is worth noting that the fully-parametric model is the same for both intake and injector but the target functions differ.

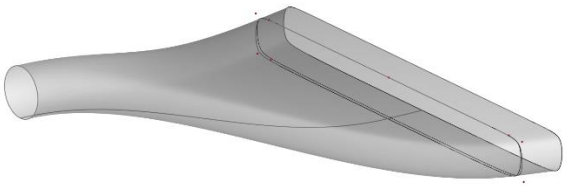


Fig.10: Generic representation of parametric injector model

First, the plausible design space is evaluated to optimise intake and injector geometry. This is achieved using a Sobol distribution of the variables within the parameter bounds. Approximately 60 variants are required to characterise the design space properly for six free variables. Based on this description, a response surface model is set up to search for actual optima. Here, another six variants were required until reaching the point of diminishing returns.

Having optimised the geometry of the intake and the injector, respectively, for generic set-ups situations that are representative of the flow situation encountered beneath the hull, an individual arrangement has to be found for each specific hull form to benefit from the PALS the most.

5.2 Arrangement

First, the hull geometry was imported into CAESES and kept fixed to model and optimise the arrangement of the PAL systems. Five optimised systems (optimised as discussed above) were placed in the vessel, with locations described by parameters giving longitudinal and transversal positions. Constraints were placed on the possible locations to take the vessel's geometric limitations into account and avoid interference between the systems. A generic arrangement is shown in Fig.11.

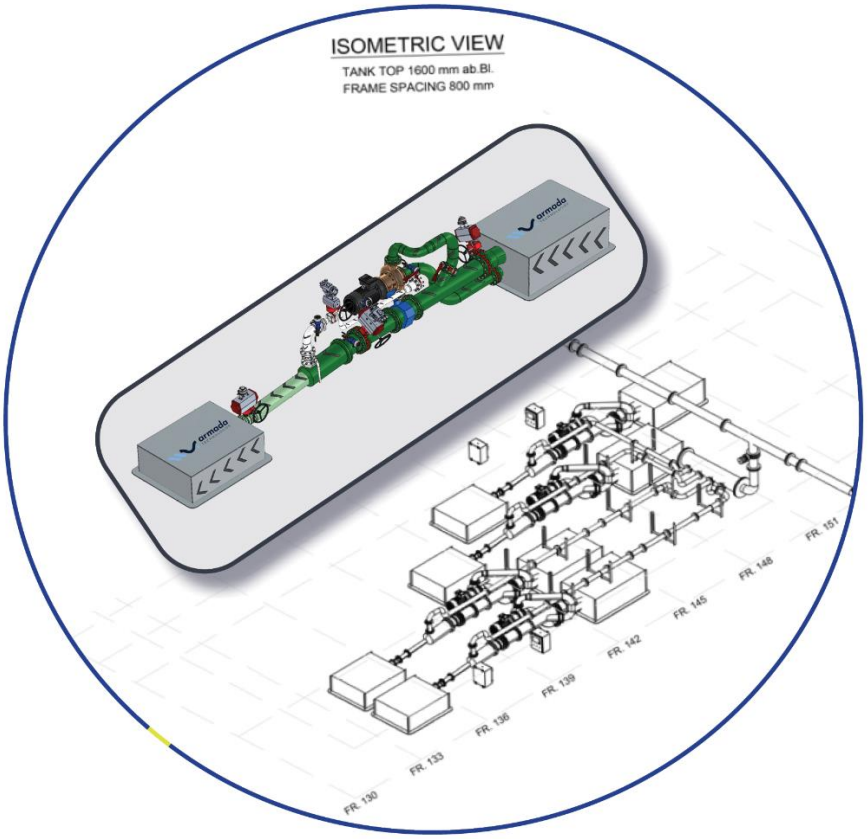


Fig.11: Generic arrangement in vessel

While the vessel's structure dictated discrete steps in the possible locations of some places, this does not lend itself well to numerical optimisation approaches. Therefore, the arrangement was initially optimised in a continuous design space (within the constraints), and moved to the nearest feasible location afterwards.

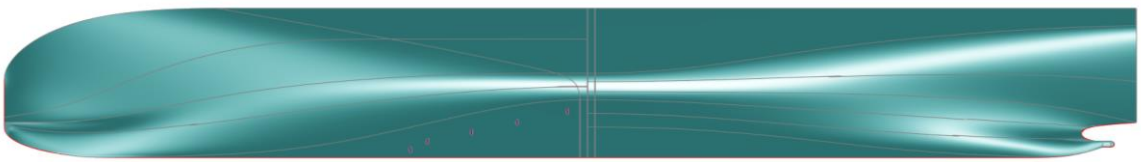


Fig.12: Global view on initial arrangement in vessel

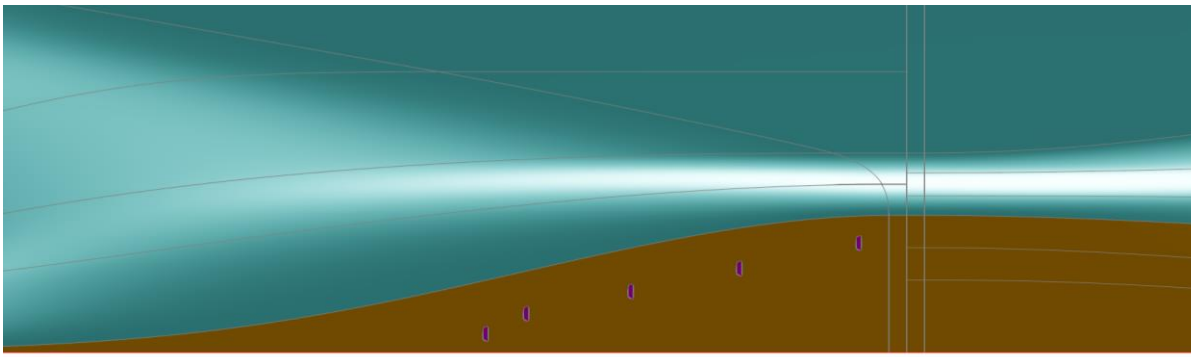


Fig.13: Close-up of initial arrangement and permissible installation region (gold)

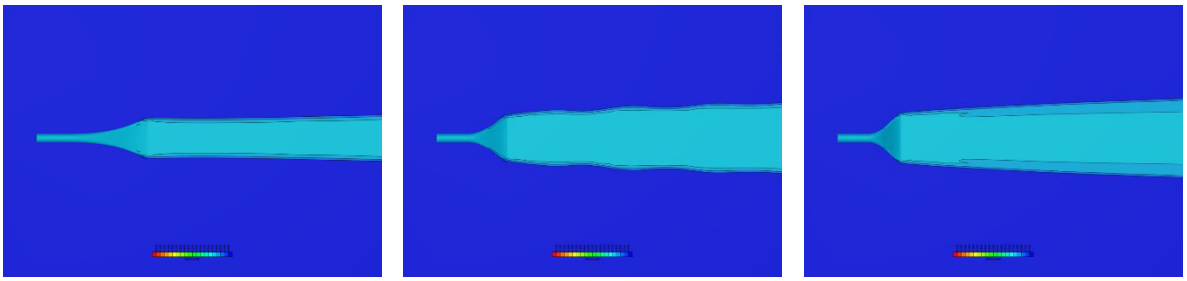
Fig.12 gives a global overview of the vessel investigated in this study and the initial arrangement before optimisation. In the close-up, Fig.13, the permissible region – the flat of bottom – is depicted in gold.

The optimisation approach is similar to that used previously for the intake/injector. A total of 70 variants were used to explore the design space and 15 for the response surface-based optimisation.

6. Exemplary Results

6.1 Intake / Injector

The design space exploration and subsequent optimisation of the injector's shape have shown that the bubble distribution downstream highly depends on the injector's shape. In Fig.14 some unfavourable bubble distributions are shown: While some geometries introduce narrow but highly concentrated bubble streams (a), others may create oscillations due to destabilising the boundary layer (b), or a highly inhomogeneous distribution (c). Ideally, a wide-spread, stable bubble stream with sufficiently high and homogeneous concentration is sought (Figure 15). With the same amount of air injected, the improvement in air coverage of the balance plate from worst to best is 15%.



(a) narrow (b) unstable (c) inhomogeneous

Fig.14: Unfavourable bubble distributions

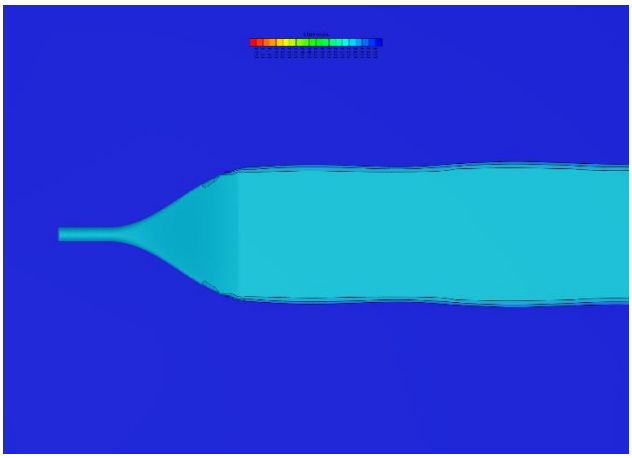


Fig.15: Favourable bubble distribution

6.2 Arrangement

Besides the obvious question on overall longitudinal installation – is it favourable to have the systems as far forward as possible to maximise covered length or is there too much air lost by disturbances due to crossflow across the forward bilge? – the quality of the air bubble coverage appears to be a determining factor.

On this particular hull shape (low block coefficient c_B), a far-aft installation, Fig.16, can harm coverage quality as the bubbles enter the lower-speed thick boundary layer region aft before the sheet stabilises.

In the optimised installation, Fig.17, only the innermost systems are brought forward and inboard significantly. Even though a gap appears in the bubble carpet, the bubble coverage on the stern gondola is improved.



Fig.16: Far-aft installation arrangement



Fig.17: Optimised arrangement

7. Conclusions

The challenge of reducing emissions in merchant shipping is pressing, driven by recent and impending regulations. For existing vessels, options are limited, making solutions such as air lubrication systems (ALS) vital. Integrating ALS into existing ships poses significant challenges, including space constraints and potentially additional engine power.

Armada's Passive Air Lubrication System (PALS) operates using the Bernoulli principle, relying on the ship's motion to generate the necessary pressure differential for system operation. This innovative approach mitigates the need for large-capacity air compressors, making it suitable for retrofitting existing vessels. Instead, by utilising the dynamic pressure head from the vessels forward motion the power to drive the venturi pump is provided by the main engine. While this results in a small increase of pressure drag the air bubbles yield a significantly larger reduction of viscous drag, giving a net reduction of total resistance. Computational Fluid Dynamics (CFD) simulations, utilising advanced models and methodologies, play a crucial role in optimising the system's components and evaluating performance.

Experimental tests at HSVA validated PALS, demonstrating effective drag reduction by creating a high-quality aerated layer. The tests identified an optimal balance of hydrodynamic phenomena that maximises drag reduction at specific operating conditions. Additionally, parametric modelling and optimisation were employed to refine the intake and injector designs, ensuring efficient bubble distribution and system arrangement within the vessel.

Overall, the development and optimisation of PALS through a combination of CFD simulations and experimental testing offer a promising solution to reduce fuel consumption and, hence, emissions in existing merchant ships, addressing regulatory requirements and contributing to more sustainable maritime operations.

Acknowledgements

This research was funded by project "RETROFIT solutions to achieve 55% GHG reduction by 2030" (RETROFIT55) - Horizon Europe programme, Grant Agreement No. 1011096068".

References

ADRIAN, R.J. (2007), *Hairpin vortex organization in wall turbulence*, Physics of Fluids 19(4). doi:10.1063/1.2717527

ELBING, B.R.; CECCIO, S.L.; WINKEL, E.S.; PFLUEGER, A.J.; MEINHART, C.D.; PERLIN, M.; DOWLING, D.R. (2008), *Bubble-induced skin-friction drag reduction and the abrupt transition to air-layer drag reduction*, J. Fluid Mechanics 612, pp.201-236

GAO, Q.; XU, J.; WANG, Z.; ZHANG, L.; MA, Y.; FENG, J. (2023), *Experimental study on bubble drag reduction by the turbulence suppression in bubble flow*, Ocean Engineering 272

HARLEMAN, M.J. (2012), *On the effect of turbulence on bubbles: experiments and numerical simulations of bubbles in wall-bounded flows*, Ph.D. Thesis, TU Delft, The Netherlands

HARRIES, S. (2020), *Practical shape optimization using CFD: State-Of-The-Art in industry and selected trends*, COMPIT Conf., Pontignano,

HASSAN, Y.A.; GUTIÉRREZ-TORRES, C.C. (2006), *Investigation of drag reduction mechanism by microbubble injection within a channel boundary layer using particle tracking velocimetry*, Nuclear Engineering and Technology 38(8), pp.763-778

HASSAN, Y.A.; GUTIÉRREZ-TORRES, C.C.; BARBOSA-SALDAÑA, J.G.; JUÁREZ-BADILLO, J.A. (2008), *Drag reduction by microbubble injection in a channel flow*, Revista Mexicana de Física 54(1), pp.8-14

HIRT, C.W.; NICHOLS, B.D. (1981), *Volume of fluid (VOF) method for the dynamics of free boundaries*, J. Computational Physics, 1/39

IMO (2023), *IMO strategy on reduction of GHG emissions from ships*, MEPC.377(80), Int. Mar. Org., London

ISSA, R.I. (1985), *Solution of the Implicitly Discretized Fluid Flow Equations by Operator-Splitting*, J. Computational Physics, 62, pp.40-65

JACOB, B.; ANDERSON, W.A.; BELWARD, J.A. (2010), *Drag reduction by microbubbles in a turbulent boundary layer*, Physics of Fluids 22

JANG, J.; LEE, S.J.; LEE, D.K.; YOU, D.J.; OH, S.J.; LEE, I. (2014), *Experimental investigation of frictional resistance reduction with air layer on the hull bottom of a ship*, Int. J. Naval Architecture and Ocean Eng. 6(2), pp.363-379

JIMÉNEZ, J.; PINELLI, A. (1999), *The autonomous cycle of near-wall turbulence*, J. Fluid Mechanics 389, pp.335-359

KANAI, A.; MIYATA, H. (2001), *Direct numerical simulation of wall turbulent flows with microbubbles*, Int. J. Numerical Methods in Fluids 35(5), pp.593-615

KAWAMURA, T.; KAKUGAWA, A.; KODAMA, Y. (2002), *Controlling the size of microbubbles for drag reduction*, 3rd Symp. Smart Control of Turbulence, http://www.nmri.go.jp/turbulence/PDF/symposium/FY2001/Kawamura.pdf

KAWAMURA, T.; TAKAHASHI, T.; KODAMA, Y.; KAKUGAWA, A.; TAKEDA, H. (2003), *Effect of bubble size on the microbubble drag reduction of a turbulent boundary layer*, ASME/JSME Joint Fluids Engineering Conf. 2A, pp.647-654

KODAMA, Y.; KAKUGAWA, A.; TAKAHASHI, T.; NAGAYA, S.; SUGIYAMA, K. (2002), *Microbubbles: Drag reduction mechanism and applicability to ships*, 24th Symp. Naval Hydrodynamics, pp.1-19

LEGENDRE, D.; MAGNAUDET, J.; MOUGIN, G. (2003), *Hydrodynamic interactions between two spherical bubbles rising side by side in a viscous liquid*, J. Fluid Mechanics 497, pp.133-166.

MADAVAN, N.K.; DEUTSCH, S.; MERKLE, C.L. (1984), *Reduction of turbulent skin friction by*

microbubbles, Physics of Fluids 27(2), pp.356-363

McCORMICK, J.M.; SIDDIQUI, M.U. (1989), *Microbubble formulation and splitting in a turbulent boundary layer for turbulence reduction*, Advances in Fluids Dynamics, pp.168-217

MENTER, F.R.; KUNTZ, M.; LANGTRY, R. (2003), *Ten Years of Industrial Experience with the SST Turbulence Model*, Turbulence, Heat and Mass Transfer 4, Begell House, pp.625-632

MERKLE, C.L.; DEUTSCH, S. (1990), *Drag Reduction in liquid boundary layers by gas injection*, in The Smithsonian/NASA Astrophysics Data System, pp.351-412

MEYER, J.; RENZSCH, H.; GRAF, K.; SLAWIG, T. (2016), *Advanced CFD-Simulations of free-surface flows around modern sailing yachts using a newly developed OpenFOAM solver*, 22nd Chesapeake Sailing Yacht Symposium, Annapolis

MURAI, Y. (2014), *Frictional drag reduction by bubble injection*, Experiments in Fluids 55(7)

PAVLOV, G.A.; ORLOVA, I.P.; KUDRYAVTSEV, I.V.; PAVLOVA, M.V. (2020), *Air Lubricated and Air Cavity Ships*, Springer

QIN, S.; OKA, Y.; TAKAHASHI, H.; FUKUDA, K. (2017), *Stream-wise distribution of skin-friction drag reduction on a flat plate with bubble injection*, Physics of Fluids 29(3)

RENZSCH, H.; MEYER, J.; GRAF, K. (2017), *Investigation of Modern Sailing Yachts Using a New Free-Surface RANSE Code*, Int. Conf. Innovation in High Performance Sailing Yachts, Lorient

SANADA, T.; IGUCHI, M.; NAKATANI, A.; YOSHIDA, T. (2009), *Motion and coalescence of a pair of bubbles rising side by side*, Chemical Eng. Science 64(11), pp.2659-2671

SANDERS, W.C.; WINKEL, E.S.; DOWNING, D.R.; PERLIN, M.; CECCIO, S.L. (2006), *Bubble friction drag reduction in a high-Reynolds-number flat-plate turbulent boundary layer*, J. Fluid Mechanics 552, pp.353-380

SINDAGI, S.; DASH, S.K.; BANERJEE, J.; RAMESH, O. (2019), *Numerical investigation of influence of microbubble injection, distribution, void fraction and flow speed on frictional drag reduction*, Lecture Notes in Civil Engineering, Springer

STEPHANI, K.A.; BEUTNER, T.L.; WITTMER, K.; BUSHNELL, D.M. (2006), *Drag Reduction using Trapped Bubbles on a Flat Plate Surface*, American Institute of Aeronautics and Astronautics, pp.1-19

WACKERS, J.; KOREN, B.; RAVEN, H.C.; VAN DER PLOEG, A.; STARKE, A.R.; DENG, G.B.; QUEUTEY, P.; VISONNEAU, M.; HINO, T.; OHASHI, K. (2010), *Free-surface viscous flow solution methods for ship hydrodynamics*, Archives of Computational Methods in Engineering 18, pp.1-41

How to Retrofit 400 kW of Green Hydrogen Power into an Offshore Supply Vessel as an Add-on System

Frederike Engels, E-Cap Marine GmbH, Hamburg/Germany, fen@ecap-marine.com
Josefin Klindt, E-Cap Marine GmbH, Hamburg/Germany, jkl@ecap-marine.com
Lars Ravens, E-Cap Marine GmbH, Hamburg/Germany, lra@ecap-marine.com

Abstract

In February 2024 we finalized the commissioning of a 400kW fuel cell (FC) power system onboard the Offshore Supply Vessel (OSV) "Coastal Liberty". Its travel route lies in the nature reserve zone Wadden Sea in the North Sea and the OSV shall deliver emission free power for that zone. Our FC power system is a 20-ft.-unit equipped with the fuel cells, batteries, inverters, power management components, and all relevant safety components. The hydrogen tank is designed as a 10-ft.-unit while the hydrogen valve system is also included in the FC power container. The FC power container is class approved by DNV and witnessed by Dutch flag with an Alternative Design Approach. This paper highlights the challenges and lessons learnt from our experience. In addition, it gives insights into the operation of the system and the safety philosophy of the very first German DNV approved hydrogen powered vessel.

1. Introduction

The obstacles and insights from this project have been so significant that we decided to write a paper on this topic. First, let's introduce eCap Marine. We deliver system integration solutions for emission-free power generation. This implies that when a customer aims to reduce their company's emissions, they frequently have a specific solution in mind. This could involve a new ship, the conversion of an existing ship, or shore power delivery. We then develop a concept by conducting feasibility studies or analysing the available market possibilities.

For this particular project, the initiators were the owner of an oil rig platform in the Wadden Sea nature reserve and their logistical sub-supplier. The sub-supplier is responsible for delivering goods to the platform and transporting the residuals of the rigging process. This includes drilling mud, and due to the environmental protection of the nature reserve, even rainwater is collected and brought to shore.

Consequently, the logistician owns a fleet of offshore supply vessels, two passenger vessels, and two cargo ships. The Coastal Liberty is one of the cargo ships that travels daily to the Mittelplate, either delivering or collecting goods and liquids. It has a LOA of 43m, its beam is 9m and the draft is 1.35 to 1.6m. The crew usually consists of 4 members, and the vessel is able to carry 6 20-ft.-containers and approximately 80 tonnes of liquids.

To reduce this vessel's emissions, the logistician contacted eCap Marine and ordered a feasibility study. We did a power measurement and delivered first concepts for the conversion. Then, it took a long way from the initial idea to the realization because first details were discussed with DNV so that we received an Approval in Principle. Funding takes time, so that in the first quarter of 2022 we received the final order and started the detailed engineering phase. The project commissioning on board started in October 2023 and the sea trials were performed in February 2024. The biggest challenge, so to say, was the time frame.

This paper will focus on the challenges and learnings of the conversion of this vessel. First, it will focus on the design approach and the limitations resulting from the feasibility study, the funding programme, flag and class requirements. Later it shows a deeper insight into the solutions and safety aspects of the whole concept.

2. General requirements for the retrofit of the Coastal Liberty

The framework for the most important requirements was given by the vessel: Flag state is supposed to be the Netherlands and the class is DNV. First steps of eCap Marine thus were to investigate the space requirements, required power and endurance of the travel. This was done in the first phase: Design of the concept.

2.1. Design of the concept

For the very first ideas, we travelled to the ship and took a tour to the Mittelplate. This also gave us lots of time to measure the space that might be occupied by our solution and to have a look into the engine room. Typically, this offshore supply vessel used in the Wadden Sea has a very small draft and consequently the space in the engine room was very limited. Immediately it was decided that the space on the very aft of the ship will be used for a containerized solution and the engines in the engine room need to be retrofitted to include electric motors and new gear boxes into the powertrain.



Fig.1: Deck of the Coastal Liberty

2.1.1. Travel route requirements

From the very beginning it was clear that emission free power sources have a high footprint and will be pioneer work, so the owner decided to aim for the best option regarding space and environmental footprint: The concept shall be designed for the slow-steaming phase of the vessel, Fig.2.



Fig.1: Travel route and emission-free power generation phases of the Coastal Liberty

In order to reduce noise and exhaust emissions, the vessel is already going 5-6 kn in the zone of the nature reserve. This part of the travel route takes ~1 hour in contrast to half an hour of manoeuvring and faster speeds in the Elbe estuary. Consequently, the biggest part of pollution is the slow steaming part which then only requires a total power of 300 kW, meaning 100 kW per each of the propellers. The hotel load shall also be provided by the alternative power generation system.

The HAZID requirements from the oil rig platform led to the conclusion that it will not be possible to generate emission-free power when the vessel is in the platform. For this reason, the vessel is connected to shore power there and the emission-free power generation system is not running.

2.1.2. Power requirements

The full power required during the above-mentioned emission-free phases was measured during a power tracking day on board. The full power of 357 kW per each engine is not needed to be fully supplied by the emission-free power generation system. Slow steaming was measured to be feasible with 100 kW on each propeller, so in total 300 kW are required to power the main drive. Hotel load is assumed to be 100 kW, which results in a total power requirement of 400 kW for the emission-free power generation system.

2.1.3. Tank requirements

The system soon was chosen to be a hydrogen system, as the customer's sister company also planned to build an electrolyser in Cuxhaven. Therefore, a mobile and easy-to-swap tank solution was to be designed which leads to the tanks being able to be transported and also suitable for both, marine application as well as road transport. In the process of Approval in Principle with DNV, it was agreed, that the DNV rules are not designed to certify a compressed hydrogen tank, so the German road transport rules ADR shall be followed. The certification from a renowned certifying body will be accepted by DNV. This left only the integration on ship to be discussed with DNV.

2.1.4. Other requirements

To meet the requirements of the chosen funding programme by our customer, the solution needed to be mobile. The idea consequently was to design a plug and play solution, were only the cables are connected to the ship. As the system will not be moved daily, there is no real plug planned and the cables are firmly attached to the ship.

2.2. Solution: eCap H2 PowerPac

The emission-free power generation system consequently is designed as a 20-ft.-PowerPac which consists of:

- 2x Ballard FCwave fuel cells (in total 400kW)
- 4x Lehmann Marine COBRA (in total 280 kWh)
- DC bus
- Fuel preparation room including safety valves and pressure regulation
- CO2 extinguishing and fire detection system
- Cooling system
- Gas alarm system
- Ventilation system

The eCap H2-PowerPac, Fig.3, is responsible for the power generation as Add-On-System, meaning that the vessel is fully dependent on the existing Diesel engines, but can switch to emission-free power generation if wanted.

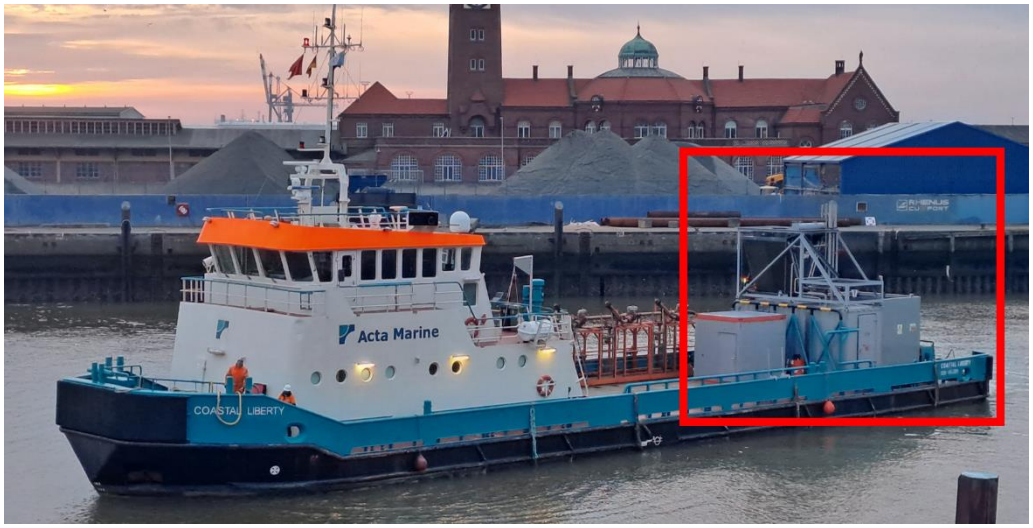


Fig.2: Coastal Liberty with the eCap H2 PowerPac on board

3. Realization of the eCap H2PowerPac

This chapter now introduces the different sub-systems and the challenges that were faced in the realisation of each of them. For a short overview: the eCap H2 PowerPac consists of three main rooms: the fuel preparation room, the fuel cell room and the electrical room. In the picture below, also the couplings are visible in front of the fuel preparation room.

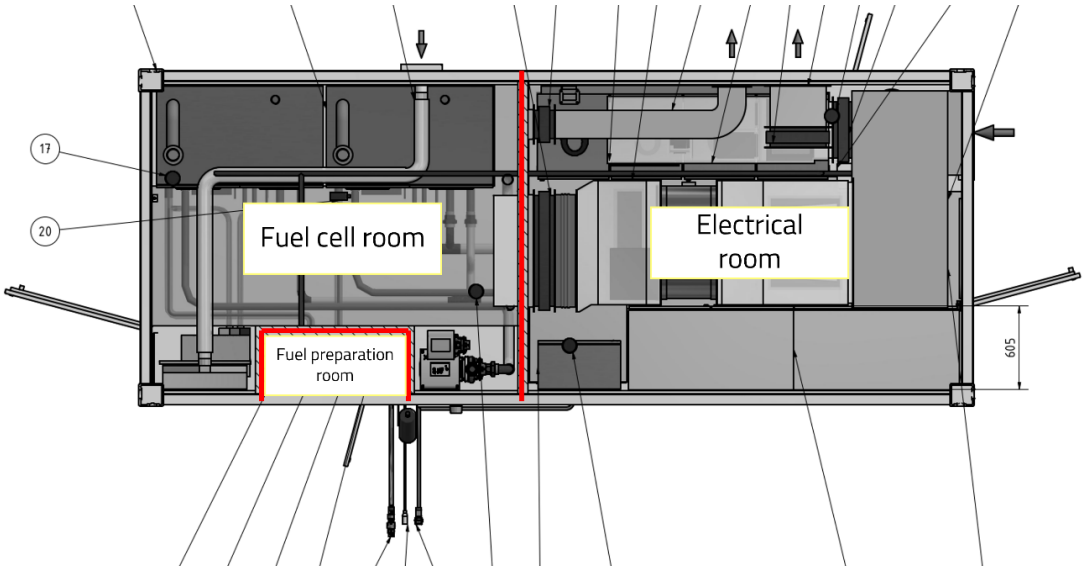


Fig.3: Rooms in the eCap H2 PowerPac

3.1. Certification

The DNV from the start of the Approval in Principle made clear that there are no rules from both, the IMO and DNV, taking hydrogen into account. The rules this project followed were in most cases the IGF code, *IMO (2015)*, and the general DNV rules for the fire extinguishing and A60 insulation, for example. The approval of this concept was done as a case-by-case approval. Therefore, not all components were obliged to have a type approval, as for the hydrogen part this was not possible. No suppliers of hydrogen components have already received a type approval and as far as we heard, this will not be possible until the DNV has its own hydrogen rules. These are outstanding and waiting for the IMO guidelines right now. The handbook for hydrogen-fuelled vessels, *DNV (2021)*, has been published already, but this book does not include specific requirements, it only describes the way of how to approve a hydrogen powered ship.

Fair enough, there is already a IMO interim guideline for the safety of ships using fuel cell power installations, *IMO (2022)*, but this is not giving any help on the, for example, hydrogen supply line. The guidelines are suitable for fuel cell suppliers to meet maritime requirements. Same is the DNV-RU-SHIP Pt.6 Ch.2 Sec.3, *DNV (2021)* which also deals with fuel cells, but no other hydrogen components.

Coming back to our specific project, it is to be noted that, the fuel cell we chose is already type approved. The Ballard FCwave consequently fulfils all rules mentioned above. Meaning: its fuel cell space is designed according to the rules and approved, the gas and fire detection and countermeasures are designed according to the rules and approved, and they leave other not fulfilled requirements to the integrator.

One major component of the certification of a case-by-case approved concept is also the HAZID workshop. This was taken by an independent society and took place in October 2022. The design was basically fix to that point in such a way, that the cause-and-effect diagrams, safety philosophy and system concepts could be fully evaluated in this workshop. Risks were identified, countermeasures decided, and the outcome evaluated.

3.2. Tank system

The tank is designed as a 10-ft.-Tanktainer and ADR certified. This makes it easy to transport and also to reproduce, as the certification is a type approval. For this purpose, the customer ordered 3 tanks in total.

It contains of 13 NPROXX Type IV bottles with a total capacity of 8125 litres of hydrogen leading to approximately 200 kg useful hydrogen at 380 bar. The coupling of that tank was a challenge in the certification process as it was needed to certify it according to both, DNV and ADR rules, *BA (2023)*. It is designed to be leakage free as a quick coupling. The tank itself is daily refuelled at an electrolyser that is 2 km away from the vessel's harbour.

The tank installation on board needed to be guided by cell guides to ease the process of craning the tank also in heavy sea. Additionally, the vessel is equipped with A60 walls around the tank to protect the tank from external fire. In event of fire, the tank will be cooled by a water spray system and taken from board.

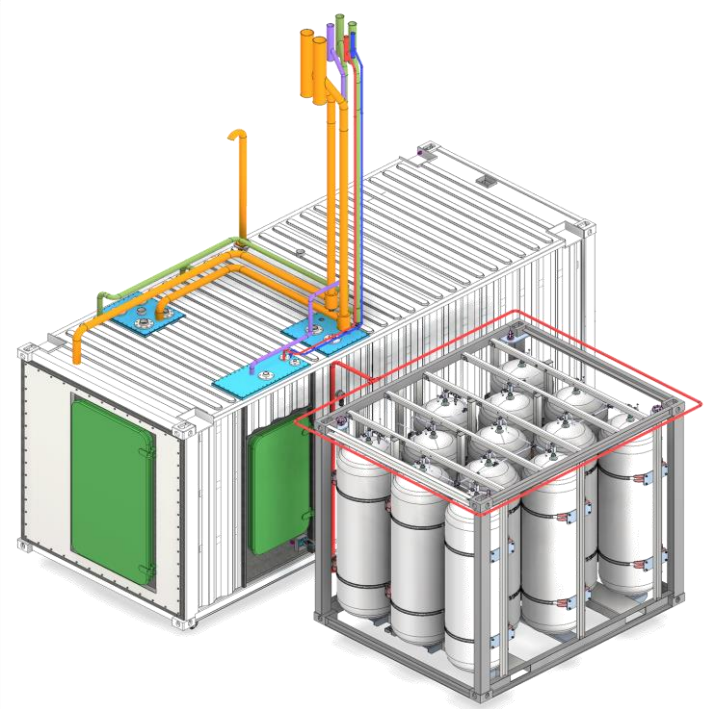


Fig.4: Concept of Tanktainer



Fig.5: The tanktainer during road transport

3.3. Hydrogen system

3.3.2. Fuel preparation room

The hydrogen system and its implementation into the eCap H2 PowerPac for sure was the most challenging part and included the most pioneer work. This project is the first DNV certified hydrogen project with pressurized hydrogen and consequently, also DNV had to face a lot of challenges in guiding us through their rules.

The intake pressure of the hydrogen differs from 380 to 20 bar, depending on the hydrogen tank's fill level. We designed a so-called fuel preparation room according to its requirements in the IGF code that regulates the hydrogen pressure and is equipped with all relevant safety valves, also including a double block and bleed valve, as prescribed by the IGF code.

The fuel preparation room is also equipped with redundant hydrogen sensors and is to be considered as ex-zone 1. All components in this room are ex-proven and the room is highly ventilated with air outlets into hazardous zones.

The main challenges in this room were the delivery of qualitatively convincing tightness tests and supplier certificates to prove the quality of the hydrogen-bearing components.

3.3.3. Vent system

The design of the vent masts was from the very start of this project a big challenge in order to fulfil the vessel's height requirements. In the IGF Code it is obliged to have one big ex-zone of 10m on the outlets of a vent line. This is not possible in the application on board the Coastal Liberty, as there is a clearance height at the oil rig platform, which the vessel needs to fulfil.

Consequently, we designed the vent masts as high as possible, but in the end, the clearance height was leading. In a HAZID workshop, a CFD calculation has been prepared by us to convince the authorities that this will not cause any major issues.

A small insight into our argumentation: hydrogen is quite a light element leading to its behaviour, that it cannot sink while it comes out of the vent mast. Also, the atoms of hydrogen are so small that they are immediately well mixed with the surrounding air. The CFD calculation also showed a high stream of the high-pressure vent mast going up in a small stream. So, the hydrogen is behaving as a stream and not even close to a cloud/circle, as assumed by the IGF code.

3.3.4. Integration of the fuel cell

The fuel cell itself is supposed to be implemented in a so-called fuel cell room. This room is non-hazardous and thus the hydrogen pipes leading to the fuel cells, each need to be double walled. Challenges with double-walled pipes are the number of welds and the DNV approval of those, meaning the welds need to be X-rayed and surveyed during commissioning.

The fuel cell room also is ventilated with high air amount because of the Ballard process air intake requirements. The process exhaust air might contain hydrogen and thus is led to the vent masts as well. This air is quite wet and contains a lot of condensates also which needs to be separated. The fuel cell exhaust purely consists of water which is led overboard.



Fig.6: The Ballard FCwave and its connections

3.4. Cooling system

A big challenge in this project was also the design of the cooling system. Here, the funding programme obligated us to choose an external cooling system. No plate heat exchanger was feasible, as this would

lead to a non-mobile, i.e. fixed, connection of the eCap H2-PowerPac with the ship. The solution here was a V-shaped cooler on top of the eCap H2-PowerPac. This coincidentally provided a perfect structural support for the vent masts. The cooling power that we calculated is 700kW for the total cooling circuit.



Fig.7: V-shaped cooler and vent masts on top of the eCap H2 PowerPac

3.5. Electrical system



Fig.8: The look into the electrical room of the eCap H2 PowerPac

The electrical room consists of all control cabinets for the 770V DC-grid, the 400V AC auxiliary grid and the 24V emergency grid. All signals are exploited here and the safety controller is also located in

this room. The eCap H2 PowerPac is completely automated and only needs input from the operator when a new tank is connected and when he wants to use the available power. Inside the electrical room, also the 280 kWh of Lehmann Marine COBRA racks are placed which ensure the delivery of power to the ship also when peak power is required. The COBRA is also type approved by DNV and in this project, the air cooled version is applied. These batteries are convenient because they do not burn, in case of major failures, a gas is lead to the atmosphere.

The challenge here in this room was to convince the DNV, that the batteries and its converters are allowed to be placed in the same room. Therefore, additional safety measures had to be installed.

Regarding the design of the electrical system, it is to be said that the insulation resistance of the fuel cells already in the FAT was quite low and therefore we needed to design countermeasures and insulation monitoring into our system.

4. Outcome and outlook

This project was a major milestone for eCap Marine, as this is the very first German hydrogen project realised and successfully working. Also, this is the first gaseous hydrogen project in Europe and together with DNV which was a lot of pioneer work for eCap Marine. We gained a lot of experience in the certification of hydrogen components. The biggest challenge was to design a full safety philosophy onto an existing ship, including the safety measures on the oil rig platform. As we were also compelled to do a HAZID workshop with the DNV, this brought a lot of clearance, but also resulted in a lot of big tasks to adapt the concept to the classes and flag's satisfaction. But this lead to a smooth commissioning, as major issues have already been detected beforehand and the approval during sea trials was eased.

Looking into the future for eCap Marine now, this looks quite interesting. A lot of customers are reaching out to us for smaller retrofits, but also bigger project for newbuilts are in the making. eCap Marine there works as an integrator for the fuel cell system and therefore we are not only responsible for the hydrogen supply line, but also for electrical integration onto the board grid. We are investigating a lot into the insulation resistance issue regarding fuel cells, but also have learnt how to ease the hydrogen supply line and the configuration of valves, regulators, sensors, etc.

Acknowledgements

This project was highly supported by EnTec Industrial Services GmbH, Wintershall DEA, TURNEO GmbH, Carlsson GmbH, Offshore Service Gesellschaft mbH, and the Hoepen GmbH. During the process of engineering and commissioning it was a pleasure to work with DNV and Ballard, to bring this vision of hydrogen powered vessels to life. Thank you also to the great team at eCap Marine, that helped throughout the whole realization of this project. There were many extra-hours, sleepless nights and problems on the way of design, construction and commissioning.

References

BA (2023), *Übereinkommen über die internationale Beförderung gefährlicher Güter auf der Strasse (ADR)*, Bundesamt für Straßen

DNV (2021), *Handbook for hydrogen-fuelled Vessels*, DNV, Hovik

DNV (2023), *DNV-RU-SHIP Pt.6 Ch.2 Sec.3*, DNV, Hovik

IMO (2022), *Interim Guidelines For The Safety Of Ships Using Fuel Cell Power Installations*, MSC.1/ Circ. 1647, Int. Mar. Org., London

IMO (2015), International Code Of Safety For Ships Using Gases Or Other Low-Flashpoint Fuels (IGF Code), MSC.391(95) , Int. Mar. Org., London

100 Years Rotor Sails: A Rediscovered Invention to Meet the Net-Zero Goal

Dirk Höflich, Norsepower, Helsinki/Finland, dirk.hoflich@norsepower.com

Abstract

Flettner rotors, named after German inventor Anton Flettner, use the Magnus effect to propel ships with wind energy. In 1924, schooner BUCKAU was retrofitted with two rotor sails. Today, modern Norsepower Rotor Sails™, featuring high-tech materials and advanced automation, are a trusted technology for shipping to reach IMO climate targets. This paper will present insights into the technology of the first rotor sails, resume the history of rotor sails until today, describe technical, practical, and safety benefits for seagoing ships, spotlight the growing market of wind propulsion and its driving factors, and look into prospects of rotor sail technology.

1. Introduction

EEXI, EEDI, CII, ETS, Fuel EU maritime, increasing bunker prices, and non the least the crisis of global warming – the challenge of de-carbonizing the shipping sector is urgently asking the industry for new solutions. But what about looking into the hidden treasures that our ancestors left us? We don't need to go back to Leonardo da Vinci – exactly 100 years ago, German Engineer and Entrepreneur Anton Flettner introduced the Flettner Rotor.

Flettner discovered that the Magnus Effect is very suitable to turn the kinetic energy of wind into propulsion force that can be used by seagoing ships - safely and with minimum manpower. Two ships with Flettner Rotors were built. Both proved the technology had a great potential to make sailing with wind force much easier, safer and more reliable than the conventional rigs of that time. In a time when steam power and fossil fuel to propel ships – fossil energy still being a rare commodity – there was great hope that the fuel consumption of cargo vessels could be reduced - and their endurance increased – considerably with the support of wind energy.

Although technically feasible, the invention did not experience financial success. No further bigger cargo ships with Flettner rotors had been built for decades until in 2010, the German company Enercon ordered one RoRo cargo ship from Lindenau Shipyard, fitted with four large rotor sails.

This project ignited many initiatives and the founding of various companies by entrepreneurs who saw the potential of wind energy directly used for ship propulsion – with modern, automated technologies of different types. Among the different technologies of wind propulsion, the rotor sail concept invented by Anton Flettner is today the solution with the largest number of installations. It seems the shipping sector has re-discovered the value of this concept, which had been hidden for almost a century – but never forgotten.

This paper is written in the memory of Mr. Anton Flettner, a great inventor and brave entrepreneur of his time – and his team of skilled engineers and seamen.

1. Historical overview

1.1. The Magnus-Effect

The German physicist Heinrich Gustav Magnus described 1852 the lateral deflection of an object moving through a fluid, caused by the rotation (spinning) of the object itself. He worked to find the reasons for the deflection of artillery bullets. Small defects in a gun barrel can make it spin, thus leading to a deviation from its natural trajectory. The rotation creates a pressure difference between the sides of the spinning object, thus creating a lateral force – the Magnus force - which depends on the direction and speed of rotation. A mathematical description of this force, considering the velocity of the airflow, the rotation speed of the object, the geometry of the object itself, and other criteria, has only been found

in the early 1920ies by a team around Professor Ludwig Prandtl at the Aeronautical Test Institute in Göttingen, Germany, *Ackeret (1925).* They found that a correlation between the theoretical lift coefficient and practical measurements with a rotating cylinder can only be achieved by avoiding the compensation of the pressure difference around the ends of the cylinder. They solved this issue by adding end disks at both ends of the cylinder – a feature that can still be found at Flettner rotors today. With end disks of an optimised size, the lift coefficient of the rotating cylinder was found to be 10 times higher than the lift of an aeroplane wing profile. It was now possible to transfer the measurements to other cylinders of the same aspect ratio (diameter/length).

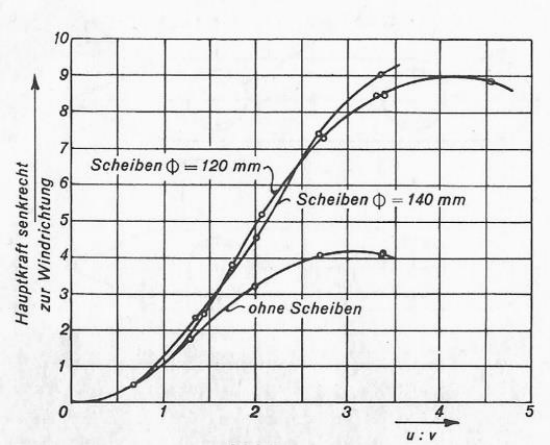


Fig.1: Magnus force versus a - different end disks, *Krupp (1925)*

Another finding of these measurements was the dependence of the Magnus force on the ratio between peripheral speed of rotation and wind speed. For a given geometry and diameter of end disks, the force reaches a maximum at a $\propto = {}^{v_{rotation}}/_{v_{wind}} = 3 \ldots 4$.

Left:

a. Air flow around a non-rotating cylinder
b. Air flow around a rotating cylinder without lateral air flow
c. Air flow around a roting cylinder with lateral air flow

Right: forces acting on a Flettner Rotor
A = Auftrieb (Lift)
W = Widerstand (Drag)
R = Resultierende (Resulting force)

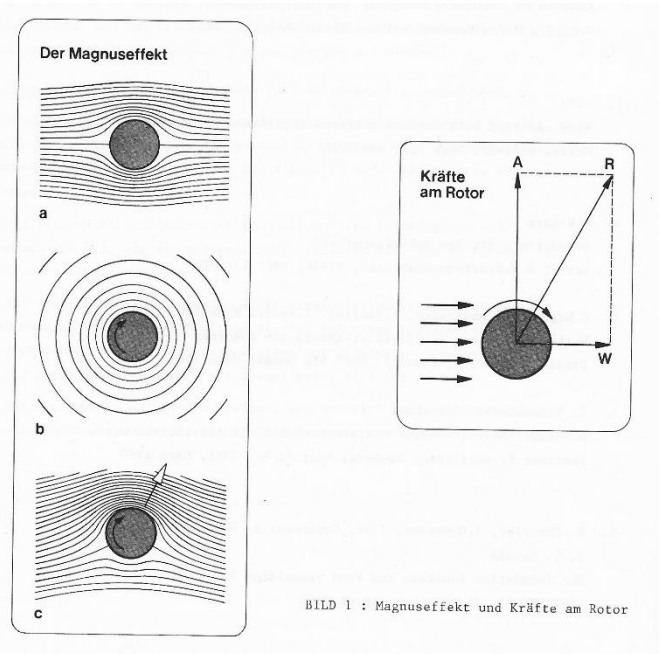


Fig.2: Explanation of the Magnus effect, *Wagner (1985)*

The scientists around Prof. Prandtl did not find a practical use of their studies. Despite the very impressive lift coefficient, the utilisation of a large rotating cylinder as an aeroplane wing, propeller, windmill blade or power generator did not seem feasible for practical operation, *Wagner (1991).*

1.2. 1922-1924 – the invention of the Flettner Rotor

A practical use case for the Magnus effect was found not too long after the results of the studies in Göttingen were reported. The 1920ies were a period of transition in shipping, from wind power to engine power. Many shipping companies decided – or were forced to – keep operating cargo vessels under sail. A trend of that time was installing auxiliary propulsion engines into traditionally rigged sailing ships, thus improving their flexibility and making them more independent from tug assistance. Anton Flettner (1855-1961), a German Engineer, Inventor and Entrepreneur, was deeply involved in technical innovations in shipping. His legendary Flettner-Rudders were a great success. To him, the operation of auxiliary engines on conventional sailing ships made it obvious that the complexity of sailing had to be reduced drastically. He did not doubt that the abundant energy of wind at sea would still be used for propulsion of ships at sea. In 1922, he started looking for suitable technologies – in cooperation with the Instituut voor Aero- en Hydro-Dynamiek, Amsterdam.

Flettner defined the following criteria for a modern wind propulsion system:

- Fast availability at any time
- Easy handling
- Small crew

The first attempts aimed at replacing fabric sails with metal profiles. Just like the famous Flettner-Rudder, a small adjustable flap could adjust these profiles with a relatively small force. Such wing profiles were tested on a small scale and in a wind tunnel at the Aeronautical Test Institute in Göttingen.

According to *Flettner (1926),* further development of profiles with a suitable control mechanism could have led to a wind propulsion system that would have been much easier to control, at a performance of 150% compared to fabric sails of the same size. This relatively small gain in performance, and the unsolved challenges of controlling such a sail in any weather conditions, caused Flettner to keep searching for a fundamentally different solution.

In 1923, during a summer vacation in Travemünde, Germany, Mr. Flettner took notice of the measurements and tests with rotating cylinders in Göttingen. It took a while until he concluded that these rotating cylinders could solve his problem – not at least due to their extremely high lift coefficient. From the very beginning, he was aware of some of the technical challenges that had to be solved:

- The large size of the cylinders
- Their resistance against severe weather conditions and ship motions
- Their power consumption
- Their drag in stormy weather, relative to their lift
- Their performance with wind from straight astern
- Their performance in upwind points of sail
- Vibrations and their impact on the ship structure

Being aware of these challenges, Flettner applied for a patent 29. August 1923. “The singular fascination of my invention consisted for me in the fact that the new sailing device would not require any manipulation; to the rotating cylinder, it would not matter at all whether the ship has the wind ahead, abeam or astern. One would not have to do anything else but to start the rotor by a turn of a handwheel, or, should the wind shift to the other side of the ship, reverse the direction of rotation. What a difference between this method of operation and the old style!”, he wrote, *Flettner (1926).*

After some practical studies with a model boat in Berlin, Mr. Flettner decided to focus on the development of the Rotor as the new wind propulsion system. He stopped all further developments regarding the wing profiles at the Aeronautical Test Institute in Göttingen and asked the scientists to prepare further tests with the rotating cylinders.

However, Prof. Prandtl's team saw huge technical challenges in the construction of large-scale rotors, and they proposed an alternative wing system with its lift increased by continuous suction of the boundary layer at the leeward back side of the profile, which was just under investigation in their wind tunnel. Flettner accepted and financed further tests with this system, which were later stopped due to unsolved challenges with their performance in extreme weather conditions.

Eventually, the whole project was reset and only the rotor sail principle was further followed. Both alternative technologies, nowadays known as “wing sails” and “suction sails”, have been tested and found inferior to rotor sails in the development objectives.

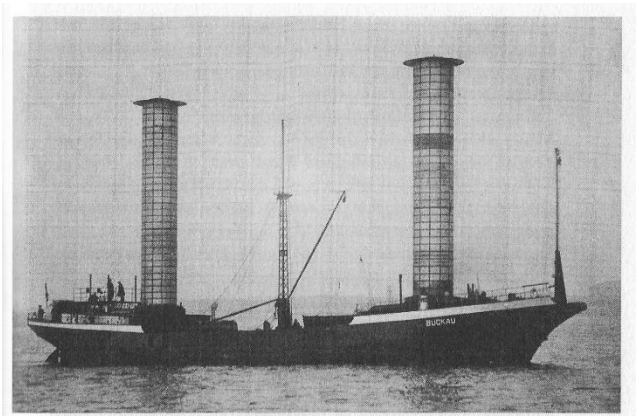
1.3. 1924-1926 – BUCKAU, design, trials, trade and marketing activities

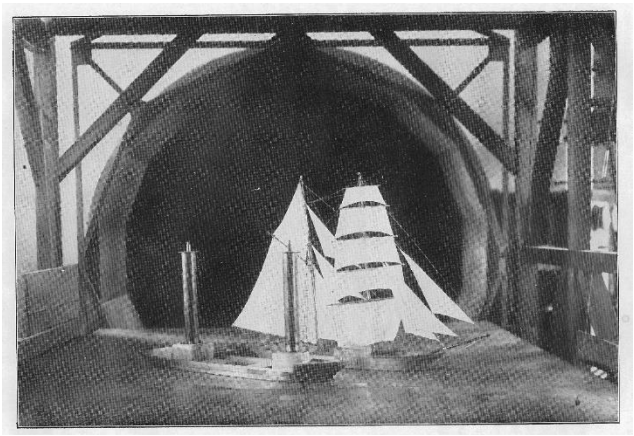
Krupp Germaniawerft built BUCKAU (HN 377) as a 3-mast schooner. 31 sailing ships of different sizes were built between 1920 and 1923 to keep the yard in operation during the economic depression in Germany after WW-1. Light steel material was in stock and found suitable for small sailing vessels for trans-Atlantic trade, most of them fitted with an auxiliary engine, *Karting (1987)*.

Anton Flettner found this ship type suitable for testing his rotor sail idea and convinced the owners to support this initiative. Four sister ships allowed a comparison of the sailing performance of the rotors with the conventional rig. The engine was a main element of the concept - rotor sails were planned as additional propulsion from the very beginning.

Table I: Technical Data of BUCKAU, *Wagner (1991)*

Built	1920
Retrofit	1924
Shipyard	Krupp Germania Werft, Kiel, Germany
Ship Owner	Hanseatische Motorschiffahrt AG
Main Data	LPP 45.0 m B 9.0 m 625 dwt 7.5 kn service speed
Rotor Sails	2 rotor sails 15.6x2.8, galvanized steel 2x11kW DC electric motors 120 rpm Aux generator 45HP (33.5kW)
Main Engine	160HP (120 kW)





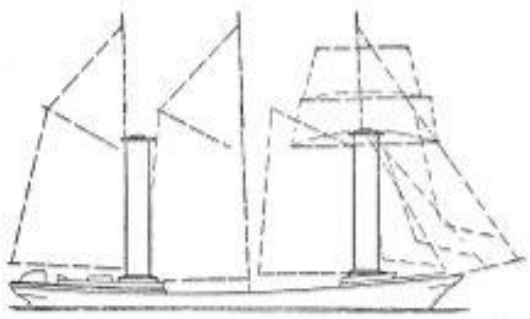


Fig.3: Comparison of Schooner rigg and Flettner Rotors, *Flettner (1926)*

In extensive tests in Göttingen wind channel, the optimum positioning and performance data of the rotor sails were investigated. The size was specified as being 10 times smaller than the area of BUCKAUs original sail area – based on the 10 times higher lift coefficient of rotor sails.

Preparations for the retrofit started in February 1924. Drawings for approval were sent to Germanischer Lloyd in March, and the assembly of the rotor sails started in June. The actual installation took place from August to October. October 1st saw the first rotation test of a rotor sail. BUCKAU left the berth on October 27th for her first sea trials with the Flettner Rotor sails. In a breeze of 4 Bft she made higher speed than she had ever made with her original schooner rig - in every point of sail - except 180° downwind, which was expected due to the characteristics of rotor sails. Her upwind point of sail had improved considerably from 45° (vier Strich) to 25° (zwei Strich) wind angle. Tacking and jibing was made by one man controlling two hand wheels at the flybridge. The ship was able to turn just by the force of rotor sails spinning in opposite directions – and she could even sail backwards, *Wagner (1991)*.

The news about the outstanding performance of the new propulsion system spread around the globe and gained the highest attention. In February 1925, BUCKAU went into regular trade and sailed from Gdansk, Poland via Grangemouth, Scotland to Hamburg, Germany. She showed an outstanding seakeeping performance crossing the stormy North Sea twice. The rotor sails worked well without any damage. In laden condition, BUCKAU was able to sail 20°-30° upwind – impossible with her conventional rig, *Flettner (1926).*

Due to the extremely high public interest, BUCKAU was chartered to perform day trips along the Baltic Sea coast to demonstrate the new rotor sail technology. In February 1926, she was bought by Flettner Rotorschiffahrt G.m.b.H, Berlin, a company founded by Anton Flettner for the purpose of marketing the rotor sail technology to investors overseas and seeking new customers.

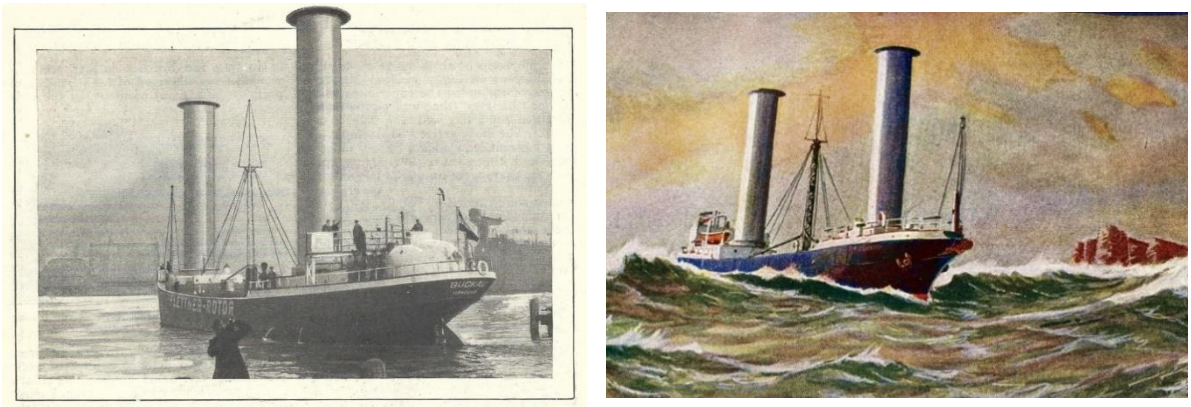


Fig.4: Artist impressions of RS Buckau, left: *Horlemann (1925)*, right: Engelien, *DSK (1926)*

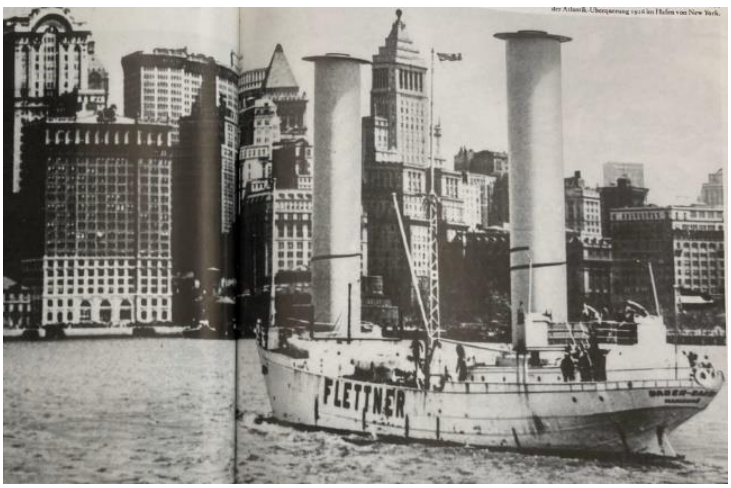


Fig.5: Baden-Baden in New York, *Broelman (1989)*

Renamed BADEN-BADEN, she crossed the Atlantic Ocean in 1926 – via the Cape Verde and the old trade wind route to New York. The 6200 nm voyage took about 40 days, at an average speed of 6.8 kn. In heavy seas, the BADEN-BADEN made 5 kn, only driven by the rotor sails. Despite the proven performance of rotor sails, no investors were found among the US shipping companies.

According to *Wagner (1991)*, the reason for the little interest in the new wind propulsion system was the low cost and high availability of crude oil and oil-based fuels for shipping. This made a return on investment in rotor sails within an acceptable period of 4-5 years unrealistic.

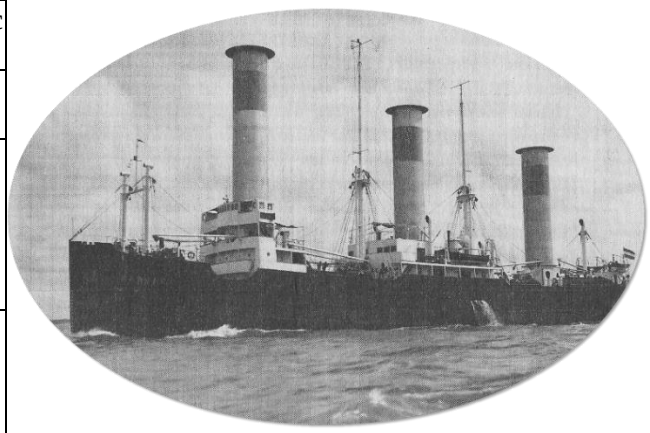
The ship was sold in 1928 to Capac Navigation Co. Inc., Panama. At that time the rotor sails were replaced by a conventional schooner rig after one of them was damaged by a lightning strike. Her last owners, J. Lau and Adolf Schenk, Costa Rica, died when the ship sank in a storm off Cartagena in November 1931, *Krupp (1925)*.

1.4. 1926 – RMS BARBARA, first commercial vessel with rotor sails

BARBARA was the first ship with rotor sails installed as a commercially viable propulsion system. The German Navy ordered the vessel to study the feasibility of rotor sails on long-distance sea voyages, seeking extended range and endurance of motor ships. The performance was compared with two sister ships without rotor sails, AMALFI and SORRENTO, sailing in a similar trade.

Table II Technical Data of BARBARA (Wagner C. D., 1991)

Built	1926
Shipyard	AG Weser, Bremen, Germany
Ship Owner	German Navy, military logistic vessel
Charterer	Reederei. Rob. M. Sloman jr., Hamburg, Germany
Main Data	LOA 90.5 m B 13.2 m 2830 dwt 10 kn service speed 2x530HP main engine
Rotor Sails	3 rotor sails 4x17m, Aluminium 41HP (30.5 kW) DC electric motors 160 rpm, 40 kN thrust each
Main Engine	2x530HP (385 kW)



Capt. Walter Lohmann, head of the logistic division of the German Navy, reported the following experiences after half a year of operation, *Lohmann (1927)*:

- The fuel consumption for the operation of one rotor was not more than 1kg per hour.
- The ratio $\frac{\text{consumed electric power}}{\text{generated propulsion power}}$ was ~1:10.
- The energy gained by wind at Bft 5 was about 600 HP (450 kW).
- The lightweight structure of the rotor sails withstands strong wind forces of Bft 10-12 in the Gulf of Biscay.
- The operation of the rotor sails was not affected by the motions of the ship.
- The stability of the ship was not affected.
- No problems were reported regarding the manoeuvrability in port.
- The Officer on duty could control the rotor sails without further assistance.

- The rotor sails increased the ship's speed by 2-3.5 kn in average wind conditions during 42% of the time at sea.
- The service speed of 10 kn with rotor sails was reached with only 50% power of the main engine. Without the main engine, the ship made 6 kn in 4-6 Bft.
- In heavy seas, the rotor sails reduced the roll motion at a constant heel of about 4° and the ship made 13 kn constant speed.

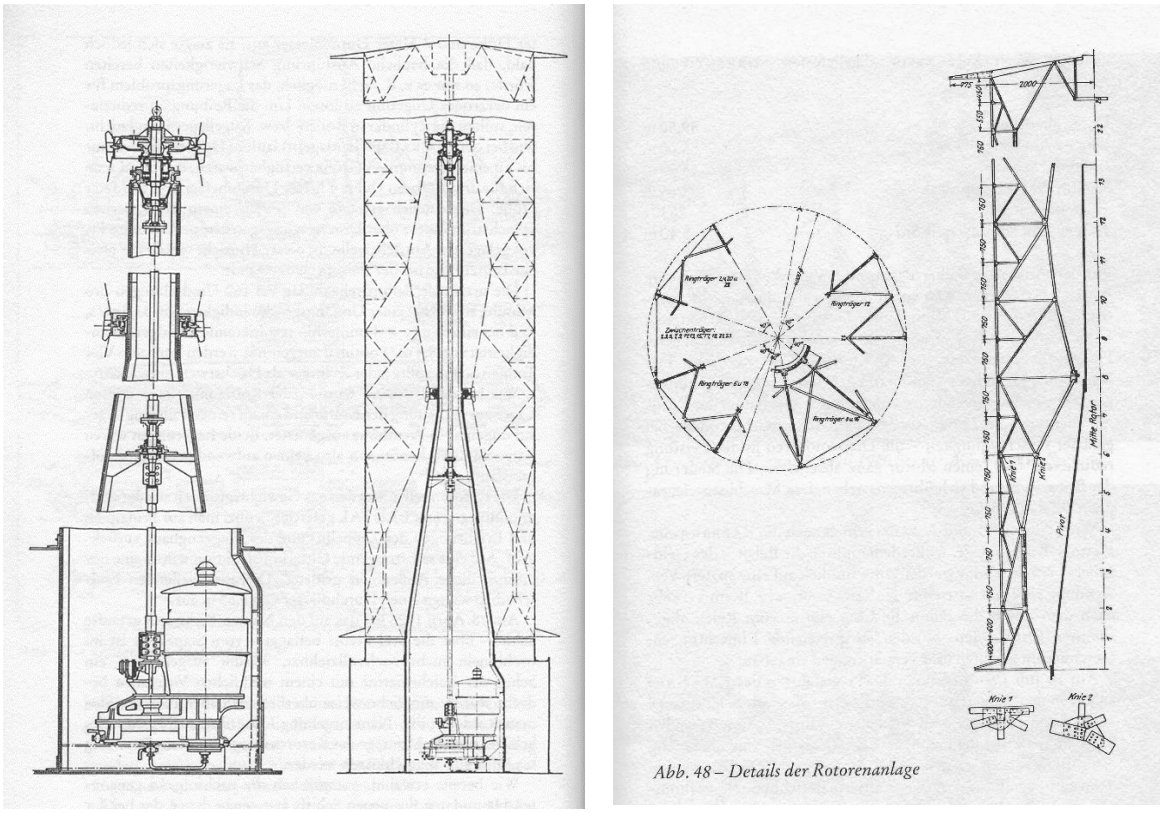


Fig.6: Details of BARBARA's Flettner Rotor, *Wagner (1991)*

During the operation by the German navy, there weren't any issues with the rotor sails and they proved to be a reliable part of the propulsion system. Due to several reasons, the concept of rotor sails was not been developed further:

- The particular situation of shipping during the global economic crisis and WW2
- Availability of crude oil and related fuels at low cost
- No incentive for saving fuel and/or reducing emissions

BARBARA was operated by Sloman until 1931. During the economic crisis of the 1930s she was laid up, then sold and operated by various owners without rotor sails until she was broken up in 1969.

1.5. 1983 – a short revival caused by high oil price

Under the rise of HFO prices in the 1970ies and 1980ies – from 20 to 75 USD/t and then to 160 USD/t - and driven by the common impression of that time of fossil energy resources becoming exhausted in not too far future, various attempts were made in Japan, Europe, and the United States to use wind energy for ship propulsion. *Wagner (1991).*

Blohm + Voss AG, Hamburg initiated a research programme to modernise the Flettner Rotor, *Wagner (1985)*. The programme consisted of two phases:

- Analysis of various routes, design criteria of rotor sails, model test and business case, and
- Detailed design, manufacturing and installation of rotor sail on a 4500 tdw chemical tanker.

However, the installation was not realised. With fuel prices going almost back to "normal" in 1986, the project came to a halt – the business case was no longer interesting for anymore. Here are some key facts about this relatively detailed design study:

- Basic assumptions and design objectives
  This study performed yet another comparison of rotor sails with other wind propulsion systems of that time, based on their resulting lift coefficient $c_R = \sqrt{{c_L}^2 + {c_D}^2}$:

Traditional Square sail	c_R @ 0.95
Solid, asymmetrical wing profile	c_R @ 1.8
Rotor sail	c_R @ 11

Turbo Sail - c_R in between solid wing and rotor sail (suction sail of J. Cousteau, tested on RV ALCYONE)

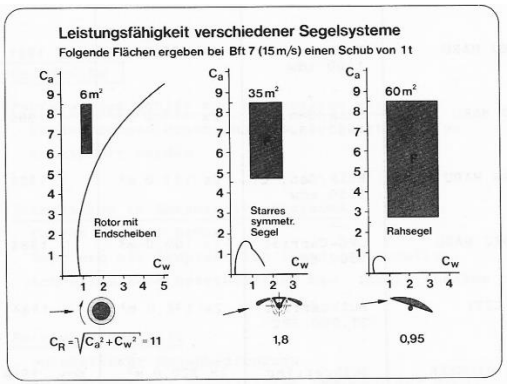
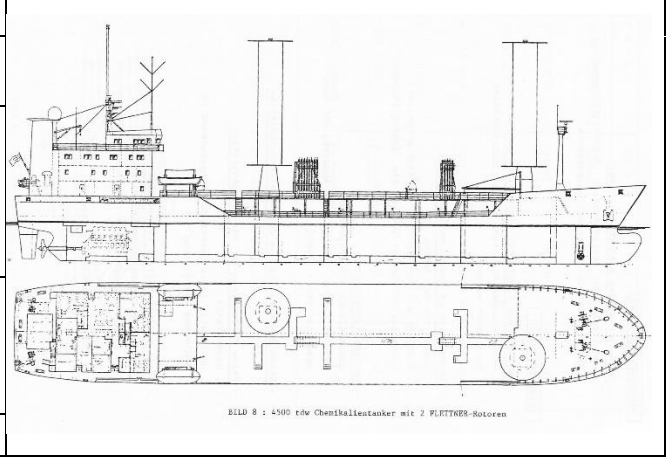


Fig.7: Performance of different sail systems, *Wagner (1985)*

- Required sail areas to generate 10 kN thrust at 15 m/s wind speed
  The study pointed out the following objectives for the installations of a wind propulsion system:
  - Economic benefit – reduction of OPEX, return of investment
  - Keep schedules – wind as additional propulsion to main engine
  - Integration into ship operation – control from the bridge, interface to main propulsion system and CPP, fast stopping and starting
  - Operational safety, no impact on ship stability – limitation of forces, no risk in gusts
  - No impact on cargo operations
  - No additional crew, reasonable training effort for operation and maintenance
  - Low technological risk – spares and services available globally.

Table III: Technical Data of the 4500 tdw project, *Wagner (1985)*

Designed	1983
Shipyard	Blohm+Voss, Hamburg, Germany
Main Data	LPP 92.0m B 15.5m 4500 dwt 12 kn service speed 2x530HP main engine
Rotor Sails	2 rotor sails 3.8x19.5 m, Aluminium 2x18 kW AC electric motors 225 rpm, 118 kN thrust each
Main Engine	1300 kW CPP



Technical details of the studied vessel are given on Table III. The 4500 tdw chemical tanker was supposed to operate on a windy route between northern Europe and Panama about 265 days per year.

The rotor sails were planned to provide 35% of the propulsion power at Bft. 5 wind force, 12 kn speed and 100° true wind angle.

The rotors were planned to be made from 4 mm aluminium with a frame structure. Two end disks of 7 m diameter were designed as a PVC composite sandwich construction. The total weight of each rotor was about 5.7 t. The rotors were carried by roller bearings and driven by an electric motor and a reduction gear.

The control system was planned to be independent of the engine control system, adjusting the speed of the rotors to the measured (apparent) wind force and angle. With variable propulsion force from the rotors, a constant ship speed could have been maintained by adjusting propeller pitch to ship speed.

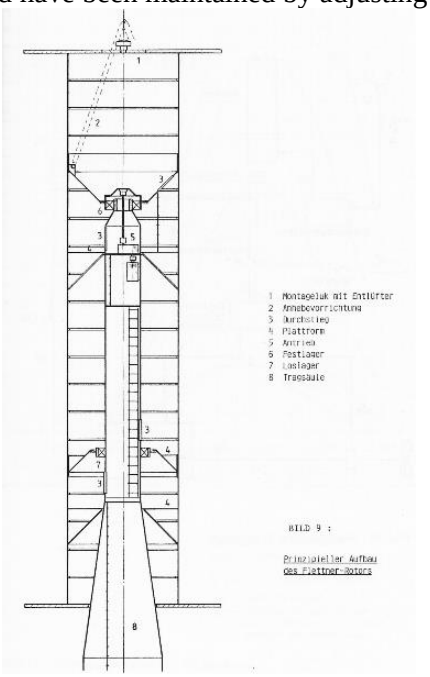


Fig.8: Sketch of the planned rotor sail, *Wagner (1985)*

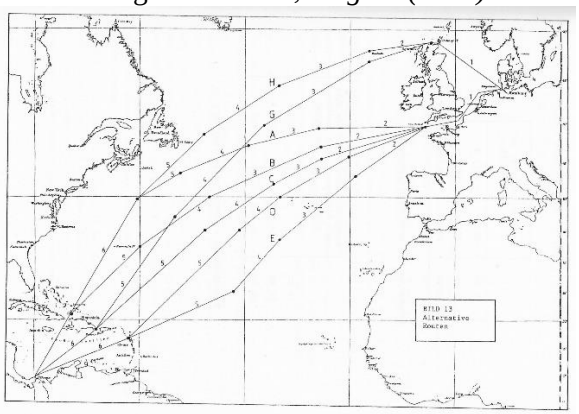
The performance of this setup:

- At Bft 5 and 110° true wind angle the rotor sails could have provided 37% of the propulsion power to maintain a speed of 12 kn,
- At Bft 7 even 100% of the propulsion power - with a power consumption of only 2x18 kW.

Table IV gives expected fuel savings based on simulations with average wind conditions and with weather routing based on actual weather conditions per year.

Table IV: Expected fuel savings, route German Bight – Panama, *Wagner (1985)*

Speed [kn]	Days at sea	Utilisation of rotor sails	Fuel saving, average wind	Fuel saving, weather routing
10	272.3	63.7%	21.7%	28.0%
12	259.0	59.4%	14.8%	21.6%
14	247.2	57.4%	11.8%	18.8%



1.6. 2010 – Enercon's E-SHIP 1

The first large-scale application of Fletter rotors in the 21st century was initiated by company Enercon GmbH, a leading supplier of wind power generation plants. The objective of shipping their eco-friendly products with an eco-friendly vessel led to the design and building of ESHIP I, delivered by Cassens Werft, Germany- in 2010. This vessel combined several "green" features, *Schmidt (2013)*. Regarding the rotor sails and aspects of the ship design influenced by wind propulsion, these were:

- Diesel-electric power generation
- Integrated power management system
- Superstructure, hull, and rudders optimised for wind propulsion

The calculation of the fundamental structure and the operation parameters of rotor sails were studied comprehensively, including:

- Static and dynamic behaviour of the structure
- Determination of basic operational parameters, e.g. lift (thrust), revolution speed
- Determination of required drive power for the rotor sails
- Integration into the ship structure

Table V. Technical data of E-Ship 1 (MINSHIP, 2022)

Built	2010
Shipyard	Lindenau Werft, Kiel Cassens Werft, Emden
Ship Owner	Enercon GmbH
Manager	Auerbach / Minship
Main Data	LOA 130:42m B 22:5m 10020 dwt 17:5 kn max. speed
Rotor Sails	4 rotor sails 25x4m, Aluminium ~100kW AC electric motors 350 rpm
Main Engine	6614 kW, 2 main engines



Enercon developed the whole rotor sail system with their own components and documentation. Full-scale tests were performed to validate the static and dynamic behaviour of the rotor sails, measure their performance, verify the power consumption, and optimize all components of the machinery and the control system. Proper balancing of the rotating elements and reduction of noise were key elements of the testing phase. The whole system was approved by Germanischer Lloyd.

After sailing 150000 nm on routes Europe-Brazil, Europe-North America, and in the Mediterranean Sea, the following features were reported:

- By aerodynamic damping and a gyroscopic effect, the rotor sails contribute to the absorption of sea disturbance,
- The rotor sails are safe to operate in all conditions,
- The operation of the rotor sails is fully automated by the control system,
- No additional crew, nor special crew training is required,
- Very little maintenance.

Enercon published considerable savings of propulsive energy by the rotor sails:

- A calculation of saved power based on trial conditions for a speed of 16.7 kn considered 2769 KW at the propeller shaft. The rotor sails should generate 1698 kW (37% of the theoretical shaft power at this speed), with 280 kW power consumption of the rotor sails
- The CFD performance model showed power savings at 12.3 m/s true wind speed for the full range of true wind angles, e.g. 15% at 40° TWA, 46% at 90° TWA, and 20% at 150° TWA.
- According to the ship managers, the rotor sails still operate without major issues and with very little maintenance. However, the company did not proceed any further with Flettner rotors as a commercial product. A sister vessel of the same type was never built.

This milestone in the history of the Flettner rotor remained a one-off ship. However, it inspired other companies to continue this development.

1.7. 2012 – modern commercialisation and outlook

There are presently eight technology providers in the business of rotor sails. They are at different levels of technological readiness. The main providers of rotor sails – in number of installations - are Norsepower (Finland, China) and Anemoi Marine (UK), *Binckert (2024)*. These companies were both founded more than a decade ago, and they are preparing themselves for an increasing order book. They offer an industrialised manufacturing process, a matured design, sophisticated control systems, and a growing international network for their sales and service activities.

There are presently about 16 vessels in operation with Flettner Rotors, and some 20 vessels more are in the order books, *Binckert (2024)*. The dimensions of modern rotor sail range from about 60 m² to 175 m², with heights up to 35 m. Considering the size of modern oceangoing cargo vessels, and compared to alternative wind propulsion technologies, these dimensions are still compact.



Fig.9: SC CONNECTOR with two Norsepower Rotor SailsTM 35x5m

2. Technical features of rotor sails for shipping

2.1. High lift – compact size

As described in , rotor sails have the highest lift coefficient of all wind propulsion systems. For a defined wind propulsion force, the arrangement of rotor sails is the most compact. This leads to the following advantages:

- Relatively little deck space consumed – more space for deck cargo, less interference with cargo operations,
- Relatively small blind sectors of bridge visibility – compliance with SOLAS without additional technical backup, and
- Relatively low air draft – many arrangements can be chosen as fixed installations – without an additional deployment system

2.2. Automation

As stated in 1.2, Anton Flettner had been most enthusiastic about the easy operation of rotor sails, Fig.10. In reality, the control algorithm is not as easy as he imagined, but the number of variables to be manipulated is relatively limited:

- Switch the rotor sails on in favourable wind conditions and off in unfavourable wind angles, too low or too high wind speed.
- Direction of rotation, based on the main direction of the apparent wind – port = clockwise / starboard = counter-clockwise
- Speed of rotation, based on the speed of the apparent wind to keep the ratio
$$\alpha = {}^{v_{rotation}}/_{v_{wind}} \cong 3.5 - 4$$
- Emergency stop



Fig.9: Controls on BUCKAU - 2 handwheels, *Flettner (1926)*

At any given true wind speed TWS, the speed of the apparent wind AWS changes with the angle AWA it hits the ship:

- In upwind points of sail: $AWS > TWS$
- In reaching point of sail: $AWS < TWS$

Modern control systems measure the apparent wind angle AWA and speed AWS constantly, and set the speed of rotation to an optimum a based on large-scale measurements of the polar diagram of the particular rotor sail assembly. Interactions between the rotor sails (if more than one is installed), and between the rotor sails and the ship structure are taken into account. These effects can be investigated by CFD, wind tunnel measurements, or full-scale trials.

This method assures an overall good performance in most conditions. In conditions of sophisticated arrangements of multiple rotor sails and complex interaction effects, a direct measurement of the individual strength and direction of each sail's lift force could further optimize the performance.

2.3. Safety against gusts

As mentioned in the historic reports, rotor sails are extremely insensitive against gusts. Any sudden increase of the TWS – with constant speed of rotation – will reduce the ratio $\alpha = {}^{v_{rotation}}/_{v_{wind}}$, thus reducing the lift coefficient of the rotor sails.

For a conventional sailing rig, or any type of wing sail or kite, the pressure increases with the square of the wind speed, and the sails must be eased immediately. Rotor sails cause only a defined maximum force with increasing wind speed, depending on their maximum rpm.

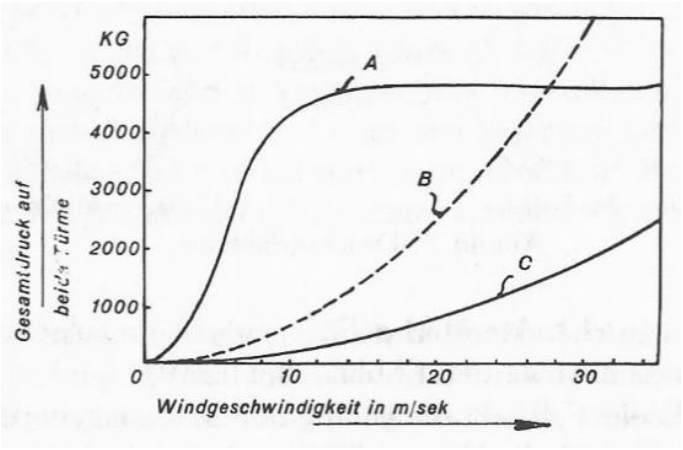


Fig.11: Comparison of drag curves for BUCKAU, total pressure vs. wind speed, *Krupp (1925)*
A. Rotating cylinders, constant peripheral speed
B. Original schooner rig with fully reefed sails
C. Cylinders not rotating

2.4. Safety against stalling of the air stream

The apparent wind angle can change relatively quickly with any change in speed or angle of the true wind. A large cargo vessel will not adjust its speed or course quickly. This means a conventional sail or a wing sail must be adjusted constantly to the AWA – a feature well known from performance yacht sailing. A delay in adjustment can lead to a disturbance of the flow around the profile, including the risk of stalling. The algorithm to control the correct sail angle in quickly changing wind directions needs high-precision sensors and quickly reacting actuators.

With sudden changes in TWS, or variable TWA over the height of the cylinder, rotor sails will not constantly operate within the optimum $\alpha = {}^{v_{rotation}}/_{v_{wind}}$. However, the slope of the a-curve is relatively flat in the highest range of performance, and the adjustment of the speed of rotation can follow with a reasonable delay. There will be a lift force in all conditions, without a risk of stalling.

2.5. Manoeuvrability

The nature of rotor sails as an active wind propulsion system means that they can easily be de-powered. The additional wind propulsion force can be switched off whenever the ship's command considers this necessary. This is extremely important in any kind of manoeuvring situation, including crash-astern or emergency turning. The drag of the non-rotating rotor sail in any wind speed is known and not critical.

2.6. Seakeeping

The experience with the BUCKAU, BARBARA and E-SHIP I already showed a positive impact on the seakeeping performance of rotor sails. Compared to the (removed) conventional rigg of BUCKAU, the weight of the rotor sails was much lighter. On modern motor ships, it is mostly the constant side force of the sails that reduces the roll motion considerably. In addition, the gyroscopic effect of the rotating masses is believed to have a roll-dampening effect, too. The Captain of SC CONNECTOR (two Norsepower Rotor Sails™ 35x5m) confirmed this positive effect: "The rotor sails have improved the ship's seakeeping behaviour very much – it is a completely different vessel now!", he said and "The rotor sails dampen the roll motion so the ship hardly rolls at all", *Sylwestrzak (2023).*

2.7. Noise / vibration

The risk of vibration generated by rotating masses was already addressed by Anton Flettner. However, by a careful balancing of the rotor, the centre of mass can be properly aligned to the centre of rotation. Additional measures can be applied to minimize the risk of frequency-induced vibrations such as defining rotation speeds to be blocked in the control system, or manipulating the masses of the fixed and rotating parts of the rotor sails.

Noise is kept within the limits of the IMO resolution MSC.337(91) for machinery spaces (inside the rotor sail) and normally unoccupied spaces (on open deck around the rotor sails). If the rotor sails are arranged close to navigation or accommodation spaces with lower noise level limits, special measures have been taken with satisfying results.

3. Modern upgrades and future developments

3.1. Modern materials for a long lifetime

The early rotors– including E-SHIP 1 – were made of metal (steel plates or aluminium). Such a structure requires high production skills and material costs. For this reason, most of the modern rotor sails utilise composite structures for the rotating components. The design lifetime of a modern wind propulsion system shall be suitable for the full lifetime of a ship.

3.2. Aerodynamic design

There have been many proposals to improve the aerodynamic performance of rotor sails. However, they still look pretty similar to the Flettner rotors on BUCKAU. Here are some of the development ideas for the future:

- “Thom fences” – a number of disks along the height of the rotor to force the air flow parallel to the rotation
- Rough surface coating to increase the friction of the boundary layer
- Special shapes of end disks
- Vertical tail profiles behind the rotor sails to improve the upwind point of sail



Fig.10 RoRo project LDA / Airbus with six rotor sails 35x5 (Norsepower)

Some of these features that work well in model tests or CFD studies may have the potential to improve the performance in certain conditions and certain points of sail. However, the industry has been working on developing reliable products in a larger scale, with good all-round performance in many operating conditions. Sooner or later there will be resources to study further optimization of the proven concepts.

More interesting is the optimum arrangement of rotor sails. The influence of superstructures and the interaction between two or more rotor sails was studied already for the projects in 1.5 and **Fehler! Verweisquelle konnte nicht gefunden werden.**. In future projects, wind tunnel tests and CFD studies will verify the arrangements of six or more rotor sails.

3.3. Automation

A basic requirement from the very beginning has been easy operation with minimum crew and minimum specific knowledge. State-of-the-art automation can take over the task of optimizing the rotor sail operation and advise the command to navigate into a more favourable point of sail with additional potential of gaining energy from the wind.

Further developments regarding optimised performance are in progress. The patented Norsepower Sentient Control™ will be able to control each rotor sail individually based on a real-time measurement of forces, thus managing the complex aerodynamic interactions between the sails and the hydrodynamic behaviour of the vessel.

3.4. Deployment systems

In some projects, the ship design, navigational requirements or cargo operations require a reduction in the height or position of the wind propulsion system. For rotor sails, there are various solutions:

- Tilting down by 90° to reduce the height during cargo operations – industry standard especially for non-geared bulk carriers
- Tilting down by any angle ≤ 90° to reduce the air draft while navigating calm waters, e.g. passing bridges
- Horizontal rolling systems to change the position of rotor sails during cargo operations

Such systems for handling heavy equipment must comply with high operational safety requirements and they add CAPEX and OPEX to the wind propulsion. They may be needed due to external restrictions, but they are not necessary for the safety of the ship in severe weather. The safest position of a rotor sail in a hurricane is locked in the upright position.

A tilting system can simplify the installation at the yard by reducing the necessary hook height of the shore crane.

A telescopic or retractable rotor sail has been in discussion. However, finding a technically feasible and economic solution will be a challenge. It should be considered that stowing a system of this size below deck will take space from the cargo holds or other useful compartments and it will require considerable structures and mechanics to handle the loads.

3.5. Lightning protection

The incident of a damaged rotor sail on BADEN-BADEN showed that the risk of a lightning strike is real for such high structures on board a ship. Each wind propulsion system must be fitted with suitable lightning protection. For rotor sails, this means creating sufficient earthing from the lightning rod on top to the steel foundation and hull.

3.6. Explosion-proof design

Various types and sizes of oil and chemical tankers are very suitable vessels for wind propulsion. Thus, the development of certified explosion-proof systems has been a natural consequence. Modern rotor sails can be delivered to comply with ATEX standards for dangerous zone 1, Class 2b. Control panels, VFD cabinet and weather station will be located in the safe zone.

3.7. Ice-prevention

Beyond 60° latitude North or South, in the Baltic Sea, and around Greenland, full ice accretion shall be applied for the stability calculation. Most wind propulsion systems cannot be operated in these conditions, so they are designed to simply survive in non-operational mode.

Due to their relatively "clean" structure, rotor sails can be fitted to prevent ice accretion during operation. With a special hydrophobic paint, the adhesion of water/ice can be avoided. With a defined minimum RPM in "idle" mode of operation, there will be sufficient centrifugal force to avoid the accretion of ice or snow on the vertical and horizontal surfaces. Additional heating is not necessary to operate the rotor sails in icy conditions. However, any unbalance of the rotating part caused by additional weight will be sensed and the system will be stopped or set to idle until the imbalance has disappeared.

3.8. Integration to power management

The ship's grid must be designed for the starting and operation of rotor sails while at sea. An integrated PMS can assure that sufficient generated power is available, and start an additional generator if needed.

If a shaft generator and controllable pitch propeller is provided, the reduction of propulsive power at the main engine – by the propulsive power of the wind propulsion system - can more than compensate for the energy consumption by the rotor sails.

3.9. Integration to engine control

In the project described in 1.5, the engine power for a set ship speed under the influence of the wind propulsion system was planned to be controlled via the measurement of the actual ship speed. An increase of the ship speed by the rotor sails would lead to a reduction of propulsion power – by adjusting the propeller pitch. This interface would require only very little interaction between the engine control system and the rotor sail control system.

If reliable real-time measurements of the present propulsion power generated by the rotor sails could be done, a more direct influence on the main engine power could be arranged. Such an integration has not become an industry standard yet.

3.10. Weather routing

In project stage, performance predictions are made based on average statistic weather conditions along defined routes. The so called "global average route" has to be used for the impact of wind propulsion on the EEDI of a vessel.

Studies have shown that fuel savings can be improved considerably – by up to xxx % - in combination with a weather routing system that considers the performance spectrum of the wind propulsion system. The actual savings will have an impact on the CII, as well as the OPEX connected to the fuel consumption (fuel cost, ETS, FEUM).

4. Conclusion

Whilst the basic technical principle of rotor sails proved to be suitable for ship operations since its early days, the fact that it had not been utilised in shipping for a long time led to doubts within the industry about its feasibility. However, the rapidly increasing numbers of installations has proven these wrong. After a century of affordable bunker prices and disregard for the environmental impacts of burning fossil fuels at a large scale, the shipping sector strives for improved energy efficiency and alternative sources of energy.

Legislative bodies like the EU and the IMO consider wind propulsion in their efforts to reduce the carbon intensity of shipping to net zero by 2050. All major classification societies have rules and regulations for wind propulsion in place, assuring a good technical basis for the design and survey of rotor sails and other technologies.

There is a growing common understanding in societies and industries globally about the urgent need to refrain from releasing greenhouse gases into the atmosphere. All this will lead to increasing cost for fossil fuels, whilst alternative fossil-free "e-fuels" are expected to be even more costly and not available in large volumes soon.

The whole scenario seems to be prepared for a breakthrough of wind propulsion to play a major role in the energy mix of future shipping – exactly 100 years after the world saw the first Flettner Rotor spinning. Rotor sails still provide the same benefits Mr. Anton Flettner had in mind when he decided to put his ideas, energy and money into this particular concept – and there is room for further development.

This is a good reason to celebrate and remind us: Nothing is stronger than an idea whose time has come! (Victor Hugo)

Acknowledgements

Special thanks to the Alfred Krupp Stiftung for sharing some very interesting historical documents about the conversion and testing of the first rotor ships BUCKAU and BARBARA. Special thanks to Minship GmbH for an interesting discussion about the performance and reliability of the rotor sails on E-SHIP 1. Special thanks to Sea Cargo Express and Capt Sylwestrzak for their continuous support in testing and improving the Norsepower Rotor Sails™ on SC CONNECTOR.

References

ACKERET, J. (1925), *Das Rotorschiff und seine physikalischen Grundlagen*, Bandenhoek & Ruprecht

BINCKERT, F. (2024), *Recensement des navires equipes de voiles*, Laboratoire de recherche en Hydrodynamique, Énergétique et Environnement Atmosphérique LHEEA, Nantes, https://cargo-cluster.fr/actualites/recensement-des-navires-equipes-de-voiles

BROELMANN, J. (1989), *Rotierend über die Meere*, Kultur & Technik, pp.16-17

DSK (1926), *Das Flettner-Rotorschiff*, Deutscher See-Kalender, pp. 80-81

FLETTNER, A. (1926), *Mein Weg zum Rotor*, Koehler & Amelang

HORLEMANN, R. (1925), *"Sailless" Ship Startles Shipping Men*, Popular Mechanics, pp.358-360

KARTING, H. (1987), *Bark, Schoner und Galeass*, Heinrich Möller Söhne

KRUPP (1925), *Das Flettner-Rotorschiff „Buckau",* Kruppsche Monatshefte, Februar

MARCHAJ, C.A. (1991), *Aerodynamik und Hydrodynamik des Segelns*, Delius Klasing

MINSHIP (2022), *Minship Fleet*, www.minship.com

SCHMIDT, A. (2013), Enercon E-Ship 1 - A Wind-Hybrid Commercial Cargo Ship, 4th Conf. Ship Efficiency, https://www.stg-online.org/onTEAM/shipefficiency/programm/06-STG_Ship_Efficiency_2013_100913_Paper.pdf

SYLWESTRZAK, C.A. (2023), *Always on schedule with rotor sails – a captain tells his story*, DNV, https://www.dnv.com/expert-story/maritime-impact/Always-on-schedule-with-rotor-sails-a-captain-tells-his-story/

WAGNER, C. (1985), *Weiterentwicklung des Flettner-Rotors zum modernen Windzusatzantrieb*, Entwicklungen in der Schiffstechnik - Statusseminar des BMFT, Bonn, pp.44-68

WAGNER, C.D. (1991), *Die Segelmaschine*, Ernst Kabel Verlag

Reimagining Proactive Cleaning: Benefits of High-Frequency Cleaning by Means of an Autonomous In-Transit Hull Grooming Robot

Stav Jacob, NakAI Robotics, Holon/Israel, stavj@nakairobotics.com
Matan Nice, NakAI Robotics, Holon/Israel, matann@nakairobotics.com

Abstract

This paper presents the advantages of high frequency cleaning of biofouling and describes the development of a robot that can achieve that. High frequency is considered to be once every 10 days on average, at which point an autonomous robot is deployed and grooms the slime layer off the hull of the ship, thus setting a new standard for what is considered proactive cleaning. High frequency hull grooming provides substantial benefits in terms of GHG emissions and a significant reduction in the migration of invasive species. Both provide a significant environmental impact and offer substantial savings for the ship operator. This paper presents the environmental and operational benefits of high frequency grooming, and provides an overview of a system that enables such a service.

1. Introduction

The accumulation of microorganisms and plants on surfaces such as ship and submarine hulls is known as biofouling. Biofouling affects any submerged object, and its effects on the shipping industry have been prevalent since the inception of marine travel, reducing ships' performance by increasing drag they experience. Biofouling on ships also negatively affects marine biodiversity due to the transportation of invasive species. According to an *IMO (2022)* report on biofouling, even a thin layer of slime (a layer of biofilm up to 0.5mm in thickness) covering up to 50% of a hull surface can increase greenhouse gases (GHG) emissions by 25-30%. *Swain et al. (2022)* estimated roughly that if all internationally operating vessels were kept clean of biofouling, the shipping industry could reduce its GHG emissions by 19%. *Schultz (2007)* quantified the effects of biofouling on the performance of US Navy ships and found that biofouling can reduce the speed of an Oliver Hazard Perry class frigate (FFG-7) by 2.7-10.7%, depending on the biofouling stage and compared to a hydraulically smooth surface when sailing speed is 30 knots. *Davidson et al. (2014)* describe in a report to the Marine Invasive Species Program in California another aspect of biofouling, which is its role as a leading vector in the transportation of invasive species. To tackle the above issues, an array of solutions has been developed, targeting biofouling at various stages.

As a preliminary preventative measure, anti-fouling (AF) coating is now applied to commercial vessels. While there are different types of AF coatings, the majority of them work by releasing biocides into the water, which slows the growth of slime. These coatings help mitigate the problem to a certain extent, however they have limited efficiency, need to be reapplied every few years, and release toxins into the water, *Soroldoni (2017*). AF coatings are sometimes complimented by ultrasonic transmitters which help further prevent the growth of biofouling, but still don't completely eliminate it. To further mitigate biofouling, periodic in-water cleaning is done at ports, and complete dry-docking of vessels is done approximately every 5 years.

Traditionally, the approach to cleaning biofouling has been mostly reactive, wherein ships are cleaned once biofouling has reached a certain level of interference. In recent years, the industry has shifted towards a proactive approach, following the understanding that maintaining a clean hull has significant advantages over cleaning a dirty one. This has been researched thoroughly and presented in *Swain et al. (2022)* and discussed in the *IMO (2022)*, where proactive cleaning is suggested to happen every 6 months, regardless of the biofouling state. A comparison between different cleaning approaches of the cumulative fuel consumption of a bulk carrier is shown in Fig.1, where proactive cleaning, considered to be once every 6 months, is shown to provide significant fuel savings.

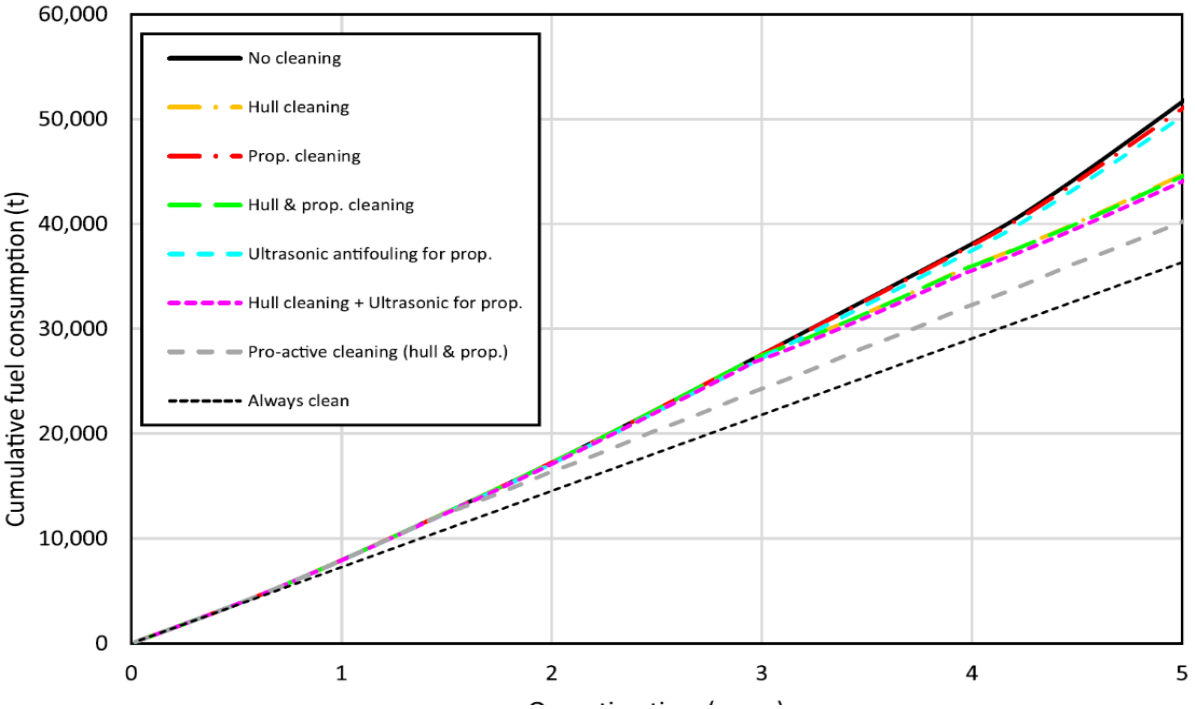


Fig.1: Comparison of the cumulative fuel consumption of a bulk carrier between different cleaning schemes. Here pro-active cleaning refers to cleaning of the hull and the propeller, and its significant advantage in terms of fuel savings is evident, *IMO (2022)*

High-frequency proactive grooming is an approach in which hull cleaning happens at close intervals, for example on a weekly or bi-weekly basis. This helps maintain a mostly clean hull, reducing drag penalties and leading to increased performance while improving fuel consumption. Moreover, high-frequency proactive grooming helps to reduce the migration of invasive species since slime gets removed soon after it is formed, preventing its development to the microfouling stage (layers 0.1 to 1 mm thick which include invertebrate larvae). Maintaining a clean hull also has significant financial benefits for ship operators, combining the reduction in fuel expenses and increase in ship efficiency by decreasing down-time for cleaning.

2. Why Hull Grooming is Better

The growth of biofouling is normally divided into three stages: Slime – an initial stage which includes a bacterial biofilm; Microfouling – includes diatoms, larva and microalgae spores; Macrofouling – macroalgae and invertebrates. While biofouling's effect already begin at the slime stage, macrofouling has traditionally been treated as significantly worse, hence most cleaning efforts have been focused on cleaning biofouling at such an advanced stage. This is considered reactive cleaning, meaning the cleaning happens after the ship's performance has been affected by biofouling. However, extensive research over the last two decades has shown that proactive cleaning has significant benefits. Proactive cleaning is described by *Scianni and Georgiades (2019)* as the removal of biofouling before it reaches the macrofouling stage.

Proactive cleaning done at a high frequency, for example on the order of once every 2 weeks, has demonstrated significant advantages, and is highlighted by *Swain et al (2022)*. A demonstration of the efficacy of high frequency grooming can be seen in Fig.2, which shows images comparing plates that were cleaned every week with those that were not cleaned at all. High frequency grooming helped maintain a clean plate and did not harm the paint, except for the case of non-copper based AF coating. High frequency hull grooming requires less force to remove the biofilm layer, leading to a less abrasive treatment to AF coatings, meaning a longer life span. The extension of the AF coating's life span assists in increasing the time interval between dry dockings, resulting in significant savings for the operator and increased ship efficiency.

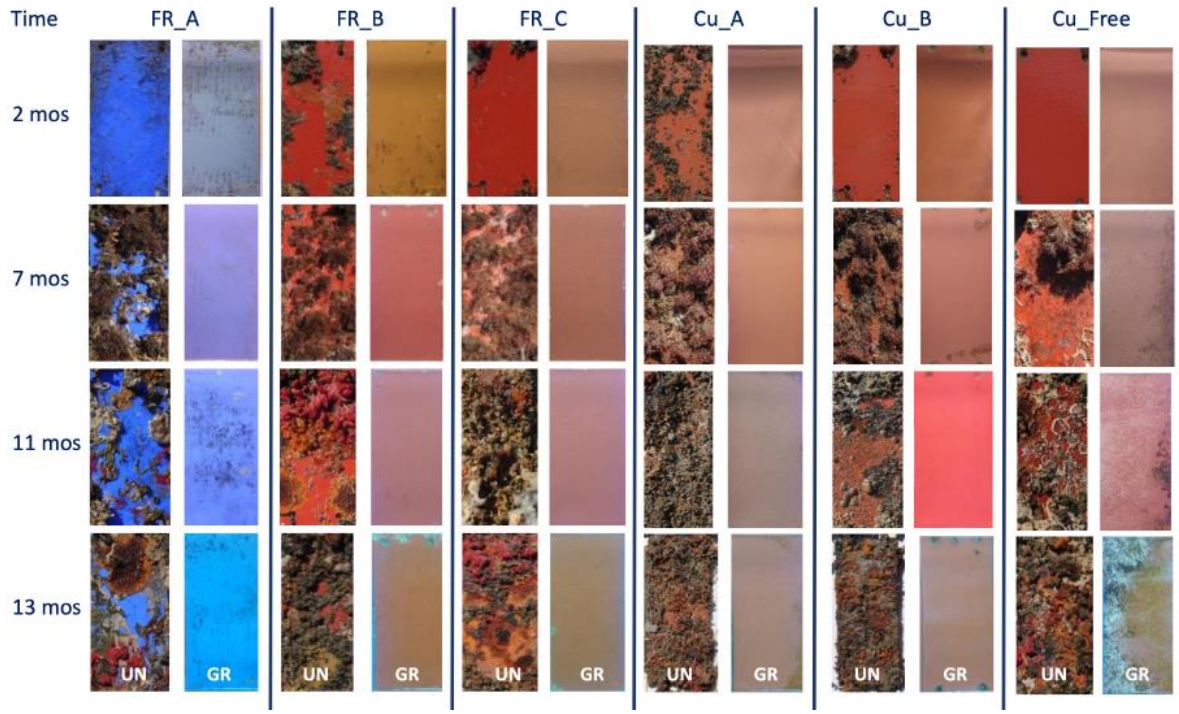


Fig.2: Comparison of the progression of fouling on six different types of AF coating between ungroomed (UN) and groomed on a weekly basis (GR) plates. The three types of coatings are Fouling Release (FR), Copper based (Cu) and copper free (Cu_Free), *Swain et al. (2022)*

Furthermore, a significant portion of a ship's power is used to overcome friction between the water and the ship's hull. The friction is determined primarily by the surface roughness of the ship's hull, which increases as biofouling development progresses. Traditionally, cleaning has been done once the friction is significant enough, meaning when the ship experiences a significant reduction in its performance, characterized by a loss of speed and increased fuel consumption. *Hunsucker et al. (2018)* showed that drag associated with ungroomed biofilm is substantially higher than that of a groomed biofilm. This continues to support evidence that grooming at a high-frequency leads to significant fuel saving, as was also presented by *Schultz (2007)*.

High frequency hull grooming holds the potential to significantly reduce the migration of invasive species. *Scianni and Georgiades (2019)* show that although proactive grooming does release microbial material into local waters, the risk of transporting highly impacting species through the slime layer is minimal, deeming this method as within an acceptable risk tolerance. Since hull grooming targets biofouling at an early stage, it prevents the biofouling from reaching an advanced biological stage, which is when invasive species are formed and transported.

3. Why Isn't Everybody Utilizing High Frequency Hull Grooming?

Despite all that is said above, hull grooming is still not a prevalent solution, and in fact, there are very few companies that offer this service. Hull cleaning was traditionally done manually by divers, which is a slow and cumbersome process, and it puts divers at risk. In recent years, thanks to advances in technology, robotics have entered the realm of hull cleaning, improving the efficiency of the process. Since the general approach is still reactive cleaning, these solutions are still required to include capture capabilities to avoid releasing invasive species into local waterways and prevent the discharge of harmful materials. This aspect makes the operation of these solutions complicated and often raises their cost.

As a result of the price and complexity associated with hull cleaning, operators and owners seeking to clean their vessels must choose between an expensive method and a slow one. Since time equals money in the shipping industry, a slow solution is also an expensive one. The shipping industry is a relatively

conservative one, and new technological solutions require a lot of work to break into the market. Therefore, there is little empirical data to showcase the real-life advantages of proactive hull grooming. Due to all these factors, there is little inherent motivation for ship owners and operators to shift their cleaning practices towards a proactive one.

In spite of the above, a variety of initiatives in the shipping industry recognize the myriad of advantages held by proactive hull grooming and are shifting the mindset towards this approach. As we enter the age of the Carbon Intensity Index, ships are rated according to their performance, providing an incentive for owners and operators to maintain their fleet at a higher standard. Additionally, regulation is becoming increasingly strict towards reactive cleaning. In Australia, according to *DAFF (2023)*, ships must clean the hull and niche areas no more than 30 days prior to entry. Simultaneously to these trends, ports are allowing proactive cleaning without capture, incorporating the understating the biofouling at an early stage poses a negligible risk of transporting invasive species. And to top all of that, a variety of improvements in technology are making robots more efficient and effective, lowering the cost of this service. All of this will surely help move the industry towards proactive hull cleaning.

4. Along Came NakAI

NakAI Robotics is developing a robotic system that will provide high frequency proactive hull grooming services. The system is designed to live on board the ship, thus allowing the cleaning to happen anywhere along the ship's route. It is comprised of three parts: Goby, the primary robot, built to operate while the ship is in transit; Plecos, a secondary robot, built to clean areas the Goby can't reach; Docking station, built to house the two robots as the ship sails. Both robots are designed to be autonomous, negating the need for significant intervention from the crew, limiting it to basic control commands by the bridge. Each robot records its track such that the system in its entirety can monitor which areas of the hull were cleaned and when, providing a holistic solution.

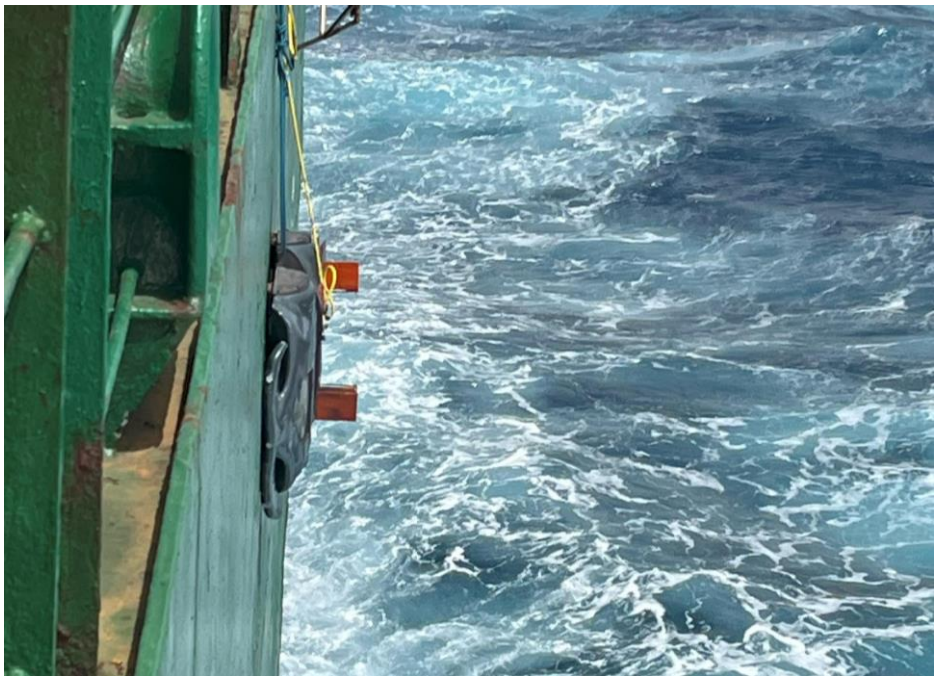


Fig.3: NakAI's Goby robot during one of the in-transit sea trials. The foils, which assist in generating additional downforce and are seen in red, are set to an open state.

The robots operate autonomously, boasting the ability to navigate a set path and avoid obstacles as they go. The robots receive an initial layout of the ship's hull, and use a unique version of SLAM algorithm to create a custom map including obstacles and landmarks in conjunction with the original map. At the end of each cleaning cycle the robots upload their path to a shared database which is held at the docking station. Upon the next cleaning round, each robot's route is optimized based on previous data, including areas the other robot covered recently. The path optimization includes other variables such as driving

efficiency, likelihood of biofouling growth, operating time limit and more. To initiate a cleaning cycle, the bridge grants permission and a time limit for the relevant robot to operate. Once a cleaning session is completed, a report is generated and sent to the bridge.

Remaining attached to the ship as it is sailing is one of NakAI's core developments. The Goby uses a unique set of adjustable foils positioned strategically to affect the robot's hydrodynamics. The foils are controlled by individual mechanisms and operate in response to measured changes in the driving motors' current consumption, indicating a change in the robot's attachment strength. They open to varying angles depending on the required amount of downforce, meaning the force that pushes the robot towards the ship's hull. In addition to the foils, the Goby generates downforce passively through its shape, designed to create a similar force to an upside-down wing as it travels through water. To further enhance its adhesion capabilities NakAI uses underbody magnets and magnetic wheels, which allow the robot to remain attached to the ship out of the water and operate while the ship is stationary.

While the Goby is at the heart of NakAI's developmental process, the Plecos is a vital addition to ensure a complete service. The Plecos is a smaller robot, capable of reaching areas the Goby cannot due to its geometry. Its compact design allows it to traverse areas of high curvature with ease, and to reach areas such as the bilge keel and near the sea chest and side thrusters. The Plecos is equipped with two brushes, one on each side of it, increasing its efficiency as it operates.

Hull grooming is widely understood to not require capture due to its low potential of transporting invasive species. However, some ports employ stricter regulations and require capture for all types of cleaning. For this reason, the Plecos includes a capture compartment which includes a filter. The capture compartment is removable, such that it can be left out in ports that don't require capture and can be easily cleaned or replaced if needed. Besides capturing invasive species, many reactive cleaning robots incorporate capture capabilities to contain toxins released while they operate. Due to its gentle cleaning nature, hull grooming does not pose a risk of releasing such toxins. Furthermore, NakAI has proved by third party testing with DHI in Denmark in April 2023, as presented by *Bohn (2023)*.



Fig.4: NakAI's Plecos. The removable capture compartment is visible in black at center of robot

To accommodate high frequency cleaning, the robots are accompanied by a docking station, where they remain parked while not in operation. The docking station is fastened at the deck level and is equipped with a variety of maintenance and communication systems to assist with the operation of the robots. It includes systems such as fresh water washing, wireless charging, satellite communication and more. The docking station sits outside the railing yet is within size limits such that there is no class change requirements. The docking station's design is customizable such that it can fit each ship's requirements and design.

NakAI is developing a novel fully autonomous high frequency hull grooming device. Currently, NakAI has installed the Goby on a ship of its first client and is in the process of implementing the Plecos as well. High frequency hull grooming offers a variety of advantages, including fuel savings and improved AF coating lifespan. Performing the cleaning during transit helps reduce time spent in ports, increasing

operational efficiency and reducing expenses for ship operators. NakAI aspires to be a significant part of the industry's shift towards this approach and believes that it will have significant positive impacts on the industry's environmental footprint.

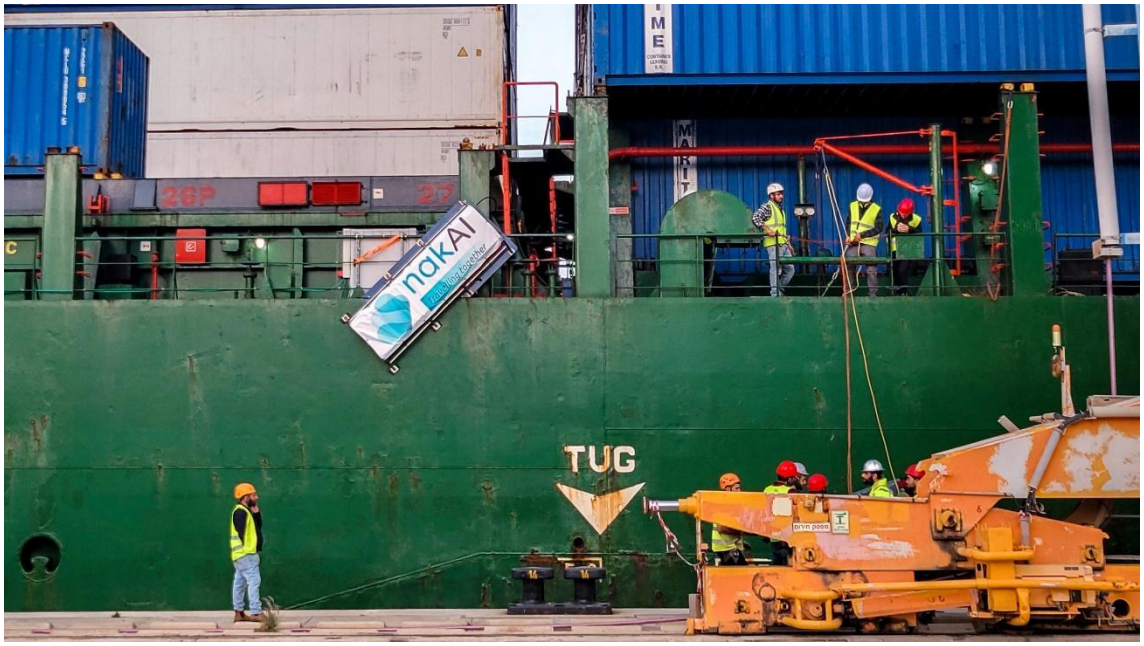


Fig.5: NakAI's team during the installation of the Goby robot. The docking station, at that stage designed only for the Goby, is visible with NakAI's logo.

5. Summary

This paper provides an overview of in-water cleaning and discusses the advantages of proactive high frequency hull grooming over reactive cleaning. The advantages can be divided into operational and environmental. The significant advantages on the operational side are fuel savings thanks to the maintenance of a clean hull, and improved AF coating lifespan thanks to gentle cleaning. On the environmental side the benefits are reduced GHG emissions as a result of the reduction in fuel consumption, and the prevention of migration of invasive species thanks to preemptive cleaning before biofouling reaches a harmful state. These points have been shown in research, yet only few companies seek to implement them in practice. This is bound to change following regulation which is trending towards proactive cleaning.

This paper also discussed NakAI's proactive hull grooming device, which is a first-of-its-kind fully autonomous in-transit cleaning robot. NakAI's robot boasts specialized hydrodynamic features which allow it to remain attached to the ship as it sails and incorporates a unique version of SLAM to navigate autonomously. The robot remains on the ship in a docking station and thus is able to clean anywhere along the route so long as the sea conditions allow. NakAI aspires to lead the industry's shift towards high frequency hull grooming to reduce the footprint of the shipping sector and preserve the world's oceans.

References

BOHN, P. (2023), *Evaluating Technologies for Growth Prevention*, 4th PortPIC Conf., Pontignano, pp. 12-15, http://data.hullpic.info/PortPIC2023_Pontignano.pdf

DAFF (2023), *Australian biofouling management requirements version 2*, Department of Agriculture, Fisheries and Forestry, Canberra

DAVIDSON, I.; SCIANNI, C.; CEBALLOS, L.; ZABIN, C.; ASHTON, G.; RUIZ, G. (2014), *Evaluating ship biofouling and emerging management tools for reducing biofouling-mediated species incursions*, Report to the Marine Invasive Species Program of the California State Lands Commission, Sacramento, California

GLOFOULING (2022), *Analysing the Impact of Marine Biofouling on the Energy Efficiency of Ships and the GHG Abatement Potential of Biofouling Management Measures*, GEF-UNDP-IMO GloFouling Partnerships Project and GIA for Marine Biosafety, Int. Mar. Org., London

HUNSUCKER, K.Z.; VORA, G.J.; HUNSUCKER, J.T.; GARDNER, H.; LEARY, D.H.; SEONG-WON, K.; BAOCHUAN, L.; SWAIN, G. (2018), *Biofilm community structure and the associated drag penalties of a groomed fouling release ship hull coating*, Biofouling 34(2), pp.162-172

SCHULTZ, M. (2007), *Effects of coating roughness and biofouling on ship resistance and powering*, Biofouling: J. Bioadhesion and Biofilm Research 23:5, pp.331-341

SCIANNI, C.; GEORGIADES, E. (2019), *Vessel In-Water Cleaning or Treatment: Identification of Environmental Risks and Science Needs for Evidence-Based Decision Making*, Front. Mar. Sci. 6:467

SOROLDONI, S.; ABREU, F.; CASTRO, Í.B.; DUARTE, F.A.; PINHO, G.L.L. (2017), *Are antifouling paint particles a continuous source of toxic chemicals to the marine environment?*, J. Hazardous Materials 330, pp.76-82

SWAIN, G.; ERDOGAN, C.; FOY, L.; GARDNER, H.; HARPER, M.; HEARIN, J.; HUNSUCKER, K.Z.; HUNSUCKER, J.T.; LIEBERMAN, K.; NANNEY, M.; RALSTON, E.; STEPHENS, A.; TRIBOU, M.; WALKER, B.; WASSICK, A. (2022), *Proactive In-Water Ship Hull Grooming as a Method to Reduce the Environmental Footprint of Ships*, Front. Mar. Sci. 8

Ultrasonic Antifouling –
An Approach to Mitigate Biofouling on Ship Hulls and Niche Areas

Ove Hagel, HASYTEC electronics, Kiel/Germany, o.hagel@hastec.com
Matti Früchtenicht, HASYTEC electronics, Kiel/Germany, m.fruechtenicht@hasytec.com

Abstract

This paper presents final results of the EU R&D project CHEK for the work packages related to ultrasonic hull protection against hull and propeller fouling. The work packages and the Dynamic Biofilm Protection intelligent (DBPi) solution are described. One work package concerns the concept and installation manual for hull surface and niche areas based on construction plans for a cruise vessel and a bulk carrier. Following simulations and laboratory tests, the DBPi hardware and software were adapted. After successful factory acceptance tests, results will be examined in real life test during a 7-month demo voyage period.

1. HASYTEC story – Role in CHEK project

HASYTEC electronics was founded in 2016 as a start-up for specialising in ultrasonic cleaning technologies. These are used in professional marine as well as in land-based industry. The use of HASYTEC ultrasound prevents the formation of biofilm as well as organic and inorganic deposits. These form the basis for the decomposition of equipment, pipes and materials through biocorrosion. HASYTEC started "showing flag" and raising perception of ultrasonic hull and propeller protection against biofouling very early on, e.g. *Kelling (2017a,b).* By 2024, the company had installed more than 10000 ultrasonic tranducers in over 850 ships worldwide.

The EU R&D project CHEK (deCarbonising sHipping by Enabling Key technology symbiosis on real vessel concept designs), https://www.projectchek.eu/, has as a goal to reduce CO_2 emissions in global shipping. The focus is on the combined application of advanced key technologies in shipbuilding. The project is described in more detail in Appendix I and *Kelling (2021).* Within the CHEK project, one focus was on drag reduction technologies to reduce fuel consumption and emissions to air. HASYTEC was in charge of the work package WP6, contributing all activities and devlopment concerning ultrasonic hull and propeller biofouling protection.

2. Ultrasonic Antifouling

2.1. Short introduction to biofouling

Biofouling is the unwanted attachment of various marine plants and animals in the marine environment. Every submerged structure is susceptible to fouling and will eventually become overgrown. On ships, its significance is manifold, and different estimates have been made of the losses incurred due to biofouling, including reduction of ships speed due to frictional resistance, leading to increased fuel consumption, docking charges for ship servicing and loss of income due to downtimes, Fig.1. Another significant aspect of biofouling is the transport of invasive species. To battle these issues, often antifouling paints, containing toxic compounds are used. However, their damaging effect to the environment is leading them to be phased out of production and use. Therefore, the need for a toxic-free solution is high.

2.2. Ultrasonic antifouling technology

The basic concept in ultrasonic antifouling is to use acoustic waves in the ultrasound range to prevent the biofouling already in the biofilm stage. Although the concept has been around since around the 1960s, the optimal parameters were not known for a long time, preventing industrial adoption.

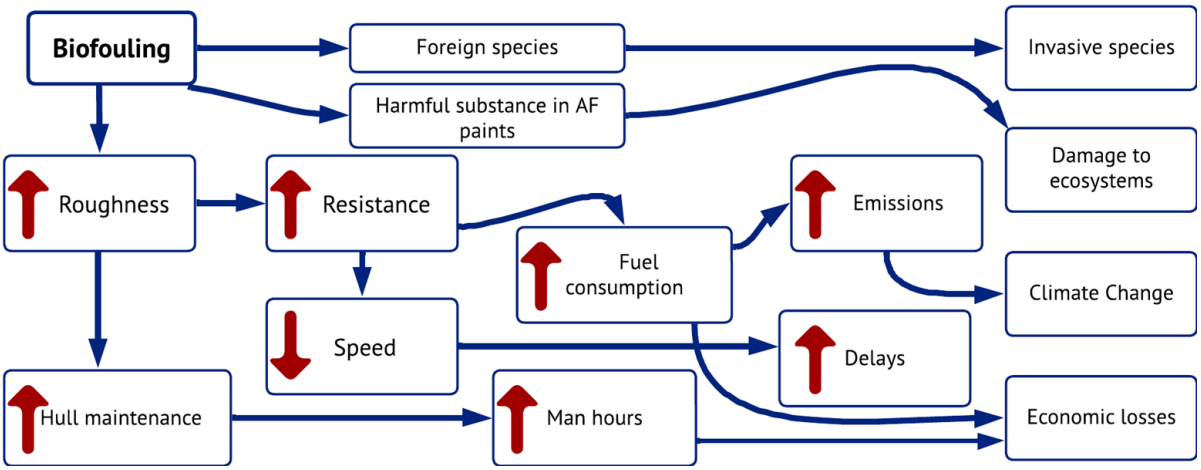


Fig.1: Effect of biofouling on shipping

To understand the wave propagation in detail, a Finite Element Analysis (FEA) approach was used now within the project, Fig.2. As coatings may lead to strong sound absorption, selecting the right paint impacts the effectiveness of the ultrasonic approach significantly and we performed lab testing to determine the most suitable coatings for ultrasonic wave transmission (Sound pressure tests and Caliometry tests for output power comparison). Once we had the concept ready, we proceeded to the prototyping.

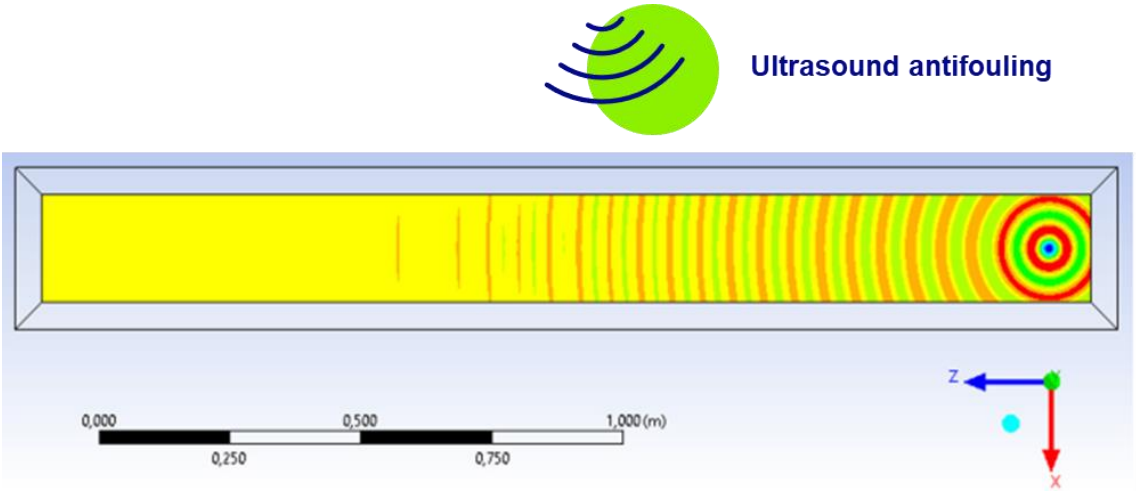


Fig.2: Laboratory testing of ultrasonic technology on coated steel plate

2.3. Installation of prototype

The development process involved several adaptations from older designs including several new features. In the hardware aspect, the control unit was adapted to host up to 16 transducers. This allows to scale up to the larger surface areas. In addition to higher power, cable lengths of up 100 m facilitated centralized installation of the system.

We used the results obtained from the simulations to develop customized transducers for ship hull applications. These were specifically designed for large-area coverage of the test patches and had an integrated measurement board that provided us with status information and environmental conditions, e.g. ambient temperatures.

The software adaptations included:

- Establishing communication with transducers

- Optimization of the software scan, aligned with the new transducers. Adjusting the frequencies, as these were in a different range.
- Design of several power programs with variable output power and pulse intervals to investigate their influence on the biofilm

Once the design was ready for production, the manufacturing of 4 hull prototype units and 12 hull transducers for testing on case vessels and 8 niche prototypes with 52 transducers was planned. That phase was challenging due to supply shortages during the Covid-19 pandemic. Nonetheless, eventually all parts were obtained and all prototypes, transducers including sensor boards and connection cables were assembled at the production facility in Kiel. Factory tests on hardware and software ensured that the prototypes worked according to specifications. For later installation on the two demo vessels, Fig.3, Table I, all parts were shipped to their destinations in Malta and China. Table II gives details of the installations. Fig.4 shows one of the installations with control unit and a typical transducer glued to the hull steel structure.

Table I: Demo vessels for installation

	MSC Seaside	Sirius Sky
Vessel type	Cruise ship	Bulk carrier
Length	323.00 m	200 m
Breadth	41.00 m	32.24 m
Tonnage	153516 tdw	34164 tdw
Built in	2017	2017



Fig.3: Demo vessels: MSC Seaside (left) and Sirius Sky (right)

Table II: Installation details

	Cruise ship	Bulk carrier
When?	November 2022	January 2022
How long?	6 days	10 days
Where?	Fincantieri shipyard, Malta	Zhoushan Jinhai yard, China
What?	Hull test patches, Seawater Supply with Sea Chests and Seawater Filters, Engine Cooling, Propeller	Hull test patches, Freshwater Generator, Propeller, Engine Cooling
Transducers installed	Niche areas: 24 Hull test patches: 6	Niche areas: 28 Hull test patches: 6

To assess the performance of the ultrasonic antifouling system, the following parameters were evaluated, Fig.5:

- Consistency and continuous operation of the software and hardware functionality
- Underwater visual inspection of the hull test patches
- Visual inspection of the seawater filters and sea chests
- Visual inspection of the propeller
- Comparison of heat exchange parameters between units with and without ultrasound antifouling

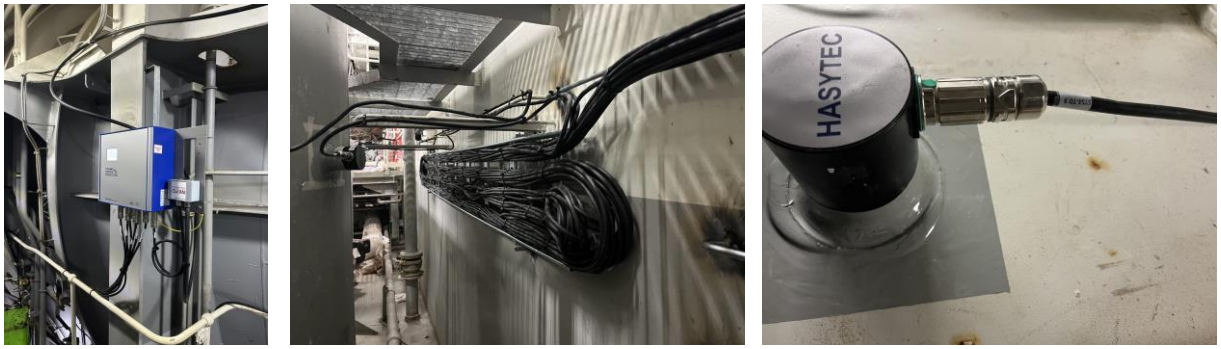


Fig.4: Installation: Control unit (left) and one transducer (center and right)


Fig.5: Monitoring of system

2.4. Results

Figs.6-8 show results from test voyage trials for niche areas.


Fig.6: Results from test voyage trials – Sea strainer after 1 year; with (left) and without (right) ultrasonic protections

The freshwater generator was also inspected, and favourable results were observed, Fig.7. No visible fouling was present. In addition, the bottom evaporator tube was also opened. This was free from any organic and inorganic deposits.

During the first underwater inspections, the sea chests were also inspected from the outside, Fig.8. Limited, but spatially inconsistent cover by barnacles were recorded on the portside.

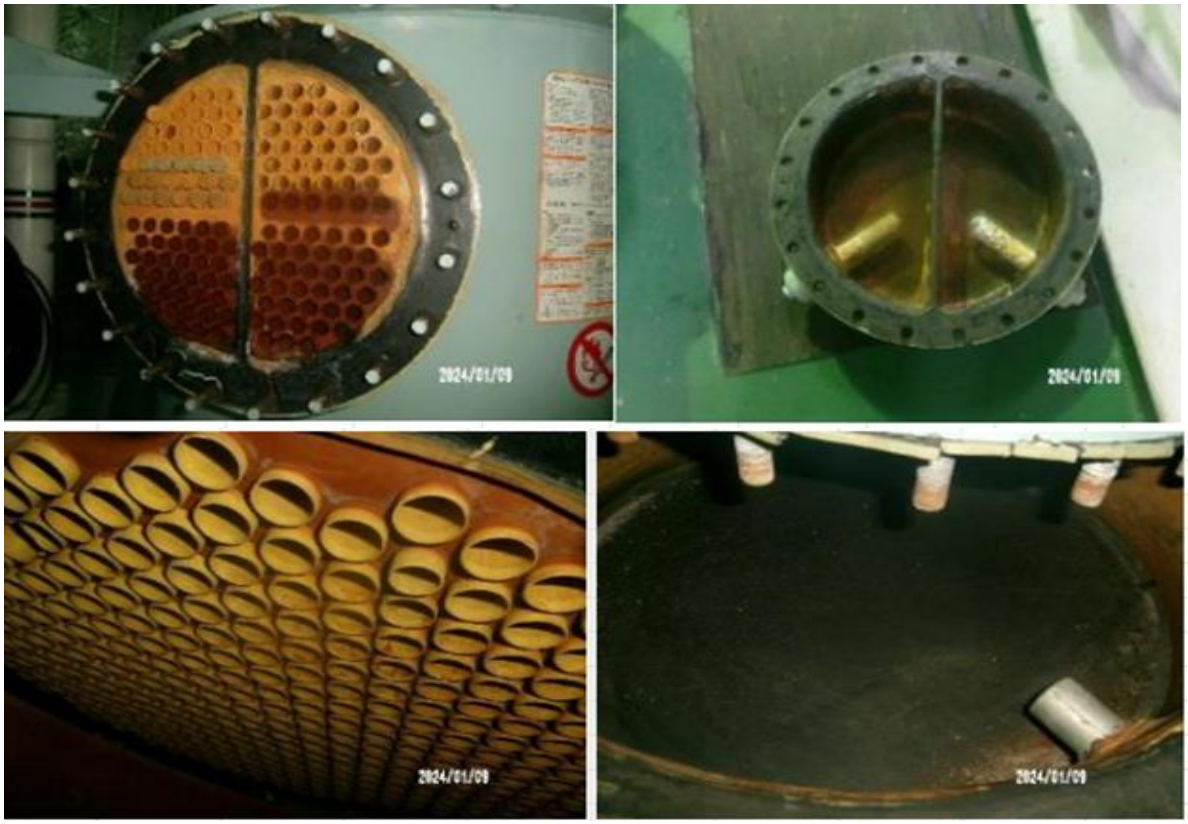


Fig.7: Results from test voyage trials – Freshwater generator


Fig.8: Results from test voyage trials – Sea chests

The results from the test hull patch inspection were favourable and only light slime was recorded after ten months of voyage, Fig.9:

- Hull Patch Examination Outcomes:
  - Performance Validation: Visual examination confirms the underwater (UW) system performs as anticipated.

- Fouling Comparison: Clear distinction noted between areas with and without transducers; areas with the UW system show significantly less fouling.

- Fouling Categories and Hull Roughness:
  - Details Provided: Descriptions of slime categories and average hull roughness for digital twin investigations are detailed in the cruise ship section.

- Fouling Condition Designation:
  - Without UW System: After a year in service, the bulk carrier's condition is designated as heavy slime.
  - With UW System: The bulk carrier equipped with the UW system is designated as light slime.



Fig.9: Hull text patches, with (top) and without (bottom) ultrasonic protection

3. Challenges and outlook

Lessons from the text voyages were:

- Inconclusive Results:
  - Favorable outcomes for the bulk carrier, less so for the cruise ship, suggesting hull transducer design may require refinement

- Transducer Development Needs:
  - Focus on reducing ultrasonic transmission losses due to impedance between hull and water
  - Explore different materials for transducer housing

- Software Implementation Challenges:
  - Difficulties in quick software changes noted
  - Future projects will develop remote access and control to quickly resolve software issues and analyze log data.

- Physical Verification and Accessibility:
  - Regular physical verification needed
  - Logistical challenges in vessel accessibility for underwater inspections due to location constraints (regulations or poor visibility)

- Vessel Selection for Future Projects:
  - Select vessels to facilitate easier and more regular data collection

- Data Collection and Impact Quantification:
  - Improved data Collection methods to better quantify reductions in waste streams, particularly biocides.
  - Better assessment of ultrasound system's impact on energy savings and maintenance costs

Acknowledgements

The CHEK project has received funding from the European Union's Horizon 2020 research and innovation program under grant agreement No 955286.

References

KELLING, J. (2017a), *Ultrasound-Based Antifouling Solutions*, 2nd HullPIC Conf., Ulrichshusen, pp.43-49, http://data.hullpic.info/hullpic2017_ulrichshusen.pdf

KELLING, J. (2017b), *Ultrasonic Technology for Biocide-Free Antifouling*, 11th HIPER Conf., Zevenwacht, pp.70-76, http://data.hiper-conf.info/Hiper2017_Zevenwacht.pdf

KELLING, J. (2021), *EU Project CHEK – Ultrasonic Antifouling and other Measures to Meet the CII Challenge*, 13th HIPER Symp., Tullamore, pp.132-139, http://data.hiper-conf.info/Hiper2021_Tullamore.pdf

Appendix I: CHEK project

The CHEK project was supported by the European Union with a total of 10 million Euro from the Horizon 2020 funding program, https://ec.europa.eu/programmes/horizon2020/en/home. The Horizon 2020 program is the biggest EU research & innovation program ever, with nearly € 80 billion of funding over 7 years. Its aim is combining European research and innovation to achieve excellent science, industrial leadership and tackling societal challenges. The CHEK project partners are:

- University of Vaasa (UV), http://www.uwasa.fi/, is a business-oriented, multidisciplinary, and international university.
- Wärtsilä, www.wartsila.com, is a provider of ship machinery, propulsion and manoeuvring solutions, supplying engines and generating sets, reduction gears, propulsion equipment, control systems, and sealing solutions for all types of vessels and offshore applications.
- Cargill Ocean Transportation, https://www.cargill.com/transportation/cargill-ocean-transportation, is a freight-trading business that provides bulk shipping services to customers across the globe.
- MSC Cruises, www.msccruises.com, is a global cruise line, which is part of the Cruises Division of MSC Group, the privately held Swiss-based shipping and logistics conglomerate.
- Lloyd's Register EMEA (LR), www.lr.org, is part of the Lloyd's Register Group, a global independent risk management and safety assurance organisation that works to enhance safety and improve the performance of assets and systems at sea, on land and in the air.
- World Maritime University (WMU), www.wmu.se, was established in 1983 by the International Maritime Organization (IMO).
- Silverstream Technologies, https://www.silverstream-tech.com/, was established in 2010 and the company specialises in Air Lubrication Technology, Silberschmidt et al. (2016), which is designed to reduce the frictional impact between the flat bottom of the ship hull and water.
- HASYTEC Electronics GmbH, https://www.hasytec.de/, is market leader in ultrasound based antifouling technology.
- Deltamarin, https://deltamarin.com/, is a ship engineering and design company.
- Climeon AB, https://climeon.com/, has well proven technology to convert waste heat to clean power.
- BAR Technologies, https://www.bartechnologies.uk/, have used its in-house tool ShipSEAT to design and optimise their own patented and trademarked wind propulsion system called WindWings, https://www.bartechnologies.uk/project/windwings/.

The project aims to combine a variety of innovative technologies to achieve its goals of significant increase (>50%) of energy efficiency and virtual elimination (>99%) of greenhouse gases, Fig. I.1:

- New energy technologies
  - Fixed wing sails
  - Fuel-cell ready hydrogen engine
- Operational technologies and practices
  - Automated vessel routing/sailing
  - Cruise vessel itinerary optimization
- Propulsion/Power supply technologies
  - Fuel-flexible gas engine incl. over-the-air software updates
  - Scalable power plant
  - Hybrid energy management
  - Waste heat recovery
  - Waste-to-power
- Drag reduction technologies
  - Gate rudder
  - Air lubrication
  - Ultrasound antifouling
  - Ship hull optimization

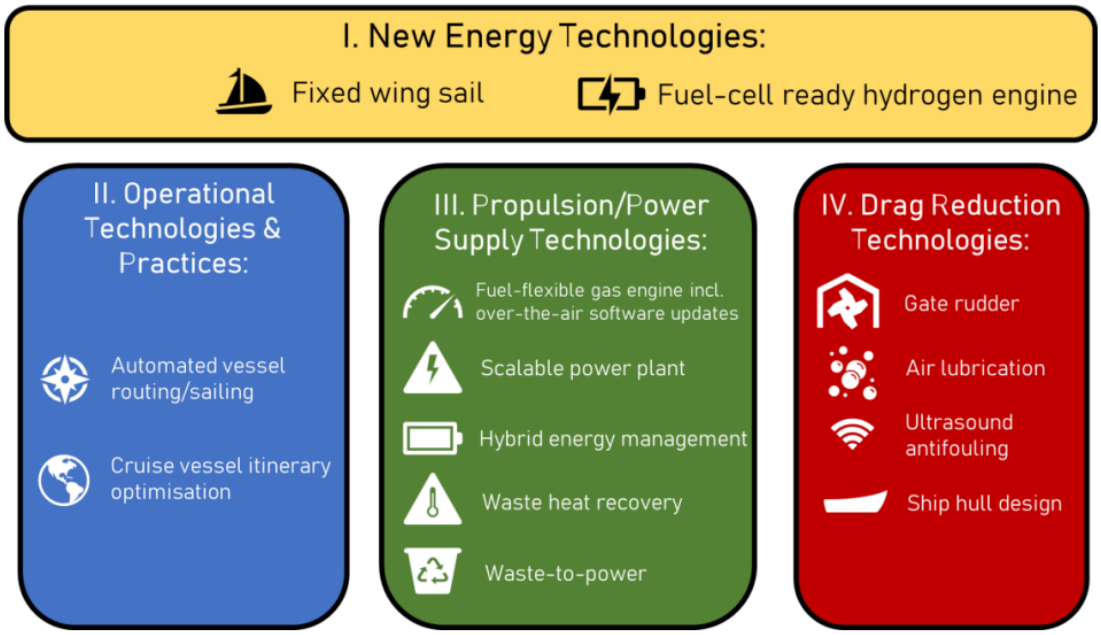


Fig.I.1: Technological synergy for emission savings

Digital Tools Enabling Net-Zero Cruise Vessels

Angela Craciun, MSC Cruises, London/UK, Angela.Craciun@msccm.co.uk
Ivana Melillo, MSC Cruises, London/UK, Ivana.Melillo@msccm.co.uk
Fotis Papadopoulos, MSC Cruises, London/UK, Fotios.Papadopoulos@msccm.co.uk
Mia Elg, Deltamarin, Helsinki/Finland, mia.elg@deltamarin.com

Abstract

Decarbonisation of shipping can be achieved through a combination of ship design and technologies, efficient operations, and clean fuels. Interdependencies between these factors should be considered during design phase and examined in real life. This paper presents energy consumption simulations and life cycle impact of various energy efficiency technologies working in synergy, combined with a hydrogen fuel system for a cruise ship. Additionally, examples from operational optimisation for both single ship and fleet level are given. This approach will steer the development of new and existing ships, with net-zero shipping remaining the ultimate goal.

1. Introduction

Decarbonisation of shipping constitutes a major challenge for the entire industry, with international, regional and local regulations being continuously introduced to support the transition towards cleaner transport. The cruise industry is committed to pursuing net zero emissions by 2050 and supports the long-term objectives of the EU Green Deal, https://www.consilium.europa.eu/en/policies/green-deal/. The gradual transition towards net-zero emissions can be supported by three main pillars:

- Ship design and technology,
- Operational efficiency and,
- Renewable fuels.

An indicative, high-level pathway towards net-zero for cruise vessels is presented in Fig.1.

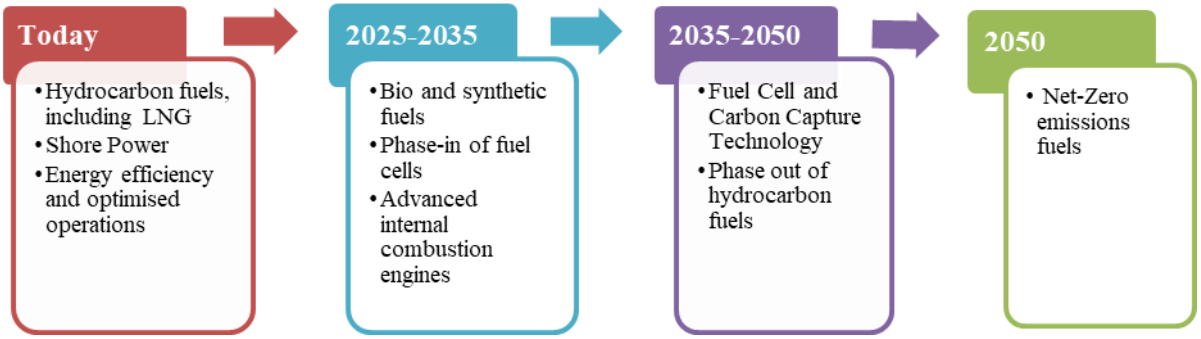


Fig.1: Roadmap to Net Zero

It is clear that the ultimate goal of net zero emissions requires the uptake of clean fuels and/or capturing of pollutants from the exhaust gases. In the short term, however, a shift towards greener shipping can be achieved by investing in optimised ship designs with energy efficient technologies, as well as in fuel efficient operations. Since it can be expected that the clean fuels will be significantly more costly than today's fossil-based fuels, energy efficient ship design and operation is expected to constitute another natural focus area of shipping decarbonisation even after the uptake of clean fuels.

Digitalisation is considered the key to improving the ability to deploy the fleet efficiently, monitor ship performance in real-time, and rely on data-driven decision making. Also, the data from operating ship can be utilised to support modelling of new conceptual ship designs, where the degree of freedom of decarbonisation through design, technologies and new fuels is large. This paper presents examples of

both new concept generation and of utilising data of operating ships to improve their performance on individual and fleet level.

Project CHEK is a three-year joint-industry project (2021-2024) focusing on decarbonisation of long-distance shipping, https://www.projectchek.eu/. One of the concept designs developed for the study is a Meraviglia class sized cruise ship illustrated in Fig.2. The technical goal of project CHEK, regarding the "CHEK cruise vessel" is to reduce green-house gas emissions by 99%, achieve 40-50% energy savings and reduce black carbon emissions by over 95% compared to the state-of-the-art existing ship in operation that is fulfilling the EEDI Phase 2 requirements.



Fig.2: CHEK vessels

2. Digital design for ship decarbonisation

The design stage constitutes the earliest phase of a vessel's lifecycle and has a crucial impact on its lifetime, as it includes the dimensioning of the ship and her systems and selecting the main components of the energy system. Retrofits along the ship's operational life are of course possible and beneficial from both maintenance and efficiency upgrade perspectives, but the early design stages present the largest degree of freedom for optimising the ship towards the desired performance.

One of the focus areas in project CHEK has been to develop a platform for ship design which allows developing and testing new technologies for improving ship environmental performance. Deltamarin develops this Future-proof vessel (FPV) design platform as a combination of various layers or dimensions of ship design. The simulations for project CHEK are performed in three different modelling generations. The first CHEK vessel related results are generated as "digital prototypes" (first model generation), where much of the historical operation is utilised directly as input to the simulations. At this stage, some components of the ship energy system are modified, to predict the possible impact of the CHEK technologies. The second round of result generation is called "digital master". For this round, new hulls for both vessels are generated, and the entire operation and propulsion profile for the cruise ship is also generated digitally, adding historical weather data to the modelling. The final simulation round, "Digital twin" includes enhancing the digital models with as much measurement data as possible from the CHEK technologies from in-lab measurements or from measurements that were provided from real vessel installations. This chapter presents the digital design and simulation results of the cruise ship in project CHEK from the final modelling round. The methods for achieving the results are explained in Chapter 3.

2.1. Introduction to the ship and technologies

Digital modelling in project CHEK starts with defining an operational profile for the vessel. The profile is based on measured data from a selected vessel in the fleet. A typical 7-day Mediterranean voyage of a Meraviglia class cruise ship, as shown in Fig.3, serves as basis for simulations. The study is based on assuming that the ship performs the same cruise constantly. This is a rather low-speed Mediterranean cruise. In reality, the speed profile over a cruise often features more significant variations.

Technology synergy is in focus of project CHEK. Regarding future fuels, there are several potential future fuels for cruise ships, such as green LNG or methanol. In the project the fuel explored is pure hydrogen, including its impact on the ship energy system.

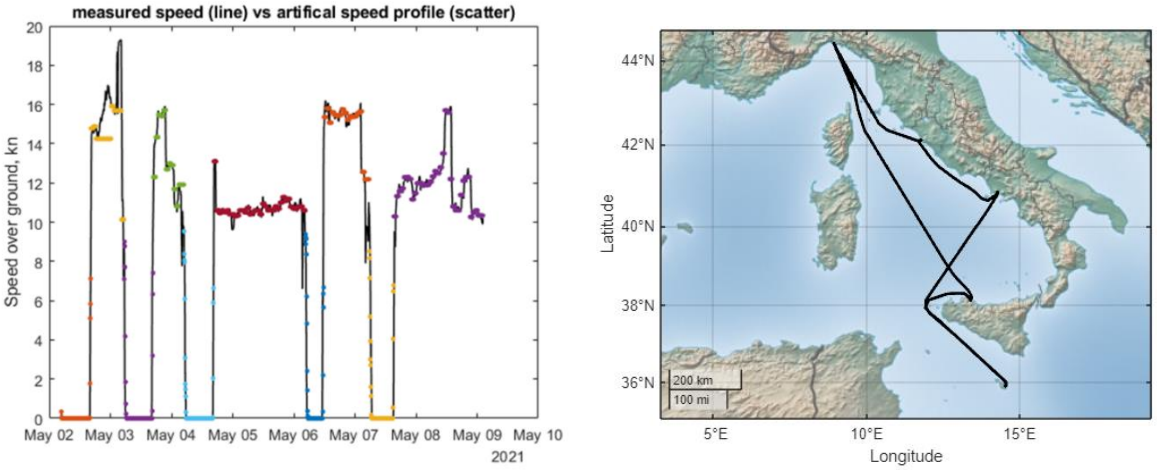


Fig.3: 7-day voyage historical profile compared to artificially generated speed profile with uniform time series

In terms of technologies, the studied selection includes: Hydrogen engine, Air lubrication system, Ultrasound antifouling system, Hull design optimisation, Fuel flexible gas engine including over-the-air software updates, Hybrid energy management, Waste heat recovery with Organic Rankine Cycle (ORC) and Waste to power. Also, automated vessel routing/sailing and Cruise itinerary optimisation tools have been developed during the project. Most of the studied technologies have already been introduced in *Melillo et al. (2023).*

In addition to the previously presented technologies, the final simulations include 10MWh battery capacity and explore preliminarily how gasification of the onboard waste would impact the ship energy system. The batteries are integrated in the ship power management system in a way that they would aim to keep the ship main machinery in an optimal consumption area by either charging or discharging them, within the allowed limits. It is also assumed that the batteries would be charged fully while the ship is on shore power. The waste-to-power concept is studied at a feasibility level, as one subtask in project CHEK. The waste would be gasified onboard the ship during port stays, producing heat which would reduce consumption of oil-fired boilers while the ship is in shore power. Gasification emissions to air are not included in the study due to unavailability of emission data for this process. As a final "new technology", a hypothetical scenario was analysed where the ship's additional heat demand in port is provided by an electrical boiler, instead of the traditional oil-fired boiler.

2.2. Achieved energy and emissions reductions

Table I illustrates the variables for simulations. Each simulation includes voyages in 12 months of the year. HFO (Heavy fuel oil) and Hydrogen stand for power plant and fuel type selection.

Table I: Simulation variables

CHEK EEDI Phase II Baseline	HFO	The Baseline energy consumption and emissions are defined based on the scaling of the clean hull condition simulation
Normal Fouling (11 %)	HFO / Hydrogen	Vessel with an average 11% resistance increase relative to clean hull due to hull fouling, used as the benchmark for actual energy savings for the CHEK vessel
Hasytec Antifouling (6 %)	HFO / Hydrogen	Vessel with an average 6% resistance increase relative to clean hull due to Hasytec's ultrasound antifouling benefit

Waste to Power	HFO / Hydrogen	Gasification in port scenario with medium temperature waste heat recovery for ship's thermal load and ORC units
1 x HP300 ORC	HFO	Climeon's Waste heat to power conversion with one HP300, 355 kWe unit
2 x HP300 ORCs	Hydrogen	Climeon's Waste heat to power conversion with two HP300, 355 kWe units
10 MWh Battery	HFO / Hydrogen	10 MWh battery is enabled in the system, including spinning reserve and load optimisation functions
Shore power	HFO / Hydrogen	Shore power connection is assumed in all ports of visit
Air Lubrication	HFO / Hydrogen	Silverstream's air lubrication model is included in the simulation of propulsion power profiles and added compressor loads
Electric Boiler	HFO / Hydrogen	Electrical heaters in ports enabled

The results regarding both fuel energy consumption and CO_2 emission production are shown in Fig.4. The illustration is made based on simulations run with different combinations of technologies so that at each step one additional change is made and the system always finds a new balance.

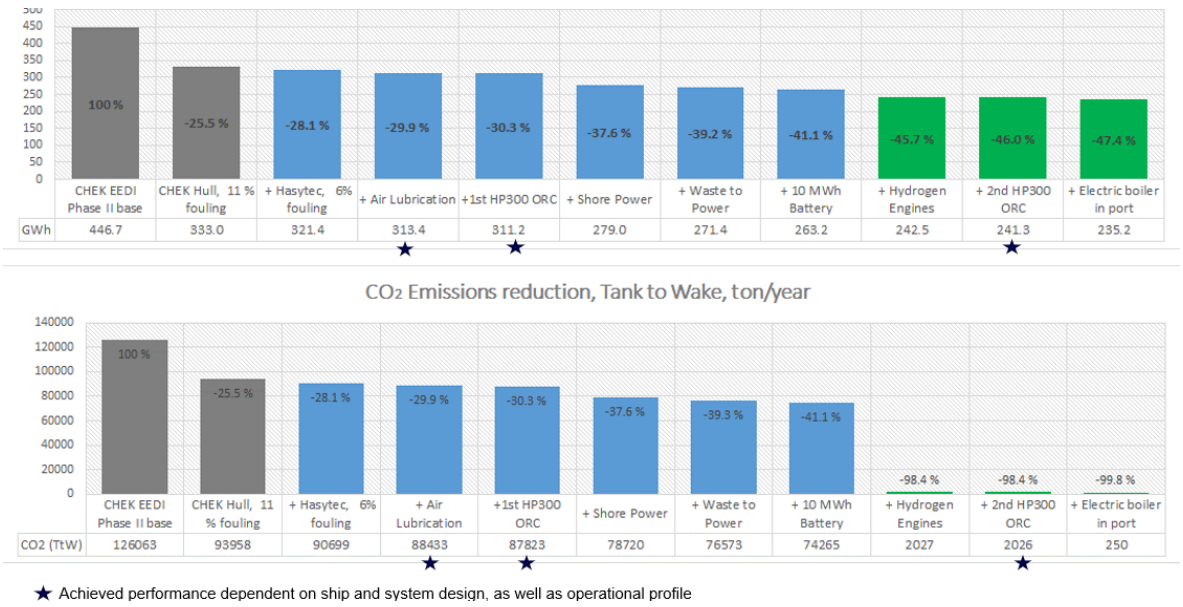


Fig.4: Effect of different combinations of technologies on energy demand and emissions

For the cruise ship the "EEDI phase 2 scaling" is significant. We can observe that on CHEK metrics this scaling alone gives 25.5% benefit for the CHEK "baseline" vessel, compared to the "CHEK EEDI2 baseline"; in other words, the baseline Meraviglia class vessel was already significantly more efficient by design compared to EEDI phase 2 requirements. The pure energy saving with "CHEK technologies" is around 30% in energy consumption, compared to sailing Meraviglia class sized ship. With the studied operational profile, over half of the ship's energy demand is for hotel and auxiliary machinery consumers. Many of the CHEK technologies, such as air lubrication or waste heat recovery with ORCs provide savings when the ship is operating at sea and the absolute saving potential grows with the ship speed. Since the simulated ship operational profile in the Mediterranean includes very moderate operational speeds, these technologies do not represent in these results their full potential. Additionally, these technologies are adapted to each unique ship design and operational profile, as such achieved savings from one ship cannot directly be extrapolated to another ship without careful consideration. Nevertheless, the focus of project CHEK is not to find typical energy savings of single technologies but to examine the entire system, where various technologies all contribute to the ultimate goal.

One can also observe interesting interactions between different technologies. Especially, introduction of shore power introduces certain changes in the ship energy system. The ship boiler consumption is considerably lifted with the shore power scenario. On the other hand, shore power enables even further fuel energy saving and decarbonisation, albeit at a high cost for the operator, if batteries are introduced to the ship, since they can be charged fully onshore.

Nevertheless, the most exciting synergies in the cruise ship case are found when introducing hydrogen fuelled engines in the ship energy system. As the results show, the hydrogen engines alone cause a certain amount of energy consumption reduction onboard. The reasons for these were partially improved power plant efficiency due to chosen power management logic and engine expected performance. Also, part of the savings is due to less boiler utilisation onboard, since hydrogen as clean fuel does not require certain heat consumers, which are required with HFO as fuel. Hydrogen fuel also enables more energy savings with heat recovery with ORCs.

In addition to operational simulations, life cycle assessment (LCA) is performed for the ship. The main results are illustrated in Fig.5. The CHEK combo includes all earlier mentioned technologies working in synergy. The CHEK technology combo already considerably reduces fuel consumption and, thus, emissions. When considering hydrogen fuel, assuming sustainable production from renewable sources, the total life cycle impact gets close to net-zero for the cruise ship.

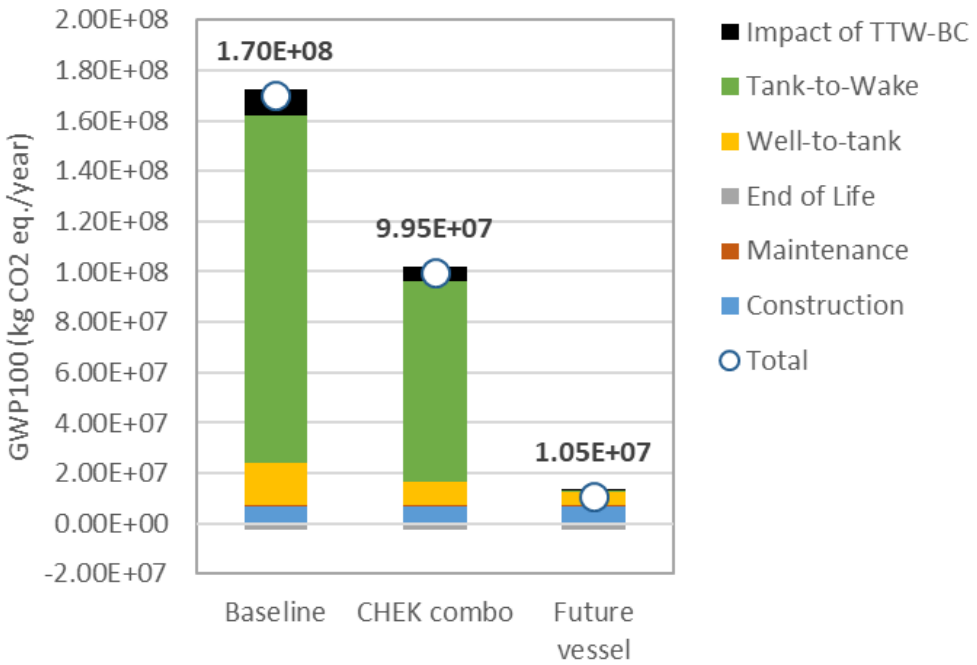


Fig.5: The main results of the CHEK cruise ship LCA

3. Digital design tools

3.1. Introduction to the future-proof vessel design platform

As stated earlier, ship decarbonisation is a combination of efficient operation, good design and technical improvements and also low carbon fuels. The operational profile is, thus, a leading driver and an integral part of the decarbonisation. To incorporate all this efficiently in ship design, new processes to support the traditional ship design process are necessary.

The future-proof vessel (FPV) design platform is a developing entity that aims to produce ship designs with low emissions. We can identify several dimensions which should be considered in the FPV design platform. One is the physical ship hull and volume dimension, which is the typical work performed for

dimensioning the vessel correctly and is required for compiling the ship specification and other documents for ship building. This layer is named DeltaWay. In project CHEK, majority of the work includes analysing the technology impact mainly on the energy flow level. Generating a hull, which serves as basis for the propulsion analysis, represents the DeltaWay layer in the project. Another dimension is the ship external forces, which are not documented in ship design materials but impact the ship operation. This layer is named DeltaSeas. A third dimension is the ship functional dimension focusing on energy system interactions and energy conversions, named DeltaKey.
Fig.6 provides a more detailed view to variables relevant for the propulsion profile (DeltaSeas) modelling and energy model (DeltaKey). DeltaKey provides as output the project key performance indicators.

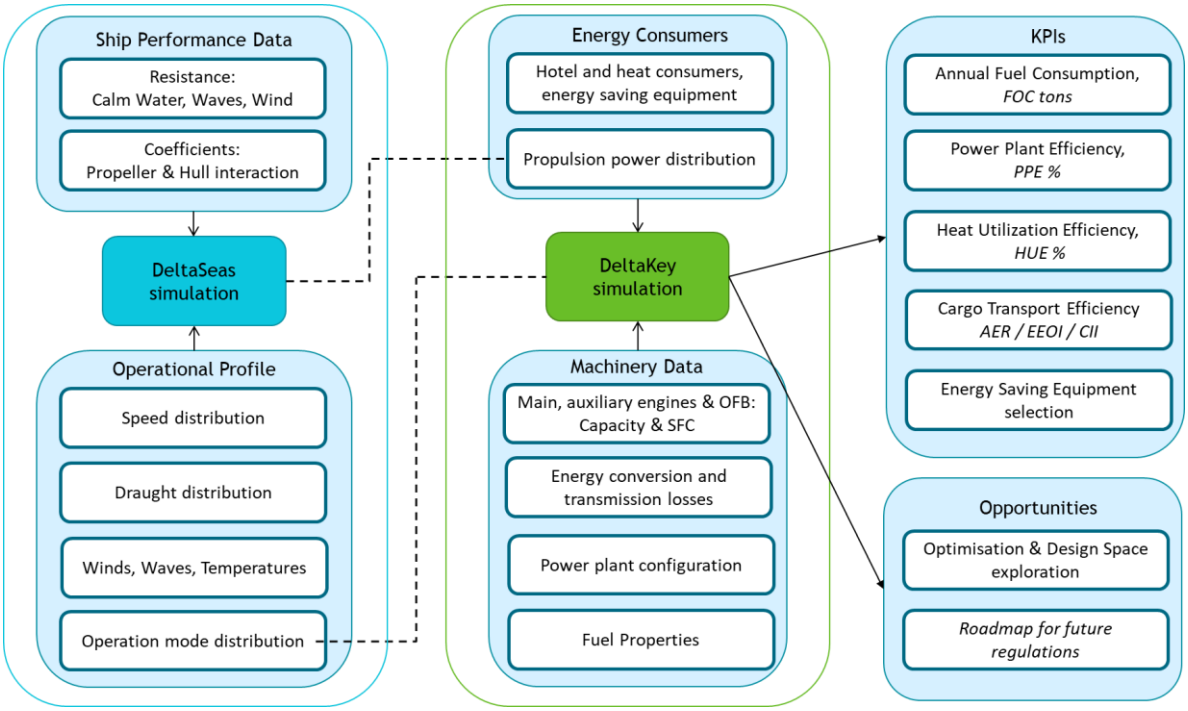


Fig.6: DeltaSeas and DeltaKey

3.2. DeltaSeas – propulsion profile model

The purpose of DeltaSeas is to collect as much relevant information as possible regarding ship operation. Typically, and in its simplest form, DeltaSeas would include a speed profile for the ship. Secondly, the weather and other margins are typically added on top of the propulsion power in form of a fixed “sea margin.”

Nevertheless, for the CHEK vessel this is not a satisfactory approach. Instead, for the ship routing, a set of geographical coordinates is generated with navigational routing software Wartsila FOS coupled with an interpolation algorithm. The seasonal weather variation is covered by assuming that the ship sails along each of the routes 12 times, starting on the first day of each month. Based on the vessel's position and assumed time the wind and wave parameters are gathered from the weather database. The structure for the data extraction algorithm, utilised in the entire cruise ship study, is shown in Fig.7.

The main databases used in the project are provided by the European Commission initiative called Copernicus, https://data.marine.copernicus.eu/product/GLOBAL_ANALYSISFORECAST_WAV_001_027/description, https://sextant.ifremer.fr/eng/Data/Catalogue#/metadata/a0e1104c-3fd3-4f81-9fcc-de00b756bd38. This initiative aggregates data provided by European meteorological institutes.

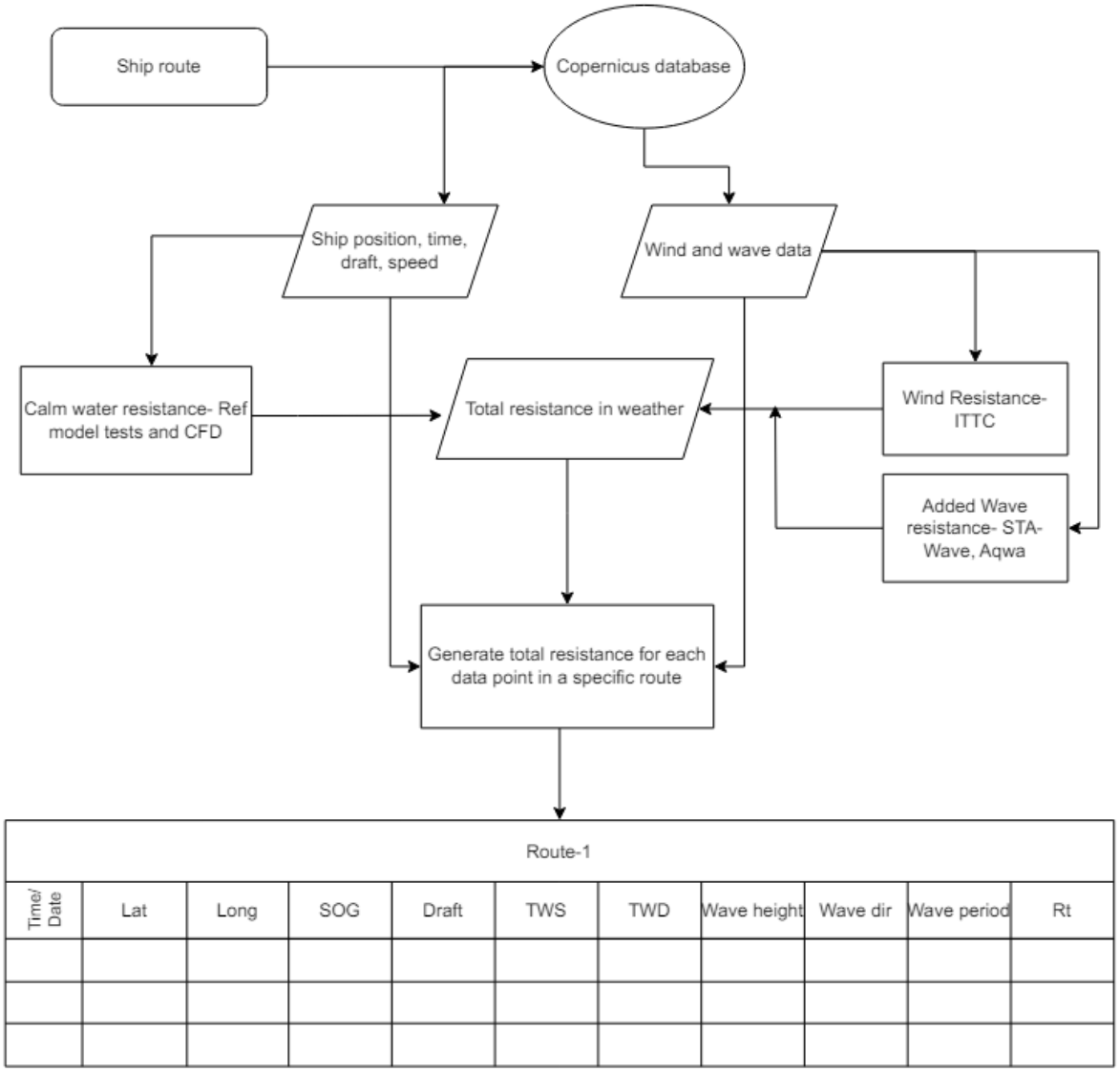


Fig.7: Algorithm for extraction and processing of data for ship added resistance

3.3. DeltaKey – Energy simulations

DeltaKey is a system level energy model. The inputs for the model include ship fuel types, machinery components and the energy requirements. The propulsion power is an input from DeltaSeas. The model is coded by Deltamarin and further developed in project CHEK on top of Matlab and Simulink tools. DeltaKey has been presented also in the CHEK bulk carrier intermediate result study earlier, *Sandberg et al. (2023).*

In project CHEK the focus is in implementing the CHEK technologies in the ship energy system. Some of the technologies are considered in the DeltaSeas code, but for instance ALS is considered both in DeltaSeas (reduced ship hull resistance) and in DeltaKey (the electricity demand). For the ORCs an entire logic for how several units would be implemented in a ship was developed during the project. DeltaKey, being fully developed and coded by Deltamarin, can be developed to also include external simulation models within.

Fig.8 illustrates the overall logic in the modelling regarding ship energy consumption and machinery utilisation for the Diesel-Electric system case, where addition of shore power, battery and ORC models are included.

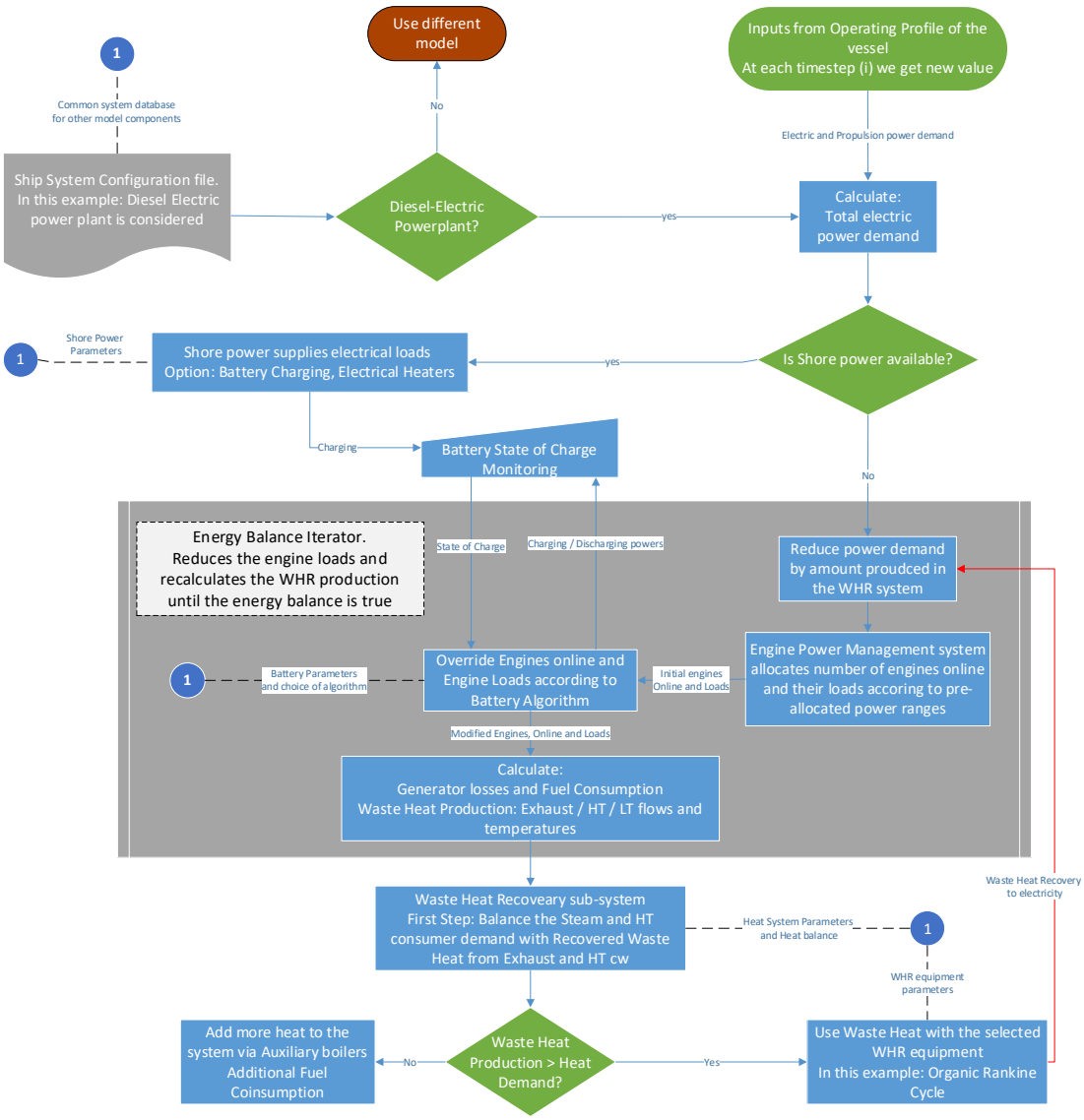


Fig.8: DeltaKey principal illustration of the logic in calculation

3.4. Life cycle assessment (LCA)

A new addition to FPV design platform is the life cycle assessment layer, developed fully in project CHEK. The scope of LCA in CHEK is illustrated in Fig.9.

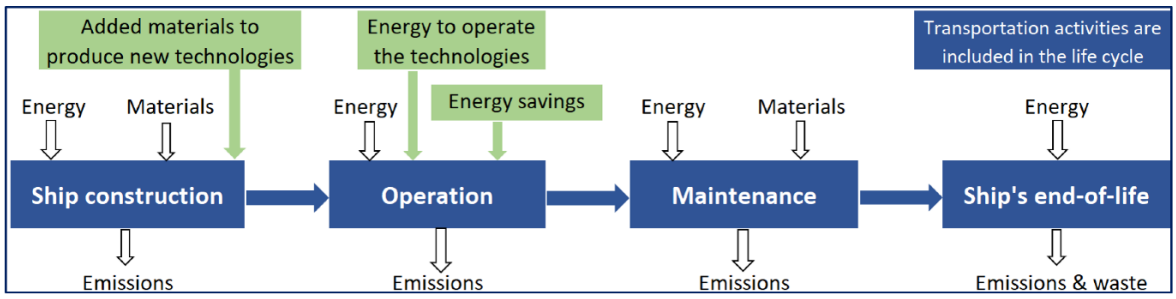


Fig.9: Life cycle analysis scope in project CHEK Fig.9: Life cycle analysis scope in project CHEK

The focus area is emissions to air from ship construction, operation, maintenance and end-of-life stages, considering the material and fuel pathways. The operational stage fuel consumption is a direct input from DeltaKey results, but regarding the other stages, the input is collected based on extensive literature research.

The digital design tools regarding ship physical dimensions and the ones for modelling operational fuel consumption, when utilised in the LCA form a "design based LCA" for the ship, which brings additional perspective in the ship or fleet strategic development. Fig.5 illustrates clearly that in the future, if majority of the ships would operate with sustainable fuels, the role of other processes than ship operation are lifted in focus regarding ship life time impact. Fig.10 illustrates how the digital design dimensions can be connected to form the design stage LCA.

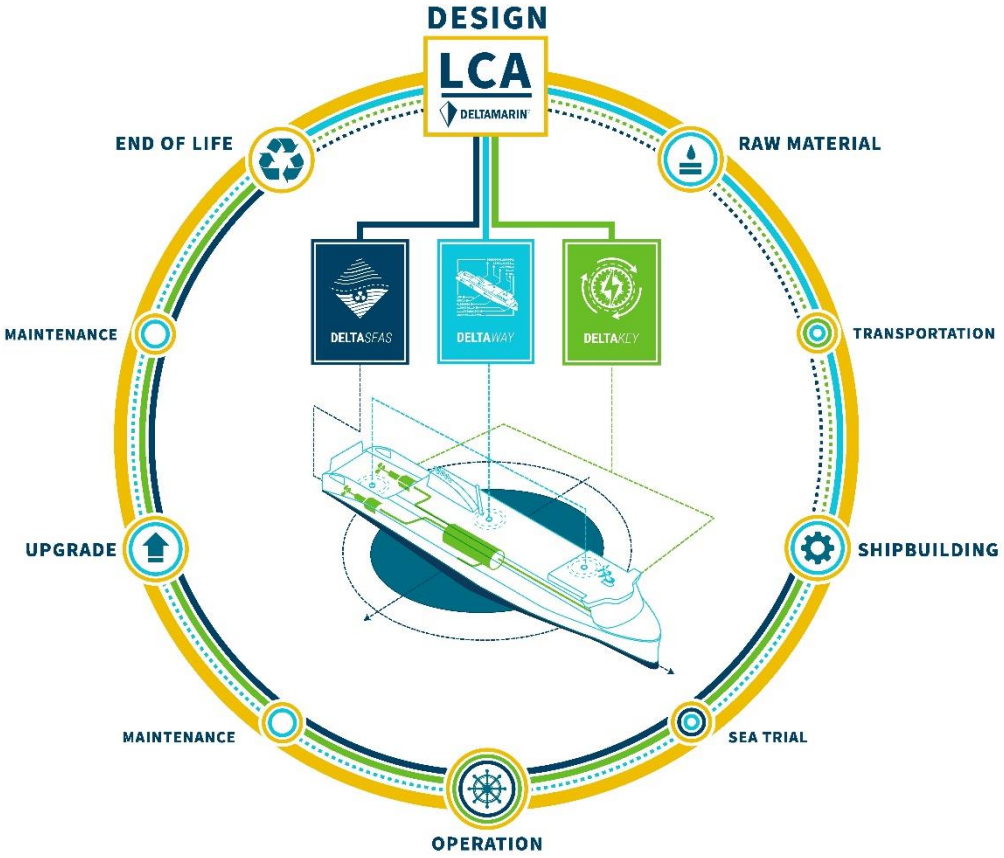


Fig.10: FPV design platform "dimensions" including design based LCA

4. Operational optimisation

4.1. Itinerary planning digitalisation

Cruise itineraries are typically set and marketed up to a year or two before they are operated. Itinerary optimisation can have a significant impact on environmental performance of the cruise operations. Decisions around port selection, timing and sequence must consider many interdependent and complex inputs to solve for optimal outcomes. *Melillo et al. (2014)* describe a cruise itinerary optimisation tool pilot developed and tested for one Meraviglia class vessel and 17 ports in West Mediterranean area. The tool represents the passage from manual to digital itinerary planning and is used as decision support system for the cruise itinerary planning process given the possibilities of planning, simulating, evaluating and performing several scenario analyses.

The tool consists of four main components: the Main Database, the Main Logic Module (Backend), the User Interface and the Solver. The system runs on four different operating modes in terms of degrees

of freedom provided by the user (optimisation of timings; optimisation of timings and sequence; optimisation of ports, timings and sequence; optimisation of some ports, timings and sequence).

Depending on the selected objective function(s) (e.g. maximisation of profit, minimisation of emissions or both), it provides as output one optimal solution or a set of efficient solutions.

The system architecture includes a stand-alone database that collects all the needed real data from the company systems for allowing the optimisation process to run, Fig.11. The tool is capable of aggregating data from different sources and different origins, considering fuel efficiency, revenue, as well as navigational or technical constraints and other itinerary related aspects.

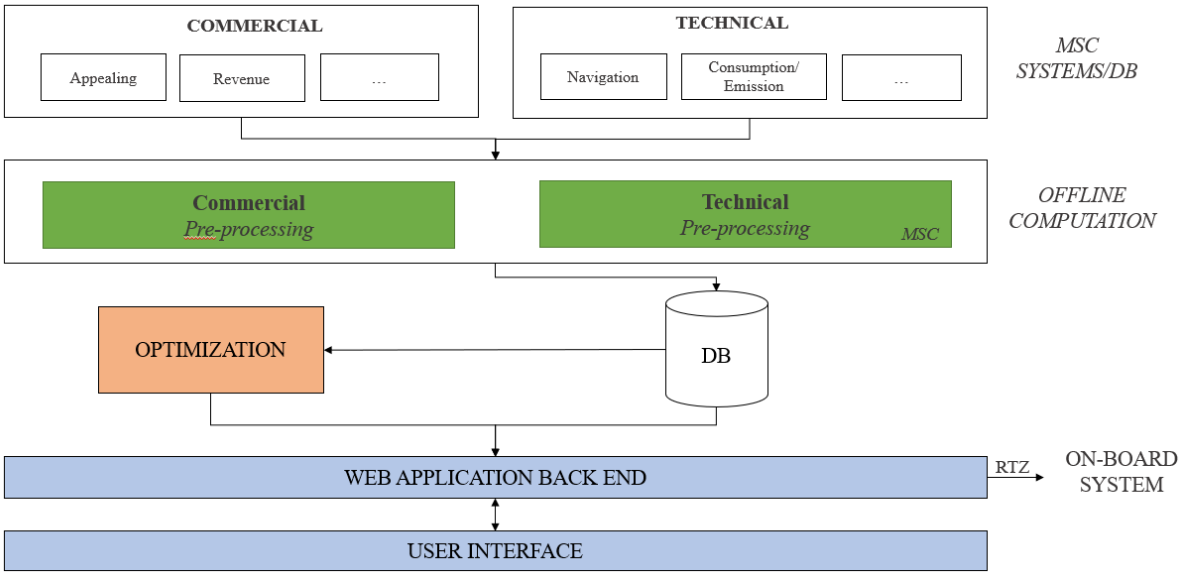


Fig.11: Cruise itinerary optimisation tool high-level design

The user interface comprises several layers - some of which are presented below - that allow the operators to select the best possible itineraries:

1. Planning: for creating the scenario to evaluate, entering the main information, and selecting the optimisation mode;
2. Revenue: comprises the touristic attractiveness of each port and the maximum embarkation/ disembarkation percentage for each port
3. Port Charges: includes the costs for each port depending on the duration of the stopover.
4. Technical layer: includes data such as “Manoeuvring” and “Ship characteristics” – including the ship model to calculate the fuel consumption;
5. Energy Efficiency: comprises the “Environmental Indexes" parameters, etc.
6. Results: the output of the tool might be, depending on the different modalities explained in *Melillo et al. (2023,2024)*, one optimal solution or a set of efficient solutions. Displayed output for each possible solution includes the main characteristics of the itinerary (i.e., ports, days, timings, stop duration), the suggested speed of sailing between each couple of ports, the level of touristic attractiveness and the economic performances, the fuel consumption, the environmental performance with all the defined indices and their values, the active hours at sea and in port. Several case study results showed that, by running the cruise itinerary optimisation tool can be obtained itineraries with improved CII, from rating D to B, reaching fuel savings up to 10%. The results of previous study also revealed the weaknesses in CII framework as a driver of absolute emission reductions for the cruise industry, since the best fuel saving itinerary is not always leading to the best CII performance.

The cruise itinerary optimisation tool has been developed to TRL4 during CHEK time frame and is being further expanded by including other elements relevant to the itinerary decisional process, enabling scalability and replicability towards all cruise vessels, other ports, basins, etc. The possibility of obtaining different itineraries for different ships with the addition of new constraints, such as, for example, visiting the same port in a limited number of itineraries and the deployment of the best ship given a certain itinerary represent key elements in the future operational development.

4.2. In-service performance monitoring and optimisation

4.2.1. Introduction

During actual operation, a system for high frequency data collection and analysis is crucial towards achieving savings in fuel and emissions. Such a system can be used to understand operational patterns and identify areas for improvement, provide suggestions to the ship's command to utilise their resources in an optimal way, enable smart data-driven decisions regarding the scheduling of interventions, and monitor the effectiveness of interventions thereafter. In addition, it acts as a feedback loop for development purposes and decision making for the future fleet, as showcased for instance in the CHEK design.

Some quantities of interest, for cruise ships in particular, would be the following:

- Ship's position, speed;
- Displacement, trim, stabiliser fin status;
- Engine configuration in use and produced power;
- Fuel flows to the diesel generators and the auxiliary boilers;
- Propulsion motors power and rpm;
- Electric power consumption of main transformers;
- Electric power consumption of major equipment (eg. air conditioning compressors, galleys, air handling units (AHU), laundry, engine room ventilation, large pumps);
- Fresh water production and consumption, running status of evaporators and reverse osmosis plants.

Indicative applications of such a performance system to enable more efficient and sustainable cruise ship operations are presented in this subchapter.

4.2.2. Propulsion power

A typical application, common for all merchant vessels, is the monitoring of propulsive performance, essentially of the ship's speed – power curve against a reference condition (e.g. model test conditions with weather corrections). This enables the operator to select the most effective coatings, detect fouling and optimise the cleaning operations for the hull and the propellers.

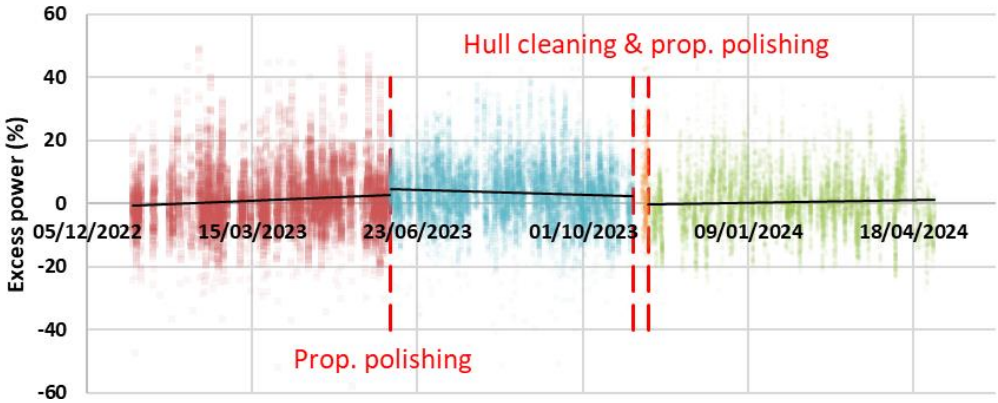


Fig.12: Meraviglia class vessel hull performance history

Fig.12 illustrates the hull performance history of a Meraviglia class ship, showcasing the effect of the development of light fouling on the propulsion power over approximately one year, which is then mitigated after a hull cleaning operation.

4.2.3. Non-propulsive (electrical / thermal) loads

Controlling non-propulsive loads on a cruise ship is of comparable importance to controlling the condition of the hull and the propellers. This can be based on parameters received through the performance system regarding the running status and power consumption of major equipment, as well as through the total power demand of groups of equipment supplied by the same transformer.

An example of the latter is shown in Fig.13, where a timeseries of the "measured" total non-propulsive electric load (calculated as the sum of relevant transformers' power) is plotted against a "predicted" load timeseries.

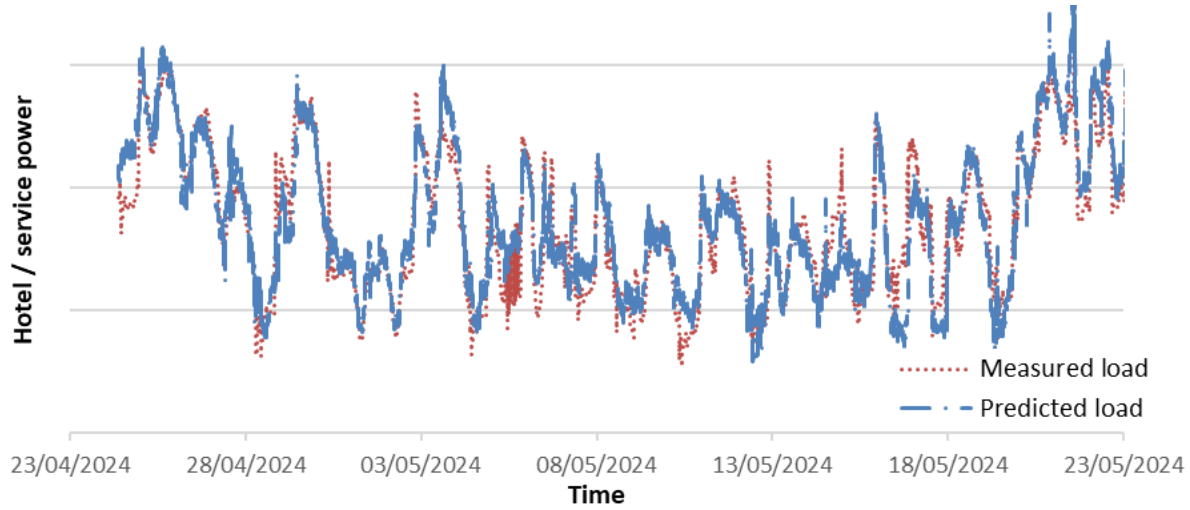


Fig.13: Measured versus predicted electric loads (Meraviglia class vessel over one month)

In this top-down approach, the measured load consists of four major components:

- Accommodation transformers' power, affected mainly by the local time, the voyage phase (at sea or in port) and the ambient conditions.
- Galley transformers' power, affected mainly by the local time.
- Air conditioning compressors power, affected mainly by the ambient conditions and the load of the compressors.
- Engine room transformers' power, affected mainly by the voyage phase (at sea or in port), the speed, the use of scrubbers and the ambient conditions.

'Digital twins' can be developed to simulate the power demand of each of the above categories, which summed up provide the total 'predicted load'. Comparison between the measured and predicted loads for each component can provide feedback on the effect of:

- Utilisation of air handling units (AHU) energy saving mode during inactive hours (affects the power of accommodation transformers);
- Energy efficient galley operation (by monitoring the galley load during inactive hours);
- Energy efficient machinery operation in port (eg. engine room ventilation).

There is significant value in sharing the related analytics with ship users, as well as setting up related alerts, in order to provide real-time support in the decision making of the ship's command. Examples include:

- Suggestion to retract the fin stabilisers if the fin angle is close to zero for a period of time;
- Suggestion to turn off an air conditioning compressor when the output power demand can be met with less compressors in use at higher load;
- Suggestion to turn off evaporator when oil fired boiler is in use, and turn on evaporator when there is steam excess from the exhaust gas boilers.

4.2.4. Power plant utilisation and efficiency

The diesel electric power systems typically present on cruise ships provides provide flexibility in operation and therefore significant opportunities for optimisation. One dimension here is the utilisation of the best possible engine combination (i.e. the one that optimises auxiliary loads, specific fuel oil consumption and emissions, including – if applicable – methane slip) for a given total power output. This can be calculated in real time based on the measured power production demand, providing advice to the ship's command in cases where a more efficient engine configuration is available to cover their given load, Fig.14.

Diesel Generators Power (MW)	18.09
Optimal Configuration At Sea	2 x 12V46F
Current Configuration	1 x 12V46F + 1 x 16V46F
Optimal Config. Check (At Sea)	0

Fig.14: Real-time actual versus optimal engine configuration example for Meraviglia class vessel

For analytics purposes, the engine configurations can also be studied over a period of time, Fig.15.

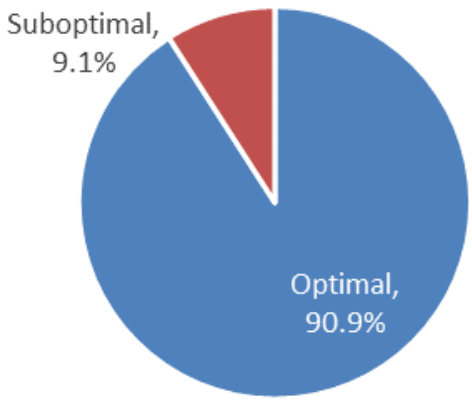


Fig.15: Engine configuration check over one month

A second dimension, which is unique to cruise ships and perhaps more interesting, is the optimisation of engine configuration on a voyage basis and in conjunction with the speed profile. In order to minimise fuel consumption and emissions over a given sea passage with fixed departure and arrival times, the optimal strategy usually involves changing the engine configuration and the ship's speed during the passage, rather than maintaining as much as possible the average speed. An example for a Meraviglia class vessel is presented in Table II, showing how a notable 7% fuel saving can be achieved by starting the passage at a speed higher than required and then slowing down, while always maintaining the engines close to their optimal load, which in this case is around 85%.

Table II: Comparison of fuel consumption over a sea passage with and without engine load optimisation – Meraviglia class vessel, 13 hours of navigation, required speed 20.7 kn

	Maintaining the average speed	Performing speed / engine load optimisation	
Average speed (kn)	20.7	20.7	
Operational speed (kn)	20.7	22.0	20.0
Time (hrs)	13.0	4.7	8.3
Propulsion power (MWe)	36	43	32
Hotel/service power (MWe)	11	11	11
Total power production (MWe)	47	54	43
Diesel Generator configuration	2x16V+2x12V	2x16V+2x12V	2x16V+1x12V
Diesel Generator load (%)	72%	83%	85%
Diesel Engine SFOC (g/kWh on MGO)	193	181	178
Fuel consumption (tonnes of MGO)	121	47	65
Total fuel consumption for the sea passage (tonnes of MGO)	**121**	**112**	

A decision support system including a digital twin of the vessel, which can also be calibrated in real time based on current hull performance and non-propulsive load requirements, can assist the ship's command to plan each leg in an optimal way. In addition, the collected data on the actual performance can be used for post-voyage analysis to identify areas for improvement and training.

Finally, monitoring the specific fuel/energy consumption of each engine provides valuable insight on their condition and enables condition-based maintenance. The monitoring system is again set up as an actual versus baseline comparison, where the baseline can be built from the engine's specifications/shop trials, with the necessary corrections for fuel type in use and the effect of ambient conditions. An example for a Meraviglia class vessel is provided in Fig.16 below.

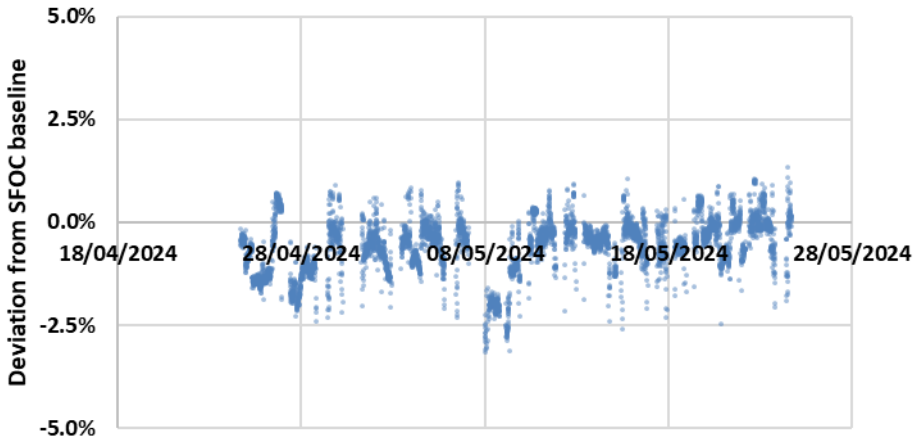


Fig.16: Deviation from SFOC baseline (Meraviglia class, one Diesel engine over one month)

5. Conclusions

The cruise industry is on a pathway to net-zero, along with the broader shipping industry and in accordance with environmental regulations.

Integrating energy efficient technologies into ship design is an important aspect of decarbonisation. It is essential to recognise that the technologies and ship design form an entity where most of the processes have cross connections. Also, the ship operations, such as operational speed have huge influence in the functioning of some of the technologies. Therefore, starting from the conceptual design stage, the ship's energy system should be developed by analysing the ship and her systems on realistic operational profile.

When introducing new fuels, several factors are considered in the ship design. In CHEK, the focus is on examining the potential interactions that the pure hydrogen could bring to the ship energy system. The simulation results reveal further energy savings on top of the energy saving technologies, due to new synergies in the ship energy system.

From an operational perspective, it is crucial to plan the itineraries in a sustainable way, aiming for fuel efficient operations with low environmental impact, while taking into account commercial and technical constraints. Another dimension is the collection and analysis of data during operation through a dedicated decision support system, that enhances optimal use of resources in real time, as well as improvement of the scheduling of interventions and assessment of their effectiveness. The presented tools for operational optimisation and the relevant examples indicate the high potential for fuel and emission savings by optimally planning and executing the operation of a given ship design.

Acknowledgements

The research presented in the paper was partially conducted under EU Horizon 2020 project deCarbonising sHipping by Enabling Key technology symbiosis on real vessel concept designs (CHEK – Contract No. 955286).

References

MELILLO, I.; CRACIUN, A.; WIDELL, K.; WIDELUND, A.; DUBOIS, A.; KELLING, J.; WILLIAMS, Y.; ELG, M.; ASTA, V. (2023), *Towards Zero-Emission Cruise Shipping*, 15th HIPER Symp., Bernried, pp.218-233, http://data.hiper-conf.info/Hiper2023_Bernried.pdf

MELILLO, I.; CRACIUN, A.; PAPADOPOULOS, F.; AMBROSINO, D.; ASTA, V.; TRAVERSA, C. (2024), *Managing CII through itinerary optimisation*, RINA Conf. Managing CII and Associated Challenges, London, pp.65-72

SANDBERG, A.; ELG, M.; MOLCHANOV, B.; KRISHNAN, A., WEJBERG, V. (2023), *Development in CII Performance of a Bulk Carrier, Transitioning from Today's State of the Art to Net-Zero Design*, 15th HIPER Symp., Bernried, pp.234-247, http://data.hiper-conf.info/Hiper2023_Bernried.pdf

Machinery Design Considerations of Future Fuel Cell Powered Vessels

Kenneth Goh, Knud E. Hansen, Perth/Australia, KEG@knudehansen.com

Abstract

As the world transitions to renewables and hydrogen economy, fuel cells will be a crucial part of enabling eco-friendly grid power and transportation. Fuel cells present a radical departure in propulsion and power generation systems compared to the standard 2-stroke engine directly coupled to the propeller used currently to propel over 95% of the global merchant fleet. The design of a merchant vessel is largely dictated by the installation requirements of the large 2-stroke engine. The study presented here examines in detail the differences between the propulsion components between a fuel cell and 2-stroke powered vessel and the machinery support systems. The changes required to the engine room and opportunities for redesign of the vessels arrangement with fuel cell propulsion has also been explored.

1. Introduction

The move towards viable fossil fuel alternative fuels presents many challenges for the shipping industry. Propulsion equipment suppliers must contend with fuels that are more difficult to make, are less energy dense, have more challenging combustion properties and difficult storage requirements. For ship designers, these alternative fuels require vessels to devote more space for fuel storage but also presents opportunities for vessel arrangements to be optimised around new types of propulsion machinery.

Knud E. Hansen identified liquid hydrogen (LH2) as the preferred future fuel, due to its better well-to-tank efficiency i.e., the energy needed to make the fuel, as shown in Fig.1.

Fuel	Energy density (MJ/kg)	Energy to produce (MJ/kg)	Well-to-Tank Efficiency	2030 Cost (USD per ton)	2030 Cost (USD per GJ)
Diesel	43	54 (Heat)	80%	500 - 1,000	12 - 23
Green Methanol (MeOH)	20	39 (Elec.)	50%	700 - 1,200	35 - 60
Green Ammonia (NH3)	19	43 (Elec.)	45%	1,000 - 1,500	53 - 79
Green 500 bar Hydrogen (500bar H2)	120	170 (Elec.)	70%	2,250 - 4,500	19 - 38
Green Liquid Hydrogen (LH2)	120	185 (Elec.)	65%	2,500 - 5,000	21 - 42

Fig.1: Well-to-tank efficiency & estimated cost of future marine fuels

As the paper explains, the advantage of hydrogen fuel comes from its very high energy per mass density, which is and six times better than either Methanol or Ammonia and nearly three times better than even fossil fuels. So even if it takes four times the energy to make hydrogen per kilogram compared to methanol or ammonia per kilogram, the well-to-tank efficiency of hydrogen is still higher.

The other fundamental reason why the well-to-tank efficiency of hydrogen fuel is better than green fuel alternatives, is that in order to make methanol or ammonia, you first need to have hydrogen as feed stock as can be seen in Fig.2.

The term ‘green fuel’ denotes the process of the fuel being produced purely using renewable energy such as wind, solar and hydro. The scaling of such renewable energy sources and the electrolysers need to produce the green fuels presents considerable challenges which are outside the scope of this study. Regardless of whether what green fuel is chosen in the future the electrolyser remains the key enabling technology.

There are two main motivations for using methanol and ammonia as future green fuels. The first is that both these fuels are easier to storage and transport, being liquids at or near room temperatures and

atmospheric pressure as can be seen in Fig.3. The other reason is that existing main machinery, such 2-stroke and 4-stroke diesel-cycle Internal Combustion Engines (ICE) can be used with relatively minor modifications to engine fuel and control systems.

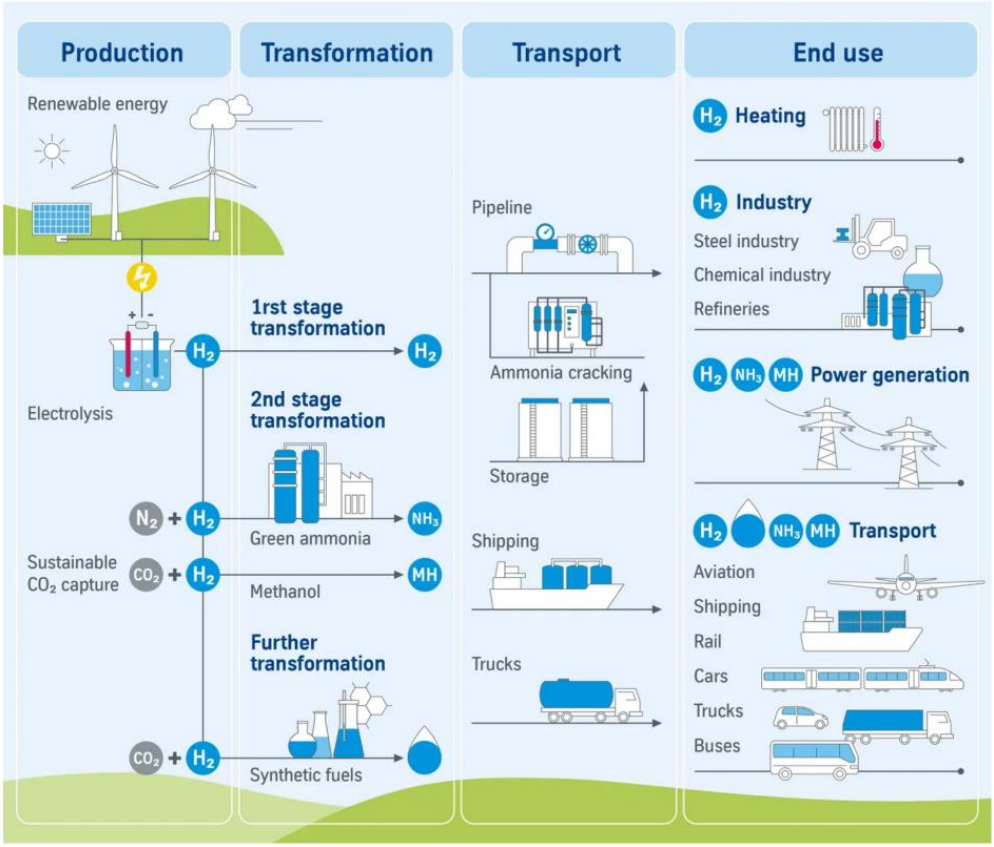


Fig.2: Well-to-tank processes for green fuels

Fuel	Storage Temp. (°C)	Storage Pressure (bar)	Tank fuel space ratio	Challenges	Tank type
Fuel Oil (HFO)	50 - 60	1	1	Heat	Integral, coated
Liquified Natural Gas (LNG)	-169	1	3 - 4	Boil-off	Pressure, membrane
Green Methanol (MeOH)	5 - 40	1	2 - 3	Corrosive, gas	Stainless steel, cofferdams
Green Ammonia (NH3)	-33	1	3 - 4	Toxic gas, boil-off	Stainless steel, cofferdams, insulated
Green 500 bar Hydrogen (500 bar H2)	5 - 40	500	15 - 20	HP, explosive	Unitary carbon fibre wrapped
Green Liquified Hydrogen (LH2)	-253	1	5 - 10	Boil-off, explosive	Unitary pressurised, membrane vacuum

Fig.3: Fuel storage requirements

While uses of green fuels will save considerable greenhouse gases from being emitted into the environment, the use of these fuels in ICEs still requires about 5% of diesel fuel to be injected into the cylinder as pilot fuel in order to start the methanol or ammonia combustion process. Such ‘green’ vessels will therefore still need to carry much of the same fuel handling and processing equipment.

We also explored the use of hydrogen fuelled Proton Exchange Membrane Fuel Cells (PEMFCs) as an alternative propulsion system to the standard 2-stroke and 4-stroke ICEs currently powering all of the global merchant fleet, Fig.4. The PEMFC’s generate electricity which is then used to power the vessel via electrical drives and motors as shown in Fig.5. This is a radical change that significantly improves the tank-to-wake efficiency and also reduce the auxiliary machinery systems required to support propulsion system, thereby reducing the vessel’s power and maintenance requirements.

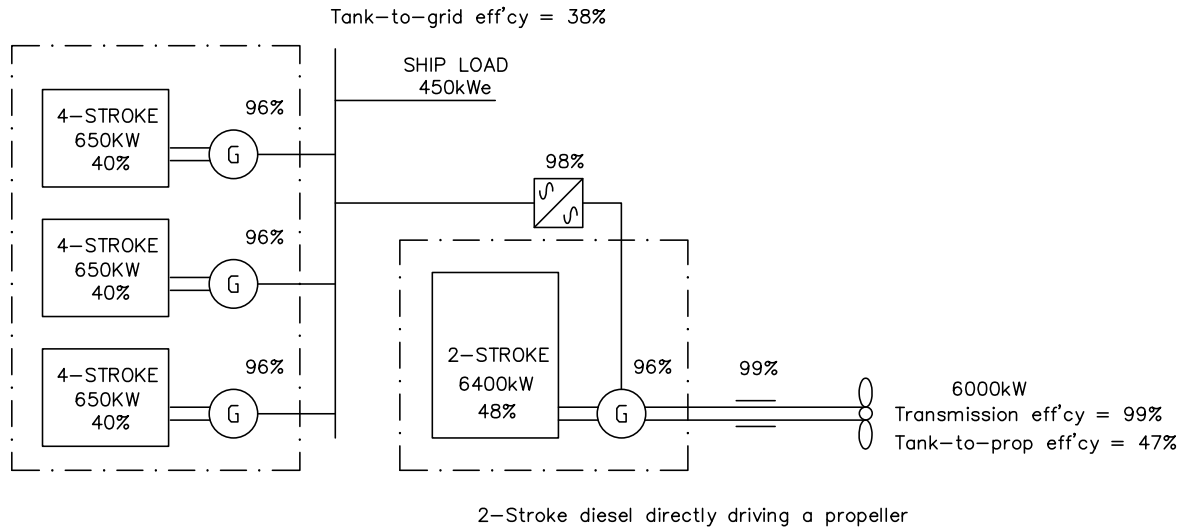


Fig.4: Typical merchant vessel ICE electrical & propulsion system

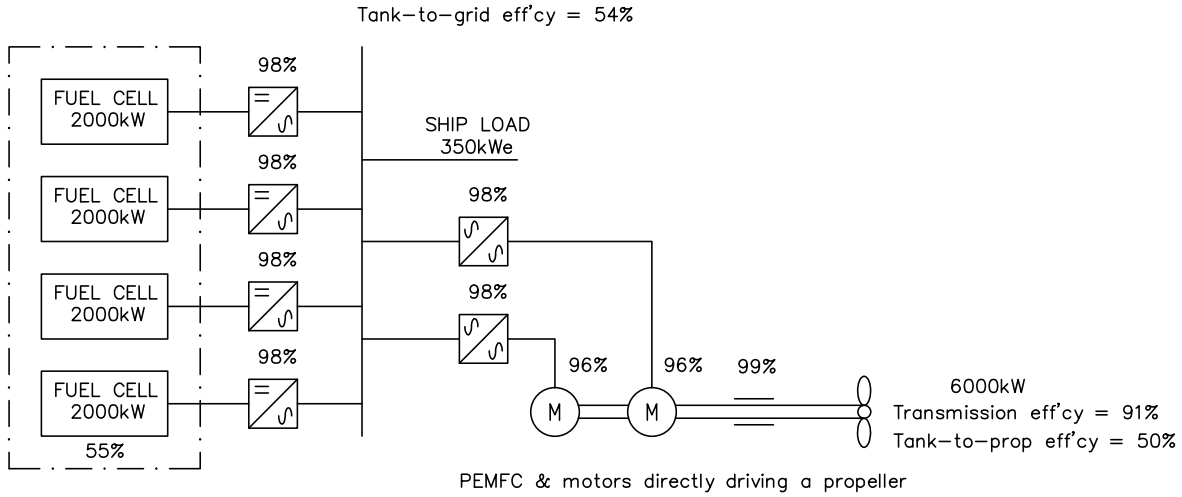


Fig.5: Proposed merchant vessel PEMFC electrical & propulsion system

2. Empirical Design Study

The study vessel is a Handymax bulk carrier, chosen for its ubiquitous utilisation, making up nearly a third of the vessels in the global bulk carrier merchant fleet. The principal particulars of a typical Handymax vessel are shown in Fig.6.

Principal Particulars	
Length overall	198.00 m
Beam	32.20 m
Depth	17.60 m
Draught	12.00 m
Deadweight	50,000 t
Hold capacity	63,500 m^3
Main engine	MAN B&W 6S–50 8,130 kW @ 108 rpm
Speed	14.5 kn
Complement	25 persons



Fig.6: Typical Handymax bulk carrier

Initially empirical data and formulas are used estimate the machinery space and fuel storage requirements of the alternative fuel and propulsion vessels. The estimations of machinery and fuel space requirements were translated into basic two-dimensional vessel arrangements to get a visual representation and comparison of various alternative fuels and propulsion systems. These arrangements can be seen in Fig.7 with the following colour code - **yellow** cargo space, **orange** machinery space, **red** fuel bunker, **crimson** tank insulation, **purple** main machinery, **green** electrical equipment, **blue** fuel cells, **black** propulsion.

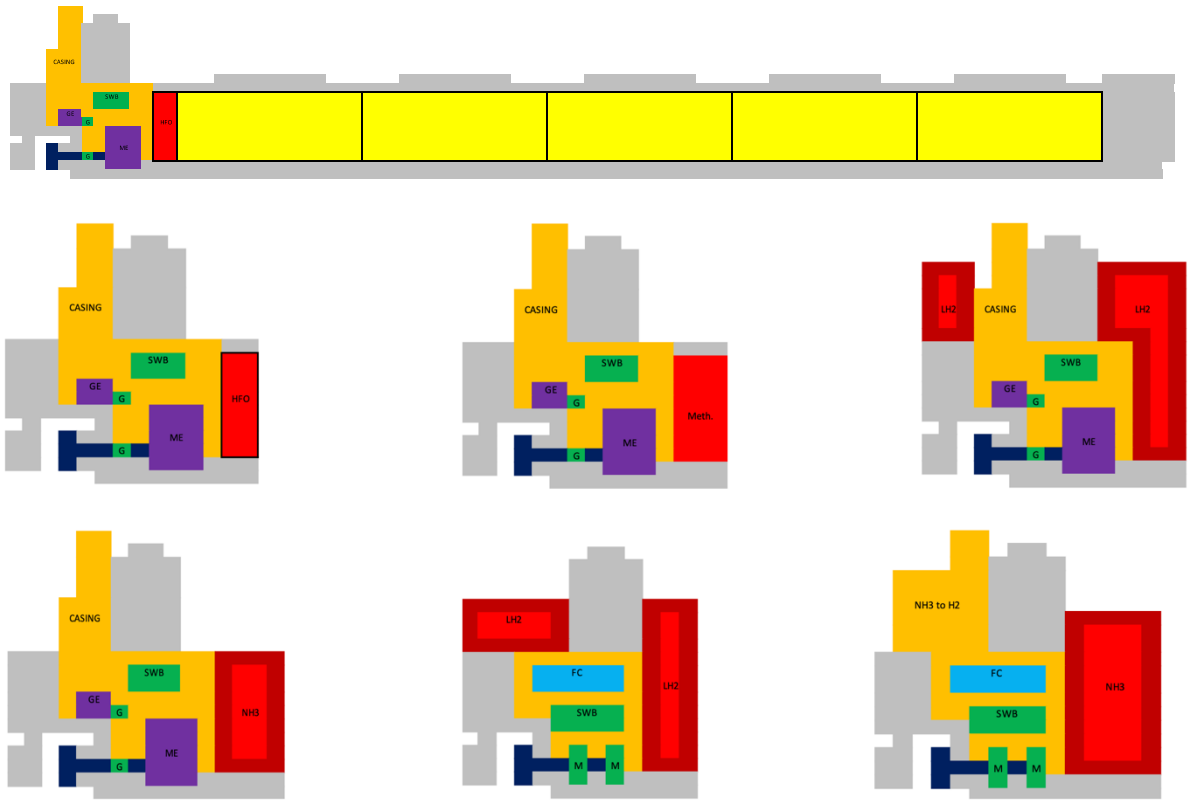


Fig.7: Engine room & fuel storage arrangements for alternative fuels & propulsion systems

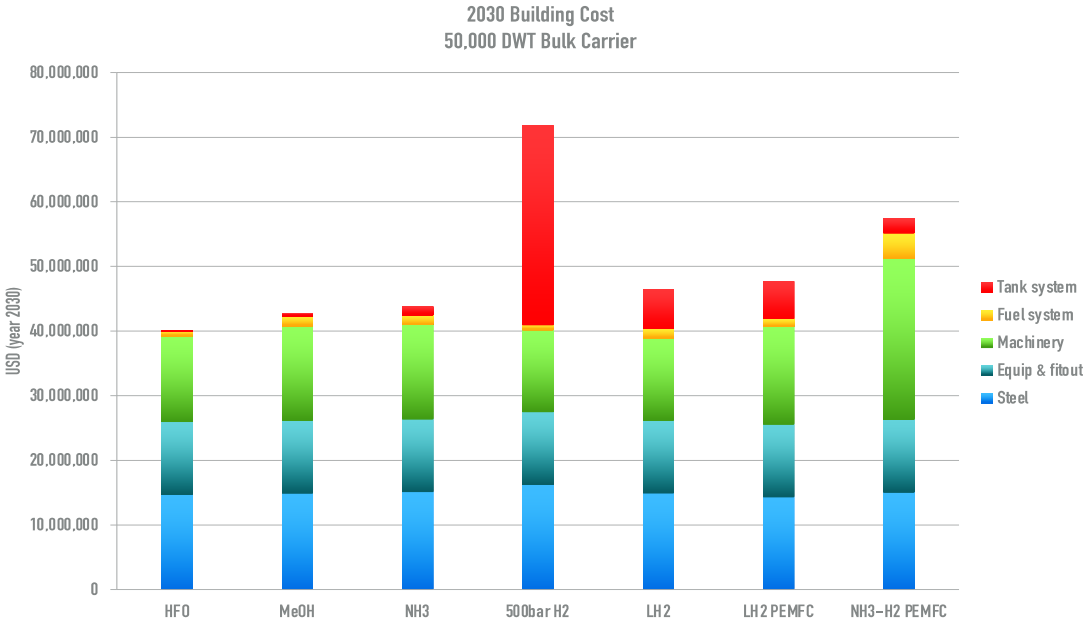


Fig.8: 2030 building costs for alternative fuels & propulsion system vessels

From this basic analysis, the vessel size and cost is estimated using regression formulas. This is combined with industry estimates for the 2030 costs of green fuel processing equipment and fuel storage tanks. The building cost for the various green fuel and propulsion options is shown in Fig.8.

A hypothetical vessel trade of shipping grain between New York and Rotterdam was calculated using industry estimates for green fuel costs. This enabled the vessel annual operating cost to be estimated with vessel financing and CO2 tax included. The resulting operating costs are shown in Figure 9.

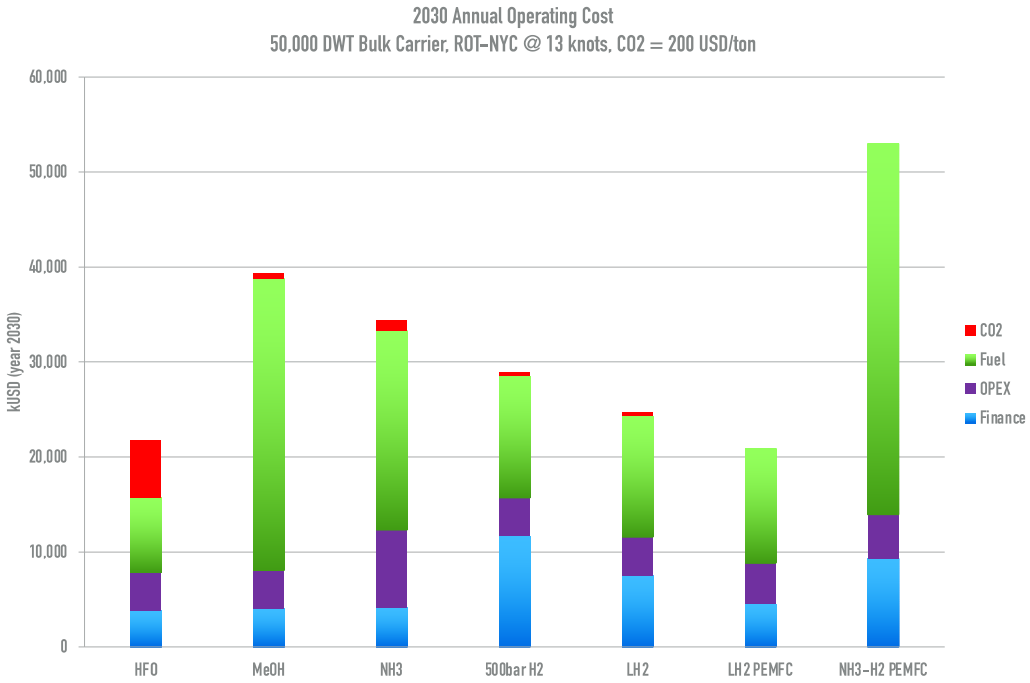


Fig.9: 2030 operating costs for alternative fuels & propulsion system vessels

3. Concept Design Study

The initial empirical design study indicates that a liquid hydrogen powered vessel using PEMFC and electric propulsion ultimately has the lowest operating costs and will be competitive with traditional fossil fuel ICE powered vessels when a CO2 tax of more than 200 USD per ton of CO2 is reached.

This vessel option was therefore selected for further development into a concept design study to verify the findings and refine the accuracy of the empirical design study. In the concept design study a more detailed investigation into the engine room design of the vessel is undertaken and considers the following requirements of electrical power and propulsion machinery and systems in the engine room.

1. Cooling
2. Heating
3. Compressed air
4. Electrical power
5. Exhaust
6. Other waste products
7. Weight
8. Space

3.1. Cooling

Much of the equipment in the engine room will give of heat due to efficiency losses. Some of this heat is rejected to the air in engine room such as an electric motor for a pump, while other high power

equipment such as generators, engines and even shaft bearings and large electrical motors and drives will require water cooling. It is normal for an ICEs cooling system to reject about half as much energy of the actual engine power produced as heat.

Large vessels such as merchant ships will use a central freshwater cooling system which will then transfer the heat to the sea through a heat exchanger. Heat rejected to the air will need to be removed mechanically by fan forced ventilation. The machinery cooling requirements for the LH2 fuelled PEMFC vessel is compared to a standard fossil fuel ICE powered vessel.

3.2. Heating

Some of the equipment in the engine room will require heating to operate correctly. For example, the bunker and service tanks of a vessel using Heavy Fuel Oil (HFO) needs to be heated to maintain its fluidity and enable the fuel to the pumped, purified and injected into ICEs. This heat is normally provided by either steam or thermal oil systems which need to be heated by either a dedicated fuel burning boiler / fluid heater or an economiser which is a boiler or fluid heater which is heated by the exhaust of the main engine. The machinery heating requirements for the LH2 fuelled PEMFC vessel are negligible compared to a standard fossil fuel ICE powered vessel.

3.3. Compressed Air

The large internal combustion engines of a standard fossil fuel powered vessel are usually started using compressed air at relatively high 30 bar pressure, which is about four times higher than the 8 bar air pressure used for air tools and other control processes on the vessel. There is no requirement for starting air for the LH2 fuelled PEMFC vessel and other compressed air requirements for process control are also significantly reduced compared to a standard fossil fuel ICE powered vessel.

3.4. Electrical Power

The electrical power needed in the engine room is largely dependent on the cooling requirements of the machinery. For example, a less efficient power generation and propulsion system will have more heat to be rejected by the vessels cooling systems which in turn requires higher pumping and ventilation flow rates which in turn demands a higher electrical load. Higher compressed air requirements will also require more electrical power for running the air compressors.

Vessel Type	Machinery Electrical Power
HFO fuel & ICE propulsion	463 kWe
LH2 fuel & PEMFC propulsion	109 kWe

Fig.10: Electrical power requirements for machinery systems

3.5. Exhaust from ICEs

Chemical processes such as the fuel combustion inside an engine produces tremendous amounts of exhaust gases with all manner of undesirable by-products, such as CO2 which has high global warming potential and nitrous oxides (NOx) and sulphur oxides (SOx) that can form acidic rain when emitted into the Earth's atmosphere. It is increasingly common to install exhaust processing equipment such as NOx reducing Selective Catalytic Reaction (SCR) reactors and SOx reducing scrubbers.

Apart from placing additional demands on the vessels electrical load, such equipment is large and mounted high up in the funnel and negatively impacts on the vessel's stability and available space. Additional toxic or highly corrosive consumables such as urea, ammonia and sodium hydroxide are also required for these emission control systems.

3.6. Exhaust from PEMFCs

The only emission produced by an LH2 fuelled PEMFC vessel is water vapour. For example, an 800 kWe PEMFC will produce about 320 kg of water vapour per hour at full power. Fresh water is a useful commodity on board any ship, being used for domestic purposes such as cooking, laundry, cleaning, personal hygiene as well as being consumed. It is also used in many machinery processes, such as fuel purification, steam generator feed water, machinery washing, fire-fighting water-mist systems, tank cleaning, flushing of seawater piping systems.

By capturing the water from the PEMFC emissions, additional electrical and heat energy is not needed to produce fresh water on board, typically through a vacuum evaporator or reverse osmosis. This is particularly relevant for passenger cruise vessels which have a high number of people on board each requiring about 300 litres of fresh water per day to meet all requirements.

For a Handymax bulk carrier with typically a crew of 20 persons, the amount for fresh water produced by a PEMFC could be up to 50 tons per day sailing. This far outweighs the requirement of 6 tons fresh water per day and opens the possibility to use more freshwater, instead of seawater for such things as cleaning and ballast water. This would lead to reduced corrosion, maintenance and painting saving both time and money for ship owners.

3.7. Other Waste Products

The processes of fuel oil and lube oil purification for necessary in support of ICEs creates sludge that needs to be collected and stored for discharge to shore facilities at considerable expense. As discussed above, the exhaust cleaning process is necessary to remove harmful gas emissions from the ICE exhaust, but this will also create toxic sludge that needs to be stored on board the vessel for shore discharge.

3.8. Equipment Weight

The weight of the power generation, propulsion machinery and any supporting systems and equipment was tallied for the standard HFO fuel ICE powered vessel and the LH2 fuelled PEMFC powered vessel for comparison and shown in Fig.11. Weight included estimations for piping, valves and electric cabling to provide a total system weight.

Vessel Type	Machinery Weight
HFO fuel & ICE propulsion	781 tons
LH2 fuel & PEMFC propulsion	572 tons

Fig.11: Weight of machinery systems

3.9. Equipment Space

The space requirements for the power generation, propulsion machinery and any supporting systems and equipment was tallied for the standard HFO fuel ICE powered vessel and the LH2 fuelled PEMFC powered vessel for comparison and shown in Fig.12. Access space for the equipment was also included to give a more realistic measurement of the space needed. Where equipment height exceeded 2.5 m, the same footprint area was added for every 2.5 m of equipment height. For example, the main engine has a base footprint of 30 m^2 and is 10 m in height, so therefore four additional 30 m^2 areas was added making the total footprint 150 m^2.

Vessel Type	Machinery Space
HFO fuel & ICE propulsion	586 m^2
LH2 fuel & PEMFC propulsion	402 m^2

Fig.12: Space requirements of machinery systems

3.10. Detailed Machinery Arrangements

The main purpose of machinery arrangements shown in Fig.7 is to give an understanding of the relative size of the main equipment and their logical location relative to each other in a two-dimensional mapping for comparative purposes. There are many ways to arrange engine rooms and fuel tanks and the model cannot be expected to encompass all possible design solutions.

For the concept design study all the main machinery and supporting equipment was arranged into a typical Handymax bulk carrier engine room space to further check the viability of using a PEMFC propulsion system for a merchant vessel. A typical arrangement for a standard fuel oil vessel with ICEs for propulsion and power generation was also generated as a check and for comparative purposes.

The standard HFO vessel with 2-stroke engine main propulsion and 4-stroke engine power generation also employs a high-pressure SCR for control of NOx emissions and a scrubber for control of SOx emissions. The aim was to try and make the fossil fuel vessel as environmentally friendly as the liquid hydrogen and fuel cell powered vessel despite the obvious CO2 emissions. A CO2 capture system was not implemented, since the maturity of such technology has not yet been adequately demonstrated. Therefore, the CO2 can only be offset by the CO2 tax in the vessel operating costs.

Two battery banks totally 2500 kWh was also added to the PEMFC vessel to allow liquid hydrogen boil-off from the two 1000 m^3 LH2 tanks to be consumed by the fuel cells for battery charging when vessel power demand is low. The battery banks serve as both an electrical energy cache and to reduce peak power demands.

4. Conclusions

A review of the previous study by the author identifies that liquid hydrogen can be made more efficiently than other green fuels proposed such as methanol and ammonia.

An initial design study using empirical formulas for vessel space and cost enabled the evaluation of a multiple vessel options with different green fuels and propulsion machinery including conventional internal combustion engines propulsion and fuel cells with electric propulsion.

The result of the initial study is that the vessel with liquid hydrogen fuel and PEM fuel cells had the lowest overall operating cost despite the slightly higher building cost. This vessel was selected for a more detailed design process to verify the findings of the initial study and arrive at a valid concept design for the machinery space.

Various machinery parameters and capabilities were assessed in the concept design including cooling, heating, exhaust, waste products, electrical power, weight and space requirements and compared for the fuel cell vessel against a typical current Handymax bulk carrier. The study found that the fuel cell vessel was feasible to arrange in the current vessel based on the reduced weight and space requirements when compared to a standard vessel.

Furthermore, the electrical power requirements of the fuel cell vessel was about a quarter when compared to a green but conventional fuelled and powered vessel.

5. Future Studies

Due to the much lower maintenance demands, a future study will examine the potential for hydrogen powered fuel cell vessels to operate with either reduced engineering crew or as an unmanned vessel.

The study will further explore the technology and options for liquid hydrogen storage and gasification. The possibility of using the cold energy in the LH2 will be investigated to reduce air conditioning loads or even the equipment cooling loads.

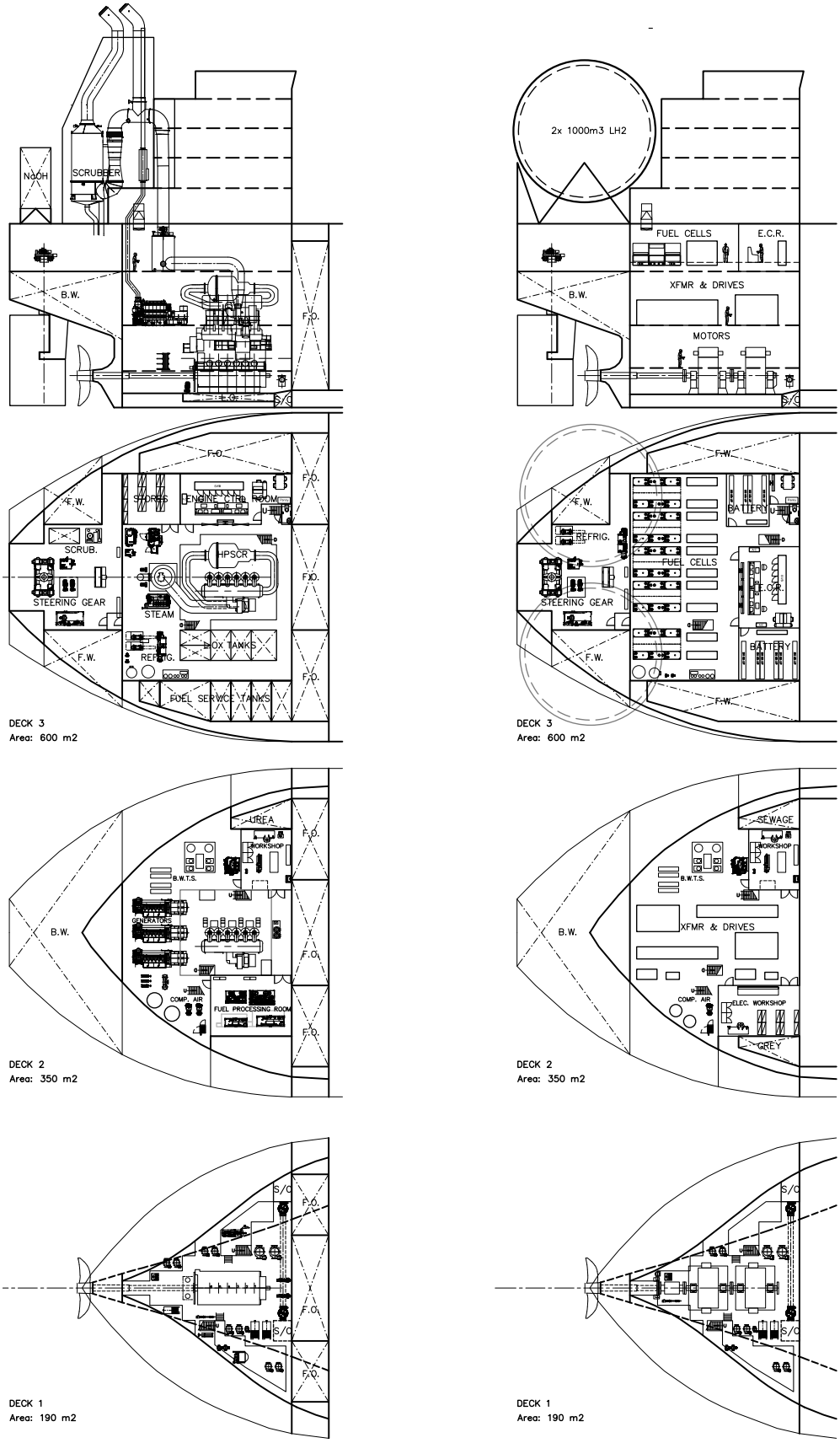


Fig.13: Detailed machinery arrangements, left: HFO fuel ICE, right: LH2 fuel PEMFC

Index by Authors

Albert 49
Arens 73
Armin 268
Bensow 197
Bertram 6,10,21,36
Bhattacharya 164
Blanco-Davis 268
Brüns 149
Castagna 89
Cederberg 43
Cerro 226
Craciun 324
Czerski 149
Dane 177
De Brie 149
Delneri xxx
Dunger 140
Elg 324
Engels 281
Früchtenicht 315
Galecka 29
Goh 339
Hagel 315
Hahn 10
Hansen 10
Hildebrandt 49
Hochkirch 10
Höflich 290
Hübler 149
Jacob 208
Jin 118
Kalajdžić 107
Kistner 252
Kanafi 184
Klindt 281
Korkmaz 197
Kudari 149
Kuusisto 184
Lindinger 131
Lu 197
Mallol 49
Marmefelt 43
Mehldau 149
Melillo 324
Melloh 140
Milliner 177
Necel 149
Nice 208
Onishi 118
Paakkari 245
Papadopoulos 324
Pearson 73
Perez Fernandez 73
Plowman 21
Ponkratov 73
Poppelier 49
Pruszko 149
Ramesh 164
Ravens 281
Reichel 149
Reimer 101
Renzsch 218,268
Routledge 268
Rozenauers 177
Sankaramoorthy 226
Snöberg 43
Spiteri 268
Sugimoto 118
Thies 218
Vasilev 107
Wakabayashi 118
Warmann 140
Wasmansdorff 131
Werner 197
Yum 252

17th Symposium on

High-Performance Marine Vehicles – "Technologies for Future Ships & Shipping"

Tullamore / Ireland, 5-7 May 2025





Topics: ultra-efficient & zero-emission ships / EEXI & CII issues / alternative fuels / electric ships
advanced designs & retrofits / shipyard 4.0 / future materials / future use of oceans / blue economy /
intelligent & connected ships / future antifouling / biomimetic marine technologies

Organiser: Volker Bertram (volker@vb-conferences.com)

Advisory Committee:

Carlo Bertorello	Naples University	**Robert Dane**	Ocius	**Richard Marioth**	Idealship
Carsten Bullemer	Maritime Data Systems	**Thomas De Nucci**	USCG Academy	**Kohei Matsuo**	NMRI
Emilio Campana	CNR	**Stefan Harries**	Friendship Systems	**Ivana Melillo**	MSC
Roy Campe	CMB	**Thomas Hildebrandt**	Numeca	**Ville Paakkari**	Norsepower
Marcel Cleijsen	Wärtsilä	**Jan Kelling**	Hasytec	**Pierre Sames**	DNV
Andrea Coraddu	TU Delft	**Jiulun Liu**	Wuhan Univ Technology	**Noah Silberschmidt**	Silverstream Technologies

Venue: The conference will be held at the Bridge House Hotel in Tullamore/Ireland

Format: Papers to the above topics are invited and will be selected by a selection committee.
Proceedings will be electronic pdf version in colour.

Deadlines:

anytime	Optional "early warning" of interest to submit paper
10.1.2025	First round of abstract selection (1/3 of available slots)
01.2.2025	**Second round of abstract selection (remaining 2/3 of slots)**
10.4.2025	Payment due for authors
15.4.2025	Final papers due (60 € surcharge for late submission)

Fees:

700 € / 350 €	regular / PhD student – early registration (by 10.4.2025)
800 € / 400 €	regular / PhD student – late registration

Fees are subject to VAT.
Fees include proceedings, lunches and coffee breaks, and conference dinner.
Fees apply also to authors.

Sponsors: Tutech Innovation, Hasytec, Idealship – further to be announced

Ship operators: tbd

Media Partner: Hansa, Royal Institution of Naval Architects

Information: volker@vb-conferences.com